

The Institute for Solid State Physics  
The University of Tokyo

# Activity Report 2018



# ISSP

## Activity Report 2018

Contents	Pages
Preface	1
Research Highlights	2 - 29
Joint Research Highlights	30 - 45
Progress of Facilities	46 - 53
Conferences and Workshops	54 - 61
Subjects of Joint Research	62 - 157
Publications	158 - 196



# Preface

We would like to offer the readers the scientific activity report of the Institute for Solid State Physics (ISSP) for the Japanese FY 2018.

ISSP was established in 1957 as a joint-use/research institute attached to the University of Tokyo. In every era, we aim to lead the frontier of “condensed matter physics and materials science” and contribute to science and technology from the view of basic research. We have promoted activities focused on research, education, and joint-use/joint-research.

The first part of the reports Research Highlights /Joint Research Highlights exhibits experimental and theoretical achievements in condensed matter physics and materials science. In 2018, the number of granted joint-research proposals is 1,330 and the total number of participants is 8,869.

The second part includes the reports on progress of facilities in 2018 as follows. (1) In International MegaGauss Science Laboratory, the pulse magnet has achieved 1,200 T as the world strongest as an in-door record by destructive methods. (2) The Supercomputer Center (SCC) has conducted “Project for advancement of software usability in materials science” for enhancing the usability of the ISSP supercomputer system since 2015. In Center of Computational Materials Science, the website "MateriApps" for information on application software in computational science has been constructed to support community members as the major contractor of K- and Post-K Computer Projects. (3) In Neutron Science Laboratory, the technical progress of High Resolution Chopper (HRC) spectrometer has been proceeded under high pressure and low temperature environment in cooperation with KEK. (4) In Laser and Synchrotron Research (LASOR) center, the powerful technique by spin- and angle-resolved photoelectron spectroscopy (SARPES) has clarified the spin-dependent electronic states in topological materials. In Synchrotron Radiation Laboratory, operand spectroscopy is available by using lasers at Harima branch.

In the following parts, eleven reports of international conferences and workshops, subjects of joint research, and list of publications have been presented.

In order to develop the international scientific network as scientific hub based upon the successful experience of JSPS Program for Advancing Strategic International Networks to Accelerate the Circulation of Talented Researchers for “Leading Research Network Topological Phenomena in Novel Quantum Matter” (TopoNet) (2014-2016), new programs including the short time (up to 3 months) international collaboration, international visiting researchers, and graduate students study abroad, as well as foreign visiting professor and international workshop programs, have been conducted since 2017.

All these facts confirm that ISSP continues to develop successfully and dynamically as the global center of excellence of condensed matter physics and materials science. We appreciate continuous support and cooperation of communities for our activities.



July, 2019  
Hatsumi MORI  
Director  
Institute for Solid State Physics,  
The University of Tokyo

# Research Highlights

## Horizontal Lines of Nodes in the Superconducting Gap of Sr<sub>2</sub>RuO<sub>4</sub>: Evidence against the Anticipated Chiral *p*-wave Scenario

Sakakibara Group

The layered-perovskite superconductor Sr<sub>2</sub>RuO<sub>4</sub> has been a leading candidate of a spin-triplet chiral *p*-wave superconductor; the spin-triplet pairing (chiral state) was suggested by the invariant spin susceptibility across  $T_c$  (time-reversal symmetry breaking in the superconducting state) [1]. However, the recently-discovered first-order superconducting transition, reminiscent of the Pauli-paramagnetic effect, under an in-plane magnetic field is likely to favor the spin-singlet scenario [2, 3]. Moreover, whereas symmetry-protected nodes are forbidden in the spin-triplet scenario, the presence of nodes has been suggested from various thermodynamic experiments. Thus, the order parameter of Sr<sub>2</sub>RuO<sub>4</sub> has remained controversial.

Recently, we have developed field-angle-resolved measurements of the specific heat as a powerful technique to identify the superconducting gap structure [4]. Here, in order to provide hints for resolving the puzzling issues

on Sr<sub>2</sub>RuO<sub>4</sub>, we have performed the field-angle-resolved measurements at low temperatures down to 0.06 K by using a high-quality single crystal ( $T_c = 1.505$  K) [5]. By subtracting the Schottky-type anomaly originating from the addenda heat capacity very precisely, we have revealed that the low-field specific heat of our sample increases in proportion to  $H^{1/2}$  with no multigap structure at 0.06 K. This behavior is in sharp contrast to the previous reports [6], and suggests that multiple gaps on the three bands ( $\alpha$ ,  $\beta$ , and  $\gamma$ ) equivalently survive up to high fields and possess nodes somewhere. In addition, the fourfold oscillation in the specific heat observed under an in-plane rotating field [6] does not change its sign even at a low temperature of  $0.04T_c$  in the low-field region (Figs. 1(a) and 1(b)).

The absence of a sign change in the fourfold specific-heat oscillation is incompatible with vertical line node scenario, such as the  $d_{x^2-y^2}$ - and  $d_{xy}$ -wave type; the present results are clearly different from the cases of vertical line node superconductors such as CeCoIn<sub>5</sub> [4]. Also, it is obvious that the present observations cannot be explained within the anticipated chiral-*p*-wave scenario. By contrast, the results favorably support the presence of horizontal line nodes; the specific-heat oscillation arises due to nodal quasiparticles that have anisotropic in-plane Fermi velocity of the cylindrical  $\gamma$  band. On the basis of microscopic theoretical calculations, the observed field and temperature variations of the specific-heat oscillation can be reproduced by assuming the presence of horizontal line nodes on cylindrical bands whose Fermi velocity is highly anisotropic within the plane (Fig. 1(c)). The agreement between the experimental and the calculated results becomes even better by taking into account the Pauli-paramagnetic effect. Our findings, in particular the presence of horizontal line nodes in the gap, challenge the historical view of Sr<sub>2</sub>RuO<sub>4</sub> and call for reconsideration of its order parameter.

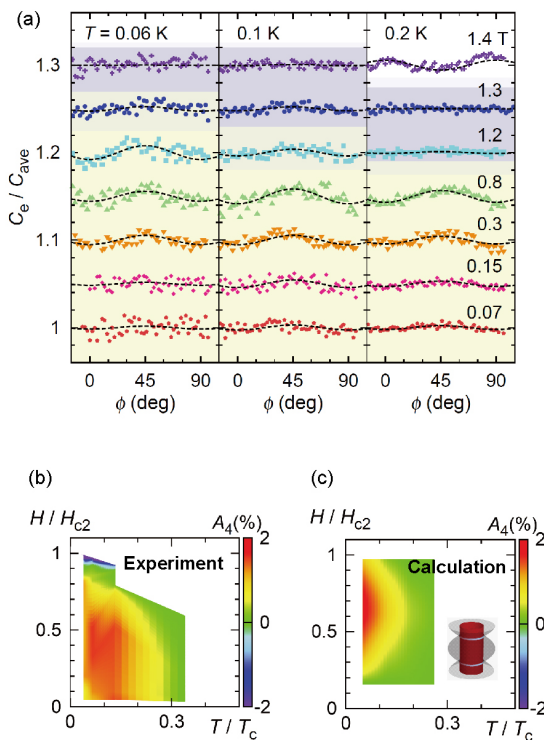


Fig. 1. (a) Field-angle dependence of the specific heat under a rotating magnetic field within the *ab* plane of Sr<sub>2</sub>RuO<sub>4</sub>. (b) The *H*-*T* phase diagram of the normalized amplitude  $A_4$  of the fourfold specific-heat oscillation. (c) The calculated results of  $A_4(T, H)$  obtained by assuming a horizontal line node gap (inset), anisotropic in-plane Fermi velocity, and the Pauli-paramagnetic effect.

### References

- [1] Y. Maeno, S. Kittaka, T. Nomura, S. Yonezawa, and K. Ishida, *J. Phys. Soc. Jpn.* **81**, 011009 (2012).
- [2] S. Yonezawa, T. Kajikawa, and Y. Maeno, *Phys. Rev. Lett.* **110**, 077003 (2013).
- [3] S. Kittaka *et al.*, *Phys. Rev. B* **90**, 220502(R) (2014).
- [4] T. Sakakibara, S. Kittaka, and K. Machida, *Rep. Prog. Phys.* **79**, 094002 (2016).
- [5] S. Kittaka *et al.*, *J. Phys. Soc. Jpn.* **87**, 093703 (2018).
- [6] K. Deguchi *et al.*, *J. Phys. Rev. Lett.* **92**, 047002 (2004).

### Authors

S. Kittaka, S. Nakamura, T. Sakakibara, N. Kikugawa<sup>a</sup>, T. Terashima<sup>a</sup>, S. Uji<sup>a,b</sup>, D. A. Sokolov<sup>c</sup>, A. P. Mackenzie<sup>c</sup>, K. Irie<sup>d</sup>, Y. Tsutsumi<sup>e,f</sup>, K. Suzuki<sup>d</sup>, and K. Machida<sup>d</sup>

<sup>a</sup>National Institute for Materials Science

<sup>b</sup>University of Tsukuba

<sup>c</sup>Max Planck Institute for Chemical Physics of Solids

<sup>d</sup>Ritsumeikan University

<sup>e</sup>The University of Tokyo

<sup>f</sup>RIKEN

# Construction of Three-Dimensional Anionic Molecular Frameworks Based on Hydrogen-Bonded Metal Dithiolene Complexes and the Crystal Solvent Effect

Mori Group

Metal organic frameworks (MOFs) and covalent organic frameworks (COFs) are a class of crystalline materials with highly periodic structures formed through coordination or covalent bonds. Extensive synthetic studies of these materials have been carried out, because of the uniqueness of their structures and the resulting functionalities, such as gas adsorption/separation, catalytic, and sensing abilities and fuel cell properties. In addition, hydrogen-bonded (H-bonded) organic frameworks (HOFs) have recently emerged as a new class of such crystalline materials. By utilizing H-bonds instead of coordination or covalent bonds, HOFs have generally better crystallinity, solution processability, and flexibility than MOFs and COFs. Such ionic frameworks are expected to show unique features different from conventional neutral ones, due to their intrinsic ionic nature and the accompanying cation–anion interactions. However, the number of ionic frameworks reported so far is limited.

Recently, we have designed and synthesized a novel metal dithiolene complex with hydrogen-bonding (H-bonding) ability,  $[\text{Au}(\text{catdt})_2]^-$  (catdt: catechol-4,5-dithiolate) and successfully constructed  $[\text{Au}(\text{catdt})_2]^-$ -based three dimensional (3D) anionic molecular frameworks in two kinds of salts,  $(\text{Ph}_4\text{P})[\text{Au}(\text{catdt})_2] \cdot 0.5\text{H}_2\text{O}$  (**1a**) and  $(\text{Ph}_4\text{P})[\text{Au}(\text{catdt})_2] \cdot \text{Et}_2\text{O} \cdot n(\text{solv})$  (**1b**; solv =  $\text{Et}_2\text{O}$  and/or acetone). To our knowledge, these are the first examples of the 3D molecular frameworks based on H-bonded metal dithiolene complexes. Importantly, these frameworks are constructed through 3D intermolecular H-bonds between  $[\text{Au}(\text{catdt})_2]^-$  molecules, and have tubular channels occupied by large  $\text{Ph}_4\text{P}^+$  cations, where multiple cation–anion short contacts are formed to stabilize the 3D framework structures. Furthermore, in addition to **1a** and **1b** with 3D frameworks, we have obtained  $(\text{Ph}_4\text{P})[\text{Au}(\text{catdt})_2] \cdot 2\text{THF}$  (**1c**) having a 2D layered structure. A detailed comparison of the structures of these compounds reveals that the included solvent molecules play an important role in regulating the intermolecular interactions and assembled structures. Interestingly, we have found that, due to the differences in the H-bonding ability and molecular size of  $\text{H}_2\text{O}$  and  $\text{Et}_2\text{O}$ , the wall structures of the 3D frameworks in **1a** without voids and **1b** with voids are qualitatively different. [1]

Three kinds of 1:1 salts of  $\text{Ph}_4\text{P}^+$  and  $[\text{Au}(\text{catdt})_2]^-$ , that is,  $(\text{Ph}_4\text{P})[\text{Au}(\text{catdt})_2] \cdot 0.5\text{H}_2\text{O}$  (**1a**),  $(\text{Ph}_4\text{P})[\text{Au}(\text{catdt})_2] \cdot \text{Et}_2\text{O} \cdot n(\text{solv})$  (**1b**; solv =  $\text{Et}_2\text{O}$  and/or acetone), and  $(\text{Ph}_4\text{P})[\text{Au}(\text{catdt})_2] \cdot 2\text{THF}$  (**1c**), were synthesized, and their structures and chemical compositions were determined by single crystal X-ray analysis. Recrystallization of the obtained powder from acetone/hexane, acetone/ $\text{Et}_2\text{O}$  or THF/hexane provided the salt **1a** (containing  $\text{H}_2\text{O}$ ) as yellowish brown needle-like crystals, **1b** (containing  $\text{Et}_2\text{O}$  and/or acetone) as yellow plate-like crystals or **1c** (containing THF) as green plate-like crystals, respectively.

We first compare the structures of three kinds of novel  $[\text{Au}(\text{catdt})_2]^-$ -based salts,  $(\text{Ph}_4\text{P})[\text{Au}(\text{catdt})_2] \cdot 0.5\text{H}_2\text{O}$  **1a**,  $(\text{Ph}_4\text{P})[\text{Au}(\text{catdt})_2] \cdot \text{Et}_2\text{O} \cdot n(\text{solv})$  (**1b**; solv =  $\text{Et}_2\text{O}$  and/or acetone), and  $(\text{Ph}_4\text{P})[\text{Au}(\text{catdt})_2] \cdot 2\text{THF}$  (**1c**). All of them are 1:1 salts of  $\text{Ph}_4\text{P}^+$  and  $[\text{Au}(\text{catdt})_2]^-$ ; however, their crystal structures are qualitatively different from each other,

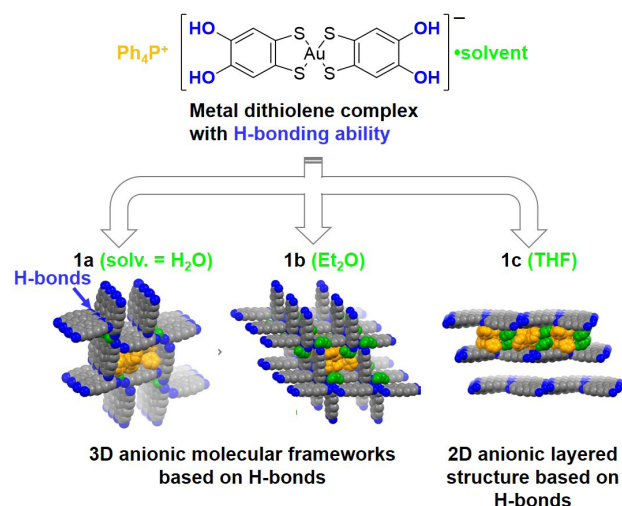


Fig. 1. On the basis of the design and synthesis of an anionic gold dithiolene complex  $[\text{Au}(\text{catdt})_2]^-$  with four hydroxyl groups, we have successfully constructed the first 3D molecular frameworks based on H-bonded metal dithiolene complexes,  $(\text{Ph}_4\text{P})[\text{Au}(\text{catdt})_2] \cdot 0.5\text{H}_2\text{O}$  (**1a**) and  $(\text{Ph}_4\text{P})[\text{Au}(\text{catdt})_2] \cdot \text{Et}_2\text{O} \cdot n(\text{solv})$  (**1b**; solv =  $\text{Et}_2\text{O}$  and/or acetone) as well as 2D layered structure of  $(\text{Ph}_4\text{P})[\text{Au}(\text{catdt})_2] \cdot 2\text{THF}$  (**1c**). The key for constructing the 3D frameworks are (i) connecting the planar  $[\text{Au}(\text{catdt})_2]^-$  molecules with 3D intermolecular H-bonds and (ii) introducing large  $\text{Ph}_4\text{P}^+$  cations into the channels. Interestingly, metal complexes are highly influenced by the solvent molecules included in the crystals (especially, the molecular size and shape and H-bonding abilities), which leads to variations in the assembled structure of the  $[\text{Au}(\text{catdt})_2]^-$  molecules; namely, a 3D framework with densely packed walls in water containing **1a**, a 3D framework with loosely packed walls in ether-containing **1b**, and a 2D layered structure in THF containing **1c**.

depending on the solvent molecules included in the crystal. The most prominent difference is the dimensionality of the assembled structures of  $[\text{Au}(\text{catdt})_2]^-$ ; namely, in the water and ether-containing salts **1a** and **1b**, this planar anionic molecule forms a 3D assembled structure (i.e., 3D framework, Fig. 1), whereas in the THF-containing salt **1c**, it forms not a 3D but a 2D structure (i.e., 2D layers). Furthermore, although both the 3D framework structures in **1a** and **1b** have tubular channels with a similar size, the structures of their walls are significantly different from each other; namely, the walls in **1a** are densely packed with  $[\text{Au}(\text{catdt})_2]^-$ , whereas those in **1b** are loosely packed to form voids, into which the cation and  $\text{Et}_2\text{O}$  molecules partially penetrate (Fig. 1). These differences should be caused by changing the intermolecular interactions between the component molecules upon the change of the crystal solvent.

We finally discuss how the crystal solvent makes differences in the intermolecular interactions and assembled structures. Here, we focus on the H-bonding ability, size, and shape of the crystal solvents.  $\text{Et}_2\text{O}$ , included in the 3D system **1b**, and THF, included in the 2D system **1c**, have proton-accepting ability due to the ether oxygen atom, which actually allows them to form the H-bonds with the catechol O–H protons of  $[\text{Au}(\text{catdt})_2]^-$  molecules. On the other hand, the overall shapes of these solvent molecules are greatly different from each other [rod-shaped ( $\text{Et}_2\text{O}$ ) vs. disk-shaped (THF)], which should contribute to the great structural difference in **1b** and **1c** (i.e., 3D vs. 2D). Namely, due to the disk shape, the THF molecules are positionally (orientationally) disordered, which leads to the formation of the THF–THF H-bonds and consequently the 2D layered structure. In contrast, the rod-shaped  $\text{Et}_2\text{O}$  molecules have no such structural disorder and additional intermolecular interactions; thus they seem to simply occupy the space

between the large  $\text{Ph}_4\text{P}^+$  and  $[\text{Au}(\text{catdt})_2]^-$  molecules without interrupting the intermolecular interactions between the  $\text{Ph}_4\text{P}^+$  and  $[\text{Au}(\text{catdt})_2]^-$  molecules for constructing the 3D framework. Meanwhile, due to the steric bulkiness of the ethyl groups in  $\text{Et}_2\text{O}$ , the walls of the 3D framework have the voids. In contrast, the water containing 3D system **1a** has no such voids and thus the wall is densely packed with the lateral  $\text{S}\cdots\text{S}$  interactions between  $[\text{Au}(\text{catdt})_2]^-$  molecules. This is probably because the solvent water molecules are involved in the wall structure, which should eliminate the above mentioned steric hindrance effect from the solvent molecules. Here, the water molecule has both proton-donating and -accepting abilities, in contrast to  $\text{Et}_2\text{O}$  and THF having only proton-accepting ability. In addition, the size of water molecule is much smaller than that of the others. These features should allow the water molecules to exist between the catechol moieties of  $[\text{Au}(\text{catdt})_2]^-$  molecules and participate in the densely packed wall structure of the 3D framework. Therefore, we have successfully illustrated the role and effect of the crystal solvent molecules on the construction of these new 3D anionic molecular frameworks based on  $[\text{Au}(\text{catdt})_2]^-$  in terms of the molecular size and shape and H-bonding abilities. As for the next step, by taking advantage of this new type of metal dithiolene complex with H-bonding abilities, we are currently investigating cooperative properties and functionalities of H-bond dynamics (e.g. dielectric properties and proton conductivity) and  $\pi$ - $d$ -electrons (e.g. electronic conductivity and magnetic properties).

#### Reference

[1] S. Yokomori, A. Ueda, T. Higashino, R. Kumai, Y. Murakami, and H. Mori, *CrystEngComm*, **21**, 2940 (2019).

#### Authors

S. Yokomori, A. Ueda, T. Higashino, R. Kumai<sup>a</sup>, Y. Murakami<sup>a</sup>, and H. Mori

<sup>a</sup>Condensed Matter Research Center (CMRC) and Photon Factory, Institute of Materials Structure Science, High Energy Accelerator Research Organization (KEK)

## Quantum Size Effects Associated with Ultra-Thinning of Layered Semimetals

Osada Group

We have investigated thickness dependence of the electronic properties of two layered semimetals, graphite and  $\text{WTe}_2$ , under magnetic fields. Their monolayer limits are known as a 2D Dirac fermion system (graphene) and a 2D quantum spin Hall insulator, respectively. Therefore, it is significant to see how their electronic properties changes associated with thinning them.

Generally, under the normal magnetic field, the band structure of the layered conductor is quantized to a set of Landau subbands with interlayer dispersion. Here, as the sample thickness approaches the de Broglie wavelength, the interlayer electron wave number is quantized, so that the bulk Landau subbands separates to discrete levels as shown in Fig. 1. This causes various size effects on electronic properties.

Bulk graphite shows a unique field-induced electronic phase transition above 30 T. Although the density wave formation due to the  $2k_F$  instability of the Landau subband was proposed as a possible mechanism of the transition,

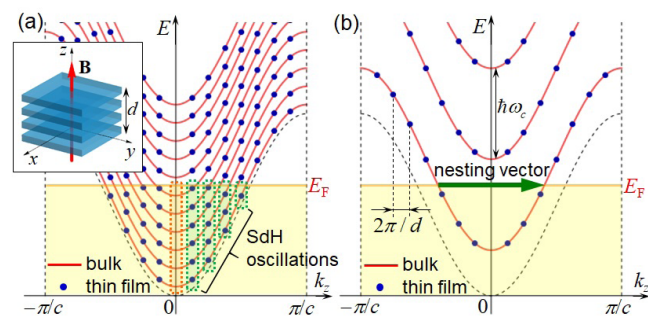


Fig. 1. Concept of the quantum size effect under magnetic fields. The Landau subbands in the bulk (red curves) are quantized into discrete levels (blue circles) due to the size effect in thin films. (a) In the low field region, several SdH oscillations with different frequencies appear in thin films, instead of the oscillation of the extremal orbit in the bulk. (b) At the high-field quantum limit, the field-induced density wave transition due to the  $2k_F$  instability of the lowest subband is suppressed by the discretization of the subband.

it has never been confirmed yet. In order to identify the high field phase, we performed transport measurements of thin-film graphite samples under the magnetic field up to 40 T, which was generated by a home-made miniature pulse magnet system. The thin-film flake was prepared on a silicon substrate by the mechanical exfoliation technique, and the device structure was fabricated using the electron beam lithography (Fig. 2(b)). As seen in Fig. 2(a), the magnetoresistance shows a saturation around 10 T, above which there exist only a few occupied Landau subbands (quasi-quantum limit). The field-induced phase transition appears above 30 T as indicated by an arrow. On the phase diagram, the phase boundaries in thin films shift to higher fields, accompanied by a reduction in temperature dependence. These results are consistently explained by the density wave model with the quantum size effect, because the  $2k_F$  instability of the Landau subband is weakened by the discretization of the subband in thin films (Fig. 1(b)). The present finding strongly suggests the density wave state standing along the interlayer direction [1].

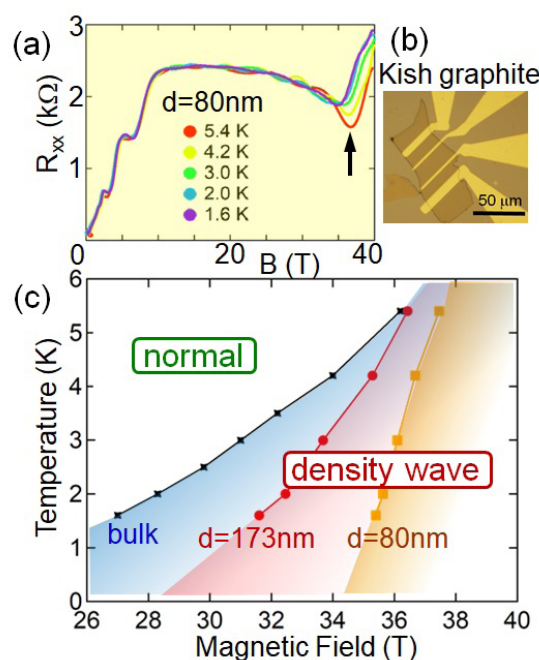


Fig. 2. Quantum size effect on the field-induced electronic phase transition in graphite. (a) Transverse magnetoresistance of a graphite thin film with the thickness of 80 nm. The arrow indicates the field-induced transition. (b) Microscope image of a Kish graphite thin film device. (c) Phase diagram of the field-induced transition in graphite thin films.

The bulk crystal of a layered transition metal dichalcogenide compound, 1T'-WTe<sub>2</sub>, is known as a 3D type-II Weyl semimetal. In order to see the change of topological states, we carried out the magnetotransport measurement of WTe<sub>2</sub> thin films with reducing their thickness. Since WTe<sub>2</sub> is degraded in the atmosphere, the mechanical exfoliation process was performed in the glove box. The clear Shubnikov-de Haas (SdH) oscillations are observed on positive magnetoresistance. The FFT spectrum of the SdH oscillations has mainly four peaks, which correspond to the extremal orbits surrounding four Fermi surfaces of the bulk. Their peak frequencies start to decrease with a film thickness of about 50 nm or less. Moreover, as the film thickness decreases, many weak subpeaks appear on the low frequency side of each main peak below about 30 nm. According to the picture of the quantum size effect (Fig. 1(a)), the observed subsidiary SdH oscillations with different frequencies originate from the 2D subbands, to which the bulk band with a Fermi surface is quantized.

#### Reference

[1] T. Taen, K. Uchida, and T. Osada, Phys. Rev. B **97**, 115122 (2018).

#### Authors

T. Osada, T. Taen, H. Adachi, T. Uchida, and K. Uchida

## Spin Thermal Hall Conductivity in a Kagomé Antiferromagnet

Yamashita and Kawashima Groups

Searching for the ground state of a kagomé Heisenberg antiferromagnet (KHA) has been one of the central issues of condensed-matter physics, because the KHA is expected to host spin-liquid phases with exotic elementary excitations.

To study the elementary excitations, we investigate the longitudinal ( $\kappa_{xx}$ ) and transverse ( $\kappa_{xy}$ ) thermal conduc-

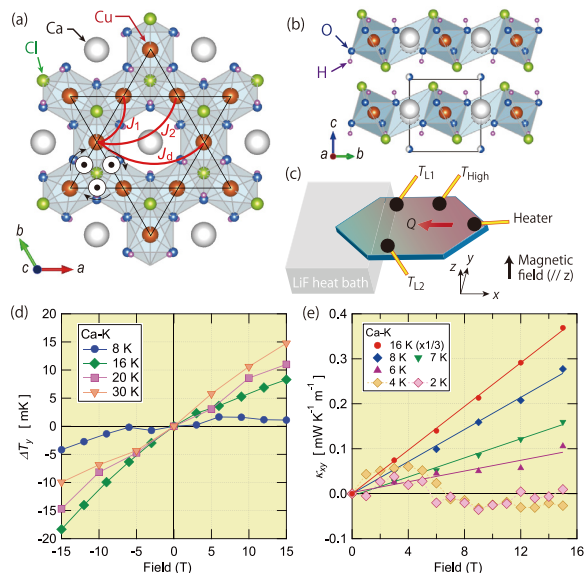


Fig. 1. (a, b) Crystal structure of Ca kwapellasilite viewed along the  $c$  axis (a) and the  $a$  axis (b). The direction of the Dzyaloshinskii-Moriya interaction ( $D$ ) is shown by the  $\odot$  symbols.  $J_1$ ,  $J_2$ , and  $J_d$  (solid red lines) represent the nearest-neighbor, next nearest-neighbor, and diagonal magnetic interactions, respectively [2]. (c) An illustration of our experimental setup. Three thermometers ( $T_{High}$ ,  $T_{L1}$ ,  $T_{L2}$ ) and a heater are attached to the sample. A heat current  $Q \parallel x$  was applied within the  $ab$  plane and a magnetic field was applied along the  $c \parallel z$  axis. (d, e) The field dependence of the transverse temperature difference  $\Delta T_y \equiv T_{L1} - T_{L2}$  (d) and  $\kappa_{xy}$  (e). Solid lines in (e) represent linear fits.

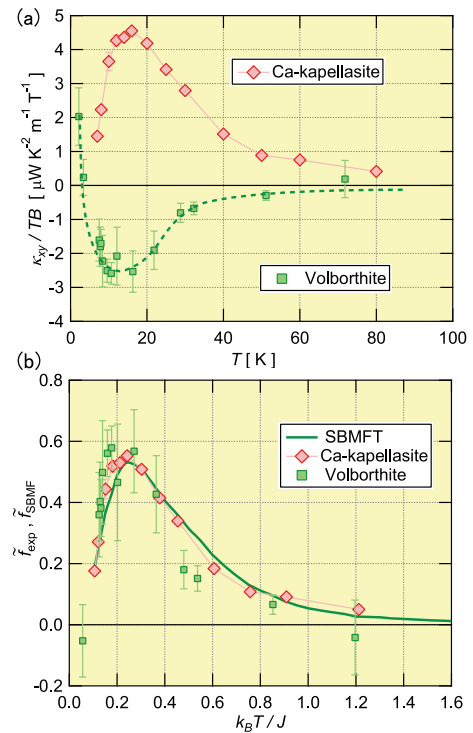


Fig. 2. (a) The temperature dependence of the thermal Hall conductivity divided by the temperature and the magnetic field ( $\kappa_{xy}/TB$ ) of Ca-kwapellasilite [1] and volborthite [4]. (b) Normalized thermal Hall conductivity of these two compounds ( $\tilde{f}_{exp}$ , symbols) and that of Schwinger-boson mean field theory ( $\tilde{f}_{SBMF}$ , solid line) show a remarkable agreement by tuning  $J$  and  $D$  as fitting parameters. The values of parameters ( $J/k_B$ ,  $D/J$ ) used for the fittings are (66, 0.12) and (60, -0.07) for Ca kwapellasilite and volborthite, respectively.

tivities of a new candidate of  $S = 1/2$  KHA Ca kwapellasilite ( $\text{CaCu}_3(\text{OH})_6\text{Cl}_2 \cdot 0.6\text{H}_2\text{O}$ ) [1]. The magnetic  $\text{Cu}^{2+}$  ions in Ca kwapellasilite form an ideal kagomé structure (Fig. 1 (a) and (b)). The fitting of the temperature dependence of the magnetic susceptibility shows that the spin Hamiltonian in Ca kwapellasilite is well approximated as an ideal KHA with the effective spin interaction energy  $J/k_B \sim 66$  K [1, 2]. Although the ground state is not a quantum spin liquid, the magnetic transition temperature  $T^* \sim 7$  K is much lower than  $J/k_B$ , providing a wide temperature range of the spin liquid phase  $T^* < T < J/k_B$  to study the elementary excitations.

Figure 1 (d) shows the field dependence of the transverse temperature difference  $\Delta T_y \equiv T_{L1} - T_{L2}$  (see Fig. 1 (c) for the experimental configuration). Remarkably, asymmetric field dependence is clearly observed, demonstrating a thermal Hall signal in this transparent insulator. By asymmetric  $\Delta T_y$  with respect to the field direction, we obtain the field dependence of  $\kappa_{xy}$  (Fig. 1 (e)) which is found to be linear to the field in the spin liquid phase.

The temperature dependence of  $\kappa_{xy}/T$  shows an increase as lowering temperature below  $J/k_B$ , which is followed by a peak at  $T \sim J/3k_B$  (Fig. 2 (a)). Quite unexpectedly, the temperature dependence and the magnitude of  $\kappa_{xy}$  of Ca kwapellasilite is similar to that of another kagomé antiferromagnet volborthite [4], whereas the  $\kappa_{xx}$  in Ca kwapellasilite is about one order of magnitude smaller than that of volborthite. Given that  $\kappa_{xx}$  is dominated by phonons in this temperature range, similar  $|\kappa_{xy}|$  in these kagomé compounds rules out phonons as the origin of  $\kappa_{xy}$ .

We find that  $\kappa_{xy}$  is well reproduced, both qualitatively and quantitatively, by spin excitations described by the Schwinger-boson mean-field theory [3] with the Dzyaloshin-

sii-Moriya interaction of  $D$ . Most remarkably, both  $\kappa_{xy}$  of Ca kagomeite and that of volborthite are found to converge to one single curve of our Schwinger-boson calculation only by choosing  $J$  and  $D$  as fitting parameters (Fig. 2 (b)). This excellent agreement demonstrates not only that the thermal Hall effect in these kagome antiferromagnets is caused by spins in the spin liquid phase, but also that the elementary excitations of this spin liquid phase are well described by the bosonic spinons. Although whether our ansatz is the only successful state for describing  $\kappa_{xy}$  or other spin liquid states – in particular spin liquids with fermionic spinons having a different  $\kappa_{xy}$  – remains an open question, our results suggest that thermal Hall conductivity of a kagome antiferromagnet has a common temperature dependence described by Schwinger bosons.

#### References

- [1] H. Doki, M. Akazawa, H.-Y. Lee, J. H. Han, K. Sugii, M. Shimozawa, N. Kawashima, M. Oda, H. Yoshida, and M. Yamashita, Phys. Rev. Lett. **121**, 097203 (2018).
- [2] H. Yoshida *et al.*, J. Phys. Soc. Jpn. **86**, 033704 (2017).
- [3] H. Lee, J. H. Han, and P. A. Lee, Phys. Rev. B **91**, 125413 (2015).
- [4] D. Watanabe *et al.*, Proc. Natl. Acad. Sci. USA **113**, 8653 (2016).

#### Authors

M. Yamashita and N. Kawashima

## Floquet-Theoretical Formulation and Analysis of High-Harmonic Generation in Solids

Tsunetsugu Group

High-harmonic generation (HHG) is a nonlinear optical phenomenon, and monochromatic input light irradiates a target medium to be converted to output with multiple high

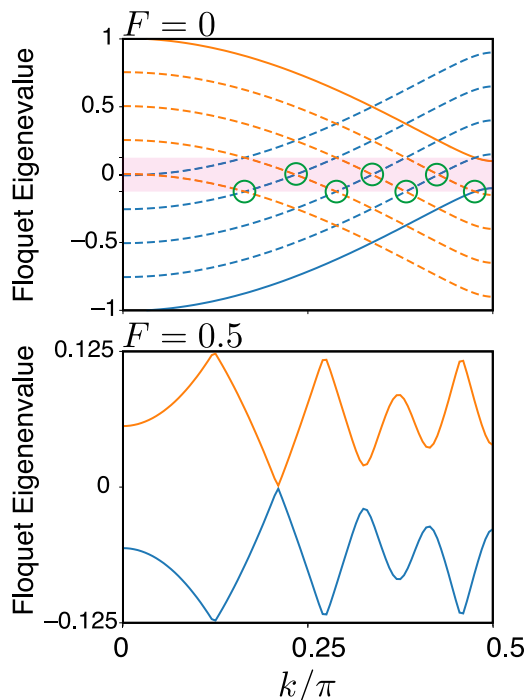


Fig. 1. Energy dispersion of Floquet bands in two cases with different electron-light coupling  $F \propto \Omega^{-1}E$  (electric field amplitude of input light): (upper) no coupling and (lower) non-zero coupling. Dimensionless frequency of input light is  $\Omega = 0.25$ . The non-zero coupling  $F$  avoids crossings of replicas of the two original energy bands (solid lines in the upper panel).

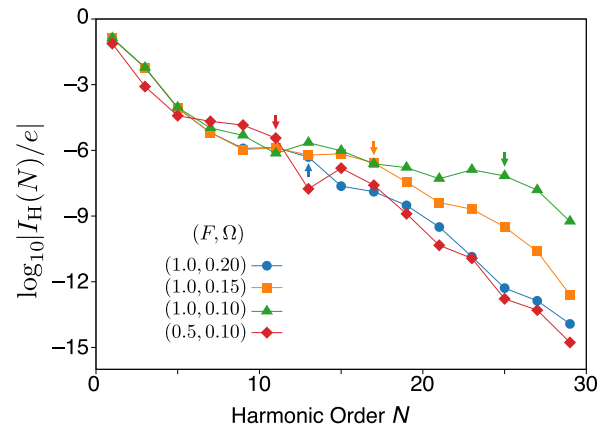


Fig. 2. High-harmonic spectrum of electric current shown in logarithmic scale. The cutoff order  $N_{\max}$  represented by the arrow is proportional to  $F/\Omega \propto E/\Omega^2$ .

harmonics, which is an indispensable technology for the state-of-the-art ultrafast physical measurements. While atomic gases were traditionally used target media, recent experiments have achieved the high-harmonic generation in bulk solids [1]. However, it remains an open problem how the interaction of light with electrons in solids results in the conversion to higher frequencies.

In this study [2], we invoke the mathematical tool known as Floquet's theorem to analyze the electron dynamics driven by light with single frequency  $\Omega$ , which induces HHG in output light. We have tailored this theoretical framework for a simple lattice electron model in one dimension. This model is a tight-binding Hamiltonian with two bands which are controlled by site-alternating potentials, and electrons acquire a time-oscillating phase in their hopping amplitude due to their coupling to input light. We have obtained an analytical solution for the time evolution of electron wave function in the limit of no potential scattering, and proceed to analyze the effects of the potential scattering by a perturbation approach. While the highest frequency of HHG in the no-scattering limit is too low to explain the related experimental data, we have found that it becomes large enough as the scattering amplitude increases.

Our result [2] also predicts that the highest order in HHG is inversely proportional to the square of the input frequency,  $N_{\max} \propto \Omega^{-2}$ , in contrast to the conventional scaling  $\propto \Omega^{-1}$  in atomic gases. This anomalous behavior deserves experimental confirmation. Besides, our Floquet-theoretical approach is general and thus applicable to various lattice systems. Therefore, for realizing effective HHG, it is useful to employ this approach and examine the effects of important characteristics of the model, such as dimensionality and symmetry of solids.

#### References

- [1] S. Ghimire *et al.*, Nat. Phys. **7**, 138 (2011).
- [2] T. N. Ikeda, K. Chinzei, and H. Tsunetsugu, Phys. Rev. A **98**, 063426 (2018).

#### Authors

T. N. Ikeda and H. Tsunetsugu

# Heat Transport via a Two-State System

Kato Group

Heat transport in macroscopic systems has been studied for long time. Recent technological progress has enabled us to measure heat transport carried by photons or phonons via a nanoscale object, for which quantum properties of the system are revealed [1]. Based on this development, we studied heat transport in the spin-boson model, in which a two-state system is coupled to two thermal reservoirs (see Fig. 1 (a)) [2]. Even though this spin-boson model is simple, it is known that there appear various physical phenomena such as the Kondo effect [3,4].

The properties of the thermal reservoirs are characterized by a spectral density function,  $I(\omega) \propto \omega^s$ . In Ref. [2], we studied thermal conductance for heat transport via a two-state system for arbitrary exponent  $s$ , comparing analytic approximations with numerical results based on the continuous-time quantum Monte Carlo method. By systematic comparison, we revealed that heat transport via a two-state system is described by one of three processes, i.e., (i) sequential tunneling, (ii) co-tunneling, and (iii) incoherent tunneling (see Fig. 1 (b)-(d)). We derived an asymptotically exact expression for the sufficiently low-temperature region (the co-tunneling regime). This formula predicts power-law temperature dependence at low temperatures. We also found that for the high-temperature or strong-coupling regions (the incoherent tunneling regime), the thermal conductance is well explained by the noninteracting-blip approximation (NIBA).

As an example, we show the temperature dependence of the thermal conductance for the ohmic reservoir ( $s = 1$ ) and  $\alpha = 0.1$  ( $\alpha$  is a dimensionless system-reservoir coupling constant) in Fig. 2. At low temperatures, the numerical result (the legends) agrees well with the asymptotically exact formula for the cotunneling process (the blue dashed line). In this regime, the thermal conductance is always proportional to  $T^3 (= T^{2s+1})$ , which is consistent with the result of Ref. [4]. At moderate temperatures and high temperatures, the numerical result deviates from the cotunneling formula, and instead agrees well with the NIBA (the black solid line). We note that the thermal conductance obtained by the NIBA is proportional to  $T^{3-\alpha}$  at low temperatures as indicated in the figure, and deviates from the low-temperature numerical results. We also show the approximate formula for the sequential tunneling (the green dot-dashed line), and the

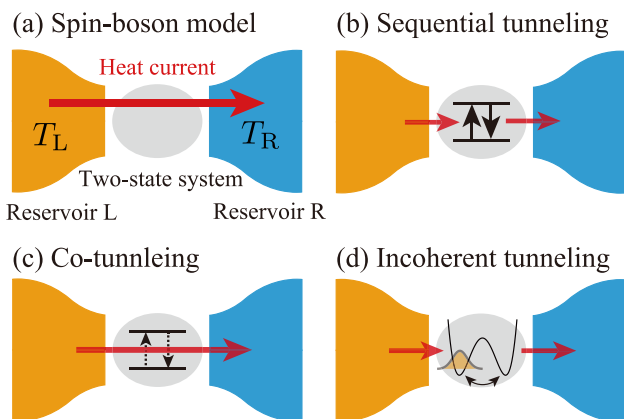


Fig. 1. (a) A schematic of the system considered in the present study. Heat transport is governed by one of three processes; (b) sequential tunneling process, (c) co-tunneling process, and (d) incoherent tunneling process.

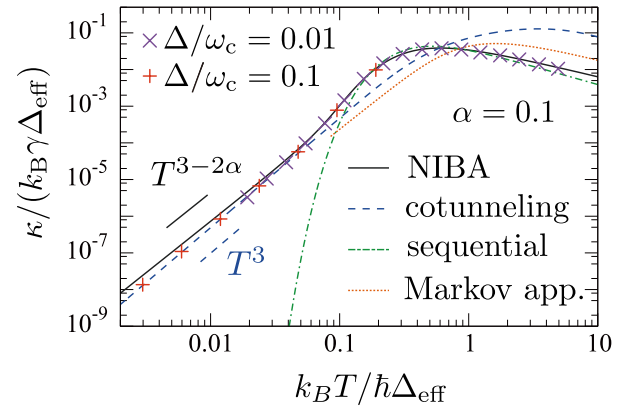


Fig. 2. Temperature dependence of the thermal conductance for the ohmic case ( $s = 1$ ).

Markov approximation for the incoherent tunneling (the orange dotted line). The former agrees with numerical data at moderate temperatures, while the latter clearly deviates from the numerical results, indicating the importance of the non-Markov properties of the system.

Our study will provide a useful basis for deep understanding of heat transport via nanoscale devices, and as well a platform for experiments attempting to access many-body effect in heat transport of mesoscopic devices.

## References

- [1] A. Ronzani *et al.*, Nat. Phys. **14**, 991 (2018).
- [2] T. Yamamoto, M. Kato, T. Kato, and K. Saito, New J. Phys. **20**, 093014 (2018).
- [3] A. J. Leggett *et al.*, Rev. Mod. Phys. **59**, 1 (1987).
- [4] K. Saito and T. Kato, Phys. Rev. Lett. **111**, 214301 (2013).

## Authors

T. Yamamoto and T. Kato

# Realization of a Current-Controlled Superconducting Device

Katsumoto Group

Ultra-high speed, low-power consumption logic device action has been predicted for Josephson superconducting junctions, which dream, however, has not come true yet for more than three decades. The device action itself had been confirmed at the beginning of the 1980s [1]. Nevertheless,

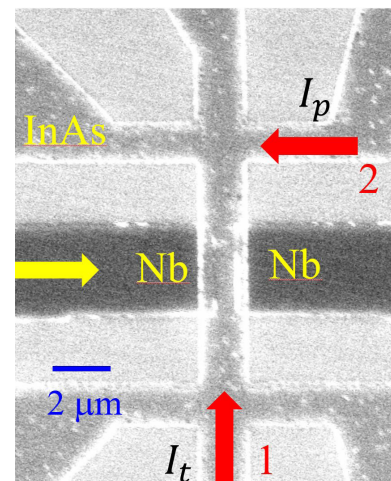


Fig. 1. Scanning electron micrograph of the sample. The yellow arrow indicates the supercurrent while two red arrows indicated the transverse (no.1) and the parallel (no.2) normal currents, respectively.

the two-terminal nature of the junction has blocked the application to the real world of logic devices. The obstacle is explained as follows. The switching to normal state occurs when the junction is “fired” by applying a bias current larger than the critical current  $J_c$  ( $J_{c1}$ ). Then to switch the next junction a current larger than its  $J_c$  ( $J_{c2}$ ) is required while the current swing of the first junction is  $J_{c1}$ . Hence for the circuit action, condition  $J_{c1} > J_{c2}$  should be fulfilled. The condition means that  $J_c$  decreases monotonically over the chain of logic gates, thus sharply limits the scalability of the circuit. The finding of a gate-controllable supercurrent through the two-dimensional electrons (2DE) on the surfaces of InAs [2], this was thought to solve the problem. However, as a voltage-driven device, the Josephson junctions have too high off-conductance, and the obstacle was realized to exist stubbornly. Therefore a current-current three(or four)-terminal device is required for the practical use.

We here report pure current-control of supercurrent, which would solve the long-standing technical problem. We prepared a 2DE in an InAs quantum well grown on an InP substrate. Figure 1 shows the sample structure, in the center of which a Nb-InAs 2DE-Nb superconducting junction is formed. Besides, the sample has six normal terminals, through which local or non-local electric currents can flow. InAs 2DE is known to have a strong Rashba-type spin-orbit interaction (RSOI), and the layered structure is design to maximize the RSOI.

One of the expected device actions is described as follows. When a supercurrent is flowing between the two Nb electrodes, a normal current is applied transverse to the supercurrent. The normal current is associated with the spin Hall effect, which causes spin accumulation at the super-normal interfaces and breaks the time-reversal symmetry locally. The normal current can thus reduce the critical current of the superconducting junction. The other is a kind of "remote reduction," in which the normal current is applied parallel to the supercurrent but at a different part of

the sample (red arrow no.2). In this case, the normal current causes the spin current, which should have a significant disorder in electron spins through the Zitterbewegung [3] and crosses the supercurrent. The disordered spin current again should lead to the reduction of the critical current.

In the experiments, the care was taken to avoid heating by the normal currents and the application of voltages due to the imbalance of the potentials at the normal electrodes. Figure 2(a) is a color plot of the resistance of the superconducting junction against the junction current and the control current. The black region corresponds to the zero-resistance state, and an apparent reduction of the critical current is observed. The current gain (the derivative of the edge line on the zero-resistance region) is larger than unity (0 dB) below 100 nA of the transverse current. The result of the remote-reduction experiment is shown in Fig. 2(b). The remote current also reduces the critical current through the sensitivity is lower, and the region for positive current gain (above 0 dB) is limited to just around the zero parallel currents.

In conclusion, we have realized a current-controlled four terminal superconducting device with finite current gains.

#### References

- [1] T. R. Gheewala, IEEE Trans. Electron Devices **27**, 1857 (1980).
- [2] H. Takayanagi and T. Kawakami, Phys. Rev. Lett. **54**, 2449 (1985).
- [3] Y. Iwasaki, Y. Hashimoto, T. Nakamura, and S. Katsumoto, Sci. Rep. **7**, 7909 (2017).

#### Authors

T. Nakamura, Y. Hashimoto and S. Katsumoto

## Magneto-Thermodynamic Properties in Submicron Wires of Pd-doped FeRh

Otani Group

An FeRh alloy with B2 order shows a first-order phase transition from antiferromagnetic (AFM) to ferromagnetic (FM) phases with raising temperature. As the transition temperature is tunable around room temperature, this is a candidate material for several applications such as heat-assisted magnetic recording, AFM memories and memristor devices. Recently, an asymmetric behavior around the AFM-FM phase transition has been reported on some tiny sample structures. Remarkably, a discontinuous and asymmetric resistance change around the phase transition was reported in submicron wires of FeRh, which is caused by suppression of the nucleation of AFM domains during the cooling process [1]. In this work, we performed resistivity measurements of submicron wires of Pd-doped FeRh as a function of temperature and external magnetic field. We further evaluated some thermal properties such as an energy loss around the temperature hysteresis in each wire to characterize those finite-size effect.

We used Pd-doped FeRh alloy in order to decrease the AFM-FM phase transition temperature. A 60-nm-thick epitaxial film of Pd-doped FeRh was prepared and fabricated into submicron wires. Detailed processes for film growth and patterning are shown in Ref. 2. As the resistivity in AFM phase is larger than that in FM phase, the electrical transport measurement can be a probe to detect the AFM-FM phase transition which is induced by sweeping temperature or external magnetic field. The resistance on 270-nm-wide wire against temperature and magnetic field is plotted in Fig. 1(a). We can see the temperature-driven and field-driven hysteresis

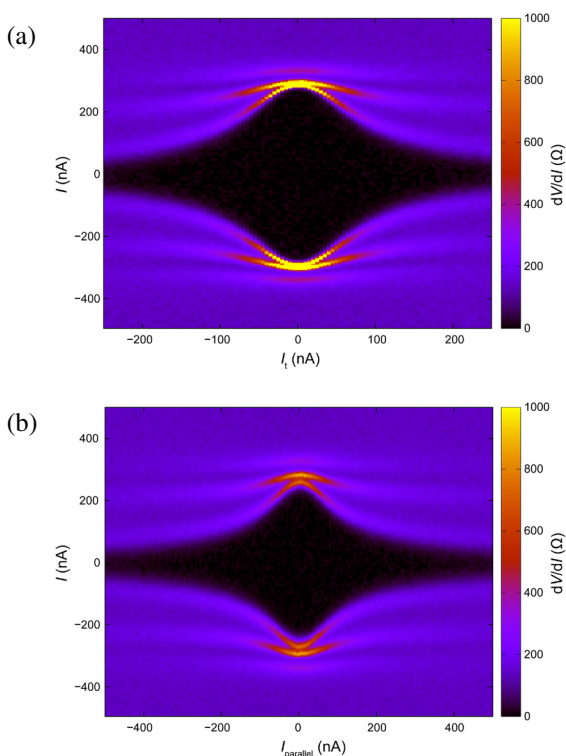


Fig. 2. (a) Color plot of the junction resistance versus the plane of transverse current and junction current. The black region corresponds to the zero-resistance state. (b) The same for the parallel current.

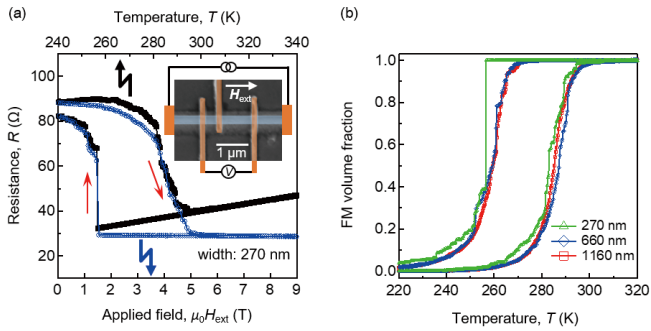


Fig. 1. Hysteresis loops due to AFM-FM transition on submicron wires of Pd-doped FeRh [2]. (a) Resistance measurements on 270-nm-wide wire of Pd-doped FeRh against temperature (black) and in-plane magnetic field (blue). The temperature-driven hysteresis loop was measured without applying a magnetic field and the field-driven one was done at a constant temperature of 240.0 K. Inset is a SEM image of the wire. (b) Volume fraction of ferromagnetic phase against temperature which were estimated from resistance of the submicron wires.

loops due to the AFM-FM phase transition. Though the resistance contains small jumps under the transition to FM phase, it showed a large discontinuous change on the opposite arm, the transition to AFM phase. These asymmetries and step-like structures in both hysteresis loops would indicate the nucleation processes of AFM and FM domains are confined by the sample size, which is also reported in Ref. 1. We further investigated how the hysteric behavior changes by the size of wires. We prepared 270-nm-, 660-nm- and 1160-nm-wide wires by the same method and measured their resistances with sweeping temperature. Under an assumption that all magnetic domains are aligned along the longitudinal direction of the wire, the volume fraction of FM domains can be calculated from the measured resistance in each wire as shown in Fig. 1(b). We can find the enhanced asymmetry in narrow wires. To evaluate this finite-size effect in wires, we estimated the energy loss around the phase transition from simple thermodynamic equations. We found the energy losses around the hysteresis loops are larger in narrower wires. Also, all wires showed larger losses than the unpatterned film. These results would suggest that the finite-size effect, probably a restriction in magnetic domain structures across the phase transition, appears in a macroscopic energy loss. This method can be a probe to characterize the rectified domain nucleation process in tiny volume samples by simple electrical measurements.

#### References

- [1] V. Uhlir *et al.*, Nature Commun. **7**, 013113 (2016).  
 [2] K. Matsumoto *et al.*, IEEE Trans. Magn. **54**, 2300904 (2018).

#### Authors

Y. Otani and K. Matsumoto

## Dynamic Interface Formation in Magnetic Thin Film Heterostructures

Komori Group

In magnetic thin film heterostructures, interaction at the interface plays a dominant role in the development of novel electronic and magnetic properties. The interlayer coupling strength primarily relies on the interfacial structure at the atomic scale, including atomic roughness, steps, and intermixing. However, the impact of the atomic scale interfacial structure on the magnetic coupling in magnetic thin film

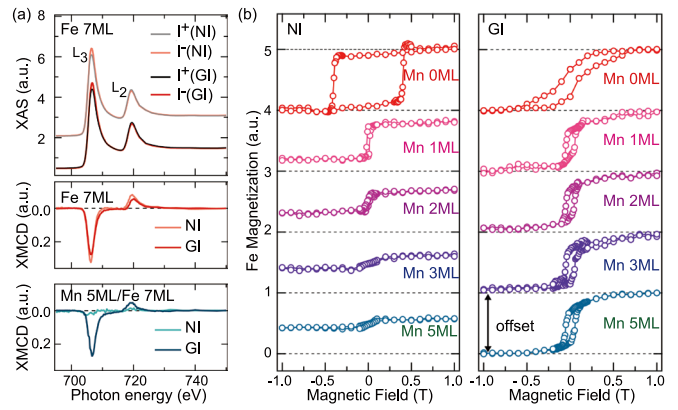


Fig. 2. (a) Fe  $L_{2,3}$  remanent XAS (upper) and XMCD (middle) of a 7-ML Fe film on Cu(001), and XMCD (lower) of a 5-ML Mn/7-ML Fe film in the normal incidence (NI) and grazing incidence (GI) geometries. Here, external magnetic field is parallel to the incident x-ray. (b) Iron magnetization curves in the heterostructures of Mn ( $x$  ML,  $x = 0, 1, 2, 3,$  and  $5$ ) overlayers on the 7-ML Fe film measured in the NI (left) and GI (right) geometries. The  $L_3$  XAS peak intensity normalized by the  $L_2$  one is plotted as a function of the magnetic field. In the GI geometry, the magnetic field is applied along the  $[100]$  direction of the Cu(001) substrate.

heterostructures has not yet been elucidated well in relation to the macroscopic magnetic properties. We use scanning tunneling microscopy (STM) and x-ray absorption spectroscopy/x-ray magnetic circular dichroism (XAS/XMCD) as complementary tools for clarifying the correlation between the atomic structure at the interface and the magnetism. Successive atomically-resolved STM characterizations of not only structural but also electronic and magnetic properties during the growth of magnetic thin film heterostructures provide crucial information on the atomic-scale interfacial factors in the dynamical process of the interface formation. The element-specific, quantitative and macroscopic observations of electronic and magnetic properties by XAS/XMCD can be linked with the microscopic interface characteristics.

We have studied fcc Fe thin films grown on Cu(001) with Mn overlayers (Mn/Fe films) as a unique system for investigating the interface interaction. [1] The electronic

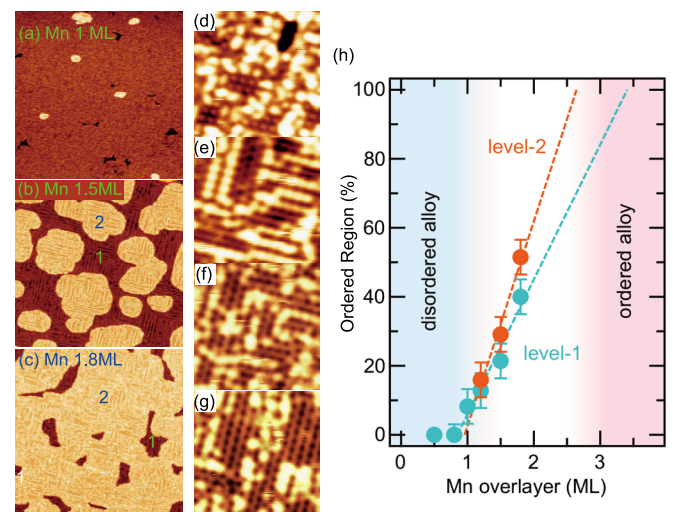


Fig. 2. (a-c) STM images of 7-ML Fe films with 1.0-ML (a), 1.5-ML (b), 1.8-ML (c) Mn overlayers. (d-g) High-resolution surface STM images of 1.0-ML (d), 1.5-ML (e), 1.8-ML (f) and second (level-2) (g) levels. The disorder alloy can be seen in each image as bright protrusions. (h) Statistical plots of the fraction of the ordered alloy region with the  $(4 \times 2)$  and  $(4 \times 4)$  reconstructions in level-1 and level-2 as a function of the average thickness of the Mn overlayer. The dashed lines are linear extrapolations of the fractions of the ordered alloy.

and magnetic properties of ferromagnetically-coupled top two layers in the fcc Fe thin film on Cu (001) [2] is susceptible to the structural changes on the atomic scale. At the interface, a collinear and homogeneous antiferromagnetic/ferromagnetic coupling is expected at the Mn/Fe interface as observed in the reference system of Mn thin films on the bulk bcc Fe(001) substrate. Thus, the fcc Fe thin film highlights the role of atomic-scale interfacial factors with the Mn overlayers.

The films were fabricated by successive deposition of Fe and Mn on Cu(001) at room temperature (RT) in an ultrahigh vacuum. The thickness of the fcc Fe layer was fixed to  $\sim 7$  monolayer (ML). The Fe layer in the Mn/Fe film exhibits a two-step spin reorientation transition (SRT) from out-of-plane to in-plane direction with increasing the thickness of the Mn overlayer as observed by XAS/XMCD measurements shown in Fig. 1. After 1 ML deposition of Mn, the coercive field in the magnetic field perpendicular to the film decreases to a value less than that in the in-plane magnetic field. Furthermore, the in-plane anisotropy gradually increases up to 3-ML Mn deposition. Corresponding atomically-resolved STM observations reveal the dynamic structure change from a disordered surface to an ordered one by the Mn deposition at RT as in Fig. 2. First, a disordered surface alloy with the Fe film is formed by the Mn deposition, which induces the first SRT. The ordered-alloy area of the surface gradually increases with increasing the amount of the deposited Mn atoms more than 1 ML on average. The ordering of the alloy completes around 3-ML Mn deposition, which corresponds to the completion of the second SRT.

The present complementary approach by XAS/XMCD and STM successfully disentangles the hidden functionality of the interface alloying, which changes and enhances the magnetic anisotropy in the Fe layer. The results will pave new ways to understand novel phenomena emerging at the interface on the atomic scale, and to improve the electronic and magnetic properties of the magnetic thin film heterostructure.

## References

- [1] S. Nakashima *et al.*, *Adv. Func. Matter.* **29**, 1804594 (2019).  
 [2] H. L. Meyerheim *et al.*, *Phys. Rev. Lett.* **103**, 267202 (2009).

## Authors

S. Nakashima, T. Miyamachi, Y. Tatetsu<sup>a</sup>, Y. Takahashi, Y. Takagi<sup>b</sup>, Y. Gohda<sup>a</sup>, T. Yokoyama<sup>b</sup>, F. Komori<sup>a</sup>  
<sup>a</sup>Tokyo Institute of Technology  
<sup>b</sup>Institute for Molecular Science

# Nanoscale Potential Mapping: Direct Visualization of Electrical Resistance at Single Surface Steps

Hasegawa Group

Atomically-thin two dimensional electron systems (2DES) have been one of the hot topics because of their unique properties originating from the low dimensionality and reduced symmetry. Among them 2DES by metallic surface states, which are formed by a few monolayer (ML) deposition of metallic elements on semiconducting substrates, have a unique status. Because of the thermal stability through the surface reconstruction, self-organized high-quality periodical structures can be formed in macroscopic dimensions. Basic properties such as atomic structure

and electronic states can be well characterized by standard surface science techniques including scanning tunneling microscopy (STM). Recent discovery of superconductivity in surface 2DES attracted further attentions.

Net and local misorientations of the substrate from a nominal plane results in the formation of steps on it. Superstructure due to the surface reconstruction inherently forms boundaries that separate domains whose periodical phases are different from each other. Both of the one-dimensional line defects disrupt the periodicity of the surface atomic arrangement and therefore work as a barrier for the electrons across them. In order to investigate the role of the line defects in electrical transport, we measured the nanometer-scale spatial distribution of local electrochemical potential of an archetypical metallic surface states; the  $7\times 7$  structure of Si(111) substrates, using an STM-based technique called scanning tunneling potentiometry (STP) [1]. Using STP, we found potential drops clearly at step edges and phase boundaries of the 2D metallic surface, demonstrating the presence of significant electrical resistance there.

Figure 1 shows STM and electrochemical potential images taken simultaneously on the  $7\times 7$  surface under the net current flow from the left to the right. A single-height (0.31 nm) steps are observed running from the upper left to the lower right in the topographic image (Fig. 1(a)). In the corresponding potential image (Fig. 1(b)), potential drops are found at the step edges, as more quantitatively presented in the inset cross-sectional plots, which was taken along the dashed A-B line in Fig. 1(a).

The steps are, however, not the only defects that disrupts the electron transport on the surface. In the potential mapping, which exhibits a ladder-like pattern, one notices several potential drops in narrow terraces separated by the steps. The potential drop due to the rungs of the ladders is more clearly displayed in a cross-sectional profile shown in the inset. The rungs correspond to boundaries that separate domains of the  $7\times 7$  reconstructed structures whose phases do not match. The potential images indicate that the phase boundaries also have electrical resistance.

From the obtained potential images and their cross-sectional plots, we can quantitatively analyze the conductivity through an individual step and phase boundary. Since the absolute value of the current density is unknown, we cannot measure the terrace, step, or phase boundary conductivity directly. But, their ratio can be estimated precisely. Since in our measurement we used low-doped substrates, the electrical conductance through the substrate is quite small. The poorly conductive substrate safely eliminates the problem of the bulk contributions in our measurements.

We estimated the conductivity ratio of the step to the

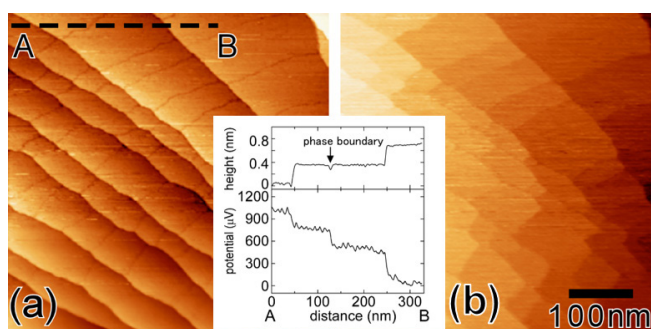


Fig. 1. STM (a) and electrochemical potential (b) images taken simultaneously on the Si(111) $7\times 7$  surface. (inset) cross-sectional plots of topographic height and potential taken along the dashed line drawn in (a).

terrace  $\sigma_s/\sigma_t$  is  $3.1 \pm 1$   $\mu\text{m}$ . The ratio means that the resistance of a single step corresponds to that the 340 nm-width terrace of the  $7 \times 7$  structure. This also implies that the contribution of the steps to the net resistance dominates when the tilting angle of the surface exceeds  $0.06^\circ$ , which is much smaller than the tolerance of the miscut angle ( $\sim 0.16^\circ$ ) for commercial wafers. The macroscopic net resistance through the  $7 \times 7$  surface states, which include both those of terraces and steps, is therefore basically determined by the step density and the misoriented angle of the substrate.

The phase boundary is found more conductive than the step: the conductivity ratio of a single phase boundary to terrace  $\sigma_{\text{ph}}/\sigma_t$  is  $16.4 \pm 10$   $\mu\text{m}$ . The density and distribution of phase domains of the  $7 \times 7$  structure are closely related with nucleation process of the  $7 \times 7$  structure from disordered  $1 \times 1$  during the cooling of the sample after the annealing to get rid of the surface oxide layer and to form the clean  $7 \times 7$  structure. The macroscopic surface conductivity, therefore, also depends on the sample preparation method; e.g. how the sample was slowly cooled after the annealing.

In fact, the electrical conductivity of the surface has been characterized in various methods including microscopic 4-probe methods, but the measured conductivity have been widely dispersed. Our results indicate that the macroscopic net conductivity are mostly determined by the density of steps and domain boundary, thus depending strongly on the misorientation of the sample and its preparation. The present study also demonstrates the importance of characterizing microscopic conductance to elucidate the intrinsic transport properties of the system.

#### References

- [1] M. Hamada and Y. Hasegawa, *Jpn. J. Appl. Phys.* **51** 125202 (2012).  
 [2] M. Hamada and Y. Hasegawa, *Phys. Rev. B* **99**, 125402 1 (2019).

#### Authors

M. Hamada and Y. Hasegawa

## Strain Relaxation at Doped Epitaxial Interfaces

Lippmaa Group

A quasi-two-dimensional quantum well is known to form by electron accumulation at an epitaxial heterointerface between  $\text{SrTiO}_3$  and  $\text{LaAlO}_3$ . The accumulation of carriers at this interface is the result of a peculiar interplay between several effects, including the polar discontinuity between  $\text{SrTiO}_3$  and  $\text{LaAlO}_3$ , tetragonal distortion of the interface layer due to the 3% epitaxial strain at the interface, field- and strain-dependent giant dielectric permittivity of  $\text{SrTiO}_3$ , and possibly due to Sr and La intermixing within the first unit cell of the interface. Although the carrier number is essentially fixed by the structure, it is possible to tune the depth distribution of the accumulated carriers by either top- or bottom-side gating, thereby changing the occupancy of the nearly degenerate  $d_{xy}$ ,  $d_{xz}$ , and  $d_{yz}$  orbitals. Due to the tetragonal distortion of the interface layer, the orbital degeneracy is partially lifted, lowering the energy of the  $d_{xy}$  orbital. Gating can then be used to shift the Fermi level below or above the level crossing, leaving the  $d_{xz}/d_{yz}$  orbitals either empty or partly filled. One unique feature of this interface is the sharply asymmetric potential profile of the quantum well due to the wide bandgap of  $\text{LaAlO}_3$ . This asymmetry leads to a

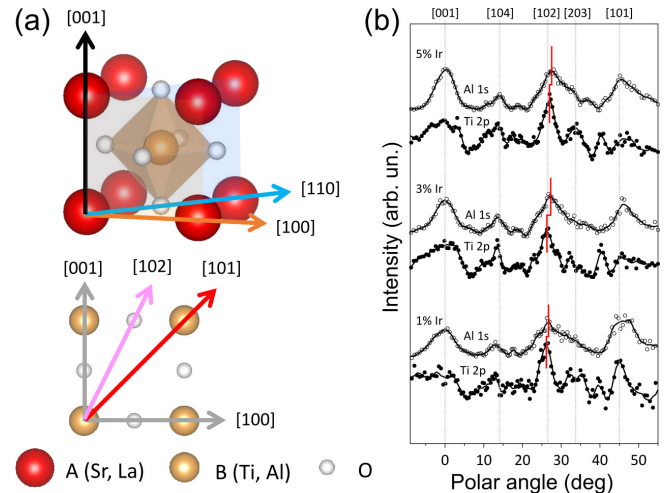


Fig. 1. Crystal FFP orientations. (a) Schematic of sample orientation and the FFP directions in the (010) plane when the emitter is a B-site atom (Al or Ti). (b) XPD polar curves for Ir-doped samples comparing Al 1s and Ti 2p emission signals for different Ir doping levels.

relatively strong Rashba-type spin-orbit coupling at the interface and this coupling strength can be tuned to some extent by gating, either because the asymmetry of the potential well is changed or due to a Lifshitz transition that occurs when the Fermi level is tuned across the  $d_{xy} - d_{xz,yz}$  crossing.

Since this level crossing energy is determined by the tetragonal distortion of the interface layer, we have turned our attention to the possibility of tuning the interfacial strain by doping the interface. Additionally, by adding heavy elements, such as Ir to the interface, it may be possible to control the spin-orbit coupling experienced by the electrons in the quantum well.

$\text{SrTiO}_3/\text{LaAlO}_3$  heterostructures with interfaces doped either with Ir or Co were grown by pulsed laser deposition and the interfacial strain relaxation was studied by hard (7940 eV) x-ray photoelectron diffraction (XPD) at SPring-8 BL47XU. It was thus possible to estimate the strain state at the interface by comparing XPD forward focusing peak (FFP) positions between La and Sr (perovskite A-site) or Al and Ti (perovskite B-site) (Fig. 1) for different interface doping levels. A shift of the La and Al FFPs towards larger angles relative to Sr and Ti showed that in all cases the  $\text{LaAlO}_3$  cap layer is under compressive strain in the out-of-plane direction due to epitaxial strain. However, the level of strain depends on interface doping, especially for Ir. One possible cause is the interdiffusion of Ir across the  $\text{SrTiO}_3/\text{LaAlO}_3$  interface. The work suggests that the interfacial strain can be tuned by doping the first unit cell layer of  $\text{LaAlO}_3$  at the interface with a larger ionic radius cation to reduce the epitaxial strain imposed on the first few unit cells of  $\text{SrTiO}_3$ . This technique may be effective for controlling the critical carrier density where the Lifshitz transition occurs and thus selecting the gate bias range where the spin-orbit coupling in the quantum well is tunable by gating.

#### Reference

- [1] M. Lee, X. L. Tan, M. Yoneda, T. Okamoto, I. Tanaka, Y. Higa, D. Peng, M. Ogi, S. Kobayashi, M. Taguchi, M. Lippmaa, M.-J. Casanove, and H. Daimon, *J. Phys. Soc. Jpn.* **87**, 084601 (2018).

#### Authors

M. Lee<sup>a</sup>, X. L. Tan<sup>a</sup>, M. Yoneda<sup>a</sup>, T. Okamoto<sup>a</sup>, I. Tanaka<sup>a</sup>, Y. Higa<sup>a</sup>, D. Peng<sup>a</sup>, M. Ogi<sup>a</sup>, S. Kobayashi<sup>a</sup>, M. Taguchi<sup>a</sup>, M. Lippmaa, M.-J. Casanove<sup>b</sup>, and H. Daimon<sup>a</sup>, *J. Phys. Soc. Jpn.* **87** (2018) 084601

<sup>a</sup>Nara Institute of Science and Technology

<sup>b</sup>University of Toulouse

# CO<sub>2</sub> Activation and Reaction on Zn-Deposited Cu Surfaces Studied by Ambient-Pressure X-Ray Photoelectron Spectroscopy

Yoshinobu and I. Matsuda Groups

It is important to understand the mechanisms of activation and hydrogenation of carbon dioxide (CO<sub>2</sub>) in order to utilize the abundant CO<sub>2</sub> effectively as a chemical feedstock. One way of utilizing CO<sub>2</sub> is methanol synthesis on Cu-based catalysts. Metallic copper in the catalysts is considered to be an active site for methanol synthesis. So far, the adsorption and reaction of CO<sub>2</sub> on Cu surfaces have been widely investigated under ultrahigh vacuum (UHV) and under ambient pressure conditions.

In this study [1], the reaction of CO<sub>2</sub> on Zn-Cu(111) and Zn-Cu(997) was systematically studied using ambient-pressure X-ray photoelectron spectroscopy (AP-XPS) at SPring-8 BL07LSU (2015B7496 and 2016A7401). AP-XPS allows adsorbate and substrate electronic states to be elucidated under reaction conditions. The aim of this study is to reveal the roles of Zn and water in the CO<sub>2</sub> reaction, and elementary steps of methanol synthesis by a series of systematic experiments performed under well-defined conditions at temperature between 299–473 K. We used Zn-deposited Cu(111) and Cu(997) single crystals as model catalytic systems. Stepped Cu surfaces are more reactive for dissociation of CO<sub>2</sub> compared to flat Cu surfaces. Recently, we have investigated adsorption states of CO<sub>2</sub> on Cu(997) surfaces under UHV, and near-ambient condition. In this study, we have focused on hydrogenation of CO<sub>2</sub> under near-ambient pressure conditions to clarify the effect of the step sites. The oxidation state of Zn-deposited Cu surfaces and the stability of reaction products depend strongly on the gas composition and sample temperature. The effect of water on the CO<sub>2</sub> activation was also examined by a set of control experiments.

In the presence of 0.8 mbar CO<sub>2</sub> and 0.4 mbar H<sub>2</sub> gases, hydrogenation products are not observed; only carbonate is formed on Zn-deposited Cu(111) and Cu(997) surfaces (not shown here). We found that the formation rate of carbonate at 299 K is significantly faster on Zn/Cu(997) than that on Zn/Cu(111), indicating that *step sites are more reactive for CO<sub>2</sub> activation than terrace sites*. On the other hand, the addition of water (D<sub>2</sub>O) in the feed gas leads to hydrogenation of CO<sub>2</sub> to formate at sample temperatures around 400 K (Fig. 1). This suggests that hydroxyl produced from dissociative adsorption of water is a reactant in the CO<sub>2</sub> hydrogenation observed under the present reaction condi-

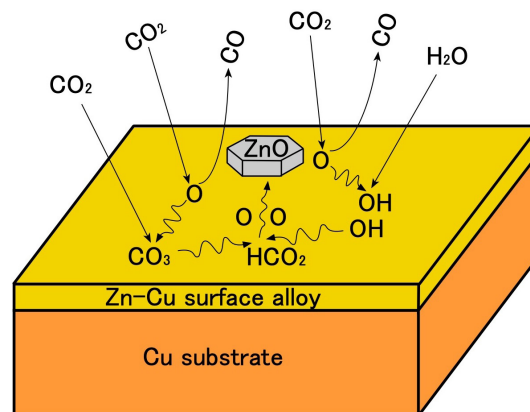


Fig. 2. Schematic diagram of proposed reactions on the Zn-deposited Cu surface in the presence of CO<sub>2</sub>, H<sub>2</sub> and H<sub>2</sub>O.

tions. Figure 2 schematically shows the proposed reactions on the Zn-deposited Cu surface in the presence of CO<sub>2</sub>, H<sub>2</sub> and H<sub>2</sub>O. We also found that the reaction products such as carbonate and formate on the Zn/Cu(997) surface are more stable than those on the bare Cu(997) surface. In particular, formate remains on Zn-deposited Cu surfaces up to 473 K, which is close to the operation temperature of industrial Cu-ZnO catalysts. We conclude that *an important role of Zn on Cu surfaces is the stabilization of reaction intermediates originated from CO<sub>2</sub>*.

## Reference

[1] T. Koitaya, S. Yamamoto, Y. Shiozawa, Y. Yoshikura, M. Hasegawa, J. Tang, K. Takeuchi, K. Mukai, S. Yoshimoto, I. Matsuda, and J. Yoshinobu, *ACS Catal.* **9**, 4539 (2019).

## Authors

T. Koitaya<sup>a</sup>, S. Yamamoto, I. Matsuda, and J. Yoshinobu  
<sup>a</sup>Institute for Molecular Science (present address)

## Biophysical Study on the Function and Molecular Mechanism of Rhodopsins

Inoue Group

Rhodopsin is photo-receptive heptahelical transmembrane proteins in which retinal chromophore is covalently bound to a conserved lysine residue in the seventh helix, and animal and microbial rhodopsin families are known so far. Animal rhodopsins present in animal retina transfer visual signal to brain and are also related to non-visual light sensing. Microbial rhodopsins show diverse functions: light-driven ion pump, light-gated ion channels, light-regulated enzyme and so on. Both types of rhodopsins are being widely used in optogenetics to control various cellular events, such as neural activity, gene expression and so on, by light. Recently, we reported third class of rhodopsin, heliorhodopsin (HeR), which is evolutionally isolated from both of microbial and animal rhodopsins [1]. The biochemical study revealed its inverted structure compared with other class of rhodopsins, and N- and C-termini of HeR faces extracellular and cytoplasmic milieus, respectively (Fig. 1). HeRs are diversely distributed from bacteria, archaea, eukaryotic algae and giant viruses. Although the function of HeR has not been clarified yet, we observed a long photo-reaction cycle up to seconds to minutes by laser flash photolysis suggesting HeR works as a signaling protein which transfers light signal to unidentified intracel-

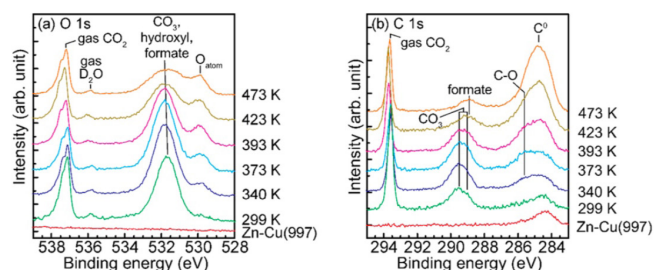


Fig. 1. A series of XPS spectra on Zn(0.25 ML)/Cu(997) surface: (a) O 1s and (b) C 1s. The spectra of bare Zn-Cu(997) surface were measured under UHV. AP-XPS measurements were first performed at 299 K in the presence of 0.8 mbar CO<sub>2</sub>, 0.4 mbar H<sub>2</sub>, and 0.05 mbar D<sub>2</sub>O, then the sample was heated up to 473 K under this ambient-pressure condition.

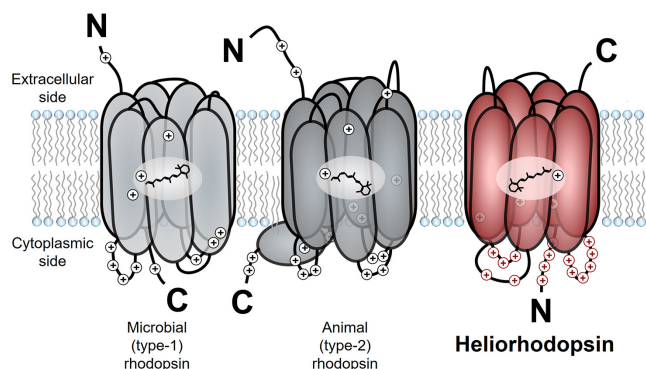


Fig. 1. Molecular structures of microbial rhodopsin, animal rhodopsin and heliorhodopsin.

lular proteins. The retinal chromophore in HeR isomerizes from all-*trans* to 13-*cis* form upon light illumination, and we dominantly observed K, M and O-intermediates in the photocycle. While the K and O intermediates show red-shifted absorption compared with that of the dark state, the absorption of M-intermediate is highly blue-shifted to 400 nm and a proton is released from retinylidene Schiff-base. A mutational study suggested that the proton is not transferred to a specific residue and it is trapped in a hydrogen bonding network, called proton accepting group (PAG), constituted from several amino-acid residues including conserved histidines and internal water molecules on the extracellular side of the protein.

Rhodopsins show wide range of absorption wavelength and the color regulation of retinal chromophore in rhodopsins to achieve longer-wavelength absorption is one of critical elemental technique to develop new types of optogenetics tools which can avoid strong light-scattering by biological tissues and phototoxicity. We reported that the mutation of the conserved proline and serine residues in sodium pump rhodopsin (KR2) induces 40-nm red-shift of the absorption without impairing sodium-transport activity [2]. Also, FTIR spectroscopy and quantum mechanical calculation revealed that the change in dipole moments of these residues lowered energy gap of  $\pi$ -electron of retinal chromophore by electrostatic interaction. Furthermore, we identified a new type of sodium pump rhodopsin from  $\alpha$ -proteobacterium, *Jannaschia seosinensis*, in which the proline residue was naturally altered to glycine and it shows 20-nm longer absorption than that of KR2. Since *J. seosinensis* is derived from solar saltern, the natural mutation of the proline occurred to use longer wavelength light in turbid environment. Since sodium pump rhodopsin can suppress the neural spiking without alterations of intracellular pH and  $\text{Cl}^-$  concentration, this red-shifted KR2 would be expected to be applied as a new type of optogenetic tool.

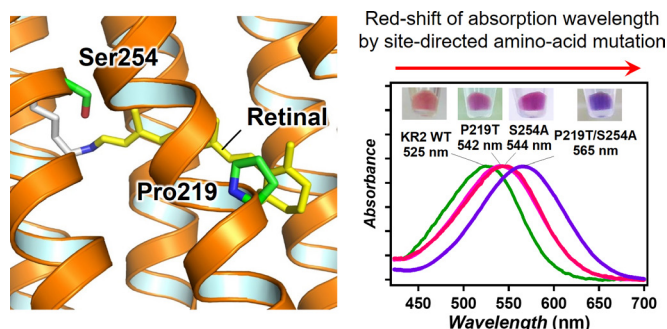


Fig. 2. Construction of light-driven sodium pump rhodopsin absorbing longer-wavelength light by site-directed amino-acid mutagenesis

## References

- [1] A. Pushkarev, K. Inoue *et al.*, Nature **558**, 595 (2018).
- [2] K. Inoue, M. d. C. Marín *et al.*, Nat. Commun. **10**, 1993 (2019).

## Author

K. Inoue

# Emergent SU(4) Symmetry and Quantum Spin-Orbital Liquid in $\alpha$ -ZrCl<sub>3</sub>

Oshikawa Group

As materials are cooled down towards the absolute zero temperature, generally they become a solid with a long-range order in location of atoms. Likewise, magnetic materials develop a magnetic long-range order at sufficiently low temperatures. However, we may expect a “quantum spin liquid” as a ground state of a magnetic material, if strong quantum fluctuations destroy the magnetic order even at zero temperature. Theoretical studies have revealed that quantum spin liquids exhibit various exotic phenomena such as fractionalization. Its realization has been one of the central topics in quantum magnetism and condensed matter physics. After intensive studies over several decades, several materials have been found to be strong candidates of quantum spin liquids. However, such candidate materials are still limited, and it is desirable to find new class of quantum spin liquid materials.

Quantum magnets often possess the (approximate) spin rotation symmetry. Mathematically it corresponds to the group of “rotations” of two-component complex vectors, SU(2). Here the two components of the vector correspond to the amplitudes of the spin pointing up and down. It is then natural to consider an extended symmetry of “rotations” of N-component complex vectors, SU(N). For a larger N, the symmetry is larger, and the quantum fluctuations would be stronger. In fact, there have been numerous theoretical studies of SU(N) “spin” systems, many of which are found to be quantum spin liquids. Experimentally, the SU(N) symmetry has been realized using nuclear spin degrees of freedom in cold atoms. However, it is still difficult to observe the SU(N) quantum spin liquid behavior in cold atoms, it is desirable to realize it in a magnetic material.

In principle, the SU(N) symmetry can appear if there are degenerate orbitals which can be occupied by electrons. For example, there are two degenerate orbitals in each atom, an electron can take 2 orbital states and 2 spin states, namely 4 states in each atom. If the system is symmetric with respect to the “rotation” of these 4 states, it is SU(4) symmetric.

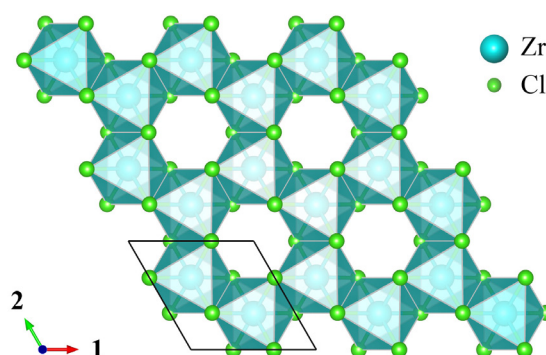


Fig. 1. Crystal structure of  $\alpha$ -ZrCl<sub>3</sub>. Zr<sup>3+</sup> ions form a honeycomb lattice.

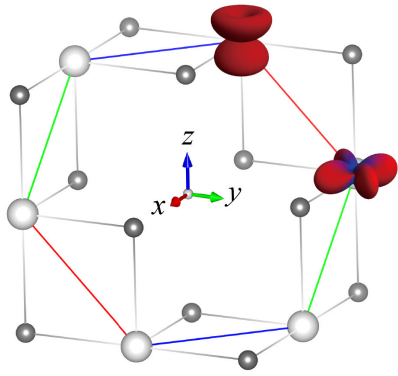


Fig. 2. Hexagonal plaquette of  $\alpha$ -ZrCl<sub>3</sub>. Hoppings between anisotropic d-orbitals are strongly orbital-dependent, and also depend on the bond directions indicated by colors (red, blue, and green).

However, since the orbital and spin are completely different degrees of freedom, there is no particular reason to expect the SU(4) symmetry. In fact, it has been known that the standard model of electrons in the presence of two degenerate orbitals, Kugel-Khomskii model, has the SU(4) symmetry only at a special point, which would require a fine-tuning. Indeed, no material has been known to possess the SU(4) symmetry, even approximately.

In this work [1], we demonstrate theoretically that the SU(4) symmetry emerges in  $\alpha$ -ZrCl<sub>3</sub> (Fig. 1). In the limit of strong spin-orbit coupling, the effective model of electrons in this material has strongly orbital-dependent hoppings (Fig. 2). As a result, the model looks far from SU(4) symmetric. However, the electron hopping between neighboring Zr ions can be identified with an SU(4) gauge field on the lattice. We find that, with an appropriate SU(4) gauge transformation on the lattice, the model is mapped to a manifestly SU(4)-symmetric one (Kugel-Khomskii model at the SU(4) point). This means that  $\alpha$ -ZrCl<sub>3</sub> has an emergent SU(4) symmetry, despite the strong spin-orbit coupling which seems to destroy even the spin SU(2) symmetry. In the strong electron repulsion limit, the effective model is reduced to the SU(4) “antiferromagnetic Heisenberg” model, which has a gapless spin liquid ground state according to a preceding theoretical study. Therefore, we expect that  $\alpha$ -ZrCl<sub>3</sub> realizes an SU(4)-symmetric quantum spin liquid. In fact, the SU(4) symmetry means that the spin and orbital degrees of freedom are intertwined and fluctuating together. In this sense, the ground state should be better called a quantum spin-orbital liquid.

#### Reference

[1] M. Yamada, M. Oshikawa, and G. Jackeli, Phys. Rev. Lett. **121**, 097201 (2018).

#### Authors

M. Yamada, M. Oshikawa, and G. Jackeli<sup>a</sup>

<sup>a</sup>University of Stuttgart and Max-Planck Institute for Solid State Research

## Tuning of Luttinger Semimetal into Weyl Semimetal by Strain and Magnetic Field

Nakatsuji, Lippmaa, Katsumoto, and Kindo Groups

In the field of condensed matter physics, there has been an intense search for topological nontrivial electronic phases in strongly correlated materials. To date, most research on topological electronic systems has been limited to weakly

correlated materials where electronic correlations play a minor role. Among newly-found topological phases, the Weyl semimetal phase has attracted the most significant attention because the Weyl fermions exhibit extremely high electrical and thermal conductivities, which may find use in ultrahigh-speed and low-power consumption devices. While the Weyl semimetal phase was experimentally discovered in the inversion symmetry broken TaAs system in 2015 [1,2], only a few candidates of the magnetic version have been found in systems with broken time reversal symmetry. Historically, a magnetic Weyl system is the first Weyl semimetal predicted for condensed matter in 2012 in the seminal paper by Wan *et al.* [3]. Notably, this prediction was specifically made for the pyrochlore iridates.

Here, we focus on a pyrochlore iridate Pr<sub>2</sub>Ir<sub>2</sub>O<sub>7</sub>. This material is known as a Luttinger semimetal where electronic correlations are strong [4]. According to theoretical predictions, the electronic state can be tuned into a Weyl semimetal state by perturbations such as lattice strain and external magnetic field [5,6]. However, experimental proof of the existence of the Weyl semimetal remains elusive because it is difficult to apply uniaxial strain on bulk single crystals. One possible solution to this problem is to use Pr<sub>2</sub>Ir<sub>2</sub>O<sub>7</sub> thin films where lattice strain can be introduced through epitaxy. To that end, more than 10 groups around the world have been working on fabricating Pr<sub>2</sub>Ir<sub>2</sub>O<sub>7</sub> thin films, but there have been no reports of success.

What makes the fabrication of the thin films difficult is the high volatility of iridium, especially at high temperatures. We therefore turned to solid-state epitaxy, namely, the deposition of precursors at room temperature by pulsed laser deposition followed by annealing in air. This synthesis route mimics bulk crystal growth and allowed us to successfully fabricate high-quality epitaxial thin films of pyrochlore Pr<sub>2</sub>Ir<sub>2</sub>O<sub>7</sub> on yttria-stabilized zirconia substrates [7]. Detailed crystal structure analysis revealed that strained and relaxed grains coexisted in the films. When Hall measurements were performed using the Pr<sub>2</sub>Ir<sub>2</sub>O<sub>7</sub> films, spontaneous Hall effect was found below 50 K even though the material shows no spontaneous magnetization nor was an external magnetic field applied to the film. This temperature of 50 K is very high, considering that bulk single crystals show spontaneous Hall effect only below 1.5 K [8]. The spontaneous Hall effect appears due to the all-in-all-out structure of the iridium 5*d* moments and the associated time reversal symmetry breaking. In this case, the theoretically predicted condition that the Weyl semimetal state appears when both the cubic symmetry and the time reversal

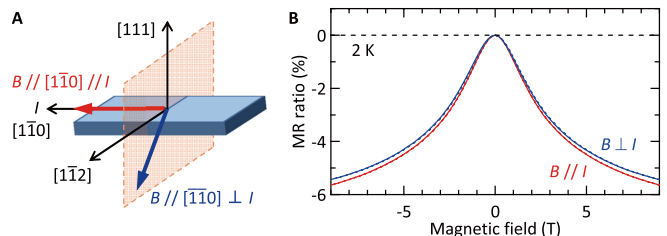


Fig. 1. Additional contribution to the negative longitudinal magneto-resistance for a Pr<sub>2</sub>Ir<sub>2</sub>O<sub>7</sub> thin film. (A) Experimental configurations. *B* and *I* represent the external magnetic field and current, respectively. For the longitudinal (*B* // *I*) and transverse (*B* ⊥ *I*) cases, *B* is applied along the [110] and [110] direction, respectively. *I* flows along the [110] direction in both cases. (B) Magnetoresistance curves as a function of *B* measured at 2 K for *B* // *I* and *B* ⊥ *I* configurations. The solid and dotted lines correspond to up and down sweeps of *B*, respectively. The difference between the two curves comes from the chiral anomaly and indicates that the film is in the Weyl semimetal state.

# Strong Electronic Correlations in a Luttinger Semimetal Pr<sub>2</sub>Ir<sub>2</sub>O<sub>7</sub>

Nakatsuji Group

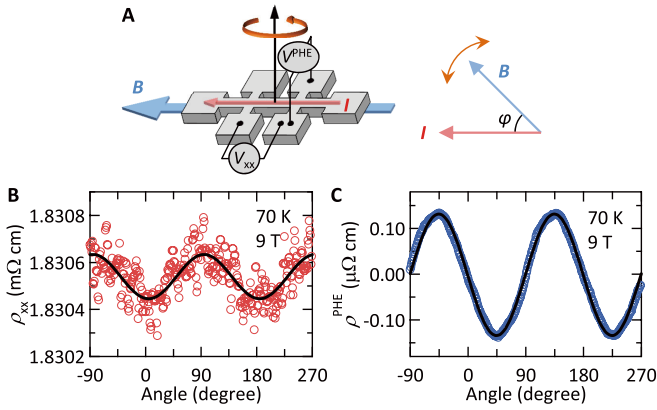


Fig. 2. Planar Hall effect in a Pr<sub>2</sub>Ir<sub>2</sub>O<sub>7</sub> thin film. (A) Experimental configuration.  $I$  flows along the  $[1\bar{1}0]$  direction and  $B$  is applied in the same plane. The angle between  $I$  and  $B$  ( $\varphi$ ) is changed by the in-plane rotation of the sample. The longitudinal and planar Hall resistance is measured by  $V_{xx}$  and  $V^{PHE}$ , respectively. (B and C) Angle dependence of the longitudinal and planar Hall resistivity, respectively, measured at 70 K and 9 T. The red and blue open circles are the experimental data, and the black solid lines are the fitting results using the equations predicted theoretically [10,11]. The experimental results agree well with the theory, suggesting that the film has been tuned into the Weyl semimetal state.

symmetry are broken is satisfied in the strained grains in the film. On the other hand, although the relaxed grains are in the Luttinger semimetal state, it is possible that they can be tuned into a magnetic Weyl semimetal when an external magnetic field is applied and the time reversal symmetry is broken. To confirm this, we examine the effects of the chiral anomaly, which is the magneto-electric response of the Weyl semimetal. As a result, we find strong evidence for the chiral anomaly in the negative longitudinal magnetoresistance [9] (Fig. 1) and the planar Hall effect [10,11] (Fig. 2). This means that the Luttinger semimetal can be modified into the Weyl semimetal by an external magnetic field.

In summary, we have successfully fabricated epitaxial thin films of Pr<sub>2</sub>Ir<sub>2</sub>O<sub>7</sub> and experimentally demonstrated that the Weyl semimetal state can be induced either by lattice strain or by applying an external magnetic field. Based on the results with the Luttinger semimetal, the research for the topological phases in strongly correlated systems, which has not been done so far, will proceed. It is expected to lead to the development of ultrahigh-speed and low-power devices utilizing the Weyl fermions having high electric and thermal conductivities.

## References

- [1] B. Q. Lv *et al.*, Phys. Rev. X **5**, 031013 (2015).
- [2] S.-Y. Xu *et al.*, Science **349**, 613 (2015).
- [3] X. Wan *et al.*, Phys. Rev. B **83**, 205101 (2011).
- [4] B. Cheng, T. Ohtsuki *et al.*, Nat. Commun. **8**, 2097 (2017).
- [5] E.-G. Moon *et al.*, Phys. Rev. Lett. **111**, 206401 (2013).
- [6] T. Kondo *et al.*, Nat. Commun. **6**, 10042 (2015).
- [7] T. Ohtsuki *et al.*, Proc. Natl. Acad. Sci. U.S.A. **116**, 8803 (2019).
- [8] Y. Machida *et al.*, Nature **463**, 210 (2010).
- [9] D. T. Son and B. Z. Spivak, Phys. Rev. B **88**, 104412 (2013).
- [10] A. A. Burkov, Phys. Rev. B **96**, 041110(R) (2017).
- [11] S. Nandy *et al.*, Phys. Rev. Lett. **119**, 176804 (2017).

## Authors

T. Ohtsuki, Z. Tian, A. Endo, M. Halim, S. Katsumoto, Y. Kohama, K. Kindo, M. Lippmaa, and S. Nakatsuji

In the field of the solid state physics, materials exhibiting novel physical properties are vigorously explored. Zero-gap semiconductors are one fascinating group of materials where topological functionalities lead to high carrier mobility and the quantum Hall effect. It is known that electrons behave as if they are massless in materials such as graphene because of the linear band dispersion near the point where the valence and the conduction bands come in contact with each other. For graphene, new phenomena were discovered one after another and it became the subject of the Nobel Prize in Physics in 2010. So far, the physics of zero-gap semiconductors have only been studied in materials where the interaction between electrons is weak.

An example of a zero-gap structure is a Luttinger semimetal with quadratic band touching whose band dispersion is parabolic near the band touching point as illustrated in Fig. 1. It was predicted more than 40 years ago that materials in a Luttinger semimetal state would show novel electronic states because of the strong electronic correlations that are unobtainable in conventional metals. However, in materials known so far, such as  $\alpha$ -Sn and HgTe, it has been difficult to identify experimentally the effects of electronic correlations because the effective mass of electrons is small and hence the electronic correlations are weak.

To clarify the effect of the strong electronic correlations, we focused on Pr<sub>2</sub>Ir<sub>2</sub>O<sub>7</sub> [1]. It is already known that Pr<sub>2</sub>Ir<sub>2</sub>O<sub>7</sub> is a Luttinger semimetal with quadratic band touching and that the effective mass of electrons is about 6 times larger than the mass of the free electron in vacuum [2]. We therefore carried out a terahertz spectroscopy study on the Pr<sub>2</sub>Ir<sub>2</sub>O<sub>7</sub> thin films and observed a very large dielectric constant of about 180 at a temperature of 5 K as shown in Fig. 2 [3]. This value is several tens of times larger than that of zero-gap semiconductors (e.g.  $\alpha$ -Sn and HgTe) known so far. Additionally, in a Luttinger semimetal state, the dielectric constant is a measure of the scale of electronic correlations. By using this fact, when the magnitude of the electronic correlations is estimated from the dielectric constant, the scale of electronic correlations is about 2 orders of magni-

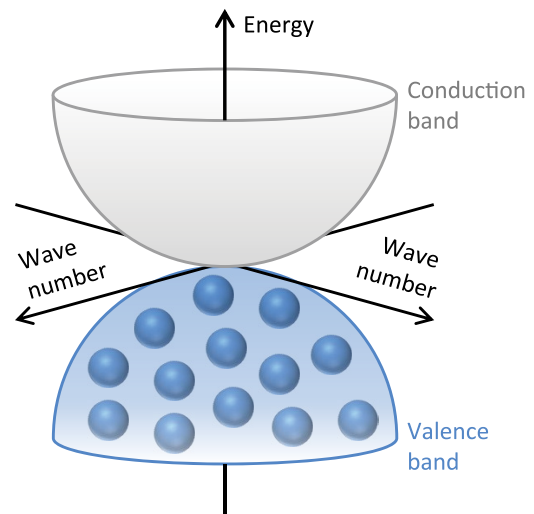


Fig. 1. Band structure of a Luttinger semimetal, which is a zero-gap semiconductor. The valence band, which is filled with electrons (blue spheres) and the empty conduction band both have a three-dimensional parabolic shape, and are in contact with each other at a single point close to the Fermi level.

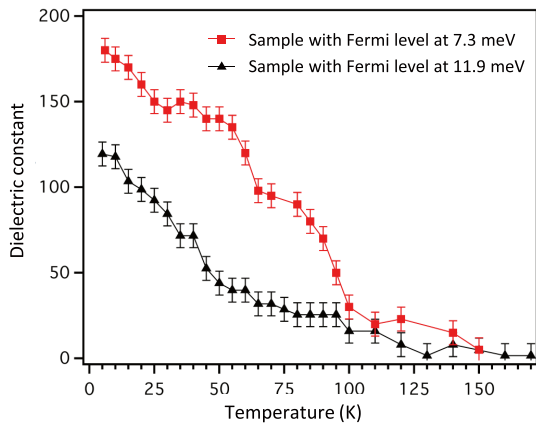


Fig. 2. Temperature dependence of the dielectric constant. The low-temperature value is several tens of times larger than that of known zero-gap semiconductors (e.g.  $\alpha$ -Sn and HgTe). The dielectric constant becomes larger when the Fermi level approaches the band touching point.

tude larger than the kinetic energy.

We have thus demonstrated that electronic correlations are indeed very strong in a Luttinger semimetal with quadratic band touching. In the future, it is expected that further understanding of the role of electronic correlations in determining the physical properties of zero-gap semiconductors will lead to the creation of novel metallic states and new functional materials.

#### References

- [1] T. Ohtsuki *et al.*, Proc. Natl. Acad. Sci. U.S.A. **116**, 8803 (2019).
- [2] T. Kondo *et al.*, Nat. Commun. **6**, 10042 (2015).
- [3] B. Cheng, T. Ohtsuki *et al.*, Nat. Commun. **8**, 2097 (2017).

#### Authors

T. Ohtsuki, B. Cheng<sup>a</sup>, D. Chaudhuri<sup>a</sup>, S. Nakatsuji, M. Lippmaa, and N. P. Armitage<sup>a</sup>

<sup>a</sup>The Johns Hopkins University

## Large Spin Hall Effect in Amorphous Mn-Sn Alloy Thin Film

Nakatsuji Group

Pure spin current contains only angular momentum without net charge flow, which greatly reduces the Joule heating. This feature makes spin current beneficial for low power spintronic devices. The spin Hall effect (SHE) converts charge current to transverse spin current, serving as an effective way to generate pure spin current. Meanwhile, as the reciprocal effect of the SHE, the inverse spin Hall effect (ISHE) converts pure spin current to transverse charge

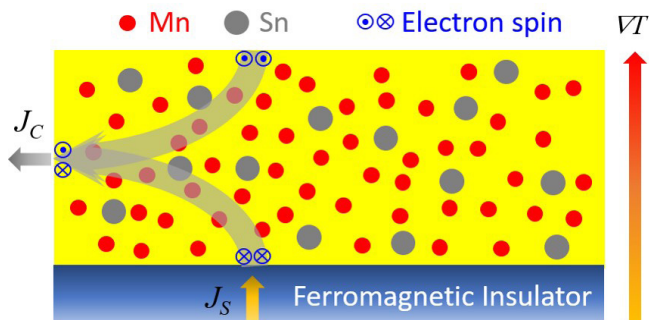


Fig. 1. Schematic of thermal spin injection from a ferromagnetic insulator into an attached metal layer.

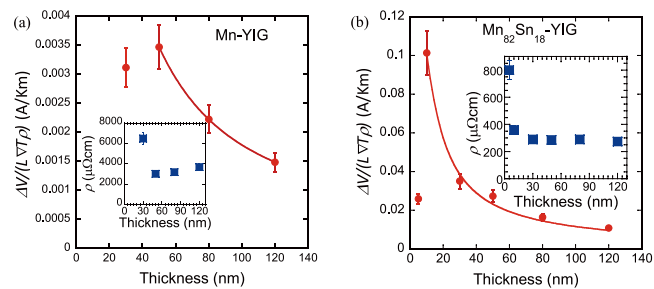


Fig. 2. Thickness dependent thermal voltage for (a) Mn and (b) Mn-Sn alloy thin films on YIG. Insets are thickness dependence of resistivity.

current, and plays an important role in pure spin current detection and conversion.

Although manipulation of pure spin current in heavy transition metals, ferromagnetic metals, and their alloys have been extensively explored in the past decade, antiferromagnets have become a new central stage due to its prominent advantages such as high frequency magnetic dynamics, negligible stray field, and perturbation insensitivity. Among these materials, the non-collinear Kagome lattice antiferromagnets  $Mn_3X$  ( $X = Sn, Ge, Ga$ ) stand out because of their large transverse electrical [1-4] and optical [5] responses to the external magnetic field as well as their negligible magnetic moment.

In our work, we used the thermally generated pure spin current from the spin Seebeck effect (SSE) in the ferrimagnetic insulator yttrium iron garnet (YIG) to study the inverse spin Hall effect in Mn and the Mn-Sn alloys (Fig. 1). A series of samples with different thicknesses are sputtering deposited onto YIG substrates. By measuring the ISHE voltage, we obtained a sizable spin Hall angle  $\theta_{SH}$  of  $-0.23\%$  (which measures the conversion efficiency between charge current and spin current), and a long spin diffusion length  $\lambda_{sd} \approx 11.5$  nm for the single element material Mn, as shown in Fig. 2 (a). Most importantly, by doping Sn in Mn, we found that the  $\theta_{SH}$  of the Mn-Sn alloy, even in its *amorphous* form, is increased by 20 times to  $-4.4\%$ , while the resistivity ( $\rho$ ) is reduced by about 10 times, as shown in Fig. 2 (b). Therefore, the energy consumption ( $\sim \rho/\theta_{SH}^2$ ) of the Mn-Sn alloy is reduced by 4000 times compared to Mn. A spin pumping measurement further corroborates the enhancement of the  $\theta_{SH}$  in the Mn-Sn alloy. These results not only serve as essential references in studying the pure spin current phenomena in Mn-based alloys, but also offer a promising method for exploring future energy efficient spin Hall materials with high spin Hall angle but low resistivity and thus low energy consumptions [6].

#### References

- [1] S. Nakatsuji, N. Kiyohara, and T. Higo, Nature **527**, 212 (2015).
- [2] M. Ikhlas, T. Tomita *et al.*, Nat. Phys. **13**, 1085 (2017).
- [3] N. Kiyohara, T. Tomita, and S. Nakatsuji, Phys. Rev. Appl. **5**, 064009 (2016); A. K. Nayak *et al.*, Sci. Adv. **2**, e1501870 (2016).
- [4] Z. H. Liu *et al.*, Sci. Rep. **7**, 515 (2017).
- [5] T. Higo *et al.*, Nat. Photon. **12**, 73 (2018).
- [6] D. Qu, T. Higo, T. Nishikawa, K. Matsumoto, K. Kondou, P. K. Muduli, Y. Otani, and S. Nakatsuji, Phys. Rev. Mater. **2**, 102001(R) (2018).

#### Authors

D. Qu, T. Higo, T. Nishikawa, K. Matsumoto, K. Kondou<sup>a</sup>, D. Nishio-Hamane, R. Ishii, P. K. Muduli, Y. Otani and S. Nakatsuji

<sup>a</sup>RIKEN-CEMS

# Large Anomalous Hall Effect in Thin Films of a Weyl Magnet Mn<sub>3</sub>Sn

Nakatsuji and Otani Groups

Recently, there has been a surge of interest in antiferromagnets (AFMs) as prospective spintronic materials for high-density and ultrafast memory devices because of their vanishingly small stray field and orders of magnitude faster spin dynamics compared to their ferromagnetic counterparts. In particular, the recently discovered functional antiferromagnet D0<sub>19</sub> Mn<sub>3</sub>Sn has attracted broad attention as the first example of a magnetic Weyl material/Weyl magnet [1-5]. This material exhibits a variety of useful functions that have never been observed before in antiferromagnets at zero magnetic field, including the anomalous Hall effect [1], the anomalous Nernst effect [2], and the magneto-optical Kerr effect [5] at room temperature. All these properties are controllable by a magnetic field and thus can be used for designing antiferromagnetic spintronics and in energy harvesting technology. It has been shown that such an antiferromagnet hosts a topological state characterized by magnetic Weyl fermions [3,4]. The discovery of the Weyl metal state in an antiferromagnet opens up a new chapter of applied research using the functional antiferromagnets. Therefore, fabrication of high quality thin films of the Weyl antiferromagnet becomes all the more important.

For the thin film fabrication, we employ DC magnetron sputtering. The films (40-400 nm) are deposited at room temperature onto a Si/SiO<sub>2</sub> substrate from the Mn<sub>3</sub>Sn target. After the deposition at room temperature, we anneal the film at 500°C for one hour, and thereby crystallizes the as-deposited amorphous film in a polycrystalline form of the Mn<sub>3</sub>Sn film. XRD measurements reveal that the films are the single phase of Mn<sub>3</sub>Sn and are in a randomly oriented polycrystalline form; all the peaks can be indexed by the hexagonal P6<sub>3</sub>/mmc symmetry of D0<sub>19</sub> Mn<sub>3</sub>Sn, with no additional peaks

due to plausible impurity phases (Fig.1(a)).

Figure 1(b) shows the temperature dependence of the longitudinal resistivity  $\rho$  and the spontaneous Hall resistivity  $\rho_H (H = 0)$  of the Mn<sub>3</sub>Sn thin film under zero field. The behavior of longitudinal resistivity  $\rho$  confirms the metallic transport consistent with the previous work on bulk single crystals [2]. The zero-field Hall resistivity  $\rho_H (H = 0)$  was obtained from  $(\rho_H (H = +0) - \rho_H (H = -0))/2$ . (Here, we use +0 and -0 to indicate zero magnetic field approached, respectively, from +5 T and -5 T in the Hall resistivity measurement at each temperature.) We have observed a sharp decrease in  $\rho_H (H = 0)$  below  $T_1 = 260$  K on cooling; this behavior agrees with the magnetic symmetry consideration in Mn<sub>3</sub>Sn that the inverse triangular spin structure breaks the global time-reversal symmetry, whereas time-reversal symmetry is restored in the low temperature helical phase. Figure 1(c) displays the field dependence of the Hall resistivity  $\rho_H (H)$  at 300 K as a function of the magnetic field applied perpendicular to the film surface. The anomalous Hall effect of the Mn<sub>3</sub>Sn films exhibit a significant change in  $\rho_H (H)$  from 1.5  $\mu\Omega\text{cm}$  to -1.5  $\mu\Omega\text{cm}$  with increasing field despite the vanishingly small magnetization; this feature is generated by the switching of the antiferromagnetic domain in real space and the large fictitious field in momentum space [6]. Notably, this is the first report on the thin film of the antiferromagnetic Mn<sub>3</sub>Sn film exhibiting the large anomalous Hall effect of the same order of magnitude as the value reported for bulk. Our fabrication of the high-quality thin film of the Weyl magnet Mn<sub>3</sub>Sn and the observation of its large anomalous Hall effect provide an important step to further develop devices useful for antiferromagnetic spintronics, such as for high-speed and high-density information storage.

## References

- [1] S. Nakatsuji, N. Kiyohara, and T. Higo, *Nature* **527**, 212 (2015).
- [2] M. Ikhlas, T. Tomita *et al.*, *Nat. Phys.* **13**, 1085 (2017).
- [3] K. Kuroda, T. Tomita *et al.*, *Nat. Mater.* **16**, 1090 (2017).
- [4] H. Yang *et al.*, *New J. Phys.* **19**, 015008 (2017).
- [5] T. Higo *et al.*, *Nat. Photon.* **12**, 73 (2018).
- [6] T. Higo, D. Qu, Y. Li, C. L. Chien, Y. Otani, and S. Nakatsuji, *Appl. Phys. Lett.* **113**, 202402 (2018).

## Authors

T. Higo, D. Qu, Y. Li<sup>a</sup>, C. L. Chien<sup>a</sup>, Y. Otani, and S. Nakatsuji  
<sup>a</sup>Johns Hopkins University

## Giant Anomalous Nernst Effect at Room Temperature in a Weyl Ferromagnet

Nakatsuji Group

The anomalous Nernst effect (ANE) is a well-known thermoelectric effect for ferromagnets, namely the generation of an electric voltage perpendicular to both magnetization and an applied temperature gradient. This transverse geometry of ANE leads to various advantages for thermoelectric modules compared to the conventional one based on Seebeck effect, such as simpler structure to efficiently cover a heat source, higher flexibility, lower production cost, and larger conversion efficiency for the same figure of merit [1]. However, the size of ANE is generally very small (on the order of  $\sim 0.1$   $\mu\text{V/K}$ ), which hinders its practical applications. Recent theoretical and experimental investigations on topological materials indicate that the intense Berry curvature of Weyl points near the Fermi energy can enhance the intrinsic ANE, rendering ANE an powerful probe to

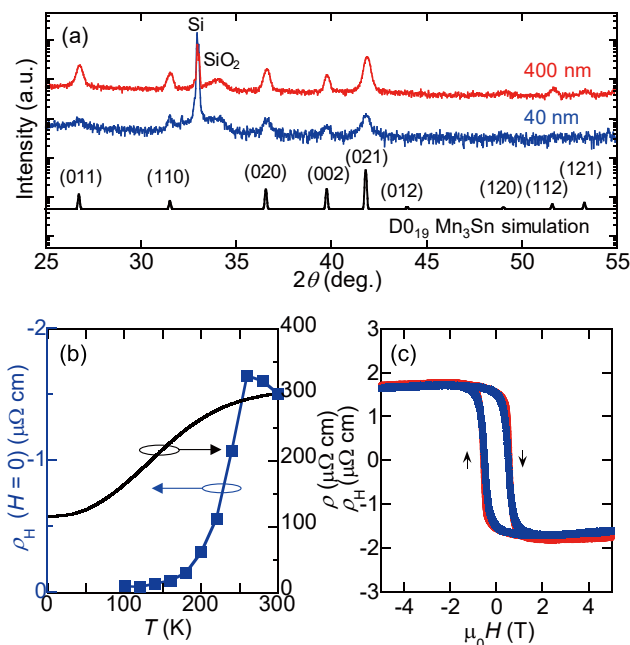


Fig. 1. (a) Room temperature spectra obtained with an X-ray diffractometer for the 40 and 400 nm thin films of Mn<sub>3</sub>Sn on a Si/SiO<sub>2</sub> substrate. The theoretical spectrum of the D0<sub>19</sub> Mn<sub>3</sub>Sn structure is shown at the bottom. (b) Temperature dependence of the resistivity  $\rho$  and the spontaneous Hall resistivity  $\rho_H$  of the Mn<sub>3</sub>Sn (40 nm) thin film. (c) Field dependence of the Hall resistivity  $\rho_H$  measured under a magnetic field applied in the perpendicular direction to the surface of the Mn<sub>3</sub>Sn thin films.

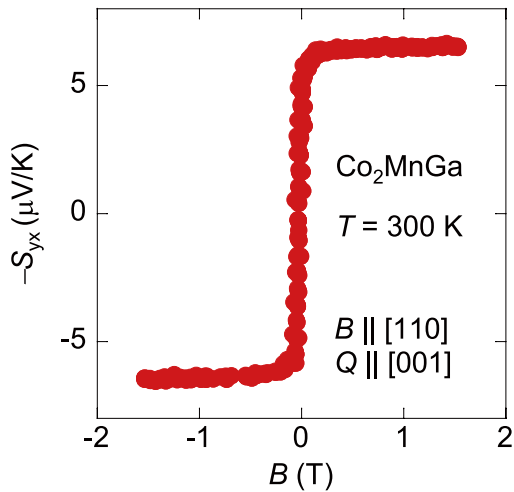


Fig. 1. Magnetic field dependence of anomalous Nernst coefficient of  $\text{Co}_2\text{MnGa}$  at room temperature.

clarify the topological electronic structure in magnetic Weyl semimetals [2-4]. In other words, a ferromagnet exhibiting a giant ANE may serve as an ideal ground for magnetic Weyl semimetal state.

In this work, we report the giant ANE in a full-Heusler ferromagnet  $\text{Co}_2\text{MnGa}$ , reaching a record high value of  $S_{yx} \sim 6 \mu\text{V/K}$  at room temperature [5] (Fig. 1). The crossover from Mott relation  $\alpha_{yx} \sim T$  to  $-\ln T$  dependence is observed on warming, where  $\alpha_{yx}$  is the transverse thermoelectric conductivity, indicating the proximity to the quantum Lifshitz transition between type-I and type-II magnetic Weyl fermion states. Our study provides a new guideline for searching new topological magnets which are useful for energy harvesting and spintronics.

#### References

- [1] M. Mizuguchi and S. Nakatsuji, *Sci. Tech. Adv. Mater.* **20**, 262 (2019).
- [2] D. Xiao *et al.*, *Rev. Mod. Phys.* **82**, 1959 (2010).
- [3] M. Ikhlas *et al.*, *Nat. Physics* **13**, 1085 (2017).
- [4] K. Kuroda *et al.*, *Nat. Mater.* **16**, 1090 (2017).
- [5] A. Sakai *et al.*, *Nat. Physics* **14**, 1110 (2018).

#### Authors

A. Sakai, Y. P. Mizuta<sup>b,c</sup>, A. A. Nugroho<sup>d</sup>, R. Sihombing<sup>d</sup>, T. Koretsune<sup>a,c</sup>, M.-T. Suzuki<sup>a,c</sup>, N. Takemori<sup>c</sup>, R. Ishii, D. N.-Hamane, R. Arita<sup>a,c</sup>, P. Goswami<sup>e,f</sup>, and S. Nakatsuji<sup>a</sup>

<sup>a</sup>CREST, Japan Science and Technology Agency (JST)

<sup>b</sup>Kanazawa University

<sup>c</sup>Center for Emergent Matter Science, RIKEN

<sup>d</sup>Bandung Institute of Technology

<sup>e</sup>University of Maryland

<sup>f</sup>Northwestern University

## Magnetic Spin Hall Effect in a Non-Collinear Antiferromagnet

Otani and Nakatsuji Groups

The conventional spin Hall effect (SHE) converts electrical currents to transverse spin currents in non-magnetic conductors in response to an electric field. The SHE has thus drawn much attention as a means to switch the magnetization of the adjacent ferromagnetic layer via spin orbit torque. New functions have been further explored in various materials in terms of spin-charge currents interconversion. The magnetic contribution to the SHE has therefore

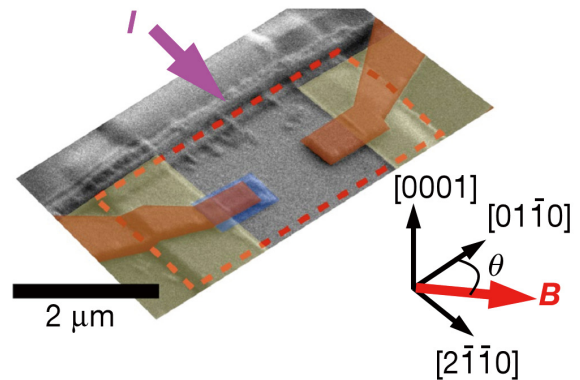


Fig. 1. Scanning electron microscope image of the spin-accumulation device. The microfabricated  $\text{Mn}_3\text{Sn}$  single crystal is indicated by the red dashed line. A NiFe ferromagnetic electrode and non-magnetic Cu electrodes are indicated by blue and brown areas, respectively. The edge of the  $\text{Mn}_3\text{Sn}$  crystal indicated by yellow area is covered with a 30-nm-thick  $\text{Al}_2\text{O}_3$  insulating layer to avoid electrical contact at the edge.

been studied intensively in these days. Here we show that antiferromagnets have richer spin Hall properties than that of non-magnetic materials. The material focused on here is  $\text{Mn}_3\text{Sn}$ , which shows non-collinear antiferromagnetic order of Mn magnetic moments that have an inverse triangular spin configuration on stacked kagome lattices [1]. We find non-trivial time reversal-symmetry-breaking counterparts of the conventional SHE, which is called magnetic spin Hall effect [2].

To study the SHE in a non-collinear antiferromagnet, we fabricated a device consisting of ferromagnetic NiFe and non-magnetic Cu electrodes formed on the top surface of a microfabricated 100-nm-thick  $\text{Mn}_3\text{Sn}$  single crystal (see Fig.1). An electric current was applied along the  $[2\bar{1}10]$  axis and the voltage was measured between electrodes aligned along the  $[01\bar{1}0]$  axis, perpendicular to the current. If current inside  $\text{Mn}_3\text{Sn}$  generated spin accumulation with a component parallel to the NiFe magnetization, it would shift the electrochemical potential across the  $\text{Mn}_3\text{Sn}/\text{NiFe}$  interface and can therefore be detected as a voltage between NiFe and the Cu electrodes. A rectangular resistance-magnetic field ( $R$ - $B$ ) hysteresis loop corresponding to the switching of NiFe magnetization is expected for a fixed polarization direction of the accumulated spins. Such a rectangular  $R$ - $B$  hysteresis loop was observed in the magnetic-field dependence of the transverse voltage between NiFe and the Cu electrodes. The results in **a** and **b** were obtained after saturation of  $\text{Mn}_3\text{Sn}$  with a sufficiently large magnetic field  $B$  of  $-0.75 \text{ T}$

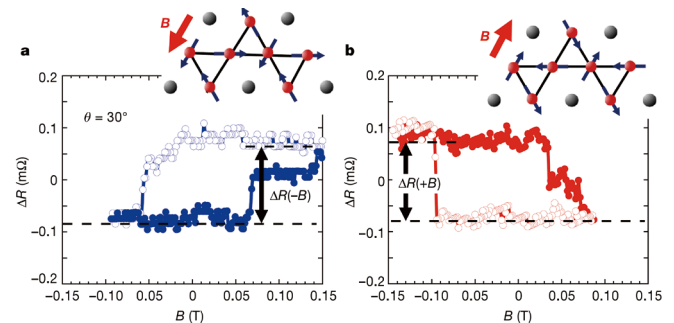


Fig. 2. Spin-accumulation signal. **a**, **b**, Magnetic-field dependence of resistance measured between the NiFe and Cu electrodes at room temperature. The results in **a** and **b** were obtained after saturation of  $\text{Mn}_3\text{Sn}$  with a sufficiently large magnetic field  $B_0$  of  $-0.75 \text{ T}$  and  $+0.75 \text{ T}$ , respectively. The corresponding spin structures of  $\text{Mn}_3\text{Sn}$  are shown in the insets.

and +0.75 T, respectively, which provide evidence that the rectangular loops originate from spin accumulation at the  $\text{Mn}_3\text{Sn}$  surface. The key observation in this work is that the spin accumulation signal changes indicate when the  $\text{Mn}_3\text{Sn}$  sub lattice moments are reversed, as illustrated in the inset. This unexpected sign change demonstrates that the dominant contribution to the SHE in  $\text{Mn}_3\text{Sn}$  is odd under time reversal. We find that in the non-collinear antiferromagnet  $\text{Mn}_3\text{Sn}$ , the SHE has an anomalous sign change when its triangularly ordered moments switch orientation. This discovery expands the horizons of antiferromagnet spintronics and spin-charge coupling mechanisms.

#### References

- [1] S. Nakatsuji *et al.*, Nature **527**, 212 (2015)  
 [2] M. Kimata *et al.*, Nature **565**, 627 (2019)

#### Authors

Y. Otani, H. Isshiki, M. Kimata, H. Chen<sup>a</sup>, K. Kondou<sup>b</sup>, S. Sugimoto, P. K. Muduli, M. Ikhlas, Y. Omori, T. Tomita, A. H. MacDonald<sup>a</sup>, and S. Nakatsuji  
<sup>a</sup>University of Texas at Austin  
<sup>b</sup>RIKEN-CEMS

## Lithium-Ion Conductivity in Single Crystals of $\text{Li}_{10}\text{GeP}_2\text{S}_{12}$

Hiroi Group

The all-solid-state lithium-ion battery has been studied extensively as a next-generation secondary battery. It uses a solid instead of a liquid electrolyte, which enables to achieve greater safety, higher energy density, wider temperature range of operation, and larger output power compared with the conventional battery. To realize this, an efficient Li-ion conductor is required, which exhibits conductivity that is either comparable to or larger than that of commercially used organic liquid electrolytes.  $\text{Li}_{10}\text{GeP}_2\text{S}_{12}$  (LGPS) is a promising candidate for the super ionic conductor; compared to other candidates, it has the highest conductivity of  $12 \text{ mS cm}^{-1}$  at room temperature and an outstanding electrochemical performance in Li batteries [1,2]. Thus, LGPS is a key compound in the materialization of the all-solid-state battery.

The high Li-ion conductivity of LGPS has been ascribed to its specific crystal structure shown in Fig. 1a. There are four partially occupied Li sites inside the rigid framework composed of the tetrahedral units of  $\text{Ge}_{0.5}\text{P}_{0.5}\text{S}_4$  and  $\text{PS}_4$ . Among them, the Li1, Li3, and Li4 sites are located in the

distorted tetrahedra of S, while the Li2 site is in the distorted octahedron of S. It has been shown that the Li diffusion between the former sites is crucial for the high conductivity, while the Li2 ions are almost immobile.

A highly anisotropic ion diffusion has been proposed based on neutron diffraction (ND) measurements and molecular dynamics calculations: a one-dimensional (1D) channel via the Li1–Li3 path along the  $c$  axis is dominant, and a two-dimensional (2D) hopping via the Li1–Li4 path in the  $\langle 110 \rangle$  direction is secondary [3]. The activation energies of the local hopping processes for the 1D and 2D paths are determined as 0.16 (0.17) and 0.26 (0.28) eV from the NMR experiments (the molecular dynamics calculations), respectively. Thus, considerable anisotropy can be expected in the atomic-scale diffusion process. In contrast, pulsed-field gradient NMR measurements, which may be sensitive to long-range Li diffusion at the micrometer scale, suggests a nearly isotropic Li diffusion.

An impedance measurement using a single crystal provides important information with which to clarify the origin of this difference and the mechanism of ion diffusion in LGPS. However, because of the lack of a sufficiently large single crystal, the Li diffusion in the bulk had not been measured thus far. Previous impedance measurements using polycrystalline samples yielded an average conductivity of  $\sim 10 \text{ mS cm}^{-1}$  and activation energy of 0.22–0.28 eV. Understanding of the true conduction mechanism in LGPS is crucial for the improvement of LGPS and for further development of a better solid electrolyte for the all-solid-state battery. In the present study, we obtain large single crystals of LGPS, a few millimeters in size, using the self-flux method (Fig. 1b), and carry out impedance measurements in the [001] and [110] directions [4]. The conductivity is, in fact, higher along [001] than along [110]; however, the difference is only a factor of 4. In addition, the activation energies are nearly equal for the two directions, suggesting a weak anisotropic 3D diffusion in LGPS, as schematically illustrated in Fig. 1c.

#### References

- [1] N. Kamaya, K. Homma, Y. Yamakawa *et al.*, Nat. Mater. **10**, 682 (2011).  
 [2] Y. Kato, S. Hori, T. Saito *et al.*, Nat. Energy **1**, 16030 (2016).  
 [3] X. Liang, L. Wang, Y. Jiang *et al.*, Chem. Mater. **27**, 5503 (2015).  
 [4] R. Iwasaki, S. Hori, R. Kanno, T. Yajima, D. Hirai, Y. Kato, and Z. Hiroi, Chem. Mater. **31**, 3694 (2019).

#### Authors

R. Iwasaki, S. Hori<sup>a</sup>, R. Kanno<sup>a</sup>, T. Yajima, D. Hirai, Y. Kato<sup>b</sup>, and Z. Hiroi  
<sup>a</sup>Tokyo Institute of Technology  
<sup>b</sup>Toyota Motor Corporation

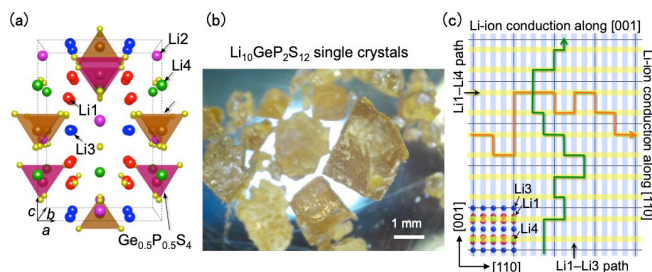


Fig. 1. (a) Crystal structure of  $\text{Li}_{10}\text{GeP}_2\text{S}_{12}$  (LGPS), (b) photograph of typical LGPS crystals of a few millimeters in size, and (c) schematic drawing illustrating the possible conducting paths of Li ions in LGPS. The one-dimensional channel via the Li1–Li3 path along the  $c$  axis is dominant, and a two-dimensional hopping via the Li1–Li4 path in the  $\langle 110 \rangle$  direction is secondary in the short-range Li-ion conduction. However, the actual long-range conduction occurs via such meandering paths as shown by the green and orange lines in (c), which give rise to weakly anisotropic Li-ion conductivity.

## From Gapless Kitaev Spin Liquid to Classical String Gas through Tensor Networks

Kawashima Group

Quantum spin liquids (QSLs) represent a state of quantum matter which is not characterized by any local order parameters even at zero temperature. These novel states are expected to exhibit long-range entanglement leading to the topological order and fractionalized excitations. For example, the Haldane phase, which is known as a symmetry-protected topological phase, is a fascinating phase one can find in the

$$|\psi_0\rangle = \left| \begin{array}{c} \text{Honeycomb lattice with no loops} \\ \text{Honeycomb lattice with one loop} \\ \text{Honeycomb lattice with two loops} \end{array} \right\rangle + \dots$$

Fig. 1. Schematic representation of the "loop-gas" state. It is a sum of all loop-gas configurations. Each configuration corresponds to a product of Pauli operators. The loop-gas configuration determines which Pauli operator is aligned on a given lattice.

S=1 quantum spin chain. The novel character that discriminates the Haldane phase from trivial gapped states was most clearly revealed by the discovery of Affleck-Kennedy-Lieb-Tasaki (AKLT) model and its exact ground state or the AKLT state. Its compact representation in the form of a matrix-product state provided a new insight into the Haldane phase. As a two-dimensional system with spin-liquid state, the Kitaev model on honeycomb lattice (KHM) is now a subject of active research, due to recent successful realizations of Kitaev materials. The model is exactly solvable and exhibits gapless and gapped Kitaev spin liquid (KSL) ground states with fractionalized excitations.

In the present work, we propose a "loop-gas" state, i.e., an exactly-solvable quantum state that has a compact and exact tensor-network representation, and a series of ansatz that starts from the loop-gas state and converges rapidly to the KHM ground-state. The loop gas state is defined by the loop-gas projector applied to a product state in which all spins are aligned in the (111) direction. The loop-gas projector is defined as tensor-network operator with bond-dimension 2, which is represented by a sum of all loop configurations each corresponding to a product of Pauli operators on all lattice points. (Fig. 1) We find that the norm of the loop gas state is exactly the same as the classical loop gas model at the critical fugacity on honeycomb lattice. The classical loop gas model appears in the low-temperature expansion of the Ising model, and therefore shares the same critical properties as the latter. These observations establishes that the correlation function of the loop-gas state is exactly the same as the correlation function of the critical Ising model. Furthermore, by defining the dimer-gas operator in an analogous way to the loop-gas operator, and applying it to the loop-gas state, we can improve the loop-gas state as an approximate to the KHM ground-state. (Fig. 2) For example, the second order approximation, which is obtained by applying the dimer-gas operator twice, achieves more than 4-digits accuracy in the energy. This is better than any other previous variational wave function. Also, note that there are only two adjustable parameters in the ansatz.

From these results, we conclude that the series of ansatz

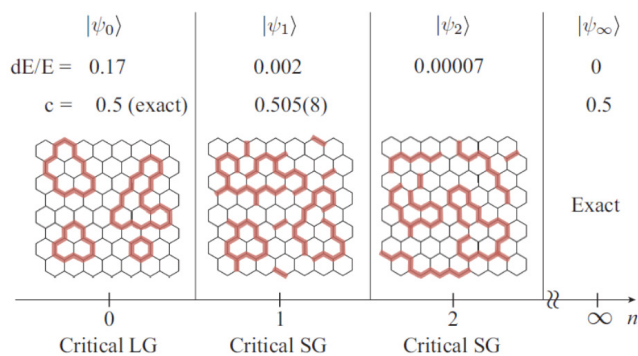


Fig. 2. The series of ansatz converging to the exact KHM ground-state. The zero-th one is the loop-gas state. The energy of the second order approximation already attains 4-digit accuracy, which has never been achieved by other numerical variational methods.

starting from the loop-gas state correctly reflects the essential properties of the family of KSLs, which is known to belong to the Ising universality class. Since the present description of KSLs does not rely on the mapping to fermions, it provides us with an alternative view point to discuss KSLs.

**Reference**

[1] Hyun-Yong Lee, Ryui Kaneko, Tsuyoshi Okubo and Naoki Kawashima: arXiv:1901.05786.

**Authors**

H.-Y. Lee, R. Kaneko, T. Okubo<sup>a</sup>, and N. Kawashima

<sup>a</sup>Department of Physics, University of Tokyo

## Evolution of Magnetic Double Helix and Quantum Criticality Near a Dome of Superconductivity in CrAs

Uwatoko Group

The study of unconventional superconductivity (SC) is one of the most vigorous research fields in condensed matter physics. Although the underlying mechanisms for the unconventional SC in cuprate, iron-based, and heavy-fermion superconductors remains elusive, extensive investigations over the last decades have evidenced quantum criticality as a candidate mechanism for these diverse classes of superconductors. The phase diagrams of these materials often feature a superconducting dome situated adjacent to a magnetically ordered state, with the optimal superconducting transition temperature ( $T_c$ ) located near a quantum critical point. The close proximity of SC to magnetic order makes it important to elucidate the nature of magnetism.

Recently, we found CrAs as the first superconductor among Cr-based compounds. The transport measurements indicated that the development of SC is accompanied by the suppression of double-helical magnetic order that is coupled with a first-order isostructural transition at ambient pressure. These observations make CrAs an ideal platform for in-depth studies on how the coupled structural and helimagnetic orders are tuned to the critical point and how the magnetism is coupled to the unconventional SC developed nearby. In combinations of elastic and inelastic neutron scattering, resistivity, and specific-heat measurements on undoped CrAs

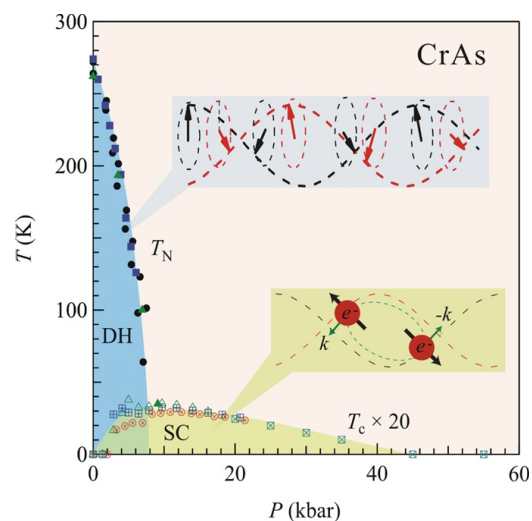


Fig. 1. Pressure dependencies of the double helical (DH) magnetic transition temperature  $T_N$  and the superconducting ( $SC$ ) transition temperature  $T_c$  for CrAs. Schematic views of the DH structure and Cooper pairing are illustrated in the figure.

and P-doped  $\text{CrAs}_{1-x}\text{P}_x$  single crystals and powders, we have studied systematically the evolutions of static helical order and dynamic spin correlations as well as the electronic properties of CrAs when its coupled structural/helical order is suppressed by either external pressure or the chemical substitutions.

Neutron diffraction on the single-crystal CrAs under hydrostatic pressure ( $P$ ) shows that the combined order is suppressed at  $P_c \approx 10$  kbar, near which bulk superconductivity develops with a maximal transition temperature  $T_c \approx 2$  K. We further show that the coupled order is also completely suppressed by phosphorus doping in  $\text{CrAs}_{1-x}\text{P}_x$  at a critical  $x_c \approx 0.05$ , above which inelastic neutron scattering evidenced persistent antiferromagnetic correlations, providing a possible link between magnetism and superconductivity. In line with the presence of antiferromagnetic fluctuations near  $P_c$  ( $x_c$ ), the  $A$  coefficient of the quadratic temperature dependence of resistivity exhibits a dramatic enhancement as  $P$  ( $x$ ) approaches  $P_c$  ( $x_c$ ), around which  $r(T)$  has a non-Fermi-liquid form. Accordingly, the electronic specific-heat coefficient of  $\text{CrAs}_{1-x}\text{P}_x$  peaks out around  $x_c$ . These properties provide clear evidences for quantum criticality, which we interpret as originating from a nearly second-order helimagnetic quantum phase transition that is concomitant with a first-order structural transition.

We propose that these results can be understood in terms of a proximity to a magnetic quantum critical point tuned by the degree of the incipient localization of the Cr-3d states, possibly via an orbital-selective Mottness mechanism. Our findings in CrAs highlight the distinct characteristics of quantum criticality in bad metals, thereby bringing out new insights into the physics of unconventional SC such as occurring in the high- $T_c$  iron pnictides.

#### References

- [1] W. Wu, J.-G. Cheng, K. Matsubayashi, P. P. Kong, F. K. Lin, C. Q. Jin, N. L. Wang, Y. Uwatoko, and J. L. Luo, *Nature Communications* **5**, 5508 (2014).  
 [2] M. Matsuda, F. K. Lin, R. Yu, J.-G. Cheng, W. Wu, J. P. Sun, J. H. Zhang, P. J. Sun, K. Matsubayashi, T. Miyake, T. Kato, J.-Q. Yan, M. B. Stone, Qimiao Si, J. L. Luo, and Y. Uwatoko, *Phys. Rev. X* **8**, 031017 (2018).

#### Authors

M. Matsuda<sup>a</sup>, F. K. Lin<sup>b</sup>, R. Yu<sup>c</sup>, J.-G. Cheng<sup>b</sup>, W. Wu<sup>b</sup>, J. P. Sun<sup>b</sup>, J. H. Zhang<sup>b</sup>, P. J. Sun<sup>b</sup>, K. Matsubayashi, T. Miyake<sup>d</sup>, T. Kato, J.-Q. Yan<sup>a</sup>, M. B. Stone<sup>a</sup>, Qimiao Si<sup>c</sup>, J. L. Luo<sup>b</sup>, and Y. Uwatoko

<sup>a</sup>Oak Ridge National Laboratory

<sup>b</sup>Institute of Physics, Chinese Academy of Sciences

<sup>c</sup>Renmin University

<sup>d</sup>Nanosystem Research Institute, AIST

<sup>e</sup>Rice University

## High- $T_c$ Superconductivity up to 55 K under High Pressure in a Heavily Electron-Doped $\text{Li}_{0.36}(\text{NH}_3)_y\text{Fe}_2\text{Se}_2$ Single Crystal

Uwatoko Group

To find out the approaches to raise the critical temperature  $T_c$  of unconventional superconductors is one of the most enduring problems in contemporary condensed matter physics. The principal route to raise the  $T_c$  of FeSe is to dope electron, which has been successfully achieved via the interlayer intercalations [ $A_x\text{Fe}_{2-y}\text{Se}_2$  ( $A = \text{K}, \text{Rb}$ ),  $A_x(\text{NH}_3)_y\text{Fe}_2\text{Se}_2$ , and  $(\text{Li},\text{Fe})\text{OHFeSe}$ ], interface charge

transfer, surface K dosing, and gate-voltage regulation. Further enhancement of  $T_c$  via adding more electrons seems to be plagued by the observed insulating state in the over doped regime. Given the limitations of electron doping, it is imperative to explore other routes to enhance  $T_c$  of these heavily electron doped (HED) FeSe materials further. In contrast to electron-doping approaches, the application of high pressure can provide an alternative means.

In this work [1], we had performed high-pressure measurement on  $\text{Li}_{0.36}(\text{NH}_3)_y\text{Fe}_2\text{Se}_2$  single crystal, which can reach an optimal  $T_c^{\text{onset}} \approx 44.3$  K at ambient pressure. From high-pressure resistivity and AC-susceptibility measurement, we can conclude that superconducting transition temperature  $T_c \approx 44$  K at ambient pressure is first suppressed to below 20 K upon increasing pressure to  $P_c \approx 2$  GPa above which the pressure dependence of  $T_c(P)$  reverses and  $T_c$  increases steadily to 55 K at 11 GPa. These results thus evidence a pressure-induced second high- $T_c$  superconducting (SC-II) phase in  $\text{Li}_{0.36}(\text{NH}_3)_y\text{Fe}_2\text{Se}_2$  with the highest  $T_c^{\text{max}} \approx 55$  K among the FeSe-based bulk materials. Also it is evident that the SC-II phase is bulk in nature for 6 GPa, whereas the sample contains two superconducting phases with different  $T_c$  above 6 GPa: The high- $T_c$  (50K) phase has a small but nearly constant volume fraction  $\sim 30\%$  to 11 GPa, whereas the low- $T_c$  (33K) phase shrinks and vanishes completely  $T_c$  above 11 GPa.

Figure 1 summarizes the pressure dependences of  $T_c^{\text{onset}}$ ,  $T_c^{\text{zero}}$ , and  $T_c^{\chi}$  for  $\text{Li}_{0.36}(\text{NH}_3)_y\text{Fe}_2\text{Se}_2$  together with the  $T_c^{\text{zero}}$  of FeSe for comparison. The temperature-pressure phase diagram depicts explicitly the evolution of the superconducting phase of  $\text{Li}_{0.36}(\text{NH}_3)_y\text{Fe}_2\text{Se}_2$  under pressure. The high- $T_c$  SC-1 phase, initially achieved at ambient pressure via doping electron through inserting lithium  $\text{Li}^+$  and ammonia in between the FeSe layers, is quickly suppressed by pressure, and the superconducting phase emerges above  $P_c \approx 2$  GPa and exists in a broad pressure range.

To further characterize the SC-II phase, we tentatively probe the information about Fermi surface under pressure by measuring the Hall effect in the normal state just above  $T_c$ . Hall data confirms that in the emergent SC-II phase the dominant electron-type carrier density undergoes a fourfold enhancement and tracks the same trend as  $T_c(P)$ . Interestingly, we find a nearly parallel scaling behavior between  $T_c$  and the inverse Hall coefficient for the SC-II phases of

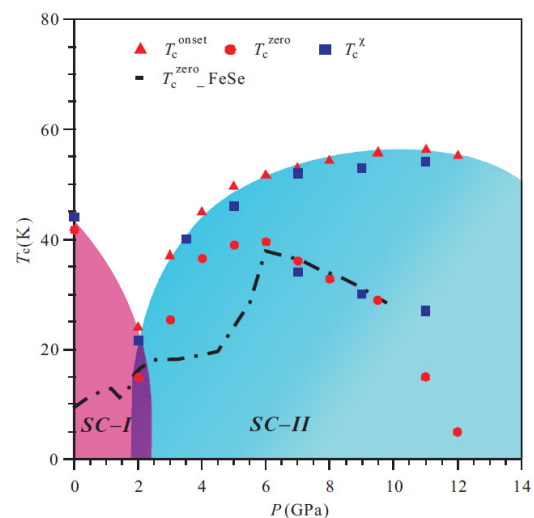


Fig. 1. The  $T$ - $P$  phase diagram of the  $\text{Li}_{0.36}(\text{NH}_3)_y\text{Fe}_2\text{Se}_2$  single crystal. The pressure dependence of the superconducting transition temperatures  $T_c$  up to 12 GPa.

$\text{Li}_{0.36}(\text{NH}_3)_y\text{Fe}_2\text{Se}_2$ .

Our present study thus demonstrates a way for high pressure to raise  $T_c$  of these HED FeSe-based materials by increasing the effective charge-carrier concentration via a possible Fermi-surface reconstruction at  $P_c$ .

#### Reference

[1] P. Shahi, J.P. Sun, S.H. Wang, Y.Y. Jiao, K.Y. Chen, S.S. Sun, H.C. Lei, Y. Uwatoko, B.S. Wang, and J-G Cheng, Phys. Rev. B, **97**, 020508 (2018).

#### Authors

P. Shahi<sup>a,b</sup>, J.P. Sun<sup>a,b</sup>, S.H. Wang<sup>c</sup>, Y.Y. Jiao<sup>a,b</sup>, K.Y. Chen<sup>a,b</sup>, S.S. Sun<sup>c</sup>, H.C. Lei<sup>c</sup>, Y. Uwatoko, B.S. Wang<sup>a,b</sup>, and J-G Cheng<sup>a,b</sup>  
<sup>a</sup>Beijing National Laboratory for Condensed Matter Physics and Institute of Physics, Chinese Academy of Sciences  
<sup>b</sup>University of Chinese Academy of Sciences  
<sup>c</sup>Beijing Key Laboratory of Opto-electronic Functional Materials & Micro-nano Devices, Renmin University of China

## Thermodynamic and Structural Studies on Super High Entropy Liquids, Alkylated Tetra-phenyl Porphyrins

### Yamamuro Group

The fusion (melting) temperature  $T_{\text{fus}}$  of molecules usually depend on molecular mass  $M$ ; the larger  $M$  is, the higher  $T_{\text{fus}}$  becomes. For example,  $T_{\text{fus}}$  of benzene ( $\text{C}_6\text{H}_6$ ,  $M = 78$ ) is 279 K while that of biphenyl ( $\text{C}_6\text{H}_5\text{-C}_6\text{H}_5$ ,  $M = 154$ ) is 342 K. This is because the intermolecular van der Waals interaction is larger in the crystalline phase with better molecular packing than that in the liquid phase with worse packing.

Recently, Nakanishi group in NIMS found a series of large molecules which exist in liquid states at room temperature. These molecules have  $\pi$ -conjugated cores such as pyrene, naphthalene, anthracene, fullerene, phthalocyanine and long alkylchains bonded to the cores [1]. We consider that these alkylated molecules are stabilized by the large entropy effect which is caused by the conformational disorder of alkylchains. This situation is similar to that of ionic liquids which are in liquid states in spite of their strong inter-ionic interactions. We collectively call this type of liquids “super-high entropy liquids (SHEL)”. The physico-

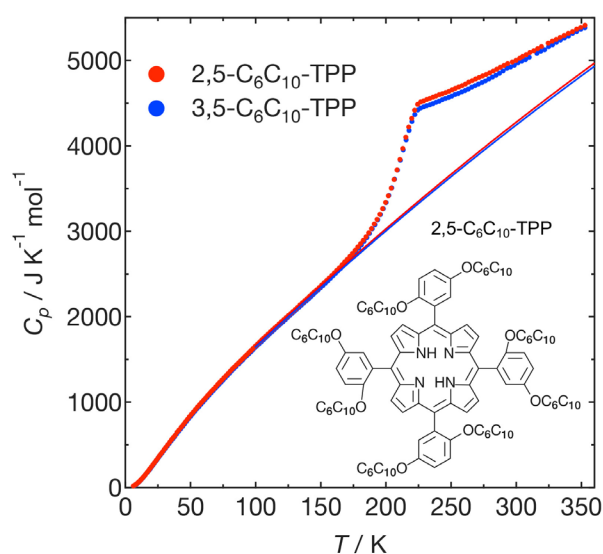


Fig. 1. Heat capacities of 2,5- $\text{C}_6\text{C}_{10}$ -TPP and 3,5- $\text{C}_6\text{C}_{10}$ -TPP. The inset shows the molecular structure of 2,5- $\text{C}_6\text{C}_{10}$ -TPP.

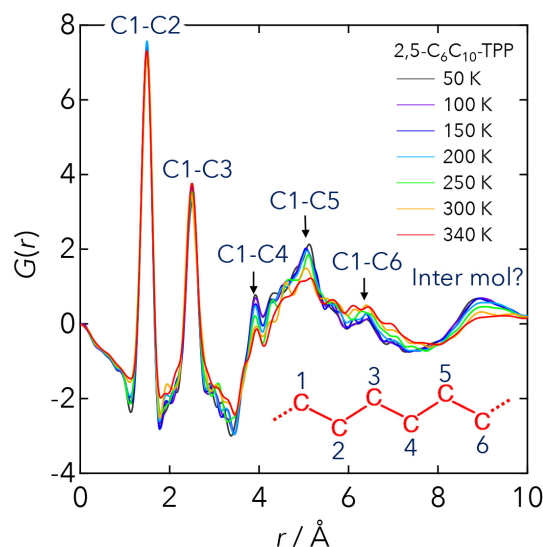


Fig. 2. Temperature dependence of the reduced pair distribution functions of 2,5- $\text{C}_6\text{C}_{10}$ -TPP calculated from the X-ray diffraction data. The distances corresponding to the intra and intermolecular correlations are given in the figure.

chemical properties of SHEL have not been studied well. As the first target we have taken 2,5- $\text{C}_6\text{C}_{10}$ -tetraphenylporphyrin (2,5- $\text{C}_6\text{C}_{10}$ -TPP) and 3,5- $\text{C}_6\text{C}_{10}$ -tetraphenylporphyrin (3,5- $\text{C}_6\text{C}_{10}$ -TPP). The molecular structure of 2,5- $\text{C}_6\text{C}_{10}$ -TPP is shown by the inset of Fig. 1; two  $-\text{OC}_6\text{C}_{10}$  groups are bonded symmetrically to a benzene ring in 3,5- $\text{C}_6\text{C}_{10}$ -TPP. It is quite interesting that  $T_{\text{fus}}$  of the alkylated molecules (2,5- $\text{C}_6\text{C}_{10}$ -TPP,  $M = 2538$ ) is lower than  $T_{\text{fus}}$  of non-alkylated molecules (TPP,  $M = 615$ ,  $T_{\text{fus}} = 723$  K).

We have measured the heat capacities of 2,5- $\text{C}_6\text{C}_{10}$ -TPP and 3,5- $\text{C}_6\text{C}_{10}$ -TPP by use of an adiabatic calorimeter in our lab. The  $C_p$  plot shown in Fig. 1 revealed that both molecules have a broad glass transition at around  $T_g = 210$  K and the  $C_p$  of 2,5- $\text{C}_6\text{C}_{10}$ -TPP is 2-3 % larger than that of 3,5- $\text{C}_6\text{C}_{10}$ -TPP at above  $T_g$ . The configurational entropies calculated from the  $C_p$  data are more than  $1000 \text{ J K}^{-1} \text{ mol}^{-1}$  at high temperature limit, which is more than 10 times larger than those of usual molecular liquids. We have also measured the X-ray diffraction of 2,5- $\text{C}_6\text{C}_{10}$ -TPP and 3,5- $\text{C}_6\text{C}_{10}$ -TPP using a diffractometer at BL04B2, SPring-8. Figure 2 shows the reduced pair-correlation function  $G(r)$  calculated from the diffraction data; a similar result is obtained in 3,5- $\text{C}_6\text{C}_{10}$ -TPP. Most of the  $G(r)$  peaks are attributed to the C-C correlations in alkylchains. The broad peak at 9 Å, maybe also at 4.5 Å, is considered to be the correlation between porphyrin rings. The present data suggest that the configurations of alkylchains and porphyrin rings of 2,5- $\text{C}_6\text{C}_{10}$ -TPP and 3,5- $\text{C}_6\text{C}_{10}$ -TPP are highly disordered at higher temperatures and becomes ordered at lower temperatures. Now we are measuring the quasielastic neutron scattering of both samples to investigate the dynamics of both alkylchains and porphyrin cores.

#### References

[1] A. Ghosh and T. Nakanishi, Chem. Commun. **53**, 10344 (2017).  
 [2] A. Ghosh, M. Yoshida, K. Suemori, H. Isago, N. Kobayashi, Y. Mizutani, Y. Kurashige, I. Kawamura, M. Nirei, O. Yamamuro, T. Takaya, K. Iwata, A. Saeki, K. Nagura, S. Ishihara, and T. Nakanishi, Nature Chem., submitted.

#### Authors

M. Nirei, H. Akiba, A. Ghosh<sup>a</sup>, T. Nakanishi<sup>a</sup>, K. Ohara<sup>b</sup>, S. Kohara<sup>a</sup>, and O. Yamamuro  
<sup>a</sup>NIMS  
<sup>b</sup>JASRI

# Magnetic States of Coupled Spin Tubes with Frustrated Geometry in CsCrF<sub>4</sub>

Masuda Group

When a theoretical model is realized in nature, small perturbation terms play important roles in the selection of the ground state in geometrically frustrated magnets. In case of a triangular spin tube, the two-dimensional network of the inter-tube interaction forms characteristic lattices. Among them Kagome-Triangular (KT) lattice in Fig. 1(a) is known to exhibit an enriched phase diagram [1] including various types of non-trivial structures: non-coplanar cuboc structure, coplanar 120° structure with the two-dimensional propagation vector of  $\mathbf{k}_{2D} = 0, \sqrt{3} \times \sqrt{3}$  structure with  $\mathbf{k}_{2D} = (1/3, 1/3)$ , and incommensurate structure as shown in Fig. 1(b). We investigate the magnetic state in the model material CsCrF<sub>4</sub> in Fig. 1(c) and 1(d) by using neutron diffraction technique. Temperature evolution of the diffraction profile was collected as shown in Fig. 2(a). Combination of representation analysis and Rietveld refinement reveals that a very rare structure, i.e., a quasi-120° structure with  $\mathbf{k}_{2D} = (1/2, 0)$  in Fig. 2(b), is realized at the base temperature. The classical calculation of the phase diagram elucidates that CsCrF<sub>4</sub> is the first experimental realization of the KT lattice having ferromagnetic Kagome bond. A single-ion anisotropy and Dzyaloshinskii-Moriya interaction play key roles in the selection of the ground state. Furthermore, a successive phase transition having an intermediate state represented by  $\mathbf{k}_{2D} = (1/3, 1/3)$  is observed. The intermediate state is a partially ordered 120° structure in Fig. 2(c) [2].

This study was originally initiated for the neutron study of the Tomonaga-Luttinger liquid predicted in a spin tube using JRR-3 research reactor before east Japan earthquake in 2010. Since the magnetic state is sensitive to impurity in the titled compound, we need to check the reproducibility of the data carefully. As a result, the quality of some samples used

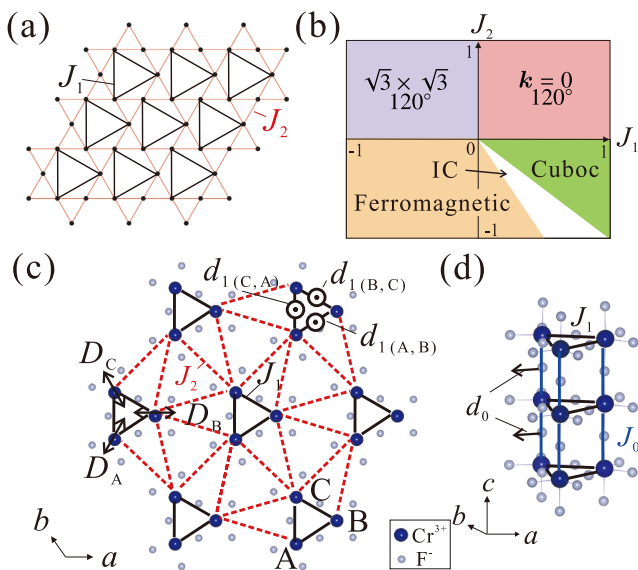


Fig. 1. Coupled spin tubes with frustrated geometry. (a) Kagome-Triangular (KT) lattice.  $J_1$  is the Triangular bond and  $J_2$  is the Kagome bond. (b) Phase diagram of the KT lattice. (c), (d) The crystal structure of CsCrF<sub>4</sub>. Blue and small gray circles represent Cr<sup>3+</sup> and F<sup>-</sup> ions, respectively.  $J_1$  is the Triangular bond and  $J_2$  is the Kagome bond. The  $\mathbf{d}_{1(\alpha\beta)}$  is DM vector ( $\alpha, \beta = A, B, C$ ).  $z^A, z^B,$  and  $z^C$  are the  $z$ -axes locally defined on the Cr sites, A, B, and C. Spin tube runs along the  $c$  axis in (d), and the tubes form the KT lattice in the  $a-b$  plane in (c).

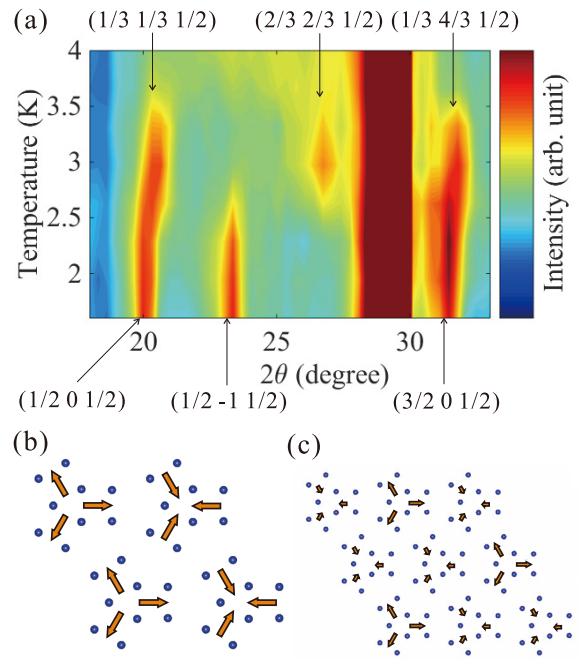


Fig. 2. Magnetic neutron diffraction profile and magnetic structures. (a) The temperature variation of diffraction profiles in the range of  $2\theta = 18^\circ$ - $33^\circ$ . (b), (c) Candidates of the magnetic structures of CsCrF<sub>4</sub> for the ground state (b) and the intermediated state (c).

at JRR-3 were not good, and we needed to redo the experiment on selected high-quality sample using foreign neutron facilities after 2010. All of the published data in Ref. [2] were, thus, collected at ECHIDNA spectrometer in ANSTO Australia. Furthermore, the difficulty of the transportation of radioactive material such as Cs after the earthquake made the situation complicated. Thanks to many people including scientists, technicians, and office staff, we completed the project.

## References

- [1] H. Ishikawa *et al.*, J. Phys. Soc. Jpn **83**, 043703 (2014).
- [2] M. Hagihala *et al.*, npj Quantum Materials **4**, 14 (2019).

## Authors

M. Hagihala, S. Hayashida, M. Avdeev<sup>a</sup>, H. Manaka<sup>b</sup>, H. Kikuchi and T. Masuda,  
<sup>a</sup>Australian Nuclear Science and Technology Organization  
<sup>b</sup>Kagoshima University

# Magnetic State Selected by Magnetic Dipole Interaction in Kagome Antiferromagnet NaBa<sub>2</sub>Mn<sub>3</sub>F<sub>11</sub>

Masuda and Hiroi Groups

Long-range magnetic dipole-dipole (MDD) interaction is ubiquitous in nature. In most bulk magnets, the MDD interaction is not necessarily a primary interaction because its energy scale is much smaller than an exchange interaction. The MDD interaction, however, plays a key role in geometrically frustrated magnets, where the geometry causes macroscopic degeneracy of the magnetic state. For instance, the origin of an exotic monopole state in pyrochlore oxides is explained by the MDD interaction [1]. The frustrated geometry and the MDD interaction are, thus, a good combination for search of a new magnetic state.

In a classical Heisenberg kagome antiferromagnet, the ground state is known to be 120° structure with an infinite

# Indoor World Record of 1200 T Achieved by the Newly Installed Electromagnetic Flux Compression Megagauss Generator

Takeyama and Y. H. Matsuda Groups

The megagauss laboratory, ISSP, UTokyo, has a long history of generations of megagauss fields, using electromagnetic flux compression (EMFC) since the original work in the late 1970s led by the Chikazumi and Miura group. The 1000 T project was revisited in 2010 and 2011, supported by the funding of the MEXT for the promotion of the basic science, and since then, we have devoted ourselves to the installation of the megagauss generation system and the technical improvements. Condenser bank units with 20 kV, 2 MJ for the seed feed coils, and two sets of the main condenser bank units, 5 MJ and 2 MJ each with 50 kV charging capability have been incorporated. The system consisting of these condenser modules has been installed, and tuning for operation was recently completed in 2019. The giant collector plates and the load coil clamping units have been placed in antiexplosion chambers. Designs of the instruments were optimized for substantial improvement in the electromagnetic field energy conversion efficiency. Using the newly installed system, we have successfully generated ultra-high magnetic fields reaching 1200 T.

The magnet coil used in the EMFC method is comprised of a single-turn steel outer (primary) coil lined with a copper plate inside (the copper-lined (CL) coil; see Fig. 1) and the so-called liner (a thin metal cylinder, made of copper) which is coaxially set inside the primary coil. A pair of seed field coils set on either side of the primary coil [1]–[3] provides the initial magnetic flux. The liner compresses the magnetic flux and generates megagauss magnetic fields. The EMFC utilizes the electric energy source stored in the condenser bank modules. A record-breaking indoor generation of magnetic field was achieved by discharging 45 kV, 3.2 MJ energy out of 5 MJ condenser units. The liner (typical size is 119 mm diameter, 1.5 mm thickness, approximately

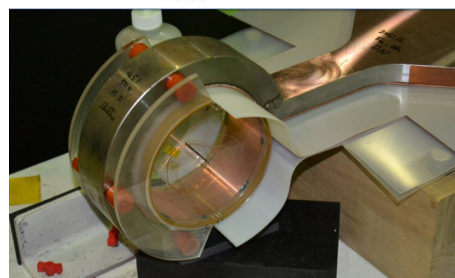
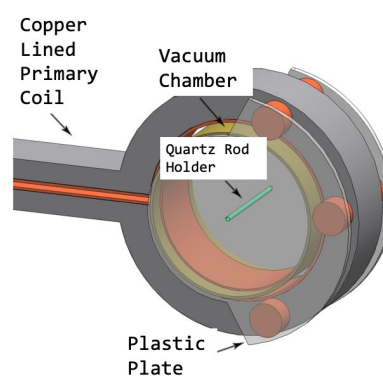


Fig. 1. Overall view of the CL coil and the measurement probe setting. The liner vacuum chamber (made of the Bakelite cylinder and the acrylic resin plastic plates) with the measurement probe is firmly furnished to the CL primary coil with high precision.

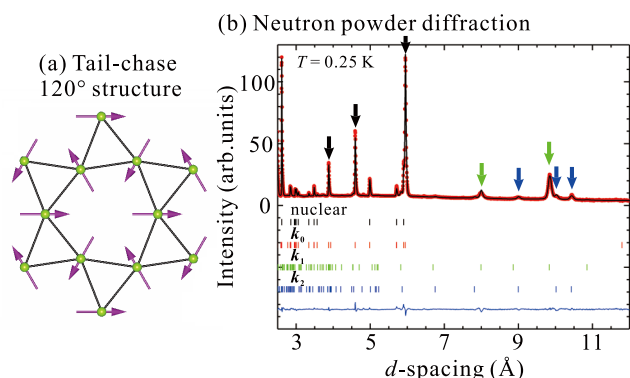


Fig. 1. (a) The tail-chase  $120^\circ$  structure on the kagome lattice. (b) Neutron diffraction profile for  $\text{NaBa}_2\text{Mn}_3\text{F}_{11}$  measured at 0.25 K. The solid square and curves show experimental data and simulation, respectively. Arrows indicate magnetic Bragg peaks.

degeneracy. A small perturbation lifts the degeneracy and selects a unique structure, e.g., an all-in all-out structure in case of Dzyaloshinskii-Moriya interaction [2]. The MDD is theoretically predicted to select a *tail-chase* structure (Fig. 1(a)) [3]. Such a structure, however, has not been experimentally identified yet to date.  $\text{NaBa}_2\text{Mn}_3\text{F}_{11}$  having a unique kagome-triangular lattice was synthesized by Hiroi group in ISSP [4]. It exhibits an antiferromagnetic transition at  $T_N = 2$  K. The estimated Curie-Weiss temperature of  $-32$  K is smaller than those of many kagome magnets, indicating that the exchange spin interaction is small. The MDD interaction may be important for the determination of the magnetic state.

Recently we carried out neutron powder diffraction experiment to identify the magnetic structure of  $\text{NaBa}_2\text{Mn}_3\text{F}_{11}$  [5]. We observed magnetic Bragg peaks at 0.25 K as shown in Fig. 1(b). They were indexed by a commensurate magnetic propagation vector  $\mathbf{k}_0 = (0,0,0)$ , and two incommensurate vectors  $\mathbf{k}_1 = (0.3209, 0.3209, 0)$  and  $\mathbf{k}_2 = (0.3338, 0.3338, 0)$ . The magnetic structure analysis by combination of Rietveld refinement and the representation analysis reveals that the tail-chase  $120^\circ$  structure modulated by the incommensurate vectors gives a satisfactory agreement with the experiment. Furthermore, we calculated the phase diagram with the parameters of the nearest- and second-neighbor exchange interaction, and MDD interaction. We identified that the MDD interaction solves the infinite degeneracy and selects the tail-chase  $120^\circ$  structure in  $\text{NaBa}_2\text{Mn}_3\text{F}_{11}$ . For the future perspective, the study of magnetic dynamics is beneficial for the search for exotic states such as zero-energy mode induced by the MDD interaction.

## References

- [1] J. S. Gardner, M. J. P. Gingras, and J. E. Greedan, *Rev. Mod. Phys.* **82**, 53 (2010).
- [2] M. Elhajal, B. Canals, and C. Lacroix, *Phys. Rev. B* **66**, 014422 (2002).
- [3] M. Maksymenko, V. R. Chandra, and R. Moessner, *Phys. Rev. B* **91**, 184407 (2015).
- [4] H. Ishikawa, T. Okubo, Y. Okamoto, and Z. Hiroi, *J. Phys. Soc. Jpn.* **83**, 043703 (2014).
- [5] S. Hayashida, H. Ishikawa, Y. Okamoto, T. Okubo, Z. Hiroi, M. Avdeev, P. Manuel, M. Hagihala, M. Soda, and T. Masuda, *Phys. Rev. B* **97**, 054411 (2018).

## Authors

S. Hayashida, H. Ishikawa, Y. Okamoto<sup>a</sup>, T. Okubo<sup>b</sup>, Z. Hiroi, M. Avdeev<sup>c</sup>, P. Manuel<sup>d</sup>, M. Hagihala, M. Soda, and T. Masuda

<sup>a</sup>Nagoya University

<sup>b</sup>Department of Physics, The University of Tokyo

<sup>c</sup>Australian Nuclear Science and Technology Organization

<sup>d</sup>ISIS Pulsed Neutron and Muon Source, Rutherford Appleton Laboratory

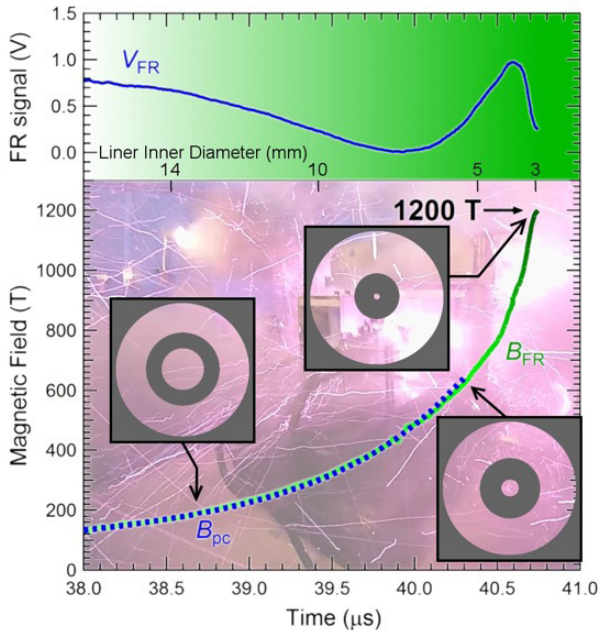


Fig. 2. Magnetic field intensity recorded up to 1200 T with an evolution of time. Upper panel: Faraday rotation signal ( $V_{FR}$ ) synchronized with the magnetic field intensity. The dotted line taken from the pickup coil ( $B_{PC}$ ), measured up to 600 T, and the green solid line measures the fields up to 1200 T by FR ( $B_{FR}$ ). The liner imploding images are shown by black circles. The estimated liner inner diameter at each magnetic field intensity is given in axis of abscissa.

50-mm length) undergoes high-speed implosion (above 5 km/s) accelerated by the magnetic force induced by a huge electric current injected to the primary coil (3–4 mega-Ampere) about its circumference, and the magnetic flux (3.2 T) initially generated in a large volume (diameter 120 mm, length 50 mm) is compressed finally into a small space (3 mm diameter, 20–30 mm length), and reaches a megagauss magnetic field of up to 1200 T. The CL coil was designed to improve the energy transfer efficiency of the imploding liner. The copper lining part bears the current, whereas the massive outer steel coil holds the inertia for the imploding liner. The measurement probes are attached to the steel outer coil as shown in Fig. 1. Thus, measurement probes are set precisely at the liner implosion center with respect to the CL coil.

The signals obtained in this work are plotted in Fig. 2. Details are provided in our recent paper [4]. The dotted line is a signal taken from the pickup coil and traced up to 600 T, which is the limit of recording because of the high-voltage induced by the rapid increase of the field. The Faraday rotation signal was intact until the very end of the liner implosion. The green solid line represents the field record after the Faraday rotation signal is converted into the magnetic field intensity. A slow-down effect was observed followed by the peak field prior to the liner “turn-around” phenomenon. Circles depicted in the graph shows images of the liner cross-section during implosion. The liner inner diameter, which corresponds to the bore of the coil, is shown as a guide in the axis of abscissa in the middle of the figure. Final diameter of the liner at 1200 T is estimated to be 3 mm. The maximum speed of the liner during the implosion is estimated to be higher than 5 km/sec, which is consistent with the “Hugoniot curve” [5], in which a field of 1200 T hits at 5.3 km/sec.

#### References

[1] N. Miura and F. Herlach, Springer Topics in Applied Physics **57**, 247 (Springer, Berlin, 1985).

- [2] F. Herlach, Rep. Prog. Phys. **62**, 859 (1999).  
 [3] N. Miura and F. Herlach, High Magnetic Fields-Science and Technology **1**, 235 (World Scientific, 2002).  
 [4] D. Nakamura, A. Ikeda, H. Sawabe, Y. H. Matsuda and S. Takeyama, Rev. Sci. Instrum. **89**, 095106 (2018).  
 [5] F. Herlach, Rep. Prog. Phys. **62**, 859 (1999).

#### Authors

S. Takeyama, D. Nakamura, H. Sawabe, Y. H. Matsuda, and A. Ikeda.

## Determination of “Diracness” in PbTe Tokunaga Group

One of the hottest research subjects in condensed matter physics is so-called topological materials, in which dynamics of charge carriers are expressed by the relativistic equations of motion that are utilized in research field of high energy physics. Since the relativistic Dirac/Weyl equations show characteristic linear dispersion relation, a great number of experimental and theoretical studies have been devoted to explore the linear dispersion as schematically shown in Fig. 1(a), which is distinguished from the parabolic one shown in Fig. 1(b). This parabolic dispersion, however, is merely the expanded view of the trace in Fig. 1(a) at around the origin. Therefore, argument based only on the appearance of the dispersion is sensuous and insufficient to quantitatively distinguish the Dirac/Weyl system from the others. As the

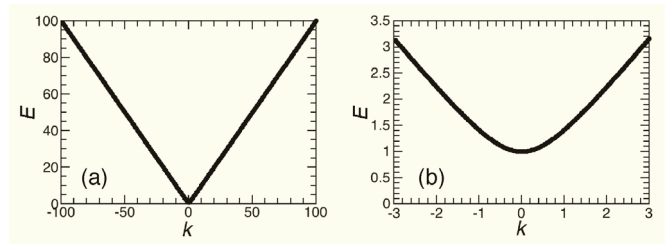


Fig. 1. (a) Schematic dispersion relation of kinetic motion of particles that is expressed by relativistic Dirac equation, which shows characteristic linear dispersion in wide range of the  $k$ -space. (b) Expanded view of the same dispersion relation with that in (a), which appears as parabolic in this region.

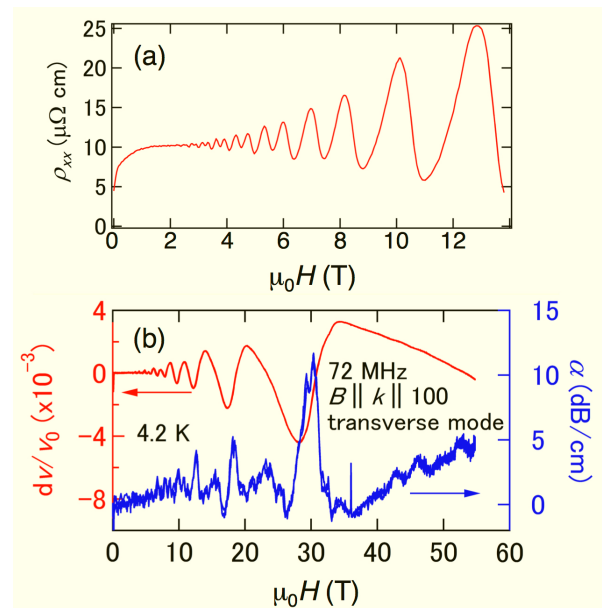


Fig. 2. (a) Transverse magnetoresistance and (b) ultrasound attenuation in single crystals of PbTe. Quantum oscillations are clearly resolved in both experiments.

quantitative indicator that characterizes similarity of a system with the ideal Dirac system, which is called as ‘‘Diracness’’ in the following, we focus on the ratio between Zeeman and cyclotron energies (ZC ratio). Recent theoretical studies revealed that this ZC ratio becomes unity for the ideal Dirac system [1,2]. Relative magnitude of the ZC ratio and unity is predicted to invert when topology of a material changes from trivial to non-trivial.

To experimentally determine the ZC ratio, we studied quantum oscillations in single crystals of PbTe through measurements of magnetoresistance (Fig. 2(a)), magnetization, and ultrasound attenuations (Fig. 2(b)) in DC and pulsed high magnetic fields [3]. By measuring quantum oscillations up to the quantum limit state and comparing the results with the standard Lifshitz-Kosevich formula [4], we determined the ZC ratio of PbTe as 0.52. In this analysis, we clarified that when the ZC ratio becomes larger than one half, peak-dip relation in the quantum oscillation will be reversed, which will appear as the phase shift in the Landau level fan diagram. The results demonstrate that observation of spin-split quantum oscillations is crucially important to discuss the origin of the phase shift.

## References

- [1] Y. Fuseya *et al.*, Phys. Rev. Lett. **115**, 216401 (2015).
- [2] H. Hayasaka and Y. Fuseya, J. Phys.: Condens. Matter **28**, 31LT01 (2016).
- [3] K. Akiba *et al.*, Phys. Rev. B **98**, 115144 (2018).
- [4] D. Shoenberg, *Magnetic Oscillations in Metals* (Cambridge University Press, 1984).

## Authors

K. Akiba, A. Miyake, H. Sakai<sup>a,b</sup>, K. Katayama<sup>a</sup>, H. Murakawa<sup>a</sup>, N. Hanasaki<sup>a</sup>, S. Takaoka<sup>a</sup>, Y. Nakanishi<sup>c</sup>, M. Yoshizawa<sup>c</sup>, and M. Tokunaga

<sup>a</sup>Osaka University

<sup>b</sup>JST-PRESTO

<sup>c</sup>Iwate University

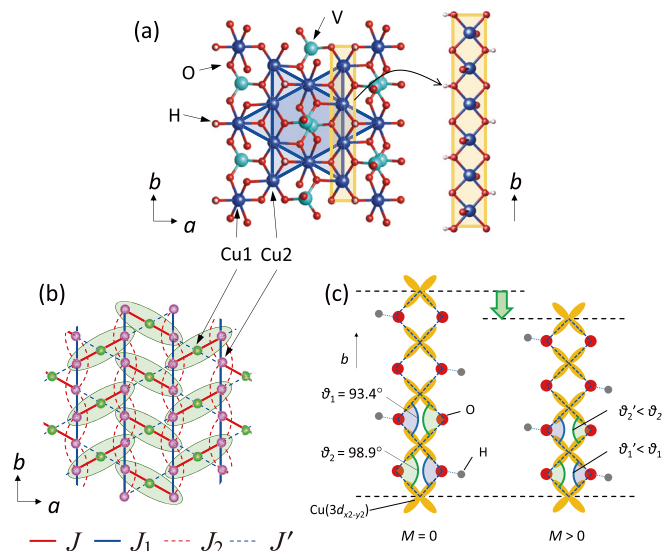


Fig. 1. (a) The lattice model of volborthite (b) Coupled trimer model for volborthite (c) A schematic drawing of the pantograph-like lattice modification of the magnetostriction in the crystallographic  $b$  axis.

Owing to the lattice deformation, the anisotropic microscopic spin model based on coupled trimers as shown in Fig. 1(b) has recently been proposed, that now attracts attention as it provides a mechanism for a field-induced spin nematic phase adjacent to the  $1/3$  magnetization plateau. In the spin nematic phase, spin directors that break the in-plane rotational symmetry are formed as a result of the Bose-Einstein condensation of bimagnon excitations. The rotational symmetry breakings take place in the lateral direction of the spin space, which thus implies that the measurement of the lateral spin-correlation in this magnet is quite important.

Figures. 2(a)-(c) shows the result of the magnetostriction

## Short-Range Spin Correlations in a Quantum Magnet Detected Through Magnetoelastic Couplings in a Kagome Quantum Spin Lattice

Y. H. Matsuda, Takeyama, and Hiroi Groups

In case of quantum magnets, magnetostriction can be a unique measure of short-range spin correlations. The spin components perpendicular to the external magnetic field is inherent in the local spin correlation. In quantum magnets, magnetostriction measurement is a direct measure of the local spin correlation.

We have recently developed a high-speed 100 MHz magnetostriction measurement system utilizing the fiber Bragg grating techniques [1] for the use in the  $\mu$ -seconds pulsed magnetic fields beyond 100 T (megagauss region) and 1000 T (kilo-Tesla region) [2]. We found later that the system can also be used in the milli-seconds pulsed magnetic fields below 100 T with an appreciable high-resolution of  $\Delta L/L \sim 10^{-6}$  [3]. Using the developed instrument, we have conducted the magnetostriction measurement for the two-dimensional quantum magnet of volborthite [4].

Volborthite ( $\text{Cu}_3\text{V}_2\text{O}_7(\text{OH})_2 \cdot 2\text{H}_2\text{O}$ ) is a fascinating example of a highly frustrated quantum magnet. In its magnetic layer, Cu ions possessing spin-1/2 moments form a deformed kagome lattice as schematically shown in Fig. 1(a).

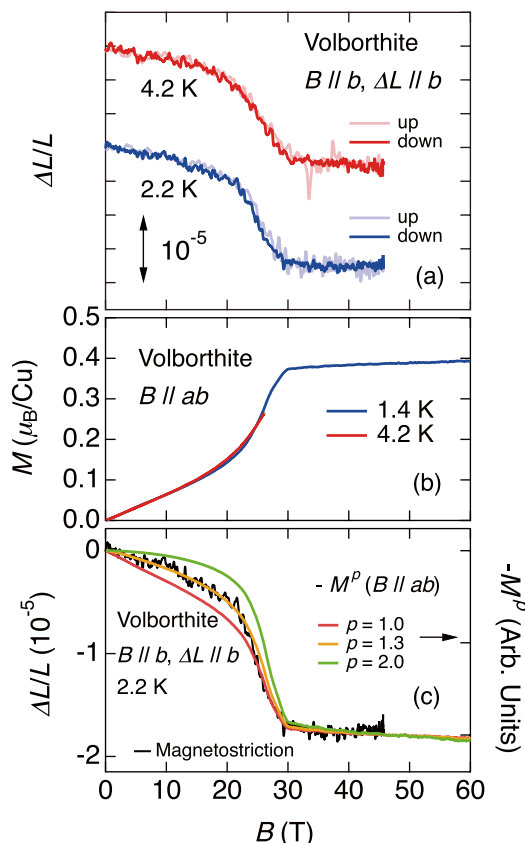


Fig. 2. (a) Magnetostriction curves of volborthite (b) Magnetization curves of volborthite (c) A comparison of the curves of magnetostriction and magnetization indicating a peculiar dependence of  $\Delta L \sim M^{1.3}$ .

measurement. A negative magnetostriction and a peculiar dependence of the magnetostriction on the magnetization as  $\Delta L \sim M^{1.3}$  are observed. The negative magnetostriction in the crystallographic  $b$  axis is understandable with a pantograph-like lattice modification. As shown in Fig. 1(c), the Cu-O-Cu chain in the  $b$  axis is responsible for the ferromagnetic superexchange interaction in the coupled trimer model. The closer the bond angles to 90 degree, the stronger the ferromagnetic exchange couplings due to the Kanamori-Goodenough rule, where, as a result, the bond length in the  $b$  axis is elongated. The story is supported by a tentative DFT+ $U$  calculations [4]. On the other hand, the peculiar dependence of the magnetostriction on the magnetization can also qualitatively understood as a manifestation of the short-range spin correlation within the exchange striction model. In the exact-diagonalization approach, it becomes clear that the spin-correlation is indeed in between the  $M^{1.0}$  and  $M^{2.0}$  and close to  $M^{1.3}$ . For further studies in the future, the spin-nematicity may show abnormal magnetoelastic response at even lower magnetic fields at around 28 T. Another possible study is the measurement beyond 100 T. The end of the 1/3 magnetization plateau may be detected in the magnetostriction measurement.

#### References

- [1] A. Ikeda, T. Nomura, Y. H. Matsuda, S. Tani, Y. Kobayashi, H. Watanabe and K. Sato, Rev. Sci. Instrum. **88**, 083906 (2017).
- [2] D. Nakamura, A. Ikeda, H. Sawabe, Y. H. Matsuda, and S. Takeyama, Rev. Sci. Instrum. **89**, 095106 (2018)
- [3] A. Ikeda, Y. H. Matsuda, and H. Tsuda, Rev. Sci. Instrum. **89**, 096103 (2018).
- [4] A. Ikeda, S. Furukawa, O. Janson, Y. H. Matsuda, S. Takeyama, T. Yajima, Z. Hiroi, and H. Ishikawa, Phys. Rev. B **99**, 140412(R) (2019).

#### Authors

A. Ikeda and Y. H. Matsuda

## Semi-Metallicity of Free-Standing Hydrogenated Monolayer Boron from MgB<sub>2</sub>

### I. Matsuda Group

Two-dimensional monatomic layers in van der Waals crystals or on solid surfaces have wide attention because of their unique physical properties and potential applications in quantum devices. There has been growing interests in layers of Xenes. Recently, borophene layers were discovered and found to have Dirac fermions. However, in contrast to graphene, these Xene layers form only on solid surfaces. It is, thus, necessary to develop technique to passivate it chemically so it can be placed on any substrate under ambient conditions.

In the present research, we synthesized a free-standing hydrogenated monolayer boron (HB) sheet and studied the electronic states via soft X-ray spectroscopy at the B K-shell absorption edge and the first-principles calculations [1]. As shown in Fig.1, the HB sheet is semi-metallic with electron and hole pockets at symmetry points of  $\Gamma$  and Y, respectively. The electron band results from the B-H-B bonds formed during synthesis from a MgB<sub>2</sub> crystal, while the hole band is kept through the process and originates from a honeycomb lattice boron layer or borophene in MgB<sub>2</sub>. Figure 2 shows a summary of the calculation for a MgB<sub>2</sub> crystal. One can find the one-to-one correspondence between wave-functions of the  $\alpha_1$ -state in HB and the  $\delta_2$ -state in MgB<sub>2</sub>. The present research reveals a relation between the surface treatment

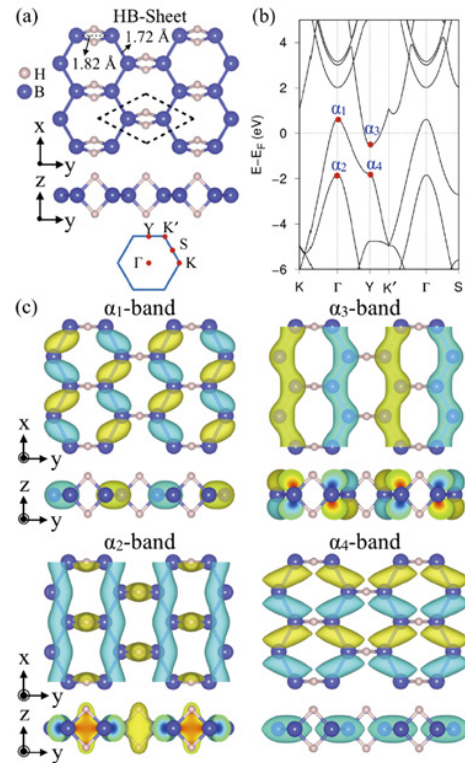


Fig. 1. (a) Atomic structure, and two-dimensional Brillouin zone of a HB sheet. (b) Calculated band structure. (c) Wave function distribution of the  $\alpha_1$ -,  $\alpha_2$ -,  $\alpha_3$ -, and  $\alpha_4$ -states. The color of wave functions corresponds to the sign of the periodic part of Bloch wave functions.

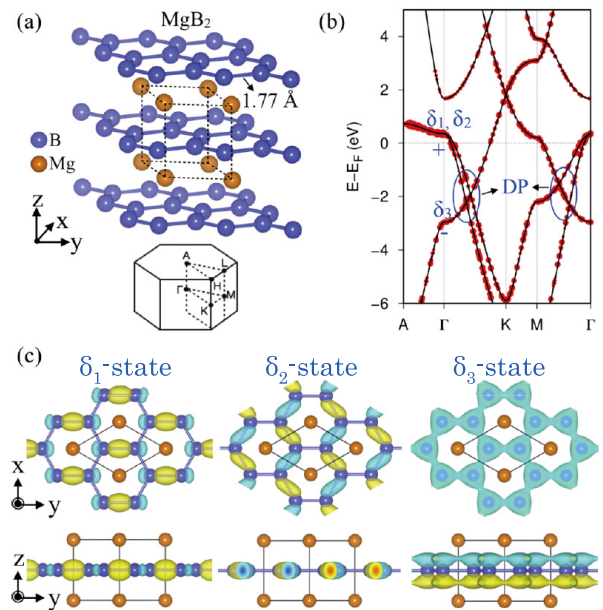


Fig. 2 (a) Atomic structure, and three-dimensional Brillouin zone of a MgB<sub>2</sub> crystal. (b) Calculated band structure. The red dots are the projected band structure of MgB<sub>2</sub> on B atoms. “DP” indicates Dirac point. Dirac points shown in (b) are “cross sections” of Dirac Nodal Loop. (c) Wave function distribution of the  $\delta_1$ -,  $\delta_2$ -, and  $\delta_3$ -states. In (c), the color of wave functions corresponds to the sign of wave functions.

of monatomic layer and evolutions of the two-dimensional states, giving clues to design novel functional layers.

#### Reference

- [1] I. Tateishi, N. T. Cuong, C.A.S. Moura, M. Cameau, R. Ishibiki, A. Fujino, S. Okada, A. Yamamoto, M. Araki, S. Ito, S. Yamamoto, M. Niibe, T. Tokushima, D.E. Weibel, T. Kondo, M. Ogata, and I. Matsuda, Phys. Rev. Materials **3**, 024004 (2019).

## Authors

I. Tateishi<sup>a</sup>, N. T. Cuong<sup>b</sup>, M. Niibe<sup>c</sup>, T. Kondo<sup>b</sup>, M. Ogata<sup>a</sup>, and I. Matsuda

<sup>a</sup>The University of Tokyo

<sup>b</sup>University of Tsukuba

<sup>c</sup>University of Hyogo

# Interfacial Carrier Dynamics of Graphene on SiC, Traced by the Full-Range Time-Resolved Core-Level Photoemission Spectroscopy at SPring-8 BL07LSU

I. Matsuda Group

Time evolutions of the Dirac Fermions in graphene layers have attracted both academic and technological interests due to observations of the various intriguing opto-electric phenomena, such as carrier multiplications and generation of a terahertz laser. Nowadays, graphene layers can be epitaxially grown on a SiC substrate in wide area and such non-equilibrium carriers in the Dirac bands have been directly probed by time-resolved photoemission spectroscopy. On the other hand, the previous studies focused only on electronic evolutions within a graphene layer and little examination was made on carrier dynamics through the graphene/substrate interfaces. Unveiling dynamic roles of the graphene/SiC interface is necessary to understanding the opto-electric properties in SiC based detectors, for example.

In the present research, we conducted measurements of time-resolved core-level photoemission spectroscopy by a combination of laser and synchrotron radiation [1]. The experiment was performed at SPring-8 soft X-ray beamline BL07LSU with the beamline laser station, BL07LASER. Figure 1 shows temporal variations of peak positions of C 1s and Si 2p during relaxation of the surface photovoltage effect, induced by the optical pumping with a laser pulse. Two C 1s components are assigned to a graphene layer (G) and a SiC substrate (SiC), while one Si 2p component originates from a SiC substrate. Thus, the high-resolution core-level spectra selectively distinguish dynamical information between overlayer and substrate. While the whole relaxation of the electron-hole recombination process takes 100 nanoseconds, one can also find difference in temporal

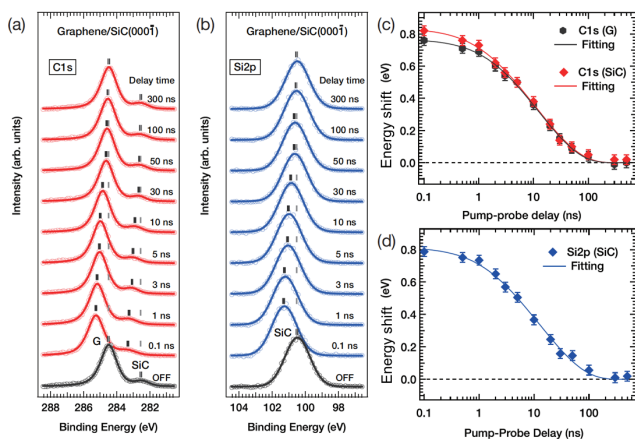


Fig. 1. Time-resolved photoemission spectra for (a) C 1s and (b) Si 2p core levels of graphene layers on the SiC substrate. In (a), graphene peaks (labeled G) and SiC peaks (labeled SiC) were distinguishably observed. The spectral energy shift measured from the laser OFF was extracted and shown as a function of time for (c) C 1s and (d) Si 2p core levels.

variation between C and SiC in the subnanosecond region. This is because carrier lifetime in the graphene layers take longer than that of the typical interface-state of SiC by the bottleneck effect of Dirac cones. When there is a buffer layer between graphene and SiC, electron-hole recombination is dominantly held at the interface and the lifetime shortens one-order of the magnitude [1]. The selective evaluations of carrier dynamics in non-uniform samples, such as hetero-junctions, allow one to design and develop novel optoelectric devices.

## Reference

[1] T. Someya, H. Fukidome, N. Endo, K. Takahashi, S. Yamamoto, and I. Matsuda, Appl. Phys. Lett. **113**, 051601 (2018).

## Authors

H. Fukidome<sup>a</sup>, S. Yamamoto, and I. Matsuda

<sup>a</sup>Tohoku University

# Polarization Resolved High Harmonic Generation in Semiconducting Gallium Selenide

Itatani Group

Recent progress in ultrafast laser technology has realized to produce strong optical fields in the mid-infrared to terahertz spectral regions. Emergence of such intense long-wavelength light sources triggers ultrafast strong-field physics for condensed matters. When crystalline materials are irradiated by intense mid-infrared pulses, for example, extreme ballistic oscillation of electrons in a conduction band with terahertz to petahertz frequencies occurs, and high-order harmonics are often produced beyond a typical bandgap of solids. So far, most of the experiments employ one-dimensional study along a specific direction. However, we show that a one-dimensional model is not suitable to investigate

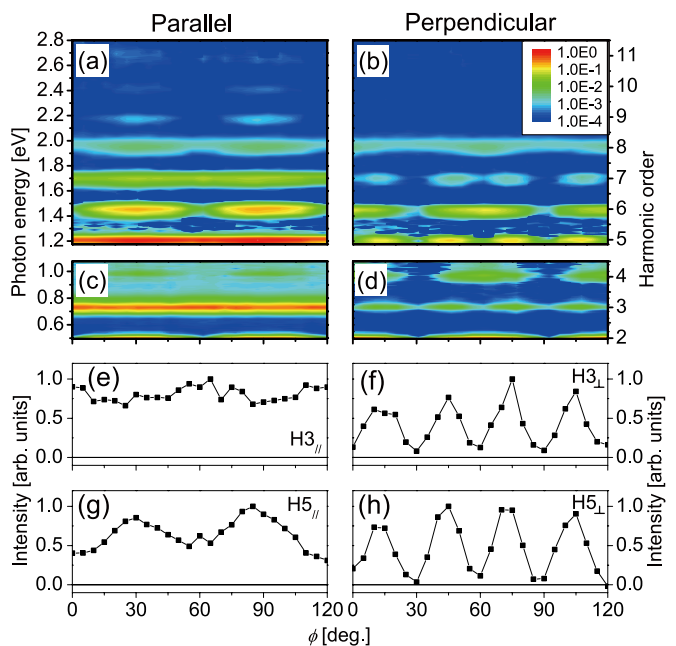


Fig. 1. Polarization resolved measurement of the crystallographic orientation dependence of high harmonics generated in GaSe with a high field amplitude of 10 MV/cm. Parallel (a, visible; c, infrared) and perpendicular (b, visible; d, infrared) polarization components of the high harmonics. Curve plots of the parallel third (e), perpendicular third (f), parallel fifth (g), and perpendicular fifth (h) harmonics.

polarization property of HHG in solids.

In this study, we investigate polarization properties of high harmonics produced in a 30- $\mu\text{m}$ -thick gallium selenide (GaSe,  $\epsilon$ -type, [001] z-cut, hexagonal structure, non-coat). The crystal is exposed to linearly polarized femtosecond mid-infrared pulses with a field amplitudes of  $\sim 10$  MV/cm that are produced from a dual-wavelength optical parametric amplifier (wavelength: 5  $\mu\text{m}$ , maximum pulse energy: 15  $\mu\text{J}$ , pulse duration: 200 fs, repetition rate: 1 kHz) [1]. The crystallographic orientation dependence of high harmonic spectra is measured after a set of wire-grid polarizers in the either parallel (Fig. 1(a), (c), (e), and (g)) or perpendicular (Fig. 1(b), (d), (f), and (h)) to the mid-infrared field. The observed high harmonics are extended up to the 11th order (2.70 eV, 460 nm) beyond the bandgap (1.98 eV, 625 nm). All even harmonics for both polarizations show modulations with  $60^\circ$  periodicities, which is consistent with the hexagonal structure of a GaSe crystal. In contrast to the even harmonics, the parallel and odd harmonics show  $60^\circ$  modulation on top of a constant offset as in Figs. 1 (e) and (g) for the third and fifth harmonics, respectively. More surprisingly, the perpendicular odd harmonics appear with  $30^\circ$  periodicity as can be seen in Figs. 1(f) and (h). This  $30^\circ$  periodicity cannot be intuitively understood from the hexagonal structure of the crystal.

To explain these results, a two-dimensional single-band

model described by the Bloch theorem is used [2]. This model assumes that (i) the intraband current dominates odd harmonics and (ii) the electron wavepacket is launched around the  $\Gamma$  point. Detailed explanation of the model and a verification of these assumptions can be found in Ref. [3]. We found that the band curvature (Figs. 2 (b) and (c)) of the lowest conduction band (Fig. 2(a)) along the electron trajectory is responsible for the source of odd-order harmonics. Based on the two-dimensional single-band model, the parallel and perpendicular odd harmonics are calculated to show  $60^\circ$  and  $30^\circ$  periodicities as can be seen in Figs. 2(d) and (e), respectively. These results well reproduce the experimental observations of the orientation dependences and the polarization property for all odd harmonics.

In summary, we have investigated a polarization property of high harmonics from a bulk GaSe crystal using femtosecond MIR pulses and their dependence on crystallographic orientation. With the 10 MV/cm electric field, the perpendicular odd harmonic emerges with a periodic modulation of  $30^\circ$ , which cannot be explained by the perturbative nonlinear optics. The underpinned physics of the perpendicular component of the odd harmonics is attributed to anisotropic momentum dependence of the band curvature along the electron trajectory, which is equivalent to the inverse effective mass. Our demonstration establishes a direct link between the band structure and HHG in a crystalline solid. Multi-dimensional analysis combined with time-resolved measurement allows to investigate electron dynamics and field-dressed structure of energy bands in future.

#### References

- [1] K. Kaneshima, N. Ishii, K. Takeuchi, and J. Itatani, Opt. Express **24**, 8660 (2016).
- [2] S. Ghimire, A. D. DiChiara, E. Sistrunk, P. Agostini, L. F. DiMauro, and D. A. Reis, Nature Phys. **7**, 138 (2011).
- [3] K. Kaneshima, Y. Shinohara, K. Takeuchi, N. Ishii, K. Imasaka, T. Kaji, S. Ashihara, K. L. Ishikawa, and J. Itatani, Phys. Rev. Lett. **120**, 243903 (2018).

#### Authors

K. Kaneshima, Y. Shinohara<sup>a</sup>, K. Takeuchi, N. Ishii, K. Imasaka<sup>b</sup>, T. Kaji<sup>b</sup>, S. Ashihara<sup>b</sup>, K. L. Ishikawa<sup>a,c</sup>, and J. Itatani<sup>a</sup>  
<sup>a</sup>Photon Science Center, School of Engineering, The University of Tokyo  
<sup>b</sup>Institute of Industrial Science, The University of Tokyo  
<sup>c</sup>Department of Nuclear Engineering and Management, School of Engineering, The University of Tokyo

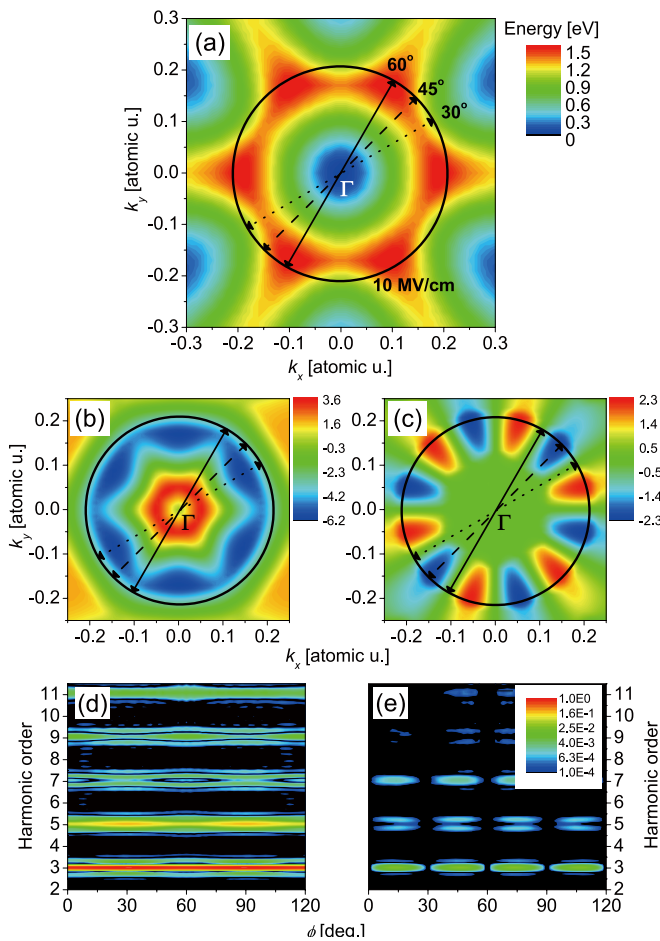


Fig. 2. Calculated results by the two-dimensional single-band model. (a) Lowest conduction band of GaSe and its band curvatures. (b) the band curvature component responsible for parallel odd harmonic generation. (c) the other band curvature component responsible for perpendicular odd harmonic generation. Three electron trajectories at  $\phi = 60^\circ$  (solid black arrows),  $45^\circ$  (dash), and  $30^\circ$  (dot) are illustrated. The maximum amplitude of electron trajectories with an electric field of 10 MV/cm is shown by the black circle. Orientation dependence of the (d) parallel and (e) perpendicular harmonics obtained by the two-dimensional single-band model with the 10-MV/cm electric field.

# Joint Research Highlights

## Spin Injection from a Ferromagnetic Insulator into a Superconductor

M. Matsuo and T. Kato

Spin injection from a ferromagnetic metal into a superconductor (SC) has been investigated for a long time. For conventional s-wave superconductors, spin injection is suppressed by a SC energy gap. Thermally excited quasiparticles in SC, however, can carry injected spins over long distances, as spin excitations in SCs have long lifetimes. Several novel techniques for spin injection have been developed so far. For example, the spin injection can be realized by the spin Seebeck effect under a temperature gradient, or by applying a spin pumping protocol using ferromagnetic resonance (FMR) under microwave irradiation.

Recently, spin injection from a ferromagnetic insulator (FI) into a SC has also been performed [1]. Although this study opens up possible applications for novel superconducting spintronic devices using FI, spin injection from a FI has been studied theoretically only in Ref. [2] in the context of the damping in the FMR experiments. In the present study [3], we considered a bilayer system composed of a s-wave singlet SC and a FI as shown in Fig. 1(a), and calculated the spin current induced by the spin Seebeck effect or spin pumping, using the perturbation theory with respect to the interface exchange interaction.

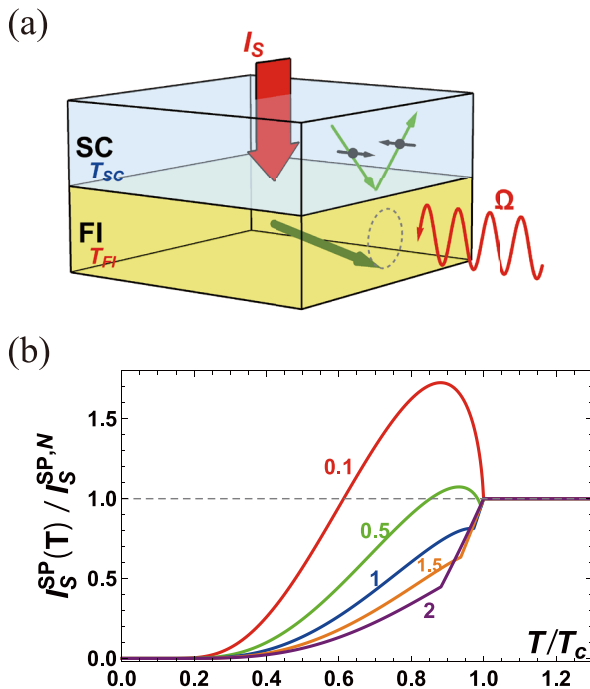


Fig. 1. (a) A schematic of the bilayer system composed of a superconductor (SC) and a ferromagnetic insulator (FI). (b) The temperature dependence of the spin current induced by spin pumping under microwave irradiation. The curves correspond to  $\hbar\Omega/k_B T_C = 0.1, 0.5, 1, 1.5,$  and  $2$  from the top to the bottom.

In Fig. 1(b), we show the temperature dependence of the spin current induced by spin pumping. Here the temperature of the bilayer system and the spin current are normalized by the SC transition temperatures  $T_C$  and the spin current for a normal metal, respectively. For small excitation frequency  $\Omega$ , the spin current is enhanced below the SC transition temperature due to a coherent factor in analogy with the NMR measurement. For  $\hbar\Omega < 2\Delta(T=0) \approx 3.54k_B T_C$ , the spin current is strongly reduced at low temperatures ( $k_B T \ll 2\Delta(T)$ ), because spin-flip excitations in the SC are suppressed due to the energy gap  $2\Delta$  in the one-electron excitation spectrum, where  $\Delta(T)$  is the SC energy gap (a function of the temperature  $T$ ). As  $\Omega$  increases, the coherence peak becomes insignificant, while there appears a kink at the temperature satisfying  $2\Delta(T) = \hbar\Omega$ . For  $\hbar\Omega > 2\Delta(T=0)$ , the spin current shows a plateau at a low temperature corresponding to its zero temperature value, ultimately recovering the normal state value (dashed line) as  $\Omega$  increases further. We also calculated the spin current induced by the spin Seebeck effect (not shown here), and discussed the effect of the SC transition.

For a realistic experimental setup, we estimated the noise power of the pure spin current following the theory developed in Ref. [4]. We have shown that the nonequilibrium spin-current noise in spin pumping experiments is much larger than the thermal noise at low temperatures, and that both noises show a coherent peak below the SC transition temperature. Finally, we proposed a possible experimental setup to measure the spin current and its noise obtained here, utilizing the inverse spin Hall effect in SCs.

This study has been performed as a joint study extended from the previous study [4] with Mamoru Matsuo, who was a visiting professor of ISSP in the academic year 2016. This study has also been performed as a collaborated project with the French group (the leader is Thierry Martin at Aix Marseille Univ., CPT, Marseille).

### References

- [1] M. Umeda *et al.*, App. Phys. Lett. **112**, 232601 (2018).
- [2] M. Inoue, M. Ichioka, and H. Adachi, Phys. Rev. B **96**, 024414 (2017).
- [3] T. Kato, Y. Ohnuma, M. Matsuo, J. Rech, T. Jonckheere, and T. Martin, Phys. Rev. B **99**, 144411 (2019).
- [4] M. Matsuo, Y. Ohnuma, T. Kato, and S. Maekawa, Phys. Rev. Lett. **120**, 037201 (2018).

### Authors

T. Kato, Y. Ohnuma<sup>a</sup>, M. Matsuo<sup>a</sup>, J. Rech<sup>b</sup>, T. Jonckheere<sup>b</sup>, and T. Martin<sup>b</sup>

<sup>a</sup>Kavli Institute for Theoretical Sciences, University of Chinese Academy of Sciences

<sup>b</sup>Aix Marseille Univ, Université de Toulon, CNRS, CPT

# Turning a Graphene into a Topological Insulator with Surface Decoration

J. Haruyama, S. Katsumoto, and T. Nakamura

Graphene once played a key role in the development of topological insulators, which exhibit an electrically inert interior yet form metallic states at their boundary (the edge states). Kane and Mele, in 2005, predicted that coupling between the spin and orbital motion of electrons turns graphene (or some honeycomb lattice) into a ‘quantum-spin-Hall (QSH)’ insulator that hosts spin-filtered metallic edge states with inherent resilience from scattering. These novel edge states underlie tantalizing technological applications for low-power electronics, spintronic devices, and fault-tolerant quantum computing. Although graphene’s intrinsic spin-orbit coupling is far too weak to produce an observable QSH phase in practice, numerous alternative platforms were subsequently discovered, including HgTe and InAs/GaSb quantum wells, WTe<sub>2</sub>, bismuthene, and the layered compound Bi<sub>14</sub>Rh<sub>3</sub>I<sub>9</sub>.

Realization of the QSH effect in graphene devices has remained an outstanding challenge dating back to the inception of the field of topological insulators. Graphene’s exceptionally weak spin-orbit coupling—stemming from carbon’s low mass—poses the primary obstacle. We experimentally study artificially enhanced spin-orbit coupling in graphene via random decoration with dilute Bi<sub>2</sub>Te<sub>3</sub> nanoparticles. Remarkably, multi-terminal resistance measurements suggest the presence of helical edge states characteristic of a QSH phase; those magnetic-field and temperature dependence, X-ray photoelectron spectra, scanning tunneling spectroscopy, and first-principles calculations further support this scenario. These observations highlight a pathway to spintronics and quantum-information applications in graphene-based QSH platforms.

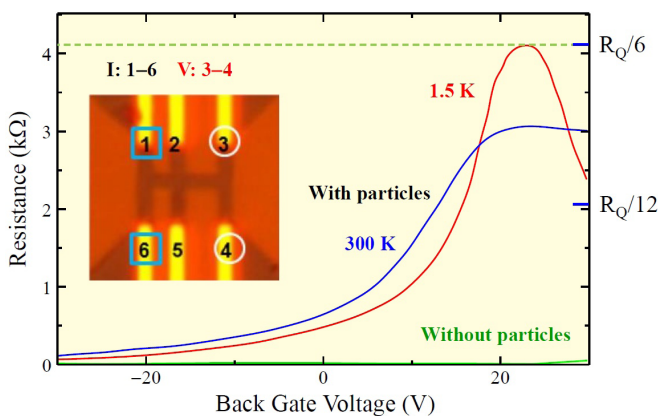


Fig. 1. Inset: AFM image of the sample. The vague dark regions are fabricated graphene with fine particles. The yellow-colored regions are Au electrodes. The blue squares indicate the current electrodes and the white circles indicate the voltage electrodes. At 1.5 K, with varying the back gate voltage, the resistance increases and hits 1/6 of the quantum resistance, which is just expected for the configuration of the electrodes and perfect conductance connection between them.

## References

[1] K. Hatsuda, H. Mine, T. Nakamura, J. Li, R. Wu, S. Katsumoto, and J. Haruyama, *Sci. Adv.* **4**, eaau6915 (2018).

## Authors

J. Haruyama<sup>a</sup>, K. Hatsuda<sup>a</sup>, S. Katsumoto, and T. Nakamura<sup>a</sup>  
<sup>a</sup>Aoyama-Gakuin University

# Coexisting Two Types of Spin Splitting Originating from Different Orbital Symmetries

K. Yaji, S. Tanaka, and F. Komori

Spin degeneracy of conducting electrons in materials can be lifted by spin-orbit interaction (SOI). Here, the symmetry of a surface or interface plays an important role in determining the spin splitting and texture of a 2D band. [1] In the framework of the Rashba model for a two-dimensional (2D) electron gas, a free-electron-like band dispersing from the  $\Gamma$  point is shifted oppositely in the wave number direction by SOI, depending on the spin direction that is perpendicular to both the surface normal and momentum of the electron. Another type of the spin-split band in the 2D system is called the Zeeman type, where the spin direction is perpendicular to the 2D plane without spin degeneracy at the symmetry point in the wave-number space. In the case of the spin-split bands of the surface 2D electron system with a three-fold lattice symmetry, either the Zeeman- or Rashba-type spin splitting has been considered to appear around a K point exclusively depending on the crystal symmetry. [1]

We have found a novel spin-dependent band structure of a Sn triangular-lattice atomic layer (TLAL) at the K point. The sample is formed by intercalation into the interface between graphene and the SiC(0001) substrate as a schematic model shown in Fig. 1(a). [2] At the K point of the Sn TLAL with the symmetry of  $C_3$  according to the lattice symmetry  $p3m1$ , the Zeeman-type spin splitting is reason-

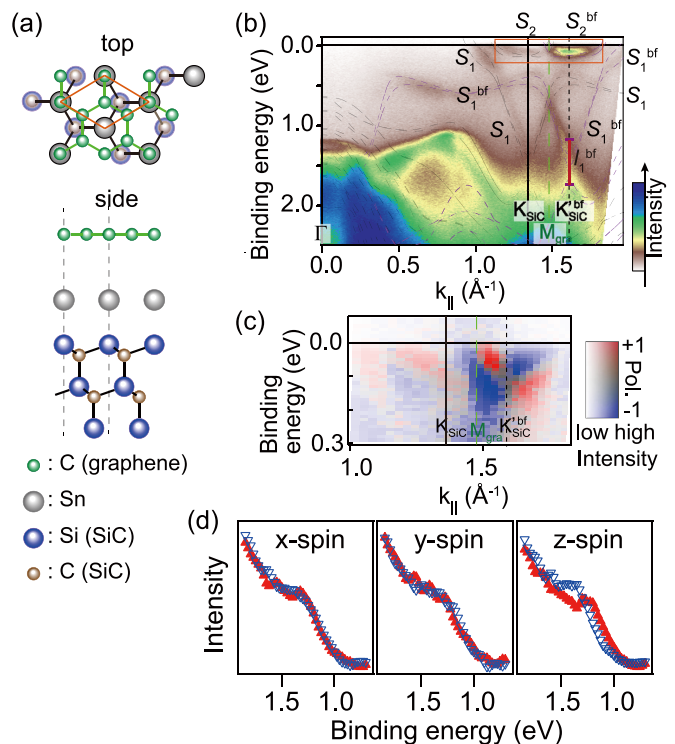


Fig. 1 (a) Atomic structure model of a Sn TLAL intercalated into the graphene/SiC(0001) interface. (b) ARPES intensity image of the Sn TLAL along  $\Gamma K_{SiC}$  with overlaying the calculated band structure. The color scale represents the photoelectron intensity, and gray (purple) dashed curves the original (back-folded) bands. Two surface bands,  $S_1$  and  $S_2$ , and their back-folded bands,  $S_1^{bf}$  and  $S_2^{bf}$ , are marked. (c) SARPES intensity images taken with the region including  $S_2$  and  $S_2^{bf}$  bands near  $E_F$  surrounded by a thin rectangle in (b). The y-spin polarization component is detected. The two-dimensional color scale represents both the photoelectron intensity and the spin polarization. (d) The x, y, and z components of the spin-resolved spectra in the region marked as  $I_1$  at  $K'_{SiC}$  of  $S_1^{bf}$  band in (b).

ably explained by the symmetry while the Rashba-type band crossing is not expected. Using our spin- and angle-resolved photoelectron spectroscopy (SARPES) with three-dimensional spin detection [4] and He I $\alpha$  ( $h\nu \sim 21.22$  eV) radiation, both the Zeeman-type and Rashba-type spin splits are confirmed at the K ( $K'$ ) point as shown in Fig. 1(b-d). [4] The surface band  $S_2$  near  $E_F$  exhibits a Rashba type inconsistently with the lattice symmetry, while the surface band  $S_1$  around 1.5 eV below  $E_F$  is the Zeeman type as expected. It should be noted that the photoelectron intensity for the back-folded band around the  $K'$  point due to the graphene-lattice scattering is stronger than that of the original one around the K point in the present experiment conditions.

We have investigated the origin of the two types in the Sn TLAL by evaluating the spin-resolved band structure and charge distribution for the spin-split bands using density functional theory calculations. The directions of the spin polarization are well reproduced by the calculation as in Fig. 2(a,b). The calculated charge distribution of the Rashba-type (Zeeman-type) band at the K point, shown in Fig. 2(c,d), corresponds to a  $C_{3v}$  ( $C_3$ ) symmetry at the K point. Theoretically, the  $C_{3v}$  symmetry allows the Rashba-type band crossing regardless of the existence of the time

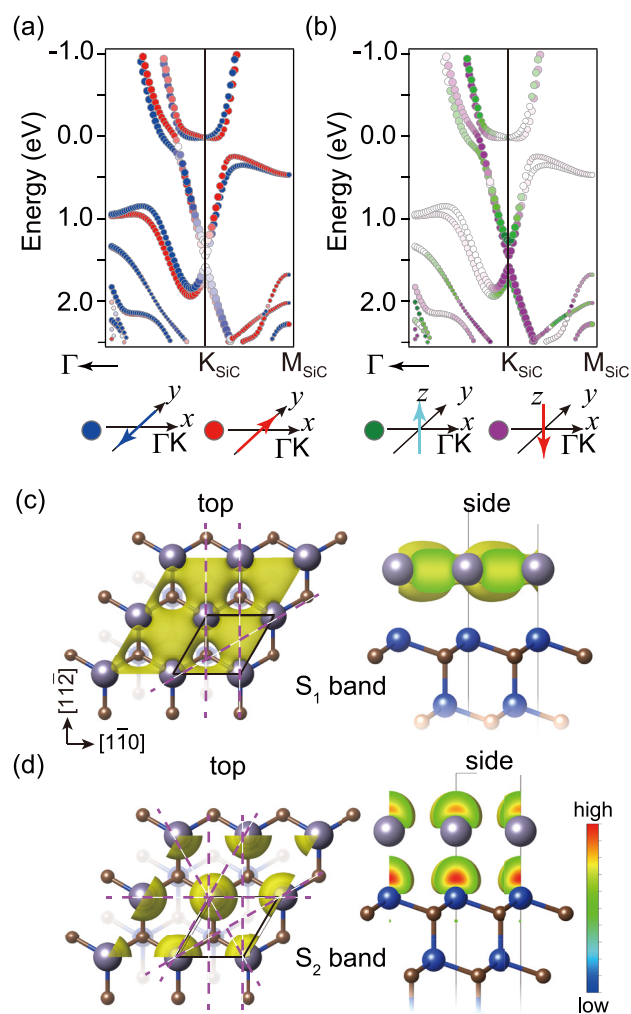


Fig. 2. (a,b) Spin polarization in the y (a) and z (b) directions for the bands around  $K_{SiC}$ , where the opposite spin directions are indicated by blue-red and green-purple colors, respectively. The diameter of the circles is proportional to the total contribution of Sn 5s and 5p. (c,d) Charge density distributions for the Zeeman-like spin-split band of  $S_1$  (c) and the Rashba-like spin-split band of  $S_2$  (d) at the  $K_{SiC}$  point. Left (right) panels represent top (side) views. In the left panels, the solid parallelograms show the unit cell of Sn/SiC(0001)-(1  $\times$  1). The dashed lines indicate the mirror planes of the charge density distribution.

reversal symmetry. [1] The symmetry of the charge density distribution, which is still a consequence of the crystal field potential for the electrons, is a key to understand the nature of the spin splitting due to SOI.

#### References

- [1] T. Oguchi and T. Shishidou, J. Phys. Condens. Matter **21**,092001 (2009).
- [2] S. Hayashi *et al.*, Appl. Phys. Express **11**, 015202 (2018).
- [3] K. Yaji *et al.*, Phys. Rev. Lett. **122**, 126403 (2019).
- [4] K. Yaji *et al.*, Rev. Sci. Instrum. **87**, 053111 (2016).

#### Authors

K. Yaji, A. Visikovskiy<sup>a</sup>, T. Iimori, K. Kuroda, S. Hayashia, T. Kajiwara<sup>a</sup>, S. Tanaka<sup>a</sup>, S. Shin, and F. Komori<sup>a</sup>  
<sup>a</sup>Kyushu University

## Advanced First-Principles Simulation of Electrochemical Interfaces

S. Kasamatsu, I. Hamada, and O. Sugino

Electrochemical interfaces have long been attracting attention as an environment for the interconversion of chemical and electric energies, but the first-principles simulation is not yet sufficiently matured because of the difficulties in (i) achieving the accuracy required for the reliable prediction and (ii) modeling the electric double layers within the density functional theory (DFT). As a step for overcoming, we studied accuracy of the random phase approximation (RPA) for the exchange and correlation (xc) of electrons and then developed an *ab initio* Monte Carlo method suitable for sampling the distribution of defects in an electrode.

Hydrogen (H) on a platinum (Pt) surface, H/Pt(111), is a typical benchmarking system for which many theoretical and experimental studies exist, but controversies still remain even for the H adsorption problem: H is presumed to adsorb on the fcc site based on indirect experiments and the conventional DFT simulations, while there exist several reports that signal from the top site can be observed spectroscopically. Since the conventional DFT, which is based on the semilocal approximation for the xc potential, was shown inaccurate for the sorption problem on Pt(111), we have tried to use more advanced xc potential called RPA [1]. The result of the calculation accurately reproduced the experimental adsorp-

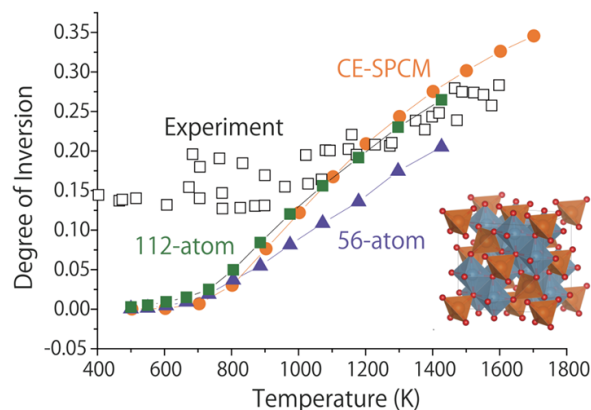


Fig. 1. Plot of the degree of conversion versus the temperature ( $T$ ) and the  $MgAl_2O_4$  spinel structure (inset). Our calculation using 112-atom and 56-atom cells well reproduced the previous simulation based on a cluster expansion model (CE-SPCM) in the whole range of  $T$  and also the neutron experiment at higher  $T$ . First-principles sampling for solids has thus made feasible.

tion energy although conventional DFT considerably overestimates it. Contrary to the conventional DFT, the DFT-RPA predicts that difference in the energy between the fcc and top sites is on the order of thermal energy at room temperature, i.e.  $k_B T_{\text{room}}$ , suggesting coexistence of the fcc and atop hydrogens. This renewed picture on the H adsorption explains why signal from the top site may be observed. We believe this is an important step for true microscopic understanding of the hydrogen evolution reaction, which is one of the most important fuel-cell reactions.

The fuel-cell reaction occurs efficiently on the Pt electrode but the efficiency needs further improvement to meet the demand of future technology. In this context, oxide electrode ( $\text{TiO}_2$  or  $\text{ZrO}_2$ ) has attracted considerable attention as a beyond Pt material. By introducing impurities and oxygen vacancies, the oxides are made active for the fuel-cell reactions. Theoretically, however, it has been extremely difficult to model this system by sampling the distribution of defects for appropriate description of the space charge layer; this is because of the large barrier existing between different configurations of defects. The *ab initio* molecular dynamics (MD) simulation is an established method for the sampling but is generally inadequate for solids. In this context, we have developed an *ab initio* Monte Carlo (MC) method of replica exchange type, which runs very efficiently on massively parallel supercomputers. Our benchmark calculation on  $\text{MgAl}_2\text{O}_4$  spinel shows that the degree of inversion, or the ratio of Al ions on Mg sites, is successfully sampled in the temperature range studied [2] (Fig. 1). This is considered as an important step for elucidation of the reason why the oxides so effectively activate the fuel-cell reactions.

## References

- [1] L. Yan, Y. Sun, Y. Yamamoto, S. Kasamatsu, I. Hamada, and O. Sugino, *J. Chem. Phys.* **149**, 164702 (2018).  
 [2] S. Kasamatsu and O. Sugino, *J. Phys.: Condensed Matter*, **31**, 085901 (2019).

## Authors

L. Yan, Y. Yamamoto, S. Kasamatsu<sup>a</sup>, O. Sugino, Y. Sun<sup>b</sup>, I. Hamada<sup>c</sup>  
<sup>a</sup>Yamagata University  
<sup>b</sup>National Institute for Materials Science  
<sup>c</sup>Osaka University

# Interfacial Hydrogen Bonding in Proton-Electron Concerted 2D Organic Bilayer on Au Substrate Probed by Soft X-Ray Spectroscopy

S. Yamamoto, H. S. Kato, and I. Matsuda

Recent developments in the molecular design of organic materials have uncovered a variety of novel functional properties. One of them is the coupling of proton dynamics and electrical conductivity, which can only be achieved in 3D organic crystals. However, reduction of dimensionality to 2D is essential in organic electronics application. In the functional materials group at ISSP, we aim to realize a 2D organic bilayer with a novel “proton-electron” functionality on a solid surface.

In this study [1], we prepared and characterized a 2D organic bilayer with “proton-electron” concerted functionality on a solid surface. A “proton-electron” concerted organic molecule, catechol-fused bis(methylthio)tetrathiafulvalene ( $\text{H}_2\text{Cat-BMT-TTF}$ ), was deposited onto an imidazole-

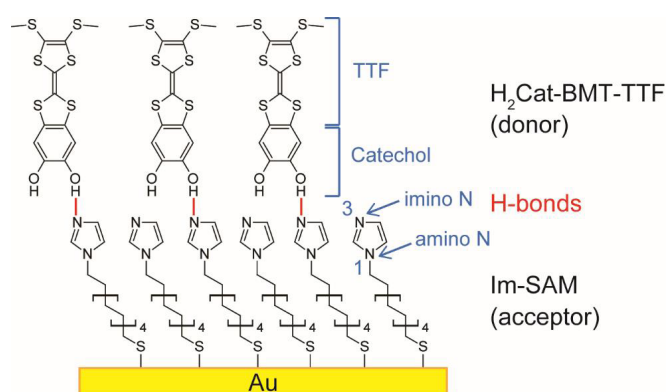


Fig. 1. Schematic structure of organic bilayer of  $\text{H}_2\text{Cat-BMT-TTF}$  and Im-SAM on Au.  $\text{H}_2\text{Cat-BMT-TTF}$  consists of catechol and tetrathiafulvalene (TTF). Im-SAM has two kinds of N atoms: imino N (N3) and amino N (N1). H-bonds are formed between the imino N atoms in Im-SAM ( $\text{H}^+$  acceptor layer) and OH groups in  $\text{H}_2\text{Cat-BMT-TTF}$  ( $\text{H}^+$  donor layer).

terminated alkanethiolate self-assembled monolayer (Im-SAM) on a Au surface (Fig. 1). In our previous study [2], the OH stretching vibrational modes of  $\text{H}_2\text{Cat-BMT-TTF}$  in the IR spectra showed a large red shift and substantial broadening upon adsorption on Im-SAM, indicating that the OH groups of  $\text{H}_2\text{Cat-BMT-TTF}$  act as the  $\text{H}^+$  donor sites. However, the counterpart  $\text{H}^+$  acceptor sites was not identified due to an overlap of vibrational peaks. Using near edge X-ray absorption fine structure (NEXAFS) spectroscopy, we succeeded in elucidating the nature of H-bonding at the  $\text{H}^+$  acceptor side (i.e., Im-SAM) because N atoms exist only in the Im-SAM layer.

N K-edge NEXAFS spectra of Im-SAM on Au before and after adsorption of  $\text{H}_2\text{Cat-BMT-TTF}$  are shown in Fig. 2. NEXAFS experiments were carried out at soft X-ray beam-line BL07LSU of SPring-8. For Im-SAM on Au, two sharp peaks are observed at 400.0 and 401.8 eV, which are ascribed to the N  $1s \rightarrow 1\pi^*$  transition of the imino N (N3) and amino N (N1) atoms, respectively, of the imidazole ring in Im-SAM. Upon adsorption of  $\text{H}_2\text{Cat-BMT-TTF}$ , the  $\pi^*$  peak of imino N (N3) shifts from 400.0 to 400.3 eV, while that of amino N (N1) remains at the same energy. The energies of the  $\pi^*$  peaks in NEXAFS are sensitive probes of local chemical environments of specific atoms. The energy shift of the  $\pi^*$  peak of imino N (N3) suggests that the local chemical environment of imino N is changed by intermo-

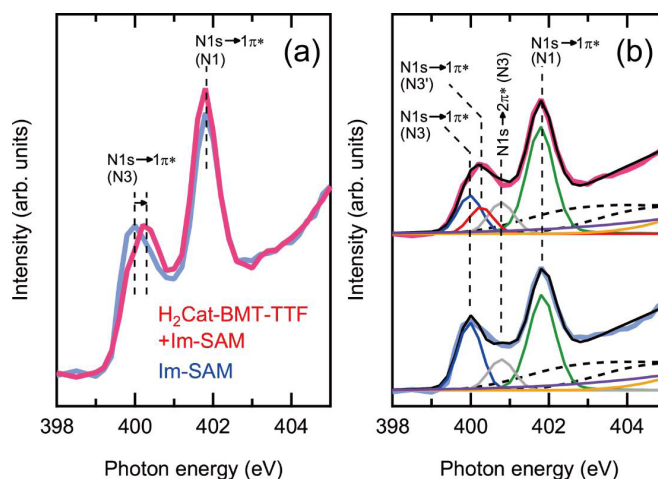


Fig. 2. N K-edge NEXAFS spectra of Im-SAM on Au before and after adsorption of  $\text{H}_2\text{Cat-BMT-TTF}$ . (a) Raw data and (b) raw data with peak fitting results.

lecular H-bonding with H<sub>2</sub>Cat-BMT-TTF. The H-bonding configuration between H<sub>2</sub>Cat-BMT-TTF and Im-SAM can be discussed based on the quantitative analysis of the coverage of each molecule. The peak fitting of N K-edge NEXAFS spectra in Fig. 2(b) reveals that the coverage of H-bonded Im-SAM is 0.41 ML. This matches the coverage of H<sub>2</sub>Cat-BMT-TTF (0.4 ML), which was estimated by X-ray photoelectron spectroscopy in our previous study [2]. This indicates that H<sub>2</sub>Cat-BMT-TTF and Im-SAM forms H-bonds in one to one fashion (Fig. 1).

In conclusion, the complete picture of H-bonding in the present organic bilayer was obtained; H-bonds form between the imino N atoms (H<sup>+</sup> acceptor sites) of Im-SAM and the OH groups (H<sup>+</sup> donor sites) of H<sub>2</sub>Cat-BMT-TTF. The present work is a steady step toward the realization of 2D organic functional materials, and the experimental methods adopted herein will serve as powerful tools for the detection of their functions.

## References

- [1] S. Yamamoto, H. S. Kato, A. Ueda, S. Yoshimoto, Y. Hirata, J. Miyawaki, K. Yamamoto, Y. Harada, H. Wadati, H. Mori, J. Yoshinobu, and I. Matsuda, *e-J. Surf. Sci. Nanotechnol.* **17**, 49-55 (2019).
- [2] H. S. Kato, S. Yoshimoto, A. Ueda, S. Yamamoto, Y. Kanematsu, M. Tachikawa, H. Mori, J. Yoshinobu, and I. Matsuda, *Langmuir* **34**, 2189 (2018).

## Authors

S. Yamamoto, H. S. Kato<sup>a</sup>, A. Ueda, S. Yoshimoto, Y. Hirata, J. Miyawaki, K. Yamamoto, Y. Harada, H. Wadati, H. Mori, J. Yoshinobu, and I. Matsuda  
<sup>a</sup>Osaka University

# Structural, Magnetic, and Transport Properties of Novel Quaternary Compounds RRu<sub>2</sub>Sn<sub>2</sub>Zn<sub>18</sub> (R = La, Pr, and Nd)

K. Wakiya, I. Umehara, and Y. Uwatoko

Cubic Pr-based intermetallic compounds are expected to show various fascinating phenomena arising from multipole degrees of freedom, when the crystal electric field (CEF) ground state of Pr<sup>3+</sup> ion is the non-Kramers  $\Gamma_3$  doublet. This is because the  $\Gamma_3$  doublet possesses not a magnetic dipole but electric quadrupoles and a magnetic octupole. Recently, PrT<sub>2</sub>X<sub>20</sub> (T: Transition metal, X = Zn, Al) with the non-Kramers doublet ground state have attracted much attention because they exhibit a coexistence of superconductivity with quadrupole ordering [1-4]. In addition, they exhibit a non-Fermi liquid behavior in the electrical resistivity and specific heat [1-4]. It is theoretically suggested that the non-Fermi liquid behavior is caused by the hybridization of quadrupoles with conduction electrons [5]. However, in order to increase our understanding of these phenomena, it is still crucial to find a new Pr compound with the  $\Gamma_3$  doublet ground state because the number of such compound is limited.

We recently focused on the isostructural compound PrRu<sub>2</sub>Zn<sub>20</sub> which shows a structural transition at  $T_S = 138$  K [6]. PrRu<sub>2</sub>Zn<sub>20</sub> shows no quadrupole ordering because the CEF ground state doublet is split into two singlets as a result of the site symmetry lowering at the structural transition. In PrT<sub>2</sub>X<sub>20</sub>, there are three distinct Zn sites: 16c, 48f, and 96g. Among these, Zn atoms at the 16c site [Zn(16c)] is encapsulated by an R<sub>2</sub>Zn<sub>12</sub> cage as shown in the inset of Fig. 1(a). A first principles calculation suggested that the large

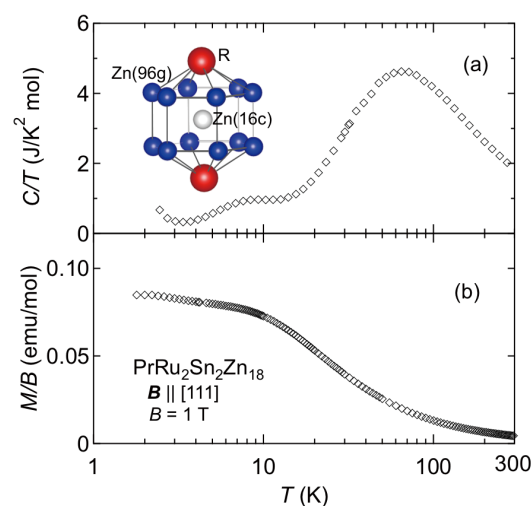


Fig. 1. (a) specific heat divided by temperature  $C/T$  and (b) magnetic susceptibility  $\chi (= M/B)$  of PrRu<sub>2</sub>Sn<sub>2</sub>Zn<sub>18</sub>. The inset (a) shows the Pr<sub>2</sub>Zn<sub>12</sub> cage surrounding the Zn atom at the 16c site [Zn(16c)]. In PrRu<sub>2</sub>Sn<sub>2</sub>Zn<sub>18</sub>, Zn atoms at the 16c site are fully replaced by Sn atoms.

cage space of R<sub>2</sub>Zn<sub>12</sub> cage induces the structural transition [7]. For RT<sub>2</sub>X<sub>20</sub> (R: Rare earth, T: Transition metal, X = Zn, Al), the cage space is evaluated by subtracting the atomic radius of the caged atom from the average distance between the atoms forming the cage and the caged atom [8]. Recently, in isostructural RT<sub>2</sub>Zn<sub>20</sub> (R = La-Nd, T = Co and Fe), it was reported that Zn(16c) can be fully replaced by the Sn atom [9]. This suggests that the structural transition in PrRu<sub>2</sub>Zn<sub>20</sub> can be suppressed by the Sn substitution because the cage space of the Pr<sub>2</sub>Zn<sub>12</sub> cage is reduced by introducing the Sn atom with a larger atomic radius into the 16c site. In this study, we synthesized Sn-substituted PrRu<sub>2</sub>Zn<sub>20</sub> using self-flux and melt growth methods in order to obtain a new cubic Pr-based compound.

The single-crystal x-ray structural analysis for obtained samples revealed that the Sn atoms selectively occupy the 16c site. Thus, the chemical formula of the obtained sample can be described as PrRu<sub>2</sub>Sn<sub>2</sub>Zn<sub>18</sub>. Figure 1(a) shows the specific heat divided by temperature,  $C/T$ , of PrRu<sub>2</sub>Sn<sub>2</sub>Zn<sub>18</sub>. No anomaly due to a structural transition is observed in  $C/T$ , suggesting that PrRu<sub>2</sub>Sn<sub>2</sub>Zn<sub>18</sub> remains cubic even at low temperatures. A broad peak at around 8 K is probably attributed to a Schottky peak due to the CEF splitting. Below 3 K,  $C/T$  increases with decreasing temperature, implying that the magnetic entropy is released even below 3 K. Figure 1 (b) shows the magnetic susceptibility  $\chi$  of PrRu<sub>2</sub>Sn<sub>2</sub>Zn<sub>18</sub>. Below 10 K,  $\chi$  shows a Van-Vleck paramagnetic behavior, indicating that the CEF ground state of PrRu<sub>2</sub>Sn<sub>2</sub>Zn<sub>18</sub> is non-magnetic. Since the Pr site has cubic symmetry, the  $J$  multiplet of Pr ion with a total angular momentum of  $J = 4$  split into four multiplets; nonmagnetic  $\Gamma_1$  singlet and  $\Gamma_3$  doublet, and magnetic  $\Gamma_4$  and  $\Gamma_5$  triplets. Considering that the magnetic entropy is released even below 3 K, the CEF ground state of PrRu<sub>2</sub>Sn<sub>2</sub>Zn<sub>18</sub> should be a nonmagnetic  $\Gamma_3$  doublet.

In conclusion, we have grown a new quaternary compound PrRu<sub>2</sub>Sn<sub>2</sub>Zn<sub>18</sub>. The structural transition in PrRu<sub>2</sub>Zn<sub>20</sub> can be suppressed by the Sn substitution. The magnetization and specific heat measurements revealed that the CEF ground state of PrRu<sub>2</sub>Sn<sub>2</sub>Zn<sub>18</sub> is probably a  $\Gamma_3$  doublet. Therefore, PrRu<sub>2</sub>Sn<sub>2</sub>Zn<sub>18</sub> is a promising material for studying the exotic phenomena arising from the multipole degrees of freedom.

## References

- [1] T. Onimaru *et al.*, Phys. Rev. Lett. **106**, 177001 (2011).
- [2] A. Sakai *et al.*, J. Phys. Soc. Jpn. **81**, 083702 (2011).
- [3] K. Matsubayashi *et al.*, Phys. Rev. Lett. **109**, 187004 (2012).
- [4] M. Tsujimoto *et al.*, Phys. Rev. Lett. **113**, 267001 (2014).
- [5] A. Tsuruta and K. Miyake, J. Phys. Soc. Jpn. **84**, 114714 (2015).
- [6] T. Onimaru *et al.*, J. Phys. Soc. Jpn. **79**, 033704 (2010).
- [7] T. Hasegawa *et al.*, J. Phys. Conf. Ser. **391**, 012016 (2012).
- [8] Z. Hiroi *et al.*, J. Phys. Soc. Jpn. **81**, 124707 (2012).
- [9] Y. Isikawa *et al.*, J. Phys. Soc. Jpn. **84**, 074707 (2015).

## Authors

K. Wakiya<sup>a</sup>, Y. Sugiyama<sup>a</sup>, M. Kishimoto<sup>b</sup>, T. D. Matsuda<sup>b</sup>, Y. Aoki<sup>b</sup>, M. Uehara<sup>a</sup>, J. Gouchi, Y. Uwatoko, and I. Umehara<sup>a</sup>  
<sup>a</sup>Yokohama National University  
<sup>b</sup>Tokyo Metropolitan University

# First-Principles Study of Anomalous Nernst Effect on Skyrmion Crystal Chern Insulator

F. Ishii, Y. P. Mizuta, and H. Sawahata

We are interested in how to achieve much higher thermoelectric conversion efficiency by effectively manipulating electron-spin degree of freedom. As one possibility, we have been studying Berry-phase-mediated thermoelectric effects, namely the contribution of the anomalous Hall conductivity (AHC) to thermoelectric power. What we target here is the anomalous Nernst effect (ANE), which is a heat-to-electricity conversion observed in magnetic materials and directly related to AHC. We discussed AHC mainly driven by an effective magnetic field, Berry curvature, induced by spin-orbit coupling and/or spin chirality.

We have so far found from computations on some models that, in the so-called 2D Skyrmion crystal (SkX) phase, where skyrmions are crystallized in two dimensions, the crystal-momentum component of effective magnetic field gives rise to the band structure that could generate large ANE when chemical potential  $\mu$  is properly tuned [1]. Although this behavior was most clearly confirmed in the simplest model of square SkX with single s-orbital per site, our subsequent computations on more realistic models of transition-metal oxides also showed possible large ANE [2]. A sizable transverse thermoelectric coefficient is predicted to arise, by means of first-principles calculations, in a SkX assumed on EuO monolayer (Fig. 1(a)) where carrier electrons are intro-

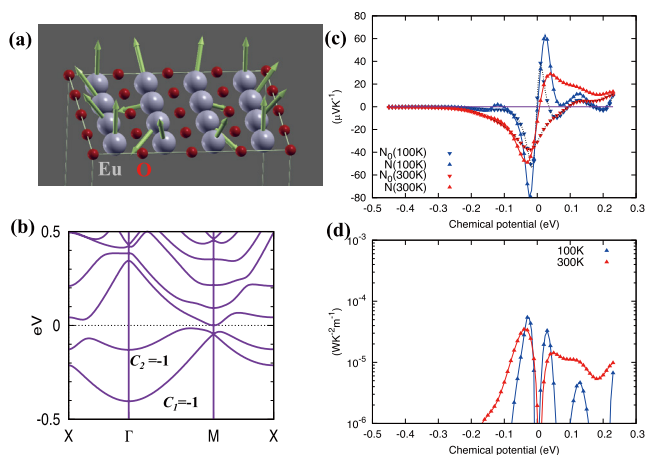


Fig. 1. (a) Calculated spin structures for skyrmion of EuO monolayer model. (b) Calculated band structure, (c) chemical potential dependence of anomalous Nernst coefficients and (d) power factors. Results are shown for different values of temperature 100K and 300K. We assumed the constant relaxation time  $\tau = 10$  fs.

duced upon a quantum anomalous Hall insulating phase of Chern number  $C = 2$ . This encourages future experiments to pursue such an effect.

Figure 1 (b) shows the band structure of electron-doped EuO monolayer. There is a narrow band gap of  $\sim 20$  meV between the valence band top and conduction band bottom. The Chern number was calculated by integrating Berry curvatures of Brillouin zone. The occupied two bands with Chern number  $C = 2$  are mainly composed of Eu 5d and 6s characters. We have calculated anomalous Nernst coefficients  $N$  and pure Nernst coefficients  $N_0 \equiv \alpha_{xy}/\sigma_{xy}$  [2] by using semiclassical Boltzmann transport theory with constant relaxation time,  $\tau = 10$  fs. The calculated chemical potential dependence of Nernst coefficients  $N$ , pure Nernst coefficients and power factor are plotted in Fig 1(c) and (d). The large anomalous Nernst coefficients up to  $60 \mu\text{V/K}$  and power factor up to  $70 \mu\text{W/mK}^2$  can be obtained.

Such  $N$  arises from the coexistence of large longitudinal thermoelectric coefficient and large Hall angle ratio, realized in the vicinity of a narrow band gap with Chern number  $C = 2$ . This demonstrates a prototype of novel class of new thermoelectric materials utilizing the nanoscale topological spin textures, motivating further studies including relevant experiments. We concluded that the SkX and narrow-gap Chern insulators could be candidate materials for thermoelectric applications.

## References

- [1] Y. P. Mizuta and F. Ishii, Sci. Rep. **6**, 28076 (2016).
- [2] Y. P. Mizuta, H. Sawahata, and F. Ishii, Phys. Rev. B **98**, 205125 (2018).

## Authors

F. Ishii<sup>a</sup>, Y.P. Mizuta<sup>b</sup>, and H. Sawahata<sup>a</sup>  
<sup>a</sup>Kanazawa University  
<sup>b</sup>Osaka University

# Heavy-Fermion State in Valence-Fluctuating Antiferromagnetic Compound EuPt<sub>2</sub>Si<sub>2</sub> under High Magnetic Field and High Pressure

T. Takeuchi, Y. Ōnuki, and T. Kida

EuPt<sub>2</sub>Si<sub>2</sub> crystallizes in the CaBe<sub>2</sub>Ge<sub>2</sub>-type tetragonal crystal structure and is known as a valence-fluctuating compound. From the  $\chi(T)$  measurement of polycrystalline samples, it is found that EuPt<sub>2</sub>Si<sub>2</sub> orders antiferromagnetically at  $T_N = 15$  K.  $\chi(T)$  at high temperatures follows the Curie-Weiss law with an effective magnetic moment of  $\mu_{\text{eff}} = 7.7 \mu_B/\text{Eu}$ , indicating that the Eu ions are essentially divalent. Here,  $\mu_{\text{eff}}$  for the Eu<sup>2+</sup> free-ion is  $7.94 \mu_B/\text{Eu}$ . On the other hand, an unusual broadening of the Mössbauer resonance line width is observed below about 100 K, suggesting that the valence is fluctuating and already deviates slightly from divalent to trivalent at room temperature. One of the intriguing findings for EuPt<sub>2</sub>Si<sub>2</sub> is the  $-\ln T$  dependence of  $\rho(T)$  below  $T \approx 100$  K. In addition, the magnetic entropy of  $S_{\text{mag}} \approx 0.6R \ln 8$  below  $T_N$  and the strongly enhanced  $\gamma \approx 200$  mJ/(K<sup>2</sup>·mol) suggest that a heavy-fermion state is realized at low temperatures in EuPt<sub>2</sub>Si<sub>2</sub>.

To obtain more insight into the heavy-fermion features in EuPt<sub>2</sub>Si<sub>2</sub>, we grew single crystals of this compound and studied the effects of a magnetic field as well as pressure on its magnetic properties.

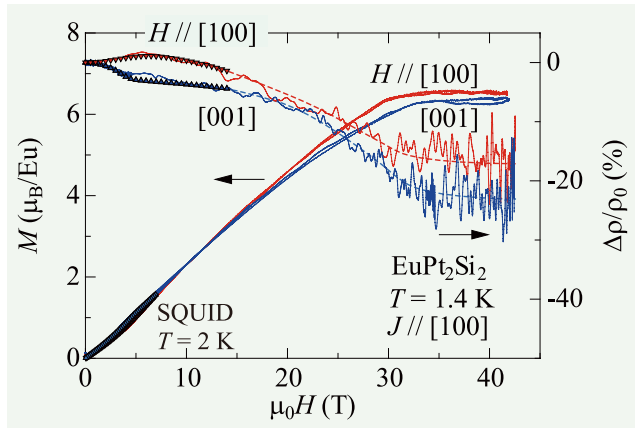


Fig. 1. High-field magnetization curves  $M(H)$  (left-hand scale) and relative changes in the magnetoresistance  $\Delta\rho/\rho_0$  for  $J // [100]$  (right-hand scale) in magnetic fields applied parallel to the [100] and [001] directions at 1.4 K. The  $M(H)$  data below 7 T were measured in static magnetic fields using a SQUID magnetometer at 2 K. The  $\Delta\rho/\rho_0$  curves below 14 T were measured using a superconducting magnet. Broken lines for  $\Delta\rho/\rho_0$  at high magnetic fields are guides to the eye.

The single crystal of  $\text{EuPt}_2\text{Si}_2$  shows two antiferromagnetic transitions at  $T_{N1} = 21$  K and  $T_{N2} = 16$  K. The  $-\ln T$  dependence of  $\rho(T)$  was observed in the temperature range from  $T_{N1}$  to about 100 K, as observed in polycrystals. The effect of magnetic field on the  $-\ln T$  dependence of  $\rho(T)$  is found to be very weak, with  $\Delta\rho/\rho_0$  of only  $\sim 0.1\%$  at  $\mu_0 H = 8$  T. Even at  $\mu_0 H = 40$  T, which was produced using a pulsed magnet,  $\Delta\rho/\rho_0$  amounted to only  $\sim 20\%$ , as shown in Fig. 1. These results suggest that the Kondo-like behavior of  $\text{EuPt}_2\text{Si}_2$  is rather stable against the application of magnetic field, which is in contrast to the Ce-based heavy-fermion compounds.

On the other hand, the pressure markedly shifts the  $-\ln T$  dependence of  $\rho(T)$  to higher temperatures, and  $T_{N1}$  is gradually decreased and suppressed to zero above  $P \simeq 4$  GPa, as indicated in Fig. 2. From the comparison of the observed magnetic, electronic, and thermal properties of  $\text{EuPt}_2\text{Si}_2$  with those of the well studied  $\text{EuCu}_2(\text{Ge}_{0.4}\text{Si}_{0.6})_2$ , [2] the anomalous features observed below 100 K in  $\rho(T)$ ,  $S(T)$ , and  $\Delta V/V$  for  $\text{EuPt}_2\text{Si}_2$  are most likely to be due to the valence fluctuation of the Eu ions. As a future problem, X-ray absorption and Mössbauer experiments are desirable to confirm the temperature dependence of the Eu valence in  $\text{EuPt}_2\text{Si}_2$ .

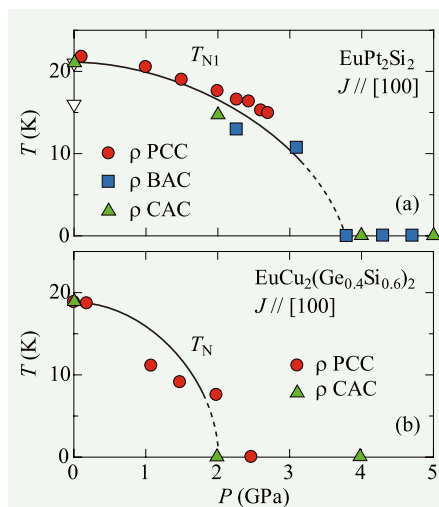


Fig. 2. Comparison of the  $P$ - $T$  phase diagrams for  $\text{EuPt}_2\text{Si}_2$  and  $\text{EuCu}_2(\text{Ge}_{0.4}\text{Si}_{0.6})_2$ , cited from Ref. [2]. The  $P$ - $T$  phase diagram for  $\text{EuCu}_2(\text{Ge}_{0.4}\text{Si}_{0.6})_2$  was obtained by the resistivity measurements for  $J // [100]$  under pressures. PCC, BAC, and CAC denote piston cylinder cell, Bridgman anvil cell, and cubic anvil cell.

## References

- [1] T. Takeuchi *et al.*, J. Phys. Soc. Jpn. **87**, 074709 (2018).
- [2] W. Iha *et al.*, J. Phys. Soc. Jpn. **87**, 064706 (2018).

## Authors

T. Takeuchi<sup>a</sup>, T. Yara<sup>b</sup>, Y. Ashitomi<sup>b</sup>, W. Iha<sup>b</sup>, M. Kakihana<sup>b</sup>, M. Nakashima<sup>c</sup>, Y. Amako<sup>c</sup>, F. Honda<sup>d</sup>, Y. Homma<sup>d</sup>, D. Aoki<sup>d</sup>, Y. Uwatoko, T. Kida<sup>a</sup>, T. Tahara<sup>a</sup>, M. Hagiwara<sup>a</sup>, Y. Haga<sup>e</sup>, M. Hedo<sup>b</sup>, T. Nakama<sup>b</sup>, and Y. Onuki<sup>b</sup>

<sup>a</sup>Osaka University

<sup>b</sup>University of the Ryukyus

<sup>c</sup>Shinshu University

<sup>d</sup>Tohoku University

<sup>e</sup>Japan Atomic Energy Agency

## Magnetolectric Behavior from Square Cupola Magnetic Units in High Magnetic Field

K. Kimura, Y. Kato, and A. Miyake

A particular class of magnetic order with broken space-inversion and time-reversal symmetries has recently attracted considerable interest because it can exhibit symmetry-dependent unique phenomena, such as linear magnetolectric (ME) effects and associated nonreciprocal optical responses. In exploring such a magnetic order, a material composed of inversion asymmetric magnetic units is fascinating, because structural asymmetry of the unit may stabilize a nontrivial non-coplanar spin arrangement due to asymmetric Dzyaloshinskii-Moriya (DM) interactions, which would lead to various magnetolectric responses. Recently, we have synthesized new antiferromagnetic insulators  $A(\text{TiO})\text{Cu}_4(\text{PO}_4)_4$  ( $A = \text{Ba}, \text{Sr}, \text{and Pb}$ ), which consists of  $\text{Cu}_4\text{O}_{12}$  convex-shaped magnetic units known as square cupola [Inset of Fig. 1(a)] [1-4]. Their crystal structure belongs to a tetragonal space group  $P4_212$  and is characterized by a layered arrangement of  $\text{Cu}_4\text{O}_{12}$  square cupolas. Interestingly, neutron diffraction study [2] reveals that below the antiferromagnetic ordering temperature  $T_N$ , four  $\text{Cu}^{2+}$  spins of each square cupola forms a magnetic quadrupole moment, which, along with magnetic monopole and toroidal moments, is known as one of cluster multipole moments that satisfy the symmetry condition for the linear ME effect. Indeed, we observed a magnetic-field-induced electric polarization in the Pb system and a sharp dielectric anomaly at  $T_N$  in the Ba and Sr systems. (The difference originates from a stacking manner of magnetic layers: the quadrupole moments stack ferroically in the Pb system, while antiferroically in the Ba

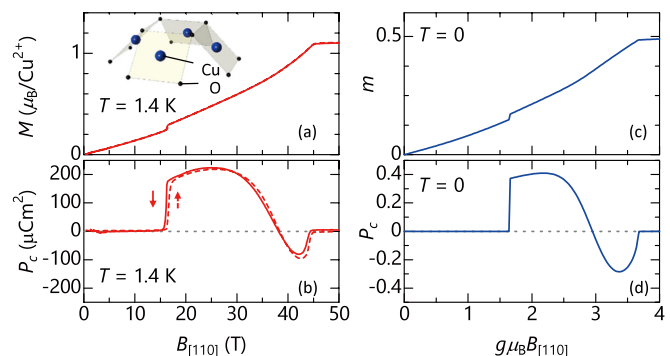
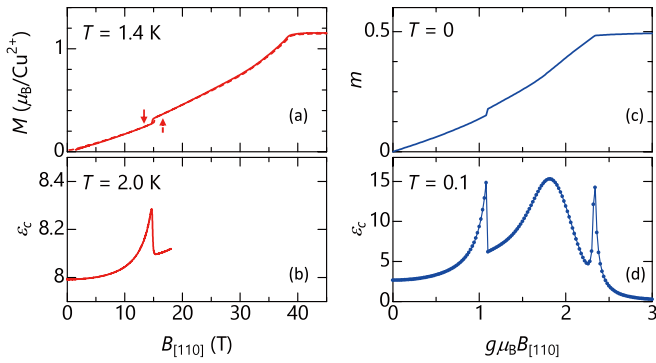


Fig. 3. Magnetic field dependence of magnetization ( $M$ ) and electric polarization along the  $c$  axis ( $P_c$ ) obtained in (a) and (b) experiments and (c) and (d) theoretical calculations for  $\text{Pb}(\text{TiO})\text{Cu}_4(\text{PO}_4)_4$  (see Ref. [5] for details). The magnetic field was applied along the [110] axis. The inset of (a) shows a  $\text{Cu}_4\text{O}_{12}$  square cupola magnetic unit.



**Fig. 2.** Magnetic field dependence of magnetization ( $M$ ) and dielectric constant along the  $c$  axis ( $\epsilon_c$ ) obtained in (a) and (b) experiments and (c) and (d) theoretical calculations for  $\text{Sr}(\text{TiO})\text{Cu}_4(\text{PO}_4)_4$  (see Ref. [6] for details). The magnetic field was applied along the [110] axis.

and Sr systems.) These results demonstrate that magnetic square cupolas are promising ME-active structural units in the low magnetic field ( $B$ ) quadrupole phase. However, their ME activity in a  $B$ -induced phase, which appears commonly in these materials above 10 T, has not been elucidated. In this study, we have investigated ME properties in the  $B$ -induced phases of the Pb [5] and Sr [6] systems.

Figures 1(a) and 1(b) show a  $B$ -dependence of electric polarization along the  $c$  axis ( $P_c$ ) in the Pb system, together with magnetization along the [110] axis ( $M_{[110]}$ ) for comparison. The  $B$  along the [110] direction ( $B_{[110]}$ ) was applied with use of a pulsed magnet. It is observed that  $P_c$  develops upon the onset of the  $B$ -induced phase at 16.4 T. A clear  $PE$  hysteresis loop was observed at steady  $B$  of 18 T, confirming the ferroelectric nature. Moreover,  $P_{[001]}$  shows a  $B$ -induced sign reversal around 35 T. On the basis of the space group  $P4_212$  in the paramagnetic phase and the existence of finite  $M_{[110]}$  and  $P_c$ , a possible maximal magnetic point group of the  $B_{[110]}$ -induced phase is  $2'$ , which supports a cluster multipole moment composed of toroidal and magnetic moments. Contrary to the Pb case, no finite  $P_c$  was observed in the  $B_{[110]}$ -induced phase of the Sr system. Instead, as shown in Figs. 2(a) and 2(b), a sharp peak in the dielectric constant along the [001] axis ( $\epsilon_c$ ) appears at the transition field of  $\sim 15.0$  T. ( $\epsilon_c$  was measured up to 18 T using a superconducting magnet.) Considering the antiferroic stacking of magnetic layers at a low  $B$  quadrupole phase, the  $B_{[110]}$ -induced phase of the Sr system is expected to be antiferroelectric with a staggered electric polarization along the  $c$  axis.

To understand the origin for the experimental results, we have constructed a spin-1/2 effective model, in which a DM interaction between neighboring spins due to convex geometry is taken into account. As shown in Figs. 1(c) and 2(c), this model well reproduces the experimental  $M$  curves in both systems, which strongly supports the validity of our model analysis. Next, we evaluated the  $B_{[110]}$  dependence of  $P_c$  in the Pb system and  $\epsilon_c$  in the Sr system on the basis of the so-called exchange striction mechanism. As shown in Figs. 1(c) and 2(c), the calculated  $P_c$  and  $\epsilon_c$  are qualitatively in good agreement with experimental results. The analysis thus indicates that the exchange striction plays a prime role for the ME behavior from  $\text{Cu}_4\text{O}_{12}$  square cupolas in the  $B_{[110]}$ -induced phase. Moreover, a cluster multipole decomposition was applied to the calculated spin arrangement of square cupolas. The result shows that both toroidal and quadrupole moments become finite in each magnetic layer. This can explain the ferroelectricity and antiferroelectricity along the  $c$  axis induced by  $B_{[110]}$ .

The present results thus demonstrate that  $\text{Cu}_4\text{O}_{12}$  square cupolas are promising ME active structural units in a broad range of a magnetic field. Distinct types of ME-active multipole moments can appear in different phases. The convex shaped geometry of  $\text{Cu}_4\text{O}_{12}$  square cupolas plays an important role for the onset of such ME active multipole moments. This implies that not only the square cupola unit, but also other types of convex-shaped structural units are worth to be explored for new magnetoelectric materials.

#### References

- [1] K. Kimura *et al.*, Nat. Commun. **7**, 13039 (2016).
- [2] Y. Kato *et al.*, Phys. Rev. Lett. **118**, 107601 (2017).
- [3] P. Babkevich *et al.*, Phys. Rev. B **96**, 214436 (2017).
- [4] K. Kimura *et al.*, Phys. Rev. B **97**, 134418 (2018).
- [5] K. Kimura *et al.*, Phys. Rev. Mater. **2**, 104415 (2018).
- [6] Y. Kato *et al.*, Phys. Rev. B **99**, 024415 (2019).

#### Authors

K. Kimura<sup>a</sup>, Y. Kato<sup>b</sup>, K. Yamauchi<sup>c</sup>, A. Miyake, M. Tokunaga, A. Matsuo, K. Kindo, M. Akaki, M. Hagiwara, S. Kimura<sup>d</sup>, M. Toyoda<sup>e</sup>, Y. Motome<sup>b</sup>, and T. Kimura<sup>a</sup>  
<sup>a</sup>Department of Advanced Materials Science, University of Tokyo  
<sup>b</sup>Department of Applied Physics, The University of Tokyo  
<sup>c</sup>ISIR-SANKEN, Osaka University  
<sup>d</sup>Institute for Materials Research, Tohoku University  
<sup>e</sup>Tokyo Institute of Technology

## Electric Dipole Spin Resonance in the Interacting Quantum Spin Dimer System $\text{KCuCl}_3$

S. Kimura, M. Matsumoto, and M. Akaki

The observation of optical transition from spin singlet to triplet states by means of high frequency electron spin resonance (ESR) measurements is known as an advantageous tool to investigate the energy spectrum of quantum spin gap systems, such as a Haldane system or a spin ladder, in high accuracy. The transition has been reported for many spin gapped system, for instance  $\text{Ni}(\text{C}_2\text{H}_8\text{N}_2)_2\text{NO}_2\text{ClO}_4$  (NENP),  $\text{CuGeO}_3$  and  $\text{SrCu}_2(\text{BO}_3)_2$ . However, the singlet-triplet transition is, in principle, forbidden in magnetic dipole transition, and therefore the origin of its finite transition probability is not so clear at the moment.

Here we report on our recent high frequency ESR study on the  $S = 1/2$  interacting dimer system  $\text{KCuCl}_3$ . By measuring polarization dependence of the ESR signal, we have clarified that the singlet-triplet transition in this compound is due to the electric dipole transition [1]. In  $\text{KCuCl}_3$ , spin dimers composed of two  $\text{Cu}^{2+}$  spins form a three dimensional network in the monoclinic crystal. Reflecting this dimer structure, the ground state of this compound is the spin singlet state, and does not order down to the lowest temperature. From the previous measurements, two sets of the singlet-triplet transitions were observed [2]. The two sets of the singlet-triplet transitions are due to two kinds of the crystallographically different dimers in the unit cell of  $\text{KCuCl}_3$ , which gives rise to superposition of two kinds of the triplet excitation modes in the momentum space. To determine the selection rules of the singlet-triplet transition, we have performed the high frequency ESR measurements by illuminating linearly polarized electromagnetic wave to the sample.

Figure 1 shows the ESR signals from the singlet-triplet transition in  $\text{KCuCl}_3$  in external magnetic fields parallel to the  $b$  axis. Our experiment showed that both the lower and

# Emergent Transport Phenomena in the Course of Multiple Topological Transitions in $\text{MnSi}_{1-x}\text{Ge}_x$

N. Kanazawa, Y. Tokura, and M. Tokunaga

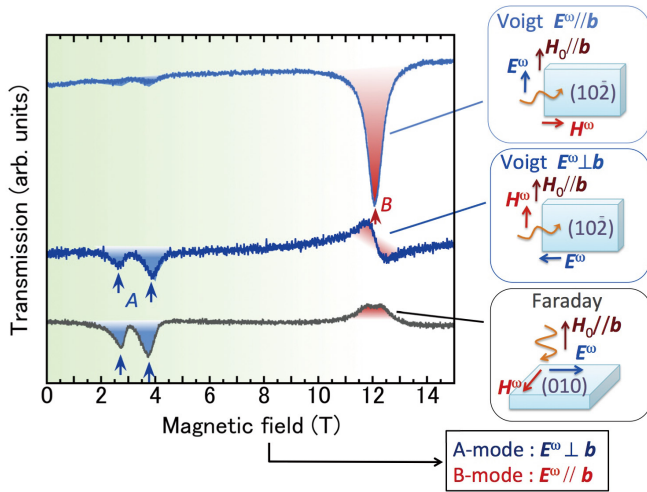


Fig. 1. ESR signals of the singlet-triplet transitions in  $\text{KCuCl}_3$ , observed in the Faraday and Voigt configurations. In the measurements in the Voigt configuration, linearly polarized electromagnetic wave is illuminated to the sample. The ESR signals *A* and *B* come from the higher and lower triplet excitation modes, respectively. The experimental result shows that both signals are electrically driven, and directions of the oscillating electric fields, which couples to *A* and *B*, are orthogonal each other.

higher energy triplet modes *A* and *B* couple with oscillating electric fields of the electromagnetic wave. Furthermore, the directions of the oscillating electric fields, which couple to the *A* and *B* modes, are orthogonal each other. These behaviors are explained by the spin dependent electric polarization. Recent studies for magnetoelectric multiferroic materials revealed that the vector spin chirality  $\mathbf{S}_i \times \mathbf{S}_j$ , which is an outer product of neighboring spin, induces an electric polarization  $\mathbf{P}$ , as  $\mathbf{P} = \hat{C} (\mathbf{S}_i \times \mathbf{S}_j)$ , where  $\hat{C}$  is a second rank tensor. Coupling between this  $\mathbf{P}$  and the oscillating electric fields  $Ee^{-i\omega t}$  can be regarded as a dynamical Dzyaloshinsky-Moriya (DM) interaction, oscillating with an angular frequency  $\omega$ . Because DM interaction has finite matrix elements between spin singlet and triplet states, the electric dipole transition between these states can occur. By taking into account the two-fold helical axis between the two dimers, the observed characteristic selection rule of the singlet-triplet transition is also explained. The electric polarization, generated by  $\mathbf{S}_i \times \mathbf{S}_j$ , can appear regardless of the local structural symmetry between the two spin sites. Therefore, electric dipole spin resonance by the spin-dependent electric polarization is universal for spin gapped systems. It is possible that the singlet-triplet transitions that were previously observed in various spin gapped materials are induced by this polarization mechanism.

## References

- [1] S. Kimura, M. Matsumoto, M. Akaki, M. Hagiwara, K. Kindo, and H. Tanaka, *Phys. Rev. B* **97**, 140406 (2018).
- [2] H. Tanaka, K. Takatsu, W. Shiramura, T. Kambe, H. Nojiri, T. Yamada, S. Okubo, H. Ohta, and M. Motokawa, *Physica B* **246-247**, 545 (1998).
- [3] H. Katsura, N. Nagaosa, and A. V. Balatsky, *Phys. Rev. Lett.* **95**, 057205 (2005).
- [4] T. A. Kaplan and S. D. Mahanti, *Phys. Rev. B* **83**, 174432 (2011).

## Authors

S. Kimura<sup>a</sup>, M. Matsumoto<sup>b</sup>, M. Akaki<sup>c</sup>, M. Hagiwara<sup>c</sup>, K. Kindo and H. Tanaka<sup>d</sup>

<sup>a</sup>Tohoku University

<sup>b</sup>Shizuoka University

<sup>c</sup>Osaka University

<sup>d</sup>Tokyo Institute of Technology

Interplay between topological spin textures and conduction electrons produces giant effective magnetic field called emergent magnetic field, leading to various electromagnetic functionalities for next-generation memory devices and energy-harvesting technology. Skyrmion and hedgehog spin structures are representative examples, which show two- and three-dimensional (2D and 3D) topological spin arrangements, respectively. Reflecting their topological properties, distinct emergent field distributions and each characteristic response are realized, i.e., flux-line- and monopole-like behaviors in skyrmion and hedgehog systems.

By synthesizing alloys of skyrmion- and hedgehog-hosting compounds ( $\text{MnSi}$  and  $\text{MnGe}$ ), we investigate the transformation process between skyrmion and hedgehog spin textures, where new type of topological phase transition is expected. We also perform high-magnetic field measurements on Hall resistivity to unravel the emergent field profiles upon complete unwinding those highly-stable magnetic knots. Precise transport measurements with  $\mu\Omega$ -resistance resolution were achieved by utilizing non-destructive pulse magnets energized by capacitor banks and a flywheel DC generator installed at International MegaGauss Science Laboratory of Institute for Solid State Physics (ISSP).

We have observed three different magnetic phases with varying composition  $x$  in  $\text{MnSi}_{1-x}\text{Ge}_x$ . As shown in the magnetic phase diagrams (Fig. 1), each magnetic phase exhibits a unique magnetic field value for the transition to ferromagnetic state (approximately 1 T for  $0 < x < 0.3$ , 10 T for  $0.3 < x < 0.7$ , and 20 T for  $0.7 < x < 1$ ), which is suggestive of the difference in topological property of the winding spin texture. In particular, we identified a new type of hedgehog lattice in  $\text{MnSi}_{1-x}\text{Ge}_x$  with intermediate composition  $x = 0.4 - 0.6$ , i.e., at the expected topological magnetic transition between the 2D skyrmion lattice (SkL) and the 3D hedgehog lattice (HL). This magnetic state consists of hedgehogs and anti-hedgehogs aligned in face-centered-cubic positions (Fig. 1). We also revealed emergent field profiles characteristic to each magnetic state as topological Hall effect (Fig. 2). There observed much difference in magnitudes and  $H$ -dependence, again contrasting the three topological phases.

In conclusion, we demonstrate the transitions among distinct topological spin textures, namely 2D SkL and two classes of 3D HLs, which are simply induced by controlling lattice constant or chemical pressure. The present study

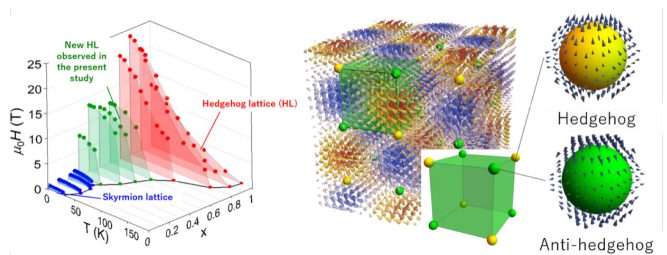


Fig. 1. (left) Variation of magnetic phase diagrams in  $\text{MnSi}_{1-x}\text{Ge}_x$ . The three colors represent different topological magnetic phases. (right) Schematic illustration of the new hedgehog lattice state identified in this study.

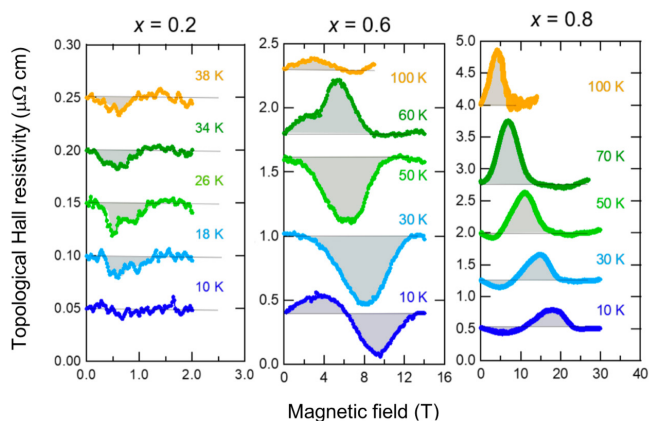


Fig. 2. Representative profiles of topological Hall resistivity for three different magnetic states ( $x = 0.2$  for SkL,  $x = 0.6$  for fcc HL, and  $x = 0.8$  for cubic HL).

suggests a new route for the direct manipulation of the spin-texture topology. Furthermore, the established precise high-field transport measurement technique will contribute to detection of emergent electromagnetic fields appearing as less-dissipative current and concomitant small resistance change.

#### References

[1] Y. Fujishiro, N. Kanazawa, T. Nakajima, X. Z. Yu, K. Ohishi, Y. Kawamura, K. Kakurai, T. Arima, H. Mitamura, A. Miyake, K. Akiba, M. Tokunaga, A. Matsuo, K. Kindo, T. Koretsune, R. Arita, and Y. Tokura, *J. Phys. Soc. Jpn.* **75**, 043707 (2006).

#### Authors

Y. Fujishiro<sup>a</sup>, N. Kanazawa<sup>a</sup>, T. Nakajima<sup>b</sup>, X. Z. Yu<sup>b</sup>, K. Ohishi<sup>c</sup>, Y. Kawamura<sup>c</sup>, K. Kakurai<sup>b,c</sup>, T. Arima<sup>b,d</sup>, H. Mitamura, A. Miyake, K. Akiba, M. Tokunaga, A. Matsuo, K. Kindo, T. Koretsune<sup>e</sup>, R. Arita<sup>a,b</sup>, and Y. Tokura<sup>a,b</sup>

<sup>a</sup>Department of Applied Physics, the University of Tokyo

<sup>b</sup>RIKEN Center for Emergent Matter Science (CEMS)

<sup>c</sup>Neutron Science and Technology Center, Comprehensive Research Organization for Science and Society (CROSS)

<sup>d</sup>Department of Advanced Materials Science, the University of Tokyo

<sup>e</sup>Tohoku University

## Ferromagnetic-to-Helimagnetic Transition in Cubic Perovskites $\text{Sr}_{1-x}\text{Ba}_x\text{CoO}_3$

H. Sakai, M. Tokunaga, and S. Ishiwata

Helimagnets have recently attracted great interest in terms of fundamental physics and (spin)electronic application, owing to their novel functions that simple ferromagnets have never attained. Typical examples include spin-spiral-driven ferroelectricity in perovskite-type manganites and current-driven motion of magnetic skyrmions in chiral magnets. However, since the helimagnetic order originates from several competing magnetic interactions, its emergence is highly limited by strong constraints on the lattice and spin systems.

Here we report the emergence of helimagnetism out of room-temperature ferromagnetism in simple cubic perovskites  $\text{Sr}_{1-x}\text{Ba}_x\text{CoO}_3$  by the negative chemical pressure (Fig. 1). By utilising a high-pressure technique, we have successfully grown a series of single crystals with systematical chemical compositions. With the isotropic lattice expansion by Ba substitution, room-temperature ferromagnetism for  $\text{SrCoO}_3$  is markedly suppressed, leading to incommensurate helimagnetism, while the simple cubic structure remains intact. High-resolution neutron diffraction the Ba-substituted

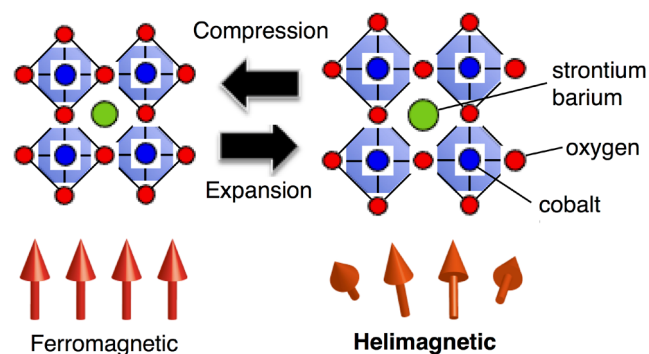


Fig. 1. Schematic illustration of the helimagnetic-ferromagnetic transition driven by the lattice expansion/compression in the cubic perovskite  $\text{Sr}_{1-x}\text{Ba}_x\text{CoO}_3$ .

compounds has revealed the helimagnetic correlation that evolves towards low temperatures in competition with ferromagnetic one [1].

Figure 2(a) shows the temperature dependence of the magnetisation  $M$  at 0.01 T for  $\text{Sr}_{1-x}\text{Ba}_x\text{CoO}_3$ , measured upon heating after a field cooling process. With increasing  $x$  from 0.1 to 0.35, the ferromagnetic Curie temperature  $T_C$  decreases systematically from 256 K to 176 K. For  $x = 0.35$ , the increase in  $M$  below  $T_C$  is largely reduced, and instead a clear drop in  $M$  upon cooling manifests itself at  $T_M$  ( $\sim 43$  K). For  $x = 0.4$ , the ferromagnetic transition disappears and the drop in  $M$  is more conspicuous. This corresponds to the onset of the helimagnetic correlations as revealed by the neutron diffraction experiments. To check the spin state of  $\text{Co}^{4+}$  ions upon Ba substitution, we have also measured the field profile of  $M$  at the lowest temperature (2–4 K) (Fig. 2(b)). For  $x = 0.1$ –0.3 with the ferromagnetic ground state, the  $M$  value is saturated above  $\sim 2$  T, whereas the saturation field is substantially enhanced with increasing  $x$  to 0.35, where the helimagnetic instability sets in. The value of  $M$  barely saturates at above  $\sim 30$  T for  $x = 0.35$ . From these data, we have found that the saturation moment is almost constant ( $\sim 2.2$ – $2.5 \mu_B/\text{Co}$ ) with  $x$  up to 0.35 in spite of a significant decrease in  $T_C$ . The spin state thus appears to remain in a nearly intermediate, i.e.,  $S = 3/2$ , configuration, which is likely to be strongly hybridised with the ligand hole states (see the inset to Fig. 2(b)).

Our results indicate that the subtle balance among the magnetic interactions can be controlled by the lattice size, i.e., bandwidth, which reflects the strong  $p$ - $d$  hybridization inherent in the unusually high-valence  $\text{Co}^{4+}$  state. The discovery of the helimagnetic order by expanding the simple

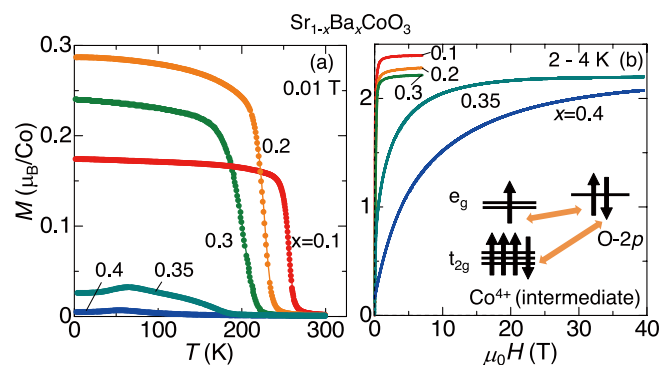


Fig. 2. (a) Temperature ( $T$ ) profiles of magnetisation ( $M$ ) at 0.01 T for  $\text{Sr}_{1-x}\text{Ba}_x\text{CoO}_3$  ( $0.1 \leq x \leq 0.4$ ) single crystals. (b) Field dependence of  $M$  at the lowest temperature (2–4 K) for  $x=0.1$ –0.4. The profiles up to  $\sim 40$  T were measured with a pulse magnet. Inset shows schematic diagram of intermediate spin configuration of  $\text{Co}^{4+}$ .  $L$  denotes an oxygen ligand hole.

cubic lattice provides a foundation for investigating the properties of many other crystalline materials.

#### Reference

[1] H. Sakai, S. Yokoyama, A. Kuwabara, J. S. White, E. Canévet, H. M. Rønnow, T. Koretsune, R. Arita, A. Miyake, M. Tokunaga, Y. Tokura, and S. Ishiwata, *Phys. Rev. Materials*, **2**, 104412 (2018).

#### Authors

H. Sakai<sup>a,b,c</sup>, S. Yokoyama<sup>a</sup>, A. Kuwabara<sup>a</sup>, A. Miyake, M. Tokunaga, Y. Tokura<sup>a</sup>, and S. Ishiwata<sup>a,c</sup>

<sup>a</sup>The University of Tokyo

<sup>b</sup>Osaka University

<sup>c</sup>PRESTO, JST

## Magnetic-Field-Induced Kondo Metal State in the Kondo Insulator YbB<sub>12</sub>

F. Iga, Y. H. Matsuda, and Y. Kohama

The Kondo effect is one of the most intensively studied many-particle correlation effects and induces intriguing phenomena such as heavy fermions and characteristic behaviors of electrons in quantum dots. There are rare materials in which insulating phases appear with development of the Kondo effect at low temperatures and they are termed Kondo insulator. Since most of the compounds with significant Kondo effect are metallic, the origin of formation of the charge gap has been attracting attention for a long time. Application of magnetic field ( $B$ ) is expected to control the electronic state of the Kondo insulator through the Zeeman effect, and the magnetic field induced insulator-metal (IM) transition actually occurs in the prototypical Kondo insulator YbB<sub>12</sub> at around 50 T [1]. The properties of the high-field metallic phase have never been well understood because the magnetic field required is rather high, which makes microscopic measurements difficult to perform.

Here we report on specific heat ( $C_p$ ) measurements of YbB<sub>12</sub> in high magnetic fields of up to 60 T. The techniques for measurements of specific heat in a pulsed magnetic field have been developed recently [2] and applied to researches of various kinds of materials. We found that the specific heat sharply increases as the IM transition takes place around 50 T. This largely enhanced value of specific heat coefficient ( $C_p/T$ ) strongly indicates that a large density of state (DOS) emerges at the Fermi energy and the electronic state corresponds to the Kondo metal state with heavy mass quasi particles.

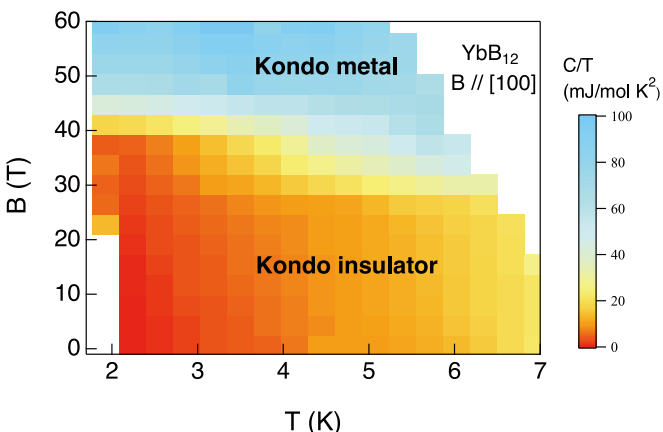


Fig. 1. The plot of the  $C_p/T$  in the  $B$ - $T$  plain with a color gradient scale. The Kondo metal phase appears in high magnetic fields.

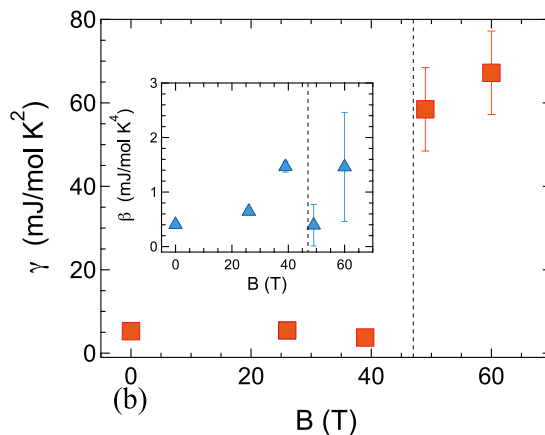


Fig. 2. Sommerfeld coefficient  $\gamma$  is plotted as a function of the magnetic field. The jump of  $\gamma$  to a large value is a direct evidence of appearance of a Kondo metal with heavy mass quasi particles.

Figure 1 shows a color plot image of the  $C_p/T$  in the  $B$ - $T$  plane. The Kondo metal state is found to appear in higher field region. Using the relation  $C_p/T = \gamma + \beta T^2$ , where the second term is due to phonon contribution with a constant  $\beta$ , the Sommerfeld coefficient  $\gamma$  is deduced from the temperature variation of  $C_p$ . The deduced  $\gamma$  is plotted as a function of the magnetic field in Fig. 2. A similar plot for  $\beta$  is shown in the inset. The vertical dashed lines denote the magnetic field where the IM transition takes place [3]. A distinct increase of  $\gamma$  occurs along with the IM transition, and the  $\gamma$  at a high-field metal phase is 58 mJ/(mol K<sup>2</sup>) and 67 mJ/(mol K<sup>2</sup>) at 49 T and 60 T, respectively. Although  $\beta$  may also have finite magnetic field dependence, it is relatively smaller than the large field-induced change in  $\gamma$  and can be ignored at low temperatures. It is also interesting to note that the obtained  $\gamma$  is as large as that in Kondo metals that exhibit strong valence fluctuations. For instance,  $\gamma$  is 50 mJ/(mol K<sup>2</sup>) in YbAl<sub>3</sub> and 130 mJ/(mol K<sup>2</sup>) in  $\alpha$ -YbAlB<sub>4</sub>. YbAl<sub>3</sub> is one of the typical valence fluctuation compounds, and  $\alpha$ -YbAlB<sub>4</sub> is the anisotropic heavy fermion compounds with significant valence fluctuations. From the value of  $\gamma$ , it is clearly concluded that the field-induced metal state in YbB<sub>12</sub> is regarded as a Kondo metal in the valence fluctuation regime [4].

We can evaluate the Kondo temperature  $T_K$  in the high-field Kondo metal phase. The entropy  $S$  in the field-induced metal can be estimated from the degeneracy  $W$  of the magnetic state of  $4f$  electrons in trivalent Yb ions. The ground state of the Yb<sup>3+</sup> ions in the cubic crystal field in YbB<sub>12</sub> is  $\Gamma_8$  and the  $W$  is 4. The excited  $\Gamma_6$  and  $\Gamma_7$  doublets are almost degenerated and located at a higher energy than  $\Gamma_8$  by about 23 meV. Since the energy gap (15 meV) collapses due to the Zeeman effect at the transition magnetic field and this energy scale is comparable to the excitation energy of the crystal field splitting (23 meV), the three  $\Gamma_{6,7,8}$  states more or less mix each other in high magnetic fields, and thus, the upper limit of  $W$  is 8. The  $S$  is safely evaluated to be between  $R \ln 4$  and  $R \ln 8$ , where  $R$  is the gas constant. Using the relation  $\gamma T_K \sim S$ ,  $T_K$  is deduced to be 172 K (for  $W = 4$ ) and 258 K (for  $W = 8$ ) at 60 T. The obtained  $T_K$  is comparable to that of  $\alpha$ -YbAlB<sub>4</sub> ( $T_K \sim 200$  K).

The theoretical work using dynamical mean field theory [5] predicts the appearance of the Kondo metal phase in high magnetic fields, whose Zeeman energy becomes comparable to the energy gap. According to this calculation, a sharp peak of DOS appears at the IM transition, and the calculated magnetization shows a steep increase at the transition that is in good agreement with the experimentally obtained results. The sharp peak can be considered as the field-induced Kondo

resonance peak. In even greater magnetic fields, the Kondo effect is expected to be sufficiently suppressed. The recent report on the magnetization process in YbB<sub>12</sub> suggests that the magnetic field for the Kondo breakdown is as high as 120 T [6].

#### References

- [1] K. Sugiyama, F. Iga, M. Kasaya, T. Kasuya, and M. Date, *J. Phys. Soc. Jpn.* **57**, 3946 (1988).
- [2] Y. Kohama, Y. Hashimoto, S. Katsumoto, M. Tokunaga, and K. Kindo, *Meas. Sci. Technol.* **24**, 115005 (2013).
- [3] F. Iga, K. Suga, K. Takeda, S. Michimura, K. Murakami, T. Takabatake, and K. Kindo, *J. Phys. Conf. Ser.* **200**, 012064 (2010).
- [4] T. T. Terashima, Y. H. Matsuda, Y. Kohama, A. Ikeda, A. Kondo, K. Kindo, and F. Iga, *Phys. Rev. Lett.* **120**, 257206 (2018).
- [5] T. Ohashi, A. Koga, S.-i. Suga, and N. Kawakami, *Phys. Rev. B* **70**, 245104 (2004).
- [6] T. T. Terashima, A. Ikeda, Y. H. Matsuda, A. Kondo, K. Kindo, and F. Iga, *J. Phys. Soc. Jpn.* **86**, 054710 (2017).

#### Authors

T. T. Terashima, Y. H. Matsuda, Y. Kohama, A. Ikeda, A. Kondo, K. Kindo, and F. Iga<sup>a</sup>  
<sup>a</sup>Ibaraki University

## Unconventional Field-Induced Spin Gap in an S = 1/2 Chiral Staggered Chain

P. A. Goddard, T. Sakakibara, and Y. Kohama

The dramatic effect of an alternating local spin environment on the properties of the spin-1/2 antiferromagnetic chain was first discovered through high-field neutron scattering and heat capacity experiments on copper-benzoate, which revealed the development of an energy gap on application of magnetic field [1]. This was perplexing until it was found that the behaviour of this system, and a handful of others, could be described by the sine-Gordon model of quantum-field theory [2,3]. Under the influence of the applied field, the gap emerges thanks to the presence of internal staggered fields and DM interactions that are a direct result of the staggered Cu(II) octahedra.

Here we report on the molecule-based chiral spin chain [Cu(pym)(H<sub>2</sub>O)<sub>4</sub>]SiF<sub>6</sub>·H<sub>2</sub>O (pym = pyrimidine), which at first glance could be a sine-Gordon chain, but with an added twist: a 4<sub>1</sub> screw (Fig.1(a)). Figure 1(b) shows the frequency

evolution of electron-spin resonance at 1.9 K. The observed resonances (black, red and blue (open) squares) cannot be explained by paramagnetic resonances of transition metals or conventional antiferromagnetic resonance. This behavior are reminiscent of excitations observed in the sine-Gordon spin chain [pym-Cu(NO<sub>3</sub>)<sub>2</sub>(H<sub>2</sub>O)<sub>2</sub>], where the branches were identified as breather modes of the sine-Gordon model, along with six other modes more difficult to classify [4]. However, the present observation *cannot* be modeled by the breather gaps proposed for sine-Gordon chains. Figure 1(c) shows the magnetic contribution ( $C_{\text{mag}}$ ) to heat capacity for a deuterated sample of [Cu(pym)(H<sub>2</sub>O)<sub>4</sub>]SiF<sub>6</sub>·H<sub>2</sub>O down to 100 mK. In zero field above 0.5 K, the nearly constant value of  $C_{\text{mag}}/T$  can be interpreted as the heat capacity of a uniform  $S = 1/2$  AF Heisenberg chain in the TLL state. The heat capacity measurement also reveal the field-induced gap in [Cu(pym)(H<sub>2</sub>O)<sub>4</sub>]SiF<sub>6</sub>·H<sub>2</sub>O. Given the similarities with the nonchiral staggered chains, the expression for the temperature dependence of  $C_{\text{mag}}$  derived from the sine-Gordon model will provide the best possible estimate of the gap at a particular magnetic field. However fitting our data to the sine-Gordon model yields a gap of  $\Delta_s = 1.98$  K at 13 T, significantly smaller than the expected value of 8.24 K, calculated using  $g_{2s}$  and  $J$  values obtained from ESR and magnetometry. More importantly, the field evolution of the gap exhibits  $\Delta_s \propto H$ , which is distinctly different from the expectation of the sine-Gordon model, where  $\Delta_s \propto H^{2/3}$ .

To recap, electron-spin resonance, magnetometry and heat capacity measurements reveal the presence of staggered  $g$  tensors, a rich low-temperature excitation spectrum, a staggered susceptibility and a spin gap that opens on the application of magnetic field. These phenomena are reminiscent of those previously observed in non-chiral sine-Gordon systems. In the present case, however, the size of the gap and its measured linear field dependence do not fit with the sine-Gordon model as it stands. We propose that the differences arise due to additional terms in the Hamiltonian resulting from the chiral structure [5].

#### References

- [1] D. C. Dender *et al.*, *Phys. Rev. Lett.* **79**, 1750 (1997).
- [2] M. Oshikawa and I. Affleck, *Phys. Rev. Lett.* **79**, 2883 (1997).
- [3] I. Affleck and M. Oshikawa, *Phys. Rev. B* **60**, 1038 (1999).
- [4] S. A. Zvyagin *et al.*, *Phys. Rev. Lett.* **93**, 027201 (2004).
- [5] J. Liu *et al.*, *Phys. Rev. Lett.* **122**, 057207 (2019).

#### Authors

J. Liu<sup>a</sup>, S. Kittaka, R. D. Johnson<sup>a</sup>, T. Lancaster<sup>b</sup>, J. Singleton<sup>c</sup>, T. Sakakibara, Y. Kohama, J. van Tol<sup>d</sup>, A. Ardavan<sup>a</sup>, B. H. Williams<sup>a</sup>, S. J. Blundell<sup>a</sup>, Z. E. Manson<sup>c</sup>, J. L. Manson<sup>c</sup>, and P. A. Goddard<sup>f</sup>  
<sup>a</sup>University of Oxford  
<sup>b</sup>Durham University  
<sup>c</sup>National High Magnetic Field Laboratory, Los Alamos National Laboratory  
<sup>d</sup>National High Magnetic Field Laboratory, Florida State University  
<sup>e</sup>Eastern Washington University  
<sup>f</sup>University of Warwick

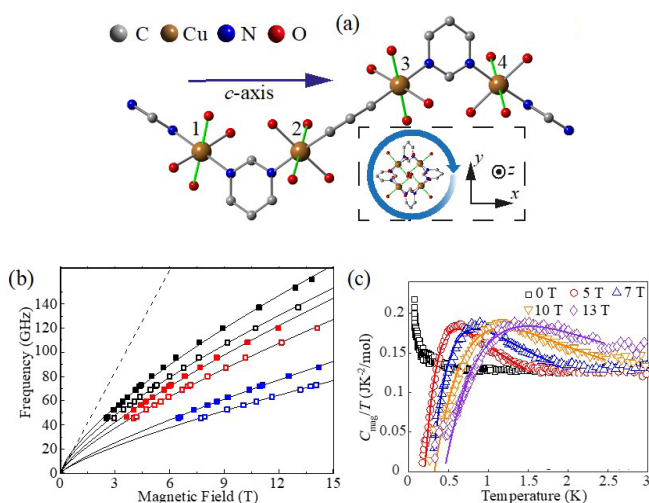


Fig. 1. (a) Chiral structure of [Cu(pym)(H<sub>2</sub>O)<sub>4</sub>]SiF<sub>6</sub>·H<sub>2</sub>O. (b) Excitations observed via electron-spin resonance at 1.9 K. (c) Temperature dependence of the magnetic contribution to heat capacity at different applied fields showing the opening of a field-induced gap. Lines are fits to a gapped model.

## Oxygen-Functionalization of Graphene Enhances CO<sub>2</sub> Adsorption under Near-Ambient Conditions

S. Yamamoto, J. Yoshinobu, and I. Matsuda

The functionalization of graphene is important in practical applications of graphene, such as in heterogeneous catalysts. The adsorption of molecules on functional-

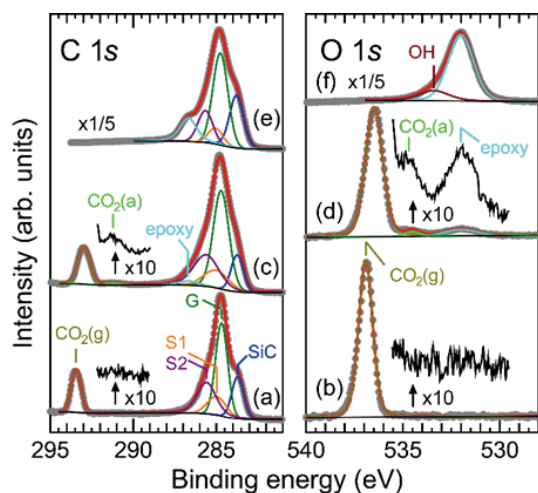


Fig. 1. (a, b) C 1s and O 1s XPS spectra of the pristine epitaxial graphene measured in 1.6 mbar CO<sub>2</sub> at 175 K. (c, d) C 1s and O 1s XPS spectra of the oxygen-functionalized epitaxial graphene measured in 1.6 mbar CO<sub>2</sub> at 175 K. (e, f) C 1s and O 1s XPS spectra of the oxygen-functionalized epitaxial graphene measured in UHV at 199 K after evacuating the CO<sub>2</sub>. The incident photon energy was 740 eV. The photon flux densities were  $1.0 \times 10^{16}$  photons/s·cm<sup>2</sup> for (a, b),  $7.3 \times 10^{16}$  photons/s·cm<sup>2</sup> for (c, d), and  $1.5 \times 10^{16}$  photons/s·cm<sup>2</sup> for (e, f). The XPS spectra were normalized with the photon flux densities.

ized graphene is an important elementary step in catalytic reactions on graphene. Despite its importance, however, experimental approaches to clarify the interactions of adsorbed molecules with functionalized graphene are limited. Especially, the experiments in ambient conditions at which catalysts are operated have been challenging.

In this study [1], the adsorption of CO<sub>2</sub> on an oxygen-functionalized epitaxial graphene surface was studied at near-ambient conditions using ambient-pressure X-ray photoelectron spectroscopy (AP-XPS). Monolayer epitaxial graphene on SiC(0001) was used in this study. The oxygen-functionalization of graphene was achieved *in-situ* by the photo-induced dissociation of CO<sub>2</sub> with X-rays on graphene in a CO<sub>2</sub> gas atmosphere. AP-XPS experiments were performed at SPring-8 BL07LSU.

Figures 1(a) and (b) shows C 1s and O 1s XPS spectra of the graphene surface measured under 1.6 mbar CO<sub>2</sub> at 175 K. Except for the spectral features of the substrate (Graphene(G), SiC, and buffer layer (S1 and S2)) and gas-phase CO<sub>2</sub> (CO<sub>2</sub>(g)), no adsorbed CO<sub>2</sub> molecules were observed on graphene under the present condition. When the photon flux density was increased by a factor of ~7 under the same conditions of CO<sub>2</sub> gas pressure and sample temperature, C 1s and O 1s XPS spectra were changed (Figs. 1(c, d)). New small peaks at 291.2 eV in C 1s and at 534.7 eV in O 1s XPS spectra were ascribed to adsorbed CO<sub>2</sub> [2]. Figures 1(e) and (f) show the C 1s and O 1s XPS spectra measured in ultrahigh vacuum after evacuating CO<sub>2</sub> gas. After gas evacuation, neither adsorbed CO<sub>2</sub> nor gas-phase CO<sub>2</sub> were observed. Therefore, CO<sub>2</sub> molecules were only present on graphene under near-ambient pressure gas at 175 K. When CO<sub>2</sub> molecules were adsorbed on the graphene surface, additional XPS features were observed at 532.0 eV in O 1s and 286.7 eV in C 1s XPS spectra (Figs. 1(c, d)). These features were assigned to epoxy (C-O-C) group on graphene. The photo-induced dissociation of CO<sub>2</sub> molecules (CO<sub>2</sub> → CO + O) at high X-ray photon flux causes the formation of epoxy groups on graphene. The oxygen-functionalized graphene surface binds CO<sub>2</sub> molecules more strongly than the pristine graphene surface.

The increase in the adsorption energy of CO<sub>2</sub> on the

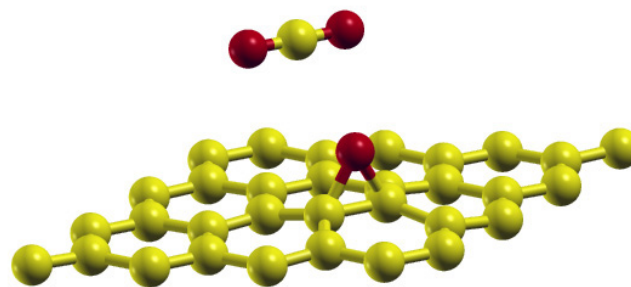


Fig. 2. The structural model of CO<sub>2</sub> adsorbed on the oxygen-functionalized graphene. The oxygen species on graphene is an epoxy (C-O-C) group.

oxygen-functionalized graphene surface was further investigated by first-principles calculations with the van der Waals density functional (vdW-DF) method. The adsorption energy of CO<sub>2</sub> was increased by ~5 kJ/mol from 20.2 kJ/mol on the pristine graphene surface [2] to 25.7 kJ/mol on the oxygen-functionalized graphene surface. This was in good agreement with the experimental value ( $\geq 5$  kJ/mol) derived from an adsorption and desorption equilibrium relationship. In addition, first-principles calculations revealed that the most stable adsorption site of CO<sub>2</sub> on the oxygen-functionalized graphene surface was not on top of the epoxy group, but on the C-C bond of graphene adjacent to the epoxy group (Fig. 2). The adsorption of CO<sub>2</sub> on the oxygen-functionalized graphene surface was stabilized by both the electrostatic interactions between the CO<sub>2</sub> and epoxy group and the vdW interactions between the CO<sub>2</sub> and graphene. The detailed understanding of the interaction between CO<sub>2</sub> and the oxygen-functionalized graphene surface obtained in the present study may assist in developing guidelines for designing novel graphene-based catalysts.

#### References

- [1] S. Yamamoto, K. Takeuchi, Y. Hamamoto, R.-Y. Liu, Y. Shiozawa, T. Koitaya, T. Someya, K. Tashima, H. Fukidome, K. Mukai, S. Yoshimoto, M. Suemitsu, Y. Morikawa, J. Yoshinobu, and I. Matsuda, *Phys. Chem. Chem. Phys.* **20**, 19532 (2018).
- [2] K. Takeuchi, S. Yamamoto, Y. Hamamoto, Y. Shiozawa, K. Tashima, H. Fukidome, T. Koitaya, K. Mukai, S. Yoshimoto, M. Suemitsu, Y. Morikawa, J. Yoshinobu, and I. Matsuda, *J. Phys. Chem. C* **121**, 2807 (2017).

#### Authors

S. Yamamoto, K. Takeuchi, Y. Hamamoto<sup>a</sup>, R.-Y. Liu, Y. Shiozawa, T. Koitaya, T. Someya, K. Tashima<sup>b</sup>, H. Fukidome<sup>b</sup>, K. Mukai, S. Yoshimoto, M. Suemitsu<sup>b</sup>, Y. Morikawa<sup>a</sup>, J. Yoshinobu, and I. Matsuda

<sup>a</sup>Osaka University  
<sup>b</sup>Tohoku University

## Ultrafast Control of a Ferroelectricity with Dynamic Repositioning of Proton in a Supermolecular Cocrystal

T. Umanodan, Y. Okimoto, and J. Itatani

Recent progress of intense THz and mid-IR (MIR) sources has opened a new opportunity in solid state physics. The small photon energy that is associated to long wavelength enables to nondestructively apply intense optical fields (~10 MV/cm or higher) to condensed matters because multiphoton ionization followed by catastrophic optical damage is unlikely to occur. When materials, especially crystalline materials, are exposed to such intense

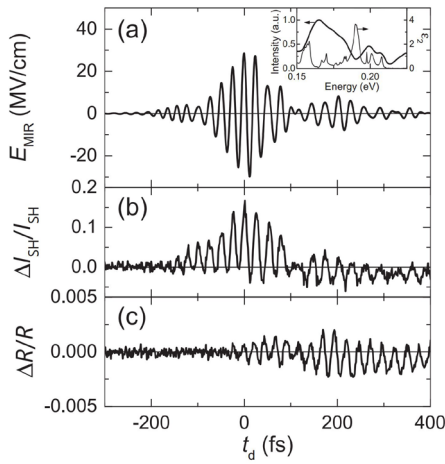


Fig. 1. (a) Waveform of the MIR pulse used for photoexcitation. The inset depicts the power spectrum of the pulse. The thin line shows the  $\epsilon_2$  spectrum of Hdppz-Hca. (b) and (c) Time profile of  $\Delta I_{SH}/I_{SH}$  (b) and relative change in the reflectivity ( $\Delta R/R$ ) (c) in the presence of a MIR field.

optical fields, many nontrivial exotic phenomena (e.g., high harmonic generation in solids) start to occur.

In this work, we explored the possibility of ultrafast control of ferroelectricity in a supraziramoferroelectric cocrystal composed of protonated 2,3-di(2-pyridinyl) pyrazine (Hdppz) and deprotonated chloranilic acid (Hca). The crystal becomes ferroelectric due to proton ordering below the Curie point ( $T_c = 402$  K), where the protons take two stable positions between the Hdppz and Hca molecules. We used intense THz and MIR pulses with stable carrier envelope phases, and probed the symmetry breaking in the presence of optical field using 6.5-fs optical pulses. This pulse duration is shorter than one oscillation period of the driving low frequency field, which allows to look into field-induced proton dynamics on sub-cycle time scales of the MIR field. We measured second harmonic of ultrashort visible pulses as a signature of inversion symmetry breaking due to proton displacement.

Figure 1(a) and (b) show the electric field waveform of the intense MIR pulses and observed change of second harmonic (SH) signals, respectively. Although the MIR field contains multiple cycles (i.e., the envelopes of the positive and negative polarity are identical), observed SH signal follows the optical waveform of the positive polarity alone. This behavior is well reproduced by a classical model depicted in Fig. 2. In this model, we included anharmonic potential and molecular vibration whose resonant frequency is within the MIR spectrum. As shown in the inset in Fig. (a), the spectrum of driving MIR pulse has an overlap with an absorption peak of C-O<sup>-</sup> stretching mode, leading to the displacement of equilibrium point in the presence of MIR fields. Contrary, with an intense THz field, the change of SH signals was observed to be proportional to the instantaneous field amplitude.

In summary, using intense THz and MIR pulses, we observed field-induced symmetry breaking in Hdppz-Hca molecular crystals. This process can be understood as the proton displacement that can follow the oscillating optical field up to  $\sim 100$  THz. The results suggest that repositioning of protons and resulting ferroelectricity can be dynamically controlled by the optical waveform of intense optical pulses. We expect that more exotic nonlinear responses will be discovered in future, leading to a foundation of PHZ optoelectronics.

## Reference

[1] T. Umanodan, K. Kaneshima, K. Takeuchi, N. Ishii, J. Itatani, H. Hirori, Y. Sanari, K. Tanaka, Y. Kanemitsu, T. Ishikawa, S. Koshihara, S. Horiuchi, and Y. Okimoto, *J. Phys. Soc. Jpn.* 88, 013705 (2019). [Selected as an Editors' Choice]

## Authors

T. Umanodan<sup>a</sup>, K. Kaneshima, K. Takeuchi, N. Ishii, J. Itatani, H. Hirori<sup>b</sup>, Y. Sanari<sup>b</sup>, K. Tanaka<sup>b</sup>, Y. Kanemitsu<sup>b</sup>, T. Ishikawa<sup>a</sup>, S. Koshihara<sup>a</sup>, S. Horiuchi<sup>c</sup>, and Y. Okimoto<sup>a</sup>

<sup>a</sup>Tokyo Institute of Technology

<sup>b</sup>Kyoto University

<sup>c</sup>National Institute of Advanced Industrial Science and Technology (AIST)

## Tensile-Strain-Dependent Spin States in Epitaxial LaCoO<sub>3</sub> Thin Films

Y. Yokoyama, H. Wadati, and Y. Harada

In transition metal compounds, charge, spin, and orbital degrees of freedom by a strong electron correlation realize various physical phenomena such as superconductivity, metal-insulator transition, and charge ordering [1]. The perovskite-type cobalt oxide LaCoO<sub>3</sub> is one of the most interesting materials because of its various electron degrees of freedom. Since the spin state of LaCoO<sub>3</sub> is sensitive to the crystal field, a spin crossover from the low-spin (LS) to high-spin (HS) state is shown by increasing the temperature [2]. Epitaxial strain can also influence the spin states and a ferromagnetism is observed in LaCoO<sub>3</sub> thin films at lower temperatures ( $\leq 85$  K) [3–5]. In previous studies, the spin states of the thin films were considered by the orderings of 3d electrons on the basis of resonant x-ray diffraction [3–5]. However, direct observations of the electronic structures are important to clarify the spin states. Since it is difficult to determine the spin states by conventional techniques such as x-ray absorption spectroscopy (XAS), we performed resonant inelastic soft x-ray scattering (RIXS) with Co 2p  $\rightarrow$  3d  $\rightarrow$  2p process (L edge) [6]. The RIXS is one of the most powerful techniques to clarify the spin states by observing the d-d excitations.

The LaCoO<sub>3</sub> epitaxial thin films (30 nm thickness) were fabricated on LSAT(110) and LSAT(111) [(LaAlO<sub>3</sub>)<sub>0.3</sub>(SrAl<sub>0.5</sub>Ta<sub>0.5</sub>O<sub>3</sub>)<sub>0.7</sub>] substrates by pulsed laser deposition

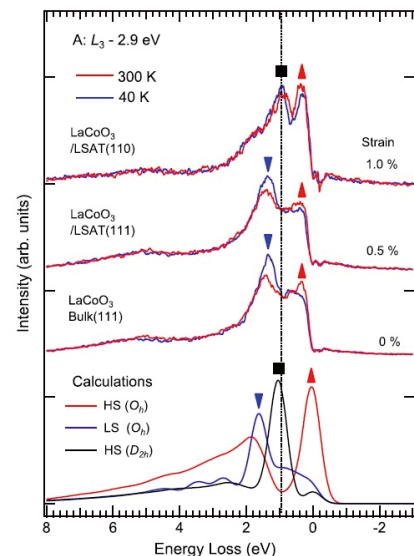


Fig. 1. Comparison of the experimental RIXS spectra excited with A:  $L_3$  -2.9 eV ( $776.5$  eV) measured at 40 and 300 K and the theoretical ones in  $O_h$  and  $D_{2h}$  symmetries.

technique. The same substrates with different orientations enable us to observe the pure strain effects on XAS and RIXS spectra. The lattice constant of the LSAT substrate is 3.868 Å, while that of the LaCoO<sub>3</sub> bulk is 3.804 Å, indicating that tensile strains are applied to the LaCoO<sub>3</sub> epitaxial thin films grown on LSAT substrates. The magnitude of the tensile strains from LSAT(110) and LSAT(111) substrates are 1.0% and 0.5%, respectively (strains are defined as the ratio of the cubic root of the unit cell volume) [3,4]. The experiments of XAS and RIXS were performed at BL07LSU HORNET, SPring-8 [7]. The RIXS measurements were performed with soft x-ray from 770 to 810 eV (Co L<sub>3</sub> and L<sub>2</sub> edge). In the range of the x-ray energy, the energy resolution is ~ 300 meV.

The comparison of the experimental RIXS spectra excited with A: L<sub>3</sub> -2.9 eV (776.5 eV) measured at 40 and 300 K and the theoretical ones with several electronic states are shown in Fig. 3. The peaks observed at around 0.3 eV is assigned to the excitations from the HS ground states. On the other hand, the peaks at 1.3 eV observed correspond to the excitations from the LS ground states. However, the peaks at 1.0 eV in LaCoO<sub>3</sub>/LSAT(110) cannot be explained by either the LS or HS with  $O_h$  symmetry. By comparing with the theoretical spectra, the peak for the HS state is shifted to 1.0 eV by lowering the symmetry from  $O_h$  to  $D_{2h}$ , indicating that the spin state of LaCoO<sub>3</sub>/LSAT(110) consists of the HS states with different local symmetries, i.e., the mixture of  $O_h$  and  $D_{2h}$  symmetries.

In this study, we performed RIXS measurements and revealed that the spin states of Co ions were different between the bulk crystal and the thin film crystals. Although it is difficult to observe the strain effects on the spin states with conventional XAS measurements, clear difference can be probed with the use of RIXS.

#### References

- [1] M. Imada *et al.*, Rev. Mod. Phys. **70**, 277 1039 (1998).
- [2] M.W. Haverkort *et al.*, Phys. Rev. Lett. **97**, 176405 (2006).
- [3] J. Fujioka *et al.*, Phys. Rev. Lett. **111**, 027206 (2013).
- [4] J. Fujioka *et al.*, Phys. Rev. B **92**, 195115 (2015).
- [5] Y. Yamasaki *et al.*, J. Phys. Soc. Jpn. **85**, 023704 (2016).
- [6] Y. Yokoyama *et al.*, Phys. Rev. Lett. **120**, 206402 (2018).
- [7] Y. Harada *et al.*, Rev. Sci. Instrum. **83**, 013116 (2012).

#### Authors

Y. Yokoyama, Y. Yamasaki, M. Taguchi, Y. Hirata, K. Takubo, J. Miyawaki, Y. Harada, D. Asakura, J. Fujioka, M. Nakamura, H. Daimon, M. Kawasaki, Y. Tokura, and H. Wadati

## Photo-Induced Semimetallic States Realized in Electron–Hole Coupled Insulators

K. Okazaki, T. Mizokawa, and S. Shin

Using light to manipulate materials into desired states is one of the goals in condensed matter physics, since light control can provide ultrafast and environmentally friendly photonics devices. However, it is generally difficult to realize a photo-induced phase which is not merely a higher entropy phase corresponding to a high-temperature phase at equilibrium.

Here, we report realization of photo-induced insulator-to-metal transitions in Ta<sub>2</sub>Ni(Se<sub>1-x</sub>S<sub>x</sub>)<sub>5</sub> including the excitonic insulator phase using time- and angle-resolved photoemission spectroscopy (TARPES) [1]. From the dynamic proper-

ties of the system, we determine that screening of excitonic correlations plays a key role in the timescale of the transition to the metallic phase, which supports the existence of an excitonic insulator phase at equilibrium. The nonequilibrium metallic state observed unexpectedly in the direct-gap excitonic insulator opens up a new avenue to optical band engineering in electron–hole coupled systems.

Figure 1 shows the time-integrated TARPES spectra before and after pumping. After photo-excitation, both the electron and hole bands cross  $E_F$  at the same Fermi momentum  $k_F \sim 0.1 \text{ \AA}^{-1}$  as schematically shown by the red and blue parabolas in Fig. 1b. This may indicate that the hybridization between the two Ta chains is sufficiently strong to lift the degeneracy. However, since this is not predicted by band-structure calculations, this behavior of the emerging of the hole and electron bands crossing  $E_F$  at the same  $k_F$  is a surprising nature of the observed non-equilibrium metallic phase, indicating that the observed nonequilibrium metallic state is entirely different from the high temperature phase in the equilibrium state.

To confirm that the observed non-equilibrium metallic phase of Ta<sub>2</sub>NiSe<sub>5</sub> can be associated with the excitonic condensation, we have performed comparative TARPES measurements on Ta<sub>2</sub>NiS<sub>5</sub>. Quite unexpectedly, an electron band emerges above  $E_F$  and the hole band below  $E_F$  shifts upward. In addition, the bottom of the electron band and the top of the hole band seems to cross  $E_F$ , and the system seems likely to be semimetallic. This may require reconsidering the nature of the insulating phase for Ta<sub>2</sub>NiS<sub>5</sub>, which had been considered as an ordinary band insulator.

The non-equilibrium metallic phases observed for both of Ta<sub>2</sub>NiSe<sub>5</sub> and Ta<sub>2</sub>NiS<sub>5</sub> should suggest that these photo-induced phase transitions are not merely transitions to higher entropy states that can be realized at high temperatures in the equilibrium state. Thus, photo-excitation can be considered to induce similar effects to pressure. Since the pressure-induced superconducting phase has been found for Ta<sub>2</sub>NiSe<sub>5</sub>, with some appropriate pumping condition probably with lower photon energy of some resonant condition, photo-induced superconductivity might be realized for

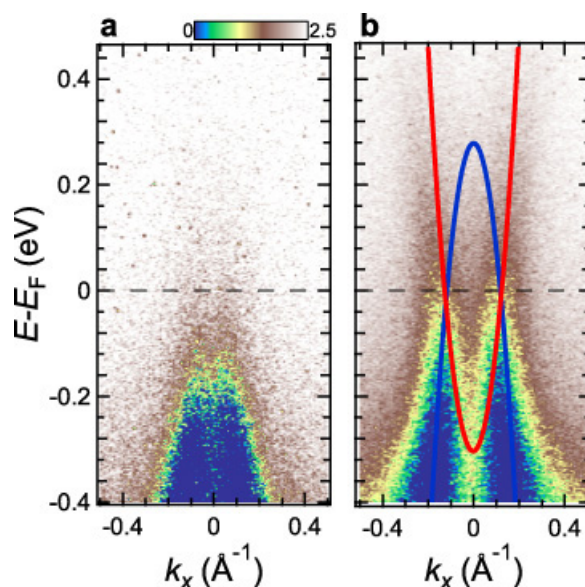


Fig. 1. TARPES spectra of Ta<sub>2</sub>NiSe<sub>5</sub> before and after pumping. **a** Energy–momentum ( $E$ - $k$ ) map before pumping, integrated in the time interval  $[-0.29, 0]$  ps. **b** Corresponding map of the transient states, integrated in  $[0, 1.2]$  ps. Red and blue parabolas indicate the electron and hole bands crossing  $E_F$  in the non-equilibrium metallic state. These spectra were acquired with a pump fluence of  $1.56 \text{ mJ/cm}^2$ .

this material. Realization of this fascinating photo-induced phase would be one of the ultimate goals of investigations of the photo-excited electronic state.

#### Reference

[1] K. Okazaki, Y. Ogawa, T. Suzuki, T. Yamamoto, T. Someya, S. Michimae, M. Watanabe, Y.-F. Lu, M. Nohara, H. Takagi, N. Katayama, H. Sawa, M. Fujisawa, T. Kanai, N. Ishii, J. Itatani, T. Mizokawa, and S. Shin, *Nat. Commun.* **9**, 4322, (2018).

#### Authors

K. Okazaki, Y. Ogawa, T. Suzuki, T. Yamamoto, T. Someya, S. Michimae, M. Watanabe, Y.-F. Lu<sup>a</sup>, M. Nohara<sup>b</sup>, H. Takagi<sup>a,c</sup>, N. Katayama<sup>d</sup>, H. Sawa<sup>d</sup>, M. Fujisawa, T. Kanai, N. Ishii, J. Itatani, T. Mizokawa<sup>c</sup>, and S. Shin

<sup>a</sup>University of Tokyo

<sup>b</sup>Okayama University

<sup>c</sup>Max Planck Institute for Solid State Research

<sup>d</sup>Nagoya University

<sup>e</sup>Waseda University

# Progress of Facilities

## Supercomputer Center

The Supercomputer Center (SCC) is a part of the Materials Design and Characterization Laboratory (MDCL) of ISSP. Its mission is to serve the whole community of computational condensed-matter physics of Japan, providing it with high performance computing environment. In particular, the SCC selectively promotes and supports large-scale computations. For this purpose, the SCC invites proposals for supercomputer-aided research projects and hosts the Steering Committee, as mentioned below, that evaluates the proposals.

The ISSP supercomputer system consists of two subsystems: System B is intended for larger total computational power and has more nodes with relatively loose connections whereas System C is intended for higher communication speed among nodes. System B is SGI ICE XA / UV hybrid system that consists of FAT nodes with large memory, CPU nodes based on Intel Xeon, and ACC node enhanced by GPGPU accelerator. Its theoretical performance is 2.6 PFLOPS. System C is HPE SGI 8600 with 0.77 PFLOPS.

In addition to the hardware administration, the SCC puts increasing effort on the software support. Since 2015, the SCC has been conducting "Project for advancement of software usability in materials science". In this project, for enhancing the usability of the ISSP supercomputer system, we perform some software-advancement activity such as developing new application software that runs efficiently on the ISSP supercomputer system, adding new functions to existing codes, help releasing private codes for public use, writing/improving manuals for public codes. Two target programs were selected in fiscal year 2018 and developed software were released as DSQSS (proposal made by A. Masaki (RIKEN)) and RESPACK (proposal made by K. Nakamura (Kyutech)). The SCC is also providing a service for porting users' software to General Purpose GPUs

(GPGPU).

All staff members of university faculties or public research institutes in Japan are invited to propose research projects (called User Program). The proposals are evaluated by the Steering Committee of SCC. Pre-reviewing is done by the Supercomputer Project Advisory Committee. In fiscal year 2018, totally 283 projects were approved. The total points applied and approved are listed on Table. 1 below. Additionally, we supported post-K and other computational materials science projects through Supercomputing Consortium for Computational Materials Science (SCCMS).

The research projects are roughly classified into the following three (the number of projects approved):

First-Principles Calculation of Materials Properties (131)  
Strongly Correlated Quantum Systems (33)  
Cooperative Phenomena in Complex, Macroscopic Systems (119)

In all the three categories, most proposals involve both methodology and applications. The results of the projects are reported in 'Activity Report 2018' of the SCC. Every year 3-4 projects are selected for "invited papers" and published at the beginning of the Activity Report. In the Activity Report 2018, the following three invited papers are included:

"Development of Open-Source Software mVMC and its Applications", Takahiro Misawa, Yuichi Motoyama, and Kota Ido (ISSP, U. Tokyo)

"First-Principles Studies on Anomalous Electron and Spin Transport Properties in Non-Trivial Spin Textures", Fumiyuki ISHII (Kanazawa U.)

"Coarse-Grained Force Field for Lipid Domain Formation Simulations", Sangjae Seo, and Wataru Shinoda (Nagoya U.)

Class	Max Points		Application	Number of Projects	Total Points			
	System B	System C			Applied		Approved	
					System B	System C	System B	System C
A	100	50	any time	20	2.0k	1.0k	2.0k	1.0k
B	1k	100	twice a year	70	64.2k	3.5k	42.6k	2.9k
C	10k	1k	twice a year	168	1395.3k	77.2k	620.0k	62.0k
D	10k	1k	any time	8	42.3k	3.0k	30.0k	2.5k
E	30k	3k	twice a year	17	490.0k	46.0k	279.5k	39.8k
S			twice a year	0	0	0	0	0
SCCMS				25	235.5k	19.1k	235.5k	19.1k
Total				308	2229.3k	149.7k	1209.6k	127.3k

Table 1. Research projects approved in 2018

The maximum points allotted to the project of each class are the sum of the points for the two systems; Computation of one node for 24 hours corresponds to one points for the CPU nodes of System B and System C. The FAT and ACC nodes require four and two points for a 1-node 24-hours use, respectively.

## Neutron Science Laboratory

The Neutron Science Laboratory (NSL) has been playing a central role in neutron scattering activities in Japan since 1961 by performing its own research programs as well as providing a strong General User Program for the university-owned various neutron scattering spectrometers installed at the JRR-3 (20MW) operated by Japan Atomic Energy Agency (JAEA) in Tokai. In 2003, the Neutron Scattering Laboratory was reorganized as the Neutron Science Laboratory to further promote the neutron science with use of the instruments in JRR-3. Under the General User Program supported by NSL, 14 university-group-owned spectrometers in the JRR-3 reactor are available for a wide scope of researches on material science, and proposals close to 300 are submitted each year, and the number of visiting users under this program reaches over 6000 person-day/year. In 2009, NSL and Neutron Science Division (KENS), High Energy Accelerator Research Organization (KEK) built a chopper spectrometer, High Resolution Chopper Spectrometer, HRC, at the beam line BL12 of MLF/J-PARC (Materials and Life Science Experimental Facility, J-PARC). HRC covers a wide energy and Q-range ( $10\mu\text{eV} < \hbar\omega < 2\text{eV}$  and  $0.02\text{\AA}^{-1} < Q < 50\text{\AA}^{-1}$ ), and therefore becomes complementary to the existing inelastic spectrometers at JRR-3. HRC started to accept general users through the J-PARC proposal system in FY2011.

Triple axis spectrometers, HRC, and a high resolution powder diffractometer are utilized for a conventional solid state physics and a variety of research fields on hard-condensed matter, while in the field of soft-condensed matter science, researches are mostly carried out by using the small angle neutron scattering (SANS-U) and/or neutron spin echo (iNSE) instruments. The upgraded time-of-flight (TOF) inelastic scattering spectrometer, AGNES, is also available through the ISSP-NSL user program.

Scientific outputs from HRC in FY2018 covers wide range in magnetism and strongly correlated electrons. One of the research highlights is the study on quantum phase transition in the singlet-ground-state antiferromagnet  $\text{CsFeCl}_3$  [1]. Even though the HRC spectrometer is designed for inelastic neutron scattering measurement, the use of white beam allows us to measure Laue spots. Temperature evolution of the Laue spot at  $\mathbf{q} = (1/3, 1/3, 0)$  at 1.4 GPa in Fig. 1(a) evidences the existence of the pressure-induced magnetic Bragg peak at the  $\mathbf{q}$  in  $\text{CsFeCl}_3$ . Combination of further measurements using a neutron diffractometer ZEBRA and magnetic structure analysis reveals a  $120^\circ$  structure with a propagation vector of  $\mathbf{k}_{\text{mag}} = (1/3, 1/3, 0)$ . The estimated critical exponent of the order parameter suggests that  $\text{CsFeCl}_3$  belongs to the universality class of  $U(1)\times Z_2$

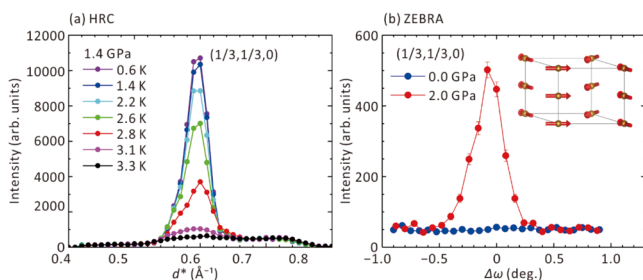


Fig. 1. (a) Temperature dependence of magnetic Bragg peak measured at HRC spectrometer. (b) Neutron diffraction profiles at 0.0 and 2.0 GPa measured at ZEBRA spectrometer. The inset exhibits the determined magnetic structure.

symmetry which is expected to realize the chiral liquid state.

Technical progress of HRC spectrometer was the development of high pressure environment. Cylinder-type cell made of CuBe alloy was designed by Prof. Uwatoko. The volume for the sample space is 5 mm in diameter and 20 mm in length. The maximum pressure is 1.4 GPa. The measurement was performed on 0.4g of  $\text{CsFeCl}_3$  sample. 1 K cryostat was used to achieve 0.7 K, and the power of the J-PARC operation was 400 kW. Well-defined spin wave was successfully measured in the pressure-induced magnetic phase in  $\text{CsFeCl}_3$ .

The NSL also operates the U.S.-Japan Cooperative Program on neutron scattering, providing further research opportunities to material scientists who utilize the neutron scattering technique for their research interests. In 2010, relocation of the U.S.-Japan triple-axis spectrometer, CTAX, was completed, and it is now open to users.

<https://neutrons.ornl.gov/ctax>

[1] S. Hayashida et al., Phys. Rev. B 97, 140405(R) (2018).

## International MegaGauss Science Laboratory

The objective of this laboratory (Fig. 1) is to study the physical properties of solid-state materials (such as semiconductors, magnetic materials, metals, insulators, superconducting materials) under ultra-high magnetic field conditions. Such a high magnetic field is also used for controlling the new material phase and functions. Our pulse magnets, at moment, can generate up to 87 Tesla (T) by non-destructive manner, and from 100 T up to 1200 T (the world strongest as an in-door record) by destructive methods. The laboratory is opened for scientists both from Japan and from overseas, especially from Asian countries, and many fruitful results are expected to come out not only from collaborative research but also from our in-house activities. One of our ultimate goals is to provide the scientific users as our joint research with magnets capable of a 100 T, millisecond long pulses in a non-destructive mode, and to offer versatile physical precision measurements. The available measuring techniques now involve magneto-optical measurements, cyclotron resonance, spin resonance, magnetization, and transport measurements. Recently, specific heat and calorimetric measurements are also possible to carry out with sufficiently high accuracy.

Our interests cover the study on quantum phase transitions (QPT) induced by high magnetic fields. Field-induced QPT has been explored in various materials such as quantum spin systems, strongly correlated electron systems and other



Fig. 1. Signboard at the entrance of the IMGSL.

magnetic materials. Non-destructive strong pulse magnets are expected to provide us with reliable and precise solid state physics measurements. The number of collaborative groups for the research is almost 56 in the FT of 2018.

A 210 MJ flywheel generator (Fig. 2), which is the world largest DC power supply (recorded in the Guinness Book of World Records) has been installed in the DC flywheel gener-



Fig. 2. The building for the flywheel generator (left hand side) and a long pulse magnet station (right hand side). The flywheel giant DC generator is 350 ton in weight and 5 m high (bottom). The generator, capable of a 51 MW output power with the 210 MJ energy storage, is planned to energize the long pulse magnet generating 100 T without destruction.

ator station at our laboratory, and used as an energy source of super-long pulse magnets. The magnet technologies are intensively devoted to the quasi-steady long pulse magnet (an order of 1-10 sec) energized by the giant DC power supply. The giant DC power source will also be used for the giant outer-magnet coil to realize a 100 T nondestructive magnet by inserting a conventional pulse magnet coil in its center bore.

Magnetic fields exceeding 100 T can only be obtained with destruction of a magnet coil, where ultra-high magnetic fields are obtained in a microsecond time scale. The project, financed by the ministry of education, culture, sports, science and technology aiming to generate 1000 T with the electromagnetic flux compression (EMFC) system

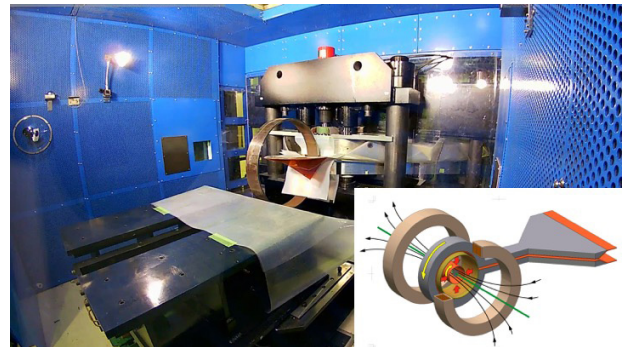


Fig. 3. (Build. C) A view of the electro-magnetic flux compression 1000-T-class megagauss generator set in side of an anti-explosive house. 1000 T project started since 2010, and finally condenser banks of 9 MJ (5 MJ + 2 MJ + 2 MJ) as a main system with the 2 MJ sub bank system for the seed field have been installed, and settled in the year of 2014.

	Alias	Type	B <sub>max</sub>	Pulse width Bore	Power source	Applications	Others
Building C Room 101-113	Electro- Magnetic Flux Compression	destructive	1200 T	$\mu$ s 10 mm	5 MJ, 50 kV 2 MJ, 50 kV	Magneto-Optical Magnetization	5 K – Room temperature
	Horizontal Single-Turn Coil	destructive	300 T 200 T	$\mu$ s 5 mm 10 mm	0.2 MJ, 50 kV	Magneto-Optical measurements Magnetization	5 K – 400 K
	Vertical Single-Turn Coil	destructive	300 T 200 T	$\mu$ s 5 mm 10 mm	0.2 MJ, 40 kV	Magneto-Optical Magnetization	2 K – Room temperature
Building C Room 114-120	Mid-Pulse Magnet	Non-destructive	60 T  70 T	40 ms 18 mm  40 ms 10 mm	0.9 MJ, 10 kV	Magneto-Optical measurements Magnetization Magneto-Transport Hall resistance Polarization Magneto-Striction Magneto-Imaging Torque Magneto- Calorimetry Heat Capacity	Independent Experiment in 5 site  Lowest temperature 0.1 K
Building C Room 121	PPMS	Steady State	14 T			Resistance Heat Capacity	Down to 0.3 K
	MPMS	Steady State	7 T			Magnetization	
Building K	Short-Pulse Magnet	Non-destructive	87 T (2-stage pulse)  85 T	5 ms 10 mm  5 ms 18 mm	0.5 MJ, 20 kV	Magnetization Magneto-Transport	2 K – Room temperature
	Long-Pulse Magnet	Non-destructive	43.5 T	1 s 30 mm	210 MJ, 2.7 kV	Resistance Magneto-Calorimetry	2 K – Room temperature

Table 1. Available Pulse Magnets, Specifications

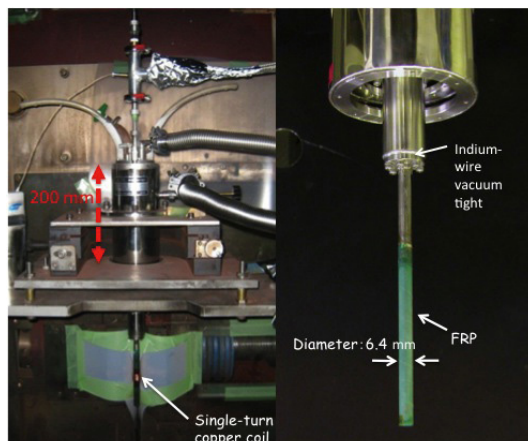


Fig. 4. Schematic picture of the H-type single-turn coil equipped with 50 kV, 200 kJ fast operating pulse power system, capable of generating 300 T within 3 mm bore coil.

(Fig. 3), has been proceeded. Our experimental techniques using the destructive magnetic fields have intensively been developed. The system which is unique to ISSP in the world scale is comprised of a power source of 5 MJ main condenser bank and 2 MJ condenser bank. Two magnet stations are constructed and both are energized from each power source. Both systems are fed with another 2 MJ condenser bank used for a seed-field coil, of which magnetic flux is to be compressed. The 2 MJ EMFC system is currently under the process for optimizing several mechanical and electrical parameters such as dimensions of coils and liners. And so far, generation of 450 T was successfully done using 1.6 MJ energy. The 5 MJ EMFC system is under conditioning the main gap switches by finely tuning control parameters. And so far, generation of 1200 T was successfully done using 3.2 MJ energy. As an easy access to the megagauss science and technology, we have the single-turn coil (STC) system capable of generating the fields of up to 300 T by a fast-capacitor of 200 kJ. We have two STC systems, one is a horizontal type (H-type, Fig. 4) and the other is a vertical type (V-type). Various kinds of laser spectroscopy experiments such as the cyclotron resonance and the Faraday rotation are possible using the H-type STC.

## Center of Computational Materials Science

The goal of the materials science is to understand and predict properties of complicated physical systems with a vast number of degrees of freedom. Since such problems cannot be solved with bare hands, it is quite natural to use computers in materials science. In fact, computer-aided science has been providing answers to many problems ranging from the most fundamental ones to the ones with direct industrial applications. In the recent trends of the hardware developments, however, the growth of computer power is mainly due to the growth in the number of the units. This fact poses a very challenging problem before us --- how can we parallelize computing tasks? In order to solve this problem in an organized way, we coordinate the use of the computational resources available to our community, and support community members through various activities such as administrating the website "MateriApps" for infor-



Fig. 1. Members of CCMS.

mation on application software in computational science. These activities are supported by funds for various governmental projects in which CCMS is involved. In particular, we are acting as the headquarters of Priority Area 7 of MEXT FLAGSHIP2020 Project (so-called "post-K computer project"). In addition to this, CCMS is involved in Priority Area 5 and Pioneering Area (CBSM2) of FLAGSHIP2020 project, Element Strategy Initiative, and Professional Development Consortium for Computational Materials Scientists (PCoMS).

The following is the selected list of meetings organized by CCMS in FY2018:

- 4/2-4/3 Joint Research Meeting of ISSP Supercomputer Joint Use and CCMS Annual Activity Report 2018 ISSP, Kashiwa
- 5/10 PCoMS Matching Workshop for industries & graduate students/postdocs The University of Tokyo Kashiwa Campus Station Satellite, Kashiwa
- 7/2-7/12 The International Summer Workshop 2018 on First Principles Electronic Structure Calculations(ISS2018) ISSP, Kashiwa
- 7/19-7/20 Post-K Project Priority Issue 7, The 3rd Annual Meeting Koshiba-Hall, Hongo, Tokyo
- 10/2-10/4 The 2nd Innovation Camp for Computational Materials Science (2nd ICCMS) The Kaike Seaside Hotel, Tottori
- 10/19 Post-K Project Exploratory Challenge 1, Sub-Challenge D, Workshop KOIL, Kashiwa
- 12/3 TIA-Takehashi Poster Workshop 2018 The University of Tokyo Kashiwa Campus Station Satellite, Kashiwa
- 12/17-12/18 Post-K Project Priority Issue 7, The 4th Symposium ISSP, Kashiwa
- 2/4 PCoMS Skill improvement training for graduate students & postdocs ISSP, Kashiwa
- 3/5 The visualization Symposium 2019 Akihabara UDX theater, Tokyo

## Laser and Synchrotron Research Center (LASOR Center)

Laser and Synchrotron Research (LASOR) Center started from October, 2012. LASOR Center aims to promote material sciences using advanced photon technologies at ISSP by combining the "Synchrotron Radiation Laboratory" and "Advanced Spectroscopy Group". These two groups have long histories since 1980's and have kept strong leaderships in each photon science fields for a long time in the world. In the past several decades, the synchrotron-

based and laser-based photon sciences have made remarkable progresses independently. However, recent progresses in both fields make it feasible to merge the synchrotron-based and laser based technologies to develop a new direction of photon and materials sciences. In the LASOR Center, extreme laser technologies such as ultrashort-pulse generation, ultraprecise control of optical pulses in the frequency domain, and high power laser sources for the generation of coherent VUV and SX light are intensively under development. The cutting edge soft X-ray beamline is also developed at the synchrotron facility SPring-8.

LASOR center aims three major spectroscopic methods [ultrafast, ultra-high resolution, and operand spectroscopy] by three groups [extreme laser science group, soft-X-ray spectroscopy and materials science group, and coherent photon science group], as illustrated in Fig. 2. Under this framework, various advanced spectroscopy, such as ultra-high resolution photoemission, time-resolved, spin-resolved spectroscopy, diffraction, light scattering, imaging, microscopy and fluorescence spectroscopy are in progress by employing new coherent light sources based on laser and synchrotron technologies that cover a wide spectral range from X-ray to terahertz. In LASOR Center, a variety of materials sciences for semiconductors, strongly-correlated materials, molecular materials, surface and interfaces, and bio-materials are studied using advanced light sources and advanced spectroscopy. Another important aim of LASOR Center is the synergy of photon and materials sciences.

Most of the research activities on the extreme laser development and their applications to materials science are performed in the ISSP buildings D and E at Kashiwa

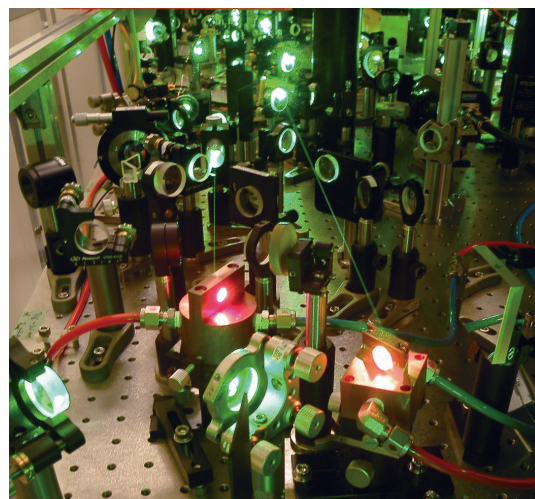


Fig. 3. Close look of a high-peak-power ultrashort-pulse laser

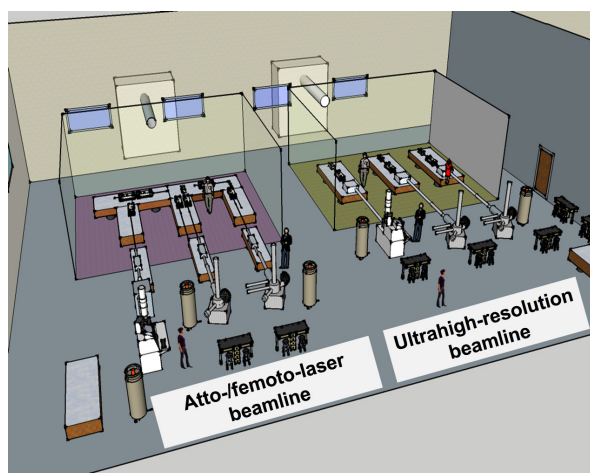


Fig. 4. Newly designed building E was constructed for new extreme VUV- and SX-lasers and new spectroscopy.

Campus where large clean rooms and the vibration-isolated floor are installed. On the other hand, the experiments utilizing the advanced synchrotron source are performed at a beamline BL07LSU in SPring-8 (Hyogo).

• Extreme Laser Science Group

The advancement of ultrashort-pulse laser technologies in the past decade has transformed the laser development at ISSP into three major directions, (i) towards ultrashort in the time domain, (ii) ultra high resolution in the spectral domain, and (iii) the extension of the spectral range, with extreme controllability of the laser sources. For ultrafast spectroscopy, we have developed carrier-envelope phase stable intense infrared light source that can produce sub-two cycle optical pulses for high harmonic and attosecond pulse generation. So far we observed coherent soft-X-ray radiation extending to a photon energy of ~330 eV. The simulation predicts the soft-X-ray field consists of single isolated attosecond pulses. For ultra-high resolution spectroscopy, fiber-laser-based light sources are intensively developed for producing EUV pulses for high resolution and time-resolved photoemission spectroscopy as well as extending the frequency comb to ultraviolet or infrared for various applications. The spectral range of intense optical pulses are being extended from visible to IR, MIR and THz ranges. Various types of high-repetition-rate ultrastable light sources are developed for laser-based ultrahigh resolution photoemission spectroscopy, high-average-power EUV generation in an enhancement cavity, and frequency comb spectroscopy



Fig. 1. Open ceremony of LASOR center on October 2012.

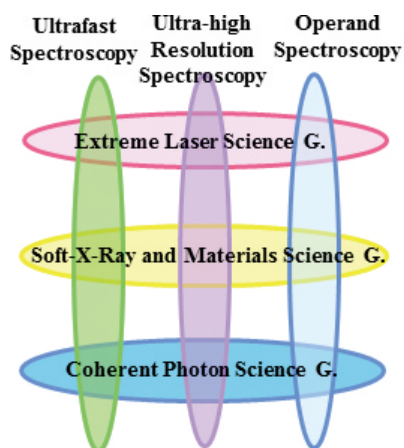


Fig. 2. Developments of advanced spectroscopy at LASOR center by three groups

for atomic physics, astronomical application, and frequency standards.

• Soft-X-ray and Materials Science Group

Recently, VUV and SX lasers have progressed very rapidly. They become very powerful for the materials science using the cutting-edge VUV and SX spectroscopy. Especially, angle resolved photoemission spectroscopy (ARPES) is very powerful to know the solid state properties. Laser has excellent properties, such as coherence, monochromaticity, polarization, ultra-short pulse, high intensity, and so on. By using monochromatic laser light, the resolution of ARPES becomes about 70- $\mu$ eV. The materials science with sub-meV resolution-ARPES is improved drastically by using high resolution laser. For example, superconducting gap anisotropy of the superconductors and Fermiology of the strongly correlated materials are studied very well. On the other hand, using pulsed laser light, the time-resolved photoemission in fs region becomes powerful to know the relaxation process of photo-excited states of the materials. Furthermore, by using CW laser with circular polarization in VUV region, the photoelectron microscopy (PEEM) is developed. The spatial resolution of nm resolution is very powerful for the study of nanomagnetic materials.

• Coherent Photon Science Group

The coherent-photon science group has main interests in exploring a variety of coherent phenomena and non-equilibrium properties of excited states in condensed matters, in

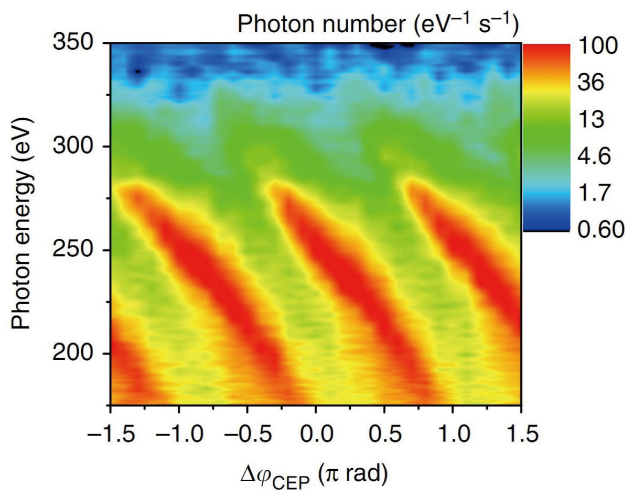


Fig. 5. Phase-dependence of high harmonic spectra in soft X rays.



Fig. 6. 10-MHz high harmonic generation in an enhancement cavity.



Fig. 7. Pump-probed photoemission system using 60-eV laser

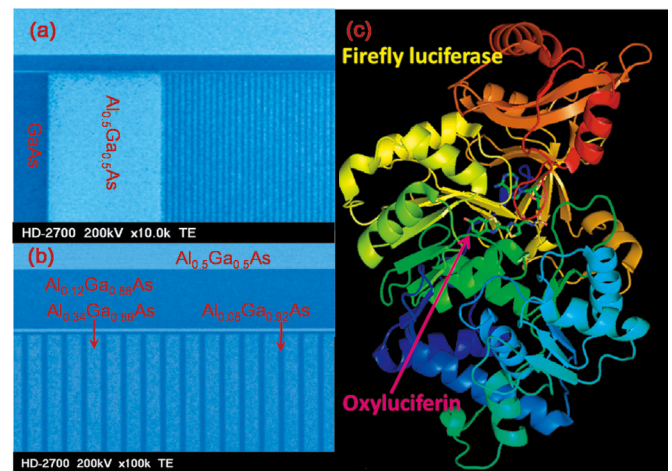


Fig. 8. Photonics devices under study: (left panel) semiconductor quantum wires and (right panel) firefly-bioluminescence system consisting of light emitter (oxyluciferin) and enzyme (luciferase)

collaborations with research groups in charge of photoemission, operant-spectroscopy and extreme laser science. This group covers a wide range of materials, from semiconductors, ferroelectrics, antiferromagnets, and superconductors to biomaterials. Various ultrafast optics technologies such as femtosecond luminescence, terahertz spectroscopy, and pump-and-probe transmission/reflection spectroscopy are applied to studies on dynamics of photo-excited carriers and photo-induced phase transitions. Coherent control of matters using phase-locked strong terahertz or mid-infrared pulse is extensively studied. Advanced photonics devices are intensively studied, such as quantum nano-structure lasers with novel low-dimensional gain physics, low-power light-standard LEDs, very efficient multi-junction tandem solar cells for satellite use, and wonderful bio-/chemi-luminescent systems for wide bio-technology applications.

## Synchrotron Radiation Laboratory

The Synchrotron Radiation Laboratory (SRL) was established in 1975 as a research division dedicated to solid state physics using synchrotron radiation (SR). Currently, SRL is composed of two research sites, the Harima branch and the E-building of the Institute for Solid State Physics.

• Brilliant soft X-ray beamline at Harima branch

In 2006, the SRL staffs have joined the Materials



Fig. 1. TR-SX station

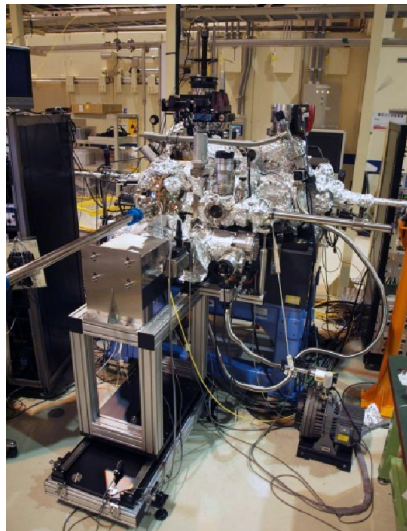


Fig. 2. 3D-nano ESCA station



Fig. 4. Ambient pressure photoemission

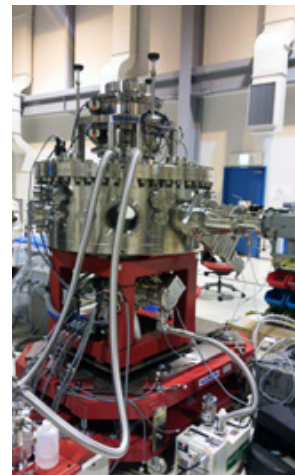


Fig. 5. Soft X-ray diffraction station

Research Division of the Synchrotron Radiation Research Organization (SRRO) of the University of Tokyo and they have played an essential role in constructing a new high brilliant soft X-ray beamline, BL07LSU, in SPring-8. The light source is the polarization-controlled 25-m long soft X-ray undulator with electromagnetic phase shifters that allow fast switching of the circularly (left, right) and linearly (vertical, horizontal) polarized photons.

The monochromator is equipped with a varied line-spacing plain grating, which covers the photon energy range from 250 eV to 2 keV. At the downstream of the beamline, a lot of experimental stations have been developed for frontier spectroscopy researches: five endstations, i.e. time-resolved soft X-ray spectroscopy (TR-SX) equipped with a two-dimensional angle-resolved time-of-flight (ARTOF) analyzer (Fig. 1), three-dimensional (3D) nano-ESCA station equipped with the Scienta R-3000 analyzer (Fig. 2), high resolution soft X-ray emission spectroscopy (XES) stations (Fig. 3) are regularly maintained by the SRL staffs and open for public use, and at free-port station many novel spectroscopic tools have been developed and installed such as ambient pressure photoemission (Fig. 4) and soft X-ray diffraction (Fig. 5) which are also open for public use from 2018, and soft X-ray resonant magneto-optical Kerr effect (MOKE), two dimensional photoelectron diffraction and so on. The beamline construction was completed in 2009 and SRL established the Harima branch laboratory in SPring-8. At SPring-8 BL07LSU, each end-station has achieved high performance: the TR-SX station have established the laser-

pump and SR-probe method with the time-resolution of 50 ps which corresponds to the SR pulse-width; the 3D nano-ESCA station reaches the spatial resolution of 70 nm; the XES station provides spectra with the energy resolution around 70 meV at 400 eV and enabled real ambient pressure experiments. Soft X-ray resonant MOKE station has been developed to make novel magneto-optical experiment using fast-switching of the polarization-controlled 25-m long soft X-ray undulator. The soft X-ray diffraction station has been fully constructed and the time-resolved measurement is available by using lasers at the TR-SX station. In 2018, 242 researchers made their experiments during the SPring-8 operation time of 4608 hours.

- High-resolution Laser SARPES at E-building

Spin- and angle-resolved photoelectron spectroscopy (SARPES) is a powerful technique to investigate the spin-dependent electronic states in solids. In FY 2014, Laser and Synchrotron Research Center (LASOR) SRL constructed a new SARPES apparatus (Fig. 6), which was designed to provide high-energy and -angular resolutions and high efficiency of spin detection using a laser light instead of the synchrotron radiation in Institute for Solid State Physics. The achieved energy resolution of 1.7 meV in SARPES spectra is the highest in the world at present. From FY 2015, the new SARPES system has been opened to outside users.

The Laser-SARPES system consists of an analysis chamber, a carousel chamber connected to a load-lock chamber, and a molecular beam epitaxy chamber, which are kept ultra-high vacuum (UHV) environment and are



Fig. 3. Soft X-ray emission station

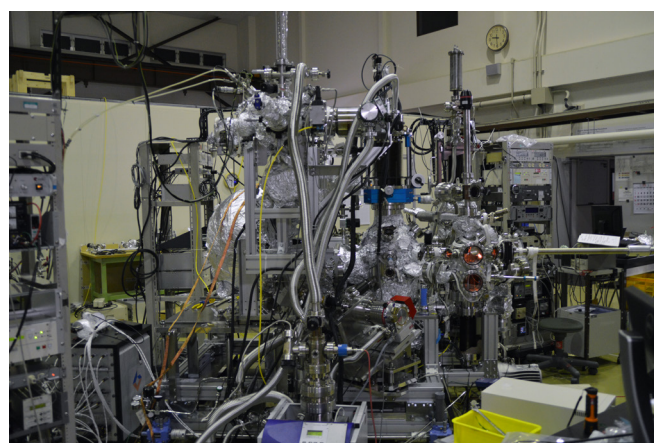


Fig. 6. Laser-SARPES system at E-building

connected each other via UHV gate valves. The electrons are excited with 6.994-eV photons, yielded by 6th harmonic of a Nd:YVO<sub>4</sub> quasi-continuous wave laser with repetition rate of 120 MHz. The hemispherical electron analyzer is a custom-made ScientaOmicron DA30-L, modified for installing the spin detectors. The spectrometer is equipped with two high-efficient spin detectors associating very low energy electron diffraction are orthogonally placed each other, which allows us to analyze the three-dimensional spin polarization of electrons. At the exit of the hemispherical analyzer, a multi-channel plate and a CCD camera are also installed, which enables us to perform the angle-resolved photoelectron spectroscopy with two-dimensional (energy-momentum) detection. The laser-SARPES machine can provide both high-resolution spin-integrated and spin-resolved photoemission spectra in various types of solids, such as spin-orbit coupled materials and ferromagnetic materials.

# Conferences and Workshops

## The International Summer WorkShop 2018 on First-Principles Electronic Structure (ISS2018)

July 2-12, 2018

T. Ozaki, F. Ishii, H. Weng, M. J. Han, M. Otani, M. Kawamura, C.-C. Lee, M. Fukuda, and Y.-T. Lee

The international summer workshop was organized in July, ISSP, the University of Tokyo to discuss recent advances of first-principles electronic structure methods and its advanced applications, and to promote international collaborations in the community, where in total 118 participants including 64 participants from abroad joined the workshop. In addition to the local organizing committee, Prof. Ishii of Kanazawa Univ., Dr. Otani of AIST, Prof. Han of KAIST, and Prof. Weng also contributed to the organization. The international workshop consisted of three parts: (i) The Summer School on DFT: Theories and Practical Aspects for July 2-6, (ii) The 3rd OpenMX developer's meeting for July 9-10, and (iii) Advanced Lecture Series for July 11-12. In the first part, fundamental issues and practical aspects of density functional theories (DFT) calculations were discussed by 15 lectures including pseudopotential theories, implementation of DFT, large-scale DFT methods, computational methods of absolute binding energies of core level, and generation of Wannier functions. Advanced applications such as topological insulators and lithium ion batteries were also discussed. In the second part, recent methodological development and applications related to the OpenMX DFT code that ISSP has been developing were presented by developers and advanced users to promote further collaboration of the community. The developments of the DC-LNO  $O(N)$  method and optical properties calculations were presented by 17 speakers. In the third part, six leading researchers gave the advanced lecture series covering methodological developments in computational physics and chemistry and its application to a wide variety of materials having not only fundamental significance and but also industrial importance. The Advanced Lecture Series highlighted the current status of first-principles electronic structure calculations and indicated a future direction of the field. In addition to this, there was a poster session of contributed participants to enhance active discussion.



# The 16th International Conference on Megagauss Magnetic Field Generation and Related Topics | ISSP International Symposium

September 25-29, 2018

S. Takeyama, Y. H. Matsuda, B. Novac, and Y. Kohama

This international conference is a series of the Megagauss conferences and was held in Japan for the first time. The conference venues are Kashiwa-no-ha Conference Center in Mitsui Garden Hotel (main venue) and The Future Center Initiative of the University of Tokyo (poster venue). Both venues are located close to the Kashiwanoha railway station of the Tsukuba Express. There are 108 participants in total including 61 participants from USA, Russia, China, Europe, and India. The topics of the Megagauss conferences are (i) generation of ultrahigh magnetic fields, (ii) high-energy and high-current pulsed power physics and technology, (iii) magnetic-flux compression technologies and their applications, (iv) high energy density physics related to fusion research, (v) high magnetic field applications in solid-state physics and for other related applications. In previous Megagauss conference, however, only a very small number of presentations have been made in solid-state-physics domain. One of the purposes to have this series of conference in Japan is to promote exchange more between researchers of pulsed power sciences and solid state physicists. The organizers encouraged not only domestic but also international solid state physicists to participate the conference. In the conference we had 42 oral and 57 poster presentations. When we count the numbers of solid-state-physics-related presentations of them, they are 15 and 37, respectively, and the numbers are considered to be large enough to boost exchanges between the pulse power and solid state physics scientists. The leaders of high magnetic field facilities of Germany, France, USA, and China presented recent results on high field properties of magnetic materials, semiconductors, superconductors, and strongly correlated systems as well as current status of their facilities. It should be noted that progress of Chinese research groups in both solid state physics and pulse power science domains is impressive. It is also found that computer simulation on high-density plasma and pulse power technology has been highly developed.



# Topological Phases and Functionality of Correlated Electron Systems 2019

February 18-20, 2019

S. Nakatsuji, Y. Otani, M. Oshikawa, C. Broholm, H. Harima, S. Miwa, and H. Wadati

For a long time, magnetism has been a central subject in strongly correlated electron systems. More recently, topology led to a new classification of band insulators, namely topological insulators. Where magnetism and topology meet, we find many intriguing phenomena including emergent "relativistic" particles and multipolar degrees of freedom. The novel physics also opens up a promising direction in spintronics and other potential practical applications. In this conference, we explored experimental and theoretical studies on subjects ranging from fundamental issues in correlated topological phases to their cutting-edge applications to spintronics. We invited 19 active researchers who are top-runners of the field around the world, and they presented their latest research results along with active discussions. On top, 11 members from ISSP, especially from Quantum Materials Group, presented their latest research, in order to enhance the collaboration between ISSP and other institutes.

The workshop was a great success. The venue was completely packed for all three days of the workshop by altogether 185 attendees. As planned, the latest results of both experiments and theories are delivered, covering a wide variety of materials such as the heterostructure of topological insulators, frustrated magnets, Weyl antiferromagnets, Kitaev spin liquids, and organic magnets. It should be noted that despite being a transdisciplinary workshop, its Q&A session was very active.

We had 74 poster presentations, 34 of them are from ISSP, and the rest are from all over Japan, including Kyoto University, and Tohoku University. Many people were staying in front of each poster and discussing with each other actively. In addition, the speakers of invited talks participated in poster sessions gave helpful comments to the students and postdocs. We believe this becomes a valuable experience for young researchers. For poster awards, five students were nominated after very competitive selections.

As aforementioned, this workshop has been a great success. We hope that groundbreaking discoveries and inventions will be made soon based on the collaboration initiated from the workshop. Lastly, we greatly appreciate everyone's generous support, including the organizers, judges, directors, secretaries, and student part-timers. Without any of the members, this could not have been accomplished.



## Computational Materials Science —Now and the Future—

April 2-3, 2018

T. Hoshi, K. Yasuoka, N. Hatano, T. Ozaki, O. Sugino, H. Noguchi, S. Kasamatsu, Y. Noguchi, Y. Higuchi, S. Morita, H. Watanabe, and N. Kawashima

This annual workshop is a joint activity between the supercomputer center (SSC/MDCL) and the center of computational materials science (CCMS), organized for the research community of the computational condensed matter physics. The objective is for the participants to exchange the information on the recent progress on the computational condensed matter research as well as the technical aspects of the high-performance computation. Every year we invite a few speakers on the topics of general interest. This year's workshop included two such special talks: one by Motoko Kotani (Tohoku U.) who talked about application of discrete geometry to material design by and the other by Teruyasu Mizoguchi (IIS, U. Tokyo) who talked about usage of artificial intelligence for analyzing crystalline interfaces. In addition to these two special invited talks, there were 14 invited oral talks and 32 poster presentations. The results of Software development/improvement project were also reported, where the target programs for FY2017 were DCORE, proposed by Hiroshi SHINAOKA (Saitama U.), and HPhi, proposed by Yohei YAMAJI (U. Tokyo).



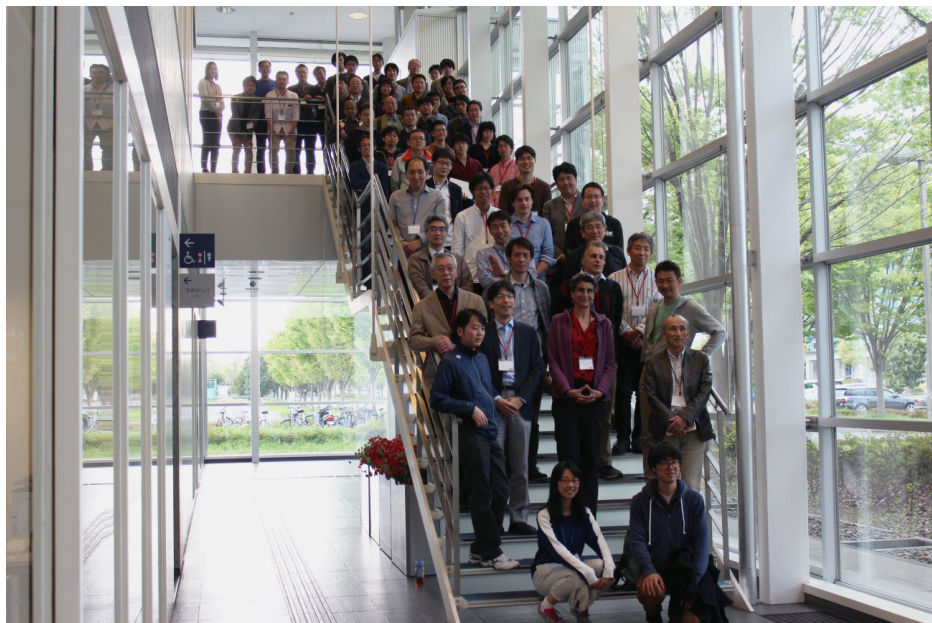
motoko kotani (Tohoku U.) who talked about application of discrete geometry to material design by and the other by Teruyasu Mizoguchi (IIS, U. Tokyo) who talked about usage of artificial intelligence for analyzing crystalline interfaces. In addition to these two special invited talks, there were 14 invited oral talks and 32 poster presentations. The results of Software development/improvement project were also reported, where the target programs for FY2017 were DCORE, proposed by Hiroshi SHINAOKA (Saitama U.), and HPhi, proposed by Yohei YAMAJI (U. Tokyo).

## Novel Phenomena in Quantum Materials driven by Multipoles and Topology

April 9-10, 2018

S. Nakatsuji, M. Oshikawa, and H. Harima

In recent years, the study of quantum materials, in particular of strongly correlated electron systems, have been enriched by the introduction of new physics based on multipoles and topology. The international workshop was planned to bring together scientists exploring the novel phenomena in new materials, and novel functionality by using spintronics and photonics, to share the latest knowledge and to fertilize new research directions. During the two days of workshop, a total of 162 people (92 on the first day and 70 on the second day) participated in the workshop, and 22 of oral and 42 of poster presentations were given by foreign and Japanese scientists. According to the questionnaires the participants filled out, the poster session was particularly well received and yielded fruitful discussions. Although it was an overcrowded schedule of 2 days, discussions were lively held everywhere even during the break time. Our workshop offered great opportunity where all the participants could share information and exchange views on the latest research results related to multipoles and topology.



## Frontier Research on Glass Transition and Related Fields

May 10-12, 2018

O. Yamamuro, H. Tanaka, T. Kanaya, K. Miyazaki, H. Hayakawa, K. Fukao, R. Nozaki, J. Habasaki, and N. Shinyashiki

This is the largest domestic workshop on the glass transition which has been held every 2 – 4 years since 2002. The glass transition is a mysterious phenomenon that a liquid is solidified without any structural change and its mechanism has not been clarified yet. In the physical properties of glasses, there are also many unsolved problems (e.g., boson peaks) originating from its non-periodic and disordered structure. Other than the works on the glass itself, there are many interesting phenomena related to the glass transition such as spin glass transition, jamming transition of granular materials, dynamical transition in proteins, etc. It is meaningful to assemble both experimental and theoretical researchers of the areas mentioned above to exchange current information and make discussion for future researches. We organized 43 oral and 45 poster presentations.

The topics of the workshop were (1) glass and supercooled liquid, (2) granular matter, jamming, rheology, (3) water and network glass, (4) biological and electrical glasses, (5) polymer and soft matter, (6) liquid-liquid transition and polyamorphism, (7) ionic conductor and ionic liquid. We had 110, 120 and 100 attendees for the first, second and third days, respectively, including many young researchers and people from outside of ISSP. There was very active and fruitful discussion throughout the workshop.



## Present and Future of Neutron Scattering Research on Condensed Matter Physics ~Future Perspective of US-Japan Cooperative Program on Neutron Scattering~

June 4-5, 2018

T. Masuda, M. Shibayama, H. Fukazawa, and Taku J Sato

Neutron Science Laboratory the University of Tokyo cooperates joint research program using triple-axis spectrometers (TAS) in JRR-3, high-resolution chopper (HRC) spectrometer in J-PARC, and cold neutron triple-axis (CTAX) spectrometer in HFIR in Oak Ridge National Laboratory. Among them CTAX has been operated under the program based on the agreement between the governments of US and Japan on cooperation research and development in science and technology in 1980, and the spectrometer has been crucial for TAS users in Japan particularly after the long shutdown of JRR-3. In addition, state-of-art inelastic spectrometers including HRC has been producing outstanding results, and the complimentary use with TAS is now popular. Furthermore in 2023 the upgrade of CTAX in large scale, the MANTA project, is planned, and the US-Japan cooperative program is getting more important. In this workshop researchers in the field of neutron scattering in US and Japan discussed the present and future of neutron scattering research on condensed matter physics. The present statuses of CTAX

and MANTA project were reviewed by US researcher, and the future of US-Japan cooperative program was discussed. Furthermore, future of spectrometers in JRR-3 was also discussed. In total 26 of oral and 9 of poster presentations were made by US and Japanese scientists, and the participants had fruitful discussions.



## New Trends in Quantum Information and Condensed Matter Physics

July 31–August 3, 2018

M. Oshikawa, T. Sasaki, T. Tomita, Y. Nakata, and M. Negoro

Quantum information science is a rapidly growing research field, aiming not only to explore information processing based on quantum theory but also to understand physics from the viewpoint of information. In the last decade, a number of novel perspectives were introduced from quantum information to many fields of physics, such as condensed matter physics, statistical mechanics, and even high energy physics, revealing that information is indeed the key to understand physics in complex quantum systems. The main goal of this workshop was to further promote these fruitful interactions between quantum information science and quantum physics. To this end, we invited active researchers from various fields, such as cold atoms, strongly correlated systems, black hole science, and quantum information and computation, both theorists and experimentalists. We also had selected talks and poster presentations. Each presentation started with a brief introduction of the topics and ended up with a huge discussion about the recent progress. In total, we had more than 660 participants in four days. This workshop provided a great opportunity to the researchers, who are willing to explore new frontiers of physics from the viewpoint of information, for future interdisciplinary collaborations.



## New Development of Science in Strongly Spin-Orbit Coupled Conductors

November 12–13, 2018

M. Tokunaga, Z. Hiroi, I. Matsuda, and Y. Fuseya

Control of physical properties via spin degrees of freedom is a fundamental subject common to various fields of material science. Strong spin-orbit interaction can make this control dramatic if the effect is properly incorporated. This workshop was held to share various on-going subjects in strongly spin-orbit coupled conductors developing independently in each research field. To this end, leading researchers from various fields got together and presented the latest researches in each field.

The workshop was started by theoretical introduction of fundamentals related to the spin-orbit coupling/interaction, and followed by bulk properties of elemental bismuth and the related materials in extreme conditions. In the following session of surface science, non-trivial band topology of pure bismuth was proposed to explain the observed surface states. Further, current status of the studies on spin-Hall and thermoelectric effects in bismuth were introduced in the spintronics and nano-materials session. In addition to the phenomena found in these  $p$ -electron systems, effects of strong spin-orbit interaction in  $d$  and  $f$  electron systems are also discussed. At the end of each session, there was a lively exchange of ideas by researchers in different area at the time of discussion.



## Upshift in the Soft X-ray Science of Synchrotron Radiation

November 30-December 1, 2018

I. Matsuda, T. Arima, Y. Harada, H. Wadati, T. Kondo, and S. Shin

The conference was organized on November 30 and December 1 to promote scientific and technological innovations of soft X-ray synchrotron radiation, motivated by the announcement on the next-generation facility by the Minister of Education, Culture, Sports, Science and Technology on July 3, 2018. It has successfully brought together more than 200 participants, including the presidents and the outstanding researchers of synchrotron radiation institutes and societies from all over Japan. The presentations at the ISSP lecture room were broadcast live to a conference room in SPring-8 through the internet. On the first day, the program focused on science and technology to be evolved at the new facility, while, on the second day, it featured experimental methods and information technologies to be developed toward researches with the light source.

With the next-generation soft X-ray synchrotron radiation, measurements are expected to be made with multi-dimensional data acquisitions or with ultra-high resolutions that have never been possible at the existing facilities. The attendance interdisciplinarily argued research topics to respond to needs in academic and industrial fields today. There was also vigorous discussion on the cutting-edge informatics to be applied in the data analysis. We were confident that the workshop was very timely and that all the arguments would become seeds of the novel science and technology.

The conference was hosted by the Institute for Solid State Physics (the University of Tokyo), Synchrotron Radiation Research Organization (the University of Tokyo), Tohoku University, and User Community of VUV·SX high-brilliant light sources.



## Liquid-Crystal-like Electronic States Generated by Quantum Many-Body Effects

December 27-28, 2018

T. Shibauchi, T. Kimura, T. Hanaguri, K. Kobayashi, K. Ohgushi, H. Kontani, and K. Okazaki

Recently, in the normal states of iron-based and cuprate superconductors, electronic states with spontaneous rotational symmetry breaking have been observed, which are called “electronic nematic” states. It has been a central issue to understand the relationship between high-temperature superconductivity and such electronic states that bear some analogy with liquid crystals. It has also been an important issue in insulating quantum spin systems that “spin liquid crystals” with broken symmetries, which differ from conventional magnetic orders (spin solids) and quantum spin liquids, may be realized. Those include spin nematic and chiral spin liquid states. These liquid-crystalline electronic states in metals and insulators are non-classical phenomena driven by quantum fluctuations and quantum many-body effects, which may have underlying principles that are important to study. This workshop aimed to provide a unique platform for developing new exchanges between different communities of superconductivity, strange metals and magnetic insulators. In two days, 25 talks and 27 poster presentations were given with lively discussions.





# Subjects of Joint Research

## 平成 30 年度 共同利用課題一覧 (前期) / Joint Research List (2018 First Term)

嘱託研究員 / Commission Researcher

No.	課題名	氏名	所属	Title	Name	Organization
担当所員：森 初果						
1	水素結合型分子導体における H/D 同位体効果による相転移機構の理論的研究	立川 仁典	横浜市立大学 大学院生命ナノシステム科学研究科	Theoretical study of phase transition mechanism induced by H/D isotope effect in hydrogen-bonded molecular conductors	Masanori Tachikawa	Yokohama City University
2	”	長嶋 雲兵	計算科学振興財団 研究部門	”	Umpei Nagashima	Foundation for Computational Science
担当所員：長谷川 幸雄						
3	極低温走査トンネル顕微鏡を用いた鉄カルコゲナイド超伝導体 FeSeTe の研究	吉田 靖雄	金沢大学 理工学域	Low-temperature STM study on iron-chalcogenide superconductor FeSeTe	Yasuo Yoshida	Kanazawa University
担当所員：秋山 英文						
4	クマリン・ケージドルシフェリンの安定構造とその電子励起状態の理論的研究	薄倉 淳子	東京理科大学 理学部	Theoretical study for equilibrium geometries and their electronic excited states of coumarin-caged luciferin	Junko Usukura	Tokyo University of Science
担当所員：上床 美也						
5	希釈冷凍機温度で使用可能な 10GPa 級超高圧発生装置の開発	松林 和幸	電気通信大学 大学院情報理工学研究科	Development of 10 GPa class high pressure apparatus for low temperature	Kazuyuki Matsubayashi	The University of Electro-Communications
6	有機伝導体の圧力効果	村田 恵三	大阪経済法科大学 21 世紀社会総合研究センター	Effect of pressure on the organic conductor	Keizo Murata	Osaka University of Economics and Law
7	圧力下 NMR 測定法に関する開発	藤原 直樹	京都大学 大学院人間・環境学研究科	Development of NMR measurement method under high pressure	Naoki Fujiwara	Kyoto University

No.	課題名	氏名	所属		Title	Name	Organization
8	希土類 122 化合物における圧力効果	繁岡 透	山口大学	大学院理工学研究科	Pressure effect of rare earth 122 compounds	Toru Shigeoka	Yamaguchi University
9	低温用マルチアンビル装置の開発	辺土 正人	琉球大学	理学部	Development of multi-anvil apparatus for low temperature	Masato Hedo	University of the Ryukyus
10	磁化測定装置の開発	名嘉 節	物質・材料研究機構	機能性材料研究拠点微粒子工学グループ	Development of the magnetometer	Takashi Naka	National Institute for Materials Science
11	高圧下 X 線回折法の開発	江藤 徹二郎	久留米工業大学	工学部	Development of High Pressure X-ray diffraction measurements	Tetsujiro Eto	Kurume Institute of Technology
12	カンチレバーを用いたトルク測定法の開発	鳥塚 潔	日本工業大学	共通教育学群	Studies on High Pressure Properties of Organic Molecular Conductors	Kiyoshi Torizuka	Nippon Institute of Technology
13	擬一次元有機物質の圧力下物性研究	糸井 充徳	日本大学	医学部	Study on pressure induced superconductivity of quasi organic conductor	Miho Itoi	Nihon University
14	磁性体の圧力効果	巨海 玄道	久留米工業大学	工学部	Effect of pressure on the Magnetic Materials	Gendo Oomi	Kurume Institute of Technology
15	3d 遷移化合物に関する圧力効果	鹿又 武	東北学院大学	工学総合研究所	Effect of pressure on the 3d transition compounds	Takeshi Kanomata	Tohoku Gakuin University
16	多重極限関連圧力装置の調整	高橋 博樹	日本大学	文理学部	Adjustment of Cubic Anvil apparatus	Hiroki Takahashi	Nihon University
担当所員：野口 博司							
17	第一原理有効模型導出プログラム RESPACK と模型解析プログラム H $\phi$ /mVMC の融合による非経験的強相関電子構造解析ソフトウェアの整備	中村 和麿	九州工業大学	大学院工学研究科	Development of first principles electronic-structure calculation software by combining effective -model derivation code (RESPACK) and model-analysis codes (H $\phi$ /mVMC)	Kazuma Nakamura	Kyushu Institute Technology
18	非自明並列を実装した量子モンテカルロソルバ - DSQSS の高度化	正木 晶子	理化学研究所	計算科学研究機構	Development of a quantum Monte Carlo Solver -DSQSS- implementing nontrivial parallelization	Akiko Masaki	RIKEN
担当：中性子科学研究施設							
19	4G における共同利用推進	佐藤 卓	東北大学	多元物質科学研究科	Research and Support of General-Use at 4G	Taku Sato	Tohoku University
20	”	奥山 大輔	東北大学	多元物質科学研究科	”	Daisuke Okuyama	Tohoku University
21	”	那波 和宏	東北大学	多元物質科学研究科	”	Kazuhiro Nawa	Tohoku University
22	6G における共同利用推進	富安 啓輔	東北大学	大学院理学研究科	Research and Support of General-Use at 6G	Keisuke Tomiyasu	Tohoku University

No.	課題名	氏名	所属		Title	Name	Organization
23	”	岩佐 和晃	茨城大学	フロンティア応用原子科学研究センター	”	Kazuaki Iwasa	Ibaraki University
24	T1-1、T1-3 における共同利用推進	大山 研司	茨城大学	大学院理工学研究科	Research and Support of General-Use at T1-1 and T1-3	Kenji Ohyama	Ibaraki University
25	T1-2、T1-3 における共同利用推進	藤田 全基	東北大学	金属材料科学研究所	Research and Support of General-Use at T1-2 and T1-3	Masaki Fujita	Tohoku University
26	T1-2、T1-3、6G における共同利用推進	南部 雄亮	東北大学	金属材料科学研究所	Research and Support of General-Use at T1-2, T1-3 and 6G	Yusuke Nambu	Tohoku University
27	”	池田 陽一	東北大学	金属材料科学研究所	”	Yoichi Ikeda	Tohoku University
28	”	鈴木 謙介	東北大学	金属材料科学研究所	”	Kensuke Suzuki	Tohoku University
29	T2-2、T1-3 における共同利用推進	木村 宏之	東北大学	多元物質科学研究所	Research and Support of General-Use at T2-2 and T1-3	Hiroyuki Kimura	Tohoku University
30	”	坂倉 輝俊	東北大学	多元物質科学研究所	”	Terutoshi Sakakura	Tohoku University
31	C1-2 における共同利用推進	杉山 正明	京都大学	複合原子力科学研究所	Research and Support of General-Use at C2-2	Masaaki Sugiyama	Kyoto University
32	C1-2、C2-3-1 における共同利用推進	井上 倫太郎	京都大学	複合原子力科学研究所	Research and Support of General-Use at C1-2 and C2-3-1	Rintaro Inoue	Kyoto University
33	C1-3-mfSANS における共同利用推進	間宮 広明	物質・材料研究機構	先端材料解析研究拠点中性子散乱グループ	Research and Support of General-Use at C1-3-mfSANS	Hiroaki Mamiya	National Institute for Materials Science
34	”	古坂 道弘	北海道大学	大学院工学研究科	”	Michihiro Furusaka	Hokkaido University
35	”	大沼 正人	北海道大学	大学院工学研究科	”	Masato Ohnuma	Hokkaido University
36	”	藤原 健	産業技術総合研究所	計量標準総合センター	”	Takeshi Fujiwara	National Institute of Advanced Industrial Science and Technology
37	C2-3-1 における共同利用推進	守島 健	京都大学	複合原子力科学研究所	Research and Support of General-Use at C2-3-1	Ken Morishima	Kyoto University
38	C3-1-2、C2-3-1 における共同利用推進	日野 正裕	京都大学	複合原子力科学研究所	Research and Support of General-Use at C3-1-2 and C2-3-1	Masahiro Hino	Kyoto University
39	C3-1-2 における共同利用推進	田崎 誠司	京都大学	大学院工学研究科	Research and Support of General-Use at C3-1-2	Seiji Tasaki	Kyoto University

No.	課題名	氏名	所属		Title	Name	Organization
40	”	小田 達郎	京都大学	複合原子力科学研究所	”	Tatsuro Oda	Kyoto University
41	C1-3、C3-1-2 における共同利用推進	北口 雅暁	名古屋大学	現象解析研究センター	Research and Support of General-Use at C1-3 and C3-1-2	Masaaki Kitaguchi	Nagoya University
42	C1-3 における共同利用推進	清水 裕彦	名古屋大学	大学院理学研究科	Research and Support of General-Use at C1-3	Hirohiko Shimizu	Nagoya University
43	”	広田 克也	名古屋大学	大学院理学研究科	”	Katsuya Hirota	Nagoya University
44	”	土川 雄介	名古屋大学	大学院理学研究科	”	Yusuke Tsuchikawa	Nagoya University
45	”	山形 豊	理化学研究所	光子工学研究領域	”	Yutaka Yamagata	RIKEN
担当所員：辛 埴							
46	スピン分解角度分解光電子分光による TaSi <sub>2</sub> のスピン構造の研究	伊藤 孝寛	名古屋大学	シンクロトロン光科学研究センター	Spin-resolved angle-resolved photoemission study of spin texture of TaSi <sub>2</sub>	Takahiro Ito	Nagoya University
47	鉄系超伝導体のレーザー光電子分光	下志万 貴博	理化学研究所	創発物性科学研究センター	Laser-ARPES on Fe superconductor	Takahiro Shimojima	RIKEN
48	有機化合物の光電子分光	金井 要	東京理科大学	理工学部	Photoemission study on organic compounds	Kaname Kanai	Tokyo University of Science
49	時間分解光電子分光を用いた強相関関係物質の研究	溝川 貴司	早稲田大学	理工学術院	Time-resolved photoemission study on strongly-correlated materials	Takashi Mizokawa	Waseda University
50	時間分解・マイクロビームラインの開発と研究	室 隆桂之	高輝度光科学研究センター	利用研究促進部門	Development of mic- and time-resolved beamline	Takayuki Muro	JASRI
51	収差補正型光電子顕微鏡の建設と利用研究	小嗣 真人	東京理科大学	基礎工学部	Construction and utilization research of aberration correction photoelectron emission microscopy	Masato Kotsugi	Tokyo University of Science
52	Mn 化合物の時間分解光電子分光	大川 万里生	東京理科大学	理学部	Time resolved Photoemission on Mn compounds	Mario Okawa	Tokyo University of Science
53	レーザー光電子分光による参加薄膜の研究	津田 俊輔	物質・材料研究機構	機能性材料研究拠点量子輸送特性グループ	Laser-Photoemission Study on Oxide Films	Shunsuke Tsuda	National Institute for Materials Science
54	インジウム原子層超伝導体におけるラッシュバースピン分裂の直接観察	内橋 隆	物質・材料研究機構	国際ナノアーキテクトゥクス研究拠点	Direct observation of Rashba effect-induced spin splitting in an indium atomic-layer superconductor	Takashi Uchihashi	National Institute for Materials Science
55	固体中のマヨラナ粒子の研究	松田 祐司	京都大学	大学院理学研究科	Study of Majorana Fermion in Solids by Laser Photoemission Spectroscopy	Yuji Matsuda	Kyoto University

No.	課題名	氏名	所属		Title	Name	Organization
56	”	佐藤 昌利	京都大学	基礎物理学研究所	”	Masatoshi Sato	Kyoto University
57	時間分解光電子分光や超高分解能光電子分光を用いた超伝導体や強相関系物質の研究	吉田 鉄平	京都大学	大学院人間・環境学研究科	Laser ARPES study on superconductors and strongly-correlated materials	Teppey Yoshida	Kyoto University
58	FeSe 超伝導体における BCS-BES クロスオーバーの研究	紺谷 浩	名古屋大学	大学院理学研究科	Study of BCS-BES crossover in FeSe superconductors	Hiroshi Kontani	Nagoya University
59	レーザー角度分解光電子分光による重い電子系超伝導体 CeCoIn <sub>5</sub> の超伝導ギャップ異方性特定	大田 由一	産業技術総合研究所	計算標準総合センター工学計測標準研究部門	Verification of superconducting-gap anisotropy of heavy fermion superconductor CeCoIn <sub>5</sub> by laser angle-resolved photoemission spectroscopy	Yuichi Ota	National Institute of Advanced Industrial Science and Technology
60	高分解能光電子分光による強相関物質の研究	横谷 尚睦	岡山大学	大学院自然科学研究科	Ultra-high resolution study on strongly correlated materials	Takayoshi Yokoya	Okayama University
61	トポロジカル超伝導体の探索	坂野 昌人	東京大学	大学院工学系研究科	Search for topological insulators	Masato Sakano	The University of Tokyo
62	60-eV レーザーを用いた時間分解光電子分光の開発	石坂 香子	東京大学	大学院工学系研究科	The development of time-resolved photoemission using 60eV laser	Kyoko Ishizaka	The University of Tokyo
63	高温超伝導体の高分解能光電子分光	藤森 淳	東京大学	大学院理学系研究科	Ultra-high resolution photoemission spectroscopy on high T <sub>c</sub> superconductor	Atsushi Fujimori	The University of Tokyo
64	重い電子系ウラン化合物の高分解能光電子分光	藤森 伸一	日本原子力研究開発機構	物質科学研究センター	Ultra high resolution photoemission study on heavy fermion Uranium compounds	Shinichi Fujimori	Japan Atomic Energy Agency
65	時間分解光電子顕微分光実験の技術開発	木下 豊彦	高輝度光科学研究センター	利用研究促進部門	Technical development of time-resolved photoemission microscopy measurement	Toyohiko Kinoshita	JASRI
66	光電子分光法を用いた各種分子性結晶の電子状態の研究及び装置の低温化	木須 孝幸	大阪大学	大学院基礎工学研究科	Research on electron state of molecular crystals using photoemission spectroscopy	Takayuki Kisu	Osaka University
67	トポロジカル絶縁体の電子状態の解明	木村 昭夫	広島大学	大学院理学研究科	Electronic-structure study of topological insulators	Akio Kimura	Hiroshima University
68	Si(111) 上単層タリウムの高次高調波を用いた時間分解光電子分光	坂本 一之	千葉大学	大学院融合科学研究科	Time-resolved ARPES investigation of monolayer Thallium on Si(111)	Kazuyuki Sakamoto	Chiba University
担当所員：原田 慈久							
69	液中プラズマ印加水の軟 X 線吸収 / 発光分光技術開発	寺嶋 和夫	東京大学	大学院新領域創成科学研究科	Technical development of soft X-ray absorption/emission spectroscopy for water processed by in-liquid plasma	Kazuo Terashima	The University of Tokyo
70	液中プラズマ印加によるナノ粒子分散特性評価と軟 X 線分光	伊藤 剛仁	東京大学	大学院新領域創成科学研究科	Characterization of nano-particle distribution in water processed by in-liquid plasma and soft X-ray spectroscopy	Tsuyohito Ito	The University of Tokyo
71	軟 X 線発光・共鳴非弾性散乱分光の磁気円・線二色性測定システムの構築	菅 滋正	大阪大学	産業科学研究所	Construction of a noble system for circular and linear dichroism in soft X-ray emission and RIXS spectroscopy	Shigemasa Suga	Osaka University

No.	課題名	氏名	所属		Title	Name	Organization
72	軟 X 線吸収/発光分光法によるリチウムイオン電池電極材料の電子物性研究	細野 英司	産業技術総合研究所	省エネルギー研究部門	Study on the electronic property of electrode materials for Li-ion batteries by soft X-ray absorption/emission spectroscopy	Eiji Hosono	National Institute of Advanced Industrial Science and Technology
73	”	朝倉 大輔	産業技術総合研究所	エネルギー技術研究部門	”	Daisuke Asakura	National Institute of Advanced Industrial Science and Technology
74	高分解能光電子分光による酸化バナジウムの研究	藤原 秀紀	大阪大学	大学院基礎工学研究科	Study on vanadium oxides by high resolution Photoemission	Hidenori Fujiwara	Osaka University
75	省エネ・創エネ・蓄電デバイスのオペランド分光	尾嶋 正治	東京大学	放射光分野融合国際卓越拠点	Operando nano-spectroscopy for energy efficient, power generation and energy storage devices	Masaharu Oshima	The University of Tokyo

担当所員：松田 巖

76	時間分解磁気光学実験の技術開発	小嗣 真人	東京理科大学	基礎工学部	Technical development of time-resolved magneto-optical experiment	Masato Kotsugi	Tokyo University of Science
----	-----------------	-------	--------	-------	---	----------------	-----------------------------

担当所員：和達 大樹

77	時間分解吸収分光による EuNi <sub>2</sub> (Si <sub>1-x</sub> Ge <sub>x</sub> ) <sub>2</sub> の価数転移ダイナミクスの解明	三村 功次郎	大阪府立大学	大学院工学研究科	Dynamics of valence transition in EuNi <sub>2</sub> (Si <sub>1-x</sub> Ge <sub>x</sub> ) <sub>2</sub> revealed by time-resolved XAS	Kojiro Mimura	Osaka Prefecture University
78	三次元 nanoESCA による実デバイスのオペランド電子状態解析	永村 直佳	物質・材料研究機構	先端材料解析研究拠点	Operando analysis of the electronic structure of actual devices by 3DnanoESCA	Naoka Nagamura	National Institute for Materials Science
79	コヒーレント共鳴軟 X 線散乱による磁気ドメイン構造の観測	山崎 裕一	物質・材料研究機構	統合型材料開発・情報基盤部門	Observation of magnetic domain structure for ferromagnetic thin films by means of resonant scattering	Yuichi Yamasaki	National Institute for Materials Science

一般研究員 / General Researcher

No.	課題名	氏名	所属		Title	Name	Organization
担当所員：榊原 俊郎							
1	超伝導対のギャップ対称性を決定する実験的、理論的研究	町田 一成	立命館大学	理工学部	Experimental and theoretical studies on gap symmetry determination in superconductors	Kazushige Machida	Ritsumeikan University
2	強相関電子系化合物の秩序相に対する結晶対称性および電子軌道の効果	横山 淳	茨城大学	理学部	Effects of crystal symmetry and electronic state in ordered phase of strongly correlated electron systems	Makoto Yokoyama	Ibaraki University
3	”	大島 佳樹	茨城大学	大学院理工学研究科	”	Yoshiki Oshima	Ibaraki University
4	磁場中比熱測定によるカゴメ近藤格子の量子臨界現象の研究	高島 敏郎	広島大学	大学院先端物質科学研究科	Study of quantum critical phenomena in the kagome Kondo lattice by specific-heat measurements in magnetic fields	Toshiro Takabatake	Hiroshima University

No.	課題名	氏名	所属		Title	Name	Organization
5	”	志村 恭通	広島大学	大学院先端物質科学研究科	”	Yasuyuki Shimura	Hiroshima University
6	”	津田 研	広島大学	大学院先端物質科学研究科	”	Suguru Tsuda	Hiroshima University
7	三元 Pt 硫化物の低温磁化測定	岡本 佳比古	名古屋大学	大学院工学研究科	Low Temperature Magnetization Measurements on a Ternary Pt Sulfide	Yoshihiko Okamoto	Nagoya University
8	(U,Th)Be <sub>13</sub> と UNi <sub>2</sub> Al <sub>3</sub> における極低温磁化・熱膨張・回転磁場中比熱測定	清水 悠晴	東北大学	金属材料研究所	Low-temperature magnetization and heat-capacity in rotated magnetic fields for (U,Th)Be <sub>13</sub> and UNi <sub>2</sub> Al <sub>3</sub>	Yusei Shimizu	Tohoku University
9	微小純良結晶を用いた超伝導体の比熱測定	加瀬 直樹	東京理科大学	理学部	Specific heat measurements using a small single crystal	Naoki Kase	Tokyo University of Science
10	磁気フラストレートした一次元量子スピン系 Rb <sub>2</sub> (Cu <sub>1-x</sub> M <sub>x</sub> ) <sub>2</sub> Mo <sub>3</sub> O <sub>12</sub> (M=Zn, Ni) の不純物置換効果	安井 幸夫	明治大学	理工学部	Impurity Doping Effect of Magnetically Frustrated One-dimensional Quantum Spin System Rb <sub>2</sub> (Cu <sub>1-x</sub> M <sub>x</sub> ) <sub>2</sub> Mo <sub>3</sub> O <sub>12</sub> (M=Zn, Ni)	Yukio Yasui	Meiji University
担当所員：山下 穰							
11	三角格子反強磁性体の低温磁性	柄木 良友	琉球大学	教育学部	Low temperature magnetism of triangular antiferromagnets	Yoshitomo Karaki	University of the Ryukyus
12	重い電子系超伝導体 CeCoIn <sub>5</sub> の超低温における dHvA 効果測定	宍戸 寛明	大阪府立大学	大学院工学研究科	dHvA effect measurements at ultra-low temperatures in a heavy fermion superconductor CeCoIn <sub>5</sub>	Hiroaki Shishido	Osaka Prefecture University
13	銅酸化物高温超伝導体における磁化分布の直接観察	芝内 孝禎	東京大学	大学院新領域創成科学研究科	Direct imaging of magnetization distribution on high-T <sub>c</sub> superconductors	Takasada Shibauchi	The University of Tokyo
14	重い電子系超伝導体 CeCoIn <sub>5</sub> の超低温における dHvA 効果測定	片山 諒	大阪府立大学	大学院工学研究科	dHvA effect measurements at ultra-low temperatures in a heavy fermion superconductor CeCoIn <sub>5</sub>	Ryo Katayama	Osaka Prefecture University
担当所員：勝本 信吾							
15	ナノセンシングデバイスに関する研究	米谷 玲皇	東京大学	大学院新領域創成科学研究科	Research on nanosensing device	Reo Kometani	The University of Tokyo
16	”	田中 航大	東京大学	大学院工学系研究科	”	Kodai Tanaka	The University of Tokyo
17	”	吉原 健太	東京大学	大学院工学系研究科	”	Kenta Yoshihara	The University of Tokyo
18	電気二重層トランジスタ構造におけるチャンネルと超伝導電極との接合の研究	石黒 亮輔	日本女子大学	理学部	Study of a junction between electric double layer transistor channel and superconducting electrodes	Ryosuke Ishiguro	Japan Women's University
19	”	相川 夕美花	日本女子大学	大学院理学研究科	”	Yumika Aikawa	Japan Women's University

No.	課題名	氏名	所属	Title	Name	Organization
担当所員：大谷 義近						
20	空間反転対称性の破れた結晶・磁気構造に発現する新奇電流応答	木俣 基	東北大学	金属材料研究所	Novel current response in non-centrosymmetric crystal and magnetic structures	Motoi Kimata Tohoku University
担当所員：小森 文夫						
21	STM を用いた L10-FeNi 表面における N サーファクタント効果の解析	高橋 優樹	東京理科大学	大学院基礎工学研究科	Study of N surfactant effect on L10-FeNi by using STM	Yuuki Takahashi Tokyo University of Science
22	Si(111) <sub>4</sub> × 1-In 基板上における In-Bi 表面合金の電子状態	中辻 寛	東京工業大学	物質理工学院	Electronic structure of In-Bi surface alloy grown on Si(111) <sub>4</sub> × 1-In substrates	Kan Nakatsuji Tokyo Institute of Technology
23	”	田中 和也	東京工業大学	物質理工学院	”	Kazuya Tanaka Tokyo Institute of Technology
24	Al-Pd-Ru 準結晶・近似結晶における空孔濃度の研究	金沢 育三	東京学芸大学	自然科学系	Positron-annihilation studies of Al-Pd-Ru quasicrystal and its approximant crystals	Ikuzo Kanazawa Tokyo Gakugei University
25	”	木村 薫	東京大学	大学院新領域創成科学研究科	”	Kaoru Kimura The University of Tokyo
26	”	大島 永康	産業技術総合研究所	分析計測標準研究部門	”	Nagayasu Oshima National Institute of Advanced Industrial Science and Technology
27	”	中村 駿	東京学芸大学	大学院教育学研究科	”	Shun Nakamura Tokyo Gakugei University
28	”	高橋 潤	東京学芸大学	大学院教育学研究科	”	Jun Takahashi Tokyo Gakugei University
29	SiC(0001) 上の Bi 吸着状態の構造および電子状態の解析	田中 悟	九州大学	大学院工学研究院	Analyses of structure and electronic states of Bi atoms on SiC(0001).	Satoru Tanaka Kyushu University
30	”	尾家 翔太郎	九州大学	大学院工学府	”	Shotaro Oie Kyushu University
31	SiC ナノ周期表面上に転写したグラフェンの電子状態の観察	田中 悟	九州大学	大学院工学研究院	Electronic structures of graphene transferred on SiC periodic nanosurfaces	Satoru Tanaka Kyushu University
32	”	安藤 寛	九州大学	大学院工学府	”	Hiroshi Ando Kyushu University
33	SiC(0001) 上の III / IV 族元素 2D オーバレイヤーの STM / STS 研究	ビシコフスキー アントン	九州大学	大学院工学研究院	The STM/STS study of group III/IV 2D overlayers on SiC(0001)	Visikovskiy Anton Kyushu University
34	”	李 文欣	埼玉工業大学	先端研究所	”	Wenxin Li Saitama Institute of Technology

No.	課題名	氏名	所属		Title	Name	Organization
35	Cu(001) 面上に形成した金属窒化物単原子層の構造 (2)	山田 正理	中央大学	理工学部	Structure of monolayer metal nitrides on Cu(001) (2)	Masamichi Yamada	Chuo University
36	金属/半導体表面上への超薄膜およびナノ構造薄膜の形成とその磁化ダイナミックスの観測	河村 紀一	日本放送協会	放送技術研究所	Study on magnetic dynamics of ultra-thin films and nano-structures on metal / semiconductor surfaces	Norikazu Kawamura	NHK Science and Technology Research Laboratories
37	STMを用いたLiO-FeNi表面におけるNサーファクタント効果の解析	小嗣 真人	東京理科大学	基礎工学部	Study of N surfactant effect on LiO-FeNi by using STM	Masato Kotsugi	Tokyo University of Science
担当所員：長谷川 幸雄							
38	エピタキシャルシリセン、ゲルマネン及びそのヘテロ構造の低温走査トンネル顕微鏡観察	高村 由起子	北陸先端科学技術大学院大学	マテリアルサイエンス系	STM investigation of epitaxial silicene, germanene, and their heterostructures	Yukiko Yamada-Takamura	JAIST
39	〃	米澤 隆宏	北陸先端科学技術大学院大学	先端科学技術研究科	〃	Takahiro Yonezawa	JAIST
担当所員：リップマー ミック							
40	傾斜組成エピタキシャル強誘電体薄膜の構造と物性	丸山 伸伍	東北大学	大学院工学研究科	Structural and physical property characterization of graded-composition epitaxial ferroelectric thin films	Shingo Maruyama	Tohoku University
41	〃	穴田 柚冬	東北大学	大学院工学研究科	〃	Yuto Anada	Tohoku university
42	新規 HfO <sub>2</sub> 基強誘電体薄膜における負の電気熱量効果の実験的検証研究	山田 智明	名古屋大学	大学院工学研究科	Experimental study on negative electrocaloric effect in HfO <sub>2</sub> -based ferroelectric thin films	Tomoaki Yamada	Nagoya University
43	〃	太田 悠登	名古屋大学	工学部	〃	Yuto Ota	Nagoya University
担当所員：吉信 淳							
44	異種二分子膜間のプロトン移動と物性の制御	加藤 浩之	大阪大学	大学院理学研究科	Proton Transfer and Property Control for Heterogeneous Bilayer	Hiroyuki Kato	Osaka University
担当所員：秋山 英文							
45	GaN 半導体における光起電力と電気的性質の相関について	小柴 俊	香川大学	大学院工学研究科	Correlation of photovoltaic electrical properties as for GaN	Shun Koshiba	Kagawa University
46	オキシルシフェリン励起状態におけるタンパク質効果の解明	樋山 みやび	群馬大学	大学院理工学府	Elucidation of protein effect for electronic excited state of oxylucifein	Miyabi Hiyama	Gunma University
47	GaN/GaP 量子井戸構造におけるアップコンバージョン発光に関する研究	矢口 裕之	埼玉大学	大学院理工学研究科	Up-conversion luminescence from GaPN/GaP quantum structures	Hiroyuki Yaguchi	Saitama University

No.	課題名	氏名	所属		Title	Name	Organization
48	”	高宮 健吾	埼玉大学	総合技術支援センター	”	Kengo Takamiya	Saitama University
49	”	高橋 涉	埼玉大学	大学院理工学研究科	”	Wataru Takahashi	Saitama University
50	”	小笠原 裕	香川大学	大学院工学研究科	”	Yutaka Ogasawara	Kagawa University
51	希薄磁性半導体 GaGdAs を用いたスピン LED の光学特性評価	宮川 勇人	香川大学	工学部	Optical properties of spin-polarized light-emitting diodes using diluted magnetic semiconductor GaGdAs	Hayato Miyagawa	Kagawa University
52	”	加藤 昇	香川大学	大学院工学研究科	”	Sho Kato	Kagawa University
53	”	高藤 誠	香川大学	大学院工学研究科	”	Makoto Takafuji	Kagawa University
54	GaN/AlN 半導体超格子の光学特性評価	小柴 俊	香川大学	大学院工学研究科	Optical characteristic evaluation of GaN/AlN semiconductor superlattice	Shun Koshiba	Kagawa University
55	”	則包 猛	香川大学	大学院工学研究科	”	Takeru Norikane	Kagawa University
担当所員：中辻 知							
56	希土類金属間化合物の強磁場程温物性研究	海老原 孝雄	静岡大学	学術院理学領域	Physical properties in rare earth intermetallic compounds at high magnetic fields in low temperature	Takao Ebihara	Shizuoka University
57	”	ジュマエダ ジャトミカ	静岡大学	大学院自然科学教育部	”	Jumaeda Jatmika	Shizuoka University
58	価数相転移に伴う格子歪みの研究	久我 健太郎	理化学研究所	放射光科学研究センター	Crystal strain associated with valence transition	Kentaro Kuga	RIKEN
担当所員：川島 直輝							
59	蜂の巣格子磁性体 RuCl <sub>3</sub> の磁場中励起	鈴木 隆史	兵庫県立大学	大学院工学研究科	Dynamical properties of honeycomb-lattice magnet RuCl <sub>3</sub> in magnetic fields	Takafumi Suzuki	University of Hyogo
60	テンソルネットワーク法の開発	原田 健自	京都大学	大学院情報学研究科	Development of tensor network method	Kenji Harada	Kyoto University
担当所員：上床 美也							
61	YbH <sub>2+x</sub> の磁性と伝導	中村 修	岡山理科大学	研究・社会連携センター	Magnetic and transport properties in YbH <sub>2+x</sub>	Osamu Nakamura	Okayama University of Science

No.	課題名	氏名	所属		Title	Name	Organization
62	ハーフホイスラー化合物の圧力下輸送特性	竹中 崇了	東京大学	大学院新領域創成科学研究科	Transport properties of half-Heusler compounds	Takaaki Takenaka	The University of Tokyo
63	”	松浦 康平	東京大学	大学院新領域創成科学研究科	”	Kohei Matsuura	The University of Tokyo
64	高圧下における Eu 化合物の価数転移の探索	大貫 惇睦	琉球大学	理学部	Investigation of valence transition on Eu compounds under high pressure	Yoshichika Onuki	University of the Ryukyus
65	”	本多 史憲	東北大学	金属材料研究所	”	Fuminori Honda	Tohoku University
66	ウラン化合物の磁性の圧力効果	本多 史憲	東北大学	金属材料研究所	Effect of Pressure on the magnetism of uranium compounds	Fuminori Honda	Tohoku University
67	Co 基ホイスラー合金における圧力誘起マルテンサイト変態に関する研究	重田 出	鹿児島大学	大学院理工学研究科	Study on pressure-induced martensitic phase transformation in Co-based Heusler alloys	Iduru Shigeta	Kagoshima University
68	有機分子性導体の高圧物性の研究	鳥塚 潔	明治大学	総合数理学部	Studies on High Pressure Properties of Organic Molecular Conductors	Kiyoshi Torizuka	Meiji University
69	三角格子反強磁性体の低温磁性	柄木 良友	琉球大学	教育学部	Low temperature magnetism of triangular antiferromagnets.	Yoshitomo Karaki	University of the Ryukyus
70	多形化合物 $R\text{Ir}_2\text{Si}_2$ (R= 希土類) の結晶育成と物質評価 4	繁岡 透	山口大学	大学院創成科学研究科	Crystal growth and characterization of polymorphic compounds $R\text{Ir}_2\text{Si}_2$ (R=rare earth) 4	Toru Shigeoka	Yamaguchi University
71	”	内間 清晴	沖縄キリスト教短期大学	総合教育系	”	Kiyoharu Uchima	Okinawa Christian Junior College
72	三元化合物 $\text{PrPd}_2\text{Si}_2$ の結晶育成 2	繁岡 透	山口大学	大学院創成科学研究科	Crystal growth of ternary compound $\text{PrPd}_2\text{Si}_2$ 2	Toru Shigeoka	Yamaguchi University
73	”	内間 清晴	沖縄キリスト教短期大学	総合教育系	”	Kiyoharu Uchima	Okinawa Christian Junior College
74	多形化合物 $R\text{Ir}_2\text{Si}_2$ (R= 希土類) の磁気特性 2	内間 清晴	沖縄キリスト教短期大学	総合教育系	Magnetic characteristics of polymorphic compounds $R\text{Ir}_2\text{Si}_2$ (R=rare earth) 2	Kiyoharu Uchima	Okinawa Christian Junior College
75	”	繁岡 透	山口大学	大学院創成科学研究科	”	Toru Shigeoka	Yamaguchi University
76	$\text{Ce}_3\text{Pd}_4$ の圧力下電気抵抗測定	角田 竜馬	新潟大学	大学院自然科学研究科	Electrical resistivity measurement of $\text{Ce}_3\text{Pd}_4$ under pressure	Ryoma Tsunoda	Niigata University
77	圧力誘起価数転移の探索と高圧下輸送特性	辺土 正人	琉球大学	理学部	Searching of pressure-induced valence transition and transport properties under high pressure	Masato Hedo	University of the Ryukyus
78	”	伊覇 航	琉球大学	大学院理工学研究科	”	Wataru Iha	University of the Ryukyus

No.	課題名	氏名	所属		Title	Name	Organization
79	鉄カルコゲナイド系化合物の単結晶育成とその圧力効果	久田 旭彦	徳島大学	大学院社会産業理工学研究部	Single-crystal growth and pressure-effect study of iron-chalcogenide compound	Akihiko Hisada	Tokushima University
80	Pd系ホイスラー合金の磁気および構造の相転移温度の高圧効果	安達 義也	山形大学	大学院理工学研究科	Pressure effect of the magnetic and structural phase transition temperature for the Pd-Heusler alloys	Yoshiya Adachi	Yamagata University
81	〃	福本 拓実	山形大学	大学院理工学研究科	〃	Takumi Fukumoto	Yamagata University
82	Eu化合物の圧力誘起近藤状態の探索	辺土 正人	琉球大学	理学部	Searching for pressure-induced Kondo state on Eu compounds	Masato Hedo	University of the Ryukyus
83	〃	松田 進弥	琉球大学	理学部	〃	Shinya Matsuda	University of the Ryukyus
84	強相関電子系化合物における圧力および磁場誘起量子相転移の探索	大橋 政司	金沢大学	理工研究域環境デザイン学系	Pressure and field induced quantum phase transition in strongly correlated electron systems	Masashi Ohashi	Kanazawa University
85	〃	前田 加衣	金沢大学	大学院自然科学研究科	〃	Kae Maeta	Kanazawa University
86	希土類ラーベス化合物 $RAI_2$ の異方的磁気体積効果	大橋 政司	金沢大学	理工研究域環境デザイン学系	Anisotropic magnetovolume effect of rare earth Laves compound $RAI_2$	Masashi Ohashi	Kanazawa University
87	〃	西川 智生	金沢大学	自然科学研究科環境デザイン学専攻	〃	Tomoki Nishikawa	Kanazawa University
88	$HoRh_2Si_2$ 単結晶の磁場中比熱測定	藤原 哲也	山口大学	大学院創成科学研究科	Specific heat measurement under magnetic field of $HoRh_2Si_2$ single crystal	Tetsuya Fujiwara	Yamaguchi University
89	〃	山本 嵩	山口大学	理学部	〃	Shu Yamamoto	Yamaguchi University
90	$HoRh_2Si_2$ の La 置換系化合物の単結晶育成 (2)	藤原 哲也	山口大学	大学院創成科学研究科	Single crystal growth of La substituted $HoRh_2Si_2$ compounds II	Tetsuya Fujiwara	Yamaguchi University
91	〃	山本 嵩	山口大学	理学部	〃	Shu Yamamoto	Yamaguchi University
92	$HoRh_2Si_2$ 単結晶の高圧力下電気抵抗測定	藤原 哲也	山口大学	大学院創成科学研究科	Resistivity measurements under hipressures of $HoRh_2Si_2$ single crystal	Tetsuya Fujiwara	Yamaguchi University
93	〃	山本 嵩	山口大学	理学部	〃	Shu Yamamoto	Yamaguchi University
94	$EuMn_2Ge_2$ 単結晶の電気抵抗測定	藤原 哲也	山口大学	大学院創成科学研究科	Resistivity measurement of $EuMn_2Ge_2$ single crystal	Tetsuya Fujiwara	Yamaguchi University
95	〃	山本 嵩	山口大学	理学部	〃	Shu Yamamoto	Yamaguchi University

No.	課題名	氏名	所属		Title	Name	Organization
96	物性測定に与える圧力媒体効果	村田 恵三	大阪経済法科大学	21世紀社会総合研究センター	Effect of pressure medium on the measurement of material properties	Keizo Murata	Osaka University of Economics and Law
97	リン系充填スクッテルダイト超伝導体の磁気特性 II	川村 幸裕	室蘭工業大学	大学院工学研究科	Magnetic properties of filled skutterudite superconductor in phosphorus system II	Yukihiro Kawamura	Muroran Institute of Technology
98	BiS <sub>2</sub> 系化合物超伝導体の圧力効果	加瀬 直樹	東京理科大学	理学部	Pressure effect of the BiS <sub>2</sub> -based superconductors	Naoki Kase	Tokyo University of Science
99	MnNiGe-CoNiGe系化合物の圧力下磁化率測定	伊藤 昌和	鹿児島大学	学術研究院理工学域理学系	Magnetic susceptibility of MnNiGe-CoNiGe under pressure	Masakazu Ito	Kagoshima University
100	”	恩田 圭二郎	鹿児島大学	大学院理工学研究科	”	Keijiro Onda	Kagoshima University
101	Yb(Co <sub>1-x</sub> Ir <sub>x</sub> ) <sub>2</sub> Zn <sub>20</sub> の基本物性評価 II	阿曾 尚文	琉球大学	理学部	Evaluation of fundamental physical properties in Yb(Co <sub>1-x</sub> Ir <sub>x</sub> ) <sub>2</sub> Zn <sub>20</sub> II	Naofumi Aso	University of the Ryukyus
102	”	佐藤 信	琉球大学	大学院理工学研究科	”	Shin Sato	University of the Ryukyus
103	YbCo <sub>2</sub> Zn <sub>20</sub> 置換系試料の圧力効果 II	阿曾 尚文	琉球大学	理学部	Pressure effect of doped YbCo <sub>2</sub> Zn <sub>20</sub> systems II	Naofumi Aso	University of the Ryukyus
104	”	盛島 実竜	琉球大学	大学院理工学研究科	”	Miiru Morishima	University of the Ryukyus
105	”	津堅 涼	琉球大学	大学院理工学研究科	”	Ryo Tsuken	University of the Ryukyus
106	セリウム化合物 CeT <sub>2</sub> X <sub>8</sub> (T: 遷移金属元素, X: Al, Ga)における高圧下物性	中島 美帆	信州大学	理学部	Pressure effect in CeT <sub>2</sub> X <sub>8</sub> (T: transition metal element, X: Al, Ga)	Miho Nakashima	Shinshu University
107	”	矢口 達志	信州大学	理学部	”	Tatsushi Yaguchi	Shinshu University
108	”	米原 直哉	信州大学	理学部	”	Naoya Yonehara	Shinshu University
109	ハーフホイスラー化合物の圧力下輸送特性	芝内 孝禎	東京大学	大学院新領域創成科学研究科	Transport properties of half-Heusler compounds	Takasada Shibauchi	The University of Tokyo
110	MnCoGeの磁気特性及び相変態に及ぼす熱処理効果	三井 好古	鹿児島大学	大学院理工学研究科	Annealing effects on magnetic properties and phase transformation in MnCoGe	Yoshifuru Mitsui	Kagoshima University
111	”	野口 滉平	鹿児島大学	理学部	”	Kohei Noguchi	Kagoshima University
112	ウラン化合物強磁性体 URh <sub>6</sub> X <sub>4</sub> (X = Si, Ge)の圧力効果	芳賀 芳範	日本原子力研究開発機構	先端基礎研究センター	Pressure effects on ferromagnetism in URh <sub>6</sub> X <sub>4</sub> (X = Si, Ge)	Yoshinori Haga	Japan Atomic Energy Agency

No.	課題名	氏名	所属		Title	Name	Organization
113	CrAlGe 系化合物の磁気特性	三井 好古	鹿児島大学	大学院理工学研究科	Magnetic properties of CrAlGe-based compound	Yoshifuru Mitsui	Kagoshima University
114	”	増満 勇人	鹿児島大学	大学院理工学研究科	”	Hayato Masumitsu	Kagoshima University
115	高圧力下における Fe 基磁性体の磁気特性	小山 佳一	鹿児島大学	大学院理工学研究科	Magnetic properties of Fe-based magnets under high pressures	Keiichi Koyama	Kagoshima University
116	”	尾上 昌平	鹿児島大学	大学院理工学研究科	”	Masahira Onoue	Kagoshima University
117	Mn-Fe 基 4 元磁性体の磁気特性	小山 佳一	鹿児島大学	大学院理工学研究科	Magnetic properties of Mn and Fe-based quaternary magnets	Keiichi Koyama	Kagoshima University
118	”	アドライン ンゴジ ム ウッド	鹿児島大学	大学院理工学研究科	”	Adline Ngozi Nwodo	Kagoshima University
119	反転対称性のない遷移金属間化合物とその関連物質の高圧下輸送特性	仲間 隆男	琉球大学	理学部	Transport properties of non-centrosymmetric transition metals compounds under high pressure	Takao Nakama	University of the Ryukyus
120	”	垣花 将司	琉球大学	大学院理工学研究科	”	Masashi Kakahana	University of the Ryukyus
121	遷移金属化合物の高圧力下の輸送特性	仲間 隆男	琉球大学	理学部	Pressure effect on transport properties of transition metal compounds	Takao Nakama	University of the Ryukyus
122	”	川勝 祥矢	琉球大学	大学院理工学研究科	”	Shoya Kawakatsu	University of the Ryukyus
123	新しい Ce および La 三元系化合物の圧力下比熱測定	本山 岳	島根大学	大学院総合理工学研究科	Specific heat measurements of new Ce and La ternary compounds under pressure	Gaku Motoyama	Shimane University
124	”	坪内 将紘	島根大学	総合理工学部	”	Masahiro Tsubouchi	Shimane University
125	DAC を用いた高圧下 X 線回折	狩野 みか	日本工業大学	共通教育系 (物理)	X-ray diffraction measurements under high pressure by using DAC	Mika Kano	Nippon Institute of Technology
担当所員：尾崎 泰助							
126	実験と計算の協奏による IV 族二次元材料の構造・電子状態解析及び制御	アントワヌ フロランス	北陸先端科学技術大学院大学	マテリアルサイエンス系	Analysis and control of crystal and electronic structures of group IV 2D materials through concerted collaboration of experiment and theory	Antoine Fleurence	JAIST
127	”	新田 寛和	北陸先端科学技術大学院大学	先端科学技術研究科	”	Hirokazu Nitta	JAIST
担当所員：益田 隆嗣							

No.	課題名	氏名	所属		Title	Name	Organization
128	重い電子系超伝導体における量子臨界揺らぎ	横山 淳	茨城大学	理学部	Quantum critical fluctuations in heavy fermion superconductors	Makoto Yokoyama	Ibaraki University
129	”	鈴木 康平	茨城大学	大学院理工学研究科	”	Kohei Suzuki	Ibaraki University
130	S=1 スピンドイマー物質 $K_2NiMo_2O_8$ と Co ダイマー磁性体 $CaCoV_2O_7$ の磁性研究	那波 和宏	東北大学	多元物質科学研究所	Magnetic properties in S = 1 spin dimer compound $K_2NiMo_2O_8$ and Co dimer magnet $CaCoV_2O_7$	Kazuhiro Nawa	Tohoku University
131	”	村崎 遼	東北大学	大学院理学研究科	”	Ryo Murasaki	Tohoku University
132	異方的三角格子 $Ca_3ReO_5Cl_2$ 単結晶試料の軸立て	那波 和宏	東北大学	多元物質科学研究所	Alignment of single crystalline samples of $Ca_3ReO_5Cl_2$ with anisotropic triangular lattice	Kazuhiro Nawa	Tohoku University
133	硫黄置換により誘起される $FeTe_{1-x}S_x$ の超伝導特性	山中 隆義	東京理科大学	理工学部	Superconductivity in sulfur substituted $FeTe_{1-x}S_x$	Takayoshi Yamanaka	Tokyo University of Science
134	”	矢口 宏	東京理科大学	理工学部	”	Hiroshi Yaguchi	Tokyo University of Science
135	”	梅澤 直樹	東京理科大学	大学院理工学研究科	”	Naoki Umezawa	Tokyo University of Science
136	$Cu_3O_8$ 三量体をもつ $Na_2Cu_3Ge_4O_{12}$ の単結晶評価	安井 幸夫	明治大学	理工学部	Characterization of Single Crystals of $Cu_3O_8$ trimer System $Na_2Cu_3Ge_4O_{12}$	Yukio Yasui	Meiji University
137	$Yb(Co_{1-x}Ir_x)_2Zn_{20}$ の極低温比熱測定	阿曾 尚文	琉球大学	理学部	Specic heat measurement at very low temperature on $Yb(Co_{1-x}Ir_x)_2Zn_{20}$	Naofumi Aso	University of the Ryukyus
138	”	瑞慶覧 長星	琉球大学	大学院理工学研究科	”	Chousei Zukeran	University of the Ryukyus
139	$Yb_{1-x}Lu_xCo_2Zn_{20}$ の極低温比熱測定	阿曾 尚文	琉球大学	理学部	Specic heat measurement at very low temperature on $Yb_{1-x}Lu_xCo_2Zn_{20}$	Naofumi Aso	University of the Ryukyus
140	”	諸見里 真嗣	琉球大学	大学院理工学研究科	”	Masatsugu Moromizato	University of the Ryukyus
141	3本足磁性体 $Cu_3(OH)_4SO_4$ の単結晶試料の結晶性の確認	萩原 雅人	高エネルギー加速器研究機構	物質構造科学研究所	Checking crystallization of three legged ladder $Cu_3(OH)_4SO_4$	Masato Hagihara	KEK
142	中性子散乱実験のための結晶方位決定	中島 多朗	理化学研究所	創発物性科学研究センター	Crystal alignment for neutron scattering experiment	Taro Nakajima	RIKEN
143	$Ce_5Si_3$ 単結晶試料の高エネルギー X線ラウエ装置による結晶方位同定 II	小林 理気	琉球大学	理学部	Alignment of $Ce_5Si_3$ single crystals by high-energy X-ray Laue diffraction II	Riki Kobayashi	University of the Ryukyus
144	空間反転対称性の破れた超伝導体の結晶性評価	古川 はづき	お茶の水女子大学	基幹研究院	Evaluation of single crystal quality of non-centrosymmetric superconductors	Hazuki Furukawa	Ochanomizu University

No.	課題名	氏名	所属		Title	Name	Organization
145	”	左右田 稔	理化学研究所	創発物性科学研究センター	”	Minoru Soda	RIKEN
担当所員：嶽山 正二郎							
146	超強磁場磁気光学による $\text{Cu}_3\text{Mo}_2\text{O}_9$ の磁化プラトーの研究 III	黒江 晴彦	上智大学	理工学部	Ultra-high magnetic field magneto-optical approach to the study of magnetization plateau in $\text{Cu}_3\text{Mo}_2\text{O}_9$ using vertical single-turn coil system III	Haruhiko Kuroe	Sophia University
担当所員：金道 浩一							
147	アンダードーブ $\text{Bi-2223}$ における超伝導揺らぎの研究	渡辺 孝夫	弘前大学	大学院理工学研究科	A study of the superconducting fluctuation using magnetotransport measurements for underdoped $\text{Bi-2223}$ single crystals	Takao Watanabe	Hirosaki University
148	”	川村 圭輔	弘前大学	大学院理工学研究科	”	Keisuke Kawamura	Hirosaki University
149	サブメガ Gauss 領域での希土類物性研究	海老原 孝雄	静岡大学	学術院理学領域	Physical property of rare earth compounds at pulse magnet	Takao Ebihara	Shizuoka University
150	”	村串 拓真	静岡大学	大学院総合科学技術研究科	”	Takuma Murakoshi	Shizuoka University
151	重い電子系化合物が示す量子臨界現象と磁気相関	横山 淳	茨城大学	理学部	Quantum critical phenomena and magnetic correlations in heavy-fermion compounds	Makoto Yokoyama	Ibaraki University
152	”	菅原 良馬	茨城大学	理学部	”	Ryoma Sugawara	Ibaraki University
153	ホイスラー化合物 $\text{Fe}_{3-x}\text{Mn}_x\text{Si}$ の強磁場物性	廣井 政彦	鹿児島大学	大学院理工学研究科	Physical properties of Heusler compounds $\text{Fe}_{3-x}\text{Mn}_x\text{Si}$ under high magnetic fields	Masahiko Hiroi	Kagoshima University
154	過剰オーバードーブ $\text{Bi-2212}$ のパルス強磁場中面間輸送特性を用いた擬ギャップ状態の研究	渡辺 孝夫	弘前大学	大学院理工学研究科	A study of the pseudogap state using interlayer magnetotransport measurements under pulsed magnetic fields for heavily overdoped $\text{Bi-2212}$	Takao Watanabe	Hirosaki University
155	”	川村 圭輔	弘前大学	大学院理工学研究科	”	Keisuke Kawamura	Hirosaki University
156	$\text{Yb}_4\text{TGe}_8$ (T: 遷移金属) およびその周辺物質の強磁場磁化測定	道岡 千城	京都大学	大学院理学研究科	High-field magnetization measurements of $\text{Yb}_4\text{TGe}_8$ (T: transition metal) and their family compounds	Chishiro Michioka	Kyoto University
157	”	引地 将仁	京都大学	大学院理学研究科	”	Masahito Hikiji	Kyoto University
158	溶液法を用いて作成したカゴメ格子反強磁性体の磁性	植田 浩明	京都大学	大学院理学研究科	Magnetism of kagome lattice fluorides synthesized using solution method	Hiroaki Ueda	Kyoto university
159	”	今西 茂	京都大学	理学部	”	Shigeru Imanishi	Kyoto University

No.	課題名	氏名	所属		Title	Name	Organization
160	幾何学的フラストレート磁性体の強磁場磁化測定	菊池 彦光	福井大学	学術研究院工学系	Magnetization measurements of the frustrated magnets	Hikomitsu Kikuchi	University of Fukui
161	”	春木 晶尋	福井大学	工学部	”	Akihiro Haruki	University of Fukui
162	(U,Th)Be <sub>13</sub> , U(Pd,Ni) <sub>2</sub> Al <sub>3</sub> , U <sub>2</sub> PtC <sub>2</sub> 及び関連物質における重い電子系化合物強磁場物性	清水 悠晴	東北大学	金属材料研究所	High-field physical properties of (U,Th)Be <sub>13</sub> , U(Pd,Ni) <sub>2</sub> Al <sub>3</sub> , U <sub>2</sub> PtC <sub>2</sub> , and other heavy-fermion systems	Yusei Shimizu	Tohoku University
163	MnNiGe-CoNiGe 系化合物の高磁場磁歪測定	伊藤 昌和	鹿児島大学	学術研究院理工学域	Magnetic strain of MnNiGe-CoNiGe system in high magnetic field	Masakazu Ito	Kagoshima University
164	”	恩田 圭二郎	鹿児島大学	大学院理工学研究科	”	Keijiro Onda	Kagoshima University
165	BiS <sub>2</sub> 系化合物超伝導体の上部臨界磁場	加瀬 直樹	東京理科大学	理学部	Upper critical field of the BiS <sub>2</sub> -based superconductors	Naoki Kase	Tokyo University of Science
166	金属ナノ結晶集合体の磁化特性	稲田 貢	関西大学	システム理工学部	Magnetic properties of metal nanocrystal assemblies	Mitsuru Inada	Kansai University
167	”	米澤 諒	関西大学	システム理工学部	”	Ryo Yonezawa	Kansai University
168	Topological insulator SmB <sub>6</sub> , YbB <sub>12</sub> の磁化特性と比熱	伊賀 文俊	茨城大学	理学部	Magnetic and thermal properties of topological insulator SmB <sub>6</sub> and YbB <sub>12</sub>	Fumitoshi Iga	Ibaraki University
169	”	松浦 航	茨城大学	大学院理工学研究科	”	Wataru Matsuura	Ibaraki University
170	高圧合成希土類 6 及び 12 ホウ化物の磁化特性と比熱	伊賀 文俊	茨城大学	理学部	Magnetic and thermal properties of rare earth hexa-borides and dodeca-borides produced by high pressure synthesis	Fumitoshi Iga	Ibaraki University
171	”	山田 貴大	茨城大学	理学部	”	Takahiro Yamada	Ibaraki University
担当所員：徳永 将史							
172	重い電子系における強磁場中の電子状態研究	海老原 孝雄	静岡大学	学術院理学領域	Electronic states at high magnetic fields in Heavy Fermion systems	Takao Ebihara	Shizuoka University
173	パルス電磁石を用いた単結晶 BiFeO <sub>3</sub> の電気磁気効果の研究	河智 史朗	東京工業大学	元素戦略研究センター	Study of magnetoelectric effect in single crystal BiFeO <sub>3</sub> using pulse magnet	Shiro Kawachi	Tokyo Institute of Technology
174	キャリア制御した Cd <sub>3</sub> As <sub>2</sub> 薄膜における表面量子ホール状態の解明	打田 正輝	東京大学	大学院工学系研究科	Investigation of surface quantum Hall states in Cd <sub>3</sub> As <sub>2</sub> films with reduced carriers	Masaki Uchida	The University of Tokyo
175	磁場誘起マルテンサイト変態における核生成と成長の実空間観察	新津 甲大	京都大学	大学院工学研究科	In-situ observations of nucleation and growth of magnetic-field-induced martensite	Kodai Niitsu	Kyoto University

No.	課題名	氏名	所属		Title	Name	Organization
176	”	矢野 凱己	京都大学	大学院工学研究科	”	Yoshiki Yano	Kyoto University
177	磁気光学顕微鏡による超伝導体中の量子渦の実空間非平衡ダイナミクス観測手法の確立	黒川 穂高	東京大学	大学院総合文化研究科	Observing the real-space nonequilibrium dynamics of vortices in superconductor with a magneto-optical microscope	Hodaka Kurokawa	The University of Tokyo
178	高移動度 EuTiO <sub>3</sub> 薄膜における磁気量子振動の観測	打田 正輝	東京大学	大学院工学系研究科	Observation of quantum magnetic oscillations in high-mobility EuTiO <sub>3</sub> thin films	Masaki Uchida	The University of Tokyo
179	”	ジュマエダ ジャトミカ	静岡大学	大学院自然科学教育部	”	Jumaeda Jatmika	Shizuoka University
180	”	鈴木 文登	静岡大学	大学院総合科学技術研究科	”	Fumito Suzuki	Shizuoka University
181	CoV 基形状記憶合金における磁場誘起マルテンサイト変態とその場組織観察	キョ キョウ	東北大学	大学院工学研究科	Magnetic field-induced martensitic transformation and in situ observation of microstructure on CoV-based shape memory alloys	Xiao Xu	Tohoku University
182	Ce <sub>2</sub> MgGe <sub>2</sub> の強磁場磁化	広瀬 雄介	新潟大学	理学部物理学科	High-field magnetization of Ce <sub>2</sub> MgGe <sub>2</sub>	Yusuke Hirose	Niigata University
183	”	本多 史憲	東北大学	金属材料研究所	”	Fuminori Honda	Tohoku University
184	逆スピネル M <sub>2</sub> XO <sub>4</sub> (M=Mn,Co, X=Ti,Sn) の強磁場磁化過程の研究	太田 寛人	東京農工大学	大学院工学府	Study of high-field magnetization curves of inverse spinel M <sub>2</sub> XO <sub>4</sub> (M=Mn,Co, X=Ti,Sn)	Hiroto Ohta	Tokyo University of Agriculture and Technology
185	”	行田 祥一郎	東京農工大学	大学院工学府	”	Shoichiro Gyoda	Tokyo University of Agriculture and Technology
186	”	徳永 柊介	東京農工大学	工学部	”	Shuusuke Tokunaga	Tokyo University of Agriculture and Technology
187	結晶構造が特異な磁性体の強磁場磁化過程	香取 浩子	東京農工大学	大学院工学研究院	High-field magnetization process of magnetic material with unique crystal structure	Hiroko Katori	Tokyo University of Agriculture and Technology
188	”	濱住 莉加	東京農工大学	大学院工学府	”	Rika Hamazumi	Tokyo University of Agriculture and Technology
189	”	羽鳥 滋	東京農工大学	工学部	”	Shigeru Hatori	Tokyo University of Agriculture and Technology
190	ホイスラー合金 NiCoMnGa のパルス強磁場下磁歪測定	木原 工	東北大学	金属材料研究所	Magnetostriction Measurements under the Pulsed High Magnetic Fields in Heusler Alloy NiCoMnGa	Takumi Kihara	Tohoku University
191	フェルミエネルギーを制御した多層ディラック電子系の強磁場輸送特性	酒井 英明	大阪大学	大学院理学研究科	High-field magneto-transport properties for a multilayered Dirac fermion system with tunable Fermi energy	Hideaki Sakai	Osaka University
192	”	西村 拓也	大阪大学	大学院理学研究科	”	Takuya Nishimura	Osaka University

No.	課題名	氏名	所属		Title	Name	Organization
193	”	藤村 飛雄吾	大阪大学	大学院理学研究科	”	Hyugo Fujimura	Osaka University
194	”	中川 賢人	大阪大学	理学部	”	Kento Nakagawa	Osaka University
195	正四角台塔型反強磁性体の強磁場中電気磁気特性の測定	木村 健太	東京大学	大学院新領域創成科学研究科	High-field magnetoelectric properties of square-cupola-based antiferromagnets	Kenta Kimura	The University of Tokyo
196	重い電子系ウラン化合物の強磁場伝導特性	芳賀 芳範	日本原子力研究開発機構	先端基礎研究センター	Transport characteristics of heavy fermion uranium compounds under high magnetic field	Yoshinori Haga	Japan Atomic Energy Agency
197	パイロクロア型モリブデン酸化物 (Nd <sub>1-x</sub> Ca <sub>x</sub> ) <sub>2</sub> Mo <sub>2</sub> O <sub>7</sub> の精密バンドフィリング制御による巨大異常ホール効果の探索	マクシミリアン ヒルシュベルガー	理化学研究所	創発物性科学研究センター	Precise band-filling controlled of large anomalous Hall effects in pyrochlore-type molybdates (Nd <sub>1-x</sub> Ca <sub>x</sub> ) <sub>2</sub> Mo <sub>2</sub> O <sub>7</sub>	Maximilian Hirschberger	RIKEN
担当所員：松田 康弘							
198	カゴメ格子反強磁性体 Li <sub>2</sub> Cr <sub>3</sub> SbO <sub>8</sub> の強磁場磁化過程測定	吉田 紘行	北海道大学	大学院理学研究科	High-field magnetization measurements on kagome lattice antiferromagnets Li <sub>2</sub> Cr <sub>3</sub> SbO <sub>8</sub>	Hiroyuki Yoshida	Hokkaido University
199	”	石井 裕人	北海道大学	大学院理学研究科	”	Yuto Ishii	Hokkaido University
200	近藤半導体 (Yb,R)B <sub>12</sub> 、価数揺動物質 (Y,Tm)B <sub>6</sub> のワンターンコイル 120T パルス磁場下での強磁場磁化過程	伊賀 文俊	茨城大学	理学部	High field magnetization of Kondo insulator (Yb,R)B <sub>12</sub> and valence fluctuation material (Y,Tm)B <sub>6</sub> by using one-turn coil in a 120 T pulse magnet	Fumitoshi Iga	Ibaraki University
201	”	中山 裕之	茨城大学	理学部	”	Hiroyuki Nakayama	Ibaraki university
担当所員：小濱 芳允							
202	キラル極性磁性体 Ni <sub>2</sub> InSbO <sub>6</sub> の磁気相転移に伴う光学スペクトル変化	荒木 勇介	東京大学	大学院新領域創成科学研究科	Magneto-optical effect in a chiral polar magnet Ni <sub>2</sub> InSbO <sub>6</sub>	Yusuke Araki	The University of Tokyo
203	”	渡辺 義人	東京大学	大学院新領域創成科学研究科	”	Yoshito Watanabe	The University of Tokyo
204	二次元超伝導体 NbSe <sub>2</sub> 薄膜の上部臨界磁場測定	松岡 秀樹	東京大学	大学院工学系研究科	Upper critical field measurement of two dimensional superconducting NbSe <sub>2</sub> thin films	Hideaki Matsuoka	The University of Tokyo
205	分子内エキサイプレックス蛍光の超強磁場効果	谷本 能文	広島大学	大学院理学研究科	Effect of ultra-high magnetic field on the intra-molecular exciplex fluorescence	Yoshifumi Tanimoto	Hiroshima University
206	キラル極性磁性体 Ni <sub>2</sub> InSbO <sub>6</sub> の磁気相転移に伴う光学スペクトル変化	有馬 孝尚	東京大学	大学院新領域創成科学研究科	Magneto-optical effect in a chiral polar magnet Ni <sub>2</sub> InSbO <sub>6</sub>	Takahisa Arima	The University of Tokyo
207	”	徳永 祐介	東京大学	大学院新領域創成科学研究科	”	Yusuke Tokunaga	The University of Tokyo

No.	課題名	氏名	所属		Title	Name	Organization
208	”	海本 祐真	東京大学	大学院新領域創成科学研究科	”	Yuma Umimoto	The University of Tokyo
担当所員：辛 埴							
209	レーザー励起光電子顕微鏡を用いた抵抗変化メモリ材料のナノ物性計測	木下 健太郎	東京理科大学	理学部	Nano physical property measurement of resistance change memory material using laser excited photo-emission microscope	Kentaro Kinoshita	Tokyo University of Science
210	”	奥田 裕司	東京理科大学	大学院理学研究科	”	Yuji Okuda	Tokyo University of Science
211	”	川並 将太郎	東京理科大学	大学院理学研究科	”	Shotaro Kawanami	Tokyo University of Science
212	”	中畝 悠介	東京理科大学	大学院理学研究科	”	Yusuke Nakaune	Tokyo University of Science
213	”	清水 敦史	東京理科大学	大学院理学研究科	”	Atsushi Shimizu	Tokyo University of Science
214	”	齋藤 修平	東京理科大学	大学院理学研究科	”	Shuheii Saitoh	Tokyo University of Science
215	有機半導体分子の吸着に伴って生じるトポロジカル表面状態の変化	金井 要	東京理科大学	理工学部物理学科	Modification of Topological surface states upon adsorption of organic semiconductors.	Kaname Kanai	Tokyo University of Science
216	”	北澤 辰也	東京理科大学	理工学部物理学科	”	Tatsuya Kitazawa	Tokyo University of Science
217	低対称性半導体基板上的Bi擬1次元構造におけるスピン偏極電子状態	大坪 嘉之	大阪大学	大学院生命機能研究科	Spin-polarized electronic states on quasi-1D Bi fabricated on low-symmetric semiconductor substrates	Yoshiyuki Ohtsubo	Osaka University
218	”	中村 拓人	大阪大学	大学院理学研究科	”	Takuto Nakamura	Osaka University
219	高分解能スピン・角度分解光電子分光によるハーフメタル強磁性体CoS <sub>2</sub> の電子構造研究	藤原 弘和	岡山大学	大学院自然科学研究科	Study on electronic structures in half-metallic ferromagnet CoS <sub>2</sub> by high-resolution spin- and angle-resolved photoemission spectroscopy	Hirokazu Fujiwara	Okayama University
220	遷移金属ダイカルコゲナイドVTe <sub>2</sub> の時間分解角度分解光電子分光	三石 夏樹	東京大学	大学院工学系研究科	Time-resolved angle-resolved photoemission study on transition metal dichalcogenides VTe <sub>2</sub>	Natsuki Mitsuishi	The University of Tokyo
221	極性ワイル半金属MoTe <sub>2</sub> におけるスピン偏極したトポロジカル表面状態の観測	坂野 昌人	東京大学	大学院工学系研究科	Observation of spin-polarized topological surface state on polar Weyl semimetal MoTe <sub>2</sub>	Masato Sakano	The University of Tokyo
222	”	深田 和宏	東京大学	大学院工学系研究科	”	Kazuhiro Fukada	The University of Tokyo
223	ミスフィット超伝導体の超伝導ギャップの観測	高橋 健吾	東京大学	大学院工学系研究科	Observation of superconducting energy gap in misfit superconductors	Kengo Takahashi	The University of Tokyo

No.	課題名	氏名	所属		Title	Name	Organization
224	トポジカル絶縁体-強磁性体界面におけるスピン偏極電子状態の観測	小林 正起	東京大学	大学院工学系研究科	Observation of spin-polarized electronic state at an interface between topological insulator and ferromagnet	Masaki Kobayashi	The University of Tokyo
225	原子層タリウム単結晶のスピン偏極電子バンド測定	坂本 一之	千葉大学	大学院工学研究科	Investigation of the spin-polarized electronic band structure of atomic layer thallium single crystal	Kazuyuki Sakamoto	Chiba University
226	トポジカル絶縁体薄膜のレーザー励起角度光電子分光による表面状態の観察	黒田 眞司	筑波大学	数理物質系	Observation of surface state on thin films of topological insulator using laser photoemission spectroscopy	Shinji Kuroda	University of Tsukuba
227	〃	伊藤 寛史	筑波大学	大学院数理物質科学研究科	〃	Hiroshi Ito	University of Tsukuba
228	遷移金属インターカレート 1T-TiS <sub>2</sub> のスピン分解角度分解光電子分光	伊藤 孝寛	名古屋大学	シンクロトロン光研究センター	Spin-resolved angle-resolved photoemission study of transition metal intercalated 1T-TiS <sub>2</sub>	Takahiro Ito	Nagoya University
229	〃	鍋平 直輝	名古屋大学	工学部	〃	Naoki Nabehira	Nagoya University
担当所員：小林 洋平							
230	次世代レーザーとレーザー加工の基礎技術研究	吉富 大	産業技術総合研究所	電子光技術研究部門	Basic research on next generation laser systems and laser machining technology	Dai Yoshitomi	National Institute of Advanced Industrial Science and Technology
231	〃	高田 英行	産業技術総合研究所	電子光技術研究部門	〃	Hideyuki Takada	National Institute of Advanced Industrial Science and Technology
232	超高速分光用ファイバーレーザーとパルス計測機器の開発	末元 徹	豊田理化学研究所		Development of fiber laser and pulse characterization instrument for ultrafast optical spectroscopy	Tohru Suemoto	Toyota Physical and Chemical Research Institute
233	青色半導体レーザー用ファイバ型光コンバイナの開発	藤本 靖	千葉工業大学	工学部	Development on fiber power combiner for GaN semiconductor lasers	Yasushi Fujimoto	Chiba Institute of Technology (CIT)
234	エルビウムドープファイバー発振器の作製	大間知 潤子	関西学院大学	理工学部	Development of a Er-doped fiber laser system	Junko Omachi	Kwansei Gakuin University
担当所員：板谷 治郎							
235	超高速レーザー分光法を用いた弾性波伝播の観測	牧野 哲征	福井大学	学術研究院工学系部門	Observation of very short stress pulses with ultrafast laser spectroscopy	Takayuki Makino	University of Fukui
236	〃	竹内 智哉	福井大学	工学部	〃	Tomoya Takeuchi	University of Fukui
237	超高速レーザー分光法を用いた弾性波伝播の観測	山出 拓史	福井大学	大学院工学研究科	Observation of very short stress pulses with ultrafast laser spectroscopy	Takuji Yamade	University of Fukui

一般研究員・大阪大学 先端強磁場科学研究センター (General Researcher・Center for Advanced High Magnetic Field Science Osaka University)

No.	課題名	氏名	所属	Title	Name	Organization
担当：萩原 政幸 (大阪大学)						
1	パルス強磁場を用いた強相関電子系物質の強磁場物性の研究	竹内 徹也	大阪大学	低温センター	Physical properties of strongly correlated electron systems under pulsed high magnetic field	Tetsuya Takeuchi Osaka University
2	〃	大貫 惇睦	琉球大学	理学部	〃	Yoshichika Onuki University of the Ryukyus
3	パルス強磁場を用いた高圧下 ESR 装置の開発と応用	櫻井 敬博	神戸大学	研究基盤センター	Development and application of high-pressure ESR system using pulse high field	Takahiro Sakurai Kobe University
4	カゴメストリップ鎖の不純物誘起磁化プラトー	浅野 貴行	福井大学	学術研究院工学系部門	Impurity induced magnetization plateau in the kagome strip chain	Takayuki Asano University of Fukui
5	カゴメ格子反強磁性体 $\text{CaCu}_3(\text{OH})_6\text{Cl}_2 \cdot 0.6\text{H}_2\text{O}$ の強磁場下 ESR 測定	吉田 紘行	北海道大学	大学院理学研究院	High-field ESR measurements on kagome lattice antiferromagnets $\text{CaCu}_3(\text{OH})_6\text{Cl}_2 \cdot 0.6\text{H}_2\text{O}$	Hiroyuki Yoshida Hokkaido University
6	〃	石井 裕人	北海道大学	大学院理学研究院	〃	Yuto Ishii Hokkaido University
7	$\text{Ce}_2\text{MgX}_2(\text{X}=\text{Si},\text{Ge})$ の強磁場磁気抵抗	広瀬 雄介	新潟大学	理学部	Magnetoresistance of $\text{Ce}_2\text{MgX}_2$ ( $\text{X}=\text{Si},\text{Ge}$ ) at high-magnetic field	Yusuke Hirose Niigata University
8	〃	本多 史憲	東北大学	金属材料研究所	〃	Fuminori Honda Tohoku University
9	パルス強磁場によるマルテンサイト変態の時間依存性に関する研究	福田 隆	大阪大学	大学院 工学研究科	Study on time dependence of martensitic transformation using pulsed high magnetic field	Takashi Fukuda Osaka University
10	フラストレート系有機磁性体の強磁場磁性	山口 博則	大阪府立大学	大学院理学系研究科	High-field magnetic properties of frustrated organic radical compounds	Hironori Yamaguchi Osaka Prefecture University
11	反強磁性絶縁体 $\text{BaMn}_2\text{Pn}_2$ の高磁場における磁気輸送特性	KHUONG KIM HUYNH	東北大学	材料科学高等研究所	Magnetotransport properties under high magnetic fields of $\text{BaMn}_2\text{Pn}_2$ antiferromagnetic insulators	Khuong Kim Huynh Tohoku University
12	1 次元配位高分子磁性体の合成と構造、量子磁性の解明	本多 善太郎	埼玉大学	大学院理工学研究科	Synthesis, structure, and quantum magnetism of one-dimensional transition metal coordination polymers	Zentaro Honda Saitama University
13	パルス強磁場用極低温実験装置の開発	野口 悟	大阪府立大学	大学院理学系研究科	Development of the cryostat for pulsed high magnetic field	Satoru Noguchi Osaka Prefecture University
14	〃	松山 友樹	大阪府立大学	生命環境科学域	〃	Tomoki Matsuyama Osaka Prefecture University
15	〃	土田 稜	大阪府立大学	生命環境科学域	〃	Ryo Tsuchida Osaka Prefecture University

No.	課題名	氏名	所属		Title	Name	Organization
16	強磁場環境下におけるタンパク質の結晶化	牧 祥	大阪大谷大学	薬学部	Protein crystallization under the magnetic field condition	Syou Maki	Osaka Ohtani University
17	単核遷移金属錯体のゼロ磁場分裂と動的磁性の関係	福田 貴光	大阪大学	大学院理学研究科	Relationship between zero-field splittings and dynamic magnetism of monocuclear transition metal complexes	Takamitsu Fukuda	Osaka University
18	〃	石崎 聡晴	大阪大学	大学院理学研究科	〃	Toshiharu Ishizaki	Osaka University
19	歪んだハニカム格子を有す反強磁性体 $\text{CaMn}_2\text{Bi}_2$ における強磁場輸送特性の研究	浦田 隆広	名古屋大学	大学院工学研究科	High field transport measurements on antiferromagnet $\text{CaMn}_2\text{Bi}_2$ with corrugated honeycomb structure	Takahiro Urata	Nagoya University
20	パルス強磁場を用いたワイル半金属の量子輸送特性の研究	村川 寛	大阪大学	大学院理学研究科	Pulsed magnetic field studies of quantum transport properties of Weyl semimetals	Hiroshi Murakawa	Osaka University
21	〃	駒田 盛是	大阪大学	大学院理学研究科	〃	Moriyoshi Komada	Osaka University
22	〃	横井 滉平	大阪大学	大学院理学研究科	〃	Kohei Yokoi	Osaka University
23	傾斜反強磁性を示す層状ディラック電子系物質の磁化測定	酒井 英明	大阪大学	大学院理学研究科	Magnetic measurements on a multilayered Dirac fermion system hosting canted antiferromagnetic order	Hideaki Sakai	Osaka University
24	〃	藤村 飛雄吾	大阪大学	大学院理学研究科	〃	Hyugo Fujimura	Osaka University
25	〃	中川 賢人	大阪大学	理学部	〃	Kento Nakagawa	Osaka University
26	$\text{SmB}_6$ 薄膜の強磁場中での磁気抵抗, ホール効果測定	穴戸 寛明	大阪府立大学	大学院工学研究科	Magnetoresistance and Hall effect measurements for $\text{SmB}_6$ thin films under high magnetic field	Hiroaki Shishido	Osaka Prefecture University
27	$\text{GaFeO}_3$ におけるスピン波の非相反性	有馬 孝尚	東京大学	大学院新領域創成科学研究科	Nonreciprocal spin waves in $\text{GaFeO}_3$	Takahisa Arima	The University of Tokyo
28	〃	近江 毅志	東京大学	大学院新領域創成科学研究科	〃	Tsuyoshi Omi	The University of Tokyo
29	フタロシアニン分子系伝導体で観測される巨大磁気抵抗に対する遷移金属置換の効果	花咲 徳亮	大阪大学	大学院理学研究科	Transition-metal Substitution Effect on Giant Magnetoresistance in Phthalocyanine-molecular Conductors	Noriaki Hanasaki	Osaka University
30	〃	清水 智可	大阪大学	理学部	〃	Tomoka Shimizu	Osaka University
31	正四角台塔型反強磁性体の強磁場中 ESR 測定	木村 健太	東京大学	大学院新領域創成科学研究科	High-field ESR measurements of square-cupola-based antiferromagnets	Kenta Kimura	The University of Tokyo
32	高温超伝導体のパルス強磁場下電流電圧特性	掛谷 一弘	京都大学	大学院工学研究科	Current-voltage characteristics in high-Tc superconductors under pulsed high magnetic fields	Itsuhiro Kakeya	Kyoto University

No.	課題名	氏名	所属		Title	Name	Organization
33	高磁場下における三角格子反強磁性体 Ag <sub>2</sub> CrO <sub>2</sub> 単結晶試料の磁気抵抗測定	新見 康洋	大阪大学	大学院理学研究科	Magnetoresistance measurements of triangular-antiferromagnet Ag <sub>2</sub> CrO <sub>2</sub> single crystal samples under high magnetic fields	Yasuhiro Niimi	Osaka University
34	Ni <sub>2</sub> MnGa 系新規ホイスラー合金の超磁歪の高速磁場応答性の研究	左近 拓男	龍谷大学	理工学部	Research on time dependences of magnetstriction of Ni <sub>2</sub> MnGa type Heusler alloys	Takuo Sakon	Ryukoku University
35	単軸性キラル磁性体の磁気特性測定 –磁気トルクと磁気共鳴測定–	戸川 欣彦	大阪府立大学	大学院工学研究科	Magnetic property of monoaxial chiral magnetic materials examined by means of magnetic torque and resonance measurements	Yoshihiko Togawa	Osaka Prefecture University
36	”	島本 雄介	大阪府立大学	大学院工学研究科	”	Yusuke Shimamoto	Osaka Prefecture University
37	CaBaCo <sub>2</sub> Fe <sub>2</sub> O <sub>7</sub> 単結晶試料の強磁場下での磁化・電気分極・ESR 測定	桑原 英樹	上智大学	理工学部	Magnetization, electric polarization, and ESR measurements for CaBaCo <sub>2</sub> Fe <sub>2</sub> O <sub>7</sub> single crystals in pulsed high magnetic fields	Hideki Kuwahara	Sophia University
38	強磁場 ESR 測定によるクロムスピネル酸化物の磁気励起の観測	木村 尚次郎	東北大学	金属材料研究所	Observation of the magnetic excitation in the chromium spinel oxides by high field ESR measurement	Shojiro Kimura	Tohoku University

物質合成・評価設備 P クラス / Materials Synthesis and Characterization P Class Researcher

No.	課題名	氏名	所属		Title	Name	Organization
1	幾何学的フラストレート系物質の単結晶育成と新奇物性の研究	松平 和之	九州工業大学	大学院工学研究科	Single crystal growth and study of novel phenomena of geometrically frustrated materials	Kazuyuki Matsuhira	Kyushu Institute of Technology
2	”	谷口 智哉	九州工業大学	大学院工学府	”	Tomoya Taniguchi	Kyushu Institute of Technology
3	電子が複合自由度を持つ遷移金属カルコゲナイドの合成と物性評価	片山 尚幸	名古屋大学	大学院工学研究科	Growth of the transition metal chalcogenides with charge, orbital and spin degrees of freedom	Naoyuki Katayama	Nagoya University
4	”	萬條 太駿	名古屋大学	大学院工学研究科	”	Taishun Manjo	Nagoya University

物質合成・評価設備 G クラス / Materials Synthesis and Characterization G Class Researcher

No.	課題名	氏名	所属		Title	Name	Organization
1	単結晶マンガン酸化物の誘電特性の研究	谷口 晴香	岩手大学	理工学部	Study of dielectric properties of single-crystalline manganite	Haruka Taniguchi	Iwate University
2	高温高圧水の固体触媒表面性質への影響の評価	大島 義人	東京大学	大学院新領域創成科学研究科	Effects of high temperature and pressure water on solid catalyst surface	Yoshito Oshima	The University of Tokyo
3	”	高橋 侑佳	東京大学	大学院新領域創成科学研究科	”	Yuka Takahashi	The University of Tokyo

No.	課題名	氏名	所属		Title	Name	Organization
4	全固体 Li 電池用電解質 (ガラスセラミックス) の研究	大友 順一郎	東京大学	大学院新領域創成科学研究科	Research on solid electrolyte (glass-ceramics) for Li battery	Junichiro Ohtomo	The University of Tokyo
5	”	陸 疎桐	東京大学	大学院新領域創成科学研究科	”	Lu Shutong	The University of Tokyo
6	新規プロトン-電子混合伝導体の開発	大友 順一郎	東京大学	大学院新領域創成科学研究科	Development of mixed proton-electron mixed conductors	Junichiro Ohtomo	The University of Tokyo
7	”	小城 元	東京大学	大学院新領域創成科学研究科	”	Gen Kojo	The University of Tokyo
8	142/5000 プロトン伝導固体酸化燃料電池によるアンモニア合成のための新しい三次元および二次元電極構造の設計と動力学解析	大友 順一郎	東京大学	大学院新領域創成科学研究科	Design of New 3-D and 2-D Electrode Structures and Kinetic Analysis for Ammonia Electrosynthesis with Proton-Conducting Solid Oxide Fuel Cells	Junichiro Ohtomo	The University of Tokyo
9	”	李 建毅	東京大学	大学院新領域創成科学研究科	”	Li Chien-i	The University of Tokyo
10	中温作動プロトン伝導型固体酸化燃料電池の新規セル設計	大友 順一郎	東京大学	大学院新領域創成科学研究科	New Cell Design of Intermediate Temperature Proton Conducting SOFC	Junichiro Ohtomo	The University of Tokyo
11	”	田所 洸	東京大学	大学院新領域創成科学研究科	”	Hiroshi Tadokoro	The University of Tokyo
12	ケミカルループ燃焼法における酸素キャリアの反応モデリング	大友 順一郎	東京大学	大学院新領域創成科学研究科	Reaction modeling in chemical looping systems with new oxygen carrier materials.	Junichiro Ohtomo	The University of Tokyo
13	”	松原 一起	東京大学	大学院新領域創成科学研究科	”	Kazuki Matsubara	The University of Tokyo
14	”	大友 順一郎	東京大学	大学院新領域創成科学研究科	”	Junichiro Ohtomo	The University of Tokyo
15	”	マーチン ケラー	東京大学	大学院新領域創成科学研究科	”	Martin Keller	The University of Tokyo
16	中温域でのアンモニア電解合成における新規電極触媒開発と反応メカニズムの解析	大友 順一郎	東京大学	大学院新領域創成科学研究科	Development of new electrochemical catalyst for ammonia electrolysis and evaluation of reaction mechanism at intermediate temperature	Junichiro Ohtomo	The University of Tokyo
17	”	長谷川 卓利	東京大学	大学院新領域創成科学研究科	”	Takuto Hasegawa	The University of Tokyo
18	アンモニア電解合成における電極触媒の界面構造制御と電位効果の検討	大友 順一郎	東京大学	大学院新領域創成科学研究科	Consideration between potential effect and control of cathode-catalyst interface structure in electrolytic synthesis of ammonia	Junichiro Ohtomo	The University of Tokyo
19	”	山本 和範	東京大学	工学部	”	Kazunori Yamamoto	The University of Tokyo
20	元素置換フェライトの磁気特性と化学組成	植田 浩明	京都大学	大学院理学研究科	Magnetic properties and chemical compositions of substituted ferrites	Hiroaki Ueda	Kyoto University

No.	課題名	氏名	所属		Title	Name	Organization
21	〃	増田 順一	京都大学	大学院理学研究科	〃	Junichi Masuda	Kyoto University
22	超臨界水を利用した微粒子合成におけるアルカリ金属種の影響	大島 義人	東京大学	大学院新領域創成科学研究科	Effect of alkali metal species for nanoparticle synthesis in supercritical water.	Yoshito Oshima	The University of Tokyo
23	〃	織田 耕彦	東京大学	大学院新領域創成科学研究科	〃	Yasuhiko Orita	The University of Tokyo
24	高温高圧水-アルコール混合溶媒を用いる二元金属ナノ粒子の合成と制御	大島 義人	東京大学	大学院新領域創成科学研究科	Control of bimetallic nanoparticle synthesis using high temperature and pressure water-alcohol mixture	Yoshito Oshima	The University of Tokyo
25	〃	劉 源	東京大学	大学院新領域創成科学研究科	〃	Liu Yuan	The University of Tokyo
26	ゼオライト触媒を利用した高温高圧水中のバイオマス化学変換	大島 義人	東京大学	大学院新領域創成科学研究科	Bio-mass conversion over zeolite under hot compressed water	Yoshito Oshima	The University of Tokyo
27	〃	アピバンボリラク チャン ウィット	東京大学	大学院新領域創成科学研究科	〃	Apibanboriak Chanwit	The University of Tokyo
28	メソポーラスマテリアル・グラフェンオキシドに担持した金属触媒のキャラクタリゼーション	佐々木 岳彦	東京大学	大学院新領域創成科学研究科	Characterization for metal catalysts supported on mesoporous materials and graphene oxides	Takehiko Sasaki	The University of Tokyo
29	〃	Etty Nurlia Kusumawati	東京大学	大学院理学系研究科	〃	Etty Nurlia Kusumawati	The University of Tokyo
30	〃	斎藤 貴仁	東京大学	大学院新領域創成科学研究科	〃	Takahito Saito	The University of Tokyo
31	触媒反応の insitu ラマン散乱測定	佐々木 岳彦	東京大学	大学院新領域創成科学研究科	In situ measurement of Raman scattering for heterogeneous catalytic reactions	Takehiko Sasaki	The University of Tokyo
32	アルカリ土類金属元素を含む充填スクッテルダイトの新物質探索	関根ちひろ	室蘭工業大学	大学院工学研究科	Search for new filled-skutterudite compounds including alkaline earth metal	Chihiro Sekine	Muroran Institute of Technology
33	〃	星野 愛	室蘭工業大学	大学院工学研究科	〃	Megumi Hoshino	Muroran Institute of Technology
34	超高圧プレスを用いた新規プロトニクス酸化物のソフト化学的合成法の検討	山口 周	東京大学	大学院工学系研究科	Oxide-Protonics materials synthesis by combined use of soft chemical method and high pressure	Shu Yamaguchi	The University of Tokyo
35	〃	田中 和彦	東京大学	大学院工学系研究科	〃	Kazuhiko Tanaka	The University of Tokyo
36	溶融亜鉛メッキ合金相の応力誘起変態	山口 周	東京大学	大学院工学系研究科	Stress-induced phase transformation of Fe-Zn alloy formed in hot-dip process	Shu Yamaguchi	The University of Tokyo
37	〃	田中 和彦	東京大学	大学院工学系研究科	〃	Kazuhiko Tanaka	The University of Tokyo

No.	課題名	氏名	所属		Title	Name	Organization
38	高圧印加による Al-Ir 1/0 近似結晶半導体の作製	木村 薫	東京大学	大学院新領域創成科学研究科	Synthesis of Al-Ir 1/0-Icosahedral Approximant Semiconductor by high-pressurization	Kaoru Kimura	The University of Tokyo
39	”	岩崎 祐昂	東京大学	大学院新領域創成科学研究科	”	Yutaka Iwasaki	The University of Tokyo
40	高圧下での MoSi <sub>2</sub> 型構造の FeAl <sub>2</sub> 結晶の作製	木村 薫	東京大学	大学院新領域創成科学研究科	High pressure synthesis of MoSi <sub>2</sub> type iron aluminide, FeAl <sub>2</sub> crystal	Kaoru Kimura	The University of Tokyo
41	”	飛田 一樹	東京大学	大学院新領域創成科学研究科	”	Kazuki Tobita	The University of Tokyo
42	アミノ酸の高圧下における圧力誘起反応の観察	藤本 千賀子	東京大学	大学院理学系研究科	Pressure-induced reaction of amino acids under high pressure	Chikako Fujimoto	The University of Tokyo
43	ナノ構造材料を用いた二次電池開発	細野 英司	産業技術総合研究所	省エネルギー研究部門	Development of secondary battery by using nanostructured materials	Eiji Hosono	National Institute of Advanced Industrial Science and Technology
44	4d および 5d 遷移金属化合物の薄膜化	平岡 奈緒香	東京大学	大学院理学系研究科	Developing new epitaxial thin films of 4d and 5d transition metal compounds	Naoka Hiraoka	The University of Tokyo
45	”	根岸 真通	東京大学	大学院理学系研究科	”	Masamichi Negishi	The University of Tokyo
46	”	山村 凌平	東京大学	大学院理学系研究科	”	Ryohhei Yamamura	The University of Tokyo
47	新しい希土類磁石の探求	齋藤 哲治	千葉工業大学	工学部	Research of new rare-earth magnets	Tetsuji Saito	Chiba Institute of Technology
48	高温高圧下で軽元素が鉄-シリケート-水系に及ぼす影響の解明	飯塚 理子	東京大学	大学院理学系研究科	Behavior of light elements in iron-silicate-water system under high pressure and high temperature	Riko Iizuka	The University of Tokyo
49	”	福山 鴻	東京大学	大学院理学系研究科	”	Ko Fukuyama	The University of Tokyo
50	Pr <sub>0.3</sub> Sr <sub>0.7</sub> Fe <sub>1-x</sub> Mn <sub>x</sub> O <sub>3</sub> (0.1 ≤ x ≤ 0.9) の高温における磁性と熱電特性に関する研究	中津川 博	横浜国立大学	大学院工学研究院	Magnetism and thermoelectric properties at high temperature in Pr <sub>0.3</sub> Sr <sub>0.7</sub> Fe <sub>1-x</sub> Mn <sub>x</sub> O <sub>3</sub> (0.1 ≤ x ≤ 0.9)	Hiroshi Nakatsugawa	Yokohama National University
51	ハーフメタル型ホイスラー合金の磁性と輸送特性に関する研究	重田 出	鹿児島大学	大学院理工学研究科	Study on the magnetic and transport properties of half-metallic Heusler alloys	Iduru Shigeta	Kagoshima University
52	逆スピネル M <sub>2</sub> XO <sub>4</sub> (M=Mn,Co, X=Ti,Sn) の弱磁場下における磁性の研究	太田 寛人	東京農工大学	大学院工学府	Low-field magnetic study on inverse spinel M <sub>2</sub> XO <sub>4</sub> (M=Mn,Co, X=Ti,Sn)	Hiroto Ohta	Tokyo University of Agriculture and Technology
53	”	行田 祥一郎	東京農工大学	大学院工学府	”	Shoichiro Gyoda	Tokyo University of Agriculture and Technology
54	”	徳永 柊介	東京農工大学	工学部	”	Shusuke Tokunaga	Tokyo University of Agriculture and Technology

No.	課題名	氏名	所属		Title	Name	Organization
55	スピングラス転移温度と物理パラメーターとの関係の研究	香取 浩子	東京農工大学	大学院工学研究科	Study of relationship between spin-glass transition temperature and physical parameter	Hiroko Katori	Tokyo University of Agriculture and Technology
56	”	柿本 和勇	東京農工大学	大学院工学府	”	Kazuo Kakimoto	Tokyo University of Agriculture and Technology
57	”	羽鳥 滋	東京農工大学	工学部	”	Shigeru Hatori	Tokyo University of Agriculture and Technology
58	四面体を基調とした構造をもつ混合原子価化合物の磁気・輸送特性	小林 慎太郎	名古屋大学	大学院工学研究科	Magnetic and transport properties of mixed-valent compounds consisting of tetrahedra	Shintaro Kobayashi	Nagoya University
59	”	中埜 彰俊	名古屋大学	大学院工学研究科	”	Akitoshi Nakano	Nagoya University
60	”	鬼頭 俊介	名古屋大学	大学院工学研究科	”	Shunsuke Kitou	Nagoya University
61	高い熱電性能を示す一次元テルル化物の合成と物性	岡本 佳比古	名古屋大学	大学院工学研究科	Synthesis and Physical Properties of One-Dimensional Tellurides with High Thermoelectric Performance	Yoshihiko Okamoto	Nagoya University
62	ホイスラー型化合物の磁気と伝導の研究	廣井 政彦	鹿児島大学	大学院理工学研究科	Study on the magnetic and electrical properties of Heusler compounds	Masahiko Hiroi	Kagoshima University
63	”	加藤 遼太	鹿児島大学	理学部	”	Ryota Kato	Kagoshima University
64	高圧印加による Li ドープ $\alpha$ 菱面体晶ボロンの作製	木村 薫	東京大学	大学院新領域創成科学研究科	Synthesis of Li-dope alpha-rhombohedral boron by high-pressurization	Kaoru Kimura	The University of Tokyo
65	”	酒井 志徳	東京大学	大学院新領域創成科学研究科	”	Munenori Sakai	The University of Tokyo
66	金属および半金属薄膜の作成	末元 徹	豊田理化学研究所		Preparation of metal and semimetal thin films	Tohru Suemoto	Toyota Physical and Chemical Research Institute
67	酸化物系融体密度・表面張力測定の超高温極限への挑戦	竹田 修	東北大学	大学院工学研究科	Measurement of density and surface tension of molten oxides at ultra-high temperature	Osamu Takeda	Tohoku University
68	希土類オルソフェライト単結晶成長と超高速テラヘルツ磁気分光	中嶋 誠	大阪大学	レーザー科学研究所	Ultrafast terahertz spin spectroscopy for rare-earth orthoferrite single crystal	Makoto Nakajima	Osaka University
69	”	加藤 康作	大阪大学	レーザー科学研究所	”	Kosaku Kato	Osaka University
70	”	邱 紅松	大阪大学	レーザー科学研究所	”	Hongsong Qiu	Osaka University
71	”	木本 翔大	大阪大学	レーザー科学研究所	”	Shodai Kimoto	Osaka University

No.	課題名	氏名	所属		Title	Name	Organization
72	”	上田 誠一郎	大阪大学	レーザー科学研究所	”	Seiichiro Ueda	Osaka University
73	新規超伝導物質合成と物性評価	芝内 孝禎	東京大学	大学院新領域創成科学研究科	Synthesis and characterization of novel superconducting materials	Takasada Shibauchi	The University of Tokyo
74	”	水上 雄太	東京大学	大学院新領域創成科学研究科	”	Yuta Mizukami	The University of Tokyo
75	”	細井 優	東京大学	大学院新領域創成科学研究科	”	Suguru Hosoi	The University of Tokyo
76	”	竹中 崇了	東京大学	大学院新領域創成科学研究科	”	Takaaki Takenaka	The University of Tokyo
77	”	石田 浩祐	東京大学	大学院新領域創成科学研究科	”	Kousuke Ishida	The University of Tokyo
78	”	杉村 優一	東京大学	大学院新領域創成科学研究科	”	Yuichi Sugimura	The University of Tokyo
79	”	田中 桜平	東京大学	大学院新領域創成科学研究科	”	Ohei Tanaka	The University of Tokyo
80	空間反転対称性を持たない新規磁性体の開発	有馬 孝尚	東京大学	大学院新領域創成科学研究科	Exploration of new noncentrosymmetric magnets	Takahisa Arima	The University of Tokyo
81	”	徳永 祐介	東京大学	大学院新領域創成科学研究科	”	Yusuke Tokunaga	The University of Tokyo
82	”	阿部 伸行	東京大学	大学院新領域創成科学研究科	”	Nobuyuki Abe	The University of Tokyo
83	”	藤間 友理	東京大学	大学院新領域創成科学研究科	”	Yuri Fujima	The University of Tokyo
84	”	佐藤 樹	東京大学	大学院新領域創成科学研究科	”	Tatsuki Sato	The University of Tokyo
85	”	吉澤 孟晃	東京大学	大学院新領域創成科学研究科	”	Takeaki Yoshizawa	The University of Tokyo
86	”	海本 祐真	東京大学	大学院新領域創成科学研究科	”	Yuma Umimoto	The University of Tokyo
87	”	蘇 丹	東京大学	大学院新領域創成科学研究科	”	Su Dan	The University of Tokyo
88	新規超伝導物質合成と物性評価	辻井 優哉	東京大学	大学院新領域創成科学研究科	Synthesis and characterization of novel superconducting materials	Masaya Tsujii	The University of Tokyo

No.	課題名	氏名	所属		Title	Name	Organization
89	コニカルらせん磁性体における複合ドメイン相関の解明	木村 剛	東京大学	大学院新領域創成科学研究科	Understanding of coupled multiferroic domains in conical spiral magnets	Tsuyoshi Kimura	The University of Tokyo
90	Cu - Ni - X (X=Co,Fe) 系単結晶性合金中の磁性微粒子析出過程と磁気特性の関係	竹田 真帆人	横浜国立大学	大学院工学研究院	Precipitation behavior and magnetic properties of fine magnetic particles in Cu - Ni base alloys single Crystal	Mahoto Takeda	Yokohama National University
91	”	又井 慎太郎	横浜国立大学	大学院工学府	”	Sintaro Matai	Yokohama National University
92	希釈強磁性元素を添加した銅合金の析出組織と磁気特性の調査	坂倉 響	横浜国立大学	大学院工学府	Microstructural evolution and magnetic properties of nano-scale particles comprising ferromagnetic element atoms in Cu alloys	Hibiki Sakakura	Yokohama National University
93	ナノ構造材料を用いた二次電池開発	太田 道広	産業技術総合研究所	省エネルギー研究部門	Development of secondary battery by using nanostructured materials	Michihiro Ohta	National Institute of Advanced Industrial Science and Technology
94	”	Priyanka Jood	産業技術総合研究所	省エネルギー研究部門	”	Priyanka Jood	National Institute of Advanced Industrial Science and Technology
95	空間反転対称性を持たない新規磁性体の開発	鷺見 浩樹	東京大学	大学院新領域創成科学研究科	Exploration of new noncentrosymmetric magnets	Hiroki Sumi	The University of Tokyo
96	”	荒木 勇介	東京大学	大学院新領域創成科学研究科	”	Yusuke Araki	The University of Tokyo
97	”	近江 毅志	東京大学	大学院新領域創成科学研究科	”	Tsuyoshi Omi	The University of Tokyo
98	”	尾亦 恭輔	東京大学	大学院新領域創成科学研究科	”	Kyosuke Omata	The University of Tokyo
99	”	西 健太	東京大学	大学院新領域創成科学研究科	”	Nishi Kenta	The University of Tokyo
100	”	山本 圭祐	東京大学	大学院新領域創成科学研究科	”	Keisuke Yamamoto	The University of Tokyo
101	”	渡辺 義人	東京大学	大学院新領域創成科学研究科	”	Yoshito Watanabe	The University of Tokyo

## 物質合成・評価設備 U クラス / Materials Synthesis and Characterization U Class Researcher

No.	課題名	氏名	所属		Title	Name	Organization
1	六方晶型バナジウム酸水素化物における圧力効果	山本 隆文	京都大学	大学院工学研究院	Pressure Effect on hexagonal vanadium Oxyhydride	Takafumi Yamamoto	Kyoto University
2	キャリアドープされたパイロクロア型イリジウム酸化物の純単結晶育成	松平 和之	九州工業大学	大学院工学研究院	Single crystal growth of carrier-doped pyrochlore iridates	Kazuyuki Matsuhira	Kyushu Institute Technology

No.	課題名	氏名	所属		Title	Name	Organization
3	”	野村 拓功	九州工業大学	工学府	”	Hironori Nomura	Kyushu Institute Technology
4	新規低次元量子磁性体 $K(NbO)Cu_4(PO_4)_4$ の低温結晶構造の研究	木村 健太	東京大学	大学院新領域創成科学研究科	Study of the low-temperature crystal structure of a new low-dimensional quantum magnet $K(NbO)Cu_4(PO_4)_4$	Kenta Kimura	The University of Tokyo
5	マイクロミキサを用いた機能性無機ナノ粒子の連続合成	陶 究	産業技術総合研究所	化学プロセス研究部門	Continuous synthesis of functional inorganic nanoparticles using a micromixer	Kiwamu Sue	National Institute of Advanced Industrial Science and Technology
6	X線用回折格子の開発	三村 秀和	東京大学	大学院工学系研究科	Development of X-ray grating	Hidekazu Mimura	The University of Tokyo
7	”	鎌田 悠	東京大学	大学院工学系研究科	”	Yu Kamata	The University of Tokyo
8	高温高圧下における下部マントル鉱物への窒素の取り込み	福山 鴻	東京大学	大学院理学系研究科	Nitrogen incorporation into the lower-mantle minerals under high pressure and high temperature	Ko Fukuyama	The University of Tokyo
9	高温高圧水中におけるゼオライトの構造安定性と触媒活性についての検討	布浦 鉄兵	東京大学	環境安全研究センター	Evaluation of structural and catalytic stability of zeolite in high temperature and high pressure water	Teppey Nunoura	The University of Tokyo
10	”	小川 拓哉	東京大学	大学院新領域創成科学研究科	”	Takuya Ogawa	The University of Tokyo
11	廃油の超臨界水ガス化工程におけるニッケル触媒の不活性化メカニズムの解明	布浦 鉄兵	東京大学	環境安全研究センター	Nickel catalyst deactivation in supercritical water gasification of waste oil	Teppey Nunoura	The University of Tokyo
12	”	ダイアン グ バタンガ	東京大学	大学院新領域創成科学研究科	”	Diane Gudatanga	The University of Tokyo
13	プラズマ風洞による宇宙往還機熱防護システムの動的酸化に関する研究	桃沢 愛	東京都市大学	工学部	Investigation on dynamic oxidation of thermal protection system (TPS) using plasma wind tunnel	Ai Momosawa	Tokyo City University
14	”	田中 聖也	東京大学	大学院工学系研究科	”	Seiya Tanaka	The University of Tokyo
15	”	山田 慎	東京大学	大学院工学系研究科	”	Shin Yamada	The University of Tokyo
16	中温作動プロトン伝導型メタルサポート固体酸化燃料電池の新規セル設計	大友 順一郎	東京大学	大学院新領域創成科学研究科	New cell design of intermediate temperature proton conducting metal supported SOFC	Junichiro Otomo	The University of Tokyo
17	”	阪田 一真	東京大学	大学院新領域創成科学研究科	”	Kazuma Sakata	The University of Tokyo
18	”	大友 順一郎	東京大学	大学院新領域創成科学研究科	”	Junichiro Otomo	The University of Tokyo
19	”	松尾 拓紀	東京大学	大学院新領域創成科学研究科	”	Hiroki Matsuo	The University of Tokyo

長期留学研究員 / Long Term Young Researcher

No.	課題名	氏名	所属		Title	Name	Organization
1	YbPd の極低温・高圧下における異常な価数揺動相の研究	大山 耕平	九州大学	大学院理学府	Study on anomalous valence fluctuation of YbPd under highpressure at extremely low temperatures	Kohei Oyama	Kyushu University
2	時間分解角度分解光電子分光による 2H-NbSe <sub>2</sub> の光励起ダイナミクスの研究	渡邊 真莉	東京理科大学	大学院理学研究科	Ultrafast dynamics in 2H-NbSe <sub>2</sub> by time-resolved photoemission spectroscopy	Mari Watanabe	Tokyo University of Science

## 平成 30 年度 共同利用課題一覧 (後期) / Joint Research List (2018 Latter Term)

嘱託研究員 / Commission Researcher

No.	課題名	氏名	所属	Title	Name	Organization
担当所員：長谷川 幸雄						
1	極低温走査トンネル顕微鏡を用いた鉄カルコゲナイド超伝導体 FeSeTe の研究	吉田 靖雄	金沢大学 理工学域	Low-temperature STM study on iron-chalcogenide superconductor FeSeTe	Yasuo Yoshida	Kanazawa University
2	走査トンネル顕微鏡による局所強磁性共鳴法の開発	安 東秀	北陸先端科学技術大学院大学 先端科学技術研究科	Development of local ferromagnetic resonance in scanning tunneling microscopy	Toshu Ann	Japan Advanced Institute of Science and Technology
3	スピン編極探針の作製・処理法の開発	岡 博文	東北大学 材料科学高等研究所	Development of fabrication and treatment methods for spin-polarized tips	Hirofumi Oka	Advanced Institute for Materials Research
4	走査トンネル顕微鏡による低次元トポロジカル物質の研究	岡田 佳憲	沖縄科学技術大学院大学 量子物質科学ユニット	Investigation of low-dimensional topological materials by scanning tunneling	Yoshinori Okada	Okinawa Institute of Science and Technology Graduate University
担当所員：川島 直輝						
5	第一原理有効模型導出プログラム RESPACK と模型解析プログラム H $\phi$ /mVMC の融合による非経験的強相関電子構造解析ソフトウェアの整備	中村 和磨	九州工業大学 大学院工学研究院	Development of first principles electronic-structure calculation software by combining effective -model derivation code (RESPACK) and model-analysis codes (H $\phi$ /mVMC)	Kazuma Nakamura	Kyushu Institute of Technology
6	スーパーコンピュータの調達に関する意見交換	笠松 秀輔	山形大学 学術研究院	Procurement of Supercomputer Systems	Shusuke Kasamatsu	Yamagata University
担当所員：上床 美也						
7	圧力下 NMR 測定法に関する開発	藤原 直樹	京都大学 大学院人間・環境学研究院	Development of NMR measurement method under high pressure	Naoki Fujiwara	Kyoto University
8	希土類 122 化合物における圧力効果	繁岡 透	山口大学 大学院理工学研究科	Pressure effect of rare earth 122 compounds	Toru Shigeoka	Yamaguchi University
9	低温用マルチアンビル装置の開発	辺土 正人	琉球大学 理学部	Development of multi-anvil apparatus for low temperature	Masato Hedo	University of the Ryukyus
10	高圧下 X 線回折法の開発	江藤 徹二郎	久留米工業大学 工学部	Development of High Pressure X-ray diffraction measurements	Tetsujiro Eto	Kurume Institute of Technology
11	カンチレバーを用いたトルク測定法の開発	鳥塚 潔	日本工業大学 共通教育群	Development of torque measurement method	Kiyoshi Torizuka	Nippon Institute of Technology
12	擬一次元有機物質の圧力下物性研究	糸井 充穂	日本大学 医学部	Study on pressure induced superconductivity of quasi organic conductor	Miho Itoi	Nihon University

No.	課題名	氏名	所属		Title	Name	Organization
13	磁性体の圧力効果	巨海 玄道	久留米工業大学	工学部	Effect of pressure on the Magnetic Materials	Gendo Oomi	Kurume Institute of Technology
14	3d 遷移化合物に関する圧力効果	鹿又 武	東北学院大学	工学総合研究所	Effect of pressure on the 3d transition compounds	Takeshi Kanomata	Tohoku Gakuin University
15	多重極限関連圧力装置の調整	高橋 博樹	日本大学	文理学部	Adjustment of Cubic Anvil apparatus	Hiroki Takahashi	Nihon University
16	ターンバックル式小型 DAC を利用した多重環境下電気抵抗測定	狩野 みか	日本工業大学	共通教育群	Electrical resistivity measurements under multi-extreme conditions by using a micro-turnbuckle DAC	Mika Kano	Nippon Institute of Technology
17	希釈冷凍機温度で使用可能な 10GPa 級超高压発生装置の開発	松林 和幸	電気通信大学	大学院情報理工学研究科	Development of 10 GPa class high pressure apparatus for low temperature	Kazuyuki Matsubayashi	The University of Electro-Communications
18	酸化物試料の作製と高压下物性測定	川中 浩史	産業技術総合研究所	電子光技術研究部門	Sample preparation and high pressure experiments	Hirofumi Kawanaka	National Institute of Advanced Industrial Science and Technology
19	有機伝導体の圧力効果	村田 惠三	大阪経済法科大学	21世紀社会総合研究センター	Effect of pressure on the organic conductor	Keizo Murata	Osaka University of Economics and Law
担当：中性子科学研究施設							
20	4G における共同利用推進	佐藤 卓	東北大学	多元物質科学研究所	Research and Support of General-Use at 4G	Taku Sato	Tohoku University
21	”	奥山 大輔	東北大学	多元物質科学研究所	”	Daisuke Okuyama	Tohoku University
22	”	那波 和宏	東北大学	多元物質科学研究所	”	Kazuhiro Nawa	Tohoku University
23	6G における共同利用推進	富安 啓輔	東北大学	大学院理学研究科	Research and Support of General-Use at 6G	Keisuke Yomiyasu	Tohoku University
24	”	岩佐 和晃	茨城大学	フロンティア応用原子科学研究センター	”	Kazuaki Iwasa	Ibaraki University
25	T1-1、T1-3 における共同利用推進	大山 研司	茨城大学	大学院理工学研究科	Research and Support of General-Use at T1-1 and T1-3	Kenji Ohoyama	Ibaraki University
26	T1-2、T1-3 における共同利用推進	藤田 全基	東北大学	金属材料科学研究所	Research and Support of General-Use at T1-2 and T1-3	Masaki Fujita	Tohoku University
27	T1-2、T1-3、6G における共同利用推進	南部 雄亮	東北大学	金属材料科学研究所	Research and Support of General-Use at T1-2, T1-3 and 6G	Yusuke Nambu	Tohoku University
28	”	池田 陽一	東北大学	金属材料科学研究所	”	Yoichi Ikeda	Tohoku University

No.	課題名	氏名	所属		Title	Name	Organization
29	”	鈴木 謙介	東北大学	金属材料科学研究 所	”	Kensuke Suzuki	Tohoku University
30	T2-2、T1-3 における共同利用推進	木村 宏之	東北大学	多元物質科学研 究所	Research and Support of General-Use at T2-2 and T1-3	Hiroyuki Kimura	Tohoku University
31	”	坂倉 輝俊	東北大学	多元物質科学研 究所	”	Terutoshi Sakakura	Tohoku University
32	C1-2 における共同利用推進	杉山 正明	京都大学	複合原子力科学 研究所	Research and Support of General-Use at C1-2	Masaaki Sugiyama	Kyoto University
33	C1-2、C2-3-1 における共同利用推進	井上 倫太郎	京都大学	複合原子力科学 研究所	Research and Support of General-Use at C1-2 and C2-3-1	Rintaro Inoue	Kyoto University
34	C1-3-mfSANS における共同利用推進	間宮 広明	物質・材料研究 機構	量子ビームユニ ット	Research and Support of General-Use at C1-3-mfSANS	Hiroaki Mamiya	National Institute for Materials Science
35	”	古坂 道弘	産業技術総合研 究所		”	Michihiro Furusaka	National Institute of Advanced Industrial Science and Technology
36	”	大沼 正人	北海道大学	大学院工学研究 科	”	Masato Ohnuma	Hokkaido University
37	”	藤原 健	産業技術総合研 究所	計量標準総合セ ンター	”	Takeshi Fujiwara	National Institute of Advanced Industrial Science and Technology
38	C2-3-1 における共同利用推進	守島 健	京都大学	複合原子力科学 研究所	Research and Support of General-Use at C2-3-1	Ken Morishima	Kyoto University
39	C3-1-2、C2-3-1 における共同利用推進	日野 正裕	京都大学	複合原子力科学 研究所	Research and Support of General-Use at C3-1-2 and C2-3-1	Masahiro Hino	Kyoto University
40	C2-1-2 における共同利用推進	田崎 誠司	京都大学	大学院工学研究 科	Research and Support of General-Use at C3-1-2	Seiji Tasaki	Kyoto University
41	”	小田 達郎	京都大学	複合原子力科学 研究所	”	Tatsuro Oda	Kyoto University
42	C1-3、C3-1-2 における共同利用推進	北口 雅暁	名古屋大学	現象解析研究セ ンター	Research and Support of General-Use at C1-3 and C3-1-2	Masaaki Kitaguchi	Nagoya University
43	C1-3 における共同利用推進	清水 裕彦	名古屋大学	大学院理学研究 科	Research and Support of General-Use at C1-3	Hirohiko Shimizu	Nagoya University
44	”	広田 克也	名古屋大学	大学院理学研究 科	”	Katsuya Hirota	Nagoya University
45	”	土川 雄介	名古屋大学	大学院理学研究 科	”	Yusuke Tsuchikawa	Nagoya University

No.	課題名	氏名	所属		Title	Name	Organization
46	”	山形 豊	理化学研究所	量子工学研究領域	”	Yutaka Yamagata	RIKEN
担当所員：辛 埴							
47	レーザー励起光電子顕微鏡を使った抵抗変化メモリ材料の研究	木下 健太郎	東京理科大学	理学部	Study on Materials for Resistive Switching Memories using laser-PEEM	Kentaro Kinoshita	Tokyo University of Science
48	FeSe 超伝導体における BCS-BES クロスオーバーの研究	紺谷 浩	名古屋大学	大学院理学研究科	Study of BCS-BES crossover in FeSe superconductors	Hiroshi Kontani	Nagoya University
49	高分解能光電子分光による強相関物質の研究	横谷 尚睦	岡山大学	大学院自然科学研究科	Ultra-high resolution study on strongly correlated materials	Takayoshi Yokoya	Okayama University
50	鉄系超伝導体のレーザー光電子分光	下志万 貴博	理化学研究所	創発物性科学研究センター	Laser-ARPES on Fe superconductor	Takahiro Shimojima	RIKEN
51	有機化合物の光電子分光	金井 要	東京理科大学	理工学部	Photoemission study on organic compounds	Kaname Kanai	Tokyo University of Science
52	時間分解光電子分光を用いた強相関物質の研究	溝川 貴司	早稲田大学	理工学術院	Time-resolved photoemission study on strongly-correlated materials	Takashi Mizokawa	Waseda University
53	トポロジカル超伝導体の探索	坂野 昌人	東京大学	大学院工学系研究科	Search for topological insulators	Masato Sakano	The University of Tokyo
54	時間分解・マイクロビームラインの開発と研究	室 隆桂之	高輝度光科学研究センター	利用研究促進部門	Development of micr- and time-resolved beamline	Takayuki Muro	Japan Synchrotron Radiation Institute
55	収差補正型光電子顕微鏡の建設と利用研究	小嗣 真人	東京理科大学	基礎工学部	Construction and utilization research of aberration correction photoelectron emission microscopy	Masato Kotsugi	Tokyo University of Science
56	60-eV レーザーを用いた時間分解光電子分光の開発	石坂 香子	東京大学	大学院工学系研究科	The development of time-resolved photoemission using 60eV laser	Kyoko Ishizaka	The University of Tokyo
57	Mn 化合物の時間分解光電子分光	大川 万里生	東京理科大学	理学部	Time resolved Photoemission on Mn compounds	Mario Okawa	Tokyo University of Science
58	レーザー光電子分光による参加薄膜の研究	津田 俊輔	物質・材料研究機構	機能性材料研究拠点量子輸送特性グループ	Laser-Photoemission Study on Oxide Films	Shunsuke Tsuda	National Institute for Materials Science
59	高温超伝導体の高分解能光電子分光	藤森 淳	東京大学	大学院理学系研究科	Ultra-high resolution photoemission spectroscopy on high Tc superconductor	Atsushi Fujimori	The University of Tokyo
60	重い電子系ウラン化合物の高分解能光電子分光	藤森 伸一	日本原子力研究開発機構	物質科学研究センター	Ultra high resolution photoemission study on heavy fermion Uranium compounds	Shinichi Fujimori	Japan Atomic Energy Agency
61	時間分解光電子顕微分光実験の技術開発	木下 豊彦	高輝度光科学研究センター	利用研究促進部門	Technical development of time-resolved photoemission microscopy measurement	Toyohiko Kinoshita	Japan Synchrotron Radiation Institute

No.	課題名	氏名	所属		Title	Name	Organization
62	光電子分光法を用いた各種分子性結晶の電子状態の研究及び装置の低温化	木須 孝幸	大阪大学	大学院基礎工学研究科	Research on electron state of molecular crystals using photoemission spectroscopy	Takayuki Kisu	Osaka University
63	トポロジカル絶縁体の電子状態の解明	木村 昭夫	広島大学	大学院理学研究科	Electronic-structure study of topological insulators	Akio Kimura	Hiroshima University
64	インジウム原子層超伝導体におけるラッシュバースピン分裂の直接観察	内橋 隆	物質・材料研究機構	国際ナノアーキテクトゥクス研究拠点	Direct observation of Rashba effect-induced spin splitting in an indium atomic-layer superconductor	Takashi Uchihashi	National Institute for Materials Science
65	Si(111) 上単層タリウムの高次高調波を用いた時間分解光電子分光	坂本 一之	千葉大学	大学院融合科学研究科	Time-resolved ARPES investigation of monolayer Thallium on Si(111)	Kszuyuki Sakamoto	Chiba University
66	スピン分解角度分解光電子分光による TaSi <sub>2</sub> のスピン構造の研究	伊藤 孝寛	名古屋大学	シンクロトロン光科学研究センター	Spin-resolved angle-resolved photoemission study of spin texture of TaSi <sub>2</sub>	Takahiro Ito	Nagoya University
67	時間分解光電子分光や超高分解能光電子分光を用いた超伝導体や強相関系物質の研究	吉田 鉄平	京都大学	大学院人間・環境学研究科	Laser ARPES study on superconductors and strongly-correlated materials	Tepei Yoshida	Kyoto University
68	固体中のマヨラナ粒子の研究	松田 祐司	京都大学	大学院理学研究科	Study of Majorana Fermion in Solids by Laser Photoemission Spectroscopy	Yuji Matsuda	Kyoto University
69	〃	佐藤 昌利	京都大学	基礎物理学研究所	〃	Masatoshi Sato	Kyoto University
担当所員：原田 慈久							
70	省エネ・創エネ・蓄電デバイスのオペランド分光	尾嶋 正治	東京大学	大学院工学研究科	Operando nano-spectroscopy for energy effect, power generation and energy storage devices	Masaharu Oshima	The University of Tokyo
71	液中プラズマ印加水の軟 X 線吸収 / 発光分光技術開発	寺嶋 和夫	東京大学	大学院新領域創成科学研究科	Technical development of soft X-ray absorption/emission spectroscopy for water processed by in-liquid plasma	Kazuo Terashima	The University of Tokyo
72	液中プラズマ印加によるナノ粒子分散特性評価と軟 X 線分光	伊藤 剛仁	東京大学	大学院新領域創成科学研究科	Characterization of nano-particle distribution in water processed by in-liquid plasma and soft X-ray spectroscopy	Tsuyohito Ito	The University of Tokyo
73	軟 X 線発光・共鳴非弾性散乱分光の磁気円・線二色性測定システムの構築	菅 滋正	大阪大学	産業科学研究所	Construction of a noble system for circular and linear dichroism in soft X-ray emission and RIXS spectroscopy	Shigemasa Suga	Osaka University
74	軟 X 線吸収 / 発光分光法によるリチウムイオン電池電極材料の電子物性研究	細野 英司	産業技術総合研究所	省エネルギー研究部門	Study on the electronic property of electrode materials for Li-ion batteries by soft X-ray absorption/emission spectroscopy	Eiji Hosono	National Institute of Advanced Industrial Science and Technology
75	〃	朝倉 大輔	産業技術総合研究所	エネルギー技術研究部門	〃	Daisuke Asakura	National Institute of Advanced Industrial Science and Technology
76	高分解能光電子分光による酸化バナジウムの研究	藤原 秀紀	大阪大学	大学院基礎工学研究科	Study on vanadium oxides by high resolution Photoemission	Hidenori Fujiwara	Osaka University
担当所員：松田 巖							

No.	課題名	氏名	所属		Title	Name	Organization
77	スピン分解光電子分光の測定技術開発	木村 真一	大阪大学	大学院生命機能研究科	Technical development of spin-resolved photoemission spectroscopy measurement	Shin-ichi Kimura	Osaka University
78	時間分解磁気光学実験の技術開発	小嗣 真人	東京理科大学	基礎工学部	Technical development of time-resolved magneto-optical experiment	Masato Kotsugi	Tokyo University of Science
担当所員：和達 大樹							
79	時間分解吸収分光による $\text{EuNi}_2(\text{Si}_{1-x}\text{Ge}_x)_2$ の価数転移ダイナミクスの解明	三村 功次郎	大阪府立大学	大学院工学研究科	Dynamics of valence transition in $\text{EuNi}_2(\text{Si}_{1-x}\text{Ge}_x)_2$ revealed by time-resolved XAS	Kojiro Mimura	Osaka Prefecture University
80	三次元 nanoESCA による実デバイスのオペランド電子状態解析	永村 直佳	物質・材料研究機構	先端材料解析研究拠点	Operando analysis of the electronic structure of actual devices by 3DnanoESCA	Naoka Ngamura	National Institute for Materials Science
81	コヒーレント共鳴軟 X 線散乱による磁気ドメイン構造の観測	山崎 裕一	物質・材料研究機構	統合型材料開発・情報基盤部門	Observation of magnetic domain structure for ferromagnetic thin films by means of resonant scattering	Yuichi Yamasaki	National Institute for Materials Science

一般研究員 / General Researcher

No.	課題名	氏名	所属		Title	Name	Organization
担当所員：榊原 俊郎							
1	$\text{Ba}^{2+}\text{-Fe}^{3+}\text{-Ti}^{4+}$ 酸化物磁性体の磁場中誘電特性	神島 謙二	埼玉大学	大学院理工学研究科	Dielectric properties of $\text{Ba}^{2+}\text{-Fe}^{3+}\text{-Ti}^{4+}$ magnetic oxides under magnetic field	Kamishima Kenji	Saitama University
2	”	米澤 豊志	埼玉大学	大学院理工学研究科	”	Atsushi Yonezawa	Saitama University
3	超伝導対のギャップ対称性を決定する実験的、理論的研究	町田 一成	立命館大学	理工学部	Experimental and theoretical studies on gap symmetry determination in superconductors	Kazushige Machida	Ritsumeikan University
4	重い電子系化合物が示す非従来型超伝導と磁性の相関	横山 淳	茨城大学	理学部	Interplay between unconventional superconductivity and magnetism in heavy-fermion compounds	Makoto Yokoyama	Ibaraki University
5	”	鈴木 康平	茨城大学	大学院理工学研究科	”	Kohei Suzuki	Ibaraki University
6	$\text{Yb}_2\text{Rh}_3\text{Si}_5$ の極低温磁化と比熱測定	中村 翔太	名古屋工業大学	工学部	Magnetization and specific heat measurements of $\text{Yb}_2\text{Rh}_3\text{Si}_5$ at very low temperature	Shota Nakamura	Nagoya Institute of Technology
7	純良な単一単結晶を用いた新規超伝導体の比熱測定	加瀬 直樹	東京理科大学	理学部	Superconducting state elucidated through specific heat measurements	Naoki Kase	Tokyo University of Science
8	トポロジカル超伝導のギャップ構造とネマチック相研究	孫 悦	青山学院大学	理工学部	Study of the gap structure and nematic phase of topological superconductors	Yue Sun	Aoyama Gakuin University

No.	課題名	氏名	所属		Title	Name	Organization
9	Rb <sub>2</sub> Cu <sub>2</sub> Mo <sub>3</sub> O <sub>12</sub> の特異な磁気特性への不純物置換効果	安井 幸夫	明治大学	理工学部	Impurity effects on anomalous magnetic properties of Rb <sub>2</sub> Cu <sub>2</sub> Mo <sub>3</sub> O <sub>12</sub>	Yukio Yasui	Meiji University
10	量子スピニアイス系 Yb <sub>2</sub> Ti <sub>2</sub> O <sub>7</sub> の誘電特性	安井 幸夫	明治大学	理工学部	Dielectric Properties of Quantum Spin Ice System Yb <sub>2</sub> Ti <sub>2</sub> O <sub>7</sub>	Yukio Yasui	Meiji University
担当所員：山下 穰							
11	三角格子反強磁性体の低温磁性	柄木 良友	琉球大学	教育学部	Low temperature magnetism of triangular antiferromagnets	Yoshitomo Karaki	University of Ryukyu
12	重い電子系化合物 YbNi <sub>2</sub> Si <sub>3</sub> の超低温磁気トルク測定	大原 繁男	名古屋工業大学	物理工学科	Magnetic torque measurements of heavy fermion YbNi <sub>2</sub> Si <sub>3</sub> at ultra low temperature	Shigeo Ohara	Nagoya Institute of Technology
13	”	中村 翔太	名古屋工業大学	工学部	”	Shota Nakamura	Nagoya Institute of Technology
14	パイロクロア酸化物 Cd <sub>2</sub> Os <sub>2</sub> O <sub>7</sub> の局所磁化測定	芝内 孝禎	東京大学	大学院新領域創成科学研究科	Local magnetization measurements on pyrochlore oxide Cd <sub>2</sub> Os <sub>2</sub> O <sub>7</sub>	Takasada Shibauchi	The University of Tokyo
15	”	向笠 清隆	東京大学	大学院新領域創成科学研究科	”	Kiyotaka Mukasa	The University of Tokyo
16	重い電子系超伝導体 CeCoIn <sub>5</sub> の超低温における dHvA 効果測定	宍戸 寛明	大阪府立大学	大学院工学研究科	dHvA effect measurements at ultra-low temperatures in a heavy fermion superconductor CeCoIn <sub>5</sub>	Hiroaki Shishido	Osaka Prefecture University
17	”	片山 諒	大阪府立大学	大学院工学研究科	”	Ryo Katayama	Osaka prefecture university
担当所員：勝本 信吾							
18	半導体 MoS <sub>2</sub> /金属 Ti 界面における超伝導状態の研究	石黒 亮輔	日本女子大学	理学部	Study of Superconducting state in semiconductor MoS <sub>2</sub> /metal Ti interface	Ishiguro Ryosuke	Japan Women's University
19	”	相川 夕美花	日本女子大学	大学院理学研究科	”	Aizawa Yumika	Japan Women's University
20	ナノ・マイクロセンシングデバイスの創製	米谷 玲皇	東京大学	大学院新領域創成科学研究科	Fabrication of nano- and microsensing devices	Reo Kometani	The University of Tokyo
21	”	田中 航大	東京大学	大学院工学系研究科	”	Kodai Tanaka	The University of Tokyo
22	”	吉原 健太	東京大学	大学院工学系研究科	”	Kenta Yoshihara	The University of Tokyo
23	”	ペンエークウ オン ケーマ ナット	東京大学	大学院新領域創成科学研究科	”	Penekwong Khemnat	The University of Tokyo

No.	課題名	氏名	所属		Title	Name	Organization
24	”	西田 裕信	東京大学	大学院新領域創成科学研究科	”	Hironobu Nishida	The University of Tokyo
25	二次元銅酸化物のホール係数測定 (II)	神戸 士郎	山形大学	大学院理工学研究科	Hall coefficient measurement of 2D curates (II)	Shiro Kambe	Yamagata University
26	”	島袋 義仁	山形大学	大学院理工学研究科	”	Yoshihito Shimabukuro	Yamagata University
27	量子ホール効果測定のための高移動度半導体試料作成	福田 昭	兵庫医科大学	物理学教室	Development of the high mobility semiconductor sample for the measurements in the quantum Hall regime	Akira Fukuda	Hyogo College of Medicine
28	”	寺澤 大樹	兵庫医科大学	物理学教室	”	Daiju Terasawa	Hyogo College of Medicine
担当所員：大谷 義近							
29	空間反転対称性の破れた結晶構造に発現する非線形電流応答	木俣 基	東北大学	金属材料研究所	Nonlinear current response in non-centrosymmetric crystal structure	Motoi Kimata	Tohoku university
担当所員：小森 文夫							
30	Al-Pd-Ru 準結晶・近似結晶における空孔濃度の研究	金沢 育三	東京学芸大学	自然科学系	Positron-annihilation studies of Al-Pd-Ru quasicrystal and its approximant crystals	Ikuzo Kanazawa	Tokyo Gakugei University
31	”	中村 駿	東京学芸大学	大学院教育学研究科	”	Shun Nakamura	Tokyo Gakugei University
32	面内圧縮された Cu(001) 表面における局所構造緩和	山田 正理	中央大学	理工学部	Local structural rearrangement on a compressed Cu(001) surface	Masamichi Yamada	ChuoUniversity
33	単層グラフェンの電子状態の解析	青柳 良英	横浜国立大学	大学院理工学府	Analysis of electrical states of monolayer graphene	Yoshihide Aoyagi	Yokohama National University
34	Si(111) <sub>4</sub> × 1-In 基板上における In-Bi 表面合金の電子状態	中辻 寛	東京工業大学	物質理工学院	Electronic structure of In-Bi surface alloy grown on Si(111) <sub>4</sub> -In substrates	Kan Nakatsuji	Tokyo Institute of Technology
35	”	田中 和也	東京工業大学	物質理工学院	”	Kazuya Tanaka	Tokyo Institute of Technology
36	単層グラフェンの電子状態の解析	大野 真也	横浜国立大学	大学院工学研究院	Analysis of electronic states of monolayer graphene	Shinya Ohno	Yokohama National University
37	金属/半導体表面上への超薄膜およびナノ構造薄膜の形成とその磁化ダイナミックスの観測	河村 紀一	日本放送協会	放送技術研究所	Study on magnetic dynamics of ultra-thin films and nano-structures on metal / semiconductor surfaces	Norikazu Kawamura	NHK Science and Technology Research Laboratories
38	STM を用いた L10-FeNi 表面における N サーファクタント効果の解析	小嗣 真人	東京理科大学	基礎工学部	Study of N surfactant effect on L10-FeNi by using STM	Masato Kotsugi	Tokyo University of Science

No.	課題名	氏名	所属	Title	Name	Organization
担当所員：長谷川 幸雄						
39	エピタキシャルシリセン、ゲルマネン及びそのヘテロ構造の低温走査トンネル顕微鏡観察	高村 由起子	北陸先端科学技術大学院大学	マテリアルサイエンス系	STM investigation of epitaxial silicene, germanene, and their heterostructures	Yukiko Takamura JAIST
40	〃	米澤 隆宏	北陸先端科学技術大学院大学	先端科学技術研究科	〃	Takahiro Yonezawa JAIST
担当所員：吉信 淳						
41	各種分光測定による機能性材料の物性と反応に関する研究	塩澤 佑一朗	山梨県	産業技術センター	The physical properties and reactivities of functional materials studied by various spectroscopies	Yuichiro Shiozawa Industrial Technology Center Yamanashi
42	電界効果による吸着分子の状態制御の赤外分光観測	野内 亮	大阪府立大学	大学院工学研究科	Field-effect control of adsorbed molecules observed by infrared spectroscopy	Ryo Nouchi Osaka Prefecture University
担当所員：秋山 英文						
43	宇宙線望遠鏡に用いる反射鏡のUV照射後の反射率測定	野田 浩司	東京大学	宇宙線研究所	Reflectance measurement of the mirrors used in cosmic ray telescopes, after an exposure to UV radiation	Koji Noda The University of Tokyo
44	フォトルミネッセンス励起分光を用いたGaPAsN混晶における局在状態に関する研究	矢口 裕之	埼玉大学	大学院理工学研究科	Photoluminescence excitation spectroscopy of localized states in GaPAsN alloys	Hiroyuki Yaguchi Saitama University
45	〃	高宮 健吾	埼玉大学	総合技術支援センター	〃	Kengo Takamiya Saitama University
46	〃	高橋 渉	埼玉大学	大学院理工学研究科	〃	Wataru Takahashi Saitama University
47	Si基板上に直接成長させたGaNの成長条件が光学特性に及ぼす影響	小柴 俊	香川大学	大学院工学研究科	Influences of growth conditions of GaN on Si substrate on optical properties	Takashi Kuraoka Kagawa University
48	〃	藏岡 賢	香川大学	大学院工学研究科	〃	Takashi Kuraoka Kagawa University
担当所員：中辻 知						
49	価数相転移に伴う格子歪みの研究II	久我健太郎	理化学研究所	放射光科学研究センター	Crystal strain associated with valence transition II	Kentaro Kuga RIKEN
50	希土類金属間化合物の強磁場低温物性研究	海老原 孝雄	静岡大学	学術院理学領域	Physical properties in rare earth intermetallic compounds at high magnetic fields in low temperature	Takao Ebihara Shizuoka University
51	〃	ジュマエダ ジャトミカ	静岡大学	創造科学技術大学院	〃	Jumaeda Jatmika Shizuoka University

No.	課題名	氏名	所属	Title	Name	Organization
担当所員：廣井 善二						
52	層状構造を有する金属間化合物のディインターカレーションと低温物性	山田 高広	東北大学	多元物質科学研究科	Characterization of electric and magnetic properties of intermetallic compounds with layered structures	Takahiyo Yamada Tohoku University
担当所員：川島 直輝						
53	蜂の巣格子 Kitaev- $\Gamma$ 模型の基底状態相図と磁気励起	鈴木 隆史	兵庫県立大学	大学院工学研究科	Ground-state phase diagram and magnetic excitation of the Kitaev- $\Gamma$ model on a honeycomb lattice	Takafumi Suzuki University of Hyogo
54	非平衡系のためのテンソルネットワーク法	原田 健自	京都大学	大学院情報学研究科	Tensor network schemes for non-equilibrium systems	Kenji Harada Kyoto University
担当所員：上床 美也						
55	キュービックアンビルセルを用いた NMR 測定開発	藤原 直樹	京都大学	大学院人間・環境学研究科	Development of NMR measurements under pressure using a cubic-anvil cell	Naoki Fujiwara Kyoto University
56	〃	桑山 昂典	京都大学	大学院人間・環境学研究科	〃	Takanori Kuwayama Kyoto University
57	BiFe <sub>1-x</sub> Co <sub>x</sub> O <sub>3</sub> における高圧下での弱強磁性相の安定性	山本 孟	東北大学	多元物質科学研究科	High pressure study of the weak ferromagnetism in BiFe <sub>1-x</sub> Co <sub>x</sub> O <sub>3</sub>	Hajime Yamamoto Tohoku University
58	YbH <sub>2+x</sub> の磁性と伝導	中村 修	岡山理科大学	研究・社会連携センター	Magnetic and transport properties in YbH <sub>2+x</sub>	Osamu Nakamura Okayama University of Science
59	多形化合物 RIr <sub>2</sub> Si <sub>2</sub> (R= 希土類) の結晶育成と物質評価 5	繁岡 透	山口大学	大学院創成科学研究科	Crystal growth and characterization of polymorphic compounds RIr <sub>2</sub> Si <sub>2</sub> (R=rare earth) 5	Toru Shigeoka Yamaguchi University
60	〃	内間 清晴	沖縄キリスト教短期大学	総合教育系	〃	Kiyoharu Uchima Okinawa Christian Junior College
61	擬三元化合物 Ce <sub>1-x</sub> MxNiC <sub>2</sub> (M = Y, La, Lu) の結晶育成と物質評価	繁岡 透	山口大学	大学院創成科学研究科	Crystal growth and characterization of pseudo-ternary compounds Ce <sub>1-x</sub> MxNiC <sub>2</sub> (M = Y, La, Lu)	Toru Shigeoka Yamaguchi University
62	〃	内間 清晴	沖縄キリスト教短期大学	総合教育系	〃	Kiyoharu Uchima Okinawa Christian Junior College
63	多形化合物 RIr <sub>2</sub> Si <sub>2</sub> (R= 希土類) 磁気特性 3	内間 清晴	沖縄キリスト教短期大学	総合教育系	Magnetic characteristics of polymorphic compounds RIr <sub>2</sub> Si <sub>2</sub> (R=rare earth) 3	Kiyoharu Uchima Okinawa Christian Junior College
64	〃	繁岡 透	山口大学	大学院創成科学研究科	〃	Toru Shigeoka Yamaguchi University
65	新規希土類化合物 R <sub>5</sub> CuSn <sub>3</sub> の磁気特性	松本 圭介	愛媛大学	大学院理工学研究科	Magnetic properties of rare-earth-based compounds R <sub>5</sub> CuSn <sub>3</sub>	Keisuke Matsumoto Ehime University

No.	課題名	氏名	所属		Title	Name	Organization
66	”	石原 憲	愛媛大学	大学院理工学研究科	”	Ken Ishihara	Ehime University
67	希土類化合物 $R_5CuSn_3$ の磁気熱量効果	松本 圭介	愛媛大学	大学院理工学研究科	Magnetocaloric effect in rare-earth-based compounds $R_5CuSn_3$	Keisuke Matsumoto	Ehime University
68	”	石原 憲	愛媛大学	大学院理工学研究科	”	Ken Ishihara	Ehime University
69	$HoRh_2Si_2$ の Co 置換系化合物の単結晶育成	藤原 哲也	山口大学	大学院創成科学研究科	Single crystal growth of Co substituted $HoRh_{2-x}Co_xSi_2$ compounds	Tetsuya Fujiwara	Yamaguchi University
70	”	山本 嵩	山口大学	大学院創成科学研究科	”	Shu Yamamoto	Yamaguchi University
71	単結晶 $Ho_{1-x}La_xRh_2Si_2$ の磁気特性	藤原 哲也	山口大学	大学院創成科学研究科	Magnetic properties of $Ho_{1-x}La_xRh_2Si_2$ single crystal	Tetsuya Fujiwara	Yamaguchi University
72	”	山本 嵩	山口大学	大学院創成科学研究科	”	Shu Yamamoto	Yamaguchi University
73	$EuMn_2Ge_2$ 単結晶の比熱測定	藤原 哲也	山口大学	大学院創成科学研究科	Specific heat measurement of $EuMn_2Ge_2$ single crystal	Tetsuya Fujiwara	Yamaguchi University
74	”	山本 嵩	山口大学	大学院創成科学研究科	”	Shu Yamamoto	Yamaguchi University
75	単結晶 $Ho_{1-x}La_xRh_2Si_2$ の電気抵抗測定	藤原 哲也	山口大学	大学院創成科学研究科	Resistivity measurements of $Ho_{1-x}La_xRh_2Si_2$ single crystal	Tetsuya Fujiwara	Yamaguchi University
76	”	山本 嵩	山口大学	大学院創成科学研究科	”	Shu Yamamoto	Yamaguchi University
77	$FeSe_{1-x}S_x$ の高置換組成における高圧下物性研究	松浦 康平	東京大学	大学院新領域創成科学研究科	The high pressure study on highly substituted $FeSe_{1-x}S_x$	Kouhei Matsuura	The University of Tokyo
78	有機反強磁性絶縁体 $\lambda$ -(BEDT-TTF) $_2$ GaCl $_4$ の超高静水圧印加によるモット相境界の決定と圧力誘起超伝導の探索	谷口 弘三	埼玉大学	大学院理工学研究科	Search for pressure-induced superconductivity and determination of the Mott phase boundary by applying quasi-hydrostatic ultra-high pressures to organic antiferromagnetic insulator, $\lambda$ -(BEDT-TTF) $_2$ GaCl $_4$	Hiromi Taniguchi	Saitama University
79	”	小林 拓矢	埼玉大学	大学院理工学研究科	”	Takuya Kobayashi	Saitama University
80	”	綱川 仁志	埼玉大学	大学院理工学研究科	”	Hitoshi Tsunakawa	Saitama University
81	”	生沼 浩介	埼玉大学	大学院理工学研究科	”	Kohsuke Oinuma	Saitama University
82	”	小澤 宏彬	埼玉大学	大学院理工学研究科	”	Hiroaki Ozawa	Saitama University

No.	課題名	氏名	所属		Title	Name	Organization
83	鉄セレン系化合物の単結晶育成とその圧力効果	久田 旭彦	徳島大学	大学院社会産業理工学研究部	Single-crystal growth and pressure-effect study of iron-selenide compound	Akihiko Hisada	Tokushima University
84	Yb(Co <sub>1-x</sub> Ir <sub>x</sub> ) <sub>2</sub> Zn <sub>20</sub> の基本物性評価 III	阿曾 尚文	琉球大学	理学部	Evaluation of fundamental physical properties in Yb(Co <sub>1-x</sub> Ir <sub>x</sub> ) <sub>2</sub> Zn <sub>20</sub> III	Naofumi Aso	University of the Ryukyus
85	〃	佐藤 信	琉球大学	大学院理工学研究科	〃	Shin Sato	University of the Ryukyus
86	YbCo <sub>2</sub> Zn <sub>20</sub> 置換系試料の圧力効果 III	阿曾 尚文	琉球大学	理学部	Pressure effect of doped YbCo <sub>2</sub> Zn <sub>20</sub> systems III	Naofumi Aso	University of the Ryukyus
87	〃	津堅 涼	琉球大学	大学院理工学研究科	〃	Ryo Tsuken	University of the Ryukyus
88	Ce 系圧力誘起超伝導体の圧力中同時測定	阿曾 尚文	琉球大学	理学部	Simultaneous measurements under pressure in Ce-based pressure-induced superconductors	Naofumi Aso	University of the Ryukyus
89	〃	盛島 実竜	琉球大学	大学院理工学研究科	〃	Miiru Morishima	University of the Ryukyus
90	希土類ラーベス化合物 RAl <sub>2</sub> の異方的磁気体積効果	大橋 政司	金沢大学	理工研究域	Anisotropic magnetovolume effect of rare earth Laves compound RAl <sub>2</sub>	Masashi Ohashi	Kanazawa University
91	〃	西川 智生	金沢大学	大学院自然科学研究科	〃	Tomoki Nishikawa	Kanazawa University
92	強相関電子系化合物における圧力および磁場誘起量子相転移の探索	大橋 政司	金沢大学	理工研究域	Pressure and field induced quantum phase transition in strongly correlated electron systems	Masashi Ohashi	Kanazawa University
93	〃	稲森 庸介	金沢大学	大学院自然科学研究科	〃	Yosuke Inamori	Knazawa University
94	1 GPa 付近の圧力媒体の異常特性の解明	村田 恵三	大阪経済法科大学	21世紀社会総合研究センター	Anomalous Properties of Pressure Medium around 1 GPa	Keizo Murata	Osaka University of Economics and Law
95	層状硫化ビスマス超伝導体 La(O,F)BiS <sub>2</sub> の高圧力下物性	加瀬 直樹	東京理科大学	理学部	Pressure effect of the BiS <sub>2</sub> -based superconductors	Naoki Kase	Tokyo University of Science
96	Cr 基三元系遍歴強磁性体の高圧磁気特性	三井 好古	鹿児島大学	大学院理工学研究科	Magnetic properties of Cr-based ternary itinerant ferromagnet under high pressure	Yoshifuru Mitsui	Kagoshima University
97	〃	増満 勇人	鹿児島大学	大学院理工学研究科	〃	Hayato Masumitsu	Kagoshima University
98	MnNiGe <sub>1-x</sub> Si <sub>x</sub> 系化合物の高圧化磁化測定	伊藤 昌和	鹿児島大学	総合科学域総合教育学系	Magnetization of MnNiGe <sub>1-x</sub> Si <sub>x</sub> system under high pressure	Masakazu Ito	Kagoshima University
99	〃	白濱 透	鹿児島大学	大学院理工学研究科	〃	Toru Shirahama	Kagoshima University

No.	課題名	氏名	所属		Title	Name	Organization
100	Co 基ホイスラー合金における圧力誘起マルテンサイト変態に関する研究	重田 出	鹿児島大学	大学院理工学研究科	Study on pressure-induced martensitic phase transformation in Co-based Heusler alloys	Iduru Shigeta	Kagoshima University
101	MnCoGe の磁気特性及び相変態と、熱処理温度の関係	三井 好古	鹿児島大学	大学院理工学研究科	Relationship between annealing temperature, magnetic and structural properties of MnCoGe	Yoshifuru Mitsui	Kagoshima University
102	〃	野口 滉平	鹿児島大学	大学院理工学研究科	〃	Kohei Noguchi	Kagosima University
103	Pd 系ホイスラー合金の磁気モーメントの高圧効果	安達 義也	山形大学	大学院理工学研究科	Pressure effect of the magnetic moments for the Pd-Heusler alloys	Yoshiya Adachi	Yamagata University
104	〃	福本 拓実	山形大学	大学院理工学研究科	〃	Takumi Fukumoto	Yamagata University
105	高圧力下における Fe 基磁性体の磁気特性	小山 佳一	鹿児島大学	大学院理工学研究科	Magnetic properties of Fe-based magnets under high pressures	Keiichi Koyama	Kagoshima University
106	〃	尾上 昌平	鹿児島大学	大学院理工学研究科	〃	Masahira Onoue	Kagoshima University
107	高圧下における Eu 化合物の価数転移の探索	大貫 惇睦	琉球大学	理学部	Investigation of valence transition on Eu compounds under high pressure	Yoshichika Onuki	University of the Ryukyus
108	〃	本多 史憲	東北大学	金属材料研究所	〃	Fuminori Honda	Tohoku University
109	反転対称性のない遷移金属間化合物とその関連物質の高圧下輸送特性	仲間 隆男	琉球大学	理学部	Transport properties of non-centrosymmetric transition metals compounds under high pressure	Takao Nakama	University of the Ryukyus
110	〃	垣花 将司	琉球大学	大学院理工学研究科	〃	Masashi Kakihana	University of the Ryukyus
111	〃	太田 譲二	琉球大学	大学院理工学研究科	〃	Jouji Ota	University of the Ryukyus
112	圧力誘起価数転移の探索と高圧下輸送特性	辺土 正人	琉球大学	理学部	Searching of pressure-induced valence transition and transport properties under high pressure	Masato Hedo	University of the Ryukyus
113	〃	伊覇 航	琉球大学	大学院理工学研究科	〃	Wataru Iha	University of the Ryukyus
114	Eu 化合物の圧力誘起近藤状態の探索	辺土 正人	琉球大学	理学部	Searching for pressure-induced Kondo state on Eu compounds	Masato Hedo	University of the Ryukyus
115	〃	松田 進弥	琉球大学	大学院理工学研究科	〃	Shinya Matsuda	University of the Ryukyus
116	遷移金属化合物の高圧力下の輸送特性	仲間 隆男	琉球大学	理学部	Pressure effect on transport properties of transition metal compounds	Takao Nakama	University of the Ryukyus

No.	課題名	氏名	所属		Title	Name	Organization
117	”	川勝 祥矢	琉球大学	大学院理工学研究科	”	Syouya Kawakatsu	University of the Ryukyus
118	トポロジカル絶縁体およびその関連物質の探索と高圧下輸送特性	辺土 正人	琉球大学	理学部	Searching of topological semiconductors and transport properties under high pressure	Masato Hedo	University of the Ryukyus
119	”	仲井間 憲李	琉球大学	大学院理工学研究科	”	Kenri Nakaima	University of the Ryukyus
120	ウラン化合物の磁性の圧力効果	本多 史憲	東北大学	金属材料研究所	Effect of Pressure on the magnetism of uranium compounds	Fuminori Honda	Tohoku University
121	ジグザグ鎖構造をもつ新しい Ce <sub>3</sub> TiBi <sub>5</sub> の圧力下比熱測定	本山 岳	島根大学	大学院自然科学研究科	Specific heat measurements of a new Ce compound with zig-zag chain structure	Gaku Motoyama	Shimane University
122	”	坪内 将紘	島根大学	大学院自然科学研究科	”	Masahiro Tsubouchi	Shimane University
123	Ce <sub>5</sub> Ge <sub>3</sub> の圧力下電気抵抗測定	広瀬 雄介	新潟大学	理学部物理学科	Electrical resistivity under pressure of Ce <sub>5</sub> Ge <sub>3</sub>	Yusuke Hirose	Niigata University
124	”	小板橋 拓斗	新潟大学	大学院自然科学研究科	”	Takuto Koitabashi	Nigata University
担当所員：尾崎 泰助							
125	実験と計算の協奏による二次元材料の構造・電子状態解析及び制御	アントワヌ フロランス	北陸先端科学技術大学院大学	マテリアルサイエンス系	Analysis and control of crystal and electronic structures of 2D materials through concerted collaboration of experiment and theory	Antoine Fleurence	JAIST
126	”	新田 寛和	北陸先端科学技術大学院大学	先端科学技術研究科	”	Hirokazu Nitta	JAIST
担当所員：益田 隆嗣							
127	単結晶 CeRh <sub>2</sub> Si <sub>2</sub> の結晶評価	齋藤 開	高エネルギー加速器研究機構	物質構造科学研究科	Evaluation on the crystallinity of single crystalline CeRh <sub>2</sub> Si <sub>2</sub>	Hiraku Saito	High Energy Accelerator Research Organization
128	重い電子系超伝導体における量子臨界揺らぎ	横山 淳	茨城大学	理学部	Quantum critical fluctuations in heavy fermion superconductors	Makoto Yokoyama	Ibaraki University
129	”	鈴木 康平	茨城大学	大学院理工学研究科	”	Kohei Suzuki	Ibaraki University
130	Yb(Co <sub>1-x</sub> Ni <sub>x</sub> ) <sub>2</sub> Zn <sub>20</sub> の極低温比熱測定	阿曾 尚文	琉球大学	理学部	Specific heat measurement at very low temperature on Yb(Co <sub>1-x</sub> Ni <sub>x</sub> ) <sub>2</sub> Zn <sub>20</sub>	Naofumi Aso	University of the Ryukyus
131	”	瑞慶覧 長星	琉球大学	大学院理工学研究科	”	Chousei Zukeran	University of the Ryukyus

No.	課題名	氏名	所属		Title	Name	Organization
132	(Yb <sub>1-x</sub> Lu <sub>x</sub> )Co <sub>2</sub> Zn <sub>20</sub> の極低温比熱測定 II	阿曾 尚文	琉球大学	理学部	Specific heat measurement at very low temperature on (Yb <sub>1-x</sub> Lu <sub>x</sub> )Co <sub>2</sub> Zn <sub>20</sub> II	Naofumi Aso	University of the Ryukyus
133	”	諸見里 真嗣	琉球大学	大学院理工学研究科	”	Masatsugu Moromizato	University of the Ryukyus
134	(Ce <sub>1-x</sub> R <sub>x</sub> ) <sub>5</sub> Si <sub>3</sub> (R=Y, Li, La, Lu) 単結晶試料の高エネルギー X 線ラウエ装置による結晶方位同定	小林 理気	琉球大学	理学部	Alignment of (Ce <sub>1-x</sub> R <sub>x</sub> ) <sub>5</sub> Si <sub>3</sub> (R=Y, Li, La, and Lu) single crystals by high-energy X-ray Laue diffraction	Riki Kobayashi	University of the Ryukyus
135	(Ce <sub>1-x</sub> R <sub>x</sub> ) <sub>5</sub> Si <sub>3</sub> (R=Y, Li, La, Lu) 単結晶試料の極低温比熱測定	小林 理気	琉球大学	理学部	Specific heat measurement at very low temperature on (Ce <sub>1-x</sub> R <sub>x</sub> ) <sub>5</sub> Si <sub>3</sub> (R=Y, Li, La, and Lu) systems	Riki Kobayashi	University of the Ryukyus
担当所員：嶽山 正二郎							
136	超強磁場磁気光学による Cu <sub>3</sub> Mo <sub>2</sub> O <sub>9</sub> の磁化プラトーの研究 IV	黒江 晴彦	上智大学	理工学部	Ultra-high magnetic field magneto-optical approach to the study of magnetization plateau in Cu <sub>3</sub> Mo <sub>2</sub> O <sub>9</sub> using vertical single-turn coil system IV	Haruhiko Kuroe	Sophia University
担当所員：金道 浩一							
137	金属ナノ結晶集合体の磁化特性	稲田 貢	関西大学	システム理工学部	Magnetic properties of metal nanocrystal assemblies	Mitsuru Inada	Kansai University
138	”	米澤 諒	関西大学	大学院理工学研究科	”	Ryo Yonezawa	Kansai University
139	幾何学的フラストレート磁性体の強磁場磁化測定	菊池 彦光	福井大学	学術研究院工学系	Magnetization measurements of the frustrated magnets	Hikomitsu Kikuchi	University of Fukui
140	サブメガガウス領域での希土類物性研究	海老原 孝雄	静岡大学	学術院理学領域	Physical property of rare earth compounds at pulse magnet	Takao Ebihara	Shizuoka University
141	”	村串 拓真	静岡大学	大学院総合科学技術研究科	”	Takuma Murakoshi	Shizuoka University
142	異常に大きな BiS <sub>2</sub> 系超伝導体の上部臨界磁場の決定	加瀬 直樹	東京理科大学	理学部	Upper critical field of the BiS <sub>2</sub> -based superconductors	Naoki Kase	Tokyo University of Science
143	Yb <sub>4</sub> TGe <sub>8</sub> (T: 遷移金属) と新規希土類化合物の強磁場磁化測定	道岡 千城	京都大学	大学院理学研究科	High-field magnetization measurements of Yb <sub>4</sub> TGe <sub>8</sub> (T: transition metal) and novel rare-earth metal compounds	Chishiro Michioka	Kyoto University
144	”	山中 俊介	京都大学	大学院理学研究科	”	Shunsuke Yamanaka	Kyoto University
145	MnNiGe(1-x)Si(x) 系化合物の高磁場磁化測定	伊藤 昌和	鹿児島大学	総合科学域総合教育学系	High magnetic field Magnetization of MnNiGe(1-x)Si(x) system	Masakazu Ito	Kagoshima University
146	”	白濱 透	鹿児島大学	大学院理工学研究科	”	Toru Shirahama	Kagoshima University

No.	課題名	氏名	所属		Title	Name	Organization
147	topological Kondo insulator $\text{SmB}_6, \text{YbB}_{12}$ の磁化特性と比熱	伊賀 文俊	茨城大学	理学部	Magnetic and thermal properties of topological Kondo insulator $\text{SmB}_6$ and $\text{YbB}_{12}$	Fumitoshi Iga	Ibaraki University
148	”	松浦 航	茨城大学	大学院理工学研究科	”	Wataru Matsuura	Ibaraki University
149	高圧合成希土類 6,12 ホウ化物の強磁場中の磁化と比熱	伊賀 文俊	茨城大学	理学部	Magnetic and thermal properties in high magnetic fields of rare earth hexa- and dodeca-borides produced by high pressure synthesis	Fumitoshi Iga	Ibaraki University
150	”	中山 裕之	茨城大学	大学院理工学研究科	”	Hiroyuki Nakayama	Ibaraki University
151	Bi 系銅酸化物高温超伝導体の磁気抵抗を用いた超伝導揺らぎの研究	渡辺 孝夫	弘前大学	大学院理工学研究科	A study of the superconducting fluctuation using magnetotransport measurements for Bi-based high-Tc cuprates	Takao Watanabe	Hirosaki University
152	”	川村 圭輔	弘前大学	大学院理工学研究科	”	Keisuke Kawamura	Hirosaki University
153	”	山口 隼平	弘前大学	大学院理工学研究科	”	Shunpei Yamaguchi	Hirosaki University
担当所員：徳永 将史							
154	強磁場下量子振動測定による Te の金属的表面状態の解明	秋葉 和人	岡山大学	大学院自然科学研究科	Investigation of the metallic surface state on Te by quantum oscillation measurements in pulsed magnetic fields	Kazuto Akiba	Okayama University
155	トーラス型フェルミ面を持つラッシュバ型半導体の量子極限伝導特性の研究	村川 寛	大阪大学	大学院理学研究科	High field study for quantum limit transport properties of tors Fermi surface in Rashba semiconductor	Hiroshi Murakawa	Osaka university
156	多層ディラック電子系 $\text{EuMnBi}_2$ のランダウ準位構造におけるスピン軌道相互作用の影響	近藤 雅起	大阪大学	大学院理学研究科	Impact of spin-orbit interaction on the Landau levels near the quantum limit for a layered Dirac material $\text{EuMnBi}_2$	Masaki Kondo	Osaka university
157	新奇重い電子系超伝導 $\text{UTe}_2$ のメタ磁性の探索	青木 大	東北大学	金属材料研究所	Search for metamagnetism in novel heavy fermion superconductor $\text{UTe}_2$	Dai Aoki	Tohoku University
158	ペロブスカイト酸化物 $\text{SrTiO}_3$ と鉄酸化物界面に形成された伝導層における強磁場下での磁気抵抗効果	大矢 忍	東京大学	大学院工学系研究科	Magnetoresistance of the transport layer between perovskite oxide $\text{SrTiO}_3$ and iron oxide under a strong magnetic field	Shinobu Ohya	The University of Tokyo
159	強磁場下における $\text{PdMnGa}$ 合金の磁化測定	許 晶	東北大学	大学院工学研究科	The magnetization measurement under strong magnetic field in $\text{PdMnGa}$ alloy	Xiao Xu	Tohoku University
160	”	伊東 達矢	東北大学	大学院工学研究科	”	Tatsuya Ito	Tohoku University
161	磁気光学顕微鏡による超伝導体中の量子渦の実空間非平衡ダイナミクス観測手法の確立	黒川 穂高	東京大学	大学院総合文化研究科	Observing the real-space nonequilibrium dynamics of vortices in superconductor with a magneto-optical microscope	Hodaka Kurokawa	The University of Tokyo
162	磁性半金属 $\text{EuP}_3$ における角度回転プローブを用いた超強磁場磁気輸送	高橋 英史	東京大学	大学院工学系研究科	Angle-dependent magnetotransport properties on the magnetic semimetal $\text{EuP}_3$	Hidefumi Takahashi	The University of Tokyo

No.	課題名	氏名	所属		Title	Name	Organization
163	”	メイヨーアレックス 浩	東京大学	大学院工学系研究科	”	Alex Hiro Mayo	The University of Tokyo
164	Ni-Mn 基ホイスラー合金におけるマルチカロリック効果の検証	木原 工	東北大学	金属材料研究所	Validation of multicaloric effects in Ni-Mn based Heusler alloys	Takumi Kihara	Tohoku University
165	重い電子系における強磁場中の電子状態研究	海老原 孝雄	静岡大学	学術院理学領域	Electronic states at high magnetic fields in Heavy Fermion systems	Takao Ebihara	Shizuoka University
166	”	鈴木 文登	静岡大学	大学院総合科学技術研究科	”	Fumito Suzuki	Shizuoka University
167	多層ディラック電子系 EuMnBi <sub>2</sub> のランダウ準位構造におけるスピン軌道相互作用の影響	酒井 英明	大阪大学	大学院理学研究科	Impact of spin-orbit interaction on the Landau levels near the quantum limit for a layered Dirac material EuMnBi <sub>2</sub>	Hideaki Sakai	Osaka University
168	”	西村 拓也	大阪大学	大学院理学研究科	”	Takuya Nishimura	Osaka University
169	”	藤村 飛雄吾	大阪大学	大学院理学研究科	”	Hyugo Fujimura	Osaka University
170	”	中川 賢人	大阪大学	大学院理学研究科	”	Kento Nakagawa	Osaka University
171	正四角台塔型反強磁性体の強磁場中電気磁気特性の測定	木村 健太	東京大学	大学院新領域創成科学研究科	High-field magnetoelectric properties of square-cupola-based antiferromagnets	Kenta Kimura	The University of Tokyo
担当所員：松田 康弘							
172	近藤半導体 (Yb,R)B <sub>12</sub> 、新規高圧合成物質のワンターンコイル 120T 強磁場磁化と伝導	伊賀 文俊	茨城大学	理学部	Magnetization and transport properties by using one-turn coil in a 120 T pulse magnet of Kondo insulator (Yb,R)B <sub>12</sub> and novel rare-earth borides produced by high-pressure synthesis	Fumitoshi Iga	Ibaraki University
173	”	山田 貴大	茨城大学	理学部	”	Takahiro Yamada	Ibaraki University
担当所員：辛 埴							
174	トポロジカル絶縁体を用いたスピン軌道トルク磁気メモリの表面状態解明	武田 崇仁	東京大学	大学院工学系研究科	Unveiling the surface state of spin-orbital torque magnetic memory using topological insulator	Takahito Takeda	The University of Tokyo
175	第二種 Weyl 半金属 WTe <sub>2</sub> の角度分解光電子分光による研究	万 宇軒	東京大学	大学院理学系研究科	Angle-resolved photoemission spectroscopy study of type-II Weyl semimetal WTe <sub>2</sub>	Wan Yuxuan	The University of Tokyo
176	半導体基板上的スピン分裂擬一次元表面状態におけるフェルミ準位調整	大坪 嘉之	大阪大学	大学院生命機能研究科	Fermi-level tuning of quasi-1D spin-split surface states on semiconductor substrates	Yoshiyuki Ohtsubo	Osaka University
177	”	中村 拓人	大阪大学	大学院理学研究科	”	Takuto Nakamura	Osaka university

No.	課題名	氏名	所属		Title	Name	Organization
178	”	徳舩 直樹	大阪大学	大学院理学研究科	”	Naoki Tokumasu	Osaka university
179	電子ホール結合系物質の時間分解光電子分光	溝川 貴司	早稲田大学	理工学術院	Time-resolved photoemission study of electron-hole coupled materials	Takashi Mizokawa	Waseda University
180	層状 MAX 相化合物 V <sub>2</sub> AlC のスピン分解角度分解光電子分光	伊藤 孝寛	名古屋大学	シンクロトロン光研究センター	Spin- and angle-resolved photoemission study of layered MAX phase compound V <sub>2</sub> AlC	Takahiro Ito	Nagoya University
181	”	鍋平 直輝	名古屋大学	大学院工学研究科	”	Naoki Nabehira	Nagoya University
182	トポジカル絶縁体を用いたスピン軌道トルク磁気メモリの表面状態解明	小林 正起	東京大学	大学院工学系研究科	Unveiling the surface state of spin-orbital torque magnetic memory using topological insulator	Masaki Kobayashi	The University of Tokyo
183	二重ジグザグ鎖構造をもつ遷移金属ダイカルコゲナイドの時間分解角度分解光電子分光	三石 夏樹	東京大学	大学院工学系研究科	Time-resolved angle-resolved photoemission study on transition metal dichalcogenides with double zigzag chains	Natsuki Mitsuishi	The University of Tokyo
184	第二種 Weyl 半金属 WTe <sub>2</sub> の角度分解光電子分光による研究	藤森 淳	東京大学	大学院理学系研究科	Angle-resolved photoemission spectroscopy study of type-II Weyl semimetal WTe <sub>2</sub>	Atsushi Fujimori	The University of Tokyo
185	レーザー励起光電子顕微鏡を用いた抵抗変化メモリ材料のナノ物性計測	木下 健太郎	東京理科大学	理学部	Nano physical property measurement of resistance change memory material using laser excited photo-emission microscope	Kentaro Kinoshita	Tokyo University of Science
186	”	中畝 悠介	東京理科大学	大学院理学研究科	”	Yusuke Nakaune	Tokyo University of Science
187	”	齋藤 修平	東京理科大学	大学院理学研究科	”	Shuhe Saitoh	Tokyo University of Science
担当所員：小林 洋平							
188	次世代レーザーとレーザー加工の基礎技術研究	吉富 大	産業技術総合研究所	電子光技術研究部門	Basic research on next generation laser systems and laser machining technology	Dai Yoshitomi	National Institute of AIST
189	”	高田 英行	産業技術総合研究所	電子光技術研究部門	”	Hideyuki Takada	National Institute of AIST
190	”	黒田 隆之助	産業技術総合研究所	先端オベラント計測技術オープンイノベーションラボラトリ	”	Ryunosuke Kuroda	National Institute of AIST
191	”	盛合 靖章	産業技術総合研究所	先端オベラント計測技術オープンイノベーションラボラトリ	”	Yasuaki Moriai	National Institute of AIST
192	”	澁谷 達則	産業技術総合研究所	分析計測標準研究部門	”	Tatsunori Shibuya	National Institute of AIST
193	”	佐藤 大輔	産業技術総合研究所	分析計測標準研究部門	”	Daisuke Satoh	National Institute of AIST

No.	課題名	氏名	所属		Title	Name	Organization
194	超高速分光用ファイバーレーザーの開発	末元 徹	豊田理化学研究所		Development of fiber laser for ultrafast optical spectroscopy	Tohru Suemoto	Toyota Physical and Chemical Research Institute
195	青色半導体レーザー用ファイバ型光コンバイナの開発	藤本 靖	千葉工業大学	工学部	Development on fiber power combiner for GaN semiconductor lasers	Yasushi Fujimoto	Chiba Institute of Technology
196	Yb ファイバーレーザーベースの光増幅システムの作製	大間知 潤子	関西学院大学	理工学部	Development of a Yb-fiber-laser based pulse amplification system	Junko Omachi	Kansei Gakuin University
197	短波長パルスレーザーによる炭素繊維の改質	森山 匡洋	東京大学	大学院理学系研究科付属フォトンサイエンス研究機構	Laser modification of carbon fiber by short wavelength pulsed laser	Masahiro Moriyama	The University of Tokyo
198	レーザー加工状態の分光測定に関する研究	山口 誠	秋田大学	大学院理工学研究科	Study on laser modification by using optical spectroscopic measurement	Makoto Yamaguchi	Akita University
199	”	富田 卓朗	徳島大学	大学院社会産業理工学研究部	”	Takuro Tomita	Tokushima University
担当所員：板谷 治郎							
200	鉛ハライド薄膜における時間分解差分吸収分光	牧野 哲征	福井大学	学術研究院工学系部門	Time-resolved differential absorption spectroscopy in lead-halide thin films	Takayuki Makino	University of Fukui
201	”	山出 拓史	福井大学	大学院工学研究科	”	Takuji Yamade	University of Fukui

一般研究員・大阪大学 先端強磁場科学研究センター / General Researcher・Center for Advanced High Magnetic Field Science Osaka University

No.	課題名	氏名	所属		Title	Name	Organization
担当：萩原 政幸（大阪大学）							
1	新しい試薬によるタンパク質の磁気浮上結晶化手法	牧 祥	大阪大谷大学	薬学部	Protein crystallization under the magnetic levitation method by using new precipitant agent	Syou Maki	Osaka Ohtani University
2	均一粒径モリブデン銅の強磁場磁化過程	浅野 貴行	福井大学	学術研究院工学系部門	High-field magnetization process on uniform particle size copper molybdate	Takayuki Asano	University of Fukui
3	ワイル半金属単結晶におけるベリー位相の磁場方位依存性の研究	村川 寛	大阪大学	大学院理学研究科	Evaluation of Berry's phase in various magnetic field direction in Weyl semimetal	Hiroshi Murakawa	Osaka University
4	”	駒田 盛是	大阪大学	大学院理学研究科	”	Moriyoshi Komada	Osaka University
5	2次元三角格子反強磁性体 Mn(OH) <sub>2</sub> の強磁場 ESR および強磁場磁化	佐藤 博彦	中央大学	理工学部	High-field ESR and high-field magnetization of two-dimensional triangular-lattice antiferromagnet Mn(OH) <sub>2</sub>	Hirohiko Sato	Chuo University

No.	課題名	氏名	所属		Title	Name	Organization
6	”	大寺 翔也	中央大学	理工学研究科	”	Shoya Ohtera	Chuo University
7	自発磁化を有する層状ディラック電子系物質におけるキャリア濃度と磁性の関係	酒井 英明	大阪大学	大学院理学研究科	Carrier density dependence of magnetic properties for a layered Dirac material with canted antiferromagnetic order	Hideaki Sakai	Osaka University
8	”	藤村 飛雄吾	大阪大学	大学院理学研究科	”	Hyugo Fujimura	Osaka University
9	”	中川 賢人	大阪大学	大学院理学研究科	”	Kento Nakagawa	Osaka University
10	フタロシアニン分子系伝導体で観測される巨大磁気抵抗に対する遷移金属置換の効果	花咲 徳亮	大阪大学	大学院理学研究科	Transition-metal-substitution Effect on Giant Magnetoresistance in Phthalocyanine-molecular Conductors	Noriaki Hanasaki	Osaka University
11	”	清水 智可	大阪大学	大学院理学研究科	”	Tomoka Shimizu	Osaka University
12	カゴメ格子反強磁性体の強磁場磁化過程測定	吉田 紘行	北海道大学	理学研究院	High-field magnetization measurements on kagome lattice antiferromagnets	Hiroyuki Yoshida	Hokkaido University
13	”	石井 裕人	北海道大学	大学院理学院	”	Yuto Ishii	Hokkaido University
14	リチウムをインターカレートしたフタロシアニン誘導体の磁性	本多 善太郎	埼玉大学	大学院理工学研究科	Magnetic properties of lithium intercalated phthalocyanine derivatives	Zentaro Honda	Saitama University
15	SmB <sub>6</sub> /SrB <sub>6</sub> 人工超格子の強磁場中での磁気抵抗、ホール効果測定	宍戸 寛明	大阪府立大学	大学院工学研究科	Magnetoresistance and Hall effect measurements for SmB <sub>6</sub> /SrB <sub>6</sub> artificial superlattices under high magnetic field	Hiroaki Shishido	Osaka Prefecture University
16	”	幸塚 祐哉	大阪府立大学	大学院工学研究科	”	Yuya Kozuka	Osaka Prefecture University
17	パルス強磁場用極低温実験装置の開発	野口 悟	大阪府立大学	大学院理学系研究科	Development of the cryostat for pulsed high magnetic field	Satoru Noguchi	Osaka Prefecture University
18	”	土田 稜	大阪府立大学	大学院理学系研究科	”	Ryo Tsuchida	Osaka Prefecture University
19	CaBaM <sub>4</sub> O <sub>7</sub> (M=(Ca,Fe)) 単結晶試料の強磁場下での磁化・電気分極・ESR 測定	桑原 英樹	上智大学	理工学部	Magnetization, electric polarization, and ESR measurements for CaBaM <sub>4</sub> O <sub>7</sub> (M=(Ca,Fe)) single crystals in pulsed high magnetic fields	Hideki Kuwahara	Sophia University
20	パルス強磁場を用いた強相関電子系物質の強磁場物性の研究	竹内 徹也	大阪大学	低温センター	Magnetic properties of strongly correlated electron systems under a pulsed high magnetic field	Tetsuya Takeuchi	Osaka University
21	”	大貫 惇睦	琉球大学	理学部	”	Yoshichika Onuki	University of the Ryukyus
22	磁性不純物をドーブしたトポロジカル結晶絶縁体の強磁場物性	浦田 隆広	名古屋大学	大学院工学研究科	Physical properties of magnetic impurity doped topological crystalline insulator under high magnetic field	Takahiro Urata	Nagoya University

No.	課題名	氏名	所属		Title	Name	Organization
23	正四角台塔反強磁性体の強磁場中 ESR 測定	木村 健太	東京大学	大学院新領域創成科学研究科	High-field ESR measurements of square-cupola-based antiferromagnets	Kenta Kimura	The University of Tokyo
24	パルス強磁場を用いた圧力下 ESR 装置の開発と応用	櫻井 敬博	神戸大学	研究基盤センター	Development and application of high-pressure ESR system using pulse high field	Takahiro Sakurai	Kobe University
25	単軸性キラル磁性体の磁気特性測定 -磁気トルクと磁気共鳴測定-	戸川 欣彦	大阪府立大学	大学院工学研究科	Magnetic property of monoaxial chiral magnetic materials examined by means of magnetic torque and resonance measurements	Yoshihiko Togawa	Osaka Prefecture University
26	〃	片山 諒	大阪府立大学	大学院工学研究科	〃	Ryo Katayama	Osaka Prefecture University
27	〃	島本 雄介	大阪府立大学	大学院工学研究科	〃	Yusuke Shimamoto	Osaka Prefecture University
28	三角格子反強磁性体の強磁場 ESR	南部 雄亮	東北大学	金属材料研究所	ESR measurements under high magnetic fields on a triangular antiferromagnet	Yusuke Nambu	Tohoku University
29	単核遷移金属錯体のゼロ磁場分裂と動的磁性の関係	福田 貴光	大阪大学	大学院理学研究科	Relationship between zero-field splittings and dynamic magnetism of monocuclear transition metal complexes	Takamitsu Fukuda	Osaka University
30	〃	石崎 聡晴	大阪大学	大学院理学研究科	〃	Toshiharu Ishizaki	Osaka University
31	強磁場電子スピン共鳴による有機磁性体の磁場誘起量子相の解明	細越 裕子	大阪府立大学	大学院理学系研究科	High-field ESR study on the field-induced quantum phases of organic radical crystals	Yuko Hosokoshi	Osaka Prefecture University
32	フェルダジラジカルから成る新規量子スピン系物質の強磁場物性	岩崎 義己	大阪府立大学	大学院理学系研究科	High-field magnetic properties of new quantum spin systems composed of verdazyl radicals	Yoshiki Iwasaki	Osaka Prefecture University
33	Ni <sub>2</sub> MnGa 系新規ホイスラー合金の超磁歪の高速磁場応答性の研究	左近 拓男	龍谷大学	理工学部	Research on time dependences of magnetstriction of Ni <sub>2</sub> MnGa type Heusler alloys	Takuo Sakon	Ryukoku University
34	ノーダルライン半金属の強磁場下量子振動測定	村川 寛	大阪大学	大学院理学研究科	High magnetic study on quantum transport properties in the nodal line semimetal	Hiroshi Murakawa	Osaka University
35	パルス磁場を用いたマルテンサイト変態の時間依存性に関する研究	福田 隆	大阪大学	大学院工学研究科	Study on time dependence of martensitic transformation using pulsed high magnetic field	Takashi Fukuda	Osaka University
36	強いスピン-軌道相互作用を活かした酸化物スピントロニクス	松野 丈夫	大阪大学	大学院理学研究科	Oxide spintronics utilizing strong spin-orbit coupling	Matsuno Jobu	Osaka university

## 物質合成・評価設備 G クラス / Materials Synthesis and Characterization G Class Researcher

No.	課題名	氏名	所属		Title	Name	Organization
1	単結晶 CaMn <sub>1-x</sub> Sb <sub>x</sub> O <sub>3</sub> の誘電特性の研究	谷口 晴香	岩手大学	理工学部	Study of dielectric properties of single crystalline CaMn <sub>1-x</sub> Sb <sub>x</sub> O <sub>3</sub>	Haruka Taniguchi	Iwate University

No.	課題名	氏名	所属		Title	Name	Organization
2	擬二次元遷移電子磁性体 $\text{Co}_3\text{Sn}_2\text{S}_2$ の低温構造	和氣 剛	京都大学	大学院工学研究科	Low temperature structure of quasi-two dimensional itinerant electron magnet $\text{Co}_3\text{Sn}_2\text{S}_2$	Takeshi Waki	Kyoto University
3	高温高圧水・アルコール中の固体酸・塩基触媒反応の速度論的検討	秋月 信	東京大学	大学院新領域創成科学研究科	Kinetics on solid acid and base catalyzed reactions in hot compressed water and alcohol	Makoto Akizuki	The University of Tokyo
4	プロトン伝導性固体電解質薄膜を用いた低温作動燃料電池・電解合成セルの開発	大友 順一郎	東京大学	大学院新領域創成科学研究科	Development of low-temperature solid oxide fuel cells and electrolysis cells using proton-conducting solid electrolyte thin films	Junichiro Otomo	The University of Tokyo
5	〃	松尾 拓紀	東京大学	大学院新領域創成科学研究科	〃	Hiroki Matsuo	The University of Tokyo
6	ケミカルループ法における酸素放出型粒子開発	大友 順一郎	東京大学	大学院新領域創成科学研究科	Development of oxygen releasing particle in chemical looping	Junichiro Otomo	The University of Tokyo
7	〃	七瀬 浩希	東京大学	大学院新領域創成科学研究科	〃	Koki Nanase	The University of Tokyo
8	新規プロトン・電子混合伝導体の開発	大友 順一郎	東京大学	大学院新領域創成科学研究科	Development of mixed proton-electron mixed conductors	Junichiro Otomo	The University of Tokyo
9	〃	小城 元	東京大学	大学院新領域創成科学研究科	〃	Gen Kojo	The University of Tokyo
10	中温域でのアンモニア電解合成における新規電極触媒開発と反応メカニズムの解析	大友 順一郎	東京大学	大学院新領域創成科学研究科	Development of new electrochemical catalyst for ammonia electrolysis and evaluation of reaction mechanism at intermediate temperature	Junichiro Otomo	The University of Tokyo
11	〃	長谷川 卓利	東京大学	大学院新領域創成科学研究科	〃	Takuto Hasegawa	The University of Tokyo
12	同位体分析によってアンモニア電解合成機構の解明	大友 順一郎	東京大学	大学院新領域創成科学研究科	A Study of the Relationship between the Mechanisms of Ammonia Electrosynthesis and Electrode Structures by Deuterium Isotopic Analysis	Junichiro Otomo	The University of Tokyo
13	〃	李 建毅	東京大学	大学院新領域創成科学研究科	〃	Li, Chien-I	The University of Tokyo
14	全固体 Li 電池用電解質 (ガラスセラミックス) の研究	大友 順一郎	東京大学	大学院新領域創成科学研究科	Research on solid electrolyte (glass-ceramics) for Li battery	Junichiro Otomo	The University of Tokyo
15	〃	陸 疎桐	東京大学	大学院新領域創成科学研究科	〃	Lu Shutong	The University of Tokyo
16	ケミカルループ法における高性能酸素キャリア材料の開発	大友 順一郎	東京大学	大学院新領域創成科学研究科	Development of oxygen carrier materials with high activity and durability for chemical looping systems	Junichiro Otomo	The University of Tokyo
17	〃	マーチン ケラー	東京大学	大学院新領域創成科学研究科	〃	Martin Keller	The University of Tokyo
18	中温作動プロトン伝導型固体酸化燃料電池の新規メタルサポートセル設計	大友 順一郎	東京大学	大学院新領域創成科学研究科	New cell design of metal supported intermediate temperature proton conducting SOFC	Junichiro Otomo	The University of Tokyo

No.	課題名	氏名	所属		Title	Name	Organization
19	”	阪田 一真	東京大学	大学院新領域創成科学研究科	”	Kazuma Sakata	The University of Tokyo
20	熱分解型ケミカルループ法のシステム設計および酸素キャリア開発	大友 順一郎	東京大学	大学院新領域創成科学研究科	Development of oxygen carrier materials and design of system design for chemical looping systems	Junichiro Otomo	The University of Tokyo
21	”	引間 脩	東京大学	大学院新領域創成科学研究科	”	Shu Hikima	The University of Tokyo
22	エネルギー貯蔵型燃料電池の電極活物質の開発	大友 順一郎	東京大学	大学院新領域創成科学研究科	Development of electrode materials of energy storage type - fuel cells	Junichiro Otomo	The University of Tokyo
23	”	中西 泰介	東京大学	大学院新領域創成科学研究科	”	Taisuke Nakanishi	The University of Tokyo
24	中温作動プロトン伝導型固体酸化物燃料電池の新規セル設計	大友 順一郎	東京大学	大学院新領域創成科学研究科	New Cell Design of Intermediate Temperature Proton Conducting SOFC	Junichiro Otomo	The University of Tokyo
25	”	田所 洸	東京大学	大学院新領域創成科学研究科	”	Hiroshi Tadokoro	The University of Tokyo
26	複合電解質及び局所電気化学測定手法の開発	大友 順一郎	東京大学	大学院新領域創成科学研究科	Development of composite electrolyte and micro electrochemical measurement method	Junichiro Otomo	The University of Tokyo
27	”	那須 雄太	東京大学	大学院新領域創成科学研究科	”	Nasu Yuta	The University of Tokyo
28	輸送現象の解明と燃料電池性能向上に向けたプロトン導電性固体電解質の合成	大友 順一郎	東京大学	大学院新領域創成科学研究科	Preparation of proton-conducting solid electrolytes for determination of charged-defect transport and improvement of solid oxide fuel cells	Junichiro Otomo	The University of Tokyo
29	”	オルティス コラレス フリアン アンドレス	東京大学	大学院新領域創成科学研究科	”	Ortiz Corrales Julian Andres	The University of Tokyo
30	ケミカルループ燃焼法における酸素キャリアの反応モデリング	大友 順一郎	東京大学	大学院新領域創成科学研究科	Reaction modeling in chemical looping systems with new oxygen carrier materials	Junichiro Otomo	The University of Tokyo
31	”	松原 一起	東京大学	大学院新領域創成科学研究科	”	Kazuki Matsubara	The University of Tokyo
32	メソポーラスマテリアル・グラフェンオキシドに担持した金属触媒のキャラクタリゼーション	佐々木 岳彦	東京大学	大学院新領域創成科学研究科	Characterization of metal catalysts loaded on mesoporous materials and graphene oxides	Takehiko Sasaki	The University of Tokyo
33	”	斎藤 貴仁	東京大学	大学院新領域創成科学研究科	”	Takahito Saito	The University of Tokyo
34	高温高圧水の固体触媒表面性質への影響の評価	大島 義人	東京大学	大学院新領域創成科学研究科	Effects of high temperature and pressure water on surface properties of solid catalyst	Yoshito Oshima	The University of Tokyo
35	”	高橋 侑佳	東京大学	大学院新領域創成科学研究科	”	Takahashi Yuka	The University of Tokyo

No.	課題名	氏名	所属		Title	Name	Organization
36	六方晶フェライトの非磁性サイト置換効果	植田 浩明	京都大学	大学院理学研究科	Non-magnetic site substitution effect of hexagonal ferrites	Hiroaki Ueda	Kyoto university
37	”	増田 順一	京都大学	大学院理学研究科	”	Jun-ichi Masuda	Kyoto University
38	高温高圧水-アルコール混合溶媒が金属酸化物ナノ粒子の合成に与える影響の解明	大島 義人	東京大学	大学院新領域創成科学研究科	Analysis of the effect of water-alcohol mixture on metal oxide nanoparticle synthesis	Yoshito Oshima	The University of Tokyo
39	”	劉 源	東京大学	大学院新領域創成科学研究科	”	Liu Yuan	The University of Tokyo
40	アンモニア電解合成における選択性向上の検討	大友 順一郎	東京大学	大学院新領域創成科学研究科	Study on promotion of selectivity in ammonia electrosynthesis	Junichiro Otomo	The University of Tokyo
41	”	山本 和範	東京大学	大学院新領域創成科学研究科	”	Kazunori Yamamoto	The University of Tokyo
42	重元素 5d 遷移金属化合物における新超伝導体探索	岡本 佳比古	名古屋大学	大学院工学研究科	Exploration of New Superconductors in 5d Electron System with Heavy Transition Metal Elements	Yoshihiko Okamoto	Nagoya University
43	超臨界水中の ZnO ナノ粒子合成における共存イオンの影響	大島 義人	東京大学	大学院新領域創成科学研究科	Effects of coexisting ions on synthesis of zinc oxide nano particles in supercritical water	Yoshito Oshima	The University of Tokyo
44	”	織田 耕彦	東京大学	大学院新領域創成科学研究科	”	Yasuhiko Orita	The University of Tokyo
45	超臨界水中のバイオマス改質反応へのゼオライトの利用	大島 義人	東京大学	大学院新領域創成科学研究科	Utilization of modified zeolites for biomass reactions in supercritical water	Yoshito Oshima	The University of Tokyo
46	”	アピバンボリラク チャンウィット	東京大学	大学院新領域創成科学研究科	”	Apibanboriak Chanwit	The University of Tokyo
47	触媒反応の insitu ラマン散乱測定	佐々木 岳彦	東京大学	大学院新領域創成科学研究科	In situ measurement of Raman scattering for heterogeneous catalytic reactions	Takehiko Sasaki	The University of Tokyo
48	超高压直接窒化反応による多窒化物の合成	丹羽 健	名古屋大学	大学院工学研究科	Synthesis of pernitrides via direct nitridation of elements under high pressure	Ken Niwa	Nagoya University
49	”	飯塚 友規	名古屋大学	大学院工学研究科	”	Tomoki Iizuka	Nagoya university
50	超高压合成法による新規遷移金属リン化合物の創製と結晶化学	丹羽 健	名古屋大学	大学院工学研究科	High pressure synthesis and crystal chemistry of novel transition metal phosphides	Ken Niwa	Nagoya University
51	”	松尾 拓	名古屋大学	大学院工学研究科	”	Taku Matsuo	Nagoya University
52	超高压プレスを用いた新規プロトニクス酸化物のソフト化学的合成法の検討	山口 周	東京大学	大学院工学系研究科	Oxide-Protonics materials synthesis by combined use of soft chemical method and high pressure	Shu Yamaguchi	The University of Tokyo

No.	課題名	氏名	所属		Title	Name	Organization
53	”	田中 和彦	東京大学	大学院工学系研究科	”	Kazuhiko Tanaka	The University of Tokyo
54	溶融亜鉛メッキ合金相の応力誘起変態	山口 周	東京大学	大学院工学系研究科	Stress-induced phase transformation of Fe-Zn alloy formed in hot-dip process	Shu Yamaguchi	The University of Tokyo
55	”	田中 和彦	東京大学	大学院工学系研究科	”	Kazuhiko Tanaka	The University of Tokyo
56	リチウムイオン伝導体 Li <sub>3</sub> BP <sub>2</sub> O <sub>8</sub> の高圧相合成	廣瀬 瑛一	名古屋大学	大学院工学研究科	High pressure synthesis of a novel lithium ion conductor Li <sub>3</sub> BP <sub>2</sub> O <sub>8</sub>	Eiichi Hirose	Nagoya University
57	超高圧力合成法による Pb- 遷移金属系新規化合物の合成	佐々木 拓也	名古屋大学	大学院工学研究科	High-pressure synthesis of novel Pb-transition metal compounds	Takuya Sasaki	Nagoya University
58	”	位田 昌鴻	名古屋大学	大学院工学研究科	”	Masahiro Inden	Nagoya University
59	高圧下におけるアミノ酸の圧力誘起反応の観察	藤本 千賀子	東京大学	大学院理学系研究科	Pressure-induced reaction of amino acids under high pressure	Fujimoto Chikako	The University of Tokyo
60	新規 MO-Al <sub>2</sub> O <sub>3</sub> 系 (M = Mg, Ca, Sr, Ba) 蛍光体の高圧力合成	佐々木 拓也	名古屋大学	大学院工学研究科	High-pressure synthesis of novel phosphors in MO-Al <sub>2</sub> O <sub>3</sub> system (M = Mg, Ca, Sr, Ba)	Takuya Sasaki	Nagoya University
61	”	森 唯人	名古屋大学	大学院工学研究科	”	Yuito Mori	Nagoya university
62	希土類元素を充填した新規スキutterdait型熱電材料の高圧合成	関根 ちひろ	室蘭工業大学	大学院工学研究科	High-pressure synthesis of new rare-earth-filled skutterudite-type thermoelectric materials	Chihiro Sekine	Muroran Institute of Technology
63	”	星野 愛	室蘭工業大学	大学院工学研究科	”	Megumi Hoshino	Muroran Institute of Technology
64	高温高圧下における下部マントル鉱物への窒素の取り込み	福山 鴻	東京大学	大学院理学系研究科	Nitrogen incorporation into the lower-mantle minerals under high pressure and high temperature	Ko Fukuyama	The University of Tokyo
65	高圧下での MoSi <sub>2</sub> 型構造の FeAl <sub>2</sub> 結晶の作製	木村 薫	東京大学	大学院新領域創成科学研究科	High pressure synthesis of MoSi <sub>2</sub> type iron aluminide, FeAl <sub>2</sub> crystal	Kaoru Kimura	The University of Tokyo
66	”	飛田 一樹	東京大学	大学院新領域創成科学研究科	”	Kazuki Tobita	The University of Tokyo
67	高圧印加による Al-Ir 1/0 近似結晶半導体の作製	木村 薫	東京大学	大学院新領域創成科学研究科	Synthesis of Al-Ir 1/0-Icosahedral Approximant Semiconductor by high-pressurization	Kaoru Kimura	The University of Tokyo
68	”	岩崎 祐昂	東京大学	大学院新領域創成科学研究科	”	Yutaka Iwasaki	The University of Tokyo
69	新しい希土類磁石の探求	齋藤 哲治	千葉工業大学	工学部	Research of new rare-earth magnets	Tetsuji Saito	Chiba Instiute of Technology

No.	課題名	氏名	所属		Title	Name	Organization
70	オレイン酸被覆水熱成長法によるセリアナノ粒子の鉄イオンドーブによる形態変化	牧之瀬 佑旗	島根大学	総合理工学部	Study of shape changing of Fe doped ceria nanoparticles synthesized by oleate-modified hydrothermal method	Yuki Makinose	Shimane University
71	プラズマ/氷界面反応場を用いたナノ構造物質の合成	榊原 教貴	東京大学	大学院新領域創成科学研究科	Synthesis of nano-structured materials with plasma/ice interface	Noritaka Sakakibara	The University of Tokyo
72	ナノ構造材料を用いた省エネルギーデバイス開発	細野 英司	産業技術総合研究所	省エネルギー研究部門	Development of devices for energy conservation by using nanostructured materials	Eiji Hosono	National Institute of Advanced Industrial Science and Technology
73	新規金属窒化物半導体の超高压創製と光学特性	長谷川 正	名古屋大学	大学院工学研究科	Synthesis and optical properties of novel semiconductive metal-nitrides in ultra-high pressures	Masashi Hasegawa	Nagoya University
74	〃	野村 俊介	名古屋大学	大学院工学研究科	〃	Shunsuke Nomura	Nagoya University
75	新規複合アニオン層状化合物の超高压合成と結晶育成および物性	長谷川 正	名古屋大学	大学院工学研究科	High pressure synthesis, crystal growth and physical properties of novel layer-structure compounds	Masashi Hasegawa	Nagoya University
76	〃	生駒 鷹秀	名古屋大学	大学院工学研究科	〃	Takahide Ikoma	Nagoya University
77	新規超伝導物質合成と物性評価	飯塚 理子	東京大学	大学院理学系研究科	Behavior of multi light elements in iron-silicate-water system under high pressure and high temperature	Riko Iizuka-Oku	The University of Tokyo
78	$\text{Pr}_{1-x}\text{Ca}_x\text{FeO}_3$ ( $0.1 \leq x \leq 0.9$ ) の高温における磁性と熱電特性に関する研究	中津川 博	横浜国立大学	大学院工学研究科	Magnetism and thermoelectric properties at high temperature in $\text{Pr}_{1-x}\text{Ca}_x\text{FeO}_3$ ( $0.1 \leq x \leq 0.9$ )	Hiroshi Nakatsugawa	Yokohama National University
79	準結晶・近似結晶の磁性に関する研究	鈴木 慎太郎	東京理科大学	基礎工学部	Magnetism of quasicrystal and approximants	Shintaro Suzuki	Tokyo University of Science
80	ハーフメタルホイスラー合金の遍歴電子磁性体のスピンゆらぎ理論による解析に関する研究	重田 出	鹿児島大学	大学院理工学研究科	Study on analysis of half-metallic Heusler alloys by the spin fluctuation theory for itinerant electron magnetism	Shigeta Iduru	Kagoshima University
81	高压印加による Li ドープ $\alpha$ 菱面体晶ボロンの作製	木村 薫	東京大学	大学院新領域創成科学研究科	Synthesis of Li-doped alpha-rhombohedral boron by high-pressure	Kaoru Kimura	The University of Tokyo
82	〃	酒井 志徳	東京大学	大学院新領域創成科学研究科	〃	Munenori Sakai	The University of Tokyo
83	貫入型三元系遷移金属炭化物窒化物の単結晶育成	和氣 剛	京都大学	大学院工学研究科	Single crystal growth of interstitial ternary transition metal nitride and carbide	Takeshi Waki	Kyoto University
84	非共面的磁気構造を有する磁性体における電子物性に関する研究	木村 剛	東京大学	大学院新領域創成科学研究科	Investigation of electronic properties in magnetic systems with non-coplanar spin structure	Tsuyoshi Kimura	The University of Tokyo
85	電子ネマティシティを有する新規超伝導物質合成と物性評価	水上 雄太	東京大学	大学院新領域創成科学研究科	Synthesis and characterization of novel superconductors with electron nematicity	Yuta Mizukami	The University of Tokyo
86	〃	竹中 崇了	東京大学	大学院新領域創成科学研究科	〃	Takaaki Takenaka	The University of Tokyo

No.	課題名	氏名	所属		Title	Name	Organization
87	”	石田 浩祐	東京大学	大学院新領域創成科学研究科	”	Kousuke Ishida	The University of Tokyo
88	”	田中 桜平	東京大学	大学院新領域創成科学研究科	”	Ohei Tanaka	The University of Tokyo
89	”	石原 滉大	東京大学	大学院新領域創成科学研究科	”	Kota Ishihara	The University of Tokyo
90	”	辻井 優哉	東京大学	大学院新領域創成科学研究科	”	Masaya Tsujii	The University of Tokyo
91	空間反転対称性を持たない新規磁性体の開発	有馬 孝尚	東京大学	大学院新領域創成科学研究科	Exploration of new noncentrosymmetric magnets	Taka-hisa Arima	The University of Tokyo
92	”	徳永 祐介	東京大学	大学院新領域創成科学研究科	”	Yusuke Tokunaga	The University of Tokyo
93	”	阿部 伸行	東京大学	大学院新領域創成科学研究科	”	Nobuyuki Abe	The University of Tokyo
94	”	鷲見 浩樹	東京大学	大学院新領域創成科学研究科	”	Hiroki Sumi	The University of Tokyo
95	”	藤間 友理	東京大学	大学院新領域創成科学研究科	”	Yuri Fujima	The University of Tokyo
96	”	荒木 勇介	東京大学	大学院新領域創成科学研究科	”	Yusuke Araki	The University of Tokyo
97	”	近江 毅志	東京大学	大学院新領域創成科学研究科	”	Tsuyoshi Omi	The University of Tokyo
98	”	海本 祐真	東京大学	大学院新領域創成科学研究科	”	Yuma Umimoto	The University of Tokyo
99	”	佐藤 樹	東京大学	大学院新領域創成科学研究科	”	Tatsuki Sato	The University of Tokyo
100	”	吉澤 孟晃	東京大学	大学院新領域創成科学研究科	”	Takeaki Yoshizawa	The University of Tokyo
101	”	尾亦 恭輔	東京大学	大学院新領域創成科学研究科	”	Kyosuke Omata	The University of Tokyo
102	”	西 健太	東京大学	大学院新領域創成科学研究科	”	Kenta Nishi	The University of Tokyo
103	”	山本 圭祐	東京大学	大学院新領域創成科学研究科	”	Keisuke Yamamoto	The University of Tokyo

No.	課題名	氏名	所属		Title	Name	Organization
104	”	渡辺 義人	東京大学	大学院新領域創成科学研究科	”	Yoshito Watanabe	The University of Tokyo
105	電子が複合自由度を持つ遷移金属カルコゲナイドの合成と物性	片山 尚幸	名古屋大学	大学院工学研究科	Growth of the transition metal chalcogenides with charge, orbital and spin degrees of freedom	Naoyuki Katayama	Nagoya University
106	”	小林 慎太郎	名古屋大学	大学院工学研究科	”	Shintaro Kobayashi	Nagoya University
107	”	前田 泰	名古屋大学	大学院工学研究科	”	Shin Maeda	Nagoya University
108	析出現象を用いた銅合金中における磁性ナノ粒子の物性調査	坂倉 響	横浜国立大学	大学院工学府	Investigation of nano-scale magnetic properties comprising ferromagnetic element atoms in copper alloys	Hibiki Sakakura	Yokohama National University
109	Cu - Ni - X (X=Co,Fe) 系単結晶性合金中の磁性微粒子析出過程と磁気特性の関係	竹田 真帆人	横浜国立大学	大学院工学研究院	Precipitation behavior and magnetic properties of fine magnetic particles in Cu - Ni base alloys single Crystal	Mahoto Takeda	Yokohama National University
110	”	又井 慎太郎	横浜国立大学	大学院工学府	”	Shintaro Matai	Yokohama National University
111	非共面的磁気構造を有する磁性体における電子物性に関する研究	木村 健太	東京大学	大学院新領域創成科学研究科	Investigation of electronic properties in magnetic systems with non-coplanar spin structure	Kenta Kimura	The University of Tokyo
112	”	勝吉 司	東京大学	大学院新領域創成科学研究科	”	Katsuyoshi Tsukasa	The University of Tokyo
113	”	三澤 龍介	東京大学	大学院新領域創成科学研究科	”	Misawa Ryusuke	The University of Tokyo

## 物質合成・評価設備 U クラス / Materials Synthesis and Characterization U Class Researcher

No.	課題名	氏名	所属		Title	Name	Organization
1	宇宙線望遠鏡に用いる反射鏡の UV 照射後の反射率測定	野田 浩司	東京大学	宇宙線研究所	Reflectance measurement of the mirrors used in cosmic ray telescopes, after an exposure to UV radiation	Koji Noda	The University of Tokyo
2	光反応による機能性酸化物薄膜の製膜機構	松林 康仁	産業技術総合研究所	センターグリーンデバイ材料研究チーム	Mechanism of photo-assisted deposition of functional oxide thin films	Yasuhito Matsubayashi	National Institute of AIST
3	PSA によるバイオガス浄化システム：自然粘土を用いた CO <sub>2</sub> 及び H <sub>2</sub> S の吸着	布浦鉄兵	東京大学	環境安全研究センター	Biohydrogen purification through utilization of pressure swing adsorption: Natural Japanese clay as an adsorbent for CO <sub>2</sub> and H <sub>2</sub> S	Tepei Nunoura	The University of Tokyo
4	”	ジェニファー チャー ウィーファン	東京大学	大学院新領域創成科学研究科	”	Jennifer Chia Wee Fern	The University of Tokyo
5	プラズマ風洞による宇宙往還機熱防護システムの動的酸化に関する研究	桃沢 愛	東京都市大学	工学部医用工学科	Investigation on dynamic oxidation of thermal protection system using plasma wind tunnel	Ai Momozawa	Tokyo City University

No.	課題名	氏名	所属		Title	Name	Organization
6	〃	田中 聖也	東京大学	大学院工学系研究科	〃	Seiya Tanaka	The University of Tokyo
7	〃	山田 慎	東京大学	大学院工学系研究科	〃	Shin Yamada	The University of Tokyo
8	高温高压水による廃棄リチウムイオン電池リサイクル技術に関する研究	布浦 鉄兵	東京大学	環境安全研究センター	Study on recycling of waste lithium ion batteries using hot compressed water	Teppey Nunoura	The University of Tokyo
9	〃	シュウ ユウメイ	東京大学	大学院新領域創成科学研究科	〃	Zhou Yiming	The University of Tokyo
10	光ファイバーセンシング技術を利用した泥岩中の化学的浸透現象に伴う岩石の局所的変形の計測	廣田 翔伍	東京大学	大学院新領域創成科学研究科	Measure of local deformation of mudstones caused by chemical osmosis with optical fiber sensing technique	Shogo Hirota	The University of Tokyo
11	マイクロミキサを用いた機能性無機ナノ粒子の連続合成	陶 究	産業技術総合研究所	化学プロセス研究部門	Continuous synthesis of functional inorganic nanoparticles using a micromixer	Sue Kiwamu	National Institute of Advanced Industrial Science and Technology
12	静電浮遊法を用いた過冷却液体急冷法によるボロン系準結晶の探索	木村 薫	東京大学	大学院新領域創成科学研究科	Search for quasicrystalline boron using rapid quenching from super-cooled liquid by levitation	Kaoru Kimura	The University of Tokyo
13	〃	高橋 昂宏	東京大学	大学院新領域創成科学研究科	〃	Takahiro Takahashi	The University of Tokyo
14	バングラデシュ南部デルタ沿岸地域における地下水水位変動と塩の起源	マスドウル ラハマン	東京大学	環境システム学専攻	Water-level fluctuations and salinity sources of groundwater systems in the southern deltaic coastal areas of Bangladesh: A multi-methodological	Masudur Rahman	The University of Tokyo

## 短期留学研究員 / Short Term Young Researcher

No.	課題名	氏名	所属		Title	Name	Organization
1	メタンの固体表面での吸着と活性化に関する研究	セプティア エカ マルシ ヤ プトラ	大阪大学	大学院工学研究科	Study on anomalous valence fluctuation of YbPd under high pressure at extremely low temperatures	Septia Eka Marsha Putra	Osaka University

平成 30 年度 中性子科学研究施設 共同利用課題一覧 / Joint Research List of Neutron Scattering Researcher 2018

No.	課題名	氏名	所属	Title	Name	Organization
・ 申請装置 4G: GPTAS						
1	GPTAS (汎用 3 軸中性子分光器) IRT 課題	佐藤 卓	東北大学	多元物質科学研究所	IRT project of GPTAS	Taku J Sato Tohoku University
2	磁性準結晶中の隠れた磁気秩序の探索	佐藤 卓	東北大学	多元物質科学研究所	Hidden magnetic order in magnetic quasicrystals	Taku J Sato Tohoku University
3	新奇三角格子系 Yb <sub>3</sub> Ni <sub>11</sub> Ge <sub>4</sub> の磁気励起	佐藤 卓	東北大学	多元物質科学研究所	Magnetic excitations in the new quantum triangular-lattice compound Yb <sub>3</sub> Ni <sub>11</sub> Ge <sub>4</sub>	Taku J Sato Tohoku University
4	時間分割中性子散乱測定による磁気構造変化過程の実時間追跡	元屋 清一郎	東京理科大学	理工学部 物理学科	Real-time observation of magnetic structural change by means of time-resolved neutron scattering	Kiyoichiro Motoya Tokyo University of Science
5	Ba <sub>2</sub> Zn <sub>2</sub> Fe <sub>12</sub> O <sub>22</sub> および BaFe <sub>12</sub> O <sub>19</sub> 系六方晶フェライトの磁気構造と超交換相互作用	内海 重宣	諏訪東京理科大学	工学部 機械工学科	Magnetic structure and superexchange interaction of hexagonal ferrite Ba <sub>2</sub> Zn <sub>2</sub> Fe <sub>12</sub> O <sub>22</sub> and BaFe <sub>12</sub> O <sub>19</sub> systems	Shigenori Utsumi Tokyo University of Science, Suwa
6	強磁性超伝導体における磁性と超伝導の研究	古川 はづき	お茶の水女子大学	基幹研究院 自然科学系	A study of magnetic state in ferromagnetic superconductors	Hazuki Furukawa Ochanomizu University
7	Sr <sub>2</sub> RuO <sub>4</sub> の非弾性散乱	古川 はづき	お茶の水女子大学	基幹研究院 自然科学系	Inelastic neutron scattering experiments on Sr <sub>2</sub> RuO <sub>4</sub>	Hazuki Furukawa Ochanomizu University
8	空間反転対称性の破れた超伝導体の非弾性散乱	古川 はづき	お茶の水女子大学	基幹研究院 自然科学系	Inelastic neutron scattering experiments on non-centrosymmetric superconductors	Hazuki Furukawa Ochanomizu University
9	トポロジカル超伝導体の非弾性散乱	古川 はづき	お茶の水女子大学	基幹研究院 自然科学系	Inelastic neutron scattering experiments on topological superconductors	Hazuki Furukawa Ochanomizu University
10	多段メタ磁性転移を示す空間反転対称性の破れた Ce 系化合物 CeTSi <sub>3</sub> (T = Pd, Pt) における磁気構造の決定	吉田 雅洋	東京大学	物性研究所附属 中性子科学研究施設	Determination of the Magnetic Structure of the Noncentrosymmetric Heavy-Electron Metamagnet CeTSi <sub>3</sub> (T = Pd, Pt)	Masahiro Yoshida The University of Tokyo
11	二次元ダイマー反強磁性体におけるトリプロン励起	那波 和宏	東北大学	多元物質科学研究所	Triplon excitations in the two-dimensional dimer antiferromagnet	Kazuhiro Nawa Tohoku University
12	強誘電体の相転移機構 (変位型及び秩序-無秩序型) に関する統一的理解の確立	重松 宏武	山口大学	教育学部	Establishment of the unified explanation about the phase transition mechanism (displacive and order-disorder type) in Ferroelectrics	Hirotake Shigematsu Yamaguchi University
13	スピンアイスにおけるトポロジカル相転移	門脇 広明	首都大学東京	理工学研究科物理学専攻	Topological phase transition in spin ice	Hiroaki Kadowaki Tokyo Metropolitan University
14	パイロクロア磁性体 Tb <sub>2</sub> Zr <sub>2</sub> O <sub>7</sub> の磁気ダイナミクスと結晶場励起	高津 浩	京都大学	工学研究科	Quantum spin fluctuations and crystal field of the pyrochlore magnet Tb <sub>2</sub> Zr <sub>2</sub> O <sub>7</sub>	Hiroshi Takatsu Kyoto University
15	DyMnO <sub>3</sub> の高圧力相の磁気秩序の探査	寺田 典樹	物質材料研究機構	中性子散乱グループ	Investigation of magnetic ordering in the high-pressure phase of DyMnO <sub>3</sub>	Noriki Terada National Institute for Materials Science

No.	課題名	氏名	所属		Title	Name	Organization
16	熱電材料 Mg <sub>3</sub> Sb <sub>2</sub> のフォノンダイナミクス	李 哲虎	産業技術総合研究所	省エネルギー研究部門	Phonon dynamics on thermoelectric material of Mg <sub>3</sub> Sb <sub>2</sub>	Chul-Ho Lee	National Institute of Advanced Industrial Science and Technology
・ 申請装置 5G: PONTA							
17	PONTA (高性能偏極中性子散乱装置) IRT 課題	益田 隆嗣	東京大学	物性研究所	IRT project of PONTA	Takatsugu Masuda	The University of Tokyo
18	時間分割中性子散乱測定による磁気構造変化過程の実時間追跡	元屋 清一郎	東京理科大学	理工学部 物理学科	Real-time observation of magnetic structural change by means of time-resolved neutron scattering	Kiyochiro Motoya	Tokyo University of Science
19	マグネトプランバイト型コバルト酸化物 SrCo <sub>12</sub> O <sub>19</sub> の電荷 - 磁気秩序	浅井 晋一郎	東京大学	物性研究所	Charge and magnetic order of magnetoplumbite-type cobalt oxide SrCo <sub>12</sub> O <sub>19</sub>	Shinichiro Asai	The University of Tokyo
20	ダブルペロブスカイト型コバルト酸化物 Sr <sub>2</sub> CoNbO <sub>6</sub> の磁気秩序	浅井 晋一郎	東京大学	物性研究所	Magnetic order of double perovskite cobalt oxide Sr <sub>2</sub> CoNbO <sub>6</sub>	Shinichiro Asai	The University of Tokyo
21	偏極中性子散乱による LaCo <sub>0.8</sub> Rh <sub>0.2</sub> O <sub>3</sub> の新奇な強磁性磁気秩序の研究	浅井 晋一郎	東京大学	物性研究所	Polarized neutron diffraction study on a novel type of ferromagnetic order of LaCo <sub>0.8</sub> Rh <sub>0.2</sub> O <sub>3</sub>	Shinichiro Asai	The University of Tokyo
22	励起子絶縁体候補物質 LaCo <sub>0.97</sub> Rh <sub>0.03</sub> O <sub>3</sub> の中性子散乱	浅井 晋一郎	東京大学	物性研究所	Neutron Scattering for Excitonic Insulator Candidate LaCo <sub>0.97</sub> Rh <sub>0.03</sub> O <sub>3</sub>	Shinichiro Asai	The University of Tokyo
23	スピン状態クロスオーバーが起こるコバルト酸化物 Sr <sub>2</sub> CoNbO <sub>6</sub> の中性子非弾性散乱研究	浅井 晋一郎	東京大学	物性研究所	Inelastic neutron scattering study of spin-state crossover for double perovskite cobalt oxide Sr <sub>2</sub> CoNbO <sub>6</sub>	Shinichiro Asai	The University of Tokyo
24	マルチフェロイック物質 Ba <sub>2</sub> CoGe <sub>2</sub> O <sub>7</sub> における磁気モーメントの完全電場制御	益田 隆嗣	東京大学	物性研究所	Full control of magnetic moment in multiferroics Ba <sub>2</sub> CoGe <sub>2</sub> O <sub>7</sub>	Takatsugu Masuda	The University of Tokyo
25	三角スピントューブ CsCrF <sub>4</sub> の圧力下中性子回折	益田 隆嗣	東京大学	物性研究所	Neutron diffraction experiment on triangular spin tube CsCrF <sub>4</sub>	Takatsugu Masuda	The University of Tokyo
26	マルチフェロイック Ca <sub>2</sub> CoSi <sub>2</sub> O <sub>7</sub> の磁場下における磁気構造解析	益田 隆嗣	東京大学	物性研究所	Magnetic structure analysis on multiferroic Ca <sub>2</sub> CoSi <sub>2</sub> O <sub>7</sub> in magnetic field	Takatsugu Masuda	The University of Tokyo
27	カイラル磁性体 CsCuCl <sub>3</sub> のカイラルらせん磁性の検証	高阪 勇輔	岡山大学	異分野基礎科学研究所	Chiral Helimagnetism in Chiral Inorganic Compound CsCuCl <sub>3</sub>	Yusuke Kousaka	Okayama University
28	URu <sub>2</sub> Si <sub>2</sub> の隠れた秩序に伴う多重極秩序の直接観測	高阪 勇輔	岡山大学	異分野基礎科学研究所	Direct Observation of the "Hidden Order" due to Multipole Ordering in URu <sub>2</sub> Si <sub>2</sub>	Yusuke Kousaka	Okayama University
29	偏極解析を用いた Zn-Nd-Zn 単分子磁石の磁気弾性散乱の検出	古府 麻衣子	日本原子力研究開発機構	中性子利用セクション	Detection of magnetic scattering of Zn-Nd-Zn single molecule magnet using polarization analysis	Maiko Kofu	Japan Atomic Energy Agency
30	鉄系超伝導体のスピン揺動	李 哲虎	産業技術総合研究所	省エネルギー研究部門	Spin fluctuations of iron-based superconductors	Chul-Ho Lee	National Institute of Advanced Industrial Science and Technology
31	磁場中の中性子回折を利用した Cu <sub>3</sub> (P <sub>2</sub> O <sub>6</sub> OD) <sub>2</sub> の基底状態の研究	長谷 正司	物質・材料研究機構	中性子散乱グループ	The investigation on the ground state of Cu <sub>3</sub> (P <sub>2</sub> O <sub>6</sub> OD) <sub>2</sub> using neutron diffraction in magnetic fields	Masashi Hase	National Institute for Materials Science

No.	課題名	氏名	所属		Title	Name	Organization
32	磁場中の中性子回折を利用した $K_2Cu_3O(SO_4)_3$ の基底状態の研究	長谷 正司	物質・材料研究機構	中性子散乱グループ	The investigation on the ground state of $K_2Cu_3O(SO_4)_3$ using neutron diffraction in magnetic fields	Masashi Hase	National Institute for Materials Science
33	メイプルリーフ化合物 $MgMn_3O_7 \cdot 3D_2O$ の磁気構造	浅井 晋一郎	東京大学	物性研究所	Magnetic Structure of Maple Leaf Compound $MgMn_3O_7 \cdot 3D_2O$	Shinichiro Asai	The University of Tokyo
・ 申請装置 6G: TOPAN							
34	TOPAN (東北大理: 3 軸型偏極中性子分光器) IRT 課題	富安 啓輔	東北大学	大学院理学研究科	IRT project of TOPAN	Keisuke Tomiyasu	Tohoku University
35	近藤半金属におけるワイルフェルミオンの磁気状態	岩佐 和晃	茨城大学	フロンティア応用原子科学研究センター	Magnetic states of Weyl fermion in Kondo semimetals	Kazuaki Iwasa	Ibaraki University
36	$PrT_2X_{20}$ (T = Rh, Ir, X = Al, Zn) における 2 チャンネル近藤効果	岩佐 和晃	茨城大学	フロンティア応用原子科学研究センター	Two-channel Kondo effect in $PrT_2X_{20}$ (T = Rh, Ir, X = Al, Zn)	Kazuaki Iwasa	Ibaraki University
37	全対称型多極子秩序による金属-非金属転移に対する磁気不純物効果	岩佐 和晃	茨城大学	フロンティア応用原子科学研究センター	Magnetic Impurity Effect on the Metal-Nonmetal Transition Associated with Totally-Symmetric Electron Multipole Ordering	Kazuaki Iwasa	Ibaraki University
38	$Pr_{1-x}LaCe_xCuO_4$ の磁気共鳴ピークの組成依存性	池内 和彦	総合科学研究機構	中性子科学センター	Doping dependence of the magnetic resonance peak in PLCCO	Kazuhiko Ikeuchi	CROSS
39	$Pr_{1-x}LaCe_xCuO_4$ の格子振動を通じたギャップ対称性の観測	池内 和彦	総合科学研究機構	中性子科学センター	Observation of the gap symmetry due to lattice vibrations in PLCCO	Kazuhiko Ikeuchi	CROSS
・ 申請装置 C1-1: HER							
40	HER (高エネルギー分解能 3 軸型中性子分光器) IRT 課題	益田 隆嗣	東京大学	物性研究所	IRT project of HER	Takatsugu Masuda	The University of Tokyo
41	磁気スカーミオン格子相におけるトポロジカルマグノンの探索	佐藤 卓	東北大学	多元物質科学研究研究所	Topological magnon band in the magnetic skyrmion lattice	Taku J Sato	Tohoku University
42	a- $Cu_2V_2O_7$ のマグノン電場効果	佐藤 卓	東北大学	多元物質科学研究研究所	Inelastic neutron scattering measurements on the a- $Cu_2V_2O_7$ under electric field	Taku J Sato	Tohoku University
43	フラストレイト近藤化合物 $Ce_5Si_3$ の磁気構造とダイマー構造の研究	小林 理気	琉球大学	理学部	Study of Magnetic and Dimer Structure in Frustrated Kondo Compound $Ce_5Si_3$	Riki Kobayashi	University of the Ryukyus
44	近藤半金属におけるワイルフェルミオンの磁気状態	岩佐 和晃	茨城大学	フロンティア応用原子科学研究センター	Magnetic states of Weyl fermion in Kondo semimetals	Kazuaki Iwasa	Ibaraki University
45	$PrT_2X_{20}$ (T = Rh, Ir, X = Al, Zn) における 2 チャンネル近藤効果	岩佐 和晃	茨城大学	フロンティア応用原子科学研究センター	Two-channel Kondo effect in $PrT_2X_{20}$ (T = Rh, Ir, X = Al, Zn)	Kazuaki Iwasa	Ibaraki University
46	全対称型多極子秩序による金属-非金属転移に対する磁気不純物効果	岩佐 和晃	茨城大学	フロンティア応用原子科学研究センター	Magnetic Impurity Effect on the Metal-Nonmetal Transition Associated with Totally-Symmetric Electron Multipole Ordering	Kazuaki Iwasa	Ibaraki University

No.	課題名	氏名	所属		Title	Name	Organization
47	Fe 置換により誘起される LSCO の異方的磁気秩序ピークの起源	藤田 全基	東北大学	金属材料研究所	Origin of isotropic magnetic peaks induced by Fe-substitution in LSCO	Masaki Fujita	Tohoku University
48	量子スピン液体の研究	門脇 広明	首都大学東京	理工学研究科物理学専攻	Quantum spin liquid	Hiroaki Kadowaki	Tokyo Metropolitan University
49	空間反転対称性をもたない超伝導体 CeRhSi <sub>3</sub> の磁気励起	阿曾 尚文	琉球大学	理学部物質地球科学科	Magnetic Fluctuations in a Non-Centrosymmetric Superconductor CeRhSi <sub>3</sub>	Naofumi Aso	University of the Ryukyus
50	広角中性子回折による化学当量的な LuFe <sub>2</sub> O <sub>4</sub> 電荷 - 磁気相関の研究	加倉井 和久	総合科学研究機構	中性子科学センター	Wide-angle neutron diffraction investigation of charge and magnetic correlations in stoichiometric LuFe <sub>2</sub> O <sub>4</sub>	Kazuhisa Kakurai	Comprehensive Research Organization for Science and Society (CROSS)
51	Ce(Co,Rh)In <sub>5</sub> のネスティングと超伝導発現機構	古川 はづき	お茶の水女子大学	基幹研究院 自然科学系	Nesting features and the superconducting mechanism in Ce(Co,Rh)In <sub>5</sub>	Hazuki Furukawa	Ochanomizu University
・ 申請装置 C1-2: SANS-U							
52	SANS-U (二次元位置測定小角散乱装置) IRT 課題	柴山 充弘	東京大学	物性研究所	IRT project of SANS-U	Mitsuhiro Shibayama	The University of Tokyo
53	アセトニトリル溶媒 Tetra-PEG ゲルの USANS 測定	Li Xiang	東京大学	物性研究所中性子科学研究施設	USANS measurement of acetonitrile solvent Tetra-PEG gel	Xiang Li	The University of Tokyo
54	温度応答性ポリマーの一本鎖収縮挙動	Li Xiang	東京大学	物性研究所中性子科学研究施設	Single-chain shrinking behavior of temperature-responsive polymers	Xiang Li	The University of Tokyo
55	モデルネットワークゲルの静的均一性評価	Li Xiang	東京大学	物性研究所中性子科学研究施設	Static homogeneity evaluation of model network gel	Xiang Li	The University of Tokyo
56	SANS・DSC 同時測定による 2 本鎖 DNA により架橋されたモデル物理ゲルの構造解析	Li Xiang	東京大学	物性研究所中性子科学研究施設	Simultaneous SANS/DSC measurement for a model physical gel crosslinked by double-stranded DNA	Xiang Li	The University of Tokyo
57	イミダゾリウム系イオン液体 + プロパノール二成分溶液の相分離メカニズムの解明	下村 拓也	室蘭工業大学	大学院工学研究科	Phase separation of imidazolium-based ionic liquid+propanol binary solutions	Takuya Shimomura	Muroran Institute of Technology
58	ブラシ状高分子中の重水素ラベルした側鎖に対する小角中性子散乱測定	中村 洋	京都大学	工学研究科高分子化学専攻	Small-angle neutron scattering from a deuterated labeled side chain in brush-like polymers	Yo Nakamura	Kyoto University
59	CV-SANS による DNA 存在下での制限分解酵素の構造解析	井上 倫太郎	京都大学	複合原子力科学研究所	Structural analysis of restriction endonuclease with the existence of DNA by contrast variation SANS (CV-SANS)	Rintaro Inoue	Kyoto University
60	植物性食品タンパク質複合体の中性子小角散乱による構造解析	佐藤 信浩	京都大学	複合原子力科学研究所	SANS analysis of plant food protein complex structure	Nobuhiro Sato	Kyoto University
61	磁性準結晶中の隠れた磁気秩序の探索	佐藤 卓	東北大学	多元物質科学研究所	Hidden magnetic order in magnetic quasicrystals	Taku J Sato	Tohoku University
62	中性子小角散乱実験による Sr <sub>2</sub> RuO <sub>4</sub> の異常金属状態の研究	古川 はづき	お茶の水女子大学	基幹研究院 自然科学系	Anomalous vortex state in Sr <sub>2</sub> RuO <sub>4</sub> studied by SANS experiments	Hazuki Furukawa	Ochanomizu University

No.	課題名	氏名	所属		Title	Name	Organization
63	空間反転対称性の破れた超伝導体のヘリカル磁束格子の観測	古川 はづき	お茶の水女子大学	基幹研究院 自然科学系	Herical vortex phase on non-centrosymmetric superconductors	Hazuki Furukawa	Ochanomizu University
64	Fe 系超伝導体の磁束研究	古川 はづき	お茶の水女子大学	基幹研究院 自然科学系	Vortex study on Fe-based superconductors	Hazuki Furukawa	Ochanomizu University
65	(Ce,Nd)CoIn <sub>5</sub> のスピン密度波と超伝導の関係	古川 はづき	お茶の水女子大学	基幹研究院 自然科学系	Spin Density Wave and Superconductivity on (Ce,Nd)CoIn <sub>5</sub>	Hazuki Furukawa	Ochanomizu University
66	強磁性超伝導体における自発的磁束格子構造の研究	古川 はづき	お茶の水女子大学	基幹研究院 自然科学系	Spontaneous vortex phase in ferromagnetic superconductors	Hazuki Furukawa	Ochanomizu University
67	トポロジカル超伝導体の磁束格子	古川 はづき	お茶の水女子大学	基幹研究院 自然科学系	Vortex phase in topological superconductors	Hazuki Furukawa	Ochanomizu University
68	歯車状両親媒性分子からなるナノキューブの溶液中での構造解析	守島 健	京都大学	複合原子力科学研究所	Structural research of nano cube formed by gear-like molecule	Ken Morishima	Kyoto University
69	分子混雑環境下のタンパク質、生体膜構造の研究	平井 光博	群馬大学	理工学府	Structural study of protein and biomembrane in molecular crowding environment	Mitsuhiro Hirai	Gunma University
70	時計蛋白質 Kai システムにおける要素蛋白質の動態解析	杉山 正明	京都大学	複合原子力科学研究所	Anayisis for Kinetics of Componet Proteins in Kai Clock Protein System	Masaaki Sugiyama	Kyoto University
71	全イオン性高分子ミセルのナノ構造と刺激応答	松岡 秀樹	京都大学	工学研究科高分子化学専攻	Nanostructure and Stimuli-responsivity of Tottaly Ionic Polymer Micelles	Hideki Matsuoka	Kyoto University
72	界面不活性の働きをする界面活性剤	貞包 浩一朗	同志社大学	生命医科学部医情報学科	Surfactant molecules behaving as surface-inactive agent	Koichiro Sadakane	Doshisha University
73	高圧条件下における 2 成分混合溶液の新奇な臨界挙動	貞包 浩一朗	同志社大学	生命医科学部医情報学科	Novel critical behavior in a mixture of water / organic solvent under high-pressure condition	Koichiro Sadakane	Doshisha University
74	コントラスト変調中性子小角散乱法によるポリビニルピロリドン保護金ナノクラスターの構造解析	遠藤 仁	高エネルギー加速器研究機構	物質構造科学研究所	Structure of Poly(N-vinyl-2-pyrrolidone)-supported Gold Nanoclusters Investigated by Means of Contrast Variation Small-Angle Neutron Scattering	Hitoshi Endo	High energy accelerator research organization
75	小角中性子散乱によるポリ(キノキサリン-2,3-ジイル)の温度依存性らせん反転の機構解明	長田 裕也	京都大学	工学研究科	Investigation of the Mechanism of the Temperature-Dependent Helix Inversion of Poly(quinoxaline-2,3-diy)s by Small-angle Neutron Scattering	Nagata Yuya	Kyoto University
76	イミダゾリウム系イオン液体中におけるエタノールクラスターの形成	高椋 利幸	佐賀大学	大学院工学系研究科	Formation of Ethanol Clusters in Imidazolium-based Ionic Liquids	Toshiyuki Takamuku	Saga University
77	中性子小角散乱によるマルチドメイン蛋白質の溶液構造解析	中川 洋	日本原子力研究開発機構	階層構造研究グループ	Analysisi of solution structure of multi-domain protein by SANS	Hiroshi Nakagawa	Japan Atomic Energy Agency
78	中性子小角散乱測定による構造材料中のナノ析出物の評価	間宮 広明	物質材料研究機構	先端材料解析研究拠点	Study on nano-precipitates in structural materials using small angle scattering technique	Hiroaki Mamiya	National Institute for Materials Science
79	中性子散乱法によるブロック共重合体の共連続ダブルワーク型相分離構造内における添加物の分布状態解析	山本 勝宏	名古屋工業大学	大学院工学研究科	Distribution of Additives in Ordered-Bicontinuous-Double-Network Structure Formed in Block Copolymer Systems Revealed by Small Angle Neutron Scattering	Katsuhiro Yamamoto	Nagoya Institute of Technology

No.	課題名	氏名	所属		Title	Name	Organization
80	金属貯蔵原子模倣 dendrimer の構造解析	Li Xiang	東京大学	物性研究所	Structure analysis of metal-storing atom-mimicking dendrimers	Xiang Li	The University of Tokyo
81	均一構造を持つ高分子ゲルにおける架橋点間相関の視覚化	Li Xiang	東京大学	物性研究所	Visualizing the correlation between branching point of homogeneous polymer gels	Xiang Li	The University of Tokyo
82	生体適合性ポリオリゴエチレングリコールメタクリレートゲルの微細構造変化の調査	呉羽 拓真	東京大学	物性研究所	Investigation of Changes in the Microscopic Structure of Poly(oligo ethylene glycol methacrylate)-based Hydrogels.	Takuma Kureha	The University of Tokyo
83	MnSi における変動電流下の磁気スキルミオンのダイナミクス	奥山 大輔	東北大学	多元物質科学研究所	Dynamics of magnetic skyrmion under alternative current in MnSi	Daisuke Okuyama	Tohoku University
84	SANS 測定による分子透過性ベシクルの Poly(propylene oxide) 層中の水和量の決定	西村 智貴	京都大学	工学研究科	Elucidating the degree of hydration of the poly (propylene oxide) block in carbohydrate-b-poly(propylene oxide) block-copolymer vesicle membranes by SANS measurements	Tomoki Nishimura	Kyoto University
85	完全に単分散な逆ミセルの構造可視化	藤井 翔太	北九州市立大学	環境技術研究所	Structural visualization of perfectly monodispersed reverse micelles	Shota Fujii	The University of Kitakyushu
・ 申請装置 C1-3: ULS							
86	ULS (高分解能後方散乱装置) IRT 課題	清水 裕彦	名古屋大学	大学院理学研究科	IRT project of ULS	Hirohiko Shimizu	Nagoya University
・ 申請装置 C1-3: mf-SANS							
87	mf-SANS (小型集束型小角散乱装置) IRT 課題	間宮 広明	物質材料研究機構	先端材料解析研究拠点	IRT project of mf-SANS	Hiroaki Mamiya	National Institute for Materials Science
・ 申請装置 C2-3-1: iNSE							
88	iNSE (中性子スピネコー分光器) IRT 課題	Li Xiang	東京大学	物性研究所中性子科学研究施設	IRT project of iNSE	Xiang Li	The University of Tokyo
89	リン脂質膜の粘弾性および単層膜間カップリングに対するアルカンの効果: 鎖長依存性	菱田 真史	筑波大学	数理物質系化学域	Effect of variety of alkanes on fluidity and inter-leaflet coupling of lipid membranes	Mafumi Hishida	Tsukuba University
90	界面不活性の働きをする界面活性剤	貞包 浩一朗	同志社大学	生命医科学部医情報学科	Surfactant molecules behaving as surface-inactive agent	Koichiro Sadakane	Doshisha University
91	マルチドメイン蛋白質の動的構造と機能発現との関係性の解析	中川 洋	日本原子力研究開発機構	階層構造研究グループ	Analysis of relationship between structural dynamics and function of multi-domain protein	Hiroshi Nakagawa	Japan Atomic Energy Agency
92	Mn <sub>1-x</sub> Fe <sub>x</sub> Si におけるスキルミオンのダイナミクス	左右田 稔	理化学研究所	創発物性科学研究センター	Slow Dynamics of Magnetic Skyrmion Mn <sub>1-x</sub> Fe <sub>x</sub> Si	Minoru Soda	RIKEN
93	磁気スキルミオン MnSi <sub>1-x</sub> Ge <sub>x</sub> におけるダイナミクス	左右田 稔	理化学研究所	創発物性科学研究センター	Dynamics of Magnetic Skyrmion MnSi <sub>1-x</sub> Ge <sub>x</sub>	Minoru Soda	RIKEN

No.	課題名	氏名	所属	Title	Name	Organization
・ 申請装置 C3-1-1: AGNES						
94	AGNES (高分解能パルス冷中性子分光器) IRT 課題	山室 修	東京大学	物性研究所	IRT project of AGNES	Osamu Yamamuro The University of Tokyo
95	PdPt 合金ナノ粒子中の水素の速いダイナミクス	山室 修	東京大学	物性研究所	Fast dynamics of hydrogen atoms in PdPt alloy nanoparticles	Osamu Yamamuro The University of Tokyo
96	PdPt 合金ナノ粒子中の水素の遅いダイナミクス	山室 修	東京大学	物性研究所	Fast dynamics of hydrogen atoms in PdPt alloy nanoparticles	Osamu Yamamuro The University of Tokyo
97	超高エントロピー液体・アルキル化テトラフェニルポルフィリンの遅い運動	山室 修	東京大学	物性研究所	Slow dynamics of super-high entropy liquids alkylated tetraphenylporphyrins	Osamu Yamamuro The University of Tokyo
・ 申請装置 C3-1-2: MINE1						
98	MINE1 (京大炉:多層膜中性子干渉計・反射率計) IRT 課題	日野 正裕	京都大学	複合原子力科学研究所	MINE1 (Multilayer neutron interferometer and reflectometer)	Masahiro Hino Kyoto University
・ 申請装置 C3-1-2: MINE2						
99	MINE2 (京大炉:多層膜中性子干渉計・反射率計) IRT 課題	日野 正裕	京都大学	複合原子力科学研究所	MINE2 (Multilayer neutron interferometer and reflectometer)	Masahiro Hino Kyoto University
100	高分子 / 水界面における生体分子の吸着状態の解析	松野 寿生	九州大学	大学院工学研究院 応用化学部門 (機能)	Analyses of adsorbed biomolecules at the polymer/water interface	Hisao Matsuno Kyushu University
101	混合液体中における高分子薄膜の膨潤挙動	田中 敬二	九州大学	大学院工学研究院 応用化学部門	Swelling Behavior of Polymer Thin Films in Mixed Non-solvents	Keiji Tanaka Kyushu University
・ 申請装置 T1-1: HQR						
102	HQR(高分解能中性子散乱装置)IRT 課題	大山 研司	茨城大学	理工学研究科	IRT project of HQR	Kenji Ohoyama Ibaraki University
103	時間分割中性子散乱測定による磁気構造変化過程の実時間追跡	元屋 清一郎	東京理科大学	理工学部 物理学科	Real-time observation of magnetic structural change by means of time-resolved neutron scattering	Kiyochiro Motoya Tokyo University of Science
104	Rb <sub>2</sub> MoO <sub>4</sub> における多形転移とソフトフォノン	重松 宏武	山口大学	教育学部	Polymorph Transition and Soft Phonon in Rb <sub>2</sub> MoO <sub>4</sub>	Hirotake Shigematsu Yamaguchi University
105	強誘電体の相転移機構 (変位型及び秩序-無秩序型) に関する統一的理解の確立	重松 宏武	山口大学	教育学部	Establishment of the unified explanation about the phase transition mechanism (displacive and order-disorder type) in Ferroelectrics	Hirotake Shigematsu Yamaguchi University
106	一軸応力による 2 等辺三角格子反強磁性体 CoNb <sub>2</sub> O <sub>6</sub> の磁区成長過程の制御	満田 節生	東京理科大学	理学部	Uniaxial-stress-control of domain growth kinetics in isosceles-triangular lattice Ising magnet CoNb <sub>2</sub> O <sub>6</sub>	Setsuo Mitsuda Tokyo University of Science

No.	課題名	氏名	所属	Title	Name	Organization
・ 申請装置 T1-2: AKANE						
107	AKANE (東北大金研: 三軸型中性子分光器) IRT 課題	藤田 全基	東北大学 金属材料研究所	IRT project of AKANE	Masaki Fujita	Tohoku University
108	Fe 置換により誘起される LSCO の異方的磁気秩序ピークの起源	藤田 全基	東北大学 金属材料研究所	Origin of isotropic magnetic peaks induced by Fe-substitution in LSCO	Masaki Fujita	Tohoku University
109	幾何学的フラストレート系 (Mn,Mg)Cr <sub>2</sub> O <sub>4</sub> におけるらせん磁気構造のクロスオーバー	高阪 勇輔	岡山大学 異分野基礎科学研究所	Crossover between conical and screw magnetic phase in (Mn,Mg)Cr <sub>2</sub> O <sub>4</sub>	Yusuke Kousaka	Okayama University
110	MPO <sub>4</sub> (M: 遷移金属) のカイラル磁気構造の検証	高阪 勇輔	岡山大学 異分野基礎科学研究所	Chiral Magnetism in New Chiral Magnetic Compounds MPO <sub>4</sub> (M: Transition Metal)	Yusuke Kousaka	Okayama University
111	CrX (Cr=Si, Ge) のカイラル磁気構造の検証	高阪 勇輔	岡山大学 異分野基礎科学研究所	Chiral Magnetic Structure in CrX (X=Si, Ge)	Yusuke Kousaka	Okayama University
112	鉄系超伝導体のスピン揺動	李 哲虎	産業技術総合研究所 省エネルギー研究部門	Spin fluctuations of iron-based superconductors	Chul-Ho Lee	National Institute of Advanced Industrial Science and Technology
・ 申請装置 T1-3 HERMES						
113	HERMES (東北大金研: 中性子粉末回折装置) IRT 課題	南部 雄亮	東北大学 金属材料研究所	IRT project of HERMES	Yusuke Nambu	Tohoku University
114	新奇量子カゴメ格子系 Yb <sub>3</sub> Ni <sub>11</sub> Ge <sub>4</sub> の短距離スピニ相関	佐藤 卓	東北大学 多元物質科学研究所	Short-range correlations in the new quantum kagome-lattice compound Yb <sub>3</sub> Ni <sub>11</sub> Ge <sub>4</sub>	Taku J Sato	Tohoku University
115	層状ペロブスカイト型酸化物の結晶構造とイオン拡散経路	八島 正知	東京工業大学 理学院	Crystal structure and ion-diffusion path of layered perovskite-type oxides	Masatomo Yashima	Tokyo Institute of Technology
116	Majumdar-Ghosh 系物質の中性子粉末回折	南部 雄亮	東北大学 金属材料研究所	Neutron powder diffraction on a Majumdar-Ghosh system	Yusuke Nambu	Tohoku University
117	希土類-遷移金属複合酸化物の磁気構造	土井 貴弘	北海道大学 大学院理学研究院	Magnetic structure of lanthanide-transition metal oxides	Yoshihiro Doi	Hokkaido University
118	量子スピンの三量体構造をもつ Na <sub>2</sub> Cu <sub>3</sub> Ge <sub>4</sub> O <sub>12</sub> の磁気構造	安井 幸夫	明治大学 理工学部	Magnetic Structure of S=1/2 linear trimer system Na <sub>2</sub> Cu <sub>3</sub> Ge <sub>4</sub> O <sub>12</sub>	Yukio Yasui	Meiji University
119	PdRu ナノ粒子の構造と触媒活性	山室 修	東京大学 物性研究所	Structure and catalytic activity of PdRu alloy nanoparticles	Osamu Yamamuro	The University of Tokyo
120	酸フッ化物アパタイトにおけるフッ素貯蔵挙動の解明	岡 研吾	中央大学 理工学部応用化学科	Investigation of the fluorine storage property of oxfluoride apatites	Kengo Oka	Chuo University
121	正方晶 Mn 化合物における過剰 Mn の結晶構造特性と磁気特性	岡田 宏成	東北学院大学 工学部	Structural and Magnetic properties of excess Mn in Tetragonal Mn Compound	Hironari Okada	Tohoku Gakuin University

No.	課題名	氏名	所属		Title	Name	Organization
122	近藤半金属におけるワイルフェルミオンの磁気状態	岩佐 和晃	茨城大学	フロンティア応用原子科学研究センター	Magnetic states of Weyl fermion in Kondo semimetals	Kazuaki Iwasa	Ibaraki University
123	熱電半導体 (Bi,Sb) <sub>2</sub> Te <sub>3</sub> 固溶体の酸化過程	栗栖 牧生	愛媛大学	理工学研究科(理学系)	Oxidation Process in (Bi,Sb) <sub>2</sub> Te <sub>3</sub> Pseud-binary Solid Solutions	Makio Kurisu	Ehime University
124	新規酸化物イオン伝導体の結晶構造解析とイオン伝導経路の解明	藤井 孝太郎	東京工業大学	理学院化学系	Crystal Structure Analysis and Investigation of Ion Diffusion Path of Novel Oxide-Ion Conductors	Kotaro Fujii	Tokyo Institute of Technology
125	T' 構造銅酸化物の超伝導発現と結晶構造の関係	藤田 全基	東北大学	金属材料研究所	Relation between superconducting mechanism and crystal structure in T' cuprate oxide	Masaki Fujita	Tohoku University
126	Co ダイマー磁性体における磁気秩序	那波 和宏	東北大学	多元物質科学研究科	Magnetic order of the Co dimer compound	Kazuhiro Nawa	Tohoku University
127	擬スピン 1/2 パイロクロア反強磁性体 Na <sub>3</sub> Co(CO <sub>3</sub> ) <sub>2</sub> Cl の磁気秩序	那波 和宏	東北大学	多元物質科学研究科	Magnetic order of the pseudo-spin-1/2 pyrochlore antiferromagnet Na <sub>3</sub> Co(CO <sub>3</sub> ) <sub>2</sub> Cl	Kazuhiro Nawa	Tohoku University
128	量子臨界点近傍にある YbCo <sub>2</sub> Zn <sub>20</sub> の置換系試料の結晶構造と磁気構造	阿曾 尚文	琉球大学	理学部物質地球科学科	Crystal and magnetic structures in doped systems of YbCo <sub>2</sub> Zn <sub>20</sub> in vicinity of a quantum critical point	Naofumi Aso	University of the Ryukyus
129	擬一次元梯子格子鉄系化合物の磁気構造解析	青山 拓也	東北大学	理学研究科物理学専攻	Magnetic structure analysis of quasi one-dimensional ladder lattice iron compound	Takuya Aoyama	Tohoku University
130	パイロクロア磁性体 Tb <sub>2</sub> M <sub>2</sub> O <sub>7</sub> (M = Zr, Hf, Pd, Pt) の結晶構造	高津 浩	京都大学	工学研究科	Structural investigation of pyrochlore oxides Tb <sub>2</sub> M <sub>2</sub> O <sub>7</sub> (M=Zr, Hf, Pd, Pt)	Hiroshi Takatsu	Kyoto University
131	新規カイラル磁性体 MPO <sub>4</sub> (M: 遷移金属) の磁気構造解析	高阪 勇輔	岡山大学	異分野基礎科学研究科	Magnetic structure analysis of new chiral magnetic compounds MPO <sub>4</sub> (M: transition metal)	Yusuke Kousaka	Okayama University
132	新規カイラル磁性体 CrX (X: Si, Ge) の磁気構造解析	高阪 勇輔	岡山大学	異分野基礎科学研究科	Magnetic structure analysis in new chiral magnetic compounds CrX (X: Si, Ge)	Yusuke Kousaka	Okayama University
133	EuFeAs <sub>2</sub> 超伝導体の磁気構造解析	荻野 拓	産業技術総合研究所	電子光技術研究部門	Investigation of magnetic structures of EuFeAs <sub>2</sub>	Hiraku Ogino	National Institute of Advanced Industrial Science and Technology
134	混合原子価クロム酸フッ化物ペロブスカイト化合物の磁気基底状態	辻本 吉廣	物質材料研究機構	機能性材料研究拠点	The magnetic ground state of chromium oxyfluoride perovskite with mixed valence states	Yoshihiro Tsujimoto	National Institute for Materials Science
135	歪んだ籠目格子遍歴磁性体 Yb <sub>3</sub> Ru <sub>4</sub> Al <sub>12</sub> の磁気構造	佐藤 卓	東北大学	多元物質科学研究科	Magnetic order in the 2D itinerant breathing kagome compound Yb <sub>3</sub> Ru <sub>4</sub> Al <sub>12</sub>	Taku J Sato	Tohoku University
136	Ga-Pd-Tb 2/1 近似結晶の磁気構造	佐藤 卓	東北大学	多元物質科学研究科	Neutron-diffraction study on antiferromagnetic structure in the Ga-Pd-Tb 2/1 quasicrystalline approximant	Taku J Sato	Tohoku University
・ 申請装置 T2-2: FONDER							
137	FONDER(中性子4軸回折装置)IRT 課題	木村 宏之	東北大学	多元物質科学研究科	IRT proposal for FONDER (Neutron 4-circle diffractometer)	Hiroyuki Kimura	Tohoku University

No.	課題名	氏名	所属		Title	Name	Organization
138	塑性歪みを加えた Pt <sub>3</sub> Fe 反強磁性体における強磁性の発現機構	小林 悟	岩手大学	理工学部	Mechanism of ferromagnetism in plastically deformed Pt <sub>3</sub> Fe antiferromagnet	Satoru Kobayashi	Iwate University
139	T' 構造 Pr <sub>1.40</sub> La <sub>0.60</sub> CuO <sub>4+y</sub> におけるスピン密度の空間分布	藤田 全基	東北大学	金属材料研究所	Spatial Spin Density Distribution in the T'-structured Pr <sub>1.40</sub> La <sub>0.60</sub> CuO <sub>4+y</sub>	Masaki Fujita	Tohoku University
140	typeIII 型反強磁性体 Pt-Mn における整合-非整合磁気相転移	高橋 美和子	筑波大学	数理物資系	Commensurate-Incommensurate Magnetic Phase Transition in Type-III Anti-ferromagnet Pt-Mn	Miwako Takahashi	Tsukuba University
・ 申請装置 Accessory							
141	アクセサリ- IRT 課題	上床 美也	東京大学	物性研究所	IRT project of Accessory	Yoshiya Uwatoko	The University of Tokyo

# 平成 30 年度 軌道放射物性研究施設 共同利用課題一覧 / Joint Research List of Synchrotron Radiation Researcher 2018

播磨分室 BL07LSU / Harima Branch BL07LSU

No.	課題名	氏名	所属		Title	Name	Organization
1	オペランド顕微光電子分光による全固体リチウムイオン電池の正極材料における Li 拡散・電子状態分布の観察	赤田 圭史	東京大学	物性研究所	Observation of Li diffusion and electronic-structure distribution in the cathode material of all-solid-state Li-ion battery by operando photoelectron spectromicroscopy	Keishi Akada	The University of Tokyo
2	単結晶マイクロワイヤー負極を用いたリチウムイオン電池におけるリチウム脱挿入のオペランド光電子分光測定	赤田 圭史	東京大学	物性研究所	Operando photoelectron spectroscopy of lithium intercalation on lithium-ion battery cell with single-particle microwire anode	Keishi Akada	The University of Tokyo
3	水系電解液を用いたオペランド軟 X 線発光分光によるリチウムイオン電池正極材料の電子状態の研究	朝倉 大輔	(国)産業技術総合研究所	省エネルギー研究部門	Electronic-structure analysis of Li-ion-battery cathode materials by operando soft x-ray emission spectroscopy with aqueous-solution based electrolyte	Daisuke Asakura	National Institute of Advanced Industrial Science and Technology
4	オペランド軟 X 線発光分光によるリチウムイオン電池電極材料の電子状態と酸化還元電位の相関の解明	朝倉 大輔	(国)産業技術総合研究所	省エネルギー研究部門	Electronic-structure analysis of Li-ion-battery cathode materials by operando soft x-ray emission spectroscopy with aqueous-solution based electrolyte	Daisuke Asakura	National Institute of Advanced Industrial Science and Technology
5	高分解能軟 X 線発光分光の励起エネルギー依存性から見る二次電池正極材料の酸化還元反応	大久保 将史	東京大学	工学系研究科	Redox reaction in cathode materials for rechargeable batteries studied by incident-energy dependent high-energy-resolution soft x-ray emission spectroscopy	Masashi Okubo	The University of Tokyo
6	高分解能軟 X 線発光分光によるナトリウムイオン電池正極材料の酸素レドックス反応の解明	大久保 将史	東京大学	工学系研究科	Clarification of the oxygen redox reaction in cathode materials for Na-ion batteries by high-energy-resolution soft x-ray emission spectroscopy	Masashi Okubo	The University of Tokyo
7	有機太陽電池における分離キャリアの再結合抑制機構の解明：時間分解軟 X 線光電子分光を用いた光励起状態の検証	小澤 健一	東京工業大学	大学院理工学研究科	Time-resolved soft X-ray photoelectron spectroscopy study of the charge carrier recombination process in organic photovoltaics	Kenichi Ozawa	Tokyo Institute of Technology
8	SiC トレンチ MOSFET の断面チャネル領域のナノ光電子分光解析	尾嶋 正治	東京大学	物性研究所	Nano photoelectron spectroscopy of sidewall channel region for SiC trench MOSFET	Masaharu Oshima	The University of Tokyo
9	斜入射共鳴軟 X 線散乱による電子-プロトン相関有機のヘテロ界面における水素結合状態の研究	加藤 浩之	大阪大学	大学院理学研究科	Study of an interface hydrogen-bond state of the electron-proton-correlated organic heterostructure	Hiroyuki Kato	Osaka University
10	雰囲気光電子分光による不均一触媒表面におけるメタン活性化のオペランド観測	小坂谷 貴典	分子科学研究所	物質分子科学研究領域	Operando observation of methane activation on heterogeneous catalysts by ambient-pressure XPS	Takanori Koitaya	Institute for Molecular Science
11	雰囲気光電子分光によるメタン活性化に対する金属-酸化物界面協奏効果の解明	小坂谷 貴典	分子科学研究所	物質分子科学研究領域	Synergetic effect at metal-oxide interface on methane activation measured by ambient-pressure XPS	Takanori Koitaya	Institute for Molecular Science
12	生体親和性ポリマーに含まれる中間水の状態評価	崔 藝涛	東京大学	物性研究所	Chemical state analysis of intermediate water bounded by biocompatible polymers	Yitao Cui	The University of Tokyo
13	Pd、および Pd を含むナノ粒子の水素吸蔵特性と粒子形状、試料温度、水素分圧依存性	坂田 修身	(国)物質・材料研究機構	National Institute	Shape, temperature, pressure dependent hydrogen-storage in Pd and Pd-based alloy nanoparticles	Osami Sakata	National Institute for Materials Science
14	X 線光電子分光による半導体・電解液界面におけるバンドアラインメントの究明	杉山 正和	東京大学	工学系研究科	Elucidation of Band Alignment at Semiconductor/Electrolyte Interface by X-ray Photoelectron Spectroscopy	Masakazu Sugiyama	The University of Tokyo
15	元素選択光電子ホログラフィーによる BaTiO <sub>3</sub> Pt(111)/Si 二次元準結晶の局所構造解析	大門 寛	奈良先端科学技術大学院大学	物質創成科学研究科	Local structure analysis of BaTiO <sub>3</sub> / Pt (111) / Si two-dimensional quasi-crystal by elemental selective photoelectron holography	Hiroshi Daimon	Nara Institute of Science and Technology

No.	課題名	氏名	所属		Title	Name	Organization
16	時間分解共鳴軟 X 線散乱によるスピン軌道液体 Ba <sub>3</sub> CuSb <sub>2</sub> O <sub>9</sub> の軌道揺らぎコヒーレントフォノンの可視化	田久保 耕	東京大学	物性研究所	Visualization of coherent phonons in a spin-orbital liquid Ba <sub>3</sub> CuSb <sub>2</sub> O <sub>9</sub> using time-resolved resonant soft x-ray scattering	Kou Takubo	The University of Tokyo
17	雰囲気 X 線光電子分光による Pd 系合金触媒表面 CO <sub>2</sub> 水素化反応過程の解明	唐 佳芸	兵庫県立大学	工学研究科	Ambient-pressure XPS studies of CO <sub>2</sub> hydrogenation on Pd-based bimetallic alloy catalysts	Jiayi Tang	University of Hyogo
18	軟 X 線分光を用いた無機粒子の液中プラズマ処理反応場のその場観察	寺嶋 和夫	東京大学	大学院新領域創成科学研究科	In-situ soft X-ray spectroscopy of plasma-induced reaction field in liquid, under modification of inorganic particles	Kazuo Terashima	The University of Tokyo
19	p+-WSe <sub>2</sub> /n-MoS <sub>2</sub> ヘテロ接合 TFET デバイス構造のオペランドポテンシャルイメージング	永村 直佳	(国)物質・材料研究機構	高エネルギー光解析グループ	Operando potential imaging of p+-WSe <sub>2</sub> /n-MoS <sub>2</sub> hetero junctions for TFET device structure	Naoka Nagamura	National Institute for Materials Science
20	サイト選択・時分割光電子ホログラフィーの確立とシリセン形成過程の観測	林 好一	名古屋工業大学	物理工学科	Development of site-selective and time-resolved photoelectron holography and its application to the structural observation of silicene formation	Kouichi Hayashi	Nagoya Institute of Technology
21	軟 X 線非弾性散乱、非弾性回折を用いた生体高分子や多糖、電解液における水の役割と水和水の電子状態の研究	原田 慈久	東京大学	物性研究所	Soft X-ray inelastic scattering and diffraction techniques applied for the study on the role of water and hydration in biopolymers, polysaccharides and electrolytes	Yoshihisa Harada	The University of Tokyo
22	時間分解軟 X 線吸収分光による Eu(Rh,Ir,Co) <sub>2</sub> Si <sub>2</sub> の光誘起価数転移の動的緩和現象の観測	平田 靖透	東京大学	物性研究所	Observation of dynamic relaxation phenomena related to photo-induced valence transition in Eu(Rh,Ir,Co) <sub>2</sub> Si <sub>2</sub> by means of time-resolved soft x-ray absorption spectroscopy	Yasuyuki Hirata	The University of Tokyo
23	3D nano-ESCA を用いた顕微 X 線分光の新展開 (II) 先進デバイス工学の援用による埋もれた界面の時空間ダイナミクスの観察	吹留 博一	東北大学	電気通信研究所	Novel development of soft x-ray spectromicroscopy using 3D nano-ESCA (II) Observation of spatio-temporal dynamics of buried interfaces with the aid of advanced device engineering	Hirokazu Fukidome	Tohoku University
24	波数分解共鳴非弾性軟 X 線散乱による VO <sub>2</sub> の金属絶縁体転移の発現機構解明	藤原 秀紀	大阪府立大学	理学系研究科	Revealing the mechanism of the metal-insulator transition in VO <sub>2</sub> probed by momentum resolved RIXS	Hidenori Fujiwara	Osaka Prefecture University
25	全固体リチウムイオン電池を用いたオペランド顕微光電子分光による電極材料の電子状態マッピング	細野 英司	(国)産業技術総合研究所	省エネルギー研究部門	Electronic-structure mapping of electrode materials by operando photoelectron spectromicroscopy using an all-solid-state Li-ion-battery	Eiji Hosono	National Institute of Advanced Industrial Science and Technology
26	全固体 Li イオン電池を用いたオペランド顕微光電子分光による遷移金属の価数変化マップ測定	細野 英司	(国)産業技術総合研究所	省エネルギー研究部門	Valence-change mapping of transition metals by operando photoelectron spectromicroscopy using an all-solid-state Li-ion-battery	Eiji Hosono	National Institute of Advanced Industrial Science and Technology
27	生体親和性高分子材料の機能発現に関わる水和水の電子状態観測	村上 大樹	九州大学	先導物質化学研究所	Observation of the electronic structure of hydrated water in biocompatible polymers.	Daiki Murakami	Kyushu University
28	生体親和性高分子中の中間水の性質解明に向けた軟 X 線吸収・発光分光解析	村上 大樹	九州大学	先導物質化学研究所	Soft X-ray absorption and emission spectroscopy of the intermediate water in biocompatible polymers.	Daiki Murakami	Kyushu University
29	共鳴非弾性軟 X 線散乱を用いたペロブスカイト Ni 酸化物の電荷秩序状態観測	山神 光平	東京大学	物性研究所	Charge order of perovskite Ni oxidation probed by resonant inelastic soft X-ray scattering	Kohei Yamagami	The University of Tokyo
30	共鳴非弾性軟 X 線散乱を用いた層状ペロブスカイト Mn 酸化物の電荷 / 軌道秩序観測	山神 光平	東京大学	物性研究所	Charge and orbital order of layered perovskite Mn oxidation probed by resonant inelastic soft X-ray scattering	Kohei Yamagami	The University of Tokyo
31	時分割コヒーレント軟 X 線回折イメージングによる超高速磁気ダイナミクス研究	山崎 裕一	(国)物質・材料研究機構	統合型材料開発・情報基盤部門	Ultra-fast magnetic dynamics revealed by time-resolved coherent soft x-ray diffraction imaging	Yuichi Yamasaki	National Institute for Materials Science
32	時間分解オペランド XPS の開発と光エネルギー変換過程実時間観測への展開	山本 達	東京大学	物性研究所	Development of time-resolved Operando XPS for the real time monitoring of light energy conversion processes	Susumu Yamamoto	The University of Tokyo

No.	課題名	氏名	所属		Title	Name	Organization
33	プラズモン増強サバティエ反応のオペランド軟X線分光観測	山本 達	東京大学	物性研究所	Plasmon-enhanced Sabatier reaction studied by Operando soft X-ray spectroscopies	Susumu Yamamoto	The University of Tokyo
34	軟X線吸収・発光分光によるルテニウム酸化物Ca <sub>2</sub> RuO <sub>4</sub> の電場誘起金属絶縁体転移の観測	吉田 鉄平	京都大学	大学院人間・環境学研究科	Observation of electric-field-induced metal-insulator transition in Ca <sub>2</sub> RuO <sub>4</sub> by soft x-ray absorption and emission spectroscopy	Tepei Yoshida	Kyoto University
35	ルテニウム酸化物Ca <sub>2</sub> RuO <sub>4</sub> の電場誘起金属絶縁体転移の空間分布観測	吉田 鉄平	京都大学	大学院人間・環境学研究科	Spatial distribution analysis of electric-field-induced metal-insulator transition in Ca <sub>2</sub> RuO <sub>4</sub> using 3D nano-ESCA	Tepei Yoshida	Kyoto University
36	単原子合金触媒Pd-Cu(111)におけるホルメート水素化反応の雰囲気XPSによるオペランド観察	吉信 淳	東京大学	大学院新領域創成科学研究科	Operando observation of hydrogenation of formate on a single atom alloy catalyst Pd-Cu(111) using AP-XPS	Jun Yoshinobu	The University of Tokyo
37	Ion-water interaction on the molecular level	Yin Zhong	ETH Zurich		Ion-water interaction on the molecular level	Yin Zhong	ETH Zurich
38	Investigation of Ferroelectric Photovoltaic Effect in BiFeO <sub>3</sub> (La,Sr)MnO <sub>3</sub> Heterostructures by Time-resolved X-ray Magnetic Circular Dichroism	Zhang Yujun	東京大学	物性研究所	Investigation of Ferroelectric Photovoltaic Effect in BiFeO <sub>3</sub> /(La,Sr)MnO <sub>3</sub> Heterostructures by Time-resolved X-ray Magnetic Circular Dichroism	Zhang Yujun	The University of Tokyo

柏キャンパス E 棟 / Laser and Synchrotron Research Laboratory in Kashiwa

No.	課題名	氏名	所属		Title	Name	Organization
1	遷移金属インターカレート 1T-TaSi <sub>2</sub> のスピン分解角度分解光電子分光	伊藤 孝寛	名古屋大学	シンクロトロン光科学研究センター	Spin-resolved angle-resolved photoemission study of transition metal intercalated 1T-TaSi <sub>2</sub>	Takahiro Ito	Nagoya University
2	層状 MAX 相化合物 V <sub>2</sub> AlC のスピン分解角度分解光電子分光	伊藤 孝寛	名古屋大学	シンクロトロン光科学研究センター	Spin- and angle-resolved photoemission study of layered MAX phase compound V <sub>2</sub> AlC	Takahiro Ito	Nagoya University
3	低対称性半導体基板上的 Bi 擬 1 次元構造におけるスピン偏極電子状態	大坪 嘉之	大阪大学	生命機能研究科	Spin-polarized electronic states on quasi-1D Bi fabricated on low-symmetric semiconductor substrates	Yoshiyuki Ohtsubo	Osaka University
4	半導体基板上的スピン分裂擬一次元表面状態におけるフェルミ準位調整	大坪 嘉之	大阪大学	生命機能研究科	Fermi-level tuning of quasi-1D spin-split surface states on semiconductor substrates	Yoshiyuki Ohtsubo	Osaka University
5	有機半導体分子の吸着に伴って生じるトポロジカル表面状態の変化	金井 要	東京理科大学	大学院理工学研究科	Modification of Topological surface states upon adsorption of organic semiconductors	Kaname Kanai	Tokyo University of Science
6	トポロジカル絶縁体の電子状態の解明	木村 昭夫	広島大学	大学院理学研究科	Electronic-structure study of topological insulators	Akio Kimura	Hiroshima University
7	銀の量子井戸状態の光電子分光	黒田 健太	東京大学	物性研究所	Controls of spin-orbit interband coupling in heavy atoms on quantum well states	Kenta Kuroda	The University of Tokyo
8	擬一次元 Bi ハライドの高次トポロジーに対応するヒンジ状態の研究	黒田 健太	東京大学	物性研究所	Hinge states of higher-order topology in quasi-1D bismuth halides	Kenta Kuroda	The University of Tokyo
9	トポロジカル絶縁体 - 強磁性体界面におけるスピン偏極電子状態の観測	小林 正起	東京大学	大学院工学系研究科	Observation of spin-polarized electronic state at an interface between topological insulator and ferromagnet	Masaki Kobayashi	The University of Tokyo

No.	課題名	氏名	所属		Title	Name	Organization
10	室温強磁性半導体 (Ga,Fe)Sb 量子井戸におけるスピンの偏極バンド構造の解明	小林 正起	東京大学	大学院工学系研究科	Elucidation of spin-polarized band structure in room-temperature ferromagnetic semiconductor (Ga,Fe)Sb quantum well	Masaki Kobayashi	The University of Tokyo
11	擬一次元新型トポロジカルスピンの分裂表面バンドの直接観測	近藤 猛	東京大学	物性研究所	Direct investigation of the spin-polarized topological surface state in a quasi-one dimensional material	Takeshi Kondo	The University of Tokyo
12	極性ワイル半金属 MoTe <sub>2</sub> におけるスピンの偏極したトポロジカル表面状態の観測	坂野 昌人	東京大学	大学院工学系研究科	Observation of spin-polarized topological surface state on polar Weyl semimetal MoTe <sub>2</sub>	Masato Sakano	The University of Tokyo
13	原子層タリウム単結晶のスピンの偏極電子バンド測定	坂本 一之	千葉大学	融合科学研究科	Investigation of the spin-polarized electronic band structure of atomic layer thallium single crystal	Kazuyuki Sakamoto	Chiba University
14	インジウム原子層超伝導体におけるラッシュバスピンの分裂の直接観察	坂本 一之	千葉大学	融合科学研究科	Direct observation of Rashba effect-induced spin splitting in an indium atomic-layer superconductor	Kazuyuki Sakamoto	Chiba University
15	Study of topological states in Fe-based superconductor	Peng Zhang	東京大学	物性研究所	Study of topological states in Fe-based superconductor	Peng Zhang	The University of Tokyo
16	グラフェンの光電子分光	矢治 光一郎	東京大学	物性研究所	Photoemission study of transferred graphene on Si(111)	Koichiro Yaji	The University of Tokyo
17	高分解能スピンの角度分解光電子分光によるハーフメタル強磁性体 CoS <sub>2</sub> の電子構造研究	横谷 尚睦	岡山大学	大学院自然科学研究科	Study on electronic structures in half-metallic ferromagnet CoS <sub>2</sub> by high-resolution spin- and angle-resolved photoemission spectroscopy	Takayoshi Yokoya	Okayama University
18	第二種 Weyl 半金属 WTe <sub>2</sub> の角度分解光電子分光による研究	万 宇軒	東京大学	大学院理学系研究科	Angle-resolved photoemission spectroscopy study of type-II semimetal WTe <sub>2</sub>	Yuxuan Wan	The University of Tokyo

平成 30 年度 スーパーコンピュータ 共同利用課題一覧 / Joint Research List of Supercomputer System 2018

No.	課題名	氏名	所属	Title	Name	Organization
1. 第一原理計算 / First-Principles Calculation of Materials Properties						
1	量子論による半導体界面形成機構と電子物性の解明	押山 淳	名古屋大学未来材料・システム研究所	Mechanisms of Semiconductor Interface Formation and its Electronic Properties based on Quantum Theory	Atsushi Oshiyama	Institute of Materials and Systems for Sustainability
2	高機能スピントロニクス材料物質の磁気・電子構造の解析	小田 竜樹	金沢大学理工研究域	Analyses on magnetic and electronic structures in high-performance spintronics materials	Tatsuki Oda	Kanazawa University
3	量子論による半導体界面形成機構と電子物性の解明	押山 淳	名古屋大学未来材料・システム研究所	Mechanisms of of Semiconductor Interface Formation and its Electronic Properties based on Quantum Theory	Atsushi Oshiyama	Institute of Materials and Systems for Sustainability
4	電極界面の機能物性	杉野 修	東京大学物性研究所	Functional property of electrodes	Osamu Sugino	The University of Tokyo
5	オーダー N 法を用いた MD/DFT 自己無撞着法による触媒反応設計	石塚 良介	大阪大学大学院基礎工学研究科	Seeking of catalytic reaction with the MD/order-N DFT self-consistent scheme	Ryosuke Ishizuka	Osaka University
6	高機能スピントロニクス材料物質の原子・磁気・電子構造の解析	小田 竜樹	金沢大学理工研究域	Analyses on atomic, magnetic, and electronic structures in high-performance spintronics materials	Tatsuki Oda	Kanazawa University
7	実空間差分法に基づく第一原理電子状態・輸送特性計算コード RSPACE の開発とシミュレーション	小野 倫也	筑波大学計算科学研究センター	Development of first-principles electronic-structure and transport calculation method based on real-space finite-difference approach	Tomoya Ono	University of Tsukuba
8	第一原理シミュレーション手法の開発と応用：構造探索から超伝導まで	常行 真司	東京大学大学院理学系研究科	Development and application of first-principles simulation methods: from structure prediction to superconductivity	Shinji Tsuneyuki	The University of Tokyo
9	トポロジカル熱電変換物質の第一原理的研究	石井 史之	金沢大学ナノマテリアル研究所	First-principles study of topological thermoelectric materials	Fumiyuki Ishii	Kanazawa University
10	自己無撞着 GW を用いた XPS 計算	野口 良史	静岡大学工学部	XPS simulation using self-consistent GW method	Yoshifumi Noguchi	Shizuoka University
11	非類似性を利用した自己組織化過程解析	重田 育照	筑波大学大学院数理物質科学研究科	Analyses on self-organization processes using dissimilarity sampling	Yasuteru Shigeta	University of Tsukuba
12	第一原理計算と流体力学の融合による窒化物半導体 MOVPE 成長のマルチフィジックスシミュレーション	白石 賢二	名古屋大学未来材料・システム研究所	Multiphysics Simulation of MOVPE Growth of Nitride Semiconductor Based on Unification of First Principles Calculations and Fluid Dynamics	Kenji Shiraishi	Nagoya University
13	レプリカ交換法と第一原理計算を基盤とした構造・物性予測フレームワークの開発	笠松 秀輔	東京大学物性研究所	Development of Structure/Property Prediction Framework Based on Replica Exchange Method Combined with Ab Initio Calculations	Shusuke Kasamatsu	The University of Tokyo
14	ナノデバイスに関連する諸特性の理論解析	渡邊 聡	東京大学大学院工学系研究科	Theoretical Analyses on Various Properties Concerning Nanodevices	Satoshi Watanabe	The University of Tokyo
15	ナノデバイスに関連する諸特性の理論解析	渡邊 聡	東京大学大学院工学系研究科	Theoretical Analyses on Various Properties Concerning Nanodevices	Satoshi Watanabe	The University of Tokyo

No.	課題名	氏名	所属	Title	Name	Organization
16	第一原理計算でせまる超伝導体における電荷・スピン揺らぎの定量的競合	明石 遼介	東京大学大学院理学系研究科	First-principles quantitative approach to the interplay of charge and spin fluctuations in superconductors	Ryosuke Akashi	The University of Tokyo
17	電場下の金属 / 固体界面における金属原子のイオン化・拡散の研究：半導体・有機固体基板への展開	中山 隆史	千葉大学理学部物理学科	First-principles study of ionization and diffusion of metal atoms at metal/solid interfaces in electric fields: toward semiconductor and organic substrates	Takashi Nakayama	Chiba University
18	新規二次電池材料に関する第一原理計算	山田 淳夫	東京大学工学系研究科	First-principles investigations of battery materials	Atsuo Yamada	The University of Tokyo
19	太陽光エネルギー変換における基礎過程の研究と材料設計指針獲得のための大規模第一原理計算	山下 晃一	東京大学大学院工学系研究科	Large scale ab initio calculations on the fundamental processes of solar energy convergence devices and on designing principles for new materials	Koichi Yamashita	The University of Tokyo
20	トポロジカル物質の第一原理電子状態計算	山内 邦彦	大阪大学産業科学研究所	First-Principles DFT Calculations for Topological Matter	Kunihiko Yamauchi	Osaka University
21	スピン変換物質の第一原理的研究	石井 史之	金沢大学ナノマテリアル研究所	First-principles study of spin conversion materials	Fumiyuki Ishii	Kanazawa University
22	ルチル型 TiO <sub>2</sub> (110) 表面上での酸素吸着反応における欠陥濃度依存性	泰岡 顕治	慶應義塾大学理工学部機械工学科	The Effect of Defect Density on O <sub>2</sub> Absorption Reactions on Rutile TiO <sub>2</sub> (110) Surfaces	Kenji Yasuoka	Keio University
23	ギ酸分解触媒及び酸素吸蔵材料の省貴金属化	國貞 雄治	北海道大学大学院工学研究院	Reduction of Rare Metals in Formic Acid Decomposition Catalysts and Oxygen Storage Materials	Yuji Kunisada	Hokkaido University
24	強磁性 f-d 金属間化合物の微視的電子状態第一原理計算と中間スケール磁区構造実験データの統合解析	松本 宗久	東京大学物性研究所	Integration of ab initio data of microscopic electronic structure and experimental data of mesoscopic domain structure for ferromagnetic f-d intermetallics	Munehisa Matsumoto	The University of Tokyo
25	ナノ構造の励起電子・陽電子・原子動力学と光学応答の第一原理計算	渡辺 一之	東京理科大学理学部	First-Principles Study of Excited Electron, Positron and Atom Dynamics and Optical Responses of Nanostructures	Kazuyuki Watanabe	Tokyo University of Science
26	超並列電子状態計算とデータ駆動科学の融合による大規模デバイス材料研究	星 健夫	鳥取大学大学院工学研究科	Large-scale device-material research by massively parallel electronic structure calculation and data-driven science	Takeo Hoshi	Tottori University
27	ナノ構造の励起電子・陽電子・原子動力学と光学応答の第一原理計算	渡辺 一之	東京理科大学理学部	First-Principles Study of Excited Electron, Positron and Atom Dynamics and Optical Responses of Nanostructures	Kazuyuki Watanabe	Tokyo University of Science
28	電池・触媒界面物性に関する第一原理 "サンプリング" 研究	館山 佳尚	物質・材料研究機構	DFT sampling studies on interfacial properties of batteries and catalysts	Yoshitaka Tateyama	National Institute for Materials Science
29	ファン・デル・ワールズ密度汎関数を用いた金属表面への分子吸着の研究	濱田 幾太郎	大阪大学工学研究科	van der Waals density functional study of molecular adsorption on metal surfaces	Ikutaro Hamada	Osaka University
30	表面 Bi ナノ構造の Rashba 効果	合田 義弘	東京工業大学物質理工学院材料系	Rashba effects in surface-Bi nanostructures	Yoshihiro Gohda	Tokyo Institute of Technology
31	ナノ構造の量子伝導の第一原理計算	小林 伸彦	筑波大学 数理物質系	First-principles study of quantum transport in nanostructures	Nobuhiko Kobayashi	University of Tsukuba
32	高圧力下における共有結合性液体・ガラスの構造と電子状態の第一原理計算	下條 冬樹	熊本大学大学院自然科学研究科	First-Principles Molecular-Dynamics Study of Structural and Electronic Properties of Covalent Liquids and Glass under Pressure	Fuyuki Shimojo	Kumamoto University

No.	課題名	氏名	所属	Title	Name	Organization
33	酸化物表面の Lewis 酸塩基中和による吸着分子の Brønsted 酸性発現機構の解明	山口 周	東京大学大学院工学系研究科	Bronsted Acidity on Oxide Surface Induced by Neutralization of Lewis Acid Sites by Molecules	Shu Yamaguchi	The University of Tokyo
34	高性能フッ素ポリマーエレクトレットの開発	鈴木 雄二	東京大学大学院工学系研究科	Development of High-performance Polymer Electret	Yuji Suzuki	The University of Tokyo
35	Nd-Fe-B 磁石の副相探索及び界面の大規模第一原理計算	立津 慶幸	名桜大学	First-principles calculations of a search for subphases and large-scale calculations for the grain boundaries of Nd-Fe-B magnets	Yasutomi Tatetsu	Meio University
36	第一原理計算によるトリチウム透過防止用金属酸化物中の水素同位体マイクロ挙動に関する研究	毛 偉	工学系研究科総合研究機構	First-principles calculation of microscopic behaviors of hydrogen in metal oxides for tritium permeation barrier	Wei Mao	The University of Tokyo
37	ギ酸分解触媒及び酸素吸蔵材料の省貴金属化	國貞 雄治	北海道大学大学院工学研究院	Reduction of Rare Metals in Formic Acid Decomposition Catalysts and Oxygen Storage Materials	Yuji Kunisada	Hokkaido University
38	ワイドギャップ半導体におけるミュオン及び陽電子実験に関わる第一原理計算	斎藤 峯雄	金沢大学理工研究域数物科学系	First-principles calculation for muon and positron experiments of wide gap semiconductors	Mineo Saito	Kanazawa University
39	第一原理メタダイナミクス計算による CARE 加工プロセスの解明 - エッチングにより形成される表面粗さの検討 -	稲垣 耕司	大阪大学大学院工学研究科	First-principles meta-dynamics analysis of Catalyst Referred Etching method -Analysis of surface roughness formed by etching-	Kouji Inagaki	Osaka University
40	第一原理計算を用いたクラスレート化合物の熱電特性解析	大西 正人	東京大学機械工学専攻	Analysis of Thermoelectric Properties of Clathrate Compounds with Ab Initio Calculations	Masato Ohnishi	The University of Tokyo
41	新しい構造探索法の開発と新機能性物質の探索	下司 雅章	大阪大学ナノサイエンスデザイン教育研究センター	Development of new structural search method and search for new functional materials	Masaaki Geshi	Osaka University
42	第一原理計算によるナノ物質の構造・機能の解明と予測	武次 徹也	北海道大学大学院理学研究院	Ab initio study on the structure and functions of nanomaterials	Tetsuya Taketsugu	Hokkaido University
43	アモルファス磁性体および永久磁石内アモルファス相界面に対する第一原理計算およびグラフ解析手法の開発	寺澤 麻子	東京工業大学	First principles calculations and development of graph analysis method for magnetic alloys and amorphous grain boundary phases in permanent magnets	Asako Terasawa	Tokyo Institute of Technology
44	電場中での担持金属触媒表面状態の評価	関根 泰	早稲田大学先進理工学研究所	Elucidation of the surface of supported metal catalyst in an electric field	Yasushi Sekine	Waseda University
45	第一原理分子動力学法に基づくガラスの静的構造に関する研究	高良 明英	熊本大学学生支援部	Ab initio molecular dynamics study of static structure of glasses	Akihide Koura	Kumamoto University
46	分子動力学計算による生体高分子複合体の自由エネルギー計算	館野 賢	兵庫県立大学大学院生命理学研究科	Molecular dynamics free energy calculations of functional mechanisms of biological macromolecular complex systems	Masaru Tateno	University of Hyogo
47	第一原理計算による有機強誘電体・圧電体の物性予測	石橋 章司	産業技術総合研究所	Prediction of properties of organic ferroelectrics and piezoelectrics by first-principles calculation	Shoji Ishibashi	National Institute of Advanced Industrial Science and Technology
48	トポロジカル解析と系の秩序パラメータ	赤木 和人	東北大学材料科学高等研究所	Topological Analysis and Order Parameter of the System	Kazuto Akagi	Tohoku University
49	燃料電池電極触媒及び水素透過膜の省貴金属化	坂口 紀史	北海道大学大学院工学研究院	Reduction of Rare Metals in Fuel Cell Catalysts and Hydrogen Permeable Membrane	Norihito Sakaguchi	Hokkaido University

No.	課題名	氏名	所属	Title	Name	Organization
50	ワイドギャップ半導体におけるミュオン及び陽電子実験に関わる第一原理計算	斎藤 峯雄	金沢大学理工研究域	First-principles calculation for muon and positron experiments of wide gap semiconductors	Mineo Saito	Kanazawa University
51	マテリアルズインフォマティクスを用いた新材料開発	山下 智樹	国立研究開発法人物質・材料研究機構	Developments of new materials using materials informatics	Tomoki Yamashita	National Institute for Materials Science
52	原子吸着 Si 表面系の原子構造・電子状態	服部 賢	奈良先端科学技術大学院大学物質創成科学研究科	Atomic structure and electronic states for Si surfaces with adsorbates	Ken Hattori	Nara Institute of Science and Technology
53	絶縁体非線形光吸収の第一原理計算	篠原 康	東京大学工学系研究科	First-principles calculations for nonlinear light absorption of insulators	Yasushi Shinohara	The University of Tokyo
54	第一原理計算を用いた環境発電・エネルギー貯蔵デバイス材料の理論設計	舩田 浩義	大阪大学産業科学研究所	Theoretical design of energy harvesting and storage device materials by first-principles calculations	Hiroyoshi Momida	Osaka University
55	ルチル型 TiO <sub>2</sub> (110) 表面における温度由来の欠陥安定性に関する研究	泰岡 顕治	慶應義塾大学理工学部	Study on the Temperature Induced Stability of Defects on Rutile TiO <sub>2</sub> (110) Surfaces	Kenji Yasuoka	Keio University
56	機能性材料界面の原子構造および特性発現機構の解明	幾原 雄一	東京大学大学院工学系研究科	Atomic structure and properties of functional materials	Yuichi Ikuhara	The University of Tokyo
57	第四次革新的手法を用いた産業応用酵素および創薬標的タンパク質の理論的研究	常盤 広明	立教大学理学部	Theoretical Study of Industrial Enzyme and Drug Target Protein using the Fourth Revolution	Hiroaki Tokiwa	Rikkyo University
58	高性能フッ素ポリマーエレクトレットの開発	鈴木 雄二	東京大学大学院工学系研究科	Development of High-performance Polymer Electret	Yuji Suzuki	The University of Tokyo
59	浸透圧調整物質の水中での相互作用に関する第一原理分子動力学計算	大戸 達彦	大阪大学大学院基礎工学研究科	Interaction between osmolytes in water revealed by ab initio molecular dynamics simulation	Tatsuhiko Ohto	Osaka University
60	第一原理熱力学・統計力学手法を用いた不均一触媒反応課程の研究	森川 良忠	大阪大学 大学院工学研究科	First-principles Thermodynamics and Statistical Mechanics Simulations of Catalytic Reactions at Solid Surfaces	Yoshitada Morikawa	Osaka University
61	ゲルマニウム二次元結晶に関する第一原理計算	洗平 昌晃	名古屋大学未来材料・システム研究所	First-principles study on two-dimensional crystals of germanium	Masaaki Araidai	Nagoya University
62	純水による SiC 単結晶の触媒表面基準エッチングのメカニズム解明	ブイ ヴァンフォー	大阪大学大学院工学研究科	Study on removal mechanism in catalyst referred etching of single crystalline SiC with pure water	Vanpho Bui	Osaka University
63	GaN 中の欠陥に起因した振動モード変調の研究	小田 将人	和歌山大学システム工学部	Modulation of phonon modes originate from impurities in GaN	Masato Oda	Wakayama University
64	深海熱水噴出孔における持続的な化学反応過程の第一原理分子動力学シミュレーション	島村 孝平	神戸大学大学院システム情報学研究科	Ab initio molecular dynamics simulation of sustained chemical reaction processes in deep-sea hydrothermal vents	Kohei Shimamura	Kobe University
65	超分子自己組織化膜 / 水界面の第一原理分子動力学シミュレーション	大戸 達彦	大阪大学大学院基礎工学研究科	First-principles molecular dynamics simulation of the interface between water and a supramolecular self-assembled monolayer	Tatsuhiko Ohto	Osaka University
66	Fe/Pd(001)2 層膜の磁気特性に Pd 層の量子井戸状態が与える影響に関する研究	佐藤 徹哉	慶應義塾大学理工学部	Magnetic properties of Fe/Pd(001) bilayer affected by quantum-well states in Pd layer	Tetsuya Sato	Keio University

No.	課題名	氏名	所属	Title	Name	Organization
67	軽元素含有による超高圧環境下の液体鉄合金の輸送特性変化: 第一原理分子動力学シミュレーション	大村 訓史	広島工業大学工学部	Effects of light elements on transport properties of liquid Fe alloy under ultrahigh pressure condition : ab initio molecular-dynamics simulations	Satoshi Ohmura	Hiroshima Institute of Technology
68	ナノグラフェンに現れる動的効果の理論解析	草部 浩一	大阪大学大学院基礎工学研究科	Theoretical analysis of dynamical effects of nanographene	Koichi Kusakabe	Osaka University
69	高効率な原子層水分解光触媒の理論的探索 II	鈴木 達夫	東京都立産業技術高等専門学校	Theoretical search for high-efficient monolayer water-splitting photocatalysts II	Tatsuo Suzuki	Tokyo Metropolitan College of Industrial Technology
70	エキシトニック絶縁体 Ta <sub>2</sub> NiSe <sub>5</sub> に対する第一原理低エネルギー有効模型導出	中村 和磨	九州工業大学	Ab initio derivation of effective low-energy model for excitonic insulator Ta <sub>2</sub> NiSe <sub>5</sub>	Kazuma Nakamura	Kyushu Institute of Technology
71	ドーピンググラフェン・水界面の第一原理分子動力学シミュレーション	大戸 達彦	大阪大学大学院基礎工学研究科	Ab initio molecular dynamics simulation of doped-graphene/ water interfaces	Tatsuhiko Ohto	Osaka University
72	第一原理による機能性材料の原子構造および電子状態の解明	幾原 雄一	東京大学大学院工学系研究科	Ab initio study on atomic and electronic structure of functional materials	Yuichi Ikuhara	The University of Tokyo
73	実空間差分法に基づく第一原理電子状態・輸送特性計算コード RSPACE の開発とシミュレーション	小野 倫也	筑波大学計算科学研究センター	Development of first-principles electronic-structure and transport calculation method based on real-space finite-difference approach	Tomoya Ono	University of Tsukuba
74	時間に依存した電子輸送計算手法の開発と原子層状物質への応用	江上 喜幸	北海道大学大学院工学研究院	Development of a time-dependent electron-transport simulator and its application to atomic-layered materials	Yoshiyuki Egami	Hokkaido University
75	純水による SiC 単結晶の触媒表面基準エッチングのメカニズム解明	ブイ ヴァンフォー	大阪大学大学院工学研究科	Study on removal mechanism in catalyst referred etching of single crystalline SiC with pure water	Vanpho Bui	Osaka University
76	第一原理計算によるモデルリアル触媒上の表面反応の探求	水上 渉	九州大学総合理工学研究院	Exploration of surface reactions on model real catalyst	Wataru Mizukami	Kyushu University
77	第一原理計算によるグラフェンの電子特性の解明	藤本 義隆	東京工業大学大学院理工学研究科	First-principles study of electronic properties of graphene layers	Yoshitaka Fujimoto	Tokyo Institute of Technology
78	第一原理計算による有限温度下での有機半導体のバンド計算	柳澤 将	琉球大学理学部	First-principles band structure calculation of organic crystals at finite-temperature	Susumu Yanagisawa	University of the Ryukyus
79	van der Waals 密度汎関数法による有機-金属界面電子状態の理論的解明	濱本 雄治	大阪大学 大学院工学研究科	van der Waals density functional study of organic-metal interfaces	Yuji Hamamoto	Osaka University
80	第一原理多体摂動計算ソフトウェア RESPACK の整備	中村 和磨	九州工業大学	Development of ab initio many-body perturbation calculation software RESPACK	Kazuma Nakamura	Kyushu Institute of Technology
81	時間に依存した電子輸送計算手法の開発と原子層状物質への応用	江上 喜幸	北海道大学大学院工学研究院	Development of a time-dependent electron-transport simulator and its application to atomic-layered materials	Yoshiyuki Egami	Hokkaido University
82	スピン依存ファン・デル・ワールズ密度汎関数法による磁性分子複合体・結晶・界面系の構造解析と電子相関効果の調査	小幡 正雄	金沢大学理工研究域	Analysis on atomic structure in magnetic molecular complex, crystal and interface using spin dependent van der Waals density functional and investigation of electron correlation effect	Masao Obata	Kanazawa University
83	磁性分子複合体・結晶・界面系の原子・磁気構造の解析と電子相関効果の調査	小幡 正雄	金沢大学理工研究域	Analysis on atomic and magnetic structure in magnetic molecular complex, crystal and interface and investigation of electron correlation effect	Masao Obata	Kanazawa University

No.	課題名	氏名	所属	Title	Name	Organization
84	半導体表面界面における構造的素励起の物性の研究	影島 博之	島根大学大学院自然科学研究科	Study on physical properties of structural elementary excitations of semiconductor surfaces and interfaces	Hiroyuki Kageshima	Shimane University
85	燃料電池活性サイトおよび光触媒の密度汎関数法による第一原理計算	西館 数芽	岩手大学理工学部	Density functional calculations of the catalytic site of fuel cell and photocatalyst	Kazume Nishidate	IWATE University
86	第一原理メタヒューリスティクス法によるナノ炭素機能設計	鶴田 健二	岡山大学大学院自然科学研究科	Ab-initio Metaheuristics for Functional Design of Nanocarbon	Kenji Tsuruta	Okayama University
87	遷移金属ジカルコゲナイドにおけるスピン-バレー分極と異常量子ホール伝導	ハシュミ アルカム	筑波大学計算科学研究センター	Spin-valley polarization & quantum anomalous Hall conductivity in Transition metal dichalcogenides	Arqum Hashmi	University of Tsukuba
88	第一原理計算による高温水中の多価アルコールの反応過程の研究	佐々木 岳彦	東京大学大学院新領域創成科学研究科	Reaction processes of polyalcohols in high temperature water by First Principles Calculations	Takehiko Sasaki	The University of Tokyo
89	Sb系テラヘルツトランジスタのための歪バンド構造設計	藤代 博記	東京理科大学	Strained Band-Structure Engineering for Antimonide-Based Terahertz Transistors	Hiroki Fujishiro	Tokyo University of Science
90	照射損傷と格子間原子との相互作用の研究	大澤 一人	九州大学応用力学研究所	Study of interaction between radiation damage and interstitial atom	Kazuhito Ohsawa	Kyushu University
91	量子井戸状態を用いたバンドエンジニアリングによる表面・界面スピン物性の開拓と制御	櫻木 俊輔	東京大学物性研究所	Development and control of surface and interface spin texture by band engineering using quantum-well state	Shunsuke Sakuragi	The University of Tokyo
92	第一原理分子動力学計算による有機分子膜の金属基板上での構造の探索	柳澤 将	琉球大学理学部	Search for adsorption geometry of an organic molecular layer on a metal surface with the first-principles molecular dynamics	Susumu Yanagisawa	University of the Ryukyus
93	プロトン伝導性固体電解質のイオン電導機構解析	大友 順一郎	東京大学大学院新領域創成科学研究科	Analysis of ion conduction in materials of proton-conducting solid electrolyte	Junichiro Otomo	The University of Tokyo
94	希土類磁石材料混晶の安定性と磁気特性	赤井 久純	東京大学物性研究所	Stability and magnetic properties of rare earth mixed crystal magnet materials	Hisazumi Akai	The University of Tokyo
95	高精度な第一原理手法に基づくモデルパラメータの決定方法の研究	榎原 寛史	鳥取大学大学院工学研究科	Development of the determination technique of model parameters based on the accurate ab-initio quantum simulation	Hirofumi Sakakibara	Tottori University
96	凝集誘起発光についての理論的研究	山本 典史	千葉工業大学	Theoretical Study on the Aggregation-Induced Emission	Norifumi Yamamoto	Chiba Institute of Technology
97	Yb <sub>2</sub> O <sub>3</sub> 完全結晶の電子構造に関する研究	牧野 哲征	福井大学大学院工学研究科	Study on electronic structures in Yb <sub>2</sub> O <sub>3</sub> crystals	Takayuki Makino	University of Fukui
98	d0 強磁性体および固体表面における陽電子状態の第一原理計算	萩原 聡	国立研究開発法人量子科学技術研究開発機構	First-principles study on positron states in d0 ferromagnetics and at solid surfaces	Satoshi Hagiwara	The National Institutes for Quantum and Radiological Science and Technology
99	第一原理分子動力学計算を用いたセミクラスレートハイドレートの振動スペクトル計算	平塚 将起	工学院大学機械工学科	Ab initio molecular dynamics study on the vibrational spectra of semi-clathrate hydrates	Masaki Hiratsuka	Kogakuin University
100	数値モデルを用いたアモルファス磁性体および永久磁石内アモルファス相界面の第一原理計算および解析	寺澤 麻子	東京工業大学	First principles calculations and mathematical analyses of amorphous magnetic alloys and amorphous grain boundary phases in permanent magnets	Asako Terasawa	Tokyo Institute of Technology

No.	課題名	氏名	所属	Title	Name	Organization
101	BCN系およびMX2系新規二次元物質およびナノチューブの生成機構と電子状態に関する研究	島田 敏宏	北海道大学大学院工学研究院	Formation mechanism and electronic structures of novel two dimensional materials and nanotubes - BCN and MX2 systems	Toshihiro Shimada	Hokkaido University
102	四重極型配置の局在スピンス系による電気磁気効果の理論的解明	豊田 雅之	東京工業大学理学院物理学系	Theoretical Study on Magnetoelectric Effects of Localized Spin Systems in Quadrupole Alignment	Masayuki Toyoda	Tokyo Institute of Technology
103	電子でバイスのための自己組織化ナノインターフェイスの理論	レービガー ハンネス	横浜国立大学大学院工学研究院	Theory of self-organized nano-structures for electronic devices	Hannes Raebiger	Yokohama National University
104	ケイ酸塩物質における圧力誘起構造変化の分子動力学解析	三澤 賢明	九州産業大学理工学部	Molecular dynamics study on pressure-induced transformation of silicates	Masaaki Misawa	Kyushu Sangyo University
105	触媒インフォマティクスに向けた酸化物の表面物性計算	日沼 洋陽	千葉大学先進科学センター	Calculation of oxide surface properties for catalyst informatics	Yoyo Hinuma	Chiba University
106	ケージド化合物の水溶液中における電子状態の解明	樋山 みやび	群馬大学	Elucidation of electronic states for caged compounds in aqueous solution	Miyabi Hiyama	Gunma University
107	固体表面上での小分子活性化、および素反応データベースの構築	蒲池 高志	福岡工業大学	Database construction for activation and reaction of small molecules on solid surfaces	Takashi Kamachi	Fukuoka Institute of Technology
108	電界下におけるナノスケール炭素物質の物性解明	岡田 晋	筑波大学大学院数理物質科学研究科	Physical properties of nanoscale carbon materials under an external electric field	Susumu Okada	University of Tsukuba
109	第一原理計算を用いた TABA セミクラスレートハイドレートの相平衡条件の計算	平塚 将起	工学院大学機械工学科	Ab initio calculations to determine the phase equilibrium conditions of TBAB semicathrate hydrates	Masaki Hiratsuka	Kogakuin University
110	固体表面・界面、微粒子の新規電子物性の探索と実現	稲岡 毅	琉球大学理学部	Search and realization of novel electronic properties of solid surfaces and interfaces and of small particles	Takeshi Inaoka	University of the Ryukyus
111	第一原理計算に基づくマグネシウム合金の欠陥場の解析	松中 大介	信州大学工学部	First-principles Study of Defects of Magnesium Alloys	Matsunaka Daisuke	Shinshu University
112	第一原理的アプローチによる電子状態と超伝導	池田 浩章	立命館大学理工学部	Electronic structure and superconductivity based on a first-principles approach	Hiroaki Ikeda	Ritsumeikan University
113	硫化鉛ナノ構造の化学ドーピング効果	首藤 健一	横浜国立大学・工学部	Chemical doping of nano-structured PbS	Ken-Ichi Shudo	Yokohama National University
114	触媒インフォマティクス構築に向けた固体触媒の電子状態計算	鳥屋尾 隆	北海道大学 触媒科学研究所	Calculation of catalyst electronic structures for catalyst informatics	Takashi Toyao	Hokkaido university
115	第一原理的アプローチの発展と超伝導の解析	池田 浩章	立命館大学理工学部	Development of the first-principles approach and analysis of superconductivity	Hiroaki Ikeda	Ritsumeikan University
116	Yb <sub>2</sub> O <sub>3</sub> 完全結晶の光学遷移と状態密度に関する研究	牧野 哲征	福井大学大学院工学研究科	Study on optical transition and density of states in Yb <sub>2</sub> O <sub>3</sub>	Takayuki Makino	University of Fukui
117	プロトン伝導体を用いた触媒表面反応の理論解析	大友 順一郎	東京大学大学院新領域創成科学研究科	Theoretical analysis of catalytic surface reaction with proton conductors	Junichiro Otomo	The University of Tokyo

No.	課題名	氏名	所属	Title	Name	Organization
118	ナノ粒子の表面緩和および溶媒効果に関する研究	横 哲	東北大学材料科学高等研究所	Structural study on surface reconstruction and solvent effects of nanoparticles	Akira Yoko	Tohoku University
119	第一原理計算による Fe 系形状記憶合金および Mg 合金における長周期積層欠陥構造の形成メカニズムの解明	圓谷 貴夫	熊本大学大学院先導機構	First-principles study on the formation mechanism of long-period stacking ordered structure in Fe based shape memory alloys and Mg alloys	Takao Tsumuraya	Kumamoto University
120	新たなナノスケール表面界面の電子物性の研究	小林 功佳	お茶の水女子大学理学部	Study on electronic properties in new nanoscale surfaces and interfaces	Katsuyoshi Kobayashi	Ochanomizu University
121	希土類磁石材料混晶の安定性と磁気特性	赤井 久純	東京大学物性研究所	Stability and magnetic properties of rare earth mixed crystal magnet materials	Hisazumi Akai	The University of Tokyo
122	原子層のコヒーレントフォノン分光	ヌグラハ アフ マド リドワン トレスナ	東北大学理学研究科	Coherent phonon spectroscopy of atomic layer materials	Ahmad Ridwan Tresna Nugraha	Tohoku University
123	層状ペロブスカイトにおける強誘電ドメイン構造の第一原理計算	北中 佑樹	東京大学	First-principles calculations for ferroelectric domain structure of layer-structured perovskites	Yuuki Kitanaka	The University of Tokyo
124	第一原理計算によるナノ粒子・ナノクラスターの構造に関する研究	横 哲	東北大学材料科学高等研究所	Structural study for nanoparticle/nanocluster using first-principles calculation	Akira Yoko	Tohoku University
125	金属・合金表面上で進行する酸化・還元過程の原子レベル反応シミュレーション	笠井 秀明	国立明石工業高等専門学校	Atomic-scale Simulation for Redox Processes on Metal/Alloy Surfaces	Hideaki Kasai	National Institute of Technology, Akashi College
126	Sternheimer-GW による層状物質のバンドギャップ推定	太田 優一	東京都立産業技術研究センター	Estimation of band gap for layered materials by Sternheimer-GW	Yuichi Ota	Tokyo Metropolitan Industrial Technology Research Institute
127	長波長の光を吸収する光合成色素設計のための励起状態データベースの作成	小松 勇	自然科学研究機構アストロバイオリロジーセンター	Constructing the database of excited states for designing photosynthetic pigments to absorb the longer wavelength radiation	Yu Komatsu	National Institutes of Natural Sciences AstroBiology Center
128	半導体デバイス中のキャリアダイナミクスとそのデバイス特性に関する研究	村口 正和	北海道科学大学	Study on carrier dynamics in semiconductor devices and their device characteristics	Masakazu Muraguchi	Hokkaido University of Science
129	表面超構造および薄膜のバンド計算	秋山 了太	東京大学理学系研究科	Band calculations of surface superstructures and thin films	Ryota Akiyama	The University of Tokyo
130	金属 Cr のスピン密度波状態に対する格子歪み効果の解析	小田 洋平	福島工業高等専門学校	Analysis of lattice strain effect on spin-density wave state in metallic chromium	Yohei Kota	Fukushima College
131	メタン活性触媒の理論デザイン	中西 寛	明石工業高等専門学校	Rational Design of Catalysts for Methane Activation	Hiroshi Nakanishi	National Institute of Technology, Akashi College
2. 強相関 / Strongly Correlated Quantum Systems						
132	負のフント結合をもつ多軌道系における超伝導と量子スピン液体	三澤 貴宏	東京大学物性研究所	Superconductivity and quantum spin liquid in multi-orbital systems with inverted Hund's rule coupling	Takahiro Misawa	The University of Tokyo
133	強相関電子系における分数励起の数値的研究	山地 洋平	東京大学大学院工学系研究科	Numerical studies on fractional excitations in strongly correlated electron systems	Youhei Yamaji	The University of Tokyo

No.	課題名	氏名	所属	Title	Name	Organization
134	テンソルネットワーク変分モンテカルロ法を用いた銅酸化物高温超伝導体の有効ハミルトニアンの高精度解析	今田 正俊	東京大学工学系研究科	Highly accurate analysis of an effective Hamiltonian for high Tc cuprates by the many-variable variational Monte Carlo method combined with tensor network	Masatoshi Imada	The University of Tokyo
135	スピン軌道結合物質が示す新規量子現象の数値的研究	求 幸年	東京大学大学院工学系研究科	Numerical study on novel quantum phenomena in spin-orbit coupled materials	Yukitoshi Motome	The University of Tokyo
136	強相関系の外場下応答とトポロジカル現象	川上 則雄	京都大学大学院理学研究科	Study of response to external fields and topological phenomena in strongly correlated quantum systems	Norio Kawakami	Kyoto University
137	多バンド系における第一原理計算とモデル計算による電子相関と超伝導に関する研究	黒木 和彦	大阪大学	First principles and model study of electron correlation and superconductivity in multiband systems	Kazuhiko Kuroki	Osaka University
138	スピン軌道結合物質が示す量子磁性の数値的研究	求 幸年	東京大学大学院工学系研究科	Numerical study on quantum magnetism in spin-orbit coupled materials	Yukitoshi Motome	The University of Tokyo
139	強相関系の磁性，トポロジカル相形成と外場下応答	川上 則雄	京都大学大学院理学研究科	Study of magnetism, topological phase formation, and response to external fields in strongly correlated quantum systems	Norio Kawakami	Kyoto University
140	二層型強相関電子系における非従来型超伝導に関する数値研究	黒木 和彦	大阪大学	Numerical study on unconventional superconductivity in bilayer strongly correlated systems	Kazuhiko Kuroki	Osaka University
141	二成分冷却フェルミ原子気体における Tan のコンタクトの高精度数値解析	大越 孝洋	東京大学大学院工学系研究科	Highly accurate numerical analysis of Tan's contact of two-component cold Fermi gases	Takahiro Ohgoe	The University of Tokyo
142	近藤格子模型において発現するスキルミオン結晶に対する磁気異方性の効果	速水 賢	北海道大学理学部	Effect of magnetic anisotropy on skyrmion crystal in the Kondo lattice model	Satoru Hayami	Hokkaido University
143	多軌道 TRILEX の実装と応用 ー弱相関側からのアプローチと強相関側からのアプローチをつなぐ新手法ー	野村 悠祐	東京大学大学院物理工学専攻	Implementation and application of multi-orbital TRILEX -a new method to bridge weak-coupling and strong coupling methods-	Yusuke Nomura	The University of Toyko
144	希土類系のマルチチャンネル近藤効果	堀田 貴嗣	首都大学東京理学研究科	Multi-channel Kondo Effect in Rare-Earth Systems	Takashi Hotta	Tokyo Metropolitan University
145	強相関電子系において現れる超伝導と軌道秩序との競合	古賀 昌久	東京工業大学	Competition between superconductivity and orbital order emerging in strongly correlated electron systems	Akihisa Koga	Tokyo Institute of Technology
146	第一原理計算と動的平均場理論による多バンド系の超伝導	大野 義章	新潟大学	First-principles calculation and dynamical mean-field theory for superconductivity in multi-band systems	Yoshiaki Ono	Niigata University
147	強相関電子系のフィリング制御による磁性相の安定性	古賀 昌久	東京工業大学	Stability of magnetic phases in strongly correlated electron systems with various electron filling	Akihisa Koga	Tokyo Institute of Technology
148	強相関トポロジカル系が創発する異常物性	吉田 恒也	筑波大学数理物質系	Anomalous phenomena induced for correlated topological systems	Tsuneya Yoshida	University of Tsukuba
149	キタエフスピン液体におけるマヨラナ粒子の磁場中ダイナミクス	求 幸年	東京大学大学院工学系研究科	Dynamics of Majorana particles in Kitaev spin liquids in a magnetic field	Yukitoshi Motome	The University of Tokyo
150	ハバードモデルにおける超伝導及び磁性状態の研究	山田 篤志	千葉大学理学研究科	Superconductivity and magnetic properties of the Hubbard model	Atsushi Yamada	Chiba University

No.	課題名	氏名	所属	Title	Name	Organization
151	強相関効果が創発する非エルミート物性	吉田 恒也	筑波大学数理物質系	Non-Hermitian properties induced by strong correlations	Tsuneya Yoshida	University of Tsukuba
152	強相関系における非従来型電子秩序の数値的研究	星野 晋太郎	埼玉大学	Numerical approach to unconventional electronic orderings in strongly correlated systems	Shintaro Hoshino	Saitama University
153	強相関遷移金属化合物の動的平均場近似計算	品岡 寛	埼玉大学理学部物理学科	Dynamical mean-field calculations of strongly correlated transition metal compounds	Hiroshi Shinaoka	Saitama University
154	横磁場イジングモデルにおけるランダムネスの効果	堀田 知佐	東京大学総合文化研究科	Study on the bond random transverse Ising model	Chisa Hotta	The University of Tokyo
155	機械学習と多変数変分波動関数を用いた相分類	本山 裕一	東京大学物性研究所	Drawing phase diagram from many-variable variational wave functions with machine learning	Yuichi Motoyama	The University of Tokyo
156	相関磁性体におけるオプトスピントロニクス	石原 純夫	東北大学大学院理学研究科	Opto-spintronics in correlated magnets	Sumio Ishihara	Tohoku University
157	多体分極と量子ダイナミクスの数値的研究	押川 正毅	東京大学物性研究所	Numerical study of many-body polarization and quantum dynamics	Masaki Oshikawa	The University of Tokyo
158	相互作用の強い系における複合量子ダイナミクス	石原 純夫	東北大学大学院理学研究科	Complexed quantum dynamics in strongly interacting systems	Sumio Ishihara	Tohoku University
159	Numerical study of d-wave superconductors in equilibrium	シャラレ サイヤッド	東京大学物性研究所	Numerical study of d-wave superconductors in equilibrium	Sharareh Sayyad	The University of Tokyo
160	ダイマー内電荷自由度がもたらす分子性導体の新奇現象	渡部 洋	早稲田大学高等研究所	Novel phenomena induced by intradimer charge degree of freedom in molecular conductors	Hiroshi Watanabe	Waseda Institute for Advanced Study
161	最適化量子変分モンテカルロ法による強相関電子系の研究	柳沢 孝	産業技術総合研究所	Optimization variational Monte Carlo study of strongly correlated electron systems	Takashi Yanagisawa	National Institute of Advanced Industrial Science and Technology
162	最適化モンテカルロ法および第一原理計算による強相関電子系の研究	柳沢 孝	産業技術総合研究所	Study of strongly correlated electron systems based on optimization Monte Carlo method and first-principles calculations	Takashi Yanagisawa	National Institute of Advanced Industrial Science and Technology
163	発散する状態密度をもつ系における近藤効果	野田 数人	独立行政法人 国立高等専門学校機構 香川高等専門学校	Kondo effects on a system with divergent density of states	Kazuto Noda	Kagawa Collage
164	有機ディラック電子系 $\alpha$ -(BEDT-TTF) <sub>2</sub> I <sub>3</sub> および $\alpha$ -(BETS) <sub>2</sub> I <sub>3</sub> の電子相関効果	小林 晃人	名古屋大学大学院理学研究科	Electron Correlation Effect in Organic Dirac Electron Systems $\alpha$ -(BEDT-TTF) <sub>2</sub> I <sub>3</sub> and $\alpha$ -(BETS) <sub>2</sub> I <sub>3</sub>	Akito Kobayashi	Nagoya University
3. 巨視系の協同現象 / Cooperative Phenomena in Complex, Macroscopic Systems						
165	機械学習ソルバーを用いたフラストレーションのある量子スピン系の研究	今田 正俊	東京大学工学系研究科	Study on frustrated quantum spin systems using machine-learning solvers	Masatoshi Imada	The University of Tokyo
166	テンソルネットワーク法による非磁性相の探求	川島 直輝	東京大学物性研究所	Tensornetwork Method and Its Application to Non-Magnetic States	Naoki Kawashima	The University of Tokyo

No.	課題名	氏名	所属	Title	Name	Organization
167	テンソルネットワーク法による非磁性相の探求	川島 直輝	東京大学物性研究所	Tensornetwork Method and Its Application to Non-Magnetic States	Naoki Kawashima	The University of Tokyo
168	高分子流体の非平衡ダイナミクスの解析	村島 隆浩	東北大学大学院理学研究科	Numerical analysis of non-equilibrium dynamics of polymeric liquid	Takahiro Murashima	Tohoku University
169	カルマン渦キャビテーションの分子動力学シミュレーション	浅野 優太	東京大学物性研究所	Molecular Dynamics Simulation of a Karman-Vortex Cavitation	Yuta Asano	The University of Tokyo
170	低エネルギーフェルミオン励起に基づく銅酸化物の擬ギャップ・超伝導機構の解明	今田 正俊	東京大学工学系研究科	Mechanism of pseudogap and superconductivity with low-energy fermionic excitations in high-Tc cuprates	Masatoshi Imada	The University of Tokyo
171	フラストレート磁性体における新奇秩序	川村 光	大阪大学理学研究科	Novel order in frustrated magnets	Hikaru Kawamura	Osaka University
172	全原子・粗視化分子動力学シミュレーションによるソフトマターの分子論的解析	篠田 渉	名古屋大学大学院工学研究科	Molecular basis analysis of Soft Materials using All-Atom and Coarse-Grained Molecular Dynamics Simulations	Wataru Shinoda	Nagoya University
173	Nonequilibrium investigation of high temperature superconductors	シャラレ サイヤッド	東京大学物性研究所	Nonequilibrium investigation of high temperature superconductors	Sharareh Sayyad	The University of Tokyo
174	生体膜の構造形成	野口 博司	東京大学物性研究所	Structure formation of biomembranes	Hiroshi Noguchi	The University of Tokyo
175	保存電荷描像に基づく古典・量子スピン液体の構造形成と磁気相関	宇田川 将文	学習院大学理学部	Gauge charge picture of spin liquids: Structure formation and magnetic correlation	Masafumi Udagawa	Gakushuin University
176	再生材料の機械・熱物性解明に向けた分子シミュレーション	塩見 淳一郎	東京大学工学系研究科	Understanding Mechanical and Thermal Properties of Sustainable Materials through Molecular Simulations	Junichiro Shiomi	The University of Tokyo
177	量子状態の動的外場による制御	宮下 精二	東京大学理学系研究科	Manipulation of quantum state by external fields	Seiji Miyashita	The University of Tokyo
178	ハイゼンベルグ模型の励起ダイナミクスの研究	正木 晶子	理化学研究所	Study of excitation dynamics of Heisenberg models	Akiko Masaki-Kato	RIKEN
179	分子動力学シミュレーションによるアミロイドベータペプチド全長のオリゴマー形成過程の研究	奥村 久士	分子科学研究所計算科学研究センター	Oligomerization process of full-length amyloid-beta peptides studied by molecular dynamics simulations	Hisashi Okumura	Institute for Molecular Science
180	ランダムなトポロジカル、非トポロジカル系のスケーリング理論	大槻 東巳	上智大学理工学部	Scaling theories of random topological and non topological systems	Tomi Ohtsuki	Sophia University
181	蛋白質物性に強く関与するソフトモードの効率的サンプリングシミュレーション	北尾 彰朗	東京工業大学生命理工学院	Efficient sampling simulation of the soft modes significantly contribute to protein properties	Akio Kitao	The University of Tokyo
182	スピントラップの量子相転移の数値的研究	坂井 徹	兵庫県立大学大学院物質理学研究科	Numerical Study on Quantum Phase Transitions of the Spin Tubes	Toru Sakai	University of Hyogo
183	ハニカム格子キタエフ物質における新規秩序の探索	大久保 毅	東京大学大学院理学系研究科	Novel phases in honeycomb lattice Kitaev materials	Tsuyoshi Okubo	The University of Tokyo

No.	課題名	氏名	所属	Title	Name	Organization
184	量子多体系におけるトポロジカルな秩序と量子ダイナミクス	藤堂 眞治	東京大学大学院理学系研究科	Topological Order and Quantum Dynamics in Quantum Many-body Systems	Synge Todo	The University of Tokyo
185	生体膜の構造形成	野口 博司	東京大学物性研究所	Structure formation of biomembranes	Hiroshi Noguchi	The University of Tokyo
186	微視的第一原理電子状態データと巨視的実験観測データ統合のための粗視化グリーン関数とReverse Monte Carloによる階層間架橋	松本 宗久	東京大学物性研究所	Bridging space-time scales via coarse grained Green's function and reverse Monte Carlo between microscopic electronic structure and macroscopic observation	Munehisa Matsumoto	The University of Tokyo
187	電子格子相互作用のあるハミルトニアンに対する機械学習ソルバーの開発	野村 悠祐	東京大学大学院物理工学専攻	Development of machine-learning solvers for Hamiltonians with electron-phonon interactions	Yusuke Nomura	The University of Toyko
188	ファインマン・ダイアグラム展開に基づく量子モンテカルロ法の開発と冷却フェルミ原子系の研究	大越 孝洋	東京大学大学院工学系研究科	Development of the diagrammatic Monte Carlo method and its application to cold Fermi gases	Takahiro Ohgoe	The University of Tokyo
189	動的密度行列繰り込み群法によるフラストレート量子スピン系のスピンドダイナミクスの研究	遠山 貴己	東京理科大学理学部	Dynamical DMRG study of spin dynamics in frustrated quantum spin systems	Takami Tohyama	Tokyo University of Science
190	蜂の巣格子磁性体 RuCl <sub>3</sub> の有効模型に対するラマンスペクトル	鈴木 隆史	兵庫県立大学大学院工学研究科	Raman spectra in the effective models for honeycomb-lattice magnet RuCl <sub>3</sub>	Takafumi Suzuki	University of Hyogo
191	マテリアルズ・インフォマティクスによる熱機能材料の探索	塩見 淳一郎	東京大学工学系研究科	Screening for Thermal Functional Materials using Materials Informatics	Junichiro Shiomi	The University of Tokyo
192	産業・医療応用のためのタンパク質の理論物性解析と分子設計	新井 宗仁	東京大学大学院総合文化研究科	Theoretical analysis and design of proteins for industrial and pharmaceutical applications	Munehito Arai	The University of Tokyo
193	非平衡系における相転移の数値的研究	原田 健自	京都大学大学院情報学研究科	Numerical study of phase transition in non-equilibrium systems	Kenji Harada	Kyoto University
194	動的スケーリング解析によるトポロジカル相転移の研究	尾関 之康	電気通信大学情報理工学研究科	Study on topological phase transitions by dynamical scaling analysis	Yukiyasu Ozeki	The University of Electro-Communications
195	数値的手法によるトポロジカル相とバルク・エッジ対応の研究	初貝 安弘	筑波大学大学院数理物質科学研究科	Numerical studies of topological phases and bulk-edge correspondence	Yasuhiro Hatsugai	University of Tsukuba
196	蜂の巣格子キタエフハイゼンベルク模型の磁場中動的性質	鈴木 隆史	兵庫県立大学大学院工学研究科	Dynamical properties of honeycomb-lattice Kitaev-Heisenberg models in magnetic fields	Takafumi Suzuki	University of Hyogo
197	キャビテーションの分子動力学シミュレーション	浅野 優太	東京大学物性研究所	A Molecular Dynamics Study of the Cavitation	Yuta Asano	The University of Tokyo
198	大規模粗視化分子動力学法による結晶性高分子の凝集プロセスと機械的特性	樋口 祐次	東京大学物性研究所	Assembly process and mechanical properties of crystalline polymers by large-scale coarse-grained molecular dynamics simulation	Yuji Higuchi	The University of Tokyo
199	フラストレート磁性体における新奇秩序	川村 光	大阪大学理学研究科	Novel order in frustrated magnets	Hikaru Kawamura	Osaka University
200	高分子材料の破壊と補強に関する粗視化 MD シミュレーション	萩田 克美	防衛大学校応用科学群	Coarse grained MD simulation for fracture and reinforcement of polymer materials	Katsumi Hagita	National Defense Academy

No.	課題名	氏名	所属	Title	Name	Organization
201	メタダイナミクス法を組み合わせた大規模分子動力学シミュレーションによるリン酸カルシウム結晶形成機構解析	灘 浩樹	産業技術総合研究所	Analysis of Formation Mechanism of Calcium Phosphate Crystal by Large-Scale Molecular Dynamics Simulation Combined with Metadynamics Method	Hiroki Nada	National Institute for Advanced Industrial Science and Technology
202	鉄カルコゲナイド超伝導体の圧力効果	Jeschke Harald	岡山大学異分野基礎科学研究所	Effects of pressure in iron chalcogenide superconductors	Harald Jeschke	Okayama University
203	粗視化スピン模型の構築と温度揺らぎのある保磁力解析	檜原 太一	東京大学理学系研究科	Construction of coarse-graining spin model and analysis of the coercivity	Taichi Hinokihara	The University of Tokyo
204	量子スピン液体の分数励起ダイナミクス	宇田川 将文	学習院大学理学部	Dynamics of fractional excitations in quantum spin liquid	Masafumi Udagawa	Gakushuin University
205	スピン・フラストレーション系における量子スピン液体の数値対角化による研究	坂井 徹	兵庫県立大学大学院物質理学研究科	Numerical Diagonalization Study on the Quantum Spin Liquid in Frustrated Spin Systems	Toru Sakai	University of Hyogo
206	拡張準古典方程式による渦糸フローホール効果の微視的計算	北 孝文	北海道大学理学部	Microscopic calculation of the flux-flow Hall effect based on the augmented quasiclassical equations	Takafumi Kita	Hokkaido University
207	動的スケーリング解析によるトポロジカル相転移の研究 II	尾関 之康	電気通信大学情報理工学研究所	Study on topological phase transitions by dynamical scaling analysis II	Yukiyasu Ozeki	The University of Electro-Communications
208	カイラル磁性の統計学的研究	福島 孝治	東京大学大学院総合文化研究科	Statistical-mechanical study for chiral magnets	Koji Hukushima	The University of Tokyo
209	量子スピン系の低エネルギー状態に関する数値的研究	中野 博生	兵庫県立大学大学院物質理学研究科	Numerical study on low-energy states of quantum spin systems	Hiroki Nakano	University of Hyogo
210	シェル・モデルを用いた強誘電体の分子動力学シミュレーション IV	橋本 保	産業技術総合研究所	Molecular dynamics simulation of ferroelectrics using a shell model IV	Tamotsu Hashimoto	National Institute of Advanced Industrial Science and Technology
211	データ駆動科学の物質科学への応用	福島 孝治	東京大学大学院総合文化研究科	Data-driven science for material science	Koji Hukushima	The University of Tokyo
212	量子スピン系の半古典ダイナミクスの研究	森 貴司	東京大学理学部物理学科	Semiclassical dynamics of quantum spin systems	Takashi Mori	The University of Tokyo
213	拡張アンサンブル法による複雑系の研究	岡本 祐幸	名古屋大学大学院理学研究科	Study on complex systems by generalized-ensemble algorithms	Yuko Okamoto	Nagoya University
214	フラストレートハニカム磁性体における多重 Q 秩序相	下川 統久朗	沖縄科学技術大学院大学	Multiple-Q states of the frustrated Heisenberg model on the honeycomb lattice	Tokuro Shimokawa	Okinawa Institute of Science and Technology Graduate University
215	フラストレートハニカム磁性体の多重 Q 秩序相	下川 統久朗	沖縄科学技術大学院大学	Multiple-Q states of the frustrated Heisenberg model on the honeycomb lattice	Tokuro Shimokawa	Okinawa Institute of Science and Technology Graduate University
216	スピンパイエルス系におけるランダムネスの効果	安田 千寿	琉球大学理学部	Randomness Effects on Spin-Peierls System	Chitoshi Yasuda	University of the Ryukyus
217	マニフォールドラーニングを用いたタンパク質-リガンド複合体の解離定数の定量計算	吉留 崇	東北大学大学院工学研究科	Quantitative computation of the dissociation rate of a protein-ligand complex using a manifold-learning technique	Takashi Yoshidome	Tohoku University

No.	課題名	氏名	所属	Title	Name	Organization
218	摩擦の物理	松川 宏	青山学院大学理工学部	Physics of Friction	Hiroshi Matsukawa	Aoyama Gakuin University
219	キャリア注入した二次元層状物質の電子構造及び超伝導の圧力依存性	Jeschke Harald	岡山大学異分野基礎科学研究所	Doping effect on electronic structure and superconductivity in two-dimensional layered materials	Harald Jeschke	Okayama University
220	メソポーラスシリカの界面との相互作用が水のダイナミクスに及ぼす影響	水口 朋子	京都工芸繊維大学	Effect of interface on the dynamics of water confined in mesoporous silica	Tomoko Mizuguchi	Kyoto Institute of Technology
221	相転移を起こす系における固有状態熱化仮説の数値的研究	伊與田 英輝	東京大学工学系研究科	Numerical study of eigenstate thermalization hypothesis in phase transition	Eiki Iyoda	The University of Tokyo
222	量子スピン系の低エネルギー状態に関する数値的研究	中野 博生	兵庫県立大学大学院物質物理学研究科	Numerical study on low-energy states of quantum spin systems	Hiroki Nakano	University of Hyogo
223	相平衡とポリアモルフィズム	瀧崎 員弘	愛媛大学理工学研究科	Phase equilibria and polyamorphism	Kazuhiro Fuchizaki	Ehime University
224	固体高次高調波における緩和効果の影響	篠原 康	東京大学工学系研究科	Relaxation effect on high-order harmonic generation from crystalline solids	Yasushi Shinohara	The University of Tokyo
225	電極と接して電気二重層を形成するイオン液体の構造化とダイナミクスの解析	福井 賢一	大阪大学大学院基礎工学研究科	Analysis on Structuring and Dynamics of Ionic Liquid Forming Electric Double Layer at Electrode Interfaces	Ken-Ichi Fukui	Osaka University
226	相平衡とポリアモルフィズム	瀧崎 員弘	愛媛大学理工学研究科	Phase equilibria and polyamorphism	Kazuhiro Fuchizaki	Ehime University
227	フラストレート量子スピン鎖の磁気励起とスピン伝導	大西 弘明	日本原子力研究開発機構 先端基礎研究センター	Magnetic excitation and spin transport in frustrated quantum spin chain	Hiroaki Onishi	Japan Atomic Energy Agency
228	Bose-Einstein 凝縮相における多体効果の解析	北 孝文	北海道大学理学部	Analysis of many-body effects in Bose-Einstein condensate	Takafumi Kita	Hokkaido University
229	フラストレート・ベクトルスピン模型におけるスピングラス転移	吉野 元	大阪大学サイバーメディアセンター	Spinglass transitions in frustrated vector spin models	Hajime Yoshino	Osaka University
230	乱流熱流動のRANS-LES ハイブリッド解析	森本 賢一	東京大学大学院工学系研究科	RANS-LES Hybrid Analysis of Turbulent Heat Transfer	Kenichi Morimoto	The University of Tokyo
231	機械学習を用いた複数種類入力による有効モデル推定手法の開発	田村 亮	国立研究開発法人 物質・材料研究機構	Development of effective model estimation method by machine learning for multiple input measured data	Ryo Tamura	National Institute for Materials Science
232	多波高木方程式の「キュービックアルゴリズム」による解法の研究	沖津 康平	東京大学 大学院工学系研究科	Study on 'cubic algorithm' for solving n-beam Takagi-Taupin equation	Kouhei Okitsu	The University of Tokyo
233	ゼオライト合成における相選択性の理論的、実験的検討	大久保 達也	東京大学大学院工学系研究科	Theoretical and experimental investigation on phase selectivity in zeolite syntheses	Tatsuya Okubo	The University of Tokyo
234	量子アニーリングの性能向上を目指した統計力学研究	田中 宗	早稲田大学 グリーン・コンピューティング・システム研究機構	Study on quantum annealing from a viewpoint of statistical mechanics	Shu Tanaka	Waseda University

No.	課題名	氏名	所属	Title	Name	Organization
235	量子モンテカルロ法を用いた1次元相互作用電子系の輸送特性評価	加藤 岳生	東京大学物性研究所	Transport properties of one-dimensional interacting electron systems by a quantum Monte Carlo method	Takeo Kato	The University of Tokyo
236	異方的形状細胞の込み合いによる集団運動転移の数値的研究	松下 勝義	大阪大学理学研究科	Numerical study of collective motion transition of crowding cells with anisotropic shape.	Katsuyoshi Matsushita	Osaka University
237	大規模分子動力学データの圧縮方法の検討	渡辺 宙志	東京大学物性研究所	Data compression for molecular dynamics simulation on the basis of multiresolution analysis	Hiroshi Watanabe	The University of Tokyo
238	コロイド分散系のダイナミクスに対するSchmidt数の影響	田中 肇	東京大学生産技術研究所	Schmidt number dependence on dynamics in colloidal suspensions	Hajime Tanaka	The University of Tokyo
239	ソフトマテリアルの秩序構造とその光学的性質の計算	福田 順一	九州大学大学院理学研究院	Calculation of ordered structures and their optical properties of soft materials	Jun-Ichi Fukuda	Kyushu University
240	荷電コロイド系の動的な構造形成	高江 恭平	東京大学生産技術研究所	Dynamics of structure formation in charged colloids	Kyohei Takae	The University of Tokyo
241	剛体球コロイド系の結晶核形成に対する流体力学的相互作用の影響	田中 肇	東京大学生産技術研究所	Hydrodynamic effects on crystal nucleation in a hard-sphere colloidal system	Hajime Tanaka	The University of Tokyo
242	地震の統計モデルの数値シミュレーション	川村 光	大阪大学理学研究科	Numerical simulations on statistical models of earthquakes	Hikaru Kawamura	Osaka University
243	テンソルネットワーク法による量子多体問題ソルバー開発	森田 悟史	東京大学物性研究所	Quantum many-body problem solver with tensor network methods	Satoshi Morita	The University of Tokyo
244	2次元古典Heisenberg反強磁性体のスピン伝導・熱伝導	青山 和司	大阪大学大学院理学研究科	Transport properties of the classical antiferromagnetic Heisenberg model in two dimension	Kazushi Aoyama	Osaka University
245	ペーストの流れと揺れの記憶の数値実験	中原 明生	日本大学理工学部	Numerical simulation for memory effect in paste of flow and vibration	Akio Nakahara	Nihon University
246	フェムト秒領域における電子・格子・光相互作用系の非断熱ダイナミクス	石田 邦夫	宇都宮大学大学院工学研究科	Ultrafast nonadiabatic dynamics of electron-phonon-photon system	Kunio Ishida	Utsunomiya University
247	シリカガラスの圧力誘起相転移過程における中間状態の圧縮挙動と不均質構造の研究	若林 大佑	高エネルギー加速器研究機構物質構造科学研究所	Compression behavior and inhomogeneous structure of silica glass in its intermediate state in structural transformations	Daisuke Wakabayashi	High Energy Accelerator Research Organization
248	高密度剛体球系における非平衡相転移と遅い緩和	磯部 雅晴	名古屋工業大学	Nonequilibrium phase transition and slow dynamics in the dense hard sphere systems	Masaharu Isobe	Nagoya Institute of Technology
249	空間構造をもつ一次元量子スピン系の数値的研究	利根川 孝	神戸大学大学院理学研究科	Numerical Study of the One-Dimensional Quantum Spin Systems with Spatial Structures	Takashi Tonegawa	Kobe University
250	有機電解液のナノ空間中挙動の解明	大場 友則	千葉大学大学院理学研究院	Organic Electrolyte Solution in Nanospaces	Tomonori Ohba	Chiba University
251	ソフトマテリアルの秩序構造とその光学的性質の計算	福田 順一	九州大学大学院理学研究院	Calculation of ordered structures and their optical properties of soft materials	Jun-Ichi Fukuda	Kyushu University

No.	課題名	氏名	所属	Title	Name	Organization
252	固有状態熱化仮説を用いた非平衡定常状態の解析	白井 達彦	東京大学物性研究所	Application of Eigenstate Thermalization Hypothesis to Non-equilibrium steady states	Tatsuhiko Shirai	The University of Tokyo
253	地震の統計モデルの数値シミュレーション	川村 光	大阪大学理学研究科	Numerical simulations on statistical models of earthquakes	Hikaru Kawamura	Osaka University
254	ナノ構造によるトポロジカル状態の実現と操作	苅宿 俊風	物材機構	Realization and Manipulation of Topological States by Nanostructures	Toshikaze Kariyado	NIMS
255	長波長の光を吸収する光合成色素設計のための励起状態データベースの作成	小松 勇	自然科学研究機構アストロバイオロジーセンター	Constructing the database of excited states for designing photosynthetic pigments to absorb the longer wavelength radiation	Yu Komatsu	National Institutes of Natural Sciences AstroBiology Center
256	フェーズフィールド法を用いたアメーバ細胞運動動態モデリング	斉藤 稔	東京大学理学系研究科	Phase field simulation for amoeboid cells	Nen Saito	The University of Tokyo
257	コロイド粒子系における大規模分子シミュレーション	寺尾 貴道	岐阜大学工学部	Molecular simulation of colloidal suspensions	Takamichi Terao	Gifu University
258	変形下における環状ゲルの環と軸分子の分子ダイナミクス解析	眞弓 皓一	東京大学大学院新領域創成科学研究科	Study on Dynamics of Ring and Axial Molecules of Slide-Ring Gel Under Deformation	Koichi Mayumi	The University of Tokyo
259	ハミルトニアン行列の低ランク行列近似を用いた全固有値計算と量子スピン系への応用	五十嵐 亮	東京大学情報基盤センター	Full diagonalization using low-rank approximation to Hamiltonian matrices and its application to quantum spin models	Ryo Igarashi	The University of Tokyo
260	機械ひずみを用いたナノ材料フォノン・電子輸送特性制御	塩見 淳一郎	東京大学工学系研究科	Control of phonon and electron transport properties using mechanical strain	Junichiro Shiomi	The University of Tokyo
261	フェムト秒領域における電子・格子・光相互作用系の非断熱ダイナミクス	石田 邦夫	宇都宮大学大学院工学研究科	Ultrafast nonadiabatic dynamics of electron-phonon-photon systems	Kunio Ishida	Utsunomiya University
262	ランダム媒質の光学特性値	町田 学	浜松医科大学フォトニクス医学研究部	Optical properties of random media	Manabu Machida	Hamamatsu University School of Medicine
263	三角格子 Heisenberg 反強磁性体における動的スピン相関の理論研究	青山 和司	大阪大学大学院理学研究科	Theoretical study of dynamical spin correlations in Heisenberg antiferromagnets on the triangular lattice	Kazushi Aoyama	Osaka University
264	強磁性超伝導における渦糸の数値的研究	常次 宏一	東京大学物性研究所	Numerical study of vortices in ferromagnetic superconductor	Hirokazu Tsunetsugu	The University of Tokyo
265	込み合い細胞組織運動の不安定性の数値解析	松下 勝義	大阪大学理学研究科	Numerical Analysis of Instability in Motion of Crowding Cellular Tissue	Katsuyoshi Matsushita	Osaka University
266	最大エントロピー法やスパースモデリングを用いた状態密度の推定	松田 康弘	東京大学物性研究所	Estimation of the density of states using Maximum entropy method and Sparse modeling	Yasuhiro Matsuda	Institute for Solid State Physics
267	コロイド粒子系における大規模分子シミュレーション	寺尾 貴道	岐阜大学工学部	Molecular simulation of colloidal suspensions	Takamichi Terao	Gifu University
268	空間構造をもつ一次元量子スピン系の数値的研究	利根川 孝	神戸大学大学院理学研究科	Numerical Study of the One-Dimensional Quantum Spin Systems with Spatial Structures	Takashi Tonegawa	Kobe University

No.	課題名	氏名	所属	Title	Name	Organization
269	二体自己無撞着法を用いた多層系銅酸化物の超伝導の理論的研究	西口 和孝	神戸大学大学院科学技術イノベーション研究科	Theoretical study for superconductivity in multilayer cuprates with two-particle self-consistent approach	Kazutaka Nishiguchi	Kobe University
270	カゴメ格子反強磁性体, および関連した系の諸問題の理論的研究	福元 好志	東京理科大学	Theoretical studies on kagome antiferromagnets and related systems	Fukumoto Yoshiyuki	Tokyo University of Science
271	1次元フラストレート量子スピン系の数値的研究	飛田 和男	埼玉大学大学院理工学研究科	Numerical Study of One Dimensional Frustrated Quantum Spin Systems	Kazuo Hida	Saitama University
272	フラストレート型遍歴磁性体における多重スピン密度波と磁気スキルミオンの理論	内田 尚志	北海道科学大学	Theory of multiple spin density waves and magnetic skyrmions in frustrated itinerant magnets	Takashi Uchida	Hokkaido University of Science
273	有機電解液のナノ空間中挙動の解明	大場 友則	千葉大学大学院理学研究院	Organic Electrolyte Solution in Nanospaces	Tomonori Ohba	Chiba University
274	モンテカルロ法によるスピンアイス系のエントロピー磁場角度変化のシミュレーション	橋高 俊一郎	東京大学物性研究所	Field-angle dependence of the entropy in the spin-ice system calculated by the Monte-Carlo method	Shunichiro Kittaka	The University of Tokyo
275	ペーストの流れの記憶の数値実験	中原 明生	日本大学理工学部	Numerical simulation for memory of flow in paste	Akio Nakahara	Nihon University
276	ナノ構造材料および界面の力学物性モデリング	米津 明生	中央大学理工学部	Mechanical modeling of nano structured materials and interfaces	Akio Yonezu	Chuo University
277	セブennaノゴールド	デニコラ アントニオ	山形大学工学部	7NANOGOLDS	Antonio De Nicola	Yamagata University
278	有向パーコレーション転移点近傍における界面の成長とゆらぎに関する数値的研究	平岩 徹也	東京大学大学院理学系研究科	Numerical simulation of interfacial growth and fluctuation near the directed percolation transition	Tetsuya Hiraiwa	The University of Tokyo
279	非平衡定常系に拡張された熱力学関数による構造形成の研究	中川 尚子	茨城大学理学部	Macroscopic properties characterized by an extended thermodynamic functions to nonequilibrium	Naoko Nakagawa	Ibaraki University
280	河川ネットワークの統計的性質	湯川 論	大阪大学大学院理学研究科	Statistical Properties of a River Network	Satoshi Yukawa	Osaka University
281	Kardar-Parisi-Zhang 界面の初期条件依存普遍性に関する数値的研究	竹内 一将	東京大学大学院理学系研究科	Numerical investigations of initial-condition-dependent universality of Kardar-Parisi-Zhang interfaces	Kazumasa Takeuchi	The University of Tokyo
282	バイナリーランダムネスのアンダーソン局在のフラクタル性	羽田野 直道	東京大学生産技術研究所	Fractality of the Anderson localization with binary randomness	Naomichi Hatano	The University of Tokyo
283	空気分子を含む水の結晶化機構に関する大規模分子動力学シミュレーション研究	灘 浩樹	産業技術総合研究所	Large-Scale Molecular Dynamics Simulation Study on the Crystallization Mechanism of Water Including Air Molecules	Hiroki Nada	National Institute for Advanced Industrial Science and Technology

平成 30 年度 スーパーコンピュータ 計算物質科学スパコン共用事業 課題一覧  
/ Supercomputing Consortium for Computational Materials Science Project List of Supercomputer System 2018

前期 / The first half term							
No.	課題名	氏名	所属		Title	Name	Organization
1	高機能半導体デバイス	押山 淳	名古屋大学	未来材料・システム研究所	Exploration of new-functionality and high-performance semiconductor devices	Atsushi Oshiyama	Nagoya University
2	電子の強相関と強い電子格子相互作用が生む創発物性	今田 正俊	東京大学	大学院工学系研究科	Emergent Phenomena from Combined Strong Electron Correlation and Electron-Phonon Coupling	Masatoshi Imada	The University of Tokyo
3	第一原理フェーズ・フィールド・マッピング	香山 正憲	産業技術総合研究所		First-Principles Phase Field Mapping	Masanori Kohyama	National Institute of Advanced Industrial Science and Technology
4	重点課題 5 「エネルギー変換 (化学エネルギー)」	杉野 修	東京大学	物性研究所	Priority project 5 -- energy conversion (chemical energy)	Osamu Sugino	The University of Tokyo
5	電解質液体の階層動力学と機能物性の分子動力学計算	芝 隼人	東北大学	金属材料研究所	Molecular dynamics simulation of the hierarchical dynamics and functional dynamics of electrolyte liquids	Hayato Shiba	Tohoku University
6	量子ドット系における多体相関効果をもたらすスピン緩和率変動に関する研究	吉見 一慶	東京大学	物性研究所	Study of many-body correlation effects on spin relaxation rate in quantum dots	Kazuyoshi Yoshimi	The University of Tokyo
7	トポロジカルディラック半金属におけるスピンホール磁化スイッチング	三澤 貴宏	東京大学	物性研究所	Spin Hall magnetization switching in topological Dirac semimetal	Takahiro Misawa	The University of Tokyo
8	ナノ界面高強度パルス光励起ダイナミクス	矢花 一浩	筑波大学	計算科学研究センター	Dynamics in nano-interface excited by high-intensity pulsed light	Kazuhiro Yabana	University of Tsukuba
9	テンソルネットワーク法の物性物理学への応用	川島 直輝	東京大学	物性研究所	Application of Tensor Network Methods to Condensed Matter Physics	Naoki Kawashima	The University of Tokyo
10	有機 / 無機界面の物性に関する計算	尾形 修司	名古屋工業大学	大学院工学研究科	Simulation of organic-inorganic interfaces	Shuji Ogata	Nagoya Institute of Technology
11	ポスト京課題 7 サブ課題 G ④大型実験施設との連携	遠山 貴巳	東京理科大学	理学部第一部	Cooperation Research with Big Experimental Facilities	Takami Tohyama	Tokyo University of Science
12	エネルギーの変換・貯蔵 — 電気エネルギー：全電池シミュレータの基盤技術の開発研究	岡崎 進	名古屋大学	大学院工学研究科	Conversion and storage of energy - Fuel cells and secondary batteries: Research and development of fundamental technologies of battery simulators.	Susumu Okazaki	Nagoya University
13	グリーン関数法とフラグメント分子軌道法に基づいた励起状態理論の開発	藤田 貴敏	分子科学研究所		Development of an excited-state theory based on many-body Green' s functions and fragment molecular orbital method	Takatoshi Fujita	Institute for Molecular Science
14	第一原理計算と多階層連結シミュレーションによるマテリアルデザイン	福島 鉄也	大阪大学	ナノサイエンスデザイン教育研究センター	First-principles materials design by multi-scale simulation	Tetsuya Fukushima	Osaka University

No.	課題名	氏名	所属		Title	Name	Organization
15	ナトリウム二次電池材料の電子論	小口 多美夫	大阪大学	産業科学研究所	Electron Theory on Sodium Secondary-Battery Materials	Tamio Oguchi	Osaka University
16	貴金属フリーの汎用元素ナノ触媒に向けた第一原理計算	武次 徹也	北海道大学	大学院理学研究院	Ab initio study on abundant nano-catalysts free from precious metals	Tetsuya Taketsugu	Hokkaido University
17	永久磁石材料開発	三宅 隆	産業技術総合研究所		Development of permanent magnet materials	Takashi Miyake	National Institute of Advanced Industrial Science and Technology
19	B、C、Nを用いた電子デバイス新物質の設計研究	斎藤 晋	東京工業大学	理学院	Materials design using B, C, and N for next-generation device	Susumu Saito	Tokyo Institute of Technology
20	磁性材料における界面磁気特性の第一原理計算	合田 義弘	東京工業大学	物質理工学院	First-principles calculations of interface magnetic properties at magnetic materials	Yoshihiro Gohda	Tokyo Institute of Technology
21	複雑混相流動のマルチスケールシミュレーション	川勝 年洋	東北大学	大学院理学研究科	Multiscale simulations on complex multiphase flows	Toshihiro Kawakatsu	Tohoku University
22	複雑流体の分子動力学計算	野口 博司	東京大学	物性研究所	Molecular Dynamics Simulation of Complex Fluids	Hiroshi Noguchi	The University of Tokyo
23	電極界面でのイオン輸送と脱溶媒和過程の分子シミュレーション	森田 明弘	東北大学	大学院理学研究科	Molecular simulation of ion transport and desolvation at electrode interface	Akihiro Morita	Tohoku University
24	経路積分分子動力学法を用いた含水鉱物結晶の計算 II	飯高 敏晃	理化学研究所		Computational study of hydrous minerals using the path integral molecular dynamics method II	Toshiaki Iitaka	RIKEN

後期 / The second half term

No.	課題名	氏名	所属		Title	Name	Organization
25	テンソルネットワークと機械学習を組み合わせた高精度量子格子模型ソルバーの超伝導機構解明への応用	今田 正俊	東京大学	大学院工学系研究科	Applications of highly accurate lattice model solvers with tensor network and machine learning for mechanisms of superconductivity	Masatoshi Imada	The University of Tokyo
26	第一原理フェーズ・フィールド・マッピング	香山 正憲	産業技術総合研究所		First-Principles Phase Field Mapping	Masanori Kohyama	National Institute of Advanced Industrial Science and Technology
27	普遍的ガラス性緩和の数値研究—分子性液体から電解質液体まで	芝 隼人	東北大学	金属材料研究所	Numerical simulations of universal features of slow glassy dynamics – from molecular liquids to electrolytes	Hayato Shiba	Tohoku University
28	量子ドット系における異方的空間ポテンシャルがもたらすスピン緩和率変動に関する研究	吉見 一慶	東京大学	物性研究所	Study of spatial anisotropy potential effects on spin relaxation rate in quantum dots	Kazuyoshi Yoshimi	The University of Tokyo
29	第一原理有効模型導出ソフトウェア RESPACK を用いた強相関量子系の解析	三澤 貴宏	東京大学	物性研究所	Study of correlated quantum many-body systems using RESPACK	Takahiro Misawa	The University of Tokyo
30	光・電子融合デバイス	矢花 一浩	筑波大学	計算科学研究センター	Unified Photonic-Electronic Devices	Kazuhiro Yabana	University of Tsukuba

No.	課題名	氏名	所属		Title	Name	Organization
31	テンソルネットワーク法の物性物理学への応用	川島 直輝	東京大学	物性研究所	Tensor Network Method and Its Application to Condensed Matter Physics	Naoki Kawashima	The University of Tokyo
32	エネルギーの変換・貯蔵 - 電気エネルギー：全電池シミュレータの基盤技術の開発研究	岡崎 進	名古屋大学	大学院工学研究科	Conversion and storage of energy - Fuel cells and secondary batteries : Research and development of fundamental technologies of battery simulators	Susumu Okazaki	Nagoya University
33	貴金属フリーの汎用元素ナノ触媒に向けた第一原理計算	武次 徹也	北海道大学	大学院理学研究院	Ab initio study toward abundant element nanocatalysts with less precious metals	Tetsuya Taketsugu	Hokkaido University
34	酸素レドックス反応を伴う電極材料の理論的設計	山田 淳夫	東京大学	大学院工学系研究科	Theoretical design of electrode materials with oxygen redox activity	Atsuo Yamada	The University of Tokyo
35	複雑流体の分子動力学計算	野口 博司	東京大学	物性研究所	Molecular Dynamics Simulation of Complex Fluids	Hiroshi Noguchi	The University of Tokyo
36	オーダー N 第一原理分子動力学法による珪酸塩融体の構造研究	飯高 敏晃	理化学研究所		Structure study of silicate melts using linear scaling ab initio molecular dynamics	Toshiaki Iitaka	RIKEN
37	超並列電子状態計算とデータ駆動科学の融合による大規模デバイス材料研究	星 健夫	鳥取大学大学院	工学研究科機械宇宙工学専攻応用数理工学講座	Large-scale device-material research by massively parallel electronic structure calculation and data-driven science	Takeo Hoshi	Tottori University



# Publications

## Division of Condensed Matter Science

### Takigawa group

We have been performing nuclear magnetic resonance experiments on various quantum spin systems and strongly correlated electron systems to explore novel quantum phases with exotic ordering and fluctuation phenomena. The major achievements in the year 2018 include: (1)  $^{31}\text{P}$ -NMR study on the  $J_1$ - $J_2$  frustrated square lattice antiferromagnet  $\text{RbMoOPO}_4\text{Cl}$  under high pressure, which revealed a first-order transition between low pressure columnar-type to high pressure Neel-type antiferromagnetic structures, (2) discovery of sequential electronic and structural transitions in the spin-orbit coupled metallic pyrochlore compound  $\text{Cd}_2\text{Re}_2\text{O}_7\text{Cd}_2$  by  $^{111}\text{Cd}$ -NMR measurements, which revealed breaking of inversion and cubic symmetries taking place at slightly different temperatures, (3)  $^{51}\text{V}$ -NMR investigation on the spin structure of a Neel-type skyrmion material  $\text{GaV}_4\text{Se}_8$  and first microscopic observation of the deformation of spin texture of the skyrmion lattice by oblique magnetic fields.

1. \*Inelastic Neutron Scattering Study of the Spin Dynamics in the Breathing Pyrochlore System  $\text{LiGa}_{0.95}\text{In}_{0.05}\text{Cr}_4\text{O}_8$ : Y. Tanaka, R. Wawrzynczak, M. D. Le, T. Guidi, Y. Okamoto, T. Yajima, Z. Hiroi, M. Takigawa and G. J. Nilsen, *J. Phys. Soc. Jpn.* **87** (2018) 073710.
2. †\*Field-enhanced quantum fluctuation in an  $S = 1/2$  frustrated square lattice: H. Yamaguchi, Y. Sasaki, T. Okubo, M. Yoshida, T. Kida, M. Hagiwara, Y. Kono, S. Kittaka, T. Sakakibara, M. Takigawa, Y. Iwasaki and Y. Hosokoshi, *Phys. Rev. B* **98** (2018) 094402 (1-6).
3. \*Universal geometric frustration in pyrochlores: B. A. Trump, S. M. Koohpayeh, K. J. T. Livi, J. -J. Wen, K. E. Arpino, Q. M. Ramasse, R. Brydson, M. Feygenson, H. Takeda, M. Takigawa, K. Kimura, S. Nakatsuji, C. L. Broholm and T. M. McQueen, *Nat. Commun.* **9** (2018) 2619 (1-10).

### Sakakibara group

We study magnetism and superconductivity of materials having low characteristic temperatures. These include heavy-electron systems, quantum spin systems and frustrated spin systems. The followings are some selected achievements in the fiscal year 2018. (1) We studied the superconducting gap symmetry of a candidate triplet superconductor  $\text{Sr}_2\text{RuO}_4$ . We found that the fourfold angular oscillation of the heat capacity under an in-plane rotating magnetic field does not change its sign even at very low temperature of  $0.04T_c$ . The results can be explained by Doppler-shifted quasiparticles around horizontal line nodes on the Fermi surface, in disagreement with the chiral p-wave scenario. (2) We developed a new technique for measuring the thermodynamic entropy as a function of the magnetic field angle. When the magnetic field is rotated under adiabatic conditions, the sample temperature changes owing to the field-angle variation of its entropy. By investigating this effect, the rotational magnetocaloric effect, the field-angle dependence of the entropy can be determined. (3) We developed an experimental method of low-temperature magnetization measurements with an in-situ two-axis alignment of the sample orientation. The sample alignment can be done within an accuracy of 0.02 deg. using a piezo-stepper-driven goniometer combined with a home-made tilting stage. This technique is useful to study magnetic phase transitions of strongly anisotropic systems.

1. Field-rotational Magnetocaloric Effect: A New Experimental Technique for Accurate Measurement of the Anisotropic Magnetic Entropy: S. Kittaka, S. Nakamura, H. Kadowaki, H. Takatsu and T. Sakakibara, *J. Phys. Soc. Jpn.* **87** (2018) 073601 (1-5).
2. Giant Hall Resistivity and Magnetoresistance in Cubic Chiral Antiferromagnet  $\text{EuPtSi}$ : M. Kakihana, D. Aoki, A. Nakamura, F. Honda, M. Nakashima, Y. Amako, S. Nakamura, T. Sakakibara, M. Hedo, T. Nakama and Y. Onuki, *J. Phys. Soc. Jpn.* **87** (2018) 023701 (1-4).
3. Low-Temperature Magnetization Measurements with Precise Two-Axis Alignment of the Sample Orientation: S. Nakamura, A. Kasahara, S. Kittaka, Y. Kono, Y. Onuki and T. Sakakibara, *J. Phys. Soc. Jpn.* **87** (2018) 1140018 (1-5).
4. †\*Magnetic-field-induced Quantum Phase in  $S = 1/2$  Frustrated Trellis Lattice: H. Yamaguchi, D. Yoshizawa, T. Kida, M. Hagiwara, A. Matsuo, Y. Kono, T. Sakakibara, Y. Tamekuni, H. Miyagai and Y. Hosokoshi, *J. Phys. Soc. Jpn.* **87** (2018) 043701 (1-5).

---

\* Joint research among groups within ISSP.

5. Searching for Gap Zeros in  $\text{Sr}_2\text{RuO}_4$  via Field-Angle-Dependent Specific-Heat Measurement: S. Kittaka, S. Nakamura, T. Sakakibara, N. Kikugawa, T. Terashima, S. Uji, D. A. Sokolov, A. P. Mackenzie, K. Irie, Y. Tsutsumi, K. Suzuki and K. Machida, *J. Phys. Soc. Jpn.* **87** (2018) 093703 (1-5).
6. \*Disorder-sensitive nodelike small gap in FeSe: Y. Sun, S. Kittaka, S. Nakamura, T. Sakakibara, P. Zhang, S. Shin, K. Irie, T. Nomoto, K. Machida, J. Chen and T. Tamegai, *Phys. Rev. B* **98** (2018) 064505 (1-7).
7. †\*Field-enhanced quantum fluctuation in an  $S = 1/2$  frustrated square lattice: H. Yamaguchi, Y. Sasaki, T. Okubo, M. Yoshida, T. Kida, M. Hagiwara, Y. Kono, S. Kittaka, T. Sakakibara, M. Takigawa, Y. Iwasaki and Y. Hosokoshi, *Phys. Rev. B* **98** (2018) 094402 (1-6).
8. †Field-induced quantum magnetism in the verdazyl-based charge-transfer salt [o-MePy-V-(p-Br)<sub>2</sub>FeCl<sub>4</sub>]: Y. Iwasaki, T. Kida, M. Hagiwara, T. Kawakami, Y. Kono, S. Kittaka, T. Sakakibara, Y. Hosokoshi and H. Yamaguchi, *Phys. Rev. B* **98** (2018) 224411 (1-8).
9. †Metamagnetic crossover in the quasikagome Ising Kondo-lattice compound CeIrSn: S. Tsuda, C. L. Yang, Y. Shimura, K. Umeo, H. Fukuoka, Y. Yamane, T. Onimaru, T. Takabatake, N. Kikugawa, T. Terashima, H. T. Hirose, S. Uji, S. Kittaka and T. Sakakibara, *Phys. Rev. B* **98** (2018) 155147 (1-7).
10. Quasi-one-dimensional Bose-Einstein condensation in the spin-1/2 ferromagnetic-leg ladder 3-I-V: Y. Kono, S. Kittaka, H. Yamaguchi, Y. Hosokoshi and T. Sakakibara, *Phys. Rev. B* **97** (2018) 100406 (1-5).
11. Fermi surface in the absence of a Fermi liquid in the Kondo insulator  $\text{SmB}_6$ : M. Hartstein, W. H. Toews, Y. -T. Hsu, B. Zeng, X. Chen, M. Ciomaga Hatnean, Q. R. Zhang, S. Nakamura, A. S. Padgett, G. Rodway-Gant, J. Berk, M. K. Kingston, G. H. Zhang, M. K. Chan, S. Yamashita, T. Sakakibara, Y. Takano, J. -H. Park, L. Balicas, N. Harrison, N. Shitsevalova, G. Balakrishnan, G. G. Lonzarich, R. W. Hill, M. Sutherland and S. E. Sebastian, *Nature Phys.* **14** (2018) 166-172.
12. Investigation of the tricritical point of the ising ferromagnet URhGe by angle-resolved measurements: S. Nakamura, S. Kittaka, T. Sakakibara, Y. Shimizu, Y. Kono, Y. Haga, J. Pospíšil and E. Yamamoto, *AIP Advances* **8** (2018) 101305 (1-5).
13. †Superconducting symmetries and magnetic responses of uranium heavy-fermion systems  $\text{UBe}_{13}$  and  $\text{UPd}_2\text{Al}_3$ : Y. Shimizu, S. Kittaka, T. Sakakibara and D. Aoki, *Physica B: Condensed Matter* **536** (2018) 553-557.
14. †\*Quantum valence criticality in a correlated metal: K. Kuga, Y. Matsumoto, M. Okawa, S. Suzuki, T. Tomita, K. Sone, Y. Shimura, T. Sakakibara, D. Nishio-Hamane, Y. Karaki, Y. Takata, M. Matsunami, R. Eguchi, M. Taguchi, A. Chainani, S. Shin, K. Tamasaku, Y. Nishino, M. Yabashi, T. Ishikawa and S. Nakatsuji, *Sci. Adv.* **4** (2018) eaao3547 (1-6).
15. Magnetization study on the ising ferromagnet URhGe with high-precision angle-resolved magnetic field near the hard axis: S. Nakamura, T. Sakakibara, Y. Shimizu, S. Kittaka, Y. Kono, Y. Haga, J. Pospisil and E. Yamamoto, *Progress in nuclear science and technology* **5** (2018) 123-127.
16. †Anisotropic magnetic-field response of quantum critical fluctuations in Ni-doped  $\text{CeCoIn}_5$ : M. Yokoyama, K. Suzuki, K. Tenya, S. Nakamura, Y. Kono, S. Kittaka and T. Sakakibara, *Phys. Rev. B* **99** (2019) 054506 (1-6).
17. †\* $S=1/2$  ferromagnetic Heisenberg chain in a verdazyl-based complex: N. Uemoto, Y. Kono, S. Kittaka, T. Sakakibara, T. Yajima, Y. Iwasaki, S. Miyamoto, Y. Hosokoshi and H. Yamaguchi, *Phys. Rev. B* **99** (2019) 094418 (1-6).
18. \*Unconventional field-induced spin gap in an  $S = 1/2$  chiral staggered chain: J. Liu, S. Kittaka, R. D. Johnson, T. Lancaster, J. Singleton, T. Sakakibara, Y. Kohama, J. van Tol, A. Ardavan, B. H. Williams, S. J. Blundell, Z. E. Manson, J. L. Manson and P. A. Goddard, *Phys Rev Lett* **122** (2019) 057207.

## Mori group

We have successfully developed and unveiled unprecedented functional properties for the molecular materials. The major achievements in 2018 are (1) to develop anhydrous organic proton conductors with dicarboxylic acids and imidazoles as an electrolyte of a fuel cell for medium temperatures, (2) to fabricate successfully and characterize the hydrogen-bonded molecular bilayer of catechol-fused TTF and imidazole-terminated alkanethiolate on Au(111), and (3) to estimate the thermoelectric property of the organic conductors,  $\beta^1\text{-(BEDT-TTF)}_3(\text{CoCl}_4)_{2-x}(\text{GaCl}_4)_x$ , as thermoelectric materials.

1. Antiferromagnetic Ordering in Organic Conductor  $\lambda\text{-(BEDT-TTF)}_2\text{GaCl}_4$  Probed by  $^{13}\text{C}$  NMR: Y. Saito, S. Fukuoka, T. Kobayashi, A. Kawamoto and H. Mori, *J. Phys. Soc. Jpn.* **87** (2018) 013707 (1-4).

---

† Joint research with outside partners.

2. Size effects on supercooling phenomena in strongly correlated electron systems: IrTe<sub>2</sub> and  $\theta$ -(BEDT-TTF)<sub>2</sub>RbZn(SCN)<sub>4</sub>: H. Oike, M. Suda, M. Kamitani, A. Ueda, H. Mori, Y. Tokura, H. M. Yamamoto and F. Kagawa, *Phys. Rev. B* **97** (2018) 085102 (1-7).
3. †\*Strong Hydrogen Bonds at the Interface between Proton-Donating and -Accepting Self-Assembled Monolayers on Au(111): H. S. Kato, S. Yoshimoto, A. Ueda, S. Yamamoto, Y. Kanematsu, M. Tachikawa, H. Mori, J. Yoshinobu and I. Matsuda, *Langmuir* **34** (2018) 2189-2197.
4. Anisotropic Proton Conductivity Arising from Hydrogen-Bond Patterns in Anhydrous Organic Single Crystals, Imidazolium Carboxylates: Y. Sunairi, A. Ueda, J. Yoshida, K. Suzuki and H. Mori, *J. Phys. Chem. C* **122** (2018) 11623.
5. The thermoelectric power of band-filling controlled organic conductors,  $\beta'$ -(BEDT-TTF)<sub>3</sub>(CoCl<sub>4</sub>)<sub>2-x</sub>(GaCl<sub>4</sub>)<sub>x</sub>: Y. Kiyota, T. Kawamoto, H. Mori and T. Mori, *J. Mater. Chem. A* **6** (2018) 2004-2010.
6. A phenol-fused tetrathiafulvalene: modulation of hydrogen-bond patterns and electrical conductivity in the charge-transfer salt: A. Ueda and H. Mori, *Mater. Chem. Front.* **2** (2018) 566-572.
7. Charge Order and Poor Glass-forming Ability of an Anisotropic Triangular-lattice System,  $\theta$ -(BEDT-TTF)<sub>2</sub>TiCo(SCN)<sub>4</sub>, Investigated by NMR: K. Miyagawa, T. Sato, H. Hashimoto, M. Kodama, K. Ohnoh, A. Ueda, H. Mori and K. Kanoda, *J. Phys. Soc. Jpn.* **88** (2019) 034705.
8. Hysteretic Current–Voltage Characteristics in the Deuterium-Dynamics-Triggered Charge-Ordered Phase of  $\kappa$ -D<sub>3</sub>(Cat-EDT-TTF)<sub>2</sub>: A. Ueda, K. Kishimoto, Y. Sunairi, J. Yoshida, H. Yamakawa, T. Miyamoto, T. Terashige, H. Okamoto and H. Mori, *J. Phys. Soc. Jpn.* **88** (2019) 034710.
9. \*Direct Evidence of Interfacial Hydrogen Bonding in Proton-Electron Concerted 2D Organic Bilayer on Au Substrate: S. Yamamoto, H. S. Kato, A. Ueda, S. Yoshimoto, Y. Hirata, J. Miyawaki, K. Yamamoto, Y. Harada, H. Wadati, H. Mori, J. Yoshinobu and I. Matsuda, *e-Journal of Surface Science and Nanotechnology* **17** (2019) 49-55.
10. Dynamics of Water Molecules in a 3-Fold Interpenetrated Hydrogen-Bonded Organic Framework Based on Tetrakis(4-pyridyl)methane: D. Inokuchi, Y. Hirao, K. Takahashi, K. Matsumoto, H. Mori and T. Kubo, *J. Phys. Chem. C* **123** (2019) 6599.
11. High-Temperature Cooperative Spin Crossover Transitions and Single-Crystal Reflection Spectra of [FeIII(qsal)<sub>2</sub>](CH<sub>3</sub>OSO<sub>3</sub>) and Related Compounds: K. Takahashi, K. Yamamoto, T. Yamamoto, Y. Einaga, Y. Shiota, K. Yoshizawa and H. Mori, *Crystals* **9** (2019) 81.
12. Construction of three-dimensional anionic molecular frameworks based on hydrogen-bonded metal dithiolene complexes and the crystal solvent effect: S. Yokomori, A. Ueda, T. Higashino, R. Kumai, Y. Murakami and H. Mori, *CrystEngComm* **21** (2019) 2940-2948.
13. Di- and tetramethoxy benzothienobenzothiophenes: substitution position effects on the intermolecular interactions, crystal packing and transistor properties: T. Higashino, A. Ueda and H. Mori, *New J. Chem.* **43** (2019) 884.
14. Strange metal from a frustration-driven charge order instability: T. Sato, K. Kitai, K. Miyagawa, M. Tamura, A. Ueda, H. Mori and K. Kanoda, *Nature Mater* **18** (2019) 229.
15. New  $\pi$ -extended catecholato complexes of Pt(II) and Pd(II) containing a benzothienobenzothiophene (BTBT) moiety: synthesis, electrochemical behavior and charge transfer properties: K. Tahara, Y. Ashihara, T. Higashino, Y. Ozawa, T. Kadoya, K. Sugimoto, A. Ueda, H. Mori and M. Abe, *Dalton Transactions* (2019), in print.
16. 有機結晶を舞台とした  $\pi$  電子 - プロトンカップリング物性の新展開 : 森 初果 , 日本物理学会誌 **74**、**No2** (2019) 82-92.

## Osada group

2018 (1) In order to identify the high-magnetic-field insulator phase of graphite, we investigated the phase transition in thin-film graphite samples, which were fabricated on silicon substrate by a mechanical exfoliation technique. The critical magnetic fields of the high-field transition in thin-films shift to higher fields, accompanied by a reduction in temperature dependence. These results can be qualitatively reproduced by the density-wave model with the quantum size effect. Our findings establish the density-wave state standing along the out-of-plane direction. (2) Recently, the small spin-orbit interaction (SOI) gap was proposed as an origin of the anomalous insulating behavior at low temperatures in an organic Dirac fermion system  $\alpha$ -(BEDT-TTF)<sub>2</sub>I<sub>3</sub>. We built a lattice model with plausible SOI coupling, and indicated that the gapped state is a topological insulator. This model is an organic version of the Kane-Mele model for graphene.

1. Topological Insulator State due to Finite Spin-Orbit Interaction in an Organic Dirac Fermion System: T. Osada, *J. Phys. Soc. Jpn.* **87** (2018) 075002 (1-2).

---

\* Joint research among groups within ISSP.

2. Thickness-dependent phase transition in graphite under high magnetic field: T. Taen, K. Uchida and T. Osada, *Phys. Rev. B* **97** (2018) 115122 (1-7).
3. Tunable magnetoresistance in thin-film graphite field-effect transistor by gate voltage: T. Taen, K. Uchida, T. Osada and W. Kang, *Phys. Rev. B* **98** (2018) 155136 (1-7).
4. Double carrier transport in electron doped region in black phosphorus FET: K. Hirose, T. Osada, K. Uchida, T. Taen, K. Watanabe, T. Taniguchi and Y. Akahama, *Appl. Phys. Lett.* **113** (2018) 193101 (1-4).
5. Anisotropy of Dirac cones and Van Hove singularity in an organic Dirac fermion system: A. Mori, M. Sato, T. Yajima, T. Konoike, K. Uchida and T. Osada, *Phys. Rev. B* **99** (2019) 035106 (1-5).

### Yamashita group

We have been studying (1) quantum criticality in heavy-fermion materials by ultra-low temperature cryostat, (2) thermal-Hall conductivity of exotic excitations in frustrated magnets and (3) a new technique for the study of strongly-correlated electron systems. In this year, we have published our works of (1) dHvA studies of CeCoIn<sub>5</sub> at ultralow temperatures, (2) thermal Hall measurements of Ca kagellite, and (3) thermal Hall measurements of a Kitaev candidate  $\alpha$ -RuCl<sub>3</sub>. We have performed (1) additional measurements of dHvA and Co NMR of CeCoIn<sub>5</sub> at ultralow temperatures, (2) thermal Hall measurements of another kagome compound, Cd kagellite, (3) magnetic torque measurements of organic QSL candidate  $\kappa$ -H<sub>3</sub>(Cat-EDT-TTF)<sub>2</sub>, and (4) thermal transport studies of a chiral magnet CsCuCl<sub>3</sub>.

1. Anomalous Change in the de Haas–van Alphen Oscillations of CeCoIn<sub>5</sub> at Ultralow Temperatures: H. Shishido, S. Yamada, K. Sugii, M. Shimozawa, Y. Yanase and M. Yamashita, *Phys. Rev. Lett.* **120** (2018) 177201.
2. \*Spin Thermal Hall Conductivity of a Kagome Antiferromagnet: H. Doki, M. Akazawa, H.-Y. Lee, J. H. Han, K. Sugii, M. Shimozawa, N. Kawashima, M. Oda, H. Yoshida and M. Yamashita, *Phys. Rev. Lett.* **121** (2018) 097203.
3. Unusual Thermal Hall Effect in a Kitaev Spin Liquid Candidate  $\alpha$ -RuCl<sub>3</sub>: Y. Kasahara, K. Sugii, T. Ohnishi, M. Shimozawa, M. Yamashita, N. Kurita, H. Tanaka, J. Nasu, Y. Motome, T. Shibauchi and Y. Matsuda, *Phys. Rev. Lett.* **120** (2018) 217205.

## Division of Condensed Matter Theory

### Tsunetsugu group

We have studied topics including harmonic generation in optical response of electron systems and dynamics of charge-density wave order in a planar organic material. We have also investigated spin current generation by light irradiation to a one-dimensional Mott insulator. We have also started a new project about highly out-of-equilibrium electron dynamics and studied the time evolution of the one-dimensional Hubbard model. We have used a two-reservoir quench setup and calculated charge and thermal currents using the generalized hydrodynamic theory based on Bethe ansatz.

1. Exploring the anisotropic Kondo model in and out of equilibrium with alkaline-earth atoms: M. Kanász-Nagy, Y. Ashida, T. Shi, C. P. Moca, T. N. Ikeda, S. Fölling, J. Ignacio Cirac, G. Zaránd and E. A. Demler, *Phys. Rev. B* **97** (2018) 155156.
2. Entanglement prethermalization in the Tomonaga-Luttinger model: E. Kaminishi, T. Mori, T. N. Ikeda and M. Ueda, *Phys. Rev. A* **97** (2018) 013622 (1-9).
3. Thermalization and prethermalization in isolated quantum systems: a theoretical overview: T. Mori, T. N. Ikeda, E. Kaminishi and M. Ueda, *J. Phys. B: At. Mol. Opt. Phys.* **51** (2018) 112001.
4. Nodal topology in d-wave superconducting monolayer FeSe: T. Nakayama, T. Shishidou and D. F. Agterberg, *Phys. Rev. B* **98** (2019) 214503.
5. Floquet-theoretical formulation and analysis of high-order harmonic generation in solids: T. N. Ikeda, K. Chinzei and H. Tsunetsugu, *Phys. Rev. A* **98** (2019) 063426.
6. Revisiting the Floquet-Bloch theory for an exactly solvable model of one-dimensional crystals in strong laser fields: T. N. Ikeda, *Phys. Rev. A* **97** (2019) 063413.
7. Photoinduced Dynamics of Commensurate Charge Density Wave in 1T-TaS<sub>2</sub> Based on Three-Orbital Hubbard Model: T. N. Ikeda, H. Tsunetsugu and K. Yonemitsu, *Appl. Sci.* **9** (2019) 70.

---

<sup>†</sup> Joint research with outside partners.

## Kato group

The main research subject of Kato lab. is theory of non-equilibrium properties in mesoscopic devices. We have studied (1) spin-current noise at the interface between a ferromagnetic insulator and a superconductor, (2) surface plasmon polaritons using Weyl semimetals, (3) domain wall formation in a chiral p-wave superconductor, (4) heat transport via a two-state system, (5) adiabatic electron transport via a quantum dot, and (6) Bell-state correlation in a Kondo quantum dot.

1. DC-Current Induced Domain Wall in a Chiral  $p$ -Wave Superconductor: T. Jonckheere and T. Kato, *J. Phys. Soc. Jpn.* **87** (2018) 094705 (1-6).
2. Effect of Interaction on Reservoir-Parameter-Driven Adiabatic Charge Pumping via a Single-Level Quantum Dot System: M. Hasegawa and T. Kato, *J. Phys. Soc. Jpn.* **87** (2018) 044709 (1-13).
3. Current cross-correlation in the Anderson impurity model with exchange interaction: R. Sakano, A. Oguri, Y. Nishikawa and E. Abe, *Phys. Rev. B* **97** (2018) 045127 (1-13).
4. Quantum Critical Phenomena in Heat Transport via a Two-State System: T. Yamamoto and T. Kato, *Phys. Rev. B* **98** (2018) 245412 (1-8).
5. Spin Current Noise of the Spin Seebeck Effect and Spin Pumping: M. Matsuo, Y. Ohnuma, T. Kato and S. Maekawa, *Phys. Rev. Lett.* **120** (2018) 235120 (1-5).
6. Heat transport via a local two-state system near thermal equilibrium: T. Yamamoto, M. Kato, T. Kato and K. Saito, *New J. Phys.* **20** (2018) 093014 (1-20).
7. \*Evolution of Magnetic Double Helix and Quantum Criticality near a Dome of Superconductivity in CrAs: M. Matsuda, F. K. Lin, R. Yu, J.-G. Cheng, W. Wu, J. P. Sun, J. H. Zhang, P. J. Sun, K. Matsubayashi, T. Miyake, T. Kato, J.-Q. Yan, M. B. Stone, Q.-M. Si, J. L. Luo and Y. Uwatoko, *Phys. Rev. X* **8** (2018) 031017 (1-12).
8. 国際物理オリンピック 2018 ポルトガル大会報告 : 加藤 岳生 , 大学の物理教育 **24** (2018) 112-116.
9. Surface plasmon polaritons in thin-film Weyl semimetals: T. Tamaya, T. Kato, K. Tsuchikawa, S. Konabe and S. Kawabata, *J. Phys.: Condens. Matter* **31** (2019) 305001 (1-10).
10. Bell-state correlations of quasiparticle pairs in the nonlinear current of a local Fermi liquid: R. Sakano, A. Oguri, Y. Nishikawa and E. Abe, *Phys. Rev. B* **99** (2019) 155106 (1-7).
11. Microscopic theory of spin transport at the interface between a superconductor and a ferromagnetic insulator: T. Kato, Y. Ohnuma, M. Matsuo, J. Rech, T. Jonckheere and T. Martin, *Phys. Rev. B* **99** (2019) 144411 (1-8).
12. mVMC—Open-source software for many-variable variational Monte Carlo method: T. Misawa, S. Morita, K. Yoshimi, M. Kawamura, Y. Motoyama, K. Ido, T. Ohgoe, M. Imada and T. Kato, *Comput. Phys. Commun.* **235** (2019) 447-462.
13. 非平衡状態にある近藤効果 (その 1) 非平衡グリーン関数入門 : 阪野 壘 , 固体物理 **53** (2018) 279-303.

## Division of Nanoscale Science

### Katsumoto group

Transport properties of double quantum well structures with (n-i-p-i-n)-type modulation doping were studied. For spin-injection, an iron film was deposited on top of the structure. We found peculiar magnetoresistance around zero-field. The lineshape of the magnetoresistance resembles that of anisotropic magnetoresistance. However, the origin is a kind of spin-orbit resonance due to the coexistence of Rashba and Dresselhaus type spin-orbit interactions. The anisotropy of the magnetoresistance on the in-plane angle of the magnetic field exhibited two-fold symmetry of III-V zinc-blende type crystal supporting the interpretation.

1. Frequencies of the Edge-Magnetoplasmon Excitations in Gated Quantum Hall Edges: A. Endo, K. Koike, S. Katsumoto and Y. Iye, *J. Phys. Soc. Jpn.* **87** (2018) 064709.
2. †Spin-orbit interaction in Pt or Bi<sub>2</sub>Te<sub>3</sub> nanoparticle-decorated graphene realized by a nanoneedle method: T. Namba, K. Tamura, K. Hatsuda, T. Nakamura, C. Ohata, S. Katsumoto and J. Haruyama, *Appl. Phys. Lett.* **113** (2018) 053106.
3. Frequency dependent ac transport of films of close-packed carbon nanotube arrays: A. Endo, S. Katsumoto, K. Matsuda, W. Norimatsu and M. Kusunoki, *J. Phys.: Conf. Ser.* **969** (2018) 012129.

---

\* Joint research among groups within ISSP.

4. Proximity-Induced Superconductivity in a Ferromagnetic Semiconductor (In,Fe)As: T. Nakamura, L. D. Anh, Y. Hashimoto, Y. Iwasaki, S. Ohya, M. Tanaka and S. Katsumoto, *J. Phys.: Conf. Ser.* **969** (2018) 012036.
5. †Evidence for a quantum spin Hall phase in graphene decorated with Bi<sub>2</sub>Te<sub>3</sub> nanoparticles: K. Hatsuda, H. Mine, T. Nakamura, J. Li, R. Wu, S. Katsumoto and J. Haruyama, *Sci. Adv.* **4** (2018) eaau6915.
6. Quantum Hall Edge States Probed by Plasmon Excitations: A. Endo and S. Katsumoto, *AAPPS Bulletin* **28** (2018) No.5 28 - 30.
7. Evidence for Spin-Triplet Electron Pairing in the Proximity-Induced Superconducting State of an Fe-Doped InAs Semiconductor: T. Nakamura, L. D. Anh, Y. Hashimoto, S. Ohya, M. Tanaka and S. Katsumoto, *Phys. Rev. Lett.* **122** (2019) 107001.
8. Spin Filtering Magnetoresistance in Double-Well Resonant Structures: T. Nakamura, Y. Hashimoto, T. Ke and S. Katsumoto, *Phys. Status Solidi B* **256** (2019) 1800560.
9. \*Strain-induced spontaneous Hall effect in an epitaxial thin film of a Luttinger semimetal: T. Ohtsuki, Z. Tian, A. Endo, M. Halim, S. Katsumoto, Y. Kohama, K. Kindo, M. Lippmaa and S. Nakatsuji, *Proc. Natl. Acad. Sci. USA* **116** (2019) 8803-8808.
10. Spatial distribution of thermoelectric voltages in a Hall-bar shaped two-dimensional electron system under a magnetic field: A. Endo, K. Fujita, S. Katsumoto and Y. Iye, *J. Phys. Commun.* **3** (2019) 055005 (1-19).
11. 半導体の電気伝導における Zitterbewegung (ジグザグ運動): 中村 壮智, 勝本 信吾, *日本物理学会誌* **73** (2018) 776.

## Otani group

We have studied the following topics this year; spin conversion behaviors in the bulk, the interfaces and the surfaces, magnetization dynamics in ferromagnetic nanostructures, and magneto-thermoelectric properties. In the first topic, our international collaboration with the Spanish group revealed the mechanism of the spin Hall effect in tantalum. We also succeeded in inducing the inverse Edelstein effect by decorating a copper surface with a lead phthalocyanine molecule. Furthermore, we have discovered that nonmagnetic metal/indium-tin-oxide interfaces can act as an efficient spin current source. In terms of magnetization dynamics, we have studied in collaboration with the Suemoto Group at ISSP on macroscopic magnetization control by symmetry breaking of photoinduced spin reorientation with intense terahertz magnetic near field. Apart from the above, we have also established a spin current generation by using magnon-phonon coupling.

1. Detection of the interfacial exchange field at a ferromagnetic insulator-nonmagnetic metal interface with pure spin currents: P. K. Muduli, M. Kimata, Y. Omori, T. Wakamura, S. P. Dash and Y. Otani, *Phys. Rev. B* **98** (2018) 024416.
2. Inverse Edelstein effect induced by magnon-phonon coupling: M. Xu, J. Puebla, F. Auvray, B. Rana, K. Kondou and Y. Otani, *Phys. Rev. B* **97** (2018) 180301.
3. Unveiling the mechanisms of the spin Hall effect in Ta: E. Sagasta, Y. Omori, S. Vélez, R. Llopis, C. Tollan, A. Chuvilin, L. E. Hueso, M. Gradhand, Y. Otani and F. Casanova, *Phys. Rev. B* **98** (2018) 060410.
4. Direct current modulation of spin-Hall-induced spin torque ferromagnetic resonance in platinum/permalloy bilayer thin films: S. Hirayama, S. Mitani, Y. Otani and S. Kasai, *Jpn. J. Appl. Phys.* **57** (2018) 060301.
5. \*Macroscopic Magnetization Control by Symmetry Breaking of Photoinduced Spin Reorientation with Intense Terahertz Magnetic Near Field: T. Kurihara, H. Watanabe, M. Nakajima, S. Karube, K. Oto, Y. Otani and T. Suemoto, *Phys. Rev. Lett.* **120** (2018) 107202.
6. \*Anomalous Hall effect in thin films of the Weyl antiferromagnet Mn<sub>3</sub>Sn: T. Higo, D. Qu, Y. Li, C. L. Chien, Y. Otani and S. Nakatsuji, *Appl. Phys. Lett.* **113** (2018) 202402.
7. Magnetothermodynamic Properties and Anomalous Magnetic Phase Transition in FeRh Nanowires: K. Matsumoto, M. Kimata, K. Kondou, R. C. Temple, C. H. Marrows and Y. Otani, *IEEE Trans. Magn.* **54** (2018) 23009041-5.
8. Anomalous modulation of spin torque-induced ferromagnetic resonance caused by direct currents in permalloy/platinum bilayer thin films: S. Hirayama, S. Mitani, Y. Otani and S. Kasai, *Appl. Phys. Express* **11** (2018) 013002 (1-4).
9. Active Control of Mode Crossover and Mode Hopping of Spin Waves in a Ferromagnetic Antidot Lattice: S. Choudhury, S. Majumder, S. Barman, Y. Otani and A. Barman, *Phys. Rev. Applied* **10** (2018) 064044.
10. Tunable Angle-Dependent Magnetization Dynamics in Ni<sub>80</sub>Fe<sub>20</sub> Nanocross Structures of Varying Size: K. Adhikari, S. Barman, R. Mandal, Y. Otani and A. Barman, *Phys. Rev. Applied* **10** (2018) 044010.

---

† Joint research with outside partners.

11. Voltage-Controlled Reconfigurable Spin-Wave Nanochannels and Logic Devices: B. Rana and Y. Otani, *Phys. Rev. Applied* **9** (2018) 014033 (1-15).
12. †\*Large enhancement of the spin Hall effect in Mn metal by Sn doping: D. Qu, T. Higo, T. Nishikawa, K. Matsumoto, K. Kondou, D. Nishio-Hamane, R. Ishii, P. K. Muduli, Y. Otani and S. Nakatsuji, *Phys. Rev. Materials* **2** (2018) 102001.
13. Influence of anisotropic dipolar interaction on the spin dynamics of Ni<sub>80</sub>Fe<sub>20</sub> nanodot arrays arranged in honeycomb and octagonal lattices: S. Mondal, S. Barman, S. Choudhury, Y. Otani and A. Barman, *Journal of Magnetism and Magnetic Materials* **458** (2018) 95-104.
14. Clear variation of spin splitting by changing electron distribution at non-magnetic metal/Bi<sub>2</sub>O<sub>3</sub> interfaces: H. Tsai, S. Karube, K. Kondou, N. Yamaguchi, F. Ishii and Y. Otani, *Sci Rep* **8** (2018) 5564.
15. Quantum materials for spin and charge conversion: W. Han, Y. Otani and S. Maekawa, *npj Quantum Materials* **3** (2018) 27 (1-16).
16. Field-controlled ultrafast magnetization dynamics in two-dimensional nanoscale ferromagnetic antidot arrays: A. De, S. Mondal, S. Sahoo, S. Barman, Y. Otani, R. K. Mitra and A. Barman, *Beilstein J. Nanotechnol* **9** (2018) 1123-1134.
17. Spin accumulation at nonmagnetic interface induced by direct Rashba–Edelstein effect: F. Auvray, J. Puebla, M. Xu, B. Rana, D. Hashizume and Y. Otani, *J Mater Sci: Mater Electron* **29** (2018) 15664-15670.
18. Efficient spin current generation and suppression of magnetic damping due to fast spin ejection from nonmagnetic metal/indium-tin-oxide interfaces: K. Kondou, H. Tsai, H. Isshiki and Y. Otani, *APL Materials* **6** (2018) 101105.
19. Relation between spin Hall effect and anomalous Hall effect in 3d ferromagnetic metals: Y. Omori, E. Sagasta, Y. Niimi, M. Gradhand, L. E. Hueso, F. Casanova and Y. Otani, *Phys. Rev. B* **99** (2019) 014403.
20. \*Magnetic and magnetic inverse spin Hall effects in a non-collinear antiferromagnet: M. Kimata, H. Chen, K. Kondou, S. Sugimoto, P. K. Muduli, M. Ikhlas, Y. Omori, T. Tomita, A. H. MacDonald, S. Nakatsuji and Y. Otani, *Nature* **565** (2019) 627.

## Komori group

Changes in the magnetism of epitaxially grown fcc Fe films on Cu(001) induced by single-crystal Mn overlayer are studied by scanning tunneling microscopy/spectroscopy and soft X-ray magnetic circular dichroism. Element specific magnetization curves of the Fe layer exhibit a two-step spin reorientation transition from out-of-plane to in-plane direction by increasing the Mn coverage. The atomic-scale characterizations of structural and electronic properties and the first-principles calculations successfully unravel the roles of the interface alloys and clarify the driving forces of the transition. Spin-resolved band L-gap surface bands on the noble metal (111) surfaces are quantitatively studied by spin- and angle-resolved photoelectron spectroscopy with a vacuum-ultraviolet laser. The surface-state wave function is found to be predominantly of even mirror symmetry with negligible odd contribution by SARPES using a linearly polarized light.

1. \*Surface electronic states of Au-induced nanowires on Ge(001): K. Yaji, R. Yukawa, S. Kim, Y. Ohtsubo, P. L. Fèvre, F. Bertran, A. Taleb-Ibrahimi, I. Matsuda, K. Nakatsuji, S. Shin and F. Komori, *J. Phys.: Condens. Matter* **30** (2018) 075001 (1-7).
2. \*Alkali-metal induced band structure deformation investigated by angle-resolved photoemission spectroscopy and first-principles calculations: S. Ito, B. Feng, M. Arita, T. Someya, W. -C. Chen, A. Takayama, T. Iimori, H. Namatame, M. Taniguchi, C. -M. Cheng, S. -J. Tang, F. Komori and I. Matsuda, *Phys. Rev. B* **97** (2018) 155423 (1-8)
3. †\*Giant Rashba splitting of quasi-one-dimensional surface states on Bi/InAs(110)- (2×1): T. Nakamura, Y. Ohtsubo, Y. Yamashita, S.-I. Ideta, K. Tanaka, K. Yaji, A. Harasawa, S. Shin, F. Komori, R. Yukawa, K. Horiba, H. Kumigashira and S.-I. Kimura, *Phys. Rev. B* **98** (2018) 075431.
4. \* レーザー励起スピン分解光電子分光で解き明かす光スピン制御：矢治光 一郎，黒田 健太，小森 文夫，辛 埴，*光学* **47** (2018) 142-147.
5. \*A Table-Top Formation of Bilayer Quasi-Free-Standing Epitaxial-Graphene on SiC(0001) by Microwave Annealing in Air: K.-S. Kim, G.-H. Park, H. Fukidome, T. Someya, T. Iimori, F. Komori, I. Matsuda and M. Suemitsu, *Carbon* **130** (2018) 792-798.
6. \* 物質科学、この1年「ボロフェンにおけるディラックフェルミオン」：松田 巖，*パリティ* **33** (2018) 36-38.

---

\* Joint research among groups within ISSP.

7. †Evaluation of structural vacancies for 1/1-Al–Re–Si approximant crystals by positron annihilation spectroscopy: K. Yamada, H. Suzuki, H. Kitahata, Y. Matsushita, K. Nozawa, F. Komori, R. S. Yu, Y. Kobayashi, T. Ohdaira, N. Oshima, R. Suzuki, Y. Takagiwa, K. Kimura and I. Kanazawa, *Philos. Mag.* **98** (2018) 107-117.
8. \*Discovery of 2D Anisotropic Dirac Cones: B. Feng, J. Zhang, S. Ito, M. Arita, C. Cheng, L. Chen, K. Wu, F. Komori, O. Sugino, K. Miyamoto, T. Okuda, S. Meng and I. Matsuda, *Adv. Mater.* **30** (2018) 1704025 (1-6).
9. †Triangular lattice atomic layer of Sn(1×1) at graphene/SiC(0001) interface: S. Hayashi, A. Visikovskiy, T. Kajiwara, T. Iimori, T. Shirasawa, K. Nakastuji, T. Miyamachi, S. Nakashima, K. Yaji, K. Mase, F. Komori and S. Tanaka, *Appl. Phys. Express* **11** (2018) 015202 (1-4).
10. \*Experimental Methods for Spin and Angle-Resolved Photoemission Spectroscopy Combined with Polarization Variable Laser: K. Kuroda, K. Yaji, A. Harasawa, R. Noguchi, T. Kondo, F. Komori and S. Shin, *JoVE* **136** (2018) e57090.
11. \*Rashba spin splitting of L-gap surface states on Ag(111) and Cu(111): K. Yaji, A. Harasawa, K. Kuroda, R. Li, B. Yan, F. Komori and S. Shin, *Physical Review B* **98** (2018) 041404(R).
12. Lattice distortion of square iron nitride monolayers induced by changing symmetry of substrate: T. Hattori, T. Iimori, T. Miyamachi and F. Komori, *Phys. Rev. Materials* **2** (2018) 044003 (1-7).
13. \*レーザーで電子のスピン方向を自由に制御: 矢治光 一郎, 黒田 健太, 小森 文夫, 辛 埴, レーザー加工学会誌 **25** (2018) 39-42.
14. Electronic and magnetic properties of the Fe<sub>2</sub>N monolayer film tuned by substrate symmetry: T. Hattori, T. Miyamachi, T. Yokoyama and F. Komori, *J. Phys.: Condens. Matter* **31** (2019) 255001.
15. †\*Coexistence of Two Types of Spin Splitting Originating from Different Symmetries: K. Yaji, A. Visikovskiy, T. Iimori, K. Kuroda, S. Hayashi, T. Kajiwara, S. Tanaka, F. Komori and S. Shin, *Phys. Rev. Lett.* **122** (2019) 126403.
16. †Fabrication of L1<sub>0</sub>-FeNi by pulsed-laser deposition: M. Saito, H. Ito, Y. Suzuki, M. Mizuguchi, T. Koganezawa, T. Miyamachi, F. Komori, K. Takanashi and M. Kotsugi, *Appl. Phys. Lett.* **114** (2019) 072404.
17. Dynamic Interface Formation in Magnetic Thin Film Heterostructures: S. Nakashima, T. Miyamachi, Y. Tatetsu, Y. Takahashi, Y. Takagi, Y. Gohda, T. Yokoyama and F. Komori, *Adv. Funct. Mater.* **29** (2019) 1804594.
18. †Fabrication of L1<sub>0</sub>-type FeCo ordered structure using a periodic Ni buffer layer: H. Ito, M. Saito, T. Miyamachi, F. Komori, T. Koganezawa, M. Mizuguchi and M. Kotsugi, *AIP Advances* **9** (2019) 045307.

## Hasegawa group

We performed scanning tunneling potentiometry; STM-based microscopy that enables us to obtain spatial mapping of electrochemical potential over the sample surface, on the Si(111)7×7 surface. Since the surface has the metallic surface states, electrical current flows through the surface layer created on an almost insulating low-doped substrate. We observed potential drops at the step edges and the domain boundaries of the superstructure, indicating the presence of electrical resistance there. It is found that the resistance at the step edge is rather large and thus the net conductivity of the reconstructed surface is basically determined by the step density or miscut angle of the substrate. This answers the long-standing question why the conductivity measured in macroscopic methods has dispersed so much. Our study demonstrates the importance of microscopic characterization for precise understanding of the conductivity in the two-dimensional metallic states. In the case of metallic surface states, because of the presence of the substrate, inversion symmetry is naturally broken. Therefore, superconductivity realized on the states cannot hold conventional s-wave Cooper pairing. In collaboration with Professor Shuji Hasegawa's group, Department of Physics, Univ. Tokyo, we investigated the superconductivity of a Tl-Pb monolayer formed on a Si(111) substrate by using low-temperature STM. Since previous angle-resolved photoemission spectra (ARPES) had revealed Rashba splitting in the metallic states, p-wave triplet or other unconventional pairings was expected. Our tunneling spectra clearly showed superconducting gaps on the surface whose spectrum shape cannot be explained with the BCS function. Vortices were also observed under magnetic fields. Curiously, however, even when the vortices cover the whole surface, the gaps still remain. In order to remove the gaps higher magnetic field has to be applied, which is quite unusual compared with the case of conventional s-wave superconductors. Whereas the reason of the peculiar gap behaviors is not revealed yet, the results demonstrate the possibility of unique and unconventional superconducting states on two-dimensional metallic surface states.

1. Unconventional superconductivity in the single-atom-layer alloy Si(111)-√3×√3-(Tl,Pb): T. Nakamura, H. Kim, S. Ichinokura, A. Takayama, A. V. Zotov, A. A. Saranin, Y. Hasegawa and S. Hasegawa, *Phys. Rev. B* **98** (2018) 134505 (1-6).
2. 走査プローブ顕微鏡による物性研究: 長谷川 幸雄, *固体物理* **53** (2018) 575-585.
3. SPM 特集号『プローブ顕微鏡によるナノサイエンスの最前線』企画趣旨: 長谷川 幸雄, *表面と真空* **61** (2018) 630-631.

---

† Joint research with outside partners.

4. Role of one-dimensional defects in the electrical transport through Si(111)-7×7 surface states: M. Hamada and Y. Hasegawa, *Phys. Rev. B* **99** (2019) 125402 (1-5).
5. Bulk ferromagnetic tips for spin-polarized scanning tunneling microscopy: M. Haze, H.-H. Yang, K. Asakawa, N. Watanabe, R. Yamamoto, Y. Yoshida and Y. Hasegawa, *Review of Scientific Instruments* **90** (2019) 013704 (1-5).
6. プローブ顕微鏡で切り開くこれからの研究：長谷川 幸雄，表面と真空 **61** (2018) 609-610.
7. Nanoscale Magnetic Imaging: Y. Hasegawa, M. Haze and Y. Yoshida, in: *Reference Module in Materials Science and Materials Engineering*, edited by M.S.J.Hashmi, (Elsevier, 2018), B9780128035818104370.
8. Scanning Tunneling Microscopy: Y. Hasegawa, in: *Compendium of Surface and Interface Analysis*, edited by The Surface Science Society of Japan, (Springer Singapore, 2018), 599-604.

## Lippmaa group

Noble metal doping can be an effective way of controlling the band gap width of titanate semiconductors like SrTiO<sub>3</sub>. The special feature of noble metal dopants is that they form impurity states close to the valence band top of the crystal, thereby reducing the band gap without affecting the electronic structure at the conduction band bottom. For this reason, Ir, Pt, Pd, and Rh doping in SrTiO<sub>3</sub> has been studied in the area of solar-driven photocatalysis. In our recent work, we look at the microscopic mechanism of oxide doping with noble metals and self-organized nanoscale metal segregation. We find that during thin film growth of a noble-metal-doped SrTiO<sub>3</sub> film, the metal can migrate rapidly on the film surface and aggregate in a nanoscale cluster. This cluster formation, cluster size, and areal density can be controlled by the noble metal doping level. We use transmission electron microscopy and x-ray photoelectron spectroscopy to analyze the metal nanocluster formation and growth.

1. Distortion Analysis of Ir- and Co-doped LaAlO<sub>3</sub>/SrTiO<sub>3</sub>(001) Interfaces by Hard X-ray Photoelectron Diffraction: M. Lee, X. L. Tan, M. Yoneda, T. Okamoto, I. Tanaka, Y. Higa, D. Peng, M. Ogi, S. Kobayashi, M. Taguchi, M. Lippmaa, M.-J. Casanove and H. Daimon, *J. Phys. Soc. Jpn.* **87** (2018) 084601 (1-4).
2. Pyroelectric detection of ferroelectric polarization in magnetic thin films: R. Takahashi and M. Lippmaa, *Jpn. J. Appl. Phys.* **57** (2018) 0902A1.
3. †Noble metal nanocluster formation in epitaxial perovskite thin films: M. Lee, R. Arras, R. Takahashi, B. Warot-Fonrose, H. Daimon, M.-J. Casanove and M. Lippmaa, *ACS Omega* **3** (2018) 2169-2173.
4. \*Imaging the Formation of Ferromagnetic Domains at the LaAlO<sub>3</sub>/SrTiO<sub>3</sub> Interface: Y. Motoyui, T. Taniuchi, P. Scheiderer, J. N. Lee, J. Gabel, F. Pfaff, M. Sing, M. Lippmaa, R. Claessen and S. Shin, *J. Phys. Soc. Jpn.* **88** (2019) 034717 (1-5).
5. Experimental realization of atomically flat and AlO<sub>2</sub>-terminated LaAlO<sub>3</sub>(001) substrate surfaces: J. R. Kim, J. N. Lee, J. Mun, Y. Kim, Y. J. Shin, B. Kim, S. Das, L. Wang, M. Kim, M. Lippmaa, T. H. Kim and T. W. Noh, *Phys. Rev. Mater.* **3** (2019) 023801 (1-8).
6. Synthesis and characterization of (111)-oriented BaTiO<sub>3</sub> thin films: T. Bolstad, K. Kjærnes, K. Raa, R. Takahashi, M. Lippmaa and T. Tybell, *Mater. Res. Express* **6** (2019) 056409 (1-8).
7. \*Strain-induced spontaneous Hall effect in an epitaxial thin film of a Luttinger semimetal: T. Ohtsuki, Z. Tian, A. Endo, M. Halim, S. Katsumoto, Y. Kohama, K. Kindo, M. Lippmaa and S. Nakatsuji, *Proc. Natl. Acad. Sci. USA* **116** (2019) 8803-8808.
8. Gradient Carrier Doping as a Method for Maximizing the Photon-to-Current Efficiency of a SrTiO<sub>3</sub> Water Splitting Photoanode: S. Kawasaki, R. Takahashi and M. Lippmaa, *J. Phys. Chem. C* (2019), accepted for publication.
9. 酸化物半導体中に自己組織化した金属ナノピラーによる高効率・水分解光電極反応：川崎 聖治，高橋 竜太，リップマー ミック，応用物理 **87** (2018) 366-369.

## Functional Materials Group

### Yoshinobu group

We conducted several research projects in the fiscal year 2018: (1) Systematic study of the activation and hydrogenation of CO<sub>2</sub> on Zn/Cu model catalysts by AP-XPS, IRAS, and TPD. (2) The surface chemistry of formic acid on Zn/Cu model catalysts studied by SR-PES, IRAS, and TPD. (3) Spectroscopic characterization of Hydrogen adsorption and absorption on Pd-Cu and

---

\* Joint research among groups within ISSP.

Pd-Ag surfaces by XPS. (4) LT-STM study of Zn on Cu(997). (5) The surface chemistry of hydrogen and formic acid on Pd/Cu model catalysts studied by SR-PES, IRAS, and TPD. (6) Observation of CVD processes of graphene formation on a Cu surface.

1. †\*Strong Hydrogen Bonds at the Interface between Proton-Donating and -Accepting Self-Assembled Monolayers on Au(111): H. S. Kato, S. Yoshimoto, A. Ueda, S. Yamamoto, Y. Kanematsu, M. Tachikawa, H. Mori, J. Yoshinobu and I. Matsuda, *Langmuir* **34** (2018) 2189-2197.
2. \*Atomic Structure and Local Electronic States of Single Pt Atoms Dispersed on Graphene: K. Yamazaki, Y. Maehara, C.-C. Lee, J. Yoshinobu, T. Ozaki and K. Gohara, *J. Phys. Chem. C* **122** (2018) 27292.
3. †H-D Exchange Mechanism of Butene on a D-Absorbed Pd-Au Alloy Surface: S. Ogura, S. Ohno, K. Mukai, J. Yoshinobu and K. Fukutani, *J. Phys. Chem. C* **123** (2018) 7854.
4. \*Enhancement of CO<sub>2</sub> adsorption on oxygen-functionalized epitaxial graphene surface under near-ambient conditions: S. Yamamoto, K. Takeuchi, Y. Hamamoto, R.-Y. Liu, Y. Shiozawa, T. Koitaya, T. Someya, K. Tashima, H. Fukidome, K. Mukai, S. Yoshimoto, M. Suemitsu, Y. Morikawa, J. Yoshinobu and I. Matsuda, *Phys. Chem. Chem. Phys.* **20** (2018) 19532.
5. Initial gas exposure effects on monolayer pentacene field-effect transistor studied using four gallium indium probes: S. Yoshimoto, R. Miyahara, Y. Yoshikura, J. Tang, K. Mukai and J. Yoshinobu, *Org. Electron.* **54** (2018) 34-39.
6. †An Ethynylene-Bridged Pentacene Dimer: Two-Step Synthesis and Charge-Transport Properties: K. Kawano, H. Hayashi, S. Yoshimoto, N. Aratani, M. Suzuki, J. Yoshinobu and H. Yamada, *Chem. Eur. J.* **24** (2018) 14916.
7. \*Hydrogen adsorption and absorption on a Pd-Ag alloy surface studied using in-situ X-ray photoelectron spectroscopy under ultrahigh vacuum and ambient pressure: J. Tang, S. Yamamoto, T. Koitaya, Y. Yoshikura, K. Mukai, S. Yoshimoto, I. Matsuda and J. Yoshinobu, *Applied Surface Science* **463** (2019) 1161-1167.
8. \*Mass transport in the PdCu phase structures during hydrogen adsorption and absorption studied by XPS under hydrogen atmosphere: J. Tang, S. Yamamoto, T. Koitaya, A. Yoshigoe, T. Tokunaga, K. Mukai, I. Matsuda and J. Yoshinobu, *Applied Surface Science* **480** (2019) 419-426.
9. \*CO<sub>2</sub> Activation and Reaction on Zn-Deposited Cu Surfaces Studied by Ambient-Pressure X-ray Photoelectron Spectroscopy: T. Koitaya, S. Yamamoto, Y. Shiozawa, Y. Yoshikura, M. Hasegawa, J. Tang, K. Takeuchi, K. Mukai, S. Yoshimoto, I. Matsuda and J. Yoshinobu, *ACS Catal.* **9** (2019) 4539-4550.

## Akiyama group

In 2018, we fabricated and characterized 1035nm InGaAs laser diodes for short and intense pulse generation via gain switching (NEDO project). We studied single- and multi-junction solar cells for absolute electroluminescence-efficiency standard. We made femto-second time-resolved laser photo-emission spectroscopy for solar cell systems (LASOR collaboration), and analyzed their results in comparison with model calculations and time-resolved PL spectroscopy. We made computational studies with quantum-chemistry and molecular-dynamics calculations on oxyluciferins and caged-luciferins, and corresponding experiments.

1. Coherent detection of THz-induced sideband emission from excitons in the nonperturbative regime: K. Uchida, T. Otobe, T. Mochizuki, C. Kim, M. Yoshita, K. Tanaka, H. Akiyama, L. N. Pfeiffer, K. W. West and H. Hirori, *Phys. Rev. B* **97** (2018) 165122.
2. Analysis of future generation solar cells and materials: M. Yamaguchi, L. Zhu, H. Akiyama, Y. Kanemitsu, H. Tampo, H. Shibata, K.-H. Lee, K. Araki and N. Kojima, *Jpn. J. Appl. Phys.* **57** (2018) 04FS03 (1-6).
3. Quantitative monitoring of the internal field in the depletion layer of a GaAs-based solar cell with terahertz radiation: K. Miyagawa, M. Nagai, G. Yamashita, M. Ashida, C. Kim, H. Akiyama and Y. Kanemitsu, *Appl. Phys. Lett.* **113** (2018) 163501.
4. Terahertz field-induced ionization and perturbed free induction decay of excitons in bulk GaAs: Y. Murotani, M. Takayama, F. Sekiguchi, C. Kim, H. Akiyama and R. Shimano, *J. Phys. D: Appl. Phys.* **51** (2018) 114001 (1-10).
5. Nonequilibrium Theory of the Conversion Efficiency Limit of Solar Cells Including Thermalization and Extraction of Carriers: K. Kamide, T. Mochizuki, H. Akiyama and H. Takato, *Phys. Rev. Applied* **10** (2018) 044069.
6. Revealing Solar-Cell Photovoltage Dynamics at the Picosecond Time Scale with Time-Resolved Photoemission Spectroscopy: Y. Hazama, Y. Ishida, L. Zhu, C. Kim, S. Shin and H. Akiyama, *Phys. Rev. Applied* **10** (2018) 034056.

---

† Joint research with outside partners.

- Effect of interaction between the internal cavity and external cavity on beam properties in a spectrally beam combined system: Z. Wu, T. Ito, H. Akiyama and B. Zhang, *J. Opt. Soc. Am. A* **35** (2018) 772-778.
- Absolute bioluminescence imaging at the single-cell level with a light signal at the Attowatt level: T. Enomoto, H. Kubota, K. Mori, M. Shimogawara, M. Yoshita, Y. Ohmiya and H. Akiyama, *BioTechniques* **64** (2018) 270.
- Intrinsic and extrinsic drops in open-circuit voltage and conversion efficiency in solar cells with quantum dots embedded in host materials: L. Zhu, H. Akiyama and Y. Kanemitsu, *Scientific Report* **8** (2018) 11704.
- Synthesis and quantitative characterization of coumarin-caged D-luciferin: M. Kurata, M. Hiyama, T. Narimatsu, Y. Hazama, T. Ito, Y. Hayamizu, X. Qiu, F. M. Winnik and H. Akiyama, *Journal of Photochemistry and Photobiology B: Biology* **189** (2018) 81.
- \*Nonlinear propagation effects in high harmonic generation in reflection and transmission from gallium arsenide: P. Xia, C. Kim, F. Lu, T. Kanai, H. Akiyama, J. Itatani and N. Ishii, *Optics Express* **26** (2018) 29393-29400.
- \*Femtosecond pulse generation beyond photon lifetime limit in gain-switched semiconductor lasers: T. Ito, H. Nakamae, Y. Hazama, T. Nakamura, S. Chen, M. Yoshita, C. Kim, Y. Kobayashi and H. Akiyama, *Commun. Phys.* **1** (2018) 42.

## Sugino group

In this fiscal year, we have developed a novel first-principles simulation method for defects in a material and excitons in a molecule and, in addition, have applied an advanced simulation method to a surface. The first topic is a replica exchange Monte Carlo sampling of defects in a solid, which has not been tried previously in the literature but has proven to be unexpectedly efficient. The second topic is on our progress in improving the efficiency of the Green's functional approach, which makes it possible to simulate up to 200 atoms exceeding most of our target systems. The third topic is on the problem of resolving the hydrogen adsorption on Pt(111) surface. By using an advanced exchange-correlation functional, it was finally revealed how strongly and at which site hydrogen atoms are adsorbed on the surface. This is an important step for true understanding the water splitting and fuel cell reactions.

- \*物質科学、この1年「ボロフェンにおけるディラックフェルミオン」：松田 巖，*パリティ* **33** (2018) 36-38.
- Optical properties of six isomers of three dimensionally delocalized  $\pi$ -conjugated carbon nanocage: Y. Noguchi, D. Hirose and O. Sugino, *Eur. Phys. J. B* **91** (2018) 125.
- \*Discovery of 2D Anisotropic Dirac Cones: B. Feng, J. Zhang, S. Ito, M. Arita, C. Cheng, L. Chen, K. Wu, F. Komori, O. Sugino, K. Miyamoto, T. Okuda, S. Meng and I. Matsuda, *Adv. Mater.* **30** (2018) 1704025 (1-6).
- First-principles investigation of polarization and ion conduction mechanisms in hydroxyapatite: S. Kasamatsu and O. Sugino, *Phys. Chem. Chem. Phys.* **20** (2018) 8744.
- †Hydrogen adsorption on Pt(111) revisited from random phase approximation: L. Yan, Y. Sun, Y. Yamamoto, S. Kasamatsu, I. Hamada and O. Sugino, *The Journal of Chemical Physics* **149** (2018) 164702.
- Direct coupling of first-principles calculations with replica exchange Monte Carlo sampling of ion disorder in solids: S. Kasamatsu and O. Sugino, *J. Phys.: Condens. Matter* **31** (2019) 085901.

## Inoue group

In 2018, we reported a new machine learning method to estimate the absorption wavelengths of microbial rhodopsins from their primary sequences, based on a newly constructed database of previously reported and unreported absorption maxima of microbial rhodopsins and their mutants. The chromophore structure in newly discovered heliorhodopsin was studied by international joint research.

- Resonance Raman Investigation of the Chromophore Structure of Heliorhodopsins: A. Otomo, M. Mizuno, M. Singh, W. Shihoya, K. Inoue, O. Nureki, O. Béjà, H. Kandori and Y. Mizutani, *J. Phys. Chem. Lett.* **9** (2018) 6431-6436.
- Understanding Colour Tuning Rules and Predicting Absorption Wavelengths of Microbial Rhodopsins by Data-Driven Machine-Learning Approach: M. Karasuyama, K. Inoue, R. Nakamura, H. Kandori and I. Takeuchi, *Sci. Rep.* **8** (2018) 15580.
- Ultrafast Dynamics of Heliorhodopsins: S. Tahara, M. Singh, H. Kuramochi, W. Shihoya, K. Inoue, O. Nureki, O. Béjà, Y. Mizutani, H. Kandori and T. Tahara, *J. Phys. Chem. B* **123** (2019) 2507-2512.
- Casting Light on Asgardarchaeota Metabolism in a Sunlit Microoxic Niche: P. -A. Bulzu, A. -S. Andrei, M. M. Salcher, M. Mehrshad, K. Inoue, H. Kandori, O. Béjà and R. Ghai, (2019), in print.

---

\* Joint research among groups within ISSP.

5. Heliorhodopsins are Absent in Diderm (Gram-negative) Bacteria: Some Thoughts and Possible Implications for Activity: J. Flores-Urbe, G. Hevroni, R. Ghai, A. Pushkarev, K. Inoue, H. Kandori and O. Béjà, *Environ. Microbiol. Rep.* (2019), in print.

## Quantum Materials Group

### Oshikawa group

We studied a variety of problems in quantum condensed matter physics, statistical mechanics, and field theory. In particular, we studied the electronic structure of  $\alpha$ -ZrCl<sub>3</sub>. Under the ligand field splitting and a strong spin-orbit interaction, each Zr<sup>3+</sup> has one electron each in the J=3/2 quartet states. The strong anisotropy of d-orbitals leads to highly orbital- and direction-dependent hoppings. Nevertheless, we found that, after an appropriate gauge transformation, the effective model has a global SU(4) symmetry which corresponds to the simultaneous complex rotation of the quartet states. In the presence of a strong Coulomb repulsion, the system would be described by the SU(4) antiferromagnetic "Heisenberg" model on a honeycomb lattice, which is predicted to have a gapless spin liquid state. This suggests an intriguing possibility of realizing a SU(4) spin-orbital liquid, in which spin and orbital degrees of freedom of a magnetic material are intertwined.

1. Construction of Hamiltonians by supervised learning of energy and entanglement spectra: H. Fujita, Y. O. Nakagawa, S. Sugiura and M. Oshikawa, *Phys. Rev. B* **97** (2018) 075114 (1-12).
2. †Particle statistics, frustration, and ground-state energy: W. Nie, H. Katsura and M. Oshikawa, *Phys. Rev. B* **97** (2018) 125153 (1-17).
3. Scaling of the polarization amplitude in quantum many-body systems in one dimension: R. Kobayashi, Y. O. Nakagawa, Y. Fukusumi and M. Oshikawa, *Phys. Rev. B* **97** (2018) 165133 (1-14).
4. †Unified understanding of symmetry indicators for all internal symmetry classes: S. Ono and H. Watanabe, *Phys. Rev. B* **98** (2018) 115150.
5. †Emergent SU(4) Symmetry in  $\alpha$ -ZrCl<sub>3</sub> and Crystalline Spin-Orbital Liquids: M. G. Yamada, M. Oshikawa and G. Jackeli, *Phys. Rev. Lett.* **121** (2018) 097201 (1-6).
6. 光渦レーザーによる磁性制御の展望：藤田 浩之，佐藤 正寛，*固体物理* **53**, **10** (2018) 1-15.
7. 光渦レーザーによる超高速ナノスピン構造制御：佐藤 正寛，藤田 浩之，*光学* **47**, **4** (2018) p162-.
8. 量子情報と統計力学 (特集 量子情報と物理学のフロンティア): 押川 正毅，*数理科学* **56**(6) (2018) 23-29.
9. †Inequivalent Berry Phases for the Bulk Polarization: H. Watanabe and M. Oshikawa, *Phys. Rev. X* **8** (2018) 021065 (1-15).
10. Fulde-Ferrell state in a ferromagnetic chiral superconductor with magnetic domain walls: Y. Tada, *Physical Review B* **97** (2018) 014519.
11. Decay of superconducting correlations for gauged electrons in dimensions  $D \leq 4$ : Y. Tada and T. Koma, *Journal of Mathematical Physics* **59** (2018) 031905.
12. †Crossover of correlation functions near a quantum impurity in a Tomonaga-Luttinger liquid: C.-Y. Lo, Y. Fukusumi, M. Oshikawa, Y.-J. Kao and P. Chen, *Phys. Rev. B* **99** (2019) 121103.

### Nakatsuji group

Our group explores ground state properties and spintronic functions of novel quantum phases and phase transitions in rare-earth and transition-metal based compounds. The followings are some relevant results obtained in 2018. (1) We found one order magnitude higher anomalous Nernst effect in Co<sub>2</sub>MnGa, in comparison with the previously reported value for ferromagnets, ascribable to the quantum Lifshitz transition between type-I and type-II Weyl fermions (2) We have succeeded in growing a high-quality thin film of magnetic Weyl semimetal Mn<sub>3</sub>Sn that exhibits anomalous Hall effect by a sputtering method. (3) our recent study on Mn<sub>3</sub>Sn has revealed a new type of spin Hall effect, whose sign and magnitude can be controlled by magnetization for the first time (4) We found a spin ice state with significant quantum fluctuations, namely, a quantum spin ice state in Pr<sub>2</sub>Zr<sub>2</sub>O<sub>7</sub>. (5) We established the thin film growth method of the Luttinger semimetal state of Pr<sub>2</sub>Ir<sub>2</sub>O<sub>7</sub> and reported strain-induced Weyl semimetal state in using the thin films.

---

† Joint research with outside partners.

1. Valence fluctuating compound  $\alpha$ -YbAlB<sub>4</sub> studied by <sup>174</sup>Yb Mössbauer spectroscopy and X-ray diffraction using synchrotron radiation: M. Oura, S. Ikeda, R. Masuda, Y. Kobayashi, M. Seto, Y. Yoda, N. Hirao, S. I. Kawaguchi, Y. Ohishi, S. Suzuki, K. Kuga, S. Nakatsuji and H. Kobayashi, *Physica B* **536** (2018) 162-164.
2. Spin-orbital entangled liquid state in the copper oxide Ba<sub>3</sub>CuSb<sub>2</sub>O<sub>9</sub>: H. Man, M. Halim, H. Sawa, M. Hagiwara, Y. Wakabayashi and S. Nakatsuji, *J. Phys.: Condens. Matter* **30** (2018) 443002.
3. Crystal Structure in Quadrupolar Kondo Candidate PrTr<sub>2</sub>Al<sub>20</sub> (Tr = Ti and V): D. Okuyama, M. Tsujimoto, H. Sagayama, Y. Shimura, A. Sakai, A. Magata, S. Nakatsuji and T. J. Sato, *J. Phys. Soc. Jpn.* **88** (2018) 015001.
4. Discovery of Emergent Photon and Monopoles in a Quantum Spin Liquid: Y. Tokiwa, T. Yamashita, D. Terazawa, K. Kimura, Y. Kasahara, T. Onishi, Y. Kato, M. Halim, P. Gegenwart, T. Shibauchi, S. Nakatsuji, E.-G. Moon and Y. Matsuda, *J. Phys. Soc. Jpn.* **87** (2018) 064702.
5. \*Kondo hybridization and quantum criticality in  $\beta$ -YbAlB<sub>4</sub> by laser ARPES: C. Bareille, S. Suzuki, M. Nakayama, K. Kuroda, A. H. Nevidomskyy, Y. Matsumoto, S. Nakatsuji, T. Kondo and S. Shin, *Phys. Rev. B* **97** (2018) 045112 (1-7).
6. Relaxation calorimetry at very low temperatures for systems with internal relaxation: Y. Matsumoto and S. Nakatsuji, *Rev. Sci. Instrum.* **89** (2018) 033908.
7. Magnetic Excitations across the Metal-Insulator Transition in the Pyrochlore Iridate Eu<sub>2</sub>Ir<sub>2</sub>O<sub>7</sub>: S. H. Chun, B. Yuan, D. Casa, J. Kim, C.-Y. Kim, Z. Tian, Y. Qiu, S. Nakatsuji and Y.-J. Kim, *Phys. Rev. Lett.* **120** (2018) 177203.
8. \*Anomalous Hall effect in thin films of the Weyl antiferromagnet Mn<sub>3</sub>Sn: T. Higo, D. Qu, Y. Li, C. L. Chien, Y. Otani and S. Nakatsuji, *Appl. Phys. Lett.* **113** (2018) 202402.
9. Large magneto-optical Kerr effect and imaging of magnetic octupole domains in an antiferromagnetic metal: T. Higo, H. Man, D. B. Gopman, L. Wu, T. Koretsune, O. M. J. van Erve, Y. P. Kabanov, D. Rees, Y. Li, M.-T. Suzuki, S. Patankar, M. Ikhlas, C. L. Chien, R. Arita, R. D. Shull and J. O. & S. Nakatsuji, *Nature Photon.* **12** (2018) 73-78.
10. \*Giant anomalous Nernst effect and quantum-critical scaling in a ferromagnetic semimetal: A. Sakai, Y. P. Mizuta, A. A. Nugroho, R. Sihombing, T. Koretsune, M.-T. Suzuki, N. Takemori, R. Ishii, D. Nishio-Hamane, R. Arita, P. Goswami and S. Nakatsuji, *Nature Phys.* **14** (2018) 1119-1124.
11. \*Universal geometric frustration in pyrochlores: B. A. Trump, S. M. Koohpayeh, K. J. T. Livi, J. -J. Wen, K. E. Arpino, Q. M. Ramasse, R. Brydson, M. Feygenson, H. Takeda, M. Takigawa, K. Kimura, S. Nakatsuji, C. L. Broholm and T. M. McQueen, *Nat. Commun.* **9** (2018) 2619 (1-10).
12. \*X-Ray Absorption Spectroscopy of 4f Compounds and Future Directions Toward Time-resolved Measurements: H. Wadati, K. Takubo, T. Tsuyama, Y. Yokoyama, K. Yamamoto, Y. Hirata, T. Ina, K. Nitta, M. Mizumaki, T. Togashi, S. Suzuki, Y. Matsumoto and S. Nakatsuji, *Adv. X-Ray. Chem. Anal., Japan* **49** (2018) 169-175.
13. Elastic anomalies associated with two successive transitions of PrV<sub>2</sub>Al<sub>20</sub> probed by ultrasound measurements: Y. Nakanishi, M. Taniguchi, M. M. Nakamura, J. Hasegawa, R. Ohyama, M. Nakamura, M. Yoshizawa, M. Tsujimoto and S. Nakatsuji, *Physica B: Condensed Matter* **536** (2018) 125.
14. †\*Quantum valence criticality in a correlated metal: K. Kuga, Y. Matsumoto, M. Okawa, S. Suzuki, T. Tomita, K. Sone, Y. Shimura, T. Sakakibara, D. Nishio-Hamane, Y. Karaki, Y. Takata, M. Matsunami, R. Eguchi, M. Taguchi, A. Chainani, S. Shin, K. Tamasaku, Y. Nishino, M. Yabashi, T. Ishikawa and S. Nakatsuji, *Sci. Adv.* **4** (2018) eaao3547 (1-6).
15. †\*Large enhancement of the spin Hall effect in Mn metal by Sn doping: D. Qu, T. Higo, T. Nishikawa, K. Matsumoto, K. Kondou, D. Nishio-Hamane, R. Ishii, P. K. Muduli, Y. Otani and S. Nakatsuji, *Phys. Rev. Materials* **2** (2018) 102001.
16. トポロジーを利用した反強磁性スピントロニクスとエネルギーハーベスティング: 中辻 知, まぐね /*Magnetics Japan* **13 No.5** (2018) 216-222.
17. ワイル磁性体 Mn<sub>3</sub>Sn における巨大な異常ネルンスト効果: 富田 崇弘, 日本磁気学会 第 217 回研究会資料 (2018) 23-28.
18. Evaluation of spin diffusion length and spin Hall angle of antiferromagnetic Weyl semimetal Mn<sub>3</sub>Sn: P. K. Muduli, T. Higo, T. Nishikawa, D. Qu, H. Isshiki, K. Kondou, D. Nishio-Hamane, S. Nakatsuji and Y. Otani, *Phys. Rev. B* **99** (2019) 184425.
19. 反強磁性体において実現した室温での巨大異常ネルンスト効果 - 磁気ワイルフェルミオンが織りなすトポロジカル現象: 富田 崇弘, 肥後 友也, 中辻 知, *固体物理* **54** (2019) 85-99.

---

\* Joint research among groups within ISSP.

20. \*Magnetic and magnetic inverse spin Hall effects in a non-collinear antiferromagnet: M. Kimata, H. Chen, K. Kondou, S. Sugimoto, P. K. Muduli, M. Ikhlas, Y. Omori, T. Tomita, A. H. MacDonald, S. Nakatsuji and Y. Otani, *Nature* **565** (2019) 627.
21. Energy harvesting materials based on the anomalous Nernst effect: M. Mizuguchi and S. Nakatsuji, *Sci. Technol. Adv. Mater.* **20** (2019) 262-275.
22. \*Strain-induced spontaneous Hall effect in an epitaxial thin film of a Luttinger semimetal: T. Ohtsuki, Z. Tian, A. Endo, M. Halim, S. Katsumoto, Y. Kohama, K. Kindo, M. Lippmaa and S. Nakatsuji, *Proc. Natl. Acad. Sci. USA* **116** (2019) 8803-8808.
23. 量子効果で10倍以上の磁気熱電効果を室温で実現：酒井 明人，中辻 知，*クリーンエネルギー* **28** (2019) 34-38.
24. ワイル反強磁性体 Mn<sub>3</sub>Sn における巨大な磁気光学カー効果と拡張磁気八極子ドメインの直接観測：肥後 友也，*J-Physics* **#7** (2019) 94.
25. ワイル磁性体 Co<sub>2</sub>MnGa における室温巨大異常ネルンスト効果：酒井 明人，*J-Physics* **07** (2019) 47-49.
26. Giant anisotropic magnetoresistance due to purely orbital rearrangement in the quadrupolar heavy fermion superconductor PrV<sub>2</sub>Al<sub>20</sub>: Y. Shimura, Q. Zhang, B. Zeng, D. Rhodes, R. Schönemann, M. Tsujimoto, Y. Matsumoto, A. Sakai, T. Sakakibara, K. Araki, W. Zheng, Q. Zhou, L. Balicas and S. Nakatsuji, *Phys. Rev. Lett.* (2019), accepted for publication.

## Miwa group

We have studied following topics in this year: (1) Voltage-controlled magnetic anisotropy using interface-controlled tunnel junction, (2) Spin-to-charge conversion using metal/organic interface, and (3) Reservoir computing using spintronics devices. In the topic (1), we have performed experiments using interface-controlled devices. For instance, we studied FeCoPtPd/MgO junction with various composition ratio of the Co, Pt and Pd. Specifically, we performed tunnel spectroscopy to characterize the correlation between interface electronic states and the voltage-controlled magnetic anisotropy. As a result, we find that interface resonant state enhances the voltage effect. We have also published a review paper on this topic. In the topic (2), we find that it is feasible to obtain efficient inverse Rashba-Edelstein effect at an interface between copper and lead-phthalocyanine in collaboration with Otani group. In the topic (3), we performed both experimental and theoretical study to evaluate the figure-of-merit of physical reservoir computing using spintronics devices.

1. Voltage-Controlled Magnetic Anisotropy in Fe<sub>1-x</sub>Cox/Pd/MgO system: A. K. Shukla, M. Goto, X. Xu, K. Nawaoka, J. Suwardy, T. Ohkubo, K. Hono, S. Miwa and Y. Suzuki, *Sci Rep* **8** (2018) 10362 (1-6).
2. Quantitative and systematic analysis of bias dependence of spin accumulation voltage in a nondegenerate Si-based spin valve: S. Lee, F. Rortais, R. Ohshima, Y. Ando, S. Miwa, Y. Suzuki, H. Koike and M. Shiraishi, *Phys. Rev. B* **99** (2019) 064408 (1-6).
3. Voltage-controlled magnetic anisotropy and Dzyaloshinskii-Moriya interactions in CoNi/MgO and CoNi/Pd/MgO: J. Suwardy, M. Goto, Y. Suzuki and S. Miwa, *Jpn. J. Appl. Phys.* **58** (2019) 060917 (1-4).
4. Magnetic anisotropy of ferromagnetic metals in low-symmetry systems: Y. Suzuki and S. Miwa, *Physics Letters A* **383** (2019) 1203-1206.
5. Perpendicular magnetic anisotropy and its electric-field-induced change at metal-dielectric interfaces: S. Miwa, M. Suzuki, M. Tsujikawa, T. Nozaki, T. Nakamura, M. Shirai, S. Yuasa and Y. Suzuki, *J. Phys. D: Appl. Phys.* **52** (2019) 063001 (1-22).

## Materials Design and Characterization Laboratory

### Hiroi group

We revisit the superconducting pyrochlore oxide Cd<sub>2</sub>Re<sub>2</sub>O<sub>7</sub> with a particular emphasis on the sample-quality issue. The compound has drawn attention as the only superconductor (T<sub>c</sub> = 1.0 K) that has been found in the family of α-pyrochlore oxides since its discovery in 2001. Moreover, it exhibits two characteristic structural transitions from the cubic pyrochlore structure, with the inversion symmetry broken at the first one at 200 K. Recently, it has attracted increasing attention as a candidate spin-orbit coupled metal (SOCM), in which specific Fermi liquid instability is expected to lead to an odd-parity order with spontaneous inversion-symmetry breaking and parity-mixing superconductivity. We show that a synthetic copper mineral, Cd-kapellaite, which comprises a kagomé lattice consisting of corner-sharing triangles of spin-1/2 Cu<sup>2+</sup> ions, exhibits an unprecedented

---

† Joint research with outside partners.

series of fractional magnetization plateaus in ultrahigh magnetic fields of up to 160 T. We propose that these quantum states can be interpreted as crystallizations of emergent magnons localized on the hexagon of the kagomé lattice.

1. \*Experimental and Theoretical Studies of the Metallic Conductivity in Cubic  $\text{PbVO}_3$  under High Pressure: K. Oka, T. Yamauchi, S. Kanungo, T. Shimazu, K. Oh-ishi, Y. Uwatoko, M. Azuma and T. Saha-Dasgupta, *J. Phys. Soc. Jpn.* **87** (2018) 024801 (1-6).
2. \*Formation and Control of Twin Domains in the Pyrochlore Oxide  $\text{Cd}_2\text{Re}_2\text{O}_7$ : Y. Matsubayashi, D. Hirai, M. Tokunaga and Z. Hiroi, *J. Phys. Soc. Jpn.* **87** (2018) 104604 (1-7).
3. Frustrated Magnetism of Pharmacosiderite Comprising Tetrahedral Clusters Arranged in the Primitive Cubic Lattice: R. Okuma, T. Yajima, T. Fujii, M. Takano and Z. Hiroi, *J. Phys. Soc. Jpn.* **87** (2018) 093702.
4. \*Inelastic Neutron Scattering Study of the Spin Dynamics in the Breathing Pyrochlore System  $\text{LiGa}_{0.95}\text{In}_{0.05}\text{Cr}_4\text{O}_8$ : Y. Tanaka, R. Wawrzynczak, M. D. Le, T. Guidi, Y. Okamoto, T. Yajima, Z. Hiroi, M. Takigawa and G. J. Nilsen, *J. Phys. Soc. Jpn.* **87** (2018) 073710.
5. †\*Improvement of coercivity in Nd-Fe-B nanocomposite magnets: T. Saito, S. Nozaki and D. Nishio-Hamane, *J. Magn. Mater.* **445** (2018) 49-52.
6. \*Devil's staircase of odd-number charge order modulations in divalent  $\beta$ -vanadium bronzes under pressure: T. Yamauchi, H. Ueda, K. Ohwada, H. Nakao and Y. Ueda, *Phys. Rev. B* **97** (2018) 125138.
7. \*Frustrated magnetism of the maple-leaf-lattice antiferromagnet  $\text{MgMn}_3\text{O}_7 \cdot 3\text{H}_2\text{O}$ : Y. Haraguchi, A. Matsuo, K. Kindo and Z. Hiroi, *Phys. Rev. B* **98** (2018) 064412 (1-7).
8. \*Magnetic state selected by magnetic dipole interaction in the kagome antiferromagnet  $\text{NaBa}_2\text{Mn}_3\text{F}_{11}$ : S. Hayashida, H. Ishikawa, Y. Okamoto, T. Okubo, Z. Hiroi, M. Avdeev, P. Manuel, M. Hagihala, M. Soda and T. Masuda, *Phys. Rev. B* **97** (2018) 054411 (1-7).
9. †\*Kannanite, a new mineral from Kannan Mountain, Japan: D. NISHIO-HAMANE, M. NAGASHIMA, N. OGAWA and T. MINAKAWA, *Journal of Mineralogical and Petrological Sciences* **113** (2018) 245.
10. †\*High-coercivity  $\text{SmCo}_5/\alpha$ -Fe nanocomposite magnets: T. Saito and D. Nishio-Hamane, *J. Alloys Compd.* **735** (2018) 218-223.
11. \*Giant anomalous Nernst effect and quantum-critical scaling in a ferromagnetic semimetal: A. Sakai, Y. P. Mizuta, A. A. Nugroho, R. Sihombing, T. Koretsune, M.-T. Suzuki, N. Takemori, R. Ishii, D. Nishio-Hamane, R. Arita, P. Goswami and S. Nakatsuji, *Nature Phys.* **14** (2018) 1119-1124.
12. Expanding frontiers in materials chemistry and physics with multiple anions: H. Kageyama, K. Hayashi, K. Maeda, J. Paul Attfield, Z. Hiroi, J. M. Rondinelli and K. R. Poeppelmeier, *Nat. Commun.* **9** (2018) 772 (1-15).
13. †\*Synthesis of anti-perovskite-type carbides and nitrides from metal oxides and melamine: D. Hirai, H. Tanaka, D. Nishio-Hamane and Z. Hiroi, *RSC Adv.* **8** (2018) 42025.
14. †\*Magnetic and thermoelectric properties of melt-spun ribbons of  $\text{Fe}_2\text{XAl}$  ( $\text{X} = \text{Co}, \text{Ni}$ ) Heusler compounds: T. Saito and D. Nishio-Hamane, *Journal of Applied Physics* **124** (2018) 075105.
15. †\*Quantum valence criticality in a correlated metal: K. Kuga, Y. Matsumoto, M. Okawa, S. Suzuki, T. Tomita, K. Sone, Y. Shimura, T. Sakakibara, D. Nishio-Hamane, Y. Karaki, Y. Takata, M. Matsunami, R. Eguchi, M. Taguchi, A. Chainani, S. Shin, K. Tamasaku, Y. Nishino, M. Yabashi, T. Ishikawa and S. Nakatsuji, *Sci. Adv.* **4** (2018) eaao3547 (1-6).
16. †\*Large enhancement of the spin Hall effect in Mn metal by Sn doping: D. Qu, T. Higo, T. Nishikawa, K. Matsumoto, K. Kondou, D. Nishio-Hamane, R. Ishii, P. K. Muduli, Y. Otani and S. Nakatsuji, *Phys. Rev. Materials* **2** (2018) 102001.
17. †\*Size-controllable gold nanoparticles prepared from immobilized gold-containing ionic liquids on SBA-15: E. N. Kusumawati, D. Nishio-Hamane and T. Sasaki, *Catalysis Today* **309** (2018) 109.
18. †\*Transmission electron microscopy study of the epitaxial association of hedenbergite whiskers with babingtonite: M. Nagashima and D. Nishio-Hamane, *Mineral. mag.* **82** (2018) 23.
19. †\*Aurhydrargyrumite, a Natural  $\text{Au}_6\text{Hg}_5$  Phase from Japan: D. Nishio-Hamane, T. Tanaka and T. Minakawa, *Minerals* **8** (2018) 415.

---

\* Joint research among groups within ISSP.

20. †\*Ionic Liquid Immobilized on Graphene-Oxide-Containing Palladium Metal Ions as an Efficient Catalyst for the Alkoxy, Amino, and Phenoxy Carbonylation Reactions: V. V. Gaikwad, V. B. Saptal, K. Harada, T. Sasaki, D. Nishio-Hamane and B. M. Bhanage, *ChemNanoMat* **4** (2018) 575.
21. One-dimensionalization by Geometrical Frustration in the Anisotropic Triangular Lattice of the 5d Quantum Antiferromagnet  $\text{Ca}_3\text{ReO}_5\text{Cl}_2$ : D. Hirai, K. Nawa, M. Kawamura, T. Misawa and Z. Hiroi, *J. Phys. Soc. Jpn.* **88** (2019) 044708.
22. Crystal structure and magnetic properties of the 5d transition metal oxides  $\text{AOsO}_4$  (A = K, Rb, Cs): J.-I. Yamaura and Z. Hiroi, *Phys. Rev. B* **99** (2019) 155113.
23. †\*Magnetoelastic couplings in the deformed kagome quantum spin lattice of volborthite: A. Ikeda, S. Furukawa, O. Janson, Y. H. Matsuda, S. Takeyama, T. Yajima, Z. Hiroi and H. Ishikawa, *Phys. Rev. B* **99** (2019) 140412(R) 1-5.
24. \*カゴメ銅鉱物ボルボサイトにおける軌道転移とフラストレート磁性: 広井 善二, 石川 孟, 小濱 芳允, *固体物理* **54** (2019) 117-130.
25. Weak Anisotropic Lithium-Ion Conductivity in Single Crystals of  $\text{Li}_{10}\text{GeP}_2\text{S}_{12}$ : R. Iwasaki, S. Hori, R. Kanno, T. Yajima, D. Hirai, Y. Kato and Z. Hiroi, *Chem. Mater.* **31** (2019) 3694.
26. \*A series of magnon crystals appearing under ultrahigh magnetic fields in a kagomé antiferromagnet: R. Okuma, D. Nakamura, T. Okubo, A. Miyake, A. Matsuo, K. Kindo, M. Tokunaga, N. Kawashima, S. Takeyama and Z. Hiroi, *Nature Communications* **10** (2019) 1229(7).
27. \*Possible observation of quantum spin-nematic phase in a frustrated magnet: Y. Kohama, H. Ishikawa, A. Matsuo, K. Kindo, N. Shannon and Z. Hiroi, *Proc. Nat. Acad. Sci. U.S.A.* **116** (2019) 10686-10690.
28. \*Transmission electron microscopy study of the epitaxial association of hedenbergite whiskers with babingtonite: M. Nagashima and D. Nishio-Hamane, *Mineral. Mag.* (2018) 1, accepted for publication.
29. Weak Anisotropic Lithium-Ion Conductivity in Single Crystals of  $\text{Li}_{10}\text{GeP}_2\text{S}_{12}$ : R. Iwasaki, S. Hori, R. Kanno, T. Yajima, D. Hirai, Y. Kato and Z. Hiroi, *Chem. Mater.* (2019) acs.chemmater.9b00420, in print.

## Kawashima group

We have been investigating quantum spin/boson systems and frustrated systems by means of large-scale numerical simulation. We also develop new numerical techniques. Our group's activities of 2018 include: (1) tensor-network study of frustrated quantum spin systems, such as S=1 bilinear-biquadratic model and kagome antiferromagnet, and comparison with experimental results, (2) efficient implementation of real-space renormalization group in tensor-network representation, (3) molecular-dynamics simulation of complex fluids, and (4) Monte Carlo simulation study classical statistical mechanical models.

1. Disordered quantum spin chains with long-range antiferromagnetic interactions: N. Moure, H.-Y. Lee, S. Haas, R. N. Bhatt and S. Kettmann, *Phys. Rev. B* **97** (2018) 014206 (1-6).
2. Spin-one bilinear-biquadratic model on a star lattice: H.-Y. Lee\* and N. Kawashima, *Phys. Rev. B* **97** (2018) 205123 (1-7).
3. \*Spin Thermal Hall Conductivity of a Kagome Antiferromagnet: H. Doki, M. Akazawa, H.-Y. Lee, J. H. Han, K. Sugii, M. Shimozawa, N. Kawashima, M. Oda, H. Yoshida and M. Yamashita, *Phys. Rev. Lett.* **121** (2018) 097203.
4. Tensor renormalization group with randomized singular value decomposition: S. Morita, R. Igarashi, H.-H. Zhao and N. Kawashima, *Phys. Rev. E* **97** (2018) 033310 (1-6).
5. How to experimentally probe universal features of absorbing phase transitions using steady state: K. Tamai and M. Sano, *J. Stat. Mech.* **2018** (2018) 123207 (24pages).
6. †\*Polymer effects on Kármán vortex: Molecular dynamics study: Y. Asano, H. Watanabe and H. Noguchi, *The Journal of Chemical Physics* **148** (2018) 144901.
7. Stability of velocity-Verlet- and Liouville-operator-derived algorithms to integrate non-Hamiltonian systems: H. Watanabe, *The Journal of Chemical Physics* **149** (2018) 154101(1-10).
8. Fast Algorithm for Generating Random Bit Strings and Multispin Coding for Directed Percolation: H. Watanabe, S. Morita, S. Todo and N. Kawashima, *J. Phys. Soc. Jpn.* **88** (2019) 024004 (8pages).
9. Calculation of higher-order moments by higher-order tensor renormalization group: S. Morita and N. Kawashima, *Computer Physics Communications* **236** (2019) 65-71.

---

† Joint research with outside partners.

10. \*SIMD vectorization for the Lennard-Jones potential with AVX2 and AVX-512 instructions: H. Watanabe and K. M. Nakagawa, *Computer Physics Communications* **237** (2019) 1-7.
11. \*A series of magnon crystals appearing under ultrahigh magnetic fields in a kagomé antiferromagnet: R. Okuma, D. Nakamura, T. Okubo, A. Miyake, A. Matsuo, K. Kindo, M. Tokunaga, N. Kawashima, S. Takeyama and Z. Hiroi, *Nature Communications* **10** (2019) 1229(7).

## Uwatoko group

We report a high-pressure study on the heavily electron doped  $\text{Li}_{0.36}(\text{NH}_3)_y\text{Fe}_2\text{Se}_2$  single crystal by using a cubic anvil cell apparatus. The superconducting transition temperature  $T_c \approx 44\text{K}$  at ambient pressure is first suppressed to below 20 K upon increasing pressure to  $P_c \approx 2\text{GPa}$ , above which the pressure dependence of  $T_c(P)$  reverses and  $T_c$  increases steadily to ca. 55 K at 11 GPa. These results thus evidence a pressure-induced second high- $T_c$  superconducting (SC-II) phase in  $\text{Li}_{0.36}(\text{NH}_3)_y\text{Fe}_2\text{Se}_2$  with the highest  $T_{\text{max}} \approx 55\text{K}$  among the FeSe-based bulk materials. We report two distinct superconducting states with different crystal structures and a crossover from a type-II to a type-I superconductor (SC) in  $(\text{Ba}, \text{Sr})\text{Bi}_3$ . The superconducting parameters are revealed to classify two SCs:  $\text{BaBi}_3$  is in the weak-coupling limit on the basis of  $\Delta C/\gamma n T_c \sim 0.67$  and  $2\Delta/k_B T_c \sim 3.28$  while  $\text{SrBi}_3$  is a strong-coupling SC with  $\Delta C/\gamma n T_c \sim 2.41$  and  $2\Delta/k_B T_c \sim 6.09$ . With increasing the pressure, the  $T_c$  of  $\text{BaBi}_3$  decreases linearly at first, and then shows an abrupt increase up to 6.2 K at 0.88 GPa.  $T_c$  of  $\text{SrBi}_3$  is suppressed monotonously by pressure. Possible physical mechanisms are proposed. The coexistence of superconductivity (SC) and charge density waves (CDWs) was investigated for pure and Se-doped  $1\text{T-TaS}_2$  via electrical resistivity under hydrostatic pressure. A pressure-induced superconducting state coexists with various CDWs, then bulk SC emerges along with the complete collapse of various CDWs. The superconducting transition temperature increases monotonously up to  $\sim 7.3\text{K}$  at 15 GPa without a dome-like shape. The results clarify that the superconducting Cooper pairing is associated with the CDWs' instability near  $P_c(x)$ . The electrical resistivity and magnetization of a single crystal of  $\text{Ce}_2\text{Ni}_3\text{Ge}_5$  heavy fermion compound were performed under pressure. On applying pressure, the two antiferromagnetic transitions merged at 1 GPa. At higher pressures, the antiferromagnetic transition temperature decreases, and disappears. It is suggesting that the critical pressure of  $\text{Ce}_2\text{Ni}_3\text{Ge}_5$  was 4.1 GPa. Polarized neutron analyses on  $\text{MnP}$  were applied to two different helical magnetic structures (helical-c and helical-b). Helicity was observed in the both structures. The two helical domain ratio becomes more unbalanced in the helical-b structure at a higher pressure, suggesting that the Dzyaloshinskii-Moriya interaction, which is enhanced by a local structural strain, could be related with the helical structures.

1. †Emergence of a new valence-ordered structure and collapse of the magnetic order under high pressure in  $\text{EuPtP}$ : A. Mitsuda, S. Manabe, M. Umeda, H. Wada, K. Matsubayashi, Y. Uwatoko, M. Mizumaki, N. Kawamura, K. Nitta, N. Hirao, Y. Ohishi and N. Ishimatsu, *J. Phys.: Condens. Matter* **30** (2018) 105603 (1-8).
2. Magnetic order of  $\text{Nd}_5\text{Pb}_3$  single crystals: J.-Q. Yan, M. Ochi, H. B. Cao, B. Sapiro, J.-G. Cheng, Y. Uwatoko, R. Arita, B. C. Sales and D. G. Mandrus, *J. Phys.: Condens. Matter* **30** (2018) 135801 (1-9).
3. †Direct Observation of the Quantum Phase Transition of  $\text{SrCu}_2(\text{BO}_3)_2$  by High-Pressure and Terahertz Electron Spin Resonance: T. Sakurai, Y. Hirao, K. Hijii, S. Okubo, H. Ohta, Y. Uwatoko, K. Kudo and Y. Koike, *J. Phys. Soc. Jpn.* **87** (2018) 033701 (1-4).
4. †Effects of Magnetic Field and Pressure on the Valence-Fluctuating Antiferromagnetic Compound  $\text{EuPt}_2\text{Si}_2$ : T. Takeuchi, T. Yara, Y. Ashitomi, W. Iha, M. Kakihana, M. Nakashima, Y. Amako, F. Honda, Y. Homma, D. Aoki, Y. Uwatoko, T. Kida, T. Tahara, M. Hagiwara, Y. Haga, M. Hedo, T. Nakama and Y. Onuki, *J. Phys. Soc. Jpn.* **87** (2018) 074709 (1-14).
5. †Electronic States in  $\text{EuCu}_2(\text{Ge}_{1-x}\text{Si}_x)_2$  Based on the Doniach Phase Diagram: W. Iha, T. Yara, Y. Ashitomi, M. Kakihana, T. Takeuchi, F. Honda, A. Nakamura, D. Aoki, J. Gouchi, Y. Uwatoko, T. Kida, T. Tahara, M. Hagiwara, Y. Haga, M. Hedo, T. Nakama and Y. Onuki, *J. Phys. Soc. Jpn.* **87** (2018) 064706 (1-14).
6. \*Experimental and Theoretical Studies of the Metallic Conductivity in Cubic  $\text{PbVO}_3$  under High Pressure: K. Oka, T. Yamauchi, S. Kanungo, T. Shimazu, K. Oh-ishi, Y. Uwatoko, M. Azuma and T. Saha-Dasgupta, *J. Phys. Soc. Jpn.* **87** (2018) 024801 (1-6).
7. †Pressure Effect on Magnetic Properties of Weak Itinerant Electron Ferromagnet  $\text{CrAlGe}$ : S. Yoshinaga, Y. Mitsui, R. Y. Umetsu, Y. Uwatoko and K. Koyama, *J. Phys. Soc. Jpn.* **87** (2018) 014701 (1-4).
8. †Structural, Magnetic, and Transport Properties of Novel Quaternary Compounds  $\text{RRu}_2\text{Sn}_2\text{Zn}_{18}$  (R= La, Pr, and Nd): K. Wakiya, Y. Sugiyama, M. Kishimoto, T. D. Matsuda, Y. Aoki, M. Uehara, J. Gouchi, Y. Uwatoko and I. Umehara, *J. Phys. Soc. Jpn.* **87** (2018) 094706 (1-6).
9. Time and Magnetic Field Variations of Magnetic Structure in the Triangular Lattice Magnet  $\text{Ca}_3\text{Co}_2\text{O}_6$ : K. Motoya, T. Kihara, H. Nojiri, Y. Uwatoko, M. Matsuda and T. Hong, *J. Phys. Soc. Jpn.* **87** (2018) 114703 (1-11).

---

\* Joint research among groups within ISSP.

10. High- $T_c$  superconductivity up to 55 K under high pressure in a heavily electron doped  $\text{Li}_{0.36}(\text{NH}_3)_y\text{Fe}_2\text{Se}_2$  single crystal: P. Shahi, J. P. Sun, S. H. Wang, Y. Y. Jiao, K. Y. Chen, S. S. Sun, H. C. Lei, Y. Uwatoko, B. S. Wang and J. -G. Cheng, *Phys. Rev. B* **97** (2018) 020508 (1-6).
11. †Pressure effect on the magnetic properties of the half-metallic Heusler alloy  $\text{Co}_2\text{TiSn}$ : I. Shigeta, Y. Fujimoto, R. Ooka, Y. Nishisako, M. Tsujikawa, R. Y. Umetsu, A. Nomura, K. Yubuta, Y. Miura, T. Kanomata, M. Shirai, J. Gouchi, Y. Uwatoko and M. Hiroi, *Phys. Rev. B* **97** (2018) 104414 (1-8).
12. \*Pressure-induced quantum phase transition in the quantum antiferromagnet  $\text{CsFeCl}_3$ : S. Hayashida, O. Zaharko, N. Kurita, H. Tanaka, M. Hagihala, M. Soda, S. Itoh, Y. Uwatoko and T. Masuda, *Phys. Rev. B* **97** (2018) 140405 (1-4).
13. Two distinct superconducting phases and pressure-induced crossover from type-II to type-I superconductivity in the spin-orbit-coupled superconductors  $\text{BaBi}_3$  and  $\text{SrBi}_3$ : B. Wang, X. Luo, K. Ishigaki, K. Matsubayashi, J. Cheng, Y. Sun and Y. Uwatoko, *Phys. Rev. B* **98** (2018) 220506.
14. Universal phase diagram of superconductivity and charge density wave versus high hydrostatic pressure in pure and Se-doped  $1\text{T-TaS}_2$ : B. Wang, Y. Liu, X. Luo, K. Ishigaki, K. Matsubayashi, W. Lu, Y. Sun, J. Cheng and Y. Uwatoko, *Phys. Rev. B* **97** (2018) 220504 (1-7).
15. †Magnetocaloric effect in single-crystal  $\text{HoNi}$  with a canted magnetic structure: N. Kinami, K. Wakiya, M. Uehara, J. Gouchi, Y. Uwatoko and I. Umehara, *Jpn. J. Appl. Phys.* **57** (2018) 103001 (1-4).
16. †Magnetic Phase Transition of  $\text{Mn}_{1.9}\text{Fe}_{0.1}\text{Sb}_{0.9}\text{Sn}_{0.1}$ : A. N. Nwodo, R. Kobayashi, T. Wakamori, Y. Matsumoto, Y. Mitsui, R. Y. Umetsu, M. Hiroi, K. Takahashi, Y. Uwatoko and K. Koyama, *IEEE Magn. Lett.* **9** (2018) 1 (1-4).
17. †Quasi-First Order Magnetic Transition in  $\text{Mn}_{1.9}\text{Fe}_{0.1}\text{Sb}_{0.9}\text{Sn}_{0.1}$ : A. N. Nwodo, R. Kobayashi, T. Wakamori, Y. Matsumoto, Y. Mitsui, M. Hiroi, K. Takahashi, R. Y. Umetsu, Y. Uwatoko and K. Koyama, *Mater. Trans.* **59** (2018) 348-352.
18. †Anomalous pressure effect on the Néel temperature and volume of  $\text{DyB}_6$ : T. Eto, G. Oomi, T. Sakai, Y. Uwatoko and S. Kunii, *AIP Advances* **8** (2018) 101320 (1-5).
19. †Cu-substitution effects on the magnetic properties of weak itinerant electron ferromagnet  $\text{CrAlGe}$ : H. Masumitsu, S. Yoshinaga, Y. Mitsui, R. Y. Umetsu, M. Hiroi, Y. Uwatoko and K. Koyama, *AIP Advances* **8** (2018) 101426 (1-5).
20. †Magnetic and thermodynamic properties of Heusler alloys  $\text{Ni}_{55}\text{Mn}_{26}\text{Al}_{19}$ : M. Ito, K. Onda, A. Taira, K. Sonoda, M. Hiroi and Y. Uwatoko, *AIP Advances* **8** (2018) 055712.
21. †Magnetic and transport properties of single crystalline  $\text{RCO}_x\text{Sn}_2$  ( $R = \text{Ce}$  and  $\text{La}$ ): M. Kimura, K. Wakiya, T. Tomaki, J. Gouchi, Y. Uwatoko, M. Uehara and I. Umehara, *AIP Advances* **8** (2018) 101304 (1-5).
22. †Magnetic characteristics of  $\text{RPd}_2\text{Si}_2$  ( $R = \text{Rare earth}$ ): K. Uchima, Y. Uwatoko and T. Shigeoka, *AIP Advances* **8** (2018) 101425 (1-6).
23. †Magnetic fluctuations under pressure on S-doped  $\text{FeSe}$  studied via  $^{77}\text{Se}$  NMR: T. Kuwayama, K. Matsuura, Y. Mizukami, S. Kasahara, Y. Matsuda, T. Shibauchi, Y. Uwatoko and N. Fujiwara, *AIP Advances* **8** (2018) 101308 (1-6).
24. †Magnetic properties of  $\text{Mn}_{1-x}\text{TM}_x\text{AlGe}$  ( $\text{TM} = \text{V}, \text{Fe}, \text{Cu}$ ) with  $\text{Cu}_2\text{Sb}$ -type structure: K. Noguchi, H. Masumitsu, Y. Mitsui, R. Y. Umetsu, M. Hiroi, Y. Uwatoko and K. Koyama, *AIP Advances* **8** (2018) 101433 (1-5).
25. Metal-insulator transition in Mott-insulator  $\text{FePS}_3$ : M. Tsurubayashi, K. Kodama, M. Kano, K. Ishigaki, Y. Uwatoko, T. Watanabe, K. Takase and Y. Takano, *AIP Advances* **8** (2018) 101307 (1-4).
26. Pressure effect on the antiferromagnetic compound  $\text{Ce}_2\text{Ni}_3\text{Ge}_5$ : J. Gouchi, Y. Nakamura, M. Nakashima, Y. Amako, R. Kumar and Y. Uwatoko, *AIP Advances* **8** (2018) 101323 (1-5).
27. Reemergence of high- $T_c$  superconductivity in the  $(\text{Li}_{1-x}\text{Fe}_x)\text{OHFe}_{1-y}\text{Se}$  under high pressure: J. P. Sun, P. Shahi, H. X. Zhou, Y. L. Huang, K. Y. Chen, B. S. Wang, S. L. Ni, N. N. Li, K. Zhang, W. G. Yang, Y. Uwatoko, G. Xing, J. Sun, D. J. Singh, K. Jin, F. Zhou, G. M. Zhang, X. L. Dong, Z. X. Zhao and J. -G. Cheng, *Nat. Commun.* **9** (2018) 380 (1-7).
28. \*Evolution of Magnetic Double Helix and Quantum Criticality near a Dome of Superconductivity in  $\text{CrAs}$ : M. Matsuda, F. K. Lin, R. Yu, J.-G. Cheng, W. Wu, J. P. Sun, J. H. Zhang, P. J. Sun, K. Matsubayashi, T. Miyake, T. Kato, J.-Q. Yan, M. B. Stone, Q.-M. Si, J. L. Luo and Y. Uwatoko, *Phys. Rev. X* **8** (2018) 031017 (1-12).
29. †Anisotropic lattice compression of  $\alpha$ - and  $\beta$ - $\text{CePdZn}$ : G. Oomi, T. Eto, T. Okada and Y. Uwatoko, *Physica B: Condensed Matter* **536** (2018) 293.

---

† Joint research with outside partners.

30. †Fundamental properties of a new samarium compound SmPtSi<sub>2</sub>: S. Yamaguchi, E. Takahashi, N. Kase, T. Nakano, N. Takeda, K. Matsubayashi and Y. Uwatoko, *Physica B: Condensed Matter* **536** (2018) 297-299.
31. †Magnetic characteristics of polymorphic single crystal compounds DyIr<sub>2</sub>Si<sub>2</sub>: K. Uchima, T. Shigeoka and Y. Uwatoko, *Physica B: Condensed Matter* **536** (2018) 28.
32. †Magnetic properties and effect of pressure on the electronic state of EuCo<sub>2</sub>Ge<sub>2</sub>: Y. Ashitomi, M. Kakihana, F. Honda, A. Nakamura, D. Aoki, Y. Uwatoko, M. Nakashima, Y. Amako, T. Takeuchi, T. Kida, T. Tahara, M. Hagiwara, Y. Haga, M. Hedo, T. Nakama and Y. Onuki, *Physica B: Condensed Matter* **536** (2018) 192196.
33. †Magnetic properties of new antiferromagnetic heavy-fermion compounds, Ce<sub>3</sub>TiBi<sub>5</sub> and CeTi<sub>3</sub>Bi<sub>4</sub>: G. Motoyama, M. Sezaki, J. Gouchi, K. Miyoshi, S. Nishigori, T. Mutou, K. Fujiwara and Y. Uwatoko, *Physica B: Condensed Matter* **536** (2018) 142-144.
34. Polarized neutron diffraction study in helical magnetic phases of MnP: M. Matsuda, S. E. Dissanayake, J. -G. Cheng, J. Ma, J. -Q. Yan and Y. Uwatoko, *Physica B: Condensed Matter* **551** (2018) 115-117.
35. †Pressure effects on the magnetic and transport properties of the Kondo lattice system Ce<sub>3</sub>RuSn<sub>6</sub>: K. Wakiya, T. Tomaki, M. Kimura, M. Uehara, J. Gouchi, Y. Uwatoko and I. Umehara, *Physica B: Condensed Matter* **536** (2018) 492-493.
36. †Successive magnetic transitions of the pseudo-ternary compounds Ho<sub>1-x</sub>R<sub>x</sub>Rh<sub>2</sub>Si<sub>2</sub>(R=Y, La): T. Shigeoka, K. Uchima and Y. Uwatoko, *Physica B: Condensed Matter* **536** (2018) 379-383.
37. Pressure-induced coherent sliding-layer transition in the excitonic insulator Ta<sub>2</sub>NiSe<sub>5</sub>: A. Nakano, K. Sugawara, S. Tamura, N. Katayama, K. Matsubayashi, T. Okada, Y. Uwatoko, K. Munakata, A. Nakao, H. Sagayama, R. Kumai, K. Sugimoto, N. Maejima, A. Machida, T. Watanuki and H. Sawa, *IUCrJ* **5** (2018) 158-165.
38. †Magnetic and structural properties of Mn<sub>1-x</sub>Cr<sub>x</sub>AlGe (0 < x < 1.0): H. Masumitsu, S. Yoshinaga, Y. Mitsui, R. Y. Umetsu, M. Hiroi, Y. Uwatoko and K. Koyama, *Journal of Magnetism and Magnetic Materials* **456** (2018) 104-107.
39. †Magnetic relaxation dynamics in thermally arrested Cr-modified Mn<sub>2</sub>Sb: Y. Mitsui, Y. Matsumoto, Y. Uwatoko, M. Hiroi and K. Koyama, *Journal of Magnetism and Magnetic Materials* **461** (2018) 62-68.
40. The formation of bulk β-Al<sub>3</sub> Ni phase in eutectic Al-5.69wt%Ni alloy solidified under high pressure: X. H. Wang, Z. Ran, Z. J. Wei, C. M. Zou, H. W. Wang, J. Gouchi and Y. Uwatoko, *Journal of Alloys and Compounds* **742** (2018) 670-675.
41. Cubic anvil cell apparatus for high-pressure and low-temperature physical property measurements: J.-G. Cheng, B.-S. Wang, J.-P. Sun and Y. Uwatoko, *Chinese Phys. B* **27** (2018) 077403 (1-7).
42. Pressure-induced phase transitions and superconductivity in a black phosphorus single crystal: X. Li, J. Sun, P. Shahi, M. Gao, A. H. MacDonald, Y. Uwatoko, T. Xiang, J. B. Goodenough, J. Cheng and J. Zhou, *Proc Natl Acad Sci USA* **115** (2018) 9935.
43. Effect of pressure on the self-hole-doped superconductor RbGd<sub>2</sub>Fe<sub>4</sub>As<sub>4</sub>O<sub>2</sub>: J. P. Sun, Z.-C. Wang, Z. Y. Liu, S. X. Xu, T. Eto, Y. Sui, B. S. Wang, Y. Uwatoko, G.-H. Cao and J.-G. Cheng, *J. Phys.: Condens. Matter* **31** (2019) 044001 (1-7).
44. <sup>77</sup>Se-NMR Study under Pressure on 12%-S Doped FeSe: T. Kuwayama, K. Matsuura, Y. Mizukami, S. Kasahara, Y. Matsuda, T. Shibauchi, Y. Uwatoko and N. Fujiwara, *J. Phys. Soc. Jpn.* **88** (2019) 033703.
45. Temperature–Pressure Phase Diagram of Antiferromagnet CeAl: R. Tsunoda, Y. Hirose, T. Koitabashi, Y. Sase, R. Kulkarni, A. Thamizhavel, S. K. Dhar, J. Gouchi, Y. Uwatoko and R. Settai, *J. Phys. Soc. Jpn.* **88** (2019) 034707 (1-5).
46. Exotic superconductivity in noncentrosymmetric and magnetic CeNiC<sub>2</sub> revealed under high pressure: S. Katano, M. Ito, K. Shibata, J. Gouchi, Y. Uwatoko, K. Matsubayashi, H. Soeda and H. Takahashi, *Phys. Rev. B* **99** (2019) 100501 (1-5).
47. Pressure-induced enhancement of superconductivity and quantum criticality in the 12442-type hybrid-structure superconductor KCa<sub>2</sub>F<sub>4</sub>As<sub>4</sub>F<sub>2</sub>: B. Wang, Z.-C. Wang, K. Ishigaki, K. Matsubayashi, T. Eto, J. Sun, J.-G. Cheng, G.-H. Cao and Y. Uwatoko, *Phys. Rev. B* **99** (2019) 014501 (1-6).
48. †Magnetic anisotropy of single-crystal ferromagnetic Ce<sub>3</sub>RuSn<sub>6</sub>: K. Wakiya, T. Tomaki, M. Kimura, M. Uehara, J. Gouchi, Y. Uwatoko and I. Umehara, *Journal of Magnetism and Magnetic Materials* **471** (2019) 274-277.
49. †Anomalous ferromagnetic ordering in EuCuP: W. Iha, M. Kakihana, S. Matsuda, F. Honda, Y. Haga, T. Takeuchi, M. Nakashima, Y. Amako, J. Gouchi, Y. Uwatoko, M. Hedo, T. Nakama and Y. Onuki, *Journal of Alloys and Compounds* **788** (2019) 361-366.

---

\* Joint research among groups within ISSP.

50. The effects of high pressure and superheating on the planar growth of Al<sub>3</sub>Ni phase in hypo-peritectic Al-30wt%Ni alloy: X. H. Wang, H. W. Wang, C. M. Zou, Z. J. Wei, Y. Uwatoko, J. Gouchi, D. Nishio-Hamane and H. Gotou, *Journal of Alloys and Compounds* **772** (2019) 1052-1060.
51. Enhancement of superconducting properties and flux pinning mechanism on Cr<sub>0.0005</sub>NbSe<sub>2</sub> single crystal under Hydrostatic pressure: S. Arumugam, M. Krishnan, K. Ishigaki, J. Gouchi, R. Pervin, G. Kalai Selvan, P. M. Shirage and Y. Uwatoko, *Sci Rep* **9** (2019) 347 (1-12).
52. Correction for Li et al., Pressure-induced phase transitions and superconductivity in a black phosphorus single crystal: X. Li, J. Sun, P. Shahi, M. Gao, A. H. MacDonald, Y. Uwatoko, T. Xiang, J. B. Goodenough, J. Cheng and J. Zhou, *Proc Natl Acad Sci USA* **116** (2019) 1065.
53. Nuanced superconductivity in endohedral gallide Mo<sub>8</sub>Ga<sub>41</sub>: P. Neha<sup>1</sup>, P. Sivaprakash, K. Ishigaki, G. Kalaiselvan, K. Manikandan, R. S. Dhaka and Y. Uwatoko, *Materials Research Express* **6** (2019) 016002.

## Ozaki group

In collaboration with experimental groups, we have investigated novel three kinds of surface structures and its electronic states by means of first-principles electronic structure methods based on density functional theory (DFT). (i) We identified detailed structures of two energetically competing root-13 x root-13 R13.9°silicene on Ag (111) surface which were recently revealed by scanning tunneling microscopy (STM) and atomic force microscopy (AFM). Simulations of AFM suggested that attractive interaction with the tip pulls up buckled down Si atoms which causes local flips of the buckled structures, leading to an understanding of the mechanism of experimental high-resolution AFM imaging. (ii) In single-atom catalysis, the atomic structure and local electronic states of single atoms on a supporting material remain a fundamental question. We experimentally and theoretically solved these problems for single Pt atoms dispersed on freestanding graphene using plasma sputtering. First-principles calculations elucidated that the Pt 5dxy-orbital in the step edge plays a crucial role in the formation of chemical bonds to C atoms and in the considerable charge transfer from Pt to C atoms, resulting in the large binding energy shift of the Pt 4f state. (iii) We showed that the B atoms deployed at the centers of honeycombs in boron sheets, borophene, behave as nearly perfect electron donors for filling the graphitic  $\sigma$  bonding states without forming additional in-plane bonds by first-principles calculations. It was confirmed from our the XPS binding energy calculations that the unusual energy sequence of core electrons in the borophene, verified by our high-resolution core-level photoelectron spectroscopy measurements, is originated by the hidden honeycomb bonding structure.

1. Realization of intrinsically broken Dirac cones in graphene via the momentum-resolved electronic band structure: C.-C. Lee, M. Fukuda, Y.-T. Lee and T. Ozaki, *J. Phys.: Condens. Matter* **30** (2018) 295502.
2. Efficient O(N) divide-conquer method with localized single-particle natural orbitals: T. Ozaki, M. Fukuda and G. Jiang, *Phys. Rev. B* **98** (2018) 245137.
3. \*Peculiar bonding associated with atomic doping and hidden honeycombs in borophene: C.-C. Lee, B. Feng, M. D'angelo, R. Yukawa, R.-Y. Liu, T. Kondo, H. Kumigashira, I. Matsuda and T. Ozaki, *Phys. Rev. B* **97** (2018) 075430 (1-5).
4. Reliability and applicability of magnetic-force linear response theory: Numerical parameters, predictability, and orbital resolution: H. Yoon, T. J. Kim, J. -H. Sim, S. W. Jang, T. Ozaki and M. J. Han, *Phys. Rev. B* **97** (2018) 125132.
5. Structural identification of silicene on the Ag(111) surface by atomic force microscopy: L. Feng, K. Yabuoshi, Y. Sugimoto, J. Onoda, M. Fukuda and T. Ozaki, *Phys. Rev. B* **98** (2018) 195311.
6. Tight-binding calculations of optical matrix elements for conductivity using nonorthogonal atomic orbitals: Anomalous Hall conductivity in bcc Fe: C.-C. Lee, Y.-T. Lee, M. Fukuda and T. Ozaki, *Phys. Rev. B* **98** (2018) 115115.
7. \*Atomic Structure and Local Electronic States of Single Pt Atoms Dispersed on Graphene: K. Yamazaki, Y. Maehara, C.-C. Lee, J. Yoshinobu, T. Ozaki and K. Gohara, *J. Phys. Chem. C* **122** (2018) 27292.
8. Li deposition and desolvation with electron transfer at a silicon/propylene-carbonate interface: transition-state and free-energy profiles by large-scale first-principles molecular dynamics: T. Ohwaki, T. Ozaki, Y. Okuno, T. Ikeshoji, H. Imai and M. Otani, *Phys. Chem. Chem. Phys.* **20** (2018) 11586.
9. High-Throughput Screening of Sulfide Thermoelectric Materials Using Electron Transport Calculations with OpenMX and BoltzTraP: M. Miyata, T. Ozaki, T. Takeuchi, S. Nishino, M. Inukai and M. Koyano, *Journal of Elec Materi* **47** (2018) 3254.
10. Transport properties of rocksalt-type cluster sulfides V<sub>4</sub>GeS<sub>8</sub> and Mn substitution effect: M. Miyata, T. Ozaki and M. Koyano, *Jpn. J. Appl. Phys.* **58** (2019) 061008.

---

<sup>†</sup> Joint research with outside partners.

11. OpenMX Viewer: A web-based crystalline and molecular graphical user interface program: Y.-T. Lee and T. Ozaki, *Journal of Molecular Graphics and Modelling* **89** (2019) 192.

## Noguchi group

We have studied nonequilibrium dynamics of polymer solutions and bilayer membranes. We investigated Karman vortex in polymer solution using molecular dynamics simulation. The polymer induces a reduction in the vortex shedding frequency and broadening of the lift coefficient spectrum. We also investigated the shape transformation of vesicles induced by chemical reactions. We revealed that the dynamics can be altered by the viscosity change in the membrane compared to the surrounding fluids.

1. Fracture Process of Double-Network Gels by Coarse-Grained Molecular Dynamics Simulation: Y. Higuchi, K. Saito, T. Sakai, J. P. Gong and M. Kubo, *Macromolecules* **51** (2018) 3075.
2. Bilayer sheet protrusions and budding from bilayer membranes induced by hydrolysis and condensation reactions: K. M. Nakagawa and H. Noguchi, *Soft Matter* **14** (2018) 1397-1407.
3. Fracture processes of crystalline polymers using coarse-grained molecular dynamics simulations: Y. Higuchi, *Polym J* **50** (2018) 579.
4. 短距離古典分子動力学シミュレーションコードの GPGPU 化 (2) : 中川 恒, 分子シミュレーション研究会会誌 “アンサンブル” **20** (2018) 40-45.
5. †\*Polymer effects on Kármán vortex: Molecular dynamics study: Y. Asano, H. Watanabe and H. Noguchi, *The Journal of Chemical Physics* **148** (2018) 144901.
6. Angular-momentum conservation in discretization of the Navier-Stokes equation for viscous fluids: H. Noguchi, *Phys. Rev. E* **99** (2019) 023307.
7. Limiting shapes of confined lipid vesicles: B. Kavcic, A. Sakashita, H. Noguchi and P. Zihlerl, *Soft Matter* **15** (2019) 602-614.
8. \*SIMD vectorization for the Lennard-Jones potential with AVX2 and AVX-512 instructions: H. Watanabe and K. M. Nakagawa, *Computer Physics Communications* **237** (2019) (1-7).

## Materials Synthesis and Characterization group

1. \*Experimental and Theoretical Studies of the Metallic Conductivity in Cubic  $\text{PbVO}_3$  under High Pressure: K. Oka, T. Yamauchi, S. Kanungo, T. Shimazu, K. Oh-ishi, Y. Uwatoko, M. Azuma and T. Saha-Dasgupta, *J. Phys. Soc. Jpn.* **87** (2018) 024801 (1-6).
2. †\*Improvement of coercivity in Nd-Fe-B nanocomposite magnets: T. Saito, S. Nozaki and D. Nishio-Hamane, *J. Magn. Mater.* **445** (2018) 49-52.
3. \*Devil's staircase of odd-number charge order modulations in divalent  $\beta$ -vanadium bronzes under pressure: T. Yamauchi, H. Ueda, K. Ohwada, H. Nakao and Y. Ueda, *Phys. Rev. B* **97** (2018) 125138.
4. †\*Kannanite, a new mineral from Kannan Mountain, Japan: D. Nishio-Hamane, M. Nagashima, N. Ogawa and T. Minakawa, *Journal of Mineralogical and Petrological Sciences* **113** (2018) 245.
5. †\*High-coercivity  $\text{SmCo}_5/\alpha\text{-Fe}$  nanocomposite magnets: T. Saito and D. Nishio-Hamane, *J. Alloys Compd.* **735** (2018) 218-223.
6. \*Giant anomalous Nernst effect and quantum-critical scaling in a ferromagnetic semimetal: A. Sakai, Y. P. Mizuta, A. A. Nugroho, R. Sihombing, T. Koretsune, M.-T. Suzuki, N. Takemori, R. Ishii, D. Nishio-Hamane, R. Arita, P. Goswami and S. Nakatsuji, *Nature Phys.* **14** (2018) 1119-1124.
7. †\*Synthesis of anti-perovskite-type carbides and nitrides from metal oxides and melamine: D. Hirai, H. Tanaka, D. Nishio-Hamane and Z. Hiroi, *RSC Adv.* **8** (2018) 42025.
8. †\*Magnetic and thermoelectric properties of melt-spun ribbons of  $\text{Fe}_2\text{XAl}$  (X = Co, Ni) Heusler compounds: T. Saito and D. Nishio-Hamane, *Journal of Applied Physics* **124** (2018) 075105.

---

\* Joint research among groups within ISSP.

9. †\*Quantum valence criticality in a correlated metal: K. Kuga, Y. Matsumoto, M. Okawa, S. Suzuki, T. Tomita, K. Sone, Y. Shimura, T. Sakakibara, D. Nishio-Hamane, Y. Karaki, Y. Takata, M. Matsunami, R. Eguchi, M. Taguchi, A. Chainani, S. Shin, K. Tamasaku, Y. Nishino, M. Yabashi, T. Ishikawa and S. Nakatsuji, *Sci. Adv.* **4** (2018) eaao3547 (1-6).
10. †\*Large enhancement of the spin Hall effect in Mn metal by Sn doping: D. Qu, T. Higo, T. Nishikawa, K. Matsumoto, K. Kondou, D. Nishio-Hamane, R. Ishii, P. K. Muduli, Y. Otani and S. Nakatsuji, *Phys. Rev. Materials* **2** (2018) 102001.
11. †\*Size-controllable gold nanoparticles prepared from immobilized gold-containing ionic liquids on SBA-15: E. N. Kusumawati, D. Nishio-Hamane and T. Sasaki, *Catalysis Today* **309** (2018) 109.
12. †\*Transmission electron microscopy study of the epitaxial association of hedenbergite whiskers with babingtonite: M. Nagashima and D. Nishio-Hamane, *Mineral. mag.* **82** (2018) 23.
13. †\*Aurhydrargyrumite, a Natural Au<sub>6</sub>Hg<sub>5</sub> Phase from Japan: D. Nishio-Hamane, T. Tanaka and T. Minakawa, *Minerals* **8** (2018) 415.
14. †\*Ionic Liquid Immobilized on Graphene-Oxide-Containing Palladium Metal Ions as an Efficient Catalyst for the Alkoxy, Amino, and Phenoxy Carbonylation Reactions: V. V. Gaikwad, V. B. Saptal, K. Harada, T. Sasaki, D. Nishio-Hamane and B. M. Bhanage, *ChemNanoMat* **4** (2018) 575.
15. †\*S=1/2 ferromagnetic Heisenberg chain in a verdazyl-based complex: N. Uemoto, Y. Kono, S. Kittaka, T. Sakakibara, T. Yajima, Y. Iwasaki, S. Miyamoto, Y. Hosokoshi and H. Yamaguchi, *Phys. Rev. B* **99** (2019) 094418 (1-6).
16. \*Transmission electron microscopy study of the epitaxial association of hedenbergite whiskers with babingtonite: M. Nagashima and D. Nishio-Hamane, *Mineral. Mag.* (2018) 1, accepted for publication.

## Neutron Science Laboratory

### Shibayama group

Shibayama group has been exploring the structure and dynamics of soft matter, especially polymer gels, micelles, thermoresponsive polymers, and thermosets, utilizing a combination of small-angle neutron scattering (SANS), small-angle X-ray scattering (SAXS), and dynamic light scattering (DLS). The objectives are to elucidate the relationship between the structure and variety of novel properties/functions of polymer gels/resins. The highlights of 2018 include investigations of (1) probe diffusion of sol-gel transition in isorefractive indexed solvents, (2) microscopic structure of module-assembled thermoresponsive conetwork hydrogels, (3) diffusion behavior of methanol molecules confined in cross-linked phenolic resins, (4) structure-mechanical property relationships in crosslinked phenolic resin, and (5) dynamics of thermoresponsive conetwork gels, and so on.

1. Ion Gel Network Formation in an Ionic Liquid Studied by Time-Resolved Small-Angle Neutron Scattering: K. Hashimoto, K. Fujii, K. Nishi and M. Shibayama, *J. Phys. Chem. B* **122** (2018) 9419-9424.
2. Dynamics of thermoresponsive conetwork gels composed of poly(ethylene glycol) and poly(ethyl glycidyl ether-co-methyl glycidyl ether): M. Ohira, X. Li, C. I. Gupit, H. Kamata, T. Sakai and M. Shibayama, *Polymer* **155** (2018) 75-82.
3. Two-dimensional scattering patterns and stress-strain relation of elongated clay nano composite gels: Molecular dynamics simulation analysis: K. Hagita, Y. Shudo and M. Shibayama, *Polymer* **154** (2018) 62-79.
4. Diffusion Behavior of Methanol Molecules Confined in Cross-Linked Phenolic Resins Studied Using Neutron Scattering and Molecular Dynamics Simulations: Y. Shudo, A. Izumi, K. Hagita, T. Yamada, K. Shibata and M. Shibayama, *Macromolecules* **51** (2018) 6334-6343.
5. Dynamic Fluctuations of Thermoresponsive Poly(oligo-ethylene glycol methyl ether methacrylate)-Based Hydrogels Investigated by Dynamic Light Scattering: T. Kureha, K. Hayashi, M. Ohira, X. Li and M. Shibayama, *Macromolecules* **51** (2018) 8932-8939.
6. Insight into the Microscopic Structure of Module-Assembled Thermoresponsive Conetwork Hydrogels: S. Nakagawa, X. Li, M. Shibayama, H. Kamata, T. Sakai and E. P. Gilbert, *Macromolecules* **51** (2018) 6645-6652.
7. Sulfonated Polyimide/Ionic Liquid Composite Membranes for CO<sub>2</sub> Separation: Transport Properties in Relation to Their Nanostructures: A. Ito, T. Yasuda, T. Yoshioka, A. Yoshida, X. Li, K. Hashimoto, K. Nagai, M. Shibayama and M. Watanabe, *Macromolecules* **51** (2018) 7112-7120.

---

† Joint research with outside partners.

8. Self-Healing Micellar Ion Gels Based on Multiple Hydrogen Bonding: R. Tamate, K. Hashimoto, T. Horii, M. Hirasawa, X. Li, M. Shibayama and M. Watanabe, *Adv. Mater.* **30** (2018) 1802792 (1-7).
9. Small-angle X-ray scattering study on nano-scale structures controlled by water content in a binary water/ionic liquid system: K. Hashimoto, K. Fujii, T. Kusano, K. Hirose and M. Shibayama, *Phys. Chem. Chem. Phys.* **20** (2018) 18355-18360.
10. Gels: From Soft Matter to BioMatter: M. Shibayama, X. Li and T. Sakai, *Ind. Eng. Chem. Res.* **57** (2018) 1121-1128.
11. Small-angle scattering study of tetra-poly(acrylic acid) gels: K. Morishima, X. Li, K. Oshima, Y. Mitsukami and M. Shibayama, *The Journal of Chemical Physics* **149** (2018) 163301 (1-8).
12. Molecular Dynamics Simulations of Cross-Linked Phenolic Resins Using a United-Atom Model: A. Izumi, Y. Shudo, K. Hagita and M. Shibayama, *Macromol. Theory Simul.* **27** (2018) 1700103 (1-8).
13. Evaluation of Mesh Size in Model Polymer Networks Consisting of Tetra-Arm and Linear Poly(ethylene glycol)s: Y. Tsuji, X. Li and M. Shibayama, *Gels* **4** (2018) 50.
14. Viscoelastic change of block copolymer ion gels in a photo-switchable azobenzene ionic liquid triggered by light: C. Wang, K. Hashimoto, R. Tamate, H. Kokubo, K. Morishima, X. Li, M. Shibayama, F. Lu, T. Nakanishi and M. Watanabe, *Chem. Commun.* **55** (2019) 1710-1713.
15. Network structure evolution of a hexamethylenetetramine-cured phenolic resin: A. Izumi, Y. Shudo and M. Shibayama, *Polym J* **51** (2019) 155-160.
16. Chiral crystal-like droplets displaying unidirectional rotational sliding: T. Kajitani, K. Motokawa, A. Kosaka, Y. Shoji, R. Haruki, D. Hashizume, T. Hikima, M. Takata, K. Yazawa, K. Morishima, M. Shibayama and T. Fukushima, *Nature Mater.* **18** (2019) 266-272.
17. Precision polymer network science with tetra-PEG gels—a decade history and future: M. Shibayama, X. Li and T. Sakai, *Colloid Polym Sci* **297** (2019) 1-12.
18. Rheo-SANS study on relationship between micellar structures and rheological behavior of cationic gemini surfactants in solution: H. Iwase, R. Kawai, K. Morishima, S.-I. Takata, T. Yoshimura and M. Shibayama, *Journal of Colloid and Interface Science* **538** (2019) 357-366.
19. Formation of Clusters in Whiskies During the Maturation Process: K. Morishima, N. Nakamura, K. Matsui, Y. Tanaka, H. Masunaga, S. Mori, T. Iwashita, X. Li and M. Shibayama, *Journal of Food Science* **84** (2019) 59-64.
20. 散乱を用いて不均一性を調べる：柴山 充弘，*高分子* **67** (2018) 35-38.
21. 分子動力学シミュレーションを用いたフェノール樹脂の構造 機械特性発現メカニズムの解析：首藤 靖幸，和泉 篤士，萩田 克美，柴山 充弘，*ネットワークポリマー* **39** (2018) 163-171.
22. 高強度ゲルから医療用ゲルまで：柴山 充弘，*ソフトマター* **1** (2018) 10-12.
23. Structure and Functions of Phenolic Resin: M. SHIBAYAMA, Y. SHUDO and A. IZUMI, *日本接着学会誌* **54** (2018) 451-458.
24. 高強度イオンゲル膜を用いた CO2 分離：橋本 慧，藤井 健太，柴山 充弘，*ケミカルエンジニアリング* **64** (2019) 32-38.
25. Probe Diffusion Dynamic Light Scattering of Polymer solutions and Gels: M. Shibayama and X. Li, in: *Gels and Other Soft Amorphous Solids*, Ch 4, edited by F. Horkay, J. F. Douglas, E. Del Gado, (American Chemical Society, Washington, D. C., 2018), 51-69.
26. 散乱法を用いた高分子ゲルの構造解析：柴山 充弘，『『刺激応答性高分子ハンドブック』基礎編 第4章 構造・物性解析 第2節』，宮田隆志，(エヌ・ティー・エス，東京，2018)，296-305.

## Yamamuro group

Our laboratory is studying chemical physics of complex condensed matters by using neutron scattering, X-ray diffraction, calorimetric, dielectric, and viscoelastic techniques. Our target materials are glasses, liquids, and various disordered systems. In this year, the synchrotron X-ray diffraction of glassy and liquid toluene (C<sub>6</sub>H<sub>5</sub>CH<sub>3</sub>) was measured following the previous works on carbon disulfide (CS<sub>2</sub>), propane (CH<sub>3</sub>CH<sub>2</sub>CH<sub>3</sub>) and propene (CH<sub>3</sub>CH=CH<sub>2</sub>). By means of the Reverse Monte Carlo (RMC) method combining the molecular dynamics (MD) simulations, we found that the orientational correlation between neighboring molecules steeply increased on cooling below the melting temperature and was frozen at the glass transition temperature. Another topic is the inelastic neutron scattering of vapor-deposited glassy carbon tetrachloride (CCl<sub>4</sub>). We observed the

---

\* Joint research among groups within ISSP.

$Q$ -dependence of the boson peak intensity and the dispersion-like phenomenon of acoustic phonons as observed in SiO<sub>2</sub> glass, which is a typical covalent-bond network glass. Other than the above topics, we have conducted neutron diffraction experiment of the PdRu alloy nanoparticles supported on CZ (CeO<sub>2</sub>-ZrO<sub>2</sub>). This is a high-performance catalytic system for removing CO and NO<sub>x</sub> gases. The pdf (pair-distribution function) analysis is now going on to investigate the atomic scale miscibility and local structure of the alloy.

1. Neutron Scattering Studies on Short- and Long-range Layer Structures and Related Dynamics in Imidazolium-based Ionic Liquids: F. Nemoto, M. Kofu, M. Nagao, K. Ohishi, S. Takata, J. Suzuki, T. Yamada, K. Shibata, T. Ueki, Y. Kitazawa, M. Watanabe and O. Yamamuro, *J. Chem. Phys.* **149** (2018) 054502 (1-11).
2. Two inherent crossovers of the diffusion process in glass-forming liquids: M. Kofu, A. Faraone, M. Tyagi, M. Nagao and O. Yamamuro, *Phys. Rev. E* **98** (2018) 042601 (1-6).
3. Development of adiabatic calorimetry system for enthalpy of gas absorption/adsorption and its application to H<sub>2</sub>/D<sub>2</sub> absorption into palladium nanoparticles: H. Akiba, N. Hashimoto, M. Kofu, H. Kobayashi, H. Kitagawa and O. Yamamuro, *Thermochimica Acta* **670** (2018) 87-91.
4. Neutron scattering studies of static and dynamic correlation lengths in alkali metal borate glasses: S. Kojima, V. N. Novikov, M. Kofu and O. Yamamuro, *Journal of Non-Crystalline Solids* **518** (2019) 18-23.
5. Structural and Thermodynamic Studies of Hydrogen Absorption/Desorption Processes on PdPt Nanoparticles: H. Akiba, H. Kobayashi, H. Kitagawa, K. Ikeda, T. Otomo, T. Yamamoto, S. Matsumura and O. Yamamuro, *J. Phys. Chem. C* **123** (2019) 9471.

## Masuda group

The goal of our research is to discover a new quantum phenomenon and to reveal the mechanism of it. In this fiscal year we studied the following topics; magnetic order in the rare-earth ferroborate CeFe<sub>3</sub>(BO<sub>3</sub>)<sub>4</sub>, magnetic state selected by magnetic dipole interaction in the kagome antiferromagnet NaBa<sub>2</sub>Mn<sub>3</sub>F<sub>11</sub>, polarization analysis of magnetic excitation in multiferroic Ba<sub>2</sub>CoGe<sub>2</sub>O<sub>7</sub>, pressure-induced quantum phase transition in the quantum antiferromagnet CsFeCl<sub>3</sub>, neutron spin resonance in the 112-type iron-based superconductor, crystal structure of magnetoelectric Ba<sub>2</sub>MnGe<sub>2</sub>O<sub>7</sub> at room and low temperatures by neutron diffraction.

1. Low temperature magnetic properties of Nd<sub>2</sub>Ru<sub>2</sub>O<sub>7</sub>: S. T. Ku, D. Kumar, M. R. Lees, W.-T. Lee, R. Aldus, A. Studer, P. Imperia, S. Asai, T. Masuda, S. W. Chen, J. M. Chen and L. J. Chang, *J. Phys.: Condens. Matter* **30** (2018) 155601 (1-11).
2. f-Electron States in PrPd<sub>5</sub>Al<sub>2</sub>: N. Metoki, H. Yamauchi, H. S. Suzuki, H. Kitazawa, M. Hagihara, T. Masuda, A. A. Aczel, S. Chi, T. Hong, M. Matsuda, D. Pajerowski and J. A. Fernandez-Baca, *J. Phys. Soc. Jpn.* **87** (2018) 094704 (1-8).
3. Magnetic order in the rare-earth ferroborate CeFe<sub>3</sub>(BO<sub>3</sub>)<sub>4</sub>: S. Hayashida, S. Asai, D. Kato, S. Hasegawa, M. Avdeev, H. Cao and T. Masuda, *Phys. Rev. B* **98** (2018) 224405 (1-9).
4. \*Magnetic state selected by magnetic dipole interaction in the kagome antiferromagnet NaBa<sub>2</sub>Mn<sub>3</sub>F<sub>11</sub>: S. Hayashida, H. Ishikawa, Y. Okamoto, T. Okubo, Z. Hiroi, M. Avdeev, P. Manuel, M. Hagihara, M. Soda and T. Masuda, *Phys. Rev. B* **97** (2018) 054411 (1-7).
5. Polarization analysis of magnetic excitation in multiferroic Ba<sub>2</sub>CoGe<sub>2</sub>O<sub>7</sub>: M. Soda, L.-J. Chang, M. Matsumoto, V. Ovidiu Garlea, B. Roessli, J. S. White, H. Kawano-Furukawa and T. Masuda, *Phys. Rev. B* **97** (2018) 214437 (1-6).
6. \*Pressure-induced quantum phase transition in the quantum antiferromagnet CsFeCl<sub>3</sub>: S. Hayashida, O. Zaharko, N. Kurita, H. Tanaka, M. Hagihara, M. Soda, S. Itoh, Y. Uwatoko and T. Masuda, *Phys. Rev. B* **97** (2018) 140405 (1-4).
7. Neutron Spin Resonance in the 112-Type Iron-Based Superconductor: T. Xie, D. Gong, H. Ghosh, A. Ghosh, M. Soda, T. Masuda, S. Itoh, F. Bourdarot, L.-P. Regnault, S. Danilkin, S. Li and H. Luo, *Phys. Rev. Lett.* **120** (2018) 137001 (1-7).
8. Crystal Structure of Magnetoelectric Ba<sub>2</sub>MnGe<sub>2</sub>O<sub>7</sub> at Room and Low Temperatures by Neutron Diffraction: A. Sazonov, V. Hutanu, M. Meven, G. Roth, R. Georgii, T. Masuda and B. Nafradi, *Inorg. Chem.* **57** (2018) 5089-5095.
9. Improvement for Neutron Brillouin Scattering Experiments on High Resolution Chopper Spectrometer HRC: S. Itoh, T. Yokoo, T. Masuda, H. Yoshizawa, M. Soda, M. Yoshida, T. Hawaii, D. Kawana, R. Sugiura, T. Asami and Y. Ihata, *J. Phys.: Conf. Ser.* **1021** (2018) 012028 (1-4).

---

† Joint research with outside partners.

10. YUI and HANA: control and visualization programs for HRC in J-PARC: D. Kawana, M. Soda, M. Yoshida, Y. Ikeda, T. Asami, R. Sugiura, H. Yoshizawa, T. Masuda, T. Hawaii, S. Ibuka, T. Yokoo and S. Itoh, *J. Phys.: Conf. Ser.* **1021** (2018) 012014 (1-4).
11. High resolution chopper spectrometer HRC and neutron Brillouin scattering: S. Itoh, T. Yokoo, T. Masuda, H. Yoshizawa, M. Soda, S. Ibuka, Y. Ikeda, M. Yoshida, T. Hawaii, D. Kawana, R. Sugiura, T. Asami, Y. Kawamura, T. Shinozaki and Y. Ihata, *AIP Conf. Proc.* **1969** (2018) 050002 (1-5).
12. Magnetic structure of a non-centrosymmetric CePtSi<sub>3</sub>: D. Ueta, M. Yoshida, Y. Ikeda, Y. Liu, T. Hong, T. Masuda and H. Yoshizawa, *AIP Advances* **8** (2018) 115006 (1-5).
13. Progress in High Resolution Chopper Spectrometer HRC by improving collimator and Fermi chopper: S. Itoh, T. Yokoo, T. Masuda, S. Asai, H. Saito, D. Kawana, R. Sugiura, T. Asami and Y. Ihata, *Physica B: Condensed Matter* **568** (2019) 76-80.
14. Magnetic states of coupled spin tubes with frustrated geometry in CsCrF<sub>4</sub>: M. Hagihala, S. Hayashida, M. Avdeev, H. Manaka, H. Kikuchi and T. Masuda, *npj Quantum Mater.* **4** (2019) 14 (1-9).

## International MegaGauss Science Laboratory

### Takeyama group

1000 T-class megagauss generator system has been accomplished to be used for the electro-magnetic flux compression. The system is comprised of 5 MJ and 2 MJ condenser modules, respectively, for a primary coil and 2 MJ condenser modules for the seed-magnetic field generation to be compressed. This project has started in 2010 supported by a budget from the MEXT. After long-standing struggles over 10 years with serious difficulties in the construction processes, the instruments have been finally accomplished. We could break the world record of high-magnetic fields, 1200 T, of which value was successfully recorded by the optical Faraday rotation technique with high precision and reliability.

1. †\*Ultra-high-Magnetic-Field Magnetization of Multi-Kagome-Strip (MKS) Lattice Spin-Frustrated Magnet K<sub>2</sub>Mn<sub>3</sub>(OH)<sub>2</sub>(VO<sub>4</sub>)<sub>2</sub>: D. Otsuka, H. Sato, A. Matsuo, K. Kindo, D. Nakamura and S. Takeyama, *J. Phys. Soc. Jpn.* **87** (2018) 124701 (1-7).
2. Note: An approach to 1000 T using the electro-magnetic flux compression: D. Nakamura, H. Sawabe and S. Takeyama, *Rev. Sci. Instrum.* **89** (2018) 016106 (1-3).
3. Radio frequency self-resonant coil for contactless AC-conductivity in 100 T class ultra-strong pulse magnetic fields: D. Nakamura, M. M. Altarawneh and S. Takeyama, *Meas. Sci. Technol.* **29** (2018) 035901 (1-7).
4. \*Record indoor magnetic field of 1200 T generated by electromagnetic flux-compression: D. Nakamura, A. Ikeda, H. Sawabe, Y. H. Matsuda and S. Takeyama, *Review of Scientific Instruments* **89** (2018) 095106 (1-7).
5. †\*Magnetoelastic couplings in the deformed kagome quantum spin lattice of volborthite: A. Ikeda, S. Furukawa, O. Janson, Y. H. Matsuda, S. Takeyama, T. Yajima, Z. Hiroi and H. Ishikawa, *Phys. Rev. B* **99** (2019) 140412(R) (1-5).
6. †Ultra-high magnetic field magnetic phases up to 130 T in a breathing pyrochlore antiferromagnet LiInCr<sub>4</sub>O<sub>8</sub>: M. Gen, D. Nakamura, Y. Okamoto and S. Takeyama, *Journal of Magnetism and Magnetic Materials* **473** (2019) 387-393.
7. \*A series of magnon crystals appearing under ultrahigh magnetic fields in a kagomé antiferromagnet: R. Okuma, D. Nakamura, T. Okubo, A. Miyake, A. Matsuo, K. Kindo, M. Tokunaga, N. Kawashima, S. Takeyama and Z. Hiroi, *Nature Communications* **10** (2019) 1229(7).

### Kindo group

We have succeeded in examination of various Cu-Ag strong wire. A stronger wire can suppress the deformation of the magnet after generation of high magnetic field but has a short-life frequently. We have examined the wire which has a tensile strength below 1.1 GPa. As a result, the magnet obtained long-life. Next step is to elucidate threshold between long and short life.

1. †\*Magnetic and Structural Properties of A-Site Ordered Chromium Spinel Sulfides: Alternating Antiferromagnetic and Ferromagnetic Interactions in the Breathing Pyrochlore Lattice: Y. Okamoto, M. Mori, N. Katayama, A. Miyake, M. Tokunaga, A. Matsuo, K. Kindo and K. Takenaka, *J. Phys. Soc. Jpn.* **87** (2018) 034709 (1-8).

---

\* Joint research among groups within ISSP.

2. †\*Magnetic-field-induced Quantum Phase in  $S = 1/2$  Frustrated Trellis Lattice: H. Yamaguchi, D. Yoshizawa, T. Kida, M. Hagiwara, A. Matsuo, Y. Kono, T. Sakakibara, Y. Tamekuni, H. Miyagai and Y. Hosokoshi, *J. Phys. Soc. Jpn.* **87** (2018) 043701 (1-5).
3. †Magnetism and High-magnetic Field Magnetization in Alkali Superoxide CsO<sub>2</sub>: M. Miyajima, F. Astuti, T. Kakuto, A. Matsuo, D. P. Sari, R. Asih, K. Okunishi, T. Nakano, Y. Nozue, K. Kindo, I. Watanabe and T. Kambe, *J. Phys. Soc. Jpn.* **87** (2018) 063704 (1-5).
4. Superconducting Phase Diagram of the Organic Superconductor  $\kappa$ -(BEDT-TTF)<sub>2</sub> Cu[N(CN)<sub>2</sub>]Br above 30 T: S. Imajo, Y. Nakazawa and K. Kindo, *J. Phys. Soc. Jpn.* **87** (2018) 123704 (5).
5. †\*Ultrahigh-Magnetic-Field Magnetization of Multi-Kagome-Strip (MKS) Lattice Spin-Frustrated Magnet K<sub>2</sub>Mn<sub>3</sub>(OH)<sub>2</sub>(VO<sub>4</sub>)<sub>2</sub>: D. Otsuka, H. Sato, A. Matsuo, K. Kindo, D. Nakamura and S. Takeyama, *J. Phys. Soc. Jpn.* **87** (2018) 124701 (1-7).
6. †Electric dipole spin resonance in a quantum spin dimer system driven by magnetoelectric coupling: S. Kimura, M. Matsumoto, M. Akaki, M. Hagiwara, K. Kindo and H. Tanaka, *Phys. Rev. B* **97** (2018) 140406 (1-5).
7. \*Frustrated magnetism of the maple-leaf-lattice antiferromagnet MgMn<sub>3</sub>O<sub>7</sub>·3H<sub>2</sub>O: Y. Haraguchi, A. Matsuo, K. Kindo and Z. Hiroi, *Phys. Rev. B* **98** (2018) 064412 (1-7).
8. \*High-field phase diagram and phase transitions in hexagonal manganite ErMnO<sub>3</sub>: Y. J. Liu, J. F. Wang, X. F. Sun, J. -S. Zhou, Z. C. Xia, Z. W. Ouyang, M. Yang, C. B. Liu, R. Chen, J. -G. Cheng, Y. Kohama, M. Tokunaga and K. Kindo, *Phys. Rev. B* **97** (2018) 214419 (1-5).
9. †In-plane spin canting and 1/3-magnetization-plateaulike behavior in  $S = 3/2$  Cr<sup>3+</sup> kagome lattice antiferromagnets Cs<sub>2</sub>KCr<sub>3</sub>F<sub>12</sub> and Cs<sub>2</sub>NaCr<sub>3</sub>F<sub>12</sub>: M. Goto, H. Ueda, C. Michioka, A. Matsuo, K. Kindo, K. Sugawara, S. Kobayashi, N. Katayama, H. Sawa and K. Yoshimura, *Phys. Rev. B* **97** (2018) 224421 (1-8).
10. †\*Magnetic field induced ferroelectricity and half magnetization plateau in polycrystalline R<sub>2</sub>V<sub>2</sub>O<sub>7</sub> (R = Ni, Co ): R. Chen, J. F. Wang, Z. W. Ouyang, Z. Z. He, S. M. Wang, L. Lin, J. M. Liu, C. L. Lu, Y. Liu, C. Dong, C. B. Liu, Z. C. Xia, A. Matsuo, Y. Kohama and K. Kindo, *Phys. Rev. B* **98** (2018) 184404 (1-7).
11. \*Magnetic field induced phenomena in UIrGe in fields applied along the b axis: J. Pospíšil, Y. Haga, Y. Kohama, A. Miyake, S. Kambe, N. Tateiwa, M. Vališka, P. Proschek, J. Prokleška, V. Sechovský, M. Tokunaga, K. Kindo, A. Matsuo and E. Yamamoto, *Phys. Rev. B* **98** (2018) 014430 (1-7).
12. †Quantum magnetic properties of the spin-1/2 triangular-lattice antiferromagnet Ba<sub>2</sub>La<sub>2</sub>CoTe<sub>2</sub>O<sub>12</sub>: Y. Kojima, M. Watanabe, N. Kurita, H. Tanaka, A. Matsuo, K. Kindo and M. Avdeev, *Phys. Rev. B* **98** (2018) 174406 (1-8).
13. †Revising the 4f symmetry in CeCu<sub>2</sub>Ge<sub>2</sub>: Soft x-ray absorption and hard x-ray photoemission spectroscopy: H. Aratani, Y. Nakatani, H. Fujiwara, M. Kawada, Y. Kanai, K. Yamagami, S. Fujioka, S. Hamamoto, K. Kuga, T. Kiss, A. Yamasaki, A. Higashiya, T. Kadono, S. Imada, A. Tanaka, K. Tamasaku, M. Yabashi, T. Ishikawa, A. Yasui, Y. Saitoh, Y. Narumi, K. Kindo, T. Ebihara and A. Sekiyama, *Phys. Rev. B* **98** (2018) 121113 (1-6).
14. \*Unusual magnetoelectric memory and polarization reversal in the kagome staircase compound Ni<sub>3</sub>V<sub>2</sub>O<sub>8</sub>: Y. J. Liu, J. F. Wang, Z. Z. He, C. L. Lu, Z. C. Xia, Z. W. Ouyang, C. B. Liu, R. Chen, A. Matsuo, Y. Kohama, K. Kindo and M. Tokunaga, *Phys. Rev. B* **97** (2018) 174429 (1-6).
15. †Cluster-Based Haldane State in an Edge-Shared Tetrahedral Spin-Cluster Chain: Fedotovite K<sub>2</sub>Cu<sub>3</sub>O(SO<sub>4</sub>)<sub>3</sub>: M. Fujihala, T. Sugimoto, T. Tohyama, S. Mitsuda, R. A. Mole, D. H. Yu, S. Yano, Y. Inagaki, H. Morodomi, T. Kawai, H. Sagayama, R. Kumai, Y. Murakami, K. Tomiyasu, A. Matsuo and K. Kindo, *Phys. Rev. Lett.* **120** (2018) 077201 (5).
16. †\*Magnetic-Field-Induced Kondo Metal Realized in YbB<sub>12</sub>: T. T. Terashima, Y. H. Matsuda, Y. Kohama, A. Ikeda, A. Kondo, K. Kindo and F. Iga, *Phys. Rev. Lett.* **120** (2018) 257206 (1-5).
17. \*Quantum Criticality of an Ising-like Spin-1/2 Antiferromagnetic Chain in a Transverse Magnetic Field: Z. Wang, T. Lorenz, D. I. Gorbunov, P. T. Cong, Y. Kohama, S. Niesen, O. Breunig, J. Engelmayer, A. Herman, J. Wu, K. Kindo, J. Wosnitza, S. Zherlitsyn and A. Loidl, *Phys. Rev. Lett.* **120** (2018) 207205 (1-6).
18. †Magnetic and Structural Properties of MnCoGe with Minimal Fe and Sn Substitution: M. Onoue, R. Kobayashi, Y. Mitsui, M. Hiroi, K. Takahashi, A. Kondo, K. Kindo, Y. Uwatoko and K. Koyama, *Mater. Trans.* **59** (2018) 1645-1650.
19. †Magnetic phase diagram of the frustrated  $S=1/2$  triangular-lattice magnet Cu<sub>2</sub>(NO<sub>3</sub>)(OH)<sub>3</sub>: H. Kikuchi, N. Kasamatsu, Y. Ishikawa, Y. Koizumi, Y. Fujii, A. Matsuo and K. Kindo, *J. Phys.: Conf. Ser.* **969** (2018) 012117 (1-6).

---

† Joint research with outside partners.

20. †Magnetic properties of the antiferromagnetic spin-1/2 tetramer compound  $\text{CuInVO}_5$ : M. Hase, M. Matsumoto, A. Matsuo and K. Kindo, *J. Phys.: Conf. Ser.* **969** (2018) 012100 (1-6).
21. †Magnetization and magnetic phase diagram of Heusler compounds  $\text{Fe}_{3-y}(\text{Mn}_{1-x}\text{V}_x)_y\text{Si}$  ( $y = 1$  and  $1.5$ ): M. Hiroi, S. Ishikuma, I. Shigeta, K. Koyama, A. Kondo, K. Kindo, H. Manaka and N. Terada, *J. Phys.: Conf. Ser.* **969** (2018) 012099 (1-6).
22. †Divalent ion substitution effect on Yb-site in Kondo insulator  $\text{YbB}_{12}$ : W. Matsuhra, K. Yokomichi, W. Hirano, S. Kikuchi, N. Uematsu, H. Nakayama, A. Kondo, K. Kindo and F. Iga, *AIP Advances* **8** (2018) 101329 (1-3).
23. †Magnetic properties of perovskite  $\text{Ca}_{1-x}\text{Sr}_x\text{FeO}_3$ : H. Kawanaka, E. Kawawa, Y. Nishihara, F. Iga, A. Kondo, K. Kindo and Y. Matsuda, *AIP Advances* **8** (2018) 101418 (1-4).
24. †Non-magnetic element substitution effect in Kondo insulator  $\text{YbB}_{12}$  and exotic surface effect in this alloy system: F. Iga, K. Yokomichi, W. Matsuhra, H. Nakayama, A. Kondo, K. Kindo and H. Yoshizawa, *AIP Advances* **8** (2018) 101335 (1-4).
25. †Thermodynamic properties of Heusler  $\text{Fe}_2\text{VSi}$ : M. Ito, K. Kai, T. Furuta, H. Manaka, N. Terada, M. Hiroi, A. Kondo and K. Kindo, *AIP Advances* **8** (2018) 055703 (1-5).
26. †Magnetic ordering with an XY-like anisotropy in the honeycomb lattice iridates  $\text{ZnIrO}_3$  and  $\text{MgIrO}_3$  synthesized via a metathesis reaction: Y. Haraguchi, C. Michioka, A. Matsuo, K. Kindo, H. Ueda and K. Yoshimura, *Phys. Rev. Materials* **2** (2018) 054411 (1-6).
27. \*Magnetic structural unit with convex geometry: A building block hosting an exchange-striction-driven magnetoelectric coupling: K. Kimura, Y. Kato, K. Yamauchi, A. Miyake, M. Tokunaga, A. Matsuo, K. Kindo, M. Akaki, M. Hagiwara, S. Kimura, M. Toyoda, Y. Motome and T. Kimura, *Phys. Rev. Materials* **2** (2018) 104415 (1-12).
28. †High-field Magnetism of the Honeycomb-lattice Antiferromagnet  $\text{Cu}_2(\text{pymca})_3(\text{ClO}_4)$ : A. Okutani, T. Kida, Y. Narumi, T. Shimokawa, Z. Honda, K. Kindo, T. Nakano, Y. Nozue and M. Hagiwara, *J. Phys. Soc. Jpn.* **88** (2019) 013703 (4).
29. †Reduction of the Ordered Magnetic Moment by Quantum Fluctuation in the Antiferromagnetic Spin-5/2 Dimer Compound  $\text{FeVMoO}_7$ : M. Hase, J. R. Hester, K. C. Rule, V. Yu. Pomjakushin, A. Matsuo and K. Kindo, *J. Phys. Soc. Jpn.* **88** (2019) 034711 (6).
30. †\*Difference in magnetic and ferroelectric properties between rhombohedral and hexagonal polytypes of  $\text{AgFeO}_2$ : A single-crystal study: N. Terada, Y. Ikedo, H. Sato, D. D. Khalyavin, P. Manuel, F. Orlandi, Y. Tsujimoto, Y. Matsushita, A. Miyake, A. Matsuo, M. Tokunaga and K. Kindo, *Phys. Rev. B* **99** (2019) 064402 (1-11).
31. †\*Enhancement of the effective mass at high magnetic fields in  $\text{CeRhIn}_5$ : L. Jiao, M. Smidman, Y. Kohama, Z. S. Wang, D. Graf, Z. F. Weng, Y. J. Zhang, A. Matsuo, E. D. Bauer, H. Lee, S. Kirchner, J. Singleton, K. Kindo, J. Wosnitza, F. Steglich, J. D. Thompson and H. Q. Yuan, *Phys. Rev. B* **99** (2019) 045127 (6).
32. †Evidence of low-energy singlet excited states in the spin-1/2 polyhedral clusters  $\{\text{Mo}_{72}\text{V}_{30}\}$  and  $\{\text{W}_{72}\text{V}_{30}\}$  with strongly frustrated kagome networks: T. Kihara, H. Nojiri, Y. Narumi, Y. Oshima, K. Kindo, C. Heesing, J. Schnack and A. Müller, *Phys. Rev. B* **99** (2019) 064430 (8).
33. †\*Magnetoelectric behavior from cluster multipoles in square cupolas: Study of  $\text{Sr}(\text{TiO})\text{Cu}_4(\text{PO}_4)_4$  in comparison with Ba and Pb isostructurals: Y. Kato, K. Kimura, A. Miyake, M. Tokunaga, A. Matsuo, K. Kindo, M. Akaki, M. Hagiwara, S. Kimura, T. Kimura and Y. Motome, *Phys. Rev. B* **99** (2019) 024415 (1-12).
34. †\*Topological transitions among skyrmion- and hedgehog-lattice states in cubic chiral magnets: Y. Fujishiro, N. Kanazawa, T. Nakajima, X. Z. Yu, K. Ohishi, Y. Kawamura, K. Kakurai, T. Arima, H. Mitamura, A. Miyake, K. Akiba, M. Tokunaga, A. Matsuo, K. Kindo, T. Koretsune, R. Arita and Y. Tokura, *Nat. Commun.* **10** (2019) 1059 (1-8).
35. \*Thermodynamic evidence of magnetic-field-induced complete valley polarization in bismuth: A. Iwasa, A. Kondo, S. Kawachi, K. Akiba, Y. Nakanishi, M. Yoshizawa, M. Tokunaga and K. Kindo, *Sci Rep* **9** (2019) 1672 (1-8).
36. †\*Multiple topological states in iron-based superconductors: P. Zhang, Z. Wang, X. Wu, K. Yaji, Y. Ishida, Y. Kohama, G. Dai, Y. Sun, C. Bareille, K. Kuroda, T. Kondo, K. Okazaki, K. Kindo, X. Wang, C. Jin, J. Hu, R. Thomale, K. Sumida, S. Wu, K. Miyamoto, T. Okuda, H. Ding, G. D. Gu, T. Tamegai, T. Kawakami, M. Sato and S. Shin, *Nature Phys* **15** (2019) 41-48.

---

\* Joint research among groups within ISSP.

37. \*Strain-induced spontaneous Hall effect in an epitaxial thin film of a Luttinger semimetal: T. Ohtsuki, Z. Tian, A. Endo, M. Halim, S. Katsumoto, Y. Kohama, K. Kindo, M. Lippmaa and S. Nakatsuji, *Proc. Natl. Acad. Sci. USA* **116** (2019) 8803-8808.
38. \*A series of magnon crystals appearing under ultrahigh magnetic fields in a kagomé antiferromagnet: R. Okuma, D. Nakamura, T. Okubo, A. Miyake, A. Matsuo, K. Kindo, M. Tokunaga, N. Kawashima, S. Takeyama and Z. Hiroi, *Nature Communications* **10** (2019) 1229(7).
39. \*Possible observation of quantum spin-nematic phase in a frustrated magnet: Y. Kohama, H. Ishikawa, A. Matsuo, K. Kindo, N. Shannon and Z. Hiroi, *Proc. Nat. Acad. Sci. U.S.A.* **116** (2019) 10686-10690.

## Tokunaga group

In this year, we have mainly studied magnetotransport properties on several kinds of topological semimetals. As one of the important achievements in our group, we demonstrated an experimental method to evaluate the degree of similarity between one system and ideal Dirac fermion system, “Diracness”, in a narrow-gap semiconductor PbTe through systematic studies of quantum oscillations up to the quantum limit state. We also developed international collaborations on various subjects, e.g. multiferroics, heavy fermion compounds, and topological materials.

1. \*Formation and Control of Twin Domains in the Pyrochlore Oxide  $\text{Cd}_2\text{Re}_2\text{O}_7$ : Y. Matsubayashi, D. Hirai, M. Tokunaga and Z. Hiroi, *J. Phys. Soc. Jpn.* **87** (2018) 104604 (1-7).
2. †\*Magnetic and Structural Properties of A-Site Ordered Chromium Spinel Sulfides: Alternating Antiferromagnetic and Ferromagnetic Interactions in the Breathing Pyrochlore Lattice: Y. Okamoto, M. Mori, N. Katayama, A. Miyake, M. Tokunaga, A. Matsuo, K. Kindo and K. Takenaka, *J. Phys. Soc. Jpn.* **87** (2018) 034709 (1-8).
3. \*High-field phase diagram and phase transitions in hexagonal manganite  $\text{ErMnO}_3$ : Y. J. Liu, J. F. Wang, X. F. Sun, J. -S. Zhou, Z. C. Xia, Z. W. Ouyang, M. Yang, C. B. Liu, R. Chen, J. -G. Cheng, Y. Kohama, M. Tokunaga and K. Kindo, *Phys. Rev. B* **97** (2018) 214419 (1-5).
4. †Impact of antiferromagnetic order on Landau-level splitting of quasi-two-dimensional Dirac fermions in  $\text{EuMnBi}_2$ : H. Masuda, H. Sakai, M. Tokunaga, M. Ochi, H. Takahashi, K. Akiba, A. Miyake, K. Kuroki, Y. Tokura and S. Ishiwata, *Phys. Rev. B* **98** (2018) 161108 (1-6).
5. Magnetic field effect on the chiral magnetism of noncentrosymmetric  $\text{UPtGe}$ : Experiment and theory: A. Miyake, L. M. Sandratskii, A. Nakamura, F. Honda, Y. Shimizu, D. Li, Y. Homma, M. Tokunaga and D. Aoki, *Phys. Rev. B* **98** (2018) 174436 (1-6).
6. \*Magnetic field induced phenomena in  $\text{UIrGe}$  in fields applied along the b axis: J. Pospíšil, Y. Haga, Y. Kohama, A. Miyake, S. Kambe, N. Tateiwa, M. Vališka, P. Proschek, J. Prokleška, V. Sechovský, M. Tokunaga, K. Kindo, A. Matsuo and E. Yamamoto, *Phys. Rev. B* **98** (2018) 014430 (1-7).
7. †Negative magnetoresistance suppressed through a topological phase transition in  $(\text{Cd}_{1-x}\text{Zn}_x)_3\text{As}_2$  thin films: S. Nishihaya, M. Uchida, Y. Nakazawa, K. Akiba, M. Kriener, Y. Kozuka, A. Miyake, Y. Taguchi, M. Tokunaga and M. Kawasaki, *Phys. Rev. B* **97** (2018) 245103 (1-7).
8. Quantitative evaluation of Dirac physics in PbTe: K. Akiba, A. Miyake, H. Sakai, K. Katayama, H. Murakawa, N. Hanasaki, S. Takaoka, Y. Nakanishi, M. Yoshizawa and M. Tokunaga, *Phys. Rev. B* **98** (2018) 115144 (1-11).
9. \*Unusual magnetoelectric memory and polarization reversal in the kagome staircase compound  $\text{Ni}_3\text{V}_2\text{O}_8$ : Y. J. Liu, J. F. Wang, Z. Z. He, C. L. Lu, Z. C. Xia, Z. W. Ouyang, C. B. Liu, R. Chen, A. Matsuo, Y. Kohama, K. Kindo and M. Tokunaga, *Phys. Rev. B* **97** (2018) 174429 (1-6).
10. 室温マルチフェロイック物質ビスマスフェライトの電気磁気効果: 河智 史朗, 三宅 厚志, 徳永 将史, 伊藤 利充, *固体物理* **53** (2018) 61-70.
11. †Deviation from the Kohler’s rule and Shubnikov–de Haas oscillations in type-II Weyl semimetal  $\text{WTe}_2$ : High magnetic field study up to 56 T: S. Onishi, R. Jha, A. Miyake, R. Higashinaka, T. D. Matsuda, M. Tokunaga and Y. Aoki, *AIP Advances* **8** (2018) 101330 (1-5).
12. †Large magneto-thermopower in  $\text{MnGe}$  with topological spin texture: Y. Fujishiro, N. Kanazawa, T. Shimojima, A. Nakamura, K. Ishizaka, T. Koretsune, R. Arita, A. Miyake, H. Mitamura, K. Akiba, M. Tokunaga, J. Shioyai, S. Kimura, S. Awaji, A. Tsukazaki, A. Kikkawa, Y. Taguchi and Y. Tokura, *Nat. Commun.* **9** (2018) 408 (1-7).

---

† Joint research with outside partners.

13. †Consecutive magnetic phase diagram of UCoGe-URhGe-UIrGe system: J. Pospíšil, Y. Haga, A. Miyake, S. Kambe, N. Tateiwa, Y. Tokunaga, F. Honda, A. Nakamura, Y. Homma, M. Tokunaga, D. Aoki and E. Yamamoto, *Physica B: Condensed Matter* **536** (2018) 532-534.
14. Observation of Poiseuille flow of phonons in black phosphorus: Y. Machida, A. Subedi, K. Akiba, A. Miyake, M. Tokunaga, Y. Akahama, K. Izawa and K. Behnia, *Sci. Adv.* **4** (2018) eaat3374 (1-9).
15. \*Magnetic structural unit with convex geometry: A building block hosting an exchange-striction-driven magnetoelectric coupling: K. Kimura, Y. Kato, K. Yamauchi, A. Miyake, M. Tokunaga, A. Matsuo, K. Kindo, M. Akaki, M. Hagiwara, S. Kimura, M. Toyoda, Y. Motome and T. Kimura, *Phys. Rev. Materials* **2** (2018) 104415 (1-12).
16. †Negative-pressure-induced helimagnetism in ferromagnetic cubic perovskites  $Sr_{1-x}Ba_xCoO_3$ : H. Sakai, S. Yokoyama, A. Kuwabara, J. S. White, E. Canévet, H. M. Rønnow, T. Koretsune, R. Arita, A. Miyake, M. Tokunaga, Y. Tokura and S. Ishiwata, *Phys. Rev. Materials* **2** (2018) 104412 (1-6).
17. †Magnetic-field-induced transition for reentrant martensitic transformation in Co-Cr-Ga-Si shape memory alloys: X. Xu, T. Kihara, A. Miyake, M. Tokunaga, T. Kanomata and R. Kainuma, *Journal of Magnetism and Magnetic Materials* **466** (2018) 273-276.
18. †Thermal, magnetic field- and stress-induced transformation in Heusler-type Co-Cr-Al-Si shape memory alloys: T. Odaira, X. Xu, A. Miyake, T. Omori, M. Tokunaga and R. Kainuma, *Scripta Materialia* **153** (2018) 35-39.
19. †\*Difference in magnetic and ferroelectric properties between rhombohedral and hexagonal polytypes of  $AgFeO_2$ : A single-crystal study: N. Terada, Y. Ikeda, H. Sato, D. D. Khalyavin, P. Manuel, F. Orlandi, Y. Tsujimoto, Y. Matsushita, A. Miyake, A. Matsuo, M. Tokunaga and K. Kindo, *Phys. Rev. B* **99** (2019) 064402 (1-11).
20. †Magnetic and electrical properties of the ternary compound  $U_2Ir_2Si_5$  with one-dimensional uranium zigzag chains: D. X. Li, F. Honda, A. Miyake, Y. Homma, Y. Haga, A. Nakamura, Y. Shimizu, A. Maurya, Y. J. Sato, M. Tokunaga and D. Aoki, *Phys. Rev. B* **99** (2019) 054408 (1-9).
21. †\*Magnetoelectric behavior from cluster multipoles in square cupolas: Study of  $Sr(TiO)Cu_4(PO_4)_4$  in comparison with Ba and Pb isostructurals: Y. Kato, K. Kimura, A. Miyake, M. Tokunaga, A. Matsuo, K. Kindo, M. Akaki, M. Hagiwara, S. Kimura, T. Kimura and Y. Motome, *Phys. Rev. B* **99** (2019) 024415 (1-12).
22. †\*Topological transitions among skyrmion- and hedgehog-lattice states in cubic chiral magnets: Y. Fujishiro, N. Kanazawa, T. Nakajima, X. Z. Yu, K. Ohishi, Y. Kawamura, K. Kakurai, T. Arima, H. Mitamura, A. Miyake, K. Akiba, M. Tokunaga, A. Matsuo, K. Kindo, T. Koretsune, R. Arita and Y. Tokura, *Nat. Commun.* **10** (2019) 1059 (1-8).
23. \*Thermodynamic evidence of magnetic-field-induced complete valley polarization in bismuth: A. Iwasa, A. Kondo, S. Kawachi, K. Akiba, Y. Nakanishi, M. Yoshizawa, M. Tokunaga and K. Kindo, *Sci Rep* **9** (2019) 1672 (1-8).
24. \*A series of magnon crystals appearing under ultrahigh magnetic fields in a kagomé antiferromagnet: R. Okuma, D. Nakamura, T. Okubo, A. Miyake, A. Matsuo, K. Kindo, M. Tokunaga, N. Kawashima, S. Takeyama and Z. Hiroi, *Nature Communications* **10** (2019) 1229 (7).

## Y. Matsuda group

Ultrahigh magnetic fields of up to 1200 T has been generated by the electromagnetic flux compression technique using a new 5 MJ condenser bank system installed in ISSP rather recently. It is the indoor world record of magnetic field. Several measurements such as Faraday rotation, optical transmission, magnetization, and electrical resistivity have already been done using multi-megagauss magnetic fields. Development of the technique for measuring magnetostriction has been conducted and the one using so-called Fiber Bragg Grating (FBG) was improved. The field-induced linear magnetostriction corresponding to the magnetization plateau behavior of a deformed Kagome lattice has been clearly observed. In addition, thermal properties in the Kondo insulator  $YbB_{12}$  was studied in pulsed high fields of up to 60 T, and the field-induced metallic phase has been found to be a heavy fermion metal.

1. †\*Magnetic-Field-Induced Kondo Metal Realized in  $YbB_{12}$ : T. T. Terashima, Y. H. Matsuda, Y. Kohama, A. Ikeda, A. Kondo, K. Kindo and F. Iga, *Phys. Rev. Lett.* **120** (2018) 257206 (1-5).
2. †\*100 MHz high-speed strain monitor using fiber Bragg grating and optical filter applied for magnetostriction measurements of cobaltite at magnetic fields beyond 100 T: A. Ikeda, T. Nomura, Y. H. Matsuda, S. Tani, Y. Kobayashi, H. Watanabe and K. Sato, *Physica B: Condensed Matter* **536** (2018) 847-849.

---

\* Joint research among groups within ISSP.

3. †Note: Optical filter method for high-resolution magnetostriction measurement using fiber Bragg grating under milli-second-pulsed high magnetic fields at cryogenic temperatures: A. Ikeda, Y. H. Matsuda and H. Tsuda, *Review of Scientific Instruments* **89** (2018) 096103 (3 pages).
4. \*Record indoor magnetic field of 1200 T generated by electromagnetic flux-compression: D. Nakamura, A. Ikeda, H. Sawabe, Y. H. Matsuda and S. Takeyama, *Review of Scientific Instruments* **89** (2018) 095106 (1-7).
5. †\*Magnetoelastic couplings in the deformed kagome quantum spin lattice of volborthite: A. Ikeda, S. Furukawa, O. Janson, Y. H. Matsuda, S. Takeyama, T. Yajima, Z. Hiroi and H. Ishikawa, *Phys. Rev. B* **99** (2019) 140412(R) 1-5.
6. ファイバーブラッググレーティングを用いた高速 100MHz ひずみ測定装置の構築と超強磁場中スピン格子物性の開拓：池田 暁彦，松田 康弘，*固体物理* **54** (2019) 147- 157.

## Kohama group

We have investigated various high-field properties by means of specific heat, magnetooptics and resistivity measurement techniques. In  $\text{Ni}_3\text{V}_2\text{O}_8$ ,  $\text{YbB}_{12}$  and  $\text{UIrGe}$ , the field-induced phase transitions have been detected, where the field dependence of entropy have been unveiled. We also have started to construct a new type of capacitor bank for the generation of pulsed magnetic fields with the second order timescale.

1. \*High-field phase diagram and phase transitions in hexagonal manganite  $\text{ErMnO}_3$ : Y. J. Liu, J. F. Wang, X. F. Sun, J. -S. Zhou, Z. C. Xia, Z. W. Ouyang, M. Yang, C. B. Liu, R. Chen, J. -G. Cheng, Y. Kohama, M. Tokunaga and K. Kindo, *Phys. Rev. B* **97** (2018) 214419 (1-5).
2. †\*Magnetic field induced ferroelectricity and half magnetization plateau in polycrystalline  $\text{R}_2\text{V}_2\text{O}_7$  (R = Ni, Co): R. Chen, J. F. Wang, Z. W. Ouyang, Z. Z. He, S. M. Wang, L. Lin, J. M. Liu, C. L. Lu, Y. Liu, C. Dong, C. B. Liu, Z. C. Xia, A. Matsuo, Y. Kohama and K. Kindo, *Phys. Rev. B* **98** (2018) 184404 (1-7).
3. \*Magnetic field induced phenomena in  $\text{UIrGe}$  in fields applied along the b axis: J. Pospíšil, Y. Haga, Y. Kohama, A. Miyake, S. Kambe, N. Tateiwa, M. Vališka, P. Proschek, J. Prokleška, V. Sechovský, M. Tokunaga, K. Kindo, A. Matsuo and E. Yamamoto, *Phys. Rev. B* **98** (2018) 014430 (1-7).
4. \*Unusual magnetoelectric memory and polarization reversal in the kagome staircase compound  $\text{Ni}_3\text{V}_2\text{O}_8$ : Y. J. Liu, J. F. Wang, Z. Z. He, C. L. Lu, Z. C. Xia, Z. W. Ouyang, C. B. Liu, R. Chen, A. Matsuo, Y. Kohama, K. Kindo and M. Tokunaga, *Phys. Rev. B* **97** (2018) 174429 (1-6).
5. †\*Magnetic-Field-Induced Kondo Metal Realized in  $\text{YbB}_{12}$ : T. T. Terashima, Y. H. Matsuda, Y. Kohama, A. Ikeda, A. Kondo, K. Kindo and F. Iga, *Phys. Rev. Lett.* **120** (2018) 257206 (1-5).
6. \*Quantum Criticality of an Ising-like Spin-1/2 Antiferromagnetic Chain in a Transverse Magnetic Field: Z. Wang, T. Lorenz, D. I. Gorbunov, P. T. Cong, Y. Kohama, S. Niesen, O. Breunig, J. Engelmayer, A. Herman, J. Wu, K. Kindo, J. Wosnitza, S. Zherlitsyn and A. Loidl, *Phys. Rev. Lett.* **120** (2018) 207205 (1-6).
7. Magneto-optical Transitions of GaAs/AlGaAs Multiple Quantum Wells: Y. Kim, J. D. Song and Y. Kohama, *J. Korean Phys. Soc.* **73** (2018) 338-342.
8. †\*Enhancement of the effective mass at high magnetic fields in  $\text{CeRhIn}_5$ : L. Jiao, M. Smidman, Y. Kohama, Z. S. Wang, D. Graf, Z. F. Weng, Y. J. Zhang, A. Matsuo, E. D. Bauer, H. Lee, S. Kirchner, J. Singleton, K. Kindo, J. Wosnitza, F. Steglich, J. D. Thompson and H. Q. Yuan, *Phys. Rev. B* **99** (2019) 045127 (6).
9. Viscosity measurements in pulsed magnetic fields by using a quartz-crystal microbalance: T. Nomura, S. Zherlitsyn, Y. Kohama and J. Wosnitza, *Rev. Sci. Instrum.* **90** (2019) 065101.
10. \*カゴメ銅鉍物ボルボサイトにおける軌道転移とフラストレート磁性：広井 善二，石川 孟，小濱 芳允，*固体物理* **54** (2019) 117-130.
11. \*Unconventional field-induced spin gap in an  $S = 1/2$  chiral staggered chain: J. Liu, S. Kittaka, R. D. Johnson, T. Lancaster, J. Singleton, T. Sakakibara, Y. Kohama, J. van Tol, A. Ardavan, B. H. Williams, S. J. Blundell, Z. E. Manson, J. L. Manson and P. A. Goddard, *Phys Rev Lett* **122** (2019) 057207.
12. †\*Multiple topological states in iron-based superconductors: P. Zhang, Z. Wang, X. Wu, K. Yaji, Y. Ishida, Y. Kohama, G. Dai, Y. Sun, C. Bareille, K. Kuroda, T. Kondo, K. Okazaki, K. Kindo, X. Wang, C. Jin, J. Hu, R. Thomale, K. Sumida, S. Wu, K. Miyamoto, T. Okuda, H. Ding, G. D. Gu, T. Tamegai, T. Kawakami, M. Sato and S. Shin, *Nature Phys* **15** (2019) 41-48.

---

† Joint research with outside partners.

13. Shubnikov–de Haas oscillations in the three-dimensional Dirac fermion system Ca<sub>3</sub>PbO: Y. Obata, Y. Kohama, S. Matsuishi and H. Hosono, *Phys Rev B* **99** (2019) 115133.
14. \*Strain-induced spontaneous Hall effect in an epitaxial thin film of a Luttinger semimetal: T. Ohtsuki, Z. Tian, A. Endo, M. Halim, S. Katsumoto, Y. Kohama, K. Kindo, M. Lippmaa and S. Nakatsuji, *Proc. Natl. Acad. Sci. USA* **116** (2019) 8803-8808.
15. \*Possible observation of quantum spin-nematic phase in a frustrated magnet: Y. Kohama, H. Ishikawa, A. Matsuo, K. Kindo, N. Shannon and Z. Hiroi, *Proc. Nat. Acad. Sci. U.S.A.* **116** (2019) 10686-10690.

## Laser and Synchrotron Research Center

### Shin group

We studied high T<sub>c</sub> Fe-pnictide superconductors using 7-eV laser. High resolution photoemission study with polarization dependence is very powerful for the study of the superconducting mechanism. Orbital fluctuation mechanism is also important in addition to the spin fluctuation mechanism.

1. \*Surface electronic states of Au-induced nanowires on Ge(001): K. Yaji, R. Yukawa, S. Kim, Y. Ohtsubo, P. L. Fèvre, F. Bertran, A. Taleb-Ibrahimi, I. Matsuda, K. Nakatsuji, S. Shin and F. Komori, *J. Phys.: Condens. Matter* **30** (2018) 075001 (1-7).
2. †\*Antiphase Fermi-surface modulations accompanying displacement excitation in a parent compound of iron-based superconductors: K. Okazaki, H. Suzuki, T. Suzuki, T. Yamamoto, T. Someya, Y. Ogawa, M. Okada, M. Fujisawa, T. Kanai, N. Ishi, J. Itatani, M. Nakajima, H. Eisaki, A. Fujimori and S. Shin, *Phys. Rev. B* **97** (2018) 121107(R) (1-6).
3. \*Disorder-sensitive nodelike small gap in FeSe: Y. Sun, S. Kittaka, S. Nakamura, T. Sakakibara, P. Zhang, S. Shin, K. Irie, T. Nomoto, K. Machida, J. Chen and T. Tamegai, *Phys. Rev. B* **98** (2018) 064505 (1-7).
4. †\*Giant Rashba splitting of quasi-one-dimensional surface states on Bi/InAs(110)- (2×1): T. Nakamura, Y. Ohtsubo, Y. Yamashita, S.-I. Ideta, K. Tanaka, K. Yaji, A. Harasawa, S. Shin, F. Komori, R. Yukawa, K. Horiba, H. Kumigashira and S.-I. Kimura, *Phys. Rev. B* **98** (2018) 075431.
5. \*Kondo hybridization and quantum criticality in β-YbAlB<sub>4</sub> by laser ARPES: C. Bareille, S. Suzuki, M. Nakayama, K. Kuroda, A. H. Nevidomskyy, Y. Matsumoto, S. Nakatsuji, T. Kondo and S. Shin, *Phys. Rev. B* **97** (2018) 045112 (1-7).
6. Ultrafast dynamics of an unoccupied surface resonance state in Bi<sub>2</sub>Te<sub>2</sub>Se: N. Munisa, E. E. Krasovskii, Y. Ishida, K. Sumida, J. Chen, T. Yoshikawa, E. V. Chulkov, K. A. Kokh, O. E. Tereshchenko, S. Shin and A. Kimura, *Phys. Rev. B* **97** (2018) 115303 (1-6).
7. \*Femtosecond resonant magneto-optical Kerr effect measurement on an ultrathin magnetic film in a soft X-ray free electron laser: S. Yamamoto, Y. Kubota, K. Yamamoto, Y. Takahashi, K. Maruyama, Y. Suzuki, R. Hobara, M. Fujisawa, D. Oshima, S. Owada, T. Togashi, K. Tono, M. Yabashi, Y. Hirata, S. Yamamoto, M. Kotsugi, H. Wadati, T. Kato, S. Iwata, S. Shin and I. Matsuda, *Jpn. J. Appl. Phys.* **57** (2018) 09TD02 (1-4).
8. †\*Electronic Structure of Ce-Doped and -Undoped Nd<sub>2</sub>CuO<sub>4</sub> Superconducting Thin Films Studied by Hard X-Ray Photoemission and Soft X-Ray Absorption Spectroscopy: M. Horio, Y. Krockenberger, K. Yamamoto, Y. Yokoyama, K. Takubo, Y. Hirata, S. Sakamoto, K. Koshiishi, A. Yasui, E. Ikenaga, S. Shin, H. Yamamoto, H. Wadati and A. Fujimori, *Phys. Rev. Lett.* **120** (2018) 257001 (1-6).
9. \*Element Selectivity in Second-Harmonic Generation of GaFeO<sub>3</sub> by a Soft-X-Ray Free-Electron Laser: Sh. Yamamoto, T. Omi, H. Akai, Y. Kubota, Y. Takahashi, Y. Suzuki, Y. Hirata, K. Yamamoto, R. Yukawa, K. Horiba, H. Yumoto, T. Koyama, H. Ohashi, S. Owada, K. Tono, M. Yabashi, E. Shigemasa, S. Yamamoto, M. Kotsugi, H. Wadati, H. Kumigashira, T. Arima, S. Shin and I. Matsuda, *Phys. Rev. Lett.* **120** (2018) 223902 (1-5).
10. †\*Experimental Determination of the Topological Phase Diagram in Cerium Monopnictides: K. Kuroda, M. Ochi, H. S. Suzuki, M. Hirayama, M. Nakayama, R. Noguchi, C. Bareille, S. Akebi, S. Kunisada, T. Muro, M. D. Watson, H. Kitazawa, Y. Haga, T. K. Kim, M. Hoesch, S. Shin, R. Arita and T. Kondo, *Phys. Rev. Lett.* **120** (2018) 086402 (1-6).
11. \*Observation of topological superconductivity on the surface of an iron-based superconductor: P. Zhang, K. Yaji, T. Hashimoto, Y. Ota, T. Kondo, K. Okazaki, Z. Wang, J. Wen, G. D. Gu, H. Ding and S. Shin, *Science* **360** (2018) 182-186.

---

\* Joint research among groups within ISSP.

12. \* レーザー励起スピン分解光電子分光で解き明かす光スピン制御: 矢治光 一郎, 黒田 健太, 小森 文夫, 辛 埴, 光学 **47** (2018) 142-147.
13. †\*Resonant magneto-optical Kerr effect measurement system using a high harmonic generation laser: Sh. Yamamoto, D. Oumbarek, M. Fujisawa, T. Someya, Y. Takahashi, T. Yamamoto, N. Ishiia, K. Yajia, S. Yamamoto, T. Kanai, K. Okazaki, M. Kotsugi, J. Itatani, S. Shin and I. Matsuda, *J. Electron Spectrosc. Relat. Phenom.* **222** (2018) 68-73.
14. \*Superconducting gap anisotropy sensitive to nematic domains in FeSe: T. Hashimoto, Y. Ota, H. Q. Yamamoto, Y. Suzuki, T. Shimojima, S. Watanabe, C. Chen, S. Kasahara, Y. Matsuda, T. Shibauchi, K. Okazaki and S. Shin, *Nat. Commun.* **9** (2018) 282 (1-7).
15. \*Experimental Methods for Spin and Angle-Resolved Photoemission Spectroscopy Combined with Polarization Variable Laser: K. Kuroda, K. Yaji, A. Harasawa, R. Noguchi, T. Kondo, F. Komori and S. Shin, *JoVE* **136** (2018) e57090.
16. \*Orbital-selective metal-insulator transition lifting the  $t_{2g}$  band hybridization in the Hund metal  $\text{Sr}_3(\text{Ru}_{1-x}\text{Mn}_x)_2\text{O}_7$ : M. Nakayama, T. Kondo, K. Kuroda, C. Bareille, M. D. Watson, S. Kunisada, R. Noguchi, T. K. Kim, M. Hoesch, Y. Yoshida and S. Shin, *Physical Review B* **98** (2018) 161102(R).
17. \*Rashba spin splitting of L-gap surface states on Ag(111) and Cu(111): K. Yaji, A. Harasawa, K. Kuroda, R. Li, B. Yan, F. Komori and S. Shin, *Physical Review B* **98** (2018) 041404(R).
18. †\*Superconducting Pairing of Topological Surface States in Bismuth Selenide Films on Niobium: D. Flötotto, Y. Ota, Y. Bai, C. Zhang, K. Okazaki, A. Tsuzuki, T. Hashimoto, J. N. Eckstein, S. Shin and T. -C. Chiang, *Sci. Adv.* **4** (2018) eaar7214 (1-5).
19. \* レーザーで電子のスピン方向を自由に制御: 矢治光 一郎, 黒田 健太, 小森 文夫, 辛 埴, レーザー加工学会誌 **25** (2018) 39-42.
20. †\*Photo-induced semimetallic states realised in electron-hole coupled insulators: K. Okazaki, Y. Ogawa, T. Suzuki, T. Yamamoto, T. Someya, S. Michimae, M. Watanabe, Y. Lu, M. Nohara, H. Takagi, N. Katayama, H. Sawa, M. Fujisawa, T. Kanai, N. Ishii, J. Itatani, T. Mizokawa and S. Shin, *Nat Commun* **9** (2018) 4322 (1-6).
21. \*Imaging the Formation of Ferromagnetic Domains at the  $\text{LaAlO}_3/\text{SrTiO}_3$  Interface: Y. Motoyui, T. Taniuchi, P. Scheiderer, J. N. Lee, J. Gabel, F. Pfaff, M. Sing, M. Lippmaa, R. Claessen and S. Shin, *J. Phys. Soc. Jpn.* **88** (2019) 034717 (1-5).
22. †\*Coexistence of Two Types of Spin Splitting Originating from Different Symmetries: K. Yaji, A. Visikovskiy, T. Iimori, K. Kuroda, S. Hayashi, T. Kajiwara, S. Tanaka, F. Komori and S. Shin, *Phys. Rev. Lett.* **122** (2019) 126403.
23. \*A weak topological insulator state in quasi-one-dimensional bismuth iodide: R. Noguchi, T. Takahashi, K. Kuroda, M. Ochi, T. Shirasawa, M. Sakano, C. Bareille, M. Nakayama, M. D. Watson, K. Yaji, A. Harasawa, H. Iwasawa, P. Dudin, T. K. Kim, M. Hoesch, V. Kandyba, A. Giampietri, A. Barinov, S. Shin, R. Arita, T. Sasagawa and T. Kondo, *Nature* **566** (2019) 518.
24. \*Low-energy electron-mode couplings in the surface bands of  $\text{Sr}_2\text{RuO}_4$  revealed by laser-based angle-resolved photoemission spectroscopy: S. Akebi, T. Kondo, M. Nakayama, K. Kuroda, S. Kunisada, H. Taniguchi, Y. Maeno and S. Shin, *Physical Review B* **99** (2019) 081108(R).
25. †\*Multiple topological states in iron-based superconductors: P. Zhang, Z. Wang, X. Wu, K. Yaji, Y. Ishida, Y. Kohama, G. Dai, Y. Sun, C. Bareille, K. Kuroda, T. Kondo, K. Okazaki, K. Kindo, X. Wang, C. Jin, J. Hu, R. Thomale, K. Sumida, S. Wu, K. Miyamoto, T. Okuda, H. Ding, G. D. Gu, T. Tamegai, T. Kawakami, M. Sato and S. Shin, *Nature Phys* **15** (2019) 41-48.

## I. Matsuda group

In 2018, we extended our experimental technique, developed at Spring-8 BL07LSU, to the next generation light sources. Using an X-ray free electron laser, we successfully observed the second harmonic generation of soft X-ray in a non-linear crystal of  $\text{GaFeO}_3$ . The signal was enhanced by the core-level resonance effect and, thus, it contained the element specific information. This fact indicates that the non-linear soft X-ray spectroscopy becomes an experimental probe for material science. We also designed new beamlines and experimental stations for ultimately high-brilliant soft X-ray synchrotron radiation, motivated by announcement on the next-generation facility by the Minister of Education, Culture, Sports, Science and Technology. Concerning the material science, we synthesized novel atomic layers. For examples, we fabricated a free-standing layer of borophane and also a monolayer of the Cat-TTF derivative that form interface hydrogen bonding with the self-assembled monolayer. We also examined their electronic properties and carrier dynamics by synchrotron radiation and laser.

---

† Joint research with outside partners.

1. \*Surface electronic states of Au-induced nanowires on Ge(001): K. Yaji, R. Yukawa, S. Kim, Y. Ohtsubo, P. L. Fèvre, F. Bertran, A. Taleb-Ibrahimi, I. Matsuda, K. Nakatsuji, S. Shin and F. Komori, *J. Phys.: Condens. Matter* **30** (2018) 075001 (1-7).
2. \*Alkali-metal induced band structure deformation investigated by angle-resolved photoemission spectroscopy and first-principles calculations: S. Ito, B. Feng, M. Arita, T. Someya, W. -C. Chen, A. Takayama, T. Iimori, H. Namatame, M. Taniguchi, C. -M. Cheng, S. -J. Tang, F. Komori and I. Matsuda, *Phys. Rev. B* **97** (2018) 155423 (1-8).
3. \*Peculiar bonding associated with atomic doping and hidden honeycombs in borophene: C.-C. Lee, B. Feng, M. D'angelo, R. Yukawa, R.-Y. Liu, T. Kondo, H. Kumigashira, I. Matsuda and T. Ozaki, *Phys. Rev. B* **97** (2018) 075430 (1-5).
4. \*Femtosecond resonant magneto-optical Kerr effect measurement on an ultrathin magnetic film in a soft X-ray free electron laser: S. Yamamoto, Y. Kubota, K. Yamamoto, Y. Takahashi, K. Maruyama, Y. Suzuki, R. Hobara, M. Fujisawa, D. Oshima, S. Owada, T. Togashi, K. Tono, M. Yabashi, Y. Hirata, S. Yamamoto, M. Kotsugi, H. Wadati, T. Kato, S. Iwata, S. Shin and I. Matsuda, *Jpn. J. Appl. Phys.* **57** (2018) 09TD02 (1-4).
5. \*Element Selectivity in Second-Harmonic Generation of GaFeO<sub>3</sub> by a Soft-X-Ray Free-Electron Laser: Sh. Yamamoto, T. Omi, H. Akai, Y. Kubota, Y. Takahashi, Y. Suzuki, Y. Hirata, K. Yamamoto, R. Yukawa, K. Horiba, H. Yumoto, T. Koyama, H. Ohashi, S. Owada, K. Tono, M. Yabashi, E. Shigemasa, S. Yamamoto, M. Kotsugi, H. Wadati, H. Kumigashira, T. Arima, S. Shin and I. Matsuda, *Phys. Rev. Lett.* **120** (2018) 223902 (1-5).
6. Controlling the surface photovoltage on WSe<sub>2</sub> by surface chemical modification: R.-Y. Liu, K. Ozawa, N. Terashima, Y. Natsui, B. Feng, S. Ito, W.-C. Chen, C.-M. Cheng, S. Yamamoto, H. Kato, T.-C. Chiang and I. Matsuda, *Appl. Phys. Lett.* **112** (2018) 211603 (1-5).
7. Interfacial carrier dynamics of graphene on SiC, traced by the full-range time-resolved core-level photoemission spectroscopy: T. Someya, H. Fukidome, N. Endo, K. Takahashi, S. Yamamoto and I. Matsuda, *Appl. Phys. Lett.* **113** (2018) 051601(1-4).
8. †\*Resonant magneto-optical Kerr effect measurement system using a high harmonic generation laser: Sh. Yamamoto, D. Oumbarek, M. Fujisawa, T. Someya, Y. Takahashi, T. Yamamoto, N. Ishiia, K. Yajia, S. Yamamoto, T. Kanai, K. Okazaki, M. Kotsugi, J. Itatani, S. Shin and I. Matsuda, *J. Electron Spectrosc. Relat. Phenom.* **222** (2018) 68-73.
9. \*A Table-Top Formation of Bilayer Quasi-Free-Standing Epitaxial-Graphene on SiC(0001) by Microwave Annealing in Air: K.-S. Kim, G.-H. Park, H. Fukidome, T. Someya, T. Iimori, F. Komori, I. Matsuda and M. Suemitsu, *Carbon* **130** (2018) 792-798.
10. †\*Strong Hydrogen Bonds at the Interface between Proton-Donating and -Accepting Self-Assembled Monolayers on Au(111): H. S. Kato, S. Yoshimoto, A. Ueda, S. Yamamoto, Y. Kanematsu, M. Tachikawa, H. Mori, J. Yoshinobu and I. Matsuda, *Langmuir* **34** (2018) 2189-2197.
11. \*物質科学、この1年「ボロフェンにおけるディラックフェルミオン」：松田 巖, *パリティ* **33** (2018) 36-38.
12. Correlation between Photocatalytic Activity and Carrier Lifetime: Acetic Acid on Single-Crystal Surfaces of Anatase and Rutile TiO<sub>2</sub>: K. Ozawa, S. Yamamoto, R. Yukawa, R.-Y. Liu, N. Terashima, Y. Natsui, H. Kato, K. Mase and I. Matsuda, *J. Phys. Chem. C* **122** (2018) 9562-9569.
13. \*Discovery of 2D Anisotropic Dirac Cones: B. Feng, J. Zhang, S. Ito, M. Arita, C. Cheng, L. Chen, K. Wu, F. Komori, O. Sugino, K. Miyamoto, T. Okuda, S. Meng and I. Matsuda, *Adv. Mater.* **30** (2018) 1704025 (1-6).
14. \*Enhancement of CO<sub>2</sub> adsorption on oxygen-functionalized epitaxial graphene surface under near-ambient conditions: S. Yamamoto, K. Takeuchi, Y. Hamamoto, R.-Y. Liu, Y. Shiozawa, T. Koitaya, T. Someya, K. Tashima, H. Fukidome, K. Mukai, S. Yoshimoto, M. Suemitsu, Y. Morikawa, J. Yoshinobu and I. Matsuda, *Phys. Chem. Chem. Phys.* **20** (2018) 19532.
15. Single-layer dual germanene phases on Ag(111): C.-H. Lin, A. Huang, W. W. Pai, W.-C. Chen, T.-Y. Chen, T.-R. Chang, R. Yukawa, C.-M. Cheng, C.-Y. Mou, I. Matsuda, T. -C. Chiang, H. -T. Jeng and S. -J. Tang, *Phys. Rev. Materials* **2** (2018) 024003 (1-8).
16. Time-Resolved Photoelectron Spectroscopy: I. Matsuda, *Compendium of Surface and Interface Analysis Contributed Book (Springer)* (2018).
17. Superstructure-Induced Splitting of Dirac Cones in Silicene: B. Feng, H. Zhou, Y. Feng, H. Liu, S. He, I. Matsuda, L. Chen, E. F. Schwier, K. Shimada, S. Meng and K. Wu, *Phys. Rev. Lett.* **122** (2019) 196801(1-6).

---

\* Joint research among groups within ISSP.

18. \*Direct Evidence of Interfacial Hydrogen Bonding in Proton-Electron Concerted 2D Organic Bilayer on Au Substrate: S. Yamamoto, H. S. Kato, A. Ueda, S. Yoshimoto, Y. Hirata, J. Miyawaki, K. Yamamoto, Y. Harada, H. Wadati, H. Mori, J. Yoshinobu and I. Matsuda, *e-Journal of Surface Science and Nanotechnology* **17** (2019) 49-55.
19. †Enhanced Photoresponsivity of Fullerene in the Presence of Phthalocyanine: A Time-Resolved X-ray Photoelectron Spectroscopy Study of Phthalocyanine/C<sub>60</sub>/TiO<sub>2</sub> (110): K. Ozawa, S. Yamamoto, M. D'angelo, Y. Natsui, N. Terashima, K. Mase and I. Matsuda, *J. Phys. Chem. C* **123** (2019) 4388-4395.
20. Electronic structure of a monoatomic Cu<sub>2</sub>Si layer on a Si(111) substrate: M. Cameau, R. Yukawa, C. -H. Chen, A. Huang, S. Ito, R. Ishibiki, K. Horiba, Y. Obata, T. Kondo, H. Kumigashira, H. -T. Jeng, M. D'angelo and I. Matsuda, *Phys. Rev. Materials* **3** (2019) 044004 (1-5).
21. Semimetallicity of free-standing hydrogenated monolayer boron from MgB<sub>2</sub>: I. Tateishi, N. T. Cuong, C. A. S. Moura, M. Cameau, R. Ishibiki, A. Fujino, S. Okada, A. Yamamoto, M. Araki, S. Ito, S. Yamamoto, M. Niibe, T. Tokushima, D. E. Weibel, T. Kondo, M. Ogata and I. Matsuda, *Phys. Rev. Materials* **3** (2019) 024004 (1-8).
22. \*Hydrogen adsorption and absorption on a Pd-Ag alloy surface studied using in-situ X-ray photoelectron spectroscopy under ultrahigh vacuum and ambient pressure: J. Tang, S. Yamamoto, T. Koitaya, Y. Yoshikura, K. Mukai, S. Yoshimoto, I. Matsuda and J. Yoshinobu, *Applied Surface Science* **463** (2019) 1161-1167.
23. \*Mass transport in the PdCu phase structures during hydrogen adsorption and absorption studied by XPS under hydrogen atmosphere: J. Tang, S. Yamamoto, T. Koitaya, A. Yoshigoe, T. Tokunaga, K. Mukai, I. Matsuda and J. Yoshinobu, *Applied Surface Science* **480** (2019) 419-426.
24. \*CO<sub>2</sub> Activation and Reaction on Zn-Deposited Cu Surfaces Studied by Ambient-Pressure X-ray Photoelectron Spectroscopy: T. Koitaya, S. Yamamoto, Y. Shiozawa, Y. Yoshikura, M. Hasegawa, J. Tang, K. Takeuchi, K. Mukai, S. Yoshimoto, I. Matsuda and J. Yoshinobu, *ACS Catal.* **9** (2019) 4539-4550.
25. Segmented Undulator for Extensive Polarization Controls in ≤1 nm-rad Emittance Rings: I. Matsuda, S. Yamamoto, J. Miyawaki, T. Abukawa and T. Tanaka, *e-J. Surf. Sci. Nanotechnol.* **17** (2019) 41-48.
26. Monatomic Two-Dimensional Layers: Modern Experimental Approaches for Structure, Properties, and Industrial Use: I. M. ed., (Elsevier, Amsterdam, Netherland, 2019).

## Kobayashi group

We are studying the state-of-the-art laser system including ultrashort-pulse lasers and deep-ultraviolet lasers. We aim to know "How and Why materials are broken by light?" utilizing experiment of light-matter interaction and deep-learning technology.

1. †Deep-hole drilling of amorphous silica glass by extreme ultraviolet femtosecond pulses: T. Shibuya, T. Takahashi, K. Sakaue, T.-H. Dinh, H. Hara, T. Higashiguchi, M. Ishino, Y. Koshiba, M. Nishikino, H. Ogawa, M. Tanaka, M. Washio, Y. Kobayashi and R. Kuroda, *Appl. Phys. Lett.* **113** (2018) 171902.
2. Pulse-by-pulse depth profile measurement of femtosecond laser ablation on copper: S. Tani and Y. Kobayashi, *Appl. Phys. A* **124** (2018) 265 (1-5).
3. Watt-level 193 nm source generation based on compact collinear cascaded sum frequency mixing configuration: Z. Zhao, C. Qu, H. Igarashi, H. Xuan, T. Miura, S. Ito and Y. Kobayashi, *Opt. Express* **26** (2018) 19435-19444.
4. †\*100 MHz high-speed strain monitor using fiber Bragg grating and optical filter applied for magnetostriction measurements of cobaltite at magnetic fields beyond 100 T: A. Ikeda, T. Nomura, Y. H. Matsuda, S. Tani, Y. Kobayashi, H. Watanabe and K. Sato, *Physica B: Condensed Matter* **536** (2018) 847-849.
5. High-Power, Solid-State, Deep Ultraviolet Laser Generation: H. Xuan, H. Igarashi, S. Ito, C. Qu, Z. Zhao and Y. Kobayashi, *Appl. Sci.* **8** (2018) 223 (1-13).
6. Efficient high harmonics generation by enhancement cavity driven with a post-compressed FCPA laser at 10 MHz: Z. Zhao, A. Ozawa, M. Kuwata-Gonokami and Y. Kobayashi, *High Pow Laser Sci Eng* **6** (2018) e19 (1-6).
7. \*Femtosecond pulse generation beyond photon lifetime limit in gain-switched semiconductor lasers: T. Ito, H. Nakamae, Y. Hazama, T. Nakamura, S. Chen, M. Yoshita, C. Kim, Y. Kobayashi and H. Akiyama, *Commun. Phys.* **1** (2018) 42.
8. Kerr-lens mode locking above a 20 GHz repetition rate: S. Kimura, S. Tani and Y. Kobayashi, *Optica* **6** (2019) 532-533.
9. Raman-assisted broadband mode-locked laser: S. Kimura, S. Tani and Y. Kobayashi, *Sci Rep* **9** (2019) 3738 (1-6).

---

† Joint research with outside partners.

10. Direct generation of femtosecond vortex beam from a Yb:KYW oscillator featuring a defect-spot mirror: S. Wang, Z. Zhao, I. Ito and Y. Kobayashi, *OSA Continuum* **2** (2019) 523-530.
11. Monolithic LiF or MgF<sub>2</sub> lens-window-prism device for coherent 10.7 eV beam source with 1 MHz repetition rate: Z. Zhao, K. Kuroda, A. Harasawa, T. Kondo, S. Shin and Y. Kobayashi, *Chin. Opt. Lett.* **17** (2019) 051406.
12. Improvement of conversion efficiency of DUV light generation at 221-nm using CLBO crystal: H. Igarashi, Z. Zhao, H. Xuan, C. Qu, S. Ito, Y. Tamaru, M. Tamiya, T. Miura, J. Fujimoto, H. Mizoguchi and Y. Kobayashi, in: *Proc. SPIE 10516, Nonlinear Frequency Generation and Conversion: Materials and Devices XVII* (SPIE, 2018), 1051602 (1-7).
13. TACMI コンソーシアムの展望: 小林 洋平, *光アライアンス* **29** (2018) 43.
14. レーザー加工がもたらす未来のものづくりシステムとは? AIを駆使した加工レシピの最適化へ: 小林 洋平, *OPTRONICS* **4** (2018) 167-172.
15. ものづくりを変える! NEDOのレーザー加工技術: 小林 洋平, *forcus NEDO* **68** (2018) 4.
16. カーレンズモード同期レーザーを用いた高繰り返し光周波数コムの開発: 木村 祥太, 谷 峻太郎, 小林 洋平, *光技術コンタクト* **57** (2019) 3-9.
17. \*Gerard A. Mourou 博士とチャープパルス増幅法: 渡部 俊太郎, 鍋川 康夫, 板谷 治郎, 小林 洋平, *科学* 82 巻 2 号 (2019) 131-137.

## Itatani group

We developed a high harmonic beamline for soft X-ray spectroscopy in the water window. Using a few-cycle CEP-stable intense IR source (optical parametric chirped pulse amplifier; OPCPA), attosecond pulses were produced in helium with a high pressure gas cell, resulting in broadband soft X-ray spectra that cover the entire water window (280-530 eV). We also developed an intense MIR source with a multi-plate pulse compression technique. Sub-two-cycle pulses at 3.5- $\mu\text{m}$  with a stable carrier-envelope phase were successfully produced. The maximum field amplitude at the focus was estimated to be 280 MV/cm. Using intense MIR sources, we carried out several experiments on high harmonic generation in solids. With a crystalline GaSe, we observed nontrivial polarization behavior, which was reproduced by the first-principle simulation and an intra-band current model. We also produced high harmonics in GaSe with circularly polarized pulses, and experimentally confirmed a selection rule. Collaboration with Shin and Okazaki groups was continued on time-resolved ARPES experiments.

1. †\* Antiphase Fermi-surface modulations accompanying displacement excitation in a parent compound of iron-based superconductors: K. Okazaki, H. Suzuki, T. Suzuki, T. Yamamoto, T. Someya, Y. Ogawa, M. Okada, M. Fujisawa, T. Kanai, N. Ishii, J. Itatani, M. Nakajima, H. Eisaki, A. Fujimori and S. Shin, *Phys. Rev. B* **97** (2018) 121107(R) (1-6).
2. †Polarization-Resolved Study of High Harmonics from Bulk Semiconductors: K. Kaneshima, Y. Shinohara, K. Takeuchi, N. Ishii, K. Imasaka, T. Kaji, S. Ashihara, K. L. Ishikawa and J. Itatani, *Phys. Rev. Lett.* **120** (2018) 243903.
3. †\*Resonant magneto-optical Kerr effect measurement system using a high harmonic generation laser: Sh. Yamamoto, D. Oumbarek, M. Fujisawa, T. Someya, Y. Takahashi, T. Yamamoto, N. Ishii, K. Yajia, S. Yamamoto, T. Kanai, K. Okazaki, M. Kotsugi, J. Itatani, S. Shin and I. Matsuda, *J. Electron Spectrosc. Relat. Phenom.* **222** (2018) 68-73.
4. Generation of sub-two-cycle CEP-stable optical pulses at 3.5  $\mu\text{m}$  from a KTA-based optical parametric amplifier with multiple-plate compression: F. Lu, P. Xia, Y. Matsumoto, T. Kanai, N. Ishii and J. Itatani, *Opt. Lett.* **43** (2018) 2720.
5. All-optical characterization of the two-dimensional waveform and the Gouy phase of an infrared pulse based on plasma fluorescence of gas: N. Saito, N. Ishii, T. Kanai and J. Itatani, *Opt. Express* **26** (2018) 24591.
6. †Generation of sub-two-cycle millijoule infrared pulses in an optical parametric chirped-pulse amplifier and their application to soft x-ray absorption spectroscopy with high-flux high harmonics: N. Ishii, K. Kaneshima, T. Kanai, S. Watanabe and J. Itatani, *J. Opt.* **20** (2018) 014003 (1-6).
7. †\*Photo-induced semimetallic states realised in electron-hole coupled insulators: K. Okazaki, Y. Ogawa, T. Suzuki, T. Yamamoto, T. Someya, S. Michimae, M. Watanabe, Y. Lu, M. Nohara, H. Takagi, N. Katayama, H. Sawa, M. Fujisawa, T. Kanai, N. Ishii, J. Itatani, T. Mizokawa and S. Shin, *Nat Commun* **9** (2018) 4322 (1-6).
8. \*Nonlinear propagation effects in high harmonic generation in reflection and transmission from gallium arsenide: P. Xia, C. Kim, F. Lu, T. Kanai, H. Akiyama, J. Itatani and N. Ishii, *Optics Express* **26** (2018) 29393-29400.

---

\* Joint research among groups within ISSP.

9. †Ultrafast Control of Ferroelectricity with Dynamical Repositioning of Protons in a Supramolecular Cocrystal Studied by Femtosecond Nonlinear Spectroscopy: T. Umanodan, K. Kaneshima, K. Takeuchi, N. Ishii, J. Itatani, H. Hirori, Y. Sanari, K. Tanaka, Y. Kanemitsu, T. Ishikawa, S.-Y. Koshihara, S. Horiuchi and Y. Okimoto, *J. Phys. Soc. Jpn.* **88** (2019) 013705.
10. Optical parametric amplification of carrier-envelope phase-stabilized mid-infrared pulses generated by intra-pulse difference frequency generation: N. Ishii, P. Xia, T. Kanai and J. Itatani, *Opt. Express* **27** (2019) 11447.
11. †High-order harmonic generation from hybrid organic–inorganic perovskite thin films: H. Hirori, P. Xia, Y. Shinohara, T. Otobe, Y. Sanari, H. Tahara, N. Ishii, J. Itatani, K. L. Ishikawa, T. Aharen, M. Ozaki, A. Wakamiya and Y. Kanemitsu, *APL Materials* **7** (2019) 041107.
12. \*Gerard A. Mourou 博士とチャープパルス増幅法：渡部 俊太郎，鍋川 康夫，板谷 治郎，小林 洋平，科学 82 卷 2 号 (2019) 131-137.

## Harada group

Advanced use of Resonant Inelastic X-ray Scattering is not limited to solid state physics or solution chemistry but now extending to biochemistry. Before entering real biosystems which contain extremely complex and inhomogeneous local structure and multi-elements we analyzed functional part of biosystems using model complexes like iron complexes, iron–sulfur complexes and cobalt containing polyoxometalate complexes. Charge transfer dynamics among metal sites of those complexes mediated by anionic ligands are essential to function biomaterials through catalysis, molecular binding, electron transfer and so on. We have established novel methods to obtain intact spectra of those fragile complexes to X-rays without radiation damage and published three papers this year. We have performed 13 collaborative works at BL07LSU HORNET end-station. They are well balanced in scientific topics; five of which are studies on the behavior of water at various circumstances (including international collaborations with researchers in MAX IV and Stockholm University in Sweden), four are batteries and the remaining four are solid state physics. Using beamtimes for beamline tuning we accepted some test experiments on samples from companies for future collaborations.

1. †Electronic structure and magnetic properties of the half-metallic ferrimagnet  $\text{Mn}_2\text{VAl}$  probed by soft x-ray spectroscopies: K. Nagai, H. Fujiwara, H. Aratani, S. Fujioka, H. Yomosa, Y. Nakatani, T. Kiss, A. Sekiyama, F. Kuroda, H. Fujii, T. Oguchi, A. Tanaka, J. Miyawaki, Y. Harada, Y. Takeda, Y. Saitoh, S. Suga and R. Y. Umetsu, *Phys. Rev. B* **97** (2018) 035143 (1-8).
2. †Raman and fluorescence-like components in resonant inelastic x-ray scattering on  $\text{LaAlO}_3/\text{SrTiO}_3$  heterostructures: F. Pfaff, H. Fujiwara, G. Berner, A. Yamasaki, H. Niwa, H. Kiuchi, A. Gloskovskii, W. Drube, J. Gabel, O. Kirilmaz, A. Sekiyama, J. Miyawaki, Y. Harada, S. Suga, M. Sing and R. Claessen, *Phys. Rev. B* **97** (2018) 035110 (1-8).
3. †\*Tensile-Strain-Dependent Spin States in Epitaxial  $\text{LaCoO}_3$  Thin Films: Y. Yokoyama, Y. Yamasaki, M. Taguchi, Y. Hirata, K. Takubo, J. Miyawaki, Y. Harada, D. Asakura, J. Fujioka, M. Nakamura, H. Daimon, M. Kawasaki, Y. Tokura and H. Wadati, *Phys. Rev. Lett.* **120** (2018) 206402 (1-5).
4. †Electronic Spectra of Iron–Sulfur Complexes Measured by 2p3d RIXS Spectroscopy: B. E. V. Kuiken, A. W. Hahn, B. Nayyar, C. E. Schiewer, S. C. Lee, F. Meyer, T. Weyhermüller, A. Nicolaou, Y.-T. Cui, J. Miyawaki, Y. Harada and S. DeBeer, *Inorg. Chem.* **57** (2018) 7355-7361.
5. †Probing the Valence Electronic Structure of Low-Spin Ferrous and Ferric Complexes Using 2p3d Resonant Inelastic X-ray Scattering (RIXS): A. W. Hahn, B. E. V. Kuiken, V. G. Chilkuri, N. Levin, E. Bill, T. Weyhermüller, A. Nicolaou, J. Miyawaki, Y. Harada and S. DeBeer, *Inorg. Chem.* **57** (2018) 9515-9530.
6. †Direct Observation of  $\text{Cr}^{3+}$  3d States in Ruby: Toward Experimental Mechanistic Evidence of Metal Chemistry: M. O. J. Y. Hunault, Y. Harada, J. Miyawaki, J. Wang, A. Meijerink, F. M. F. D. Groot and M. M. van Schooneveld, *J. Phys. Chem. A* **122** (2018) 4399-4413.
7. †Cobalt-to-vanadium charge transfer in polyoxometalate water oxidation catalysts revealed by 2p3d resonant inelastic X-ray scattering: B. Liu, E. N. Glass, R.-P. Wang, Y.-T. Cui, Y. Harada, D.-J. Huang, S. Schuppler, C. L. Hill and F. M. F. de Groot, *Phys. Chem. Chem. Phys.* **20** (2018) 4554-4562.
8. Resonant Inelastic X-ray Scattering (RIXS): Y. Harada, *Synchrotron Radiation News* **31** (2018) 2.
9. Resonant Inelastic X-Ray Scattering: Y. Harada, in: *Compendium of Surface and Interface Analysis*, Ch 86, edited by The Surface Science Society of Japan, (Springer, 2-40-13-402 Hongo, Bunkyo-ku, Tokyo 113-0033, 2018), 531-537.

† Joint research with outside partners.

## Wadati group

We succeeded in the observation of tensile-strain dependent spin states in epitaxial LaCoO<sub>3</sub> thin films by using soft x-ray RIXS in SPring-8 BL07LSU. We also started to use SACLA soft x-ray beam line and obtained second-harmonic generation of GaFeO<sub>3</sub>.

1. Commensurate versus incommensurate charge ordering near the superconducting dome in Ir<sub>1-x</sub>Pt<sub>x</sub>Te<sub>2</sub> revealed by resonant x-ray scattering: K. Takubo, K. Yamamoto, Y. Hirata, H. Wadati, T. Mizokawa, R. Sutarto, F. He, K. Ishii, Y. Yamasaki, H. Nakao, Y. Murakami, G. Matsuo, H. Ishii, M. Kobayashi, K. Kudo and M. Nohara, *Phys. Rev. B* **97** (2018) 205142 (1-9).
2. Thickness dependence and dimensionality effects on charge and magnetic orderings in La<sub>1/3</sub>Sr<sub>2/3</sub>FeO<sub>3</sub> thin films: K. Yamamoto, Y. Hirata, M. Horio, Y. Yokoyama, K. Takubo, M. Minohara, H. Kumigashira, Y. Yamasaki, H. Nakao, Y. Murakami, A. Fujimori and H. Wadati, *Phys. Rev. B* **97** (2018) 075134 (1-6).
3. \*Femtosecond resonant magneto-optical Kerr effect measurement on an ultrathin magnetic film in a soft X-ray free electron laser: S. Yamamoto, Y. Kubota, K. Yamamoto, Y. Takahashi, K. Maruyama, Y. Suzuki, R. Hobara, M. Fujisawa, D. Oshima, S. Owada, T. Togashi, K. Tono, M. Yabashi, Y. Hirata, S. Yamamoto, M. Kotsugi, H. Wadati, T. Kato, S. Iwata, S. Shin and I. Matsuda, *Jpn. J. Appl. Phys.* **57** (2018) 09TD02 (1-4).
4. †\*Electronic Structure of Ce-Doped and -Undoped Nd<sub>2</sub>CuO<sub>4</sub> Superconducting Thin Films Studied by Hard X-Ray Photoemission and Soft X-Ray Absorption Spectroscopy: M. Horio, Y. Krockenberger, K. Yamamoto, Y. Yokoyama, K. Takubo, Y. Hirata, S. Sakamoto, K. Koshiishi, A. Yasui, E. Ikenaga, S. Shin, H. Yamamoto, H. Wadati and A. Fujimori, *Phys. Rev. Lett.* **120** (2018) 257001 (1-6).
5. \*Element Selectivity in Second-Harmonic Generation of GaFeO<sub>3</sub> by a Soft-X-Ray Free-Electron Laser: Sh. Yamamoto, T. Omi, H. Akai, Y. Kubota, Y. Takahashi, Y. Suzuki, Y. Hirata, K. Yamamoto, R. Yukawa, K. Horiba, H. Yumoto, T. Koyama, H. Ohashi, S. Owada, K. Tono, M. Yabashi, E. Shigemasa, S. Yamamoto, M. Kotsugi, H. Wadati, H. Kumigashira, T. Arima, S. Shin and I. Matsuda, *Phys. Rev. Lett.* **120** (2018) 223902 (1-5).
6. †\*Tensile-Strain-Dependent Spin States in Epitaxial LaCoO<sub>3</sub> Thin Films: Y. Yokoyama, Y. Yamasaki, M. Taguchi, Y. Hirata, K. Takubo, J. Miyawaki, Y. Harada, D. Asakura, J. Fujioka, M. Nakamura, H. Daimon, M. Kawasaki, Y. Tokura and H. Wadati, *Phys. Rev. Lett.* **120** (2018) 206402 (1-5).
7. スピンのダイナミクスを元素別に見る (Keyword: 時間分解 XMCD) : 和達 大樹, *日本物理学会誌* **73** (2018) 4.
8. \*X-Ray Absorption Spectroscopy of 4f Compounds and Future Directions Toward Time-resolved Measurements: H. Wadati, K. Takubo, T. Tsuyama, Y. Yokoyama, K. Yamamoto, Y. Hirata, T. Ina, K. Nitta, M. Mizumaki, T. Togashi, S. Suzuki, Y. Matsumoto and S. Nakatsuji, *Adv. X-Ray. Chem. Anal., Japan* **49** (2018) 169-175.
9. Magnetic and electronic properties of B-site-ordered double-perovskite oxide La<sub>2</sub>CrMnO<sub>6</sub> thin films: K. Yoshimatsu, J. Ishimaru, K. Watarai, K. Yamamoto, Y. Hirata, H. Wadati, Y. Takeda, K. Horiba, H. Kumigashira, O. Sakata and A. Ohtomo, *Phys. Rev. B* **99** (2019) 235129 (1-8).
10. Photo-induced Spin Dynamics Revealed by Time-resolved Measurements with X-ray Free Electron Laser: K. Yamamoto and H. Wadati, *Magnetics Jpn.* **14**, No.3 (2019) 140-145.

## Kondo group

We use angle-resolved photoemission spectroscopy (ARPES) with ultrahigh energy resolution. The main findings in 2018 are as follows: (1) a weak topological insulator state in  $\alpha$ -Bi<sub>4</sub>I<sub>4</sub>, (2) Orbital-selective metal-insulator transition lifting the t<sub>2g</sub> band hybridization in the Hund metal Sr<sub>3</sub>(Ru<sub>1-x</sub>Mn<sub>x</sub>)<sub>2</sub>O<sub>7</sub>, and (3) Kondo hybridization and quantum criticality in  $\beta$ -YbAlB<sub>4</sub>.

1. \*Kondo hybridization and quantum criticality in  $\beta$ -YbAlB<sub>4</sub> by laser ARPES: C. Bareille, S. Suzuki, M. Nakayama, K. Kuroda, A. H. Nevidomskyy, Y. Matsumoto, S. Nakatsuji, T. Kondo and S. Shin, *Phys. Rev. B* **97** (2018) 045112 (1-7).
2. †\*Experimental Determination of the Topological Phase Diagram in Cerium Monopnictides: K. Kuroda, M. Ochi, H. S. Suzuki, M. Hirayama, M. Nakayama, R. Noguchi, C. Bareille, S. Akebi, S. Kunisada, T. Muro, M. D. Watson, H. Kitazawa, Y. Haga, T. K. Kim, M. Hoesch, S. Shin, R. Arita and T. Kondo, *Phys. Rev. Lett.* **120** (2018) 086402 (1-6).
3. \*Observation of topological superconductivity on the surface of an iron-based superconductor: P. Zhang, K. Yaji, T. Hashimoto, Y. Ota, T. Kondo, K. Okazaki, Z. Wang, J. Wen, G. D. Gu, H. Ding and S. Shin, *Science* **360** (2018) 182-186.

---

\* Joint research among groups within ISSP.

4. \*レーザー励起スピン分解光電子分光で解き明かす光スピン制御：矢治光 一郎，黒田 健太，小森 文夫，辛 埴，*光学* **47** (2018) 142-147.
5. \*Experimental Methods for Spin and Angle-Resolved Photoemission Spectroscopy Combined with Polarization Variable Laser: K. Kuroda, K. Yaji, A. Harasawa, R. Noguchi, T. Kondo, F. Komori and S. Shin, *JoVE* **136** (2018) e57090.
6. \*Orbital-selective metal-insulator transition lifting the t<sub>2g</sub> band hybridization in the Hund metal Sr<sub>3</sub>(Ru<sub>1-x</sub>Mn<sub>x</sub>)<sub>2</sub>O<sub>7</sub>: M. Nakayama, T. Kondo, K. Kuroda, C. Bareille, M. D. Watson, S. Kunisada, R. Noguchi, T. K. Kim, M. Hoesch, Y. Yoshida and S. Shin, *Physical Review B* **98** (2018) 161102(R).
7. \*Rashba spin splitting of L-gap surface states on Ag(111) and Cu(111): K. Yaji, A. Harasawa, K. Kuroda, R. Li, B. Yan, F. Komori and S. Shin, *Physical Review B* **98** (2018) 041404(R).
8. \*レーザーで電子のスピン方向を自由に制御：矢治光 一郎，黒田 健太，小森 文夫，辛 埴，*レーザー加工学会誌* **25** (2018) 39-42.
9. 時間分解二光子光電子分光を用いたトポジカル絶縁体表面状態における光ガルバニック効果の観測：黒田 健太，*表面と真空* **61** (2018) 302.
10. \*A weak topological insulator state in quasi-one-dimensional bismuth iodide: R. Noguchi, T. Takahashi, K. Kuroda, M. Ochi, T. Shirasawa, M. Sakano, C. Bareille, M. Nakayama, M. D. Watson, K. Yaji, A. Harasawa, H. Iwasawa, P. Dudin, T. K. Kim, M. Hoesch, V. Kandyba, A. Giampietri, A. Barinov, S. Shin, R. Arita, T. Sasagawa and T. Kondo, *Nature* **566** (2019) 518.
11. \*Low-energy electron-mode couplings in the surface bands of Sr<sub>2</sub>RuO<sub>4</sub> revealed by laser-based angle-resolved photoemission spectroscopy: S. Akebi, T. Kondo, M. Nakayama, K. Kuroda, S. Kunisada, H. Taniguchi, Y. Maeno and S. Shin, *Physical Review B* **99** (2019) 081108(R).
12. †\*Multiple topological states in iron-based superconductors: P. Zhang, Z. Wang, X. Wu, K. Yaji, Y. Ishida, Y. Kohama, G. Dai, Y. Sun, C. Bareille, K. Kuroda, T. Kondo, K. Okazaki, K. Kindo, X. Wang, C. Jin, J. Hu, R. Thomale, K. Sumida, S. Wu, K. Miyamoto, T. Okuda, H. Ding, G. D. Gu, T. Tamegai, T. Kawakami, M. Sato and S. Shin, *Nature Phys* **15** (2019) 41-48.

## Matsunaga group

Matsunaga group investigated light-matter interactions and light-induced nonequilibrium phenomena by utilizing terahertz (THz) wave, infrared, and visible light sources based on ultrafast pulsed laser technology. Polarization-sensitive THz time-domain spectroscopy system was developed with precision of several tens of micro rad between 0.5 and 2.0 THz frequency. By using this system, terahertz anomalous Hall effect in quantum materials were investigated. High-frequency THz pulse generation technique was also developed using Yb:KGW laser with 250 femtosecond pulse width. Novel pulse compression technique using a series of quartz plates were developed and evaluated, and broadband THz generation up to several tens of THz frequency with remarkable stability of carrier-envelope phase were realized.

## Okazaki group

We have investigated superconducting-gap structures of unconventional superconductors by a low-temperature and high-resolution laser ARPES apparatus and transient electronic structures in photo-excited non-equilibrium states by a time-resolved ARPES apparatus using EUV and SX lasers. In the fiscal year 2018, we have investigated the systematic S substitution dependence of the electronic structure of FeSe<sub>1-x</sub>S<sub>x</sub> in the superconducting state, and found strong evidence that this system is located in the BCS-BEC crossover regime. In addition, we have obtained strong evidence that Ta<sub>2</sub>NiSe<sub>5</sub> is an excitonic insulator from its dynamical behavior to photo-excitation, and found a photo-induced transition from an excitonic insulating state to an exotic non-equilibrium semimetallic state in this material.

1. †\*Antiphase Fermi-surface modulations accompanying displacement excitation in a parent compound of iron-based superconductors: K. Okazaki, H. Suzuki, T. Suzuki, T. Yamamoto, T. Someya, Y. Ogawa, M. Okada, M. Fujisawa, T. Kanai, N. Ishi, J. Itatani, M. Nakajima, H. Eisaki, A. Fujimori and S. Shin, *Phys. Rev. B* **97** (2018) 121107(R) (1-6).
2. \*Observation of topological superconductivity on the surface of an iron-based superconductor: P. Zhang, K. Yaji, T. Hashimoto, Y. Ota, T. Kondo, K. Okazaki, Z. Wang, J. Wen, G. D. Gu, H. Ding and S. Shin, *Science* **360** (2018) 182-186.
3. †\*Resonant magneto-optical Kerr effect measurement system using a high harmonic generation laser: Sh. Yamamoto, D. Oumbarek, M. Fujisawa, T. Someya, Y. Takahashi, T. Yamamoto, N. Ishiia, K. Yajia, S. Yamamoto, T. Kanai, K. Okazaki, M. Kotsugi, J. Itatani, S. Shin and I. Matsuda, *J. Electron Spectrosc. Relat. Phenom.* **222** (2018) 68-73.

† Joint research with outside partners.

4. \*Superconducting gap anisotropy sensitive to nematic domains in FeSe: T. Hashimoto, Y. Ota, H. Q. Yamamoto, Y. Suzuki, T. Shimojima, S. Watanabe, C. Chen, S. Kasahara, Y. Matsuda, T. Shibauchi, K. Okazaki and S. Shin, *Nat. Commun.* **9** (2018) 282 (1-7).
5. †\*Superconducting Pairing of Topological Surface States in Bismuth Selenide Films on Niobium: D. Flötotto, Y. Ota, Y. Bai, C. Zhang, K. Okazaki, A. Tsuzuki, T. Hashimoto, J. N. Eckstein, S. Shin and T. -C. Chiang, *Sci. Adv.* **4** (2018) eaar7214 (1-5).
6. †\*Photo-induced semimetallic states realised in electron–hole coupled insulators: K. Okazaki, Y. Ogawa, T. Suzuki, T. Yamamoto, T. Someya, S. Michimae, M. Watanabe, Y. Lu, M. Nohara, H. Takagi, N. Katayama, H. Sawa, M. Fujisawa, T. Kanai, N. Ishii, J. Itatani, T. Mizokawa and S. Shin, *Nat Commun* **9** (2018) 4322 (1-6).
7. †\*Multiple topological states in iron-based superconductors: P. Zhang, Z. Wang, X. Wu, K. Yaji, Y. Ishida, Y. Kohama, G. Dai, Y. Sun, C. Bareille, K. Kuroda, T. Kondo, K. Okazaki, K. Kindo, X. Wang, C. Jin, J. Hu, R. Thomale, K. Sumida, S. Wu, K. Miyamoto, T. Okuda, H. Ding, G. D. Gu, T. Tamegai, T. Kawakami, M. Sato and S. Shin, *Nature Phys* **15** (2019) 41-48.

† Joint research with outside partners.

\* Joint research between groups within ISSP.

---

\* Joint research among groups within ISSP.

The Institute for Solid State Physics (ISSP), The University of Tokyo

---

Address 5-1-5 Kashiwanoha, Kashiwa, Chiba, 277-8581, Japan

Phone +81-4-7136-3207

Home Page <https://www.issp.u-tokyo.ac.jp>